Francesco Riggi

# Messengers from the Cosmos

## An Introduction to the Physics of Cosmic Rays in Its Historical Evolution

Springer

# UNITEXT for Physics

**Series Editors**

Michele Cini, University of Rome Tor Vergata, Roma, Italy

Attilio Ferrari, University of Turin, Turin, Italy

Stefano Forte, University of Milan, Milan, Italy

Guido Montagna, University of Pavia, Pavia, Italy

Oreste Nicrosini, University of Pavia, Pavia, Italy

Luca Peliti, University of Napoli, Naples, Italy

Alberto Rotondi, Pavia, Italy

Paolo Biscari, Politecnico di Milano, Milan, Italy

Nicola Manini, University of Milan, Milan, Italy

Morten Hjorth-Jensen, University of Oslo, Oslo, Norway

Alessandro De Angelis , Physics and Astronomy, INFN Sezione di Padova, Padova, Italy

UNITEXT for Physics series publishes textbooks in physics and astronomy, characterized by a didactic style and comprehensiveness. The books are addressed to upper-undergraduate and graduate students, but also to scientists and researchers as important resources for their education, knowledge, and teaching.

Francesco Riggi

# Messengers from the Cosmos

An Introduction to the Physics of Cosmic
Rays in Its Historical Evolution

∲ Springer

Francesco Riggi
Department of Physics and Astronomy
University of Catania and INFN
Catania, Italy

# Preface

All areas of scientific investigation may be considered, especially in the eyes of those directly involved in that activity, as an exciting adventure. If we looked for a definition of "adventure", we would find that it is described as a singular and extraordinary story, or as a risky but fascinating and attractive undertaking, especially for what is unexpected and unknown, as pointed out by the very same Latin root of the word, *adventura*, what will happen. With these premises, it is not easy to find a discipline that presents, more than others, these characteristics, such as the physics of cosmic rays.

The study of the radiation of cosmic origin presented, since its inception, peculiarities capable of involving researchers in experimental activities that went beyond the boundaries of their research laboratories, pushing them to carry out their studies and their measurements in the most disparate environments of our planet. The debate about the possible nature of this radiation, whether it was linked to the phenomena of terrestrial radioactivity, which somehow began to be known already a century ago, or it was rather the result of processes that took place outside the Earth, in the whole cosmos, put the object of the investigations in a specific perspective and opened up the horizon of places where to look for clues that could have given an answer to this question.

The history of cosmic ray physics, especially in the first decades that followed the first evidence of the existence of this radiation, shows us an incessant activity by the researchers involved, who did not disdain to engage themselves in the most disparate working conditions: We will see them climbing mountains, boarding balloons, pressurized capsules or aircrafts to go to high altitudes, placing their equipment under the water of seas and lakes, or in the deepest mines, performing scientific expeditions in all the globe, from equatorial to polar regions, all to study the nature of this radiation and characterize its behavior. We must consider how this happened about a century ago, with the tools and difficulties of the time, which makes these activities even more full of adventure. We may say this is an attitude and a scientific practice that in some way still goes on today, since the research in this area, more generally in the field that we call today astroparticle physics, has reached the boundaries of space

outside the Earth and, even on our planet, makes use of environments that are among the least comfortable, with huge and complex detection apparatuses.

The first evidence of the existence of radiation of extraterrestrial origin refers, as it is well known, to the first experiences, carried out with electroscopes, of the phenomenon of air ionization. The observation of the apparently spontaneous discharge of these instruments indicated the existence of a source capable of ionizing the air inside them. Was it possible to explain this phenomenon solely on the basis of the radiation emitted by radioactive substances present in the Earth's soil? For a long time, this remained an open problem, to which the observations made by numerous experimenters gave decisive contributions, until the reasonable certainty was reached that the cause was rather to be found in a radiation coming from outside the Earth, a radiation of cosmic origin.

In the following decades, the nature of this radiation, its characteristics, and its links with the nascent physics of elementary particles became more and more defined. The experimental observations benefited from the development of equipment and detection techniques that allowed not only more detailed and precise studies of the known phenomena, but also of highlighting qualitatively new phenomena, such as the existence of enormous showers of particles in the Earth's atmosphere, produced by the arrival of a single particle of very high energy.

Looking at the events that characterized the development of this discipline in a historical key is particularly useful from an educational point of view. Indeed, it allows us to better understand how knowledge developed, and through which steps—and also which errors, or approximate knowledge—we have achieved a more correct point of view. But it is also important to see how it was possible to make a remarkable series of observations, corroborated by interpretations that turned out to be in most cases correct, although the tools and observational techniques of the past were enormously simpler than the current ones. For this reason, it was useful to discuss, even at an introductory level, what were the observational tools of the cosmic radiation, those which became from that moment on the detectors of particles and radiation.

There is another important aspect from an educational point of view in dealing with the main phenomena relating to the physics of cosmic rays. In fact, a remarkable variety of projects and teaching activities has developed around this area, especially in recent decades, in the awareness that the physics of cosmic rays can be an excellent means of introducing students and science enthusiasts to the problems and results of modern physics. This was accompanied by the possibility of using even simple detection devices, such as the Geiger counter in the first instance—but also more complex ones—to organize a multiplicity of experiments that can be carried out at low cost but with considerable potential in terms of possible scientific activities and outcomes. The author has been involved for more than twenty years in various educational projects, local or international, related to cosmic ray physics. In many cases, these activities have given rise to what is now often referred to as "citizen science", i.e., the possibility that the general public can also carry out scientific activities by learning something directly about the way in which scientific research proceeds.

If this is the spirit in which these pages were written, it must be said that it is always difficult to understand which target, which audience to turn to when writing a book. An attempt has been made to provide as broad a picture as possible of the problems and historical developments of this discipline, maintaining an understandable level, for most of the topics, even by the passionate science reader. At the same time, however, attempts have been made to present many phenomena in a quantitative way, often making use of the original results, in order to provide non-generic information on the phenomena in question. In this direction, we must consider several plots that report the data published in the original articles, in some cases slightly reworked to make them more readable.

The idea of this text is therefore to provide a working tool to those who wish to get more involved into this field of physics, whether they are students attending undergraduate courses in physics or simple science enthusiasts. To achieve this aim, an extensive bibliography has been collected, which includes, in addition to the list of the major textbooks published on the subject, also many articles of a historical and biographical nature, as well as a long list of detailed references, over 500, to the original articles cited along the text. The invitation for those wishing to further deepen their knowledge of this sector is therefore to start from this text as a guide for further reading. Another aspect that may contribute to consider this text as a working tool is the presence of a certain number of Appendices, where results obtained by numerical calculations are also presented, with an invitation to readers to implement the procedures themselves and get additional results.

Of course, although we may try to present a broad phenomenology, cosmic ray physics is strictly related to several other aspects of scientific knowledge that have only marginally been mentioned here, such as the overall picture of elementary particle physics, the physics of neutrinos, that of gravitational waves, and in general many important problems in astroparticle physics.

Instead, we wanted to give, in a specific chapter, also a picture of the different application aspects in which muons, as a penetrating charged component of the secondary cosmic radiation, play an increasingly important role, and which in recent years have given rise to numerous projects in the most diverse sectors, from the prevention of illicit transport of radioactive materials in containers to the study of the internal structure of volcanoes, to monitoring the stability of civil buildings, to name only those in which the author has been involved.

As personally engaged in various educational and research activities related to the physics of cosmic rays, I would like to thank many people with whom I have interacted in these decades. Among these, the undergraduate and Ph.D. students who collaborated to these activities, many of them are now being enrolled in research or academic Institutions. I particularly thank all the colleagues of the Extreme Energy Events (EEE) Collaboration, in which the author has participated since its beginning, with whom it was a privilege and a pleasure to collaborate. The interactions with the thousands of high-school students and teachers participating in the EEE project in recent years have provided an important framework to place many of the considerations set out in this text. Critical reading of parts of this manuscript by

several colleagues is warmly acknowledged. A special thank to the Springer staff for help in editing the manuscript. Finally, I would also like to thank the members of my family, my wife, my sons and daughter, together with our grandchildren, with whom I have sometimes tried to share the passion for investigating the world around us.

Catania, Italy                                                                                    Francesco Riggi
October 2022

# Contents

# Chapter 1
# The Discovery of the Cosmic Radiation

**Abstract** The balloon ascent made by Victor Hess in 1912, up to an altitude of 5300 m, is generally associated to the *discovery* of the cosmic rays. Related phenomena at that time were the terrestrial radioactivity, the absorption of the gamma radiation in air and the air ionization, all aspects extensively studied by the use of electroscopes. Even before the famous flight by Hess, several people contributed to these studies: Theodore Wulf with his measurements on the top of the Eiffel Tour, Julius Elster and Hans Geitel who carried out measurements of the air ionization in different locations, Albert Gockel and Karl Bergwitz performing high altitude experiments, and Domenico Pacini with his underwater measurements. The chapter reviews all these contributions and analyzes in detail, by tables and plots, the original data obtained by Victor Hess in 1911–1912 and by Werner Kolhörster in 1913–1914 at even higher altitudes, which definitely demonstrated the existence of an extraterrestrial radiation. Appendix A also provides examples and suggestions on how to perform numerical calculations of the expected gamma ray flux at the top of the Eiffel Tour, originating from ground radioactivity.

## 1.1  Introduction

August 7th, 1912, early morning: a young Austrian physicist, Victor Franz Hess (1883–1964), at that time in his thirties, is ready to leave aboard a hydrogen-filled balloon for a scientific expedition, from a location called Aussig at the time (now Ústí nad Labem, in the Czech Republic). It is not the first of his balloon flights: in the previous months he has already made other excursions, reaching almost 3000 m above sea level. Today's flight, the seventh in the series, will take him even higher, to an altitude of over 5000 m.

His aim is to verify whether the ionization of air at high altitude, measured by the discharge of the electroscopes he is carrying with him, increases significantly with altitude, confirming what he has already observed in several previous flights, carried out at lower altitudes. A few hours later Hess will have confirmation of what he is looking for: his flight, the seventh in the series, which brought him to a maximum altitude of 5350 m, will allow to establish that the cause of the electroscope discharge

phenomenon is due to something whose intensity undoubtedly increases with altitude and therefore cannot be linked to the radioactivity of terrestrial rocks.

This event has been generally associated to the *discovery* of the so-called cosmic radiation, a term that was coined many years later by the American physicist Robert Millikan (1868–1953), according to the commonly used interpretation, but which had actually been used many years before him.

Many discoveries in physics are objectively difficult to associate with defined dates or with single events, even if—often a posteriori—it becomes evident how that experiment, that formulation, that model represented a real novelty compared to the status of previous knowledge, such as to assign to them a specific role, a turning point in the history of that discipline. It is also the case of the discovery of cosmic rays, which presupposes a series of previous events, intuitions, verifications, significant contributions given by other authors, which inevitably intertwine with those events that are usually classified as "discovery".

In the specific case of the discovery of cosmic radiation and its subsequent developments many physical phenomena have played an important role, such as air conductivity and natural radioactivity, and the interpretation of the results concerned with the study of cosmic radiation involved at the same time other branches of physics, such as the knowledge of subatomic particles.

## 1.2  Terrestrial Radioactivity and First Experiences with Electroscopes

The phenomenon of the spontaneous discharge of electroscopes had already been investigated by Charles-Augustin de Coulomb (1736–1806) in 1785 [Coulomb1785]. An electroscope, in its simplest version, is a device capable of detecting the presence of an electrical charge. It may consist of two thin metal foils (for example two gold leaves), placed in contact at the upper end, through a support leaving them free to separate at the bottom; the leaflets are positioned inside an insulating container and electrically connected to an external conductor. It is a known experience that by touching the external conductor with an electrically charged body, or simply approaching the charged body to it, by induction, the leaflets diverge, both being charged with the same sign and therefore repelling each other. At the beginning of 1900 it had already been known for a long time that an electroscope gradually lost its charge, even if isolated from an electrical point of view and in the absence of any direct contact with other bodies. The speed with which the electroscope discharges depends on the pressure of the air inside it, as the observations of William Crookes (1832–1919), British physicist and chemist, had shown, suggesting that the cause of the discharge was linked to the ionization of the air [Crookes1878] (Fig. 1.1).

In those years, Charles Vernon Boys (1855–1944) had also observed the same phenomenon, concluding that this loss was due to convection processes through the air [Boys1889]. At the end of the 1800s, however, the conductivity of air was the

**Fig. 1.1** Williams Crookes (1832–1919). *Source* AIP Emilio Segrè Visual Archives

subject of very extensive studies by numerous scientists. Although the knowledge of the detailed atomic structure was yet to come, the fact that matter consisted of atoms, each corresponding to a different chemical species, and that atoms could form molecules, was already known. As well as the fact that ordinary matter is neutral, containing an equal amount of positive and negative charge. The discharge of an electroscope could therefore be interpreted based on the fact that the air is always slightly ionized, that is, it contains a small fraction of electrons and positive ions, which could be attracted by the electroscope leaves charged with the opposite sign.

Subsequently, the knowledge of the phenomena related to natural radioactivity, the discovery of cathode rays and that of X-rays had allowed to establish that these causes certainly contributed to the conductivity of the air and therefore could explain the progressive loss of electric charge by the electroscope (Fig. 1.2).

Charles Thomson Rees Wilson (1869–1959), an English physicist who had started his career working in the laboratory of Joseph Thomson (1856–1940), had already conducted, in 1896, his first observations with the prototype of what would later be the cloud chamber, investigating the conductivity of the air exposed to X-rays [Wilson1896, Wilson1897]. Further studies carried out in the following years had allowed to understand different aspects of the effect that X-rays had on the ionization of the air and on the condensation produced in the gases by these ionizing
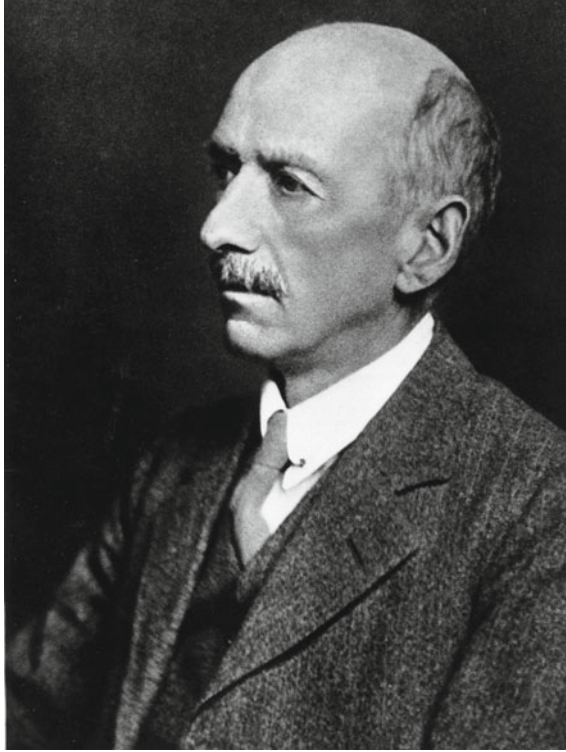
**Fig. 1.2** Charles Thomson Rees Wilson (1869–1959). *Source* AIP Emilio Segrè Visual Archives

agents [Wilson1898, Wilson1899, Wilson1900a, Wilson1900b, Wilson1901a]. In the same period, similar results on the phenomenon of the spontaneous loss, even in pure air, of the charge possessed by a charged conductor were obtained by Julius Elster (1854–1920) and Hans Geitel (1855–1923), two German physics teachers who had conducted experiments using their private laboratory [Elster1900a, Elster1900b, Geitel1901].

The overall results of this activity, carried out by numerous experimenters around the end of 1800, could therefore be summarized in the fact that a charged conductor lost its charge in the air regardless of the environmental conditions (light or dark), and that this loss was proportional to the pressure of the air, as it had been verified by experiments conducted inside sealed vessels. From a quantitative point of view, this loss of charge corresponded to about 20 ions per second for each cubic centimeter of air. It was therefore necessary to admit that an equivalent number of ions were continuously produced in the air.

Wilson had also conducted experiments expressly to establish whether this production of ions in the air could be attributed to radiation from sources extraneous to the atmosphere, such as X-rays or cathode rays, but of greater penetrating power. These experiments involved, for example, the comparison between what was

observed on the ground and what could be observed underground, at a certain depth, in a railway tunnel [Wilson 1901b]. However, since there was no appreciable difference between the results of the two measurements, Wilson concluded that ionization was an intrinsic property of air itself. The term "ionization" began to be used right from the works of this author.

We will discuss Wilson's role and contribution to cloud chamber observations later on. Instead, we still remain on the crucial issue of this period: the ionization of air and the causes that produce it.

As we have already seen, it was clear that different sources of radiation could produce the creation of ions in the air, thus discharging the electroscopes: both the X-rays and the products emitted by radioactive decay were capable of producing such effects. The prevailing opinion about the cause of this ionization was that the main source of air ionization was linked to the radioactivity of the soil rocks, in particular to the gaseous emanations emitted by certain minerals present in the rocks. In addition to those already cited, further studies by Elster and Geitel contributed to this opinion [Elster1899, Elster1901].

However, already in those years, there were also studies of the shielding effect on the discharge of electroscopes, in the underlying hypothesis that the cause was a radiation coming from above [McLennan1903a, McLennan1903b, Rutherford1903]. For example, various metal layers were used around electroscopes, to evaluate their effect on the phenomenon of discharge, and in the case of a considerable thickness (a few cm of lead) some sensitive effect was observed. Apparently, an additional amount of lead, even considerable, did not further influence the discharge of the electroscope, an aspect incomprehensible at that time but which is consistent with the modern vision of cosmic radiation.

Another phenomenology was represented by measurements made in cellars, caves or underground locations, again by Elster and Geitel [Elster1900b]. In some cases, an even faster discharge of electroscopes was observed than that observed on the surface in the open air, especially if the underground environments had been closed for several days. It is a phenomenology that today is related to the emission of radon gas produced by the radioactive decay of certain nuclei contained in the rocks.

All these measurements and related considerations revolved around the use of electroscopes, as the main tool for evaluating the ionization of air. The use of electroscopes was in fact very common at that time, for the study of issues related to electricity in the air, meteorology and for the understanding of atmospheric phenomena in everyday life [DeAngelis2014]. Many of the experimenters involved in these early studies of cosmic radiation personally contributed to the construction and improvement of these instruments, which in some way represented the first particle detectors.

Compared to the original leaf electroscopes, significant improvements [Wulf1909a] were made by Theodor Wulf (1868–1946), a German physicist, teacher in Walkenburg (Holland), a Jesuit priest, who introduced two thin quartz fibers in place of leaflets, with the possibility of observing the deviation through a microscope with a graduated scale (Fig. 1.3). Further improvements were subsequently introduced by Victor Hess and the German Werner Kolhörster (1887–1946), so much

so that the company in charge of building such devices had five different types of electroscopes in its catalog, according to the needs of the different experimenters [Walter2012]. Elster and Geitel had also dedicated themselves to improving the characteristics of these electroscopes, achieving better sensitivity [Fricke2017]. Today many of these original instruments can be viewed in collections of ancient instruments, for example at the European Center for the History of Physics in Austria [Kahlert2011], in many university or school collections, or on sites showing extensive virtual collections of electroscopes and electrometers, for example that viewable at the site of the Oak Ridge Associated Universities [ORAU].

The most common explanation of the phenomenon of the spontaneous discharge of electroscopes, linked to the conductivity of the air, was therefore associated, as we have seen, with the presence of ionizing radiation sources, in the form of radioactive impurities existing in common materials placed near the electroscope.

Although some ideas about the possibility of highly penetrating radiation of extraterrestrial origin were already circulating at that time, and it seems that even Marie Curie (1867–1934) had speculated, in 1898–1899 [Curie1898, Curie1899], about the possibility of a highly penetrating radiation coming from the Sun, no quantitative results had been obtained that could confirm these hypotheses.

In the following decade a series of quantitative investigations was carried out by various experimenters, both in Germany and in Great Britain, USA, Switzerland, Austria and also in Italy, by Domenico Pacini (1878–1934). The improvement of electrometers, by Wulf, allowed more precise measurements of air ionization, performed in different environments, on the land, on the surface of water, on lakes
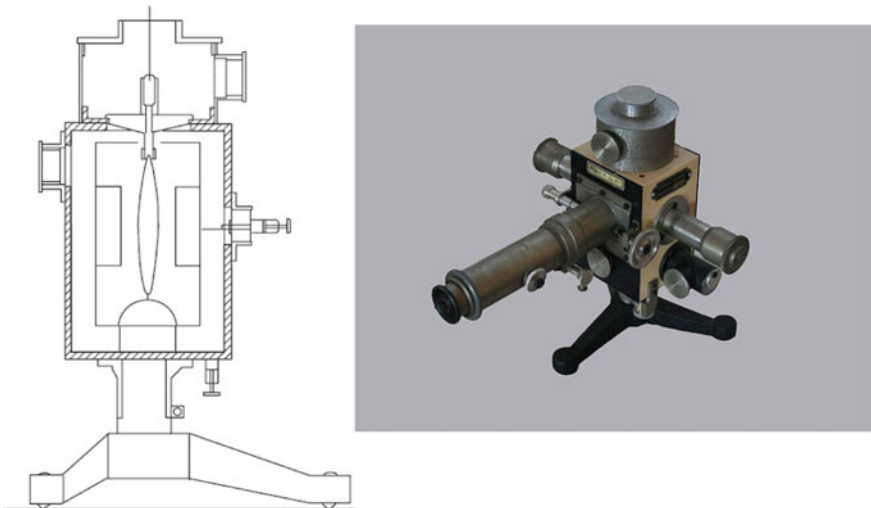


**Fig. 1.3** Left: schematic of a Wulf electroscope, in which the divergence of the fine quartz fibers can be quantitatively observed using a microscope and a graduated scale. On the right a photo of a real model of an electroscope, used by Wulf around 1912. *Source* Wikimedia Commons, A. De Angelis and C. Guaita, from the collection of R. Fricke

and on glaciers. The idea that guided these observations was linked to the fact that if this ionization had been caused by any material present in the Earth's soil, it would have had to be smaller on the surface of the water, which contained fewer radioactive impurities. The results, however, indicated only a slight decrease compared to the values observed on the ground, and therefore did not allow a clear interpretation.

One of the important consequences of these investigations was the evaluation of the absorption coefficient of gamma rays in air, water and solid ground [Eve1906, Eve1907], due to the English physicist Arthur Stewart Eve (1862–1948) (Fig. 1.4), who worked mainly in Canada. Gamma rays, made up of high-energy photons, typically produced in radioactive phenomena involving nuclei, have the greatest penetration capacity among the radiations emitted by radioactive substances present in the soil. It can be assumed as a first approximation that the gamma flux capable of crossing a given material thickness x is governed by an exponential relation, of the type

$$I = I_0 e^{-\mu x}$$

where $I_0$ and $I$ represent the original flux and that measured after a thickness x, and $\mu$ is the linear absorption coefficient, expressed for example in $cm^{-1}$ if the thickness is expressed in cm. The following table shows the value of some absorption coefficients, extracted from the original work of Eve [Eve1906] for some materials, compared with the values commonly accepted today for air at different gamma energies, tabulated on the website of the National Institute of Standards and Technology [NIST].

Based on the absorption coefficients shown in Table 1.1, the reduction of the gamma ray flux emitted in a specific direction would result in an attenuation of about 50% after a distance of 150 m of air crossed. On the other hand, these absorption coefficients are much higher in solid rocks: a 50% reduction in the gamma ray flux under the same conditions would be obtained after only 7 cm of rock crossed. From this it can be estimated that only the most superficial part of the ground can contribute significantly to the radiation present in the air.

If the emitting source were point-like, with isotropic emission, and we wanted to consider the effect produced by the gamma at a certain distance d in the air, for example the number of ions per second per unit of volume at a distance d from the source, this would be proportional to exp $(-\mu\ d)/d^2$, where the exponential term accounts for the absorption in the material and the term $1/d^2$, inversely proportional to the square of the distance, takes into account the subtended solid angle. The overall result is that the effect would diminish very quickly with distance.

In the case of radioactivity emitted from the Earth's soil, however, the emitting source is not point-like, but can be considered as a first approximation to be uniformly diffused, both horizontally and vertically, below the ground. Of course, the radioactive material present beyond a certain depth and beyond a certain distance from the place where the ionization is considered contributes little to this effect, both because there is an attenuation due to the absorption in the material (rock or air) and because the radiation is emitted isotropically in all directions and therefore is attenuated with a trend inversely proportional to the square of the distance. The problem is therefore

**Fig. 1.4** Arthur Stewart Eve (1862–1948)

**Table 1.1** Absorption coefficients for gamma rays coming from the ground, in $cm^{-1}$, for different materials

| Material | Absorption coefficient ($cm^{-1}$) |
|---|---|
| Air | 0.000044 |
| Water | 0.034 |
| Solid rock | 0.092 |
| Air (E = 1 MeV) | 0.000078 |
| Air (E = 2 MeV) | 0.000054 |
| Air (E = 3 MeV) | 0.000044 |
| Water (E = 3 MeV) | 0.039 |

The values for air, water and solid rock are extracted from [Eve1906]. The other values, corresponding to fixed gamma energies, are current values, taken from the site of the National Institute of Standards and Technology [NIST]

more complex than the absorption of the gammas emitted by a point source that travels a single path, of length x, up to the point where the flux is measured.

The situation around 1909 could be summarized by the conclusions reached up to that moment by Wulf: the result of the experiments shows that the penetrating radiation is produced by radioactive substances present in the subsoil, up to about one meter deep. If a certain fraction of this radiation comes from the atmosphere, it is however negligible compared to that due to the substances present in the subsoil and cannot be detected with the tools available at the time [Wulf1909b]. In these conclusions, as appears evident, it is not excluded that there may be an additional radiation, in addition to that due to terrestrial radioactivity, but it is quantitatively assessed that it cannot be clearly identified, given the experimental working conditions and the precision of the instruments, an absolutely reasonable and modern attitude to proceed. How then to take a step forward? We will see in the next section the results obtained in 1909 at the top of the Eiffel Tower by Wulf himself.

Even before these measurements, however, as early as 1907, the Italian physicist Domenico Pacini was also conducting experiments using electrometers (similar to those used by Wulf), in different environments (in the mountains, on the surface of a lake or sea, and finally also under a certain depth of water). In one of these measurements, conducted in a boat at a certain distance from the mainland, and with a water thickness of about 4 m under the apparatus, Pacini had observed values that were not too different (about 2/3) compared to those measured on the mainland [Pacini1910]. The absorption coefficient of gamma rays in water, measured previously, shows that already a thickness of one meter of water typically reduces the gamma ray flux to a few percent of the initial value. A thickness of a few meters therefore makes the contribution due to the radioactivity of the seabed absolutely negligible on the surface. Pacini's conclusions, even following further investigations, were clearly in favor of a significant cause of ionization due to the atmosphere, independent of the radioactivity of the soil [Pacini1912]. It would therefore seem that an important role in the awareness of the existence of a radiation of extraterrestrial origin is to be assigned to the Italian physicist, as documented in detail by Carlson and De Angelis [Carlson2011, DeAngelis2010, DeAngelis2012], although his contribution has not been adequately recognized (Fig. 1.5).

Beyond the recognition of the specific role of the many people who contributed to these studies, it can be said that around 1910 various evidence seemed to indicate the presence of something not attributable to the radioactivity of the soil or of the air circulating near the ground. The experimental working conditions of these experiments (shielding of the devices, degree of contamination of the materials …) were however not sufficiently defined and the quantitative results obtained were not precise enough to allow certain conclusions. Despite the difficulty of reconciling the results obtained with the hypothesis of radioactivity due to the Earth, a difficulty recognized by many, there was not however any real alternative, which referred to other known causes and allowed to explain in a quantitative way what was observed.

**Fig. 1.5** Domenico Pacini (1878–1934). Courtesy of Pacini family, by A. De Angelis

## 1.3   Investigations in the Atmosphere

After a long series of measurements performed in the terrestrial (or marine) environment, it was inevitable to think of obtaining more detailed information on what was happening at altitudes higher than sea level, or in the atmosphere. These are indeed different conditions: in the first case, although moving to higher altitudes, for example over the top of a high mountain, one is always close to the Earth's soil, with the presence of rocks capable of emitting radiation. If you want to investigate the behaviour of air ionization away from the presence of the soil, it is necessary to move away from it instead. Measurements of both the first and the second type had in fact been carried out by several experimenters in those years.

Elster and Geitel had compared the ionization measurements of the air at sea level and at an altitude of 3000 m, finding a slight increase at 3000 m above sea level [Elster1900a]. High altitude measurements had also been carried out by Albert Gockel (1860–1927) together with Wulf, starting from 1908. The two had carried out measurements of the ionization of the air at various altitudes, in the Alps, from 650 m up to 3000 m [Gockel1908]. However, these measurements had not allowed to highlight a clear influence of altitude on ionization, and the experimenters had therefore concluded that any cosmic radiation, if it ever existed, should have contributed to the phenomenon with a negligible intensity. Some have correctly noted [Walter2012]

how the term "cosmic radiation" has already been used in this context, well before what is commonly believed, based on the term used by Robert Millikan in 1926.

But how to get away from the ground, so as to make negligible, or at least strongly reduce, the influence of radioactivity due to the terrestrial soil? Wulf, after a campaign of measurements conducted with electroscopes in various European locations [Wulf1909b], had the opportunity in 1910 to carry out measurements at the top of the Eiffel Tower, about 300 m above the ground [Wulf1910]. The Eiffel Tower, opened to the public about twenty years earlier, in 1889, was at that time the tallest building in existence, far surpassing the Washington Monument, a 169-m-high obelisk. In addition, it had the advantage of having a very light, almost transparent structure, and therefore greatly reducing the presence of potential disturbing material under the devices used for measuring air ionization. The measurements were repeated by Wulf on different days and times, obtaining different values, measured both at the top of the Eiffel Tower and on the ground (Table 1.2; Fig. 1.6).

As can be seen from this table, the values obtained by Wulf at the top of the Eiffel Tower are slightly lower (about 15% less) than those obtained on the ground, on average 15.7 ions/(cm$^3$ s) at the top against a value of 17.9 (in the same units) on the ground. Although with large fluctuations from one measurement to another, the uncertainty associated with the average value of the set of four measurements conducted at the top of the Eiffel Tower, about 0.3 ions/(cm$^3$ s), is small enough to consider as significantly different the values obtained in the two conditions.

The main problem, however, is that the observed reduction is not compatible with what would be expected based on the absorption of gammas if they came from radioactive substances present in the soil. Such a calculation, depending on the height above the ground, is discussed in Appendix A, assuming the values of the absorption coefficients for air and rock shown in Table 1.1.

Figure 1.7 shows the average values obtained by Wulf on the ground and at the top of the Eiffel Tower, together with the trend of the expected values, as a function of the distance from the ground, according to what can be expected if the cause of this ionization at a given height was to be attributed to the gamma radiation emitted

**Table 1.2**  Values of the air ionization rate, obtained by Wulf during the measurements conducted on the Eiffel Tower [Wulf1910]

| Date | Location | Ionization rate (ions cm$^{-3}$ s$^{-1}$) |
| --- | --- | --- |
| 29.03.1910 | Ground | 17.5 |
| 30.03.1910 | 300 m | 16.2 |
| 31.03.1910 | 300 m | 14.4 |
| 01.04.1910 | 300 m | 15.0 |
| 02.04.1910 | 300 m | 17.2 |
| 03.04.1910 | Ground | 18.3 |
| Average | Ground | 17.9 |
| Average | 300 m | 15.7 |

**Fig. 1.6** Theodore Wulf (1868–1946)

by radioactive nuclei uniformly distributed in the ground, up to a depth of one meter and within a distance of 1000 m from the Eiffel Tower. Some further details of the calculation are discussed in Appendix A. The curve has been normalized to the mean of the values measured at the top. Compared to this value, as can be seen, the ionization of the air should decrease with the height above the ground, at least by a factor of 10 for a height equal to that of the Eiffel Tower, while the experimentally obtained value is only 15% smaller.

It is clear, at least to us who read these data in the light of current knowledge, that they indicate a further cause of ionization, not related to the radioactivity of the soil, and capable of compensating for the attenuation due to the distance from the ground. These data, however, were not sufficient to prove the existence of an extraterrestrial radiation, and the discrepancies were generally attributed to the influence of causes still attributable to radioactivity of terrestrial origin (residues of radioactive material in the devices, influence of radioactivity present in the material of construction of the Eiffel Tower itself, …).

How to move further away from the ground and verify if something different really happened at great heights above the Earth's surface? In fact, at the beginning of the 1900s, several possibilities were already available to courageous experimenters.
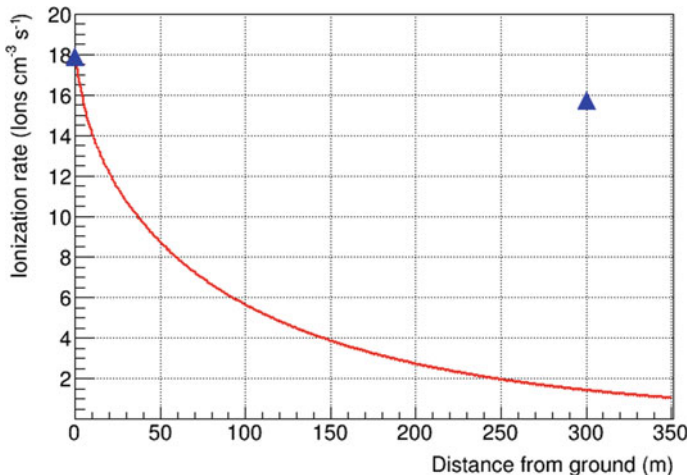
**Fig. 1.7** Average values of the ionization rate measured by Wulf on the ground and at the top of the Eiffel Tower (blue triangles). The solid red line shows the expected trend based on the contribution generated by gamma radioactive isotopes dispersed in the soil surrounding the Eiffel Tower (within a radius of 1000 m) and up to a depth of one meter underground. Further details of the calculation are given in Appendix A

The first hot-air balloons capable of carrying people on board date back to 1783, over a century earlier, and from the very beginning they had also allowed scientific explorations. A hot air balloon, or "Mongolfiera" in Italian (named after the two French brothers Joseph-Michel and Jacques-Étienne Montgolfier) consists of a balloon made of suitable fabric, with a hole in the lower part, and whose air contained inside can be heated, allowing an upward thrust capable of carrying the balloon even to great heights. Modern hot air balloons have even reached higher altitudes than commercial flights. The hot air can be produced either at the beginning, by heating the air inside the balloon with a source that remains on the ground, or by carrying with it the necessary heat source (a burner), which allows for further maneuvers to climb in quote (Fig. 1.8).

Unlike hot-air balloons, gas balloons are filled with a gas with a lower density than air (Hydrogen or Helium) but at the same temperature. They must be hermetically sealed, so as not to let the gas escape spontaneously. To climb to a higher altitude, it is necessary to lose ballast (sand), while to go back down it is possible to control the escape of a certain quantity of gas. They too, like hot air balloons, have a long history, and were available for over a century at the time of the first cosmic ray investigations [Pfotzer1972, Ziegler1989].

We also recall that in 1900 the first dirigibles were also designed, by the German von Zeppelin, huge oblong-shaped balloons, filled with gas and capable of carrying a large number of people even for civil flights, although this possibility was exploited only for a few years, also due to the numerous accidents. What about the first planes? After the first flight by the Wright brothers in 1903, which lasted just a dozen seconds,
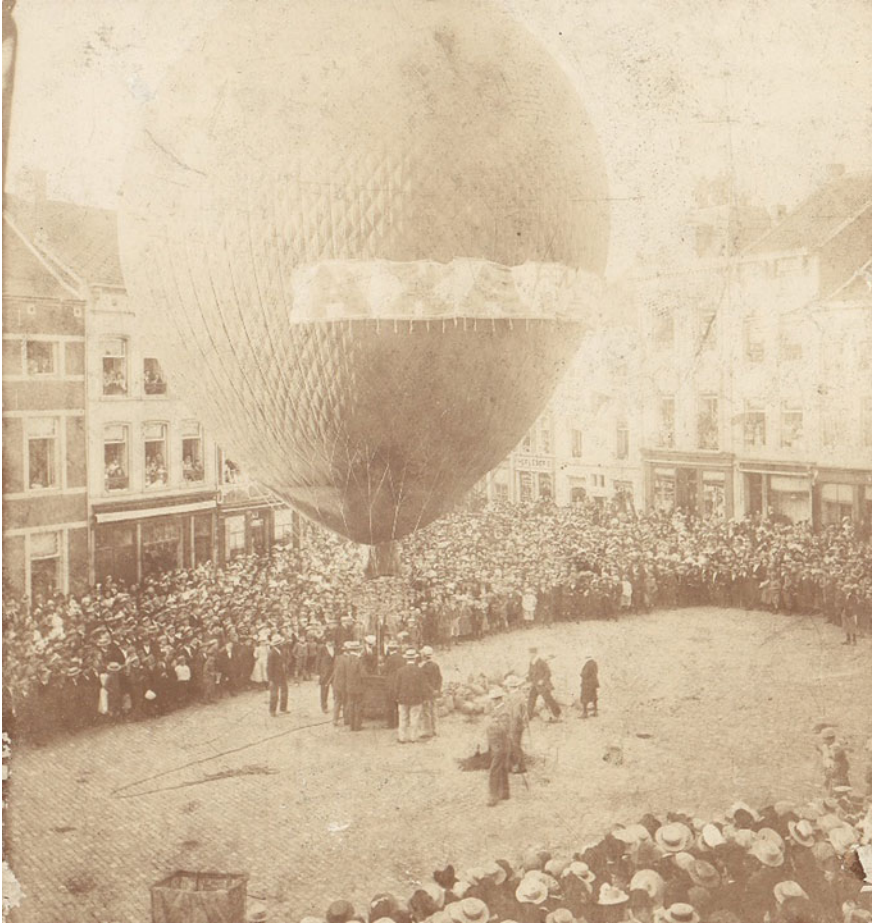
**Fig. 1.8**  Image of a hot air balloon (circa 1850–1860). *Source* Wikimedia Commons, Metropolitan Museum of Arts Collection, Creative Commons CC0 1.0 Universal Public Domain Dedication

progress had come rapidly, and by 1910 several flights had reached considerable altitudes, remaining in the air for hours.

In the early 1900s, therefore, there was no lack of means to transport measuring devices at large altitudes, an idea that in fact was pursued by numerous experimenters, who, among the various means of ascension, chose aerostatic balloons. Victor Hess's balloon ascents, remembered at the beginning, were therefore not a total novelty. The first measurements of the conductivity of air at high altitudes, aboard balloons, were made by Franz Linke (1878–1944), a German geophysicist and meteorologist, in 1902–1903, although in the context of investigations on the electric field generated by the Earth [Linke1904]. Linke had used a gold leaf electroscope up to an altitude of 5500 m, observing that around 1000 m of height the charge loss of the electrometer
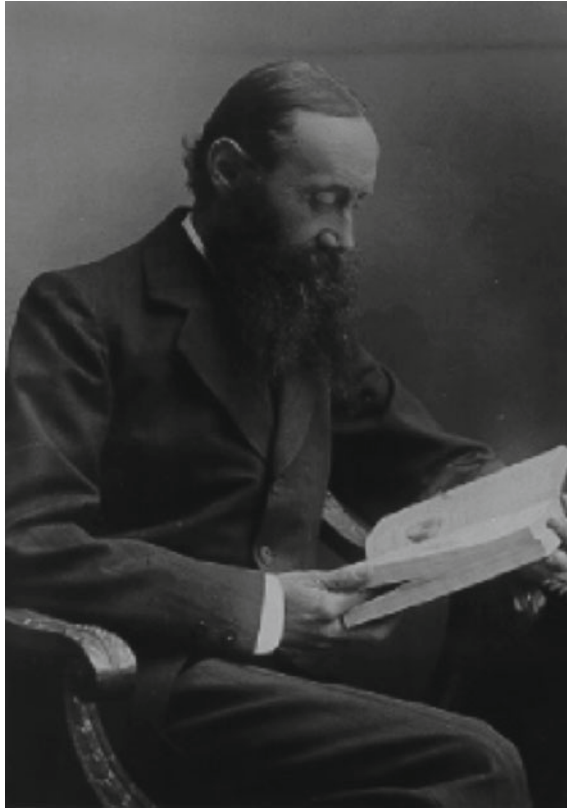
**Fig. 1.9**   Albert Gockel (1860–1927)

was less than that observed on the ground, between 1000 and 3000 m it became similar to this, and that finally, above 3000 m, became greater, up to a factor of 4 higher, at the maximum altitude reached of 5500 m, compared to what was observed on the ground. These results are strikingly similar to those observed by Hess a few years later. However, even though the activity had been conducted in collaboration with other physicists involved in such activities, such as Gockel (Fig. 1.9), it appears that they did not receive any form of recognition.

In 1908 another balloon flight was made by Karl Bergwitz (1875–1958) (Fig. 1.10), up to a height of 1300 m [Bergwitz1910], during which, even if in a much more limited interval, the same trend was noted, a decrease followed by a subsequent increase in ionization. Other balloon flights were carried out by Hermann Ebert between June 1900 and January 1901, up to a height of 3770 m, with unclear results, due to weather conditions [Ebert1901].

Subsequently, between 1909 and 1911, other flights aboard balloons were carried out by Gockel himself, at different altitudes, up to a maximum altitude of 4500 m: once again a qualitatively similar result was observed, a decrease with altitude, but

**Fig. 1.10**   Karl Bergwitz (1875–1958)

much less than expected [Gockel1910, Gockel1911]. A detailed analysis of the results obtained by Gockel during these flights has been discussed by Lacki [Lacki2014].

An interesting detail, reported by Lacki, concerns the fact that in one of the flights Gockel could have used hydrogen, instead of the usual illuminating gas. The more expensive hydrogen was promised to Gockel due to the planned dismantling of an airship, and would have allowed, as the lightest gas, to reach an altitude of 7000 m. Unfortunately, this event did not occur, and Gockel was able to carry out measurements only at moderate altitudes, for which the effect of the increase in ionization was more difficult to observe. One can only speculate on what the course of events would have been if this flight at a height of 7000 m had already been carried out by Gockel a couple of years before the ascents by Victor Hess, but that was not the case.

## 1.4  Victor Hess and the Evidence for an Extraterrestrial Radiation

When Victor Hess in turn planned to make balloon ascents for a quantitative study of the ionization of air at high altitudes and to estimate the absorption of gamma rays from the ground into the air, the problem had therefore already been addressed by several other authors, as seen above. Studies of the absorption of gammas in various materials, including air, had already been carried out and a numerous series of measurements with electroscopes, even at high altitudes, with balloons, had already been performed. However, even if many considerations about the existence of an extraterrestrial radiation, as a possible interpretation of the data obtained, had been proposed by several authors, the quality of the data collected and the quantitative information extracted from these data were not sufficient to draw definite conclusions, and above all they were unable to give a quantitative estimate of the contribution due to this hypothetical source of ionization linked to the atmosphere. Indeed, according to Millikan's perhaps too drastic comment many years later, "*Until 1910 there was no data about the penetrating radiation coming to the Earth from the outside. I cannot find any information on existence though any idea, even distantly concerning the phenomenon which we connect now with the term cosmic rays*" [Millikan1935a].

Victor Franz Hess, born in Austria, had obtained his doctorate in Physics from the University of Graz in 1910. He had therefore received his doctorate just a year before when he made his first two balloon flights, in 1911, to study absorption in air of the gammas coming from the radioactivity of the terrestrial soil. Hess was aware of Wulf's results and Eve's estimates of gamma absorption coefficients and was therefore aware of the incompatibility of the two results. His first measurements, carried out on the ground with a high intensity gamma source ($2.6 \ 10^{10}$ Bq) at distances between 10 and 90 m, were therefore aimed at a further study of the gamma absorption coefficients, using sources of known intensity, and had given results compatible with Eve's estimates, confirming the discrepancy observed in Wulf's measurements, and suggesting further measures to be taken aboard balloons to clarify the issue [Hess1911].

The first two flights, carried out in 1911, confirmed that the ionization present at still relatively low altitudes was comparable to that measured on the ground and that there was apparently no difference between what was measured during the day and during the night.

The next program also included flights at higher altitudes, with some improvements to the electroscopes to be brought on board (in particular to keep the pressure constant inside them). The idea was to maintain the same altitude for a certain duration of the flight, to verify the influence of other factors, at the same altitude with respect to the ground, and observe any variations during measurements of a certain duration. One of the three instruments was also equipped with much thinner walls, to be sensitive to electrons. The program also included some measurements during

**Table 1.3** Summary of balloon flights performed by Hess in 1912 [Hess1912]

| Date | Max height (m) | Notes |
|------|----------------|-------|
| 17.04.1912 | 2750 | Measurements made also during a partial solar eclipse, no effect observed. Slight rise around 2000 m |
| 26–27.04.1912 | 2100 | Measurements carried out also during the night; no appreciable difference observed compared to the day. Values reported up to an altitude of 1800 m |
| 20–21.05.1912 | 1200 | Night flight, values reported up to an altitude of 500 m |
| 03–04.06.1912 | 1900 | Short duration night flight due to weather conditions. Values reported up to an altitude of 1100 m |
| 19.06.1912 | 950 | Solo flight, only one instrument used |
| 28–29.06.1912 | 360 | Low altitude flight at night, with long duration measurements at the same altitude. Slight decrease observed relative to the ground |
| 07.08.1912 | 5350 | High-altitude flight, with hydrogen balloon. Detailed results reported in the text and in Table 1.4 |

the night, to get further information about the possible role of the Sun. It was therefore a consistent scientific program, carefully planned, to give possibly quantitative answers to different aspects of the problem.

This program was carried out over the course of seven different flights, between April and August 1912 (Table 1.3), supported by the Austrian Academy of Sciences, the first six departing from Vienna. A detailed description of the original article [Hess1912], through its English translation and related commentary, has been made available by De Angelis and Schultz [DeAngelis2018]. The scientific figure of Victor Hess was outlined on the occasion of the centenary of this event in [Schuster2014].

We may see in one of the historical archive photos the scene of one of these flights (Fig. 1.11). A small crowd, mostly children—we count about fifteen—look partly at the photographer, partly at the rectangular basket, in which two people are already on board. Two of the spectators are caught by the photographer's lens while they are observing in amazement the huge balloon that rises above their heads. Around the basket, weight bags marked with "Aero Club Wien" are hooked to the edges, to be used in case of need. The "light" clothing worn to climb to an altitude of several thousand meters, a normal jacket with a waistcoat and a light cap, more typical of a short hike in the hills or a picnic in the countryside, amazes in these photos.

Following the observations obtained during the first six flights of 2012, it was confirmed that the ionization rate was independent of the presence of the Sun: measurements carried out during the night and, during the first flight, even on the occasion of a solar eclipse, substantially gave the same result. As regards the dependence on altitude, the results obtained down to modest altitudes confirmed only a slight decrease in ionization with altitude, in accordance with what was found qualitatively by other authors (Linke, Bergwitz, Gockel, Wulf), and therefore suggested, as already hypothesized, that there should be an additional source of ionizing radiation beyond that linked to the emission of gamma rays from the Earth's soil.

**Fig. 1.11**   Victor F. Hess, in the center, on the occasion of one of the flights made on board a balloon

Except for the last flight, all the others used illuminating gas to fill the balloons, which did not allow reaching altitudes beyond a certain limit. The last flight, on the contrary, used hydrogen, and reached a remarkable altitude of over 5000 m, with results that opened a new chapter in the history of cosmic ray physics.

The ascent began on the morning of 7 August, at 6:12, from the locality of Aussig (Ústí nad Labem), with the presence, together with Hess, also of the pilot (W. Hoffory) and a meteorologist (E. Wolf), and had a relatively short duration: already around noon the crew had landed about fifty km from Berlin, after reaching the maximum altitude of 5350 m, and having traveled about 200 km. In the first part of the flight, up to an altitude of 1000 m, a slight decrease in ionization was observed, in accordance with what was already known, while at higher altitudes the values began to increase, reaching and exceeding the values observed on the ground. At altitudes between 3000 and 4000 m the values were significantly higher, between 20 and 40% higher than those obtained on the ground. But it was above 4000 m that the measurements with the two gamma-sensitive devices reached values that were clearly 100% higher than those observed on the ground.

Table 1.4 shows a summary of the measurements obtained during this flight. The third device, the one equipped with thin walls, sensitive to electrons, unlike the other

**Table 1.4** Summary of the average values (expressed in number of ions per cm$^3$ per second) obtained from measurements made during the August 1912 flight from Hess, up to an altitude of 5350 m [Hess1912]

| Altitude | Average for instrument #1 | Average for instrument #2 | Average for Instrument #3 (normalized value) |
|---|---|---|---|
| 0 | 16.3 | 19.6 | 11.8 |
| 0–200 m | 15.4 | 11.1 | 19.1 |
| 200–500 m | 15.5 | 10.4 | 18.8 |
| 500–1000 m | 15.6 | 10.3 | 20.8 |
| 1000–2000 m | 15.9 | 12.1 | 22.2 |
| 2000–3000 m | 17.3 | 13.3 | 31.2 |
| 3000–4000 m | 19.8 | 16.5 | 35.2 |
| 4000–5200 m | 34.4 | 27.2 | – |

two, was not pressure-tight; the air pressure, therefore, was equivalent to the external one and, especially at higher altitudes, the measured values needed to be renormalized for the estimated pressure difference. Each of the averages derives from a more or less high number of different readings, which however were taken as the balloon moved, during the ascending or descending phase. For this reason, each of these values refers to an altitude range, during which multiple readings were taken.

Figure 1.12 shows the average values measured by the three devices as a function of the height with respect to the ground, reported numerically in Table 1.4. The devices 1 and 2 (values shown with the blue and red symbols) were more shielded, therefore not very sensitive to electrons, while the device 3 (green symbols) was equipped with thin walls, which electrons could traverse. The results show for all the instruments used a slight decrease up to an altitude of around 1000 m, then a rise that becomes more and more consistent with the height. The horizontal bar for each measurement indicates the interval within which the measurements were made obtaining an average. As for the uncertainty in the measured ionization values, Hess discusses some estimates for the different instruments, reporting values between 5 and 10%.

Since the different instruments, having different calibrations, provided different values measured on the ground, it is possible to report the ionization rate measured by each instrument with respect to the value measured on the ground (Fig. 1.13). This trend is very similar for instruments 1 and 2, of the same type, while it shows a greater increase with the altitude for instrument 3, sensitive to electrons.

Between 4000 and 5000 m, the measured ionization was more than double that measured on the ground. The conclusions of Hess at the end of this investigation [Hess1912, Hess1913] report the evidence of the existence of a highly penetrating radiation, present in the upper part of the atmosphere and whose effects are however visible down to the ground.

Regarding the origin of this radiation, Hess concludes that it cannot be associated with the Sun, at least if it is assumed that it consists of gamma rays that propagate in a
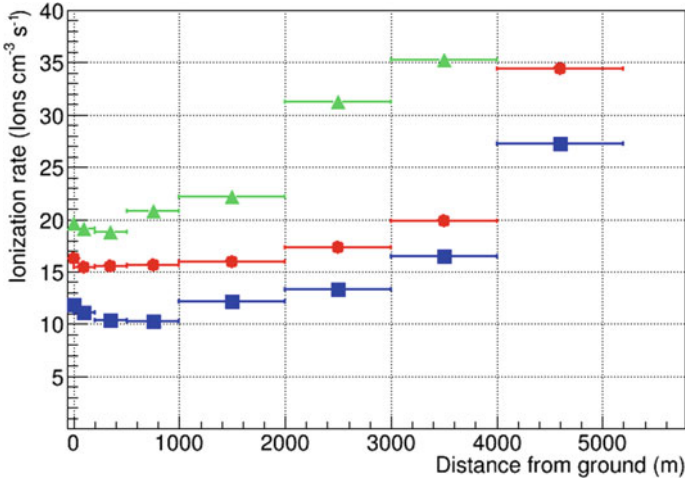
**Fig. 1.12** Evolution of the ionization rate measured at different distances from the ground, during the balloon flight performed by Hess on August 7, 1912, up to a maximum altitude of 5350 m. The symbols in blue and in red show the values measured by devices 1 and 2 (shielded), while the symbols in green show the values obtained by device 3 (also sensitive to electrons). The values were taken from the original article by Hess [Hess1912] and the horizontal bars show the altitude ranges within which the different measurements were made. Device 3 did not take data at the highest altitudes
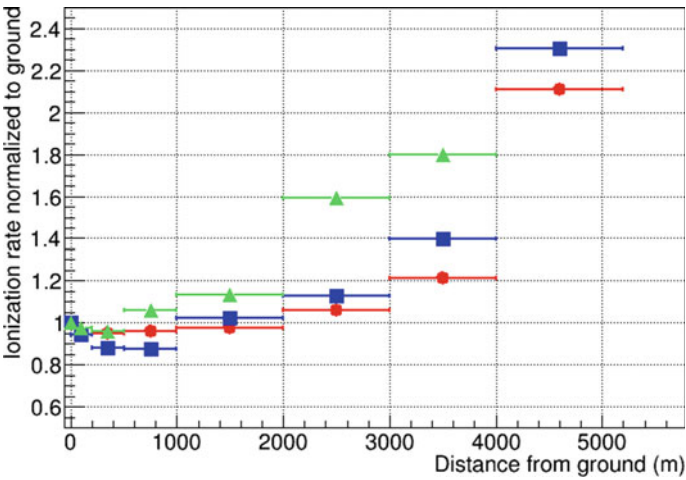


**Fig. 1.13** Values of the ionization rate, normalized to those measured on the ground, for each of the three devices used by Hess during the August 1912 flight, as a function of the distance from the ground. The different colours, relating to the three measuring devices, correspond to those also used in the previous figure

straight line. The fact that this radiation was made up of gammas was, moreover, the most plausible assumption, since of the three radiations known at that time (alpha, beta and gamma), gammas were those with a greater penetrating power.

## 1.5   Towards a Confirmation of Hess's Results

Contrary to what one might believe, the interpretation of Hess's results about the notable increase in air ionization with altitude did not immediately receive general agreement. Many physicists, perhaps most of them, continued to doubt that the cause of this ionization was due to a highly penetrating radiation of extraterrestrial origin. Indeed, the same experimental results were the subject of debate and required, in the opinion of most, further independent confirmation. This attitude, which might seem unusual, represents on the contrary what is most common in the way science usually proceeds. As the historian of science Thomas Kuhn [Kuhn1962] has pointed out in describing the structure of scientific revolutions, science is generally characterized by periods of "*normal science*", in which a *paradigm* is able to guide the research, allowing to improve the paradigm itself, to proceed to more accurate measurements, to look at applications. It may happen that during this work, however, some *anomalies* are noticed, aspects that do not completely agree with the current paradigm, and that require further reflection. As Kuhn points out, the existence of such anomalies does not in itself produce the abandonment of the existing paradigm, without which even the normal scientific practice would not be possible. On the contrary, scientists try, as far as possible, to bring the anomalies within the current paradigm, through small corrections, generalizations, extensions, which do not distort their nature. Only after an incessant work of this kind that has not given results, and especially after new hypotheses have arisen and have had the opportunity to be verified in detail, will the scientific environment be ready to abandon the old paradigm in favor of the new one, which in the meantime has been better clarified and defined. Kuhn calls this process a *scientific revolution.*

In some ways, we can look at the events related to the difficulty of reconciling the observations on the ionization of air at high altitudes with terrestrial radioactivity as a change in the current paradigm, a real revolution. As such, the anomalies about the ionization values, observed in the first measurements, gave rise to attempts at interpretations that ultimately did not upset the dominant vision, in terms of a cause linked to radioactivity, of the soil or air. This even after the results obtained by Hess. It was difficult to accept that the cause was something still unknown, and it seemed more reasonable to continue to believe that the radioactivity of natural substances, in various forms, was still the cause. This is how various considerations can be interpreted about the possibility that radioactive substances could be concentrated in the upper part of the atmosphere, or that the cause could be attributed to the electrical discharges produced during thunderstorms. Moreover, the possible influence of weather conditions had also been considered, and excluded, by Hess.

One of the physicists initially unconvinced not only of the interpretation but of the validity of the very same results provided by Hess was the German Werner Kolhörster (Fig. 1.14). At the time of Hess's achievements, in 1911–1912, Kolhörster was also very young, having just received his doctorate. Attracted by the studies of Wulf and Hess, he also had contributed to improving electroscopes for measurements to be conducted at high altitudes, in particular by making them suitable for withstanding differences in pressure between inside and outside up to 500 Torr, therefore capable of carry out measurements at constant pressure up to an altitude of 9000 m [Kolhörster1913a]. The devices also had greater sensitivity, so much so that they could make much more frequent measurements than those conducted by Hess, and therefore more correlated to the actual altitude at the time of the measurement. In the summer of 1913 Kolhörster made three balloon flights, reaching approximate altitudes of 3500, 4000 and 6200 m [Kolhörster1913b]. During this last flight, Hess's results were confirmed, with values measured even at higher altitudes. Further flights, carried out in 1914, then allowed to reach the maximum altitude of 9300 m, at which the ionization was enormously greater [Kolhörster1914]. The results obtained by Kolhörster are shown in Fig. 1.15, after subtracting the measured value at ground level. They therefore represent the differences with respect to what is observed at ground level.

No doubt remained at this point about the cause of the ionization, which could not originate from terrestrial radioactivity, and which instead showed clear evidence for a radiation coming from above. Assuming that this too was a penetrating radiation, similar to the gamma radiation emitted by the radioactive substances present on Earth, and that it was attenuated according to an exponential trend, Kolhörster was able to estimate, from the ionization values measured at various altitudes, an absorption coefficient, in a similar way to what had been done for the absorption of the radiations emitted from the ground. The value derived from these measurements indicated a much lower absorption coefficient, approximately one tenth, compared to that of the known gamma radiation. It was therefore something with a much greater penetrating power than that associated with the known radiation (Fig. 1.15).

Although many years later, illustrious physicists like Millikan continued to question the existence of this radiation, to change however their mind shortly afterwards, a new phase had now entered, in which, having established the existence of this radiation, it was now a question of characterizing it, understanding its nature, organizing and obtaining quantitative measures. A work that would engage a large part of the physics community in the following decades.

In September 1913 a scientific congress, with different sections and the participation of 7000 scientists, held in Vienna, also saw reports expressly dedicated to the debate about the origin of the radiation observed in the atmosphere. During the conference some of the scientists, including Wulf, did not recognize in the data obtained a reason to admit radiations of extraterrestrial origin, while others, including Kolhörster and Gockel confirmed Hess's hypotheses about a radiation coming from outer space, an opinion that from that moment on could be said to be accepted by most. From the measurements carried out at different altitudes it was also possible to estimate that at sea level the contribution to ionization due to radiation originating

**Fig. 1.14** Werner Kolhörster (1887–1946)
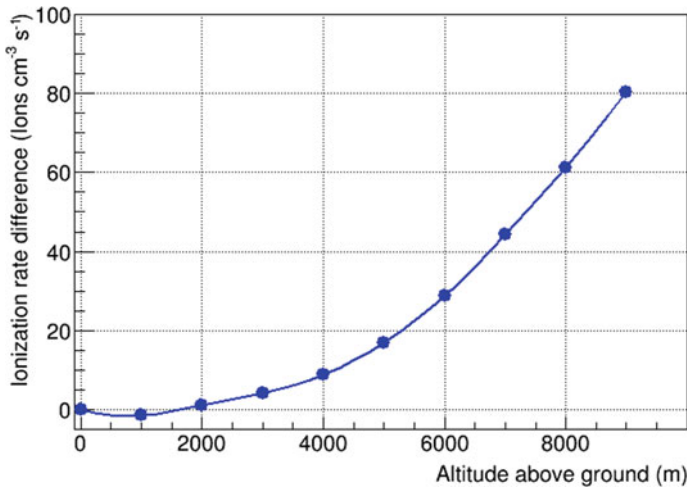


**Fig. 1.15** Difference between the ionization rate measured at different altitudes, compared to that measured on the ground, based on measurements made by Kolhörster in 1914 [Kolhörster1914]

from outside the Earth was approximately 20%, while the rest was due to natural radioactivity, which explains the initial difficulties in recognizing the origin of this radiation source.

The period immediately following the Kolhörster measurements marked a reduction in research activities, due to the war events of the First World War, with a strong downsizing of the budget allocated to this activity and a smaller number of publications of new scientific results. Sporadic activities were continued by Hess, Kolhörster

and others, both with measurements performed in the high mountains and aboard balloons, as we will see in the next chapter, but without significant improvements, so that a few researchers, including Wilson himself, continued to verify the possibility that the ionization of the air, even at high altitudes, was due to other causes.

# Chapter 2
# Confirmation of the Existence of a Cosmic Radiation

**Abstract**  Although the working conditions were not optimal, after the First World War some of the pioneers contributing to the discovery of the cosmic radiation still had the possibility to go on in Europe with their research on cosmic rays. However, in the 1920s, investigations concerning cosmic ray physics progressively moved towards the United States. The chapter discusses the important steps of this transition and the leading role of Robert Millikan to the field, with his new measurements by unmanned balloons and with the investigation of the radiation intensity under the water of lakes at various depths. Quantitative data and plots from his original papers are reported and discussed, with further analysis of the absorption effects in water reported in Appendix B. The controversial contribution of the American physicist and his first ideas of the nature of the cosmic radiation are also discussed in connection with the debate with the original findings by the European researchers, till the general acceptance of the idea of a radiation originating from the outer space.

## 2.1  Further Investigations in Europe During and After the First World War

Despite the difficulties imposed by the world conflict in those years, it cannot be said that research activities were completely absent or suspended at that time. Some European nations, in particular Germany, Austria and Switzerland, remained at the center of further studies concerning the phenomena related to *cosmic radiation*, as we will call it from this point on, even if the terminology associated with this phenomenon represents a long and complex story in itself.

The interest in carrying out further measures of air ionization moved in those years towards the possibility of organizing experiments on the mountains, at high altitudes, where, although the contribution due to the radioactivity of the soil was not negligible, as in the case of high-altitude balloon flights, the relative ease of carrying out systematic and long-lasting measurements allowed a significant benefit for the quantitative understanding of the phenomenon.

Which were the roles and contributions from the pioneers of the study of cosmic radiation at that time? Did they have the opportunity to continue working in this field and to contribute further results to this study?

Wulf, who was a Jesuit priest from the age of 20, before studying physics with Nernst in Gottingen, continued to teach physics at the Jesuit College in Valkenburg, Holland, continuously from 1904 until 1935, except for the parenthesis of the First World War, and was the author of several educational textbooks in physics, but it does not seem to have been further interested in research related to cosmic radiation.

Gockel, after the flights carried out up to an altitude of 4500 m, and after having missed the possibility of a high-altitude flight with a balloon filled with hydrogen, had no further chance to carry out other balloon flights, also due to the conditions of his work at the University of Freiburg, where, despite having been appointed professor, he did not have a lot of funds available. However, he remained active in this field, contributing to study the effects due to this radiation in various locations in Switzerland, on the Jungfraujoch (3400 m) and on the Aletsch glacier (2800 m) [Gockel1915], and also performing measurements under the ice, to evaluate the absorption of radiation. Despite his direct involvement in a specific activity of characterization of the cosmic radiation, Gockel remained largely skeptical about the extraterrestrial nature of this radiation, and in 1923, a few years before his disappearance, he still wondered whether the phenomenon of the ionization of air in the Earth's atmosphere had to do with a radiation originating from outside the Earth [Gockel1923].

During the years of the conflict, Kolhörster had served mainly in a meteorological unit, and was subsequently sent to Turkey as a member of the German military mission. He also continued some research activities on atmospheric electricity. At the end of the war, for a few years, he also had to teach at school, and was only able to resume research activities related to the study of cosmic radiation in 1922, carrying out various measurements in the mountains of Switzerland. Subsequently, from 1928, Kolhörster, together with Walter Bothe (1891–1957), who had become director of the Physikalische-Technische Reichsanstalt (PTR) in Berlin, and whom we will discuss in more detail later, began to employ the first Geiger-Müller counters, even in coincidence, for the detection of the cosmic radiation, in order to study its nature, whether it consisted of highly penetrating gammas or particles. Kolhörster, therefore, except for a brief parenthesis during the years of the conflict and in the immediately following years, always remained active in research related to the study of cosmic radiation, contributing in various ways to the understanding of its properties. Indeed, his activity was highly appreciated especially in the German context until the end of the Second World War, as we will see in the following sections.

What about Pacini, whose intuitions seemed to have preceded the hypothesis of a radiation of extraterrestrial origin? Unfortunately, for various reasons, analysed in detail by De Angelis [DeAngelis2010, DeAngelis2012], Pacini did not have the opportunity to continue this activity with significant roles in the following period. After graduating from university, he got a teaching position at the University of Rome and, subsequently, in 1928, he obtained the professorship at the University of Bari. Although he remained active in the field of experimental physics, his works

after 1913, published in Italian, were mainly devoted to spectrophotometric studies of sky light and other properties of the atmosphere. In 1913 Pacini did not have the opportunity to participate in the Conference where he could have known the latest results on the observations regarding the causes of air ionization and contribute to the debate. To the period immediately following the end of the conflict (1920) dates back the exchange of correspondence between Pacini and Hess, in which Pacini expresses his disappointment for the fact that his works on the absorption of radiation, carried out on the surface of the sea and under water, had not been mentioned. Unfortunately, Pacini's contribution was unable to be adequately exploited even in the following years.

In 1913 Hess had considered as an important task the possibility to carry out simultaneous measurements in different locations, in order to observe any correlated variation in the intensity of the radiation. Some of these measurements were actually organized, with the collaboration of several colleagues, by carrying out true "measurement working shifts" of 12 h every day [Schuster2014], perhaps the precursors of the current measurement shifts for long-term physics experiments, such as those at particle accelerators or astronomical observatories.

Measurements lasting about one year, in continuous mode, were also organized by Hess and Kofler in the Alps, between 1913 and 1914, at an altitude of about 2000 m, with electroscopes positioned outdoor, in a container with wooden walls. Being able to measure ionization over such a long period of time, and at repeated intervals throughout each day, makes this experiment perhaps the first long-duration cosmic ray flux monitoring activity. The results made it possible to evaluate any correlation between the observed values and various environmental parameters, such as temperature, pressure, time along the day [Hess1917]. For example, it was established that there was no appreciable difference between the values observed during the day and the night, and that the same daily variations were much less than those observed at sea level.

In the years following his balloon flights, Hess mainly devoted himself to activities related to natural radioactivity, also evaluating the number of alpha disintegrations per second produced by a gram of radium ($3.7 \times 10^{10}$), which allowed to establish a unit of measure of the activity of a sample, the Curie, exactly equal to the activity of one gram of radio in radioactive equilibrium, a unit still in use today. Between 1915 and 1917 he also carried out research activities related to the use of X-rays in the medical field. In 1920 Hess had become a professor at the University of Graz, but soon after he moved to the USA for a period of two years, where he still made contributions related to radioactivity and its applications.

Only a few years later, in 1923, did he return to Graz, resuming his research on cosmic rays. Despite the experimental results achieved through balloon flights at higher altitudes, both by Hess himself and by Kolhörster, the acceptance of the extraterrestrial origin of this radiation still posed some problems. As we will see in the next section, a great deal of opposition initially came from American circles, linked to the figure of Millikan, and the same priority of the evidence of this radiation was also called into question in the context of European physics, due to the contribution of Kolhörster. In the second half of the 1920s, Hess continued to contribute to the
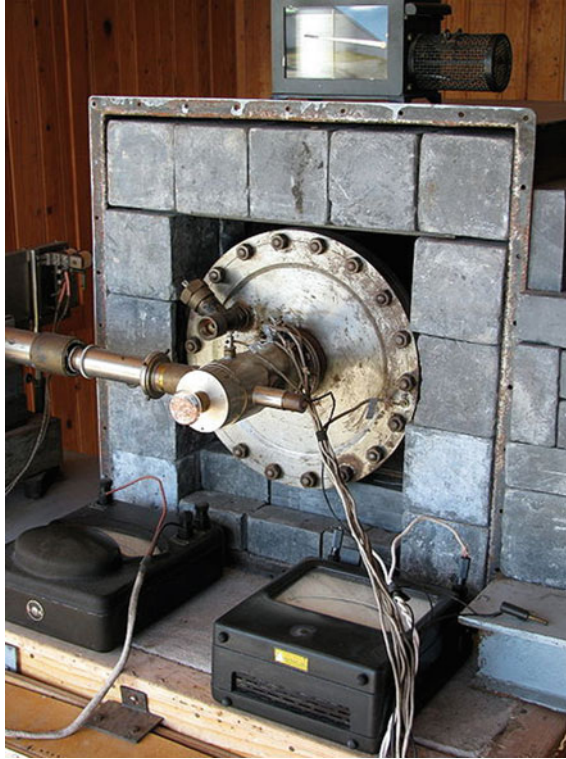
**Fig. 2.1** An apparatus for measuring cosmic radiation (ionization chamber), installed in the labora-tory for high-altitude cosmic rays on Mount Hafelekar, 1931. *Source* Wikimedia Commons, Creative Commons Attribution 3.0 Unported License

study of the cosmic radiation, through quantitative investigations of the variations observed in the mountains, at high altitudes, up to the creation in 1931 of a perma-nent observation station at an altitude of 2300 m, on Mount Hafelekar [Hess1932] (Fig. 2.1).

Among the pioneers who had contributed to the first results on cosmic radiation, the names of Hess and Kolhörster are certainly the ones that had a greater importance and continuity even in the following decades. However, starting from the early 1920s, the study of these phenomena also began in the United States, where the figure of Robert Millikan initially played a crucial role, with alternating events, in the debate about the existence and nature of this radiation.

## 2.2 Robert Millikan and the First American Contributions to Cosmic Ray Physics

In the years in which the first high-altitude balloon ascents for the study of air ionization were made in Europe (1912–1913), by researchers less than 30 years old, the name of Robert Millikan was already well known in science in the United States. Millikan, at that time nearly fifty years old, had already made his experiments on the electron charge, which ten years later, in 1923, would have given him the Nobel Prize, and held numerous positions of responsibility in the academic environment as well as organizational and managerial roles related to science. In the early 1920s he had moved from Chicago to California, where he would later establish and direct Caltech (California Institute of Technology).

Millikan's personality was complex, and together with his great scientific and organizational skills, there are some aspects of his figure, his character and above all his scientific activity that have created many problems to his biographers. One of the last steps in this area is for example the recent decision (2021) by the Caltech Management to remove the name of Millikan, along with that of numerous other colleagues, from the dedications that auditoriums, buildings, or other structures had received in the past. For what reason? For the positions that Millikan had taken at that time, belonging to the eugenics movement through the Human Betterment Foundation (HBF). The Caltech Board of Trustees assessed that "In making its recommendations regarding Millikan, the committee also considered his stances on gender, race, and ethnicity, finding them sexist, racist, xenophobic, and inexcusable by any standard" [CALTECH]. One may wonder if it is correct to notice these problems almost a century later, but probably everything is part of the renewed attention that has been given to these issues in recent years.

Apart from this paradoxical episode, the events concerning the role of Millikan, and more generally, of American physicists, on the activities concerning the study of cosmic radiation have always been the subject of attention. Millikan's attitude towards European activities concerning the study of cosmic radiation was in fact always critical, at first denying the validity and importance of these studies and the conclusions that gradually emerged about the existence of a source of radiation of extraterrestrial nature, subsequently, when he realized, through his own experiments, the real existence of this radiation, trying to minimize the European contributions in favour of the American ones. Still in 1935, that is many years after the acceptance of the ideas concerning cosmic radiation, Millikan wrote [Millikan1935a] that there was no trace until 1910 of any idea even remotely linked to what could be called "cosmic rays" [Xu1987].

Millikan, therefore, in the early 1920s, began a series of experiments in the United States related to the study of this radiation. The first measurements were carried out in March and April 1922 by Millikan and Bowen, by means of balloon flights without human intervention, up to a height of about 15 km. These results were communicated at a meeting held in May 1923 [Millikan1923]. Further measurements carried out on board airplanes, balloons and in the high mountains, were communicated during

the same meeting by his collaborators [Otis1923a, Otis1923b]. However, the full results of this activity were only published in 1926, in a series of three articles which constituted an important step in the study of cosmic radiation [Millikan1926a, Millikan1926b, Millikan1926c].

In the first of these articles [Millikan1926a], Millikan refers in the introduction to the existing situation, quoting the works of Gockel, Hess and Kolhörster (but not those of Pacini, which perhaps were not even known to him). The results of Hess and Kolhörster are expressly reported, and it is explicitly admitted that these results had immediately raised curiosity and interest in further measures to be carried out personally. The situation originating from the world conflict, although America was geographically far from the theatre of the battles, and the decision to build automatic recording devices, which avoided the physical presence of people on board the large balloons, had delayed this activity until the years 1921–1922. At that time Millikan had succeeded in having four small electroscopes built, capable of recording, by means of photographic films, the indications regarding the divergence of the fibers of the electroscope as well as the pressure and temperature. A more detailed description of these tools is given in Chap. 5.

The qualitative result obtained from these flights was that indeed, at high altitudes, the ionization was greater than that measured on the ground, in qualitative agreement with what European researchers had already found. However, from a quantitative point of view, Millikan found no congruence with the trend measured by Hess and especially by Kolhörster. The estimate of the value obtained on average at heights above 5 km was much lower than that obtained by Kolhörster. For the balloon that had reached an altitude of 15.5 km, the value obtained above 5 km was about 3 times that obtained on the ground, while Kolhörster had already reported an increase of a factor of 7 at an altitude of 9 km. The extrapolation to altitudes of 15 km, starting from the data obtained by Kolhörster, gave values enormously higher than those measured by Millikan. According to Millikan, the interpretation of these measures seems to nullify the possibility of radiation of extraterrestrial origin: "The results … constitute definite proof that there exists no radiation of cosmic origin having such characteristics as we had assumed" [Millikan1926a].

But in the final sentences of the same article, Millikan anticipates that new results, which will be published in subsequent articles (evidently partly ready), will present unambiguous evidence of cosmic radiation with extreme penetrating power. This first article, although it discusses the results obtained in the course of measurements made a few years earlier, appears to have been sent with the date of December 24, 1925, and published in April 1926.

In the following article, signed by Millikan and Otis, sent on March 1, 1926 and published in June of the same year [Millikan1926b], the results of a new series of observations, also made in the years 1922–1923, are discussed, both with balloons and in the high mountains or on board of airplanes, in different locations. In particular, some flights by plane, up to altitudes of about 5000 m, made it possible to measure values once again in qualitative, but not quantitative, agreement with what was obtained in Europe, i.e., a decrease in ionization up to moderate altitudes, around 2500 m, then a slight increase with altitude—but with absolute values well below

those reported by Hess and Kolhörster. Regarding the possible dependence of the intensity of this radiation on the particular time along the day, a further series of measurements were made in the high mountains, at Mt. Whitney (4130 m) and at Pikes Peak (4300 m), showing that this intensity was constant within the limits of observations, during the whole 24-h period and which did not depend on the position of the celestial bodies or on the Milky Way itself.

Further detailed measurements were made with different types of lead shielding around the electroscopes, the results of which allowed to understand that this radiation did not come from any privileged geographic direction (North, South). Beyond the details, the main conclusions are once again that the causes of air ionization in the various conditions are mainly attributable to local causes: "Both lines of evidence presented above point, then, to the conclusion that there is on mountain peaks a copious radiation of local origin and of a hardness not greater than that of the gamma rays of radium or thorium, but they reveal thus far no penetrating radiation of cosmic origin. If such a radiation exists at all it can at the most produce but a small part of the ionization observed in electroscopes on mountain peaks" [Millikan1926b].

Nothing new, therefore, about the conclusions on the origin of this radiation, not even in this second work? In fact, the details of the measurements reported are valuable elements that add to the knowledge existing up to that moment. But there is another aspect, which Millikan expressly mentions. Many considerations made in this field, and the same discrepancy with the values reported by other authors are based on the assumption of a gamma radiation with a given penetrating power, and Millikan is aware of the fact that assuming that cosmic radiation exists, then it must be less intense on the ground than previously assumed, or much more penetrating than previously assumed. These statements therefore leave room for further attempts to understand the phenomenon, which will come from an additional series of experiments, reported in the third of these articles of 1926, signed by Millikan and Cameron [Millikan1926c]. The article was sent to the Journal on August 7 and published in November 1926, and marks a significant step in understanding the radiation and especially in Millikan's change of opinion.

In the introductory part of this work Millikan summarizes the situation regarding the possible existence of this radiation and its penetrating power, defined by the absorption coefficient, which Millikan believes he has evaluated based on his previous work through balloon flights. Millikan also discusses the new results obtained by Kolhörster under the surface of the water (but not, again, Pacini's results). With these considerations, Millikan denies that on the basis of what has been observed so far, including his previous works, the existence of extraterrestrial radiation can be assumed, unless it is even more penetrating. This justifies a series of further measures, reported in this article, which should finally shed light on the possible existence of the radiation itself. The measurements in question concern experiments to be carried out under the surface of lakes, at different altitudes, in particular in lakes fed by melting snow, as measures conducted in the past have shown the existence of an appreciable radioactivity even in water. Millikan is therefore looking for non-radioactive lakes, located in the high mountains, where cosmic rays, if they exist, have a considerably higher intensity than at ground.

The measurements were carried out in late summer of 1925 at Lake Muir, about 3400 m above sea level, a large and very deep lake near Mount Whitney, the highest peak in the United States, excluding Alaska, and subsequently near Lake Arrowhead, at an altitude of about 1570 m, therefore significantly lower than the first, in order to compare the results obtained in the two conditions.

In Lake Muir the electroscopes were immersed to a depth of about 20 m, demonstrating a decrease to a depth of 15 m. Taking into account that the thickness of atmospheric air above the surface of the lake corresponded to about 7 m of water, this meant that the radiation measured by the electroscopes, if actually coming from the outside, would be able to cross the equivalent of $15 + 7 = 22$ m of water before being absorbed. This radiation, always assumed as gamma radiation, was therefore enormously more penetrating than any other known radiation. Millikan, in comparing this penetration capacity to that of X-rays, used in hospitals, which are arrested approximately by 1 cm of lead, realizes that the radiation observed underwater would instead be able to cross almost 2 m of the same material.

For the other observation site, Lake Arrowhead, the equivalent thickness of water, due to the atmosphere above the lake's water, differed from the first by about 1.80 m; it is as if each reading made in Lake Arrowhead therefore corresponds to a reading made in Lake Muir at a depth 1.80 m greater. The results obtained, reported in Table 2.1 and Fig. 2.2, actually show an agreement with this hypothesis. The top plot in Fig. 2.2 shows the two data series reported as a function of the depth of water actually measured in the two cases, while in the bottom graph the values originating from Lake Arrowhead (located at a lower altitude) have been shifted by the equivalent amount of water corresponding to the difference in air thickness. As it can be seen, after this shift the two series of values appear as belonging to a single set of data, that is, they actually lie on a single curve.

From this comparison Millikan is ready to draw the important conclusion "that the rays do come in definitely from above, and that their origin is entirely outside the layer of atmosphere between the levels of the two lakes". Moreover, Millikan had already used the term "cosmic" with regard to penetrating radiation in a work published in Nature in 1925 [Millikan1925].

Measurements in the lakes were also carried out in the following years in the southern hemisphere, in Bolivia and Peru, exploiting the lakes Miguilla (4570 m)

**Table 2.1** Values obtained by Millikan and Cameron with one of the two electroscopes immersed at a certain depth below the water of lakes Muir and Arrowhead [Millikan1926c]

| Depth (m) | 0.0 | 0.45 | 0.7 | 1.0 | 1.1 | 2.8 | 3.0 | 5.0 | 10 | 15 | 20 |
|---|---|---|---|---|---|---|---|---|---|---|---|
| Average ionization (ions/cm$^3$ s), Lake Muir | 13.25 | 9.7 | – | 7.75 | – | 5.9 | 5.45 | 4.75 | 4.0 | 3.6 | 3.65 |
| Average ionization (ions/cm$^3$s), Lake Arrowhead | 7.0 | – | 5.8 | 5.5 | 5.15 | – | 4.9 | 4.4 | – | 3.7 | – |
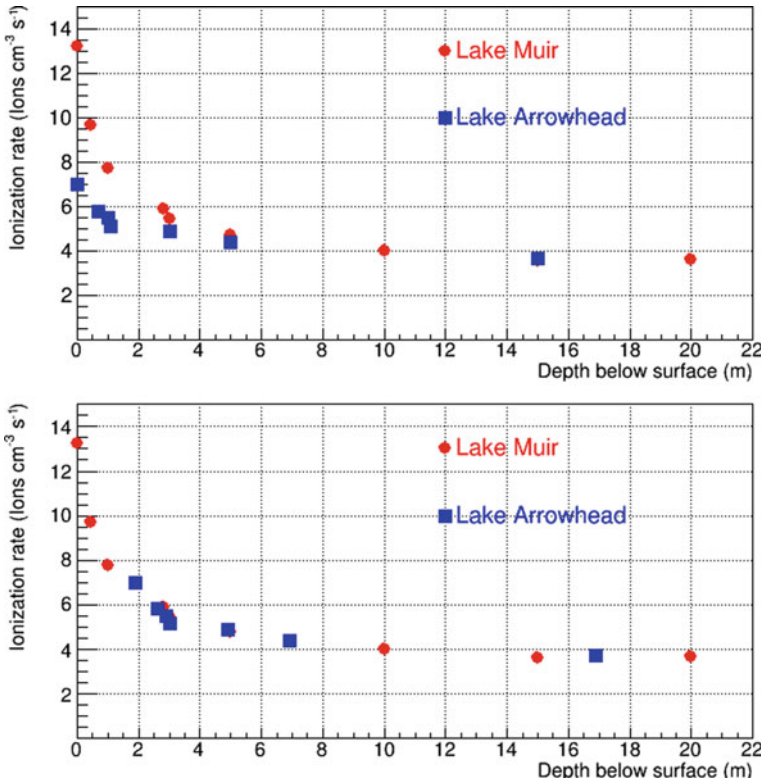
**Fig. 2.2** Average ionization values obtained by Millikan and Cameron with one of the electroscopes immersed at a certain depth in the waters of lakes Muir (dot symbols in red) and Arrowhead (square symbols in blue), taken from [Millikan1926c]. In the graph above, the values are shown as a function of the real depth in each of the two lakes. In the bottom one, the values obtained in Lake Arrowhead (located at a lower altitude) have been shifted by an amount equal to the difference in equivalent altitude in water (see text)

and Titicaca (3820 m), to verify that the results were compatible with those found in the northern hemisphere, in the United States [Millikan1928a].

To extract the absorption coefficient from these data, Millikan and Cameron use for the first time the assumption that cosmic radiation comes from every direction and not only along the vertical direction. Absorption at a given depth therefore depends on the thickness crossed along each direction (see Appendix B). The analysis of these curves also shows that the absorption cannot be represented with a single exponential curve, but rather shows two components: one that is absorbed in a smaller thickness, the other that requires larger amount of material, with two different absorption coefficients, which are estimated at $0.0030$ cm$^{-1}$ and $0.0018$ cm$^{-1}$ respectively, after including the thickness of the atmosphere in equivalent meters of water. In other words, the radiation is not homogeneous but has a certain distribution in energy (spectral composition), resulting on average more penetrating for the components

that manage to reach a certain depth. The term "soft radiation" is even used to denote the component that is most easily absorbed.

Regarding the nature of radiation, given that the most natural hypothesis was to assume that it consisted of gamma, the "soft" component is associated with electrons, in terms of the recently formulated Compton scattering process [Compton1923]. These electrons have a penetration power in the air, based on their energy, even tens of meters. We will resume later the question of the origin of cosmic radiation, on which Millikan will initially support hypotheses that he will be forced once again to abandon later.

It was this set of measurements, therefore, rather than the measurements carried out at high altitudes, which convinced Millikan of the real existence of radiation with an extraterrestrial origin. Indeed, the presentation of the results seems to suggest that without the latter evidence, obtained by Millikan, all the previous experiments would be of little significance, and could not be used as unambiguous proof of the existence of this radiation. In other words, Millikan tends to bring to himself the irrefutable proof of the existence of cosmic rays.

We recall at this point that Millikan had obtained the Nobel Prize just three years earlier, in 1923, for the measurement of the electron charge and for the study of the photoelectric effect. He was undoubtedly, at that time, the most famous physicist in the United States, so his views had a relevant social weight, especially if they could support American supremacy in science. His name, about the claims related to cosmic radiation, was in major newspapers, such as the *New York Times*, and *Time* magazine had dedicated several articles to him, writing that Millikan had announced the existence of a new radiation, the Millikan rays, capable of traversing a six-foot



**Fig. 2.3** Robert Millikan discusses with Marie Curie in Rome, on the occasion of the Conference (October 1931) dedicated to nuclear physics. *Source* Wikimedia Commons

thickness of lead. The cover of *Time* of April 25, 1927 portrays him for example while observing under the microscope, with the caption "Dr. Robert Andrews Millikan… detected the cosmic pulse". In the same period also the *Science* magazine used the term "Millikan rays". It must be said that Millikan did not do much to disprove these claims.

Naturally, Millikan's statements contained in the last of his works of 1926, and above all the use that the press made of them, created many problems for European researchers. Hess in the same year 1926 wrote that "the recent affirmation of the existence and penetrating power of this radiation (Höhenstrahlung) by Millikan and collaborators gave the inspiration to journals such as *Science* and *Scientific Monthly* to propose the term "Millikan-rays" for them. Since this is only a confirmation and an extension of the results of the ionization measurements carried out in the balloon by Gockel, myself and Kolhörster in the period between 1910 and 1913, this nomenclature must be rejected as inappropriate and unauthorized" [Hess1926]. And Kolhörster himself intervened, recalling that the so-called "Millikan rays" are none other than the "Höhenstrahlung" known for some time [Kolhörster1926].

When Hess and others expressed their disappointment at this appropriation of roles, Millikan pointed out that on no occasion had he taken the initiative to appropriate the discovery, and that the important thing was that with the contribution of all the nature of this was finally clarified, as a radiation of extraterrestrial origin [Xu1986]. It is illustrative in this context to read an article by Millikan himself, *History of Research in Cosmic rays* [Millikan1930a], published in Nature in July 1930, in which the American physicist reports his general considerations about the events that gave rise to the study of cosmic radiation and the relationship between European and American science. Despite the controversy that characterized the relationship between Millikan's school and the environment of European physicists in those years, later in 1936, when the Nobel Prize was awarded to Hess for the discovery of cosmic rays, Millikan, in congratulating him for the assignment, he publicly wrote that Gockel, Hess and Kolhörster had been the pioneers until 1914 and that further work had appeared only ten years later, when the study of these processes had entered a new era (Fig. 2.3).

## 2.3  The Acceptance of the Idea of a Cosmic Radiation

Starting from 1927 it can therefore be said that the idea of a cosmic radiation, that is, of a radiation of extraterrestrial origin, had been universally accepted, with the exception of a few physicists who continued to have doubts about the results reported. Apart from the initial attitude of Millikan and in general of the American scientific community, it must be said that a notable contribution to the understanding of the phenomenology of observations regarding the cosmic radiation certainly came from those works carried out by Millikan and collaborators around the mid-1920s, which are believed to constitute: (i) a finally unambiguous proof of the existence of radiation of extraterrestrial origin, which cannot be explained on the basis of the radioactivity

of terrestrial substances; (ii) a demonstration of the fact that this radiation has a spectral composition, with several components, subject to different absorption effects in matter; (iii) an interpretation of the soft component as constituted by energetic beta rays (electrons); (iv) a more precise estimate of the ionization present at ground level and due to cosmic radiation, evaluated in 1.4 ions/(cm$^3$ s).

From this moment a new phase begins, which will see an increasing number of experimenters contribute to the detailed knowledge of this radiation, especially in the United States. If before that period most of the articles devoted to the study of these phenomena were published in German language journals, since 1930 the situation is reversed, and most of the scientific literature concerning cosmic radiation can be found in American journals, particularly Physical Review. As an example, Fig. 2.4 shows the number of articles published in Physical Review, containing the word "cosmic" in the title or abstract of the article, in each five-years period since 1920. As the figure shows, there is literally an explosion of articles on the subject starting in the 1930s and in the following decades. It is also possible to note a decline in scientific production during the period of the Second World War. In more recent years, the term "cosmic" has been associated in scientific papers also with topics other than those strictly related to cosmic ray physics and therefore it is not significant for the purposes of these considerations.

This new period in the study of cosmic radiation is also characterized, as we will see in more detail in the following chapters, by the introduction and use of new experimental techniques, such as the Geiger counter and the cloud chamber, which will allow to achieve far superior quantitative results to those obtainable with electroscopes, and from the use of coincidence techniques involving several detectors,
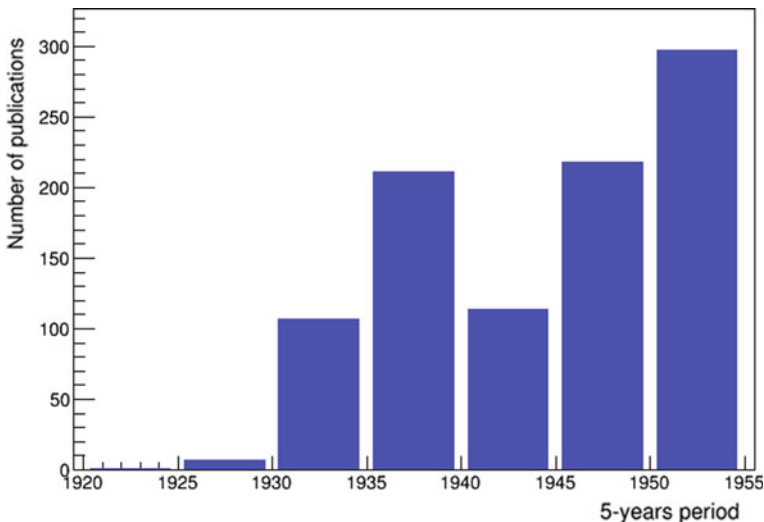


**Fig. 2.4** Number of publications that appeared in the Physical Review since 1920, containing the word "cosmic" in the title or abstract of the article, grouped by five-year periods

which permit to understand many aspects precluded to the use of inclusive measurements. These tools will allow far-reaching measurement campaigns, in the most disparate locations of the Earth, and, therefore, to highlight, in a quantitative way, the existence of specific effects that will also help in understanding the nature and the overall properties of both primary and secondary radiation. In fact, starting from the 1930s, extensive measurement campaigns of the cosmic flux and its dependence on geomagnetic phenomena began, such as the dependence on latitude and longitude, the East–West effect, and the connection with the Earth's magnetic field. These measurement campaigns will also allow answering one of the questions that remained open for at least a decade after the acceptance of the existence of cosmic radiation, namely its composition, both as regards the primary and secondary components. The discoveries concerning the existence of new particles, many of which observed in cosmic rays, and the detailed study of their properties were not extraneous to this. Finally, the experimental evidence of the existence of extensive air showers and the study of the propagation and development of these showers in the atmosphere helped to clarify the overall picture of the phenomenology of cosmic radiation, establishing a link that still lasts today between the study of this radiation and the high-energy nuclear collision processes at particle accelerators.

# Chapter 3
# The Nature of the Cosmic Radiation

**Abstract** Understanding the nature of the cosmic radiation received a strong boost from the study of the cosmic ray intensity in different locations of Earth. The influence of the magnetic field of the Earth on the cosmic ray flux is the main topic of the first part of the chapter. Magnetic field effects on cosmic rays were investigated in a series of famous worldwide measurements campaigns, carried out by the European physicists Clay, Bothe and Kolhörster, and in an extended way, by the American teams leaded by Millikan and Compton. Such effects were also theoretically studied by Lemaitre and Vallarta. As a result, new insights about the corpuscular nature of the cosmic radiation were obtained. Measurements by Compton are reported in their original form, with a discussion on the main points concerned with the nature of the radiation. Related concepts of geomagnetic coordinates and magnetic rigidity of charged particles are discussed in Appendices C and D. The second part of the chapter summarizes other contributions made in that period in various parts of the world (in different European countries, Japan, India and Soviet Union) to clarify the nature of the established extraterrestrial radiation, thus arriving to the idea of protons as the main component of the primary radiation.

## 3.1 The Influence of the Earth's Magnetic Field

Millikan's measurements, performed even at various depths under the water of lakes, had made possible to quantitatively evaluate the absorption coefficients of cosmic radiation. The evidence that this radiation had a penetrating power extremely higher than the known gamma radiation suggested by analogy that they too were extremely high-energy gamma radiations. More generally, it was natural to ask what the nature of these radiations was: those known up to that moment, following the studies on radioactivity, were—in addition to gamma radiations—beta rays, i.e. electrons, and alpha rays, nuclei of $^4$He. The latter, being absorbed very easily by matter, could therefore certainly not be a crucial component of the cosmic radiation observed at sea level.

To understand the question of the nature of cosmic radiation it must be remembered that while the gamma radiation is not deflected or influenced by electric or

magnetic fields, electrons, on the contrary, undergo the action of these fields. A moving electric charge, in fact, is equivalent to an electric current, and is subject to the same electromagnetic effects. For a phenomenon, such as that of cosmic radiation, which involves the entire Earth's atmosphere, it is natural to think of the existence of the Earth's magnetic field.

The Earth, as well as some of the other planets of the Solar System and the Sun itself, is provided with a magnetic field, which extends over large distances from the Earth's surface. As a first approximation we know that the Earth's magnetic field can be represented by a dipole, similar to the field created by a magnetized bar. However, the magnetic field generated by the Earth is more complex: the center of this dipole is displaced with respect to the center of the Earth, its axis does not coincide with the axis of rotation and the position of the magnetic poles changes over time. We know today that even the direction of the Earth's magnetic field can reverse, and that this phenomenon has occurred countless times throughout the history of our Planet (Appendix C). The extension of the Earth's magnetic field is enormous, even if the intensity of this magnetic field is weak. Therefore, it can also act on charged particles at large distances from the Earth. Leaving aside the question of the origin and detailed description of the magnetic field inside the Earth, we are interested in this context to understand the importance of the magnetic field effect for the purpose of understanding the nature of the cosmic radiation.

The Northern Lights phenomenon was already known in ancient times, so called from the end of 1500: a brightness in the sky sporadically visible in regions of high latitudes, which can take on different shapes and colours. The light emitted during these events is characterized by a spectrum that includes lines and bands, and is due to phenomena of ionization and excitation of the atoms that make up the upper part of the atmosphere. As early as the late 1800s it had been suggested by Birkeland that this phenomenon could be due to charged particles emitted by the Sun, predictably electrons, interacting with atoms in the atmosphere. The action of the Earth's magnetic field was able to deflect these particles, preferentially conveying them towards the polar regions. Experimental studies were also done in the laboratory, using a cathode ray (electron) beam and a model of the structure of the Earth with a dipolar magnetic field, observing a luminescence like that observed in the Northern Lights [Rypdal1997] (Fig. 3.1).

A theoretical study of the dynamics of these charged particles under the action of the Earth's magnetic field was carried out by the Norwegian mathematician and geophysicist Carl Størmer (1874–1957), who as early as 1903 analysed the quantitative behaviour of possible trajectories of electrons emitted during periods of intense solar activity, relating them to the observation of the phenomenon of the Northern Lights [Størmer1907]. Further developments of Størmer's theory were published in several subsequent papers [Størmer1930] and in a complete reference text [Størmer1955] (Fig. 3.2).

The action of the Earth's magnetic field on any electron is to deviate them from their trajectory, and this deviation would occur differently in the equatorial regions and in the polar regions, due to the different magnetic field. It was therefore expected that if cosmic rays were made up of electrons, they would be subject to the influence
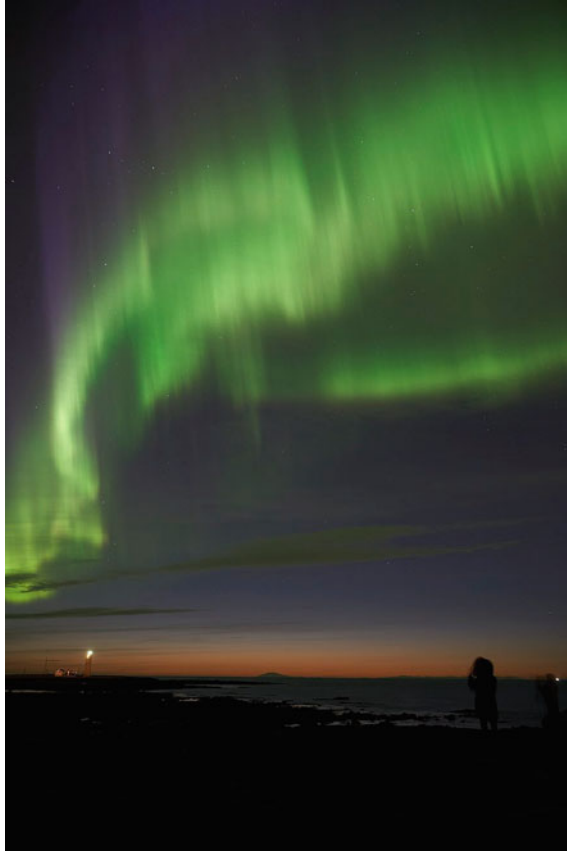
**Fig. 3.1** The image of a Northern Lights. Shows of this kind are visible above all in the regions of higher latitude, although sporadically they can also be observed in the latitudes of the regions of Northern Italy. *Source* Wikimedia Commons, under Creative Commons Attribution 2.0 Generic License

of the Earth's magnetic field, which exhibits different values in different geographical regions. On the contrary, if cosmic rays were made up of photons, their trajectories would not have to undergo any deviation. Of course, even in the case of electrons of very high energy the deviation due to the Earth's magnetic field would be very small. However, if a part of these electrons had energies lower than some GeV, they too would be deflected by the magnetic field, and we could expect differences in intensity in the flux measured at various latitudes.

The study of the behaviour of charged particles in the Earth's magnetic field received notable contributions from several other authors, apart from Størmer, especially from Georges Lemaitre (1894–1966), Belgian astronomer and priest, and from the Mexican Sandoval Vallarta (1899–1977). Georges Lemaitre is best known for his cosmological theories on the expansion of the universe and the Big Bang hypothesis.

**Fig. 3.2** Fredrik Carl Mülert Størmer (1874–1957). *Source* Wikimedia Commons, under Creative Commons Generic 2.0 License from Nasjonalbiblioteket

In the context of this issue, Lemaitre and Vallarta published several papers [Lemaitre 1933, Lemaitre1936a, Lemaitre1936b], which quantitatively analysed how low-energy particles would be deflected by the Earth's magnetic field near the geomagnetic equator but could reach the Earth near the geomagnetic poles (Figs. 3.3 and 3.4).

Calculating the trajectories of these particles is very complex. Unlike Størmer, Lemaitre and Vallarta were able to use at the Massachusetts Institute of Technology (MIT), where they both worked for a certain period, of a calculation tool, a sort of analog mechanical calculator (the Differential Analyzer developed by Vannevar Bush (1890- 1974), an electrical engineer from MIT), which allowed to solve differential equations even of high order. Lemaitre remained interested and intrigued even in the following decades by the potential of these first computers, which he was able to use directly in the 1950s.

Considerations on the possible trajectories of particles in the Earth's magnetic field placed stringent constraints on the nature of cosmic radiation. If the primary particles were photons, they would not undergo the action of the magnetic field, so their intensity should be the same both in the equatorial and polar regions. Even if photons could produce charged particles by interacting with nuclei in the upper atmosphere, they would not be significantly deviated from their original direction,

**Fig. 3.3** George Lemaitre (1894–1966). *Source* American Institute of Physics (AIP), Emilio Segrè Visual Archives

due to the low intensity of the magnetic field and to the fact that the trajectories followed would have a length of the order of a few km. If, on the other hand, the primary particles were charged particles, they would undergo the action of the Earth's magnetic field even at large distances from the Earth. Those arriving in the direction of the poles could reach the Earth, even those with a low energy, while those arriving in the equatorial plane would be strongly deflected, especially the particles with a low energy; in this case we should expect a different intensity at different latitudes. A quantitative analysis of the problem shows what must be the minimum energy that the particles must have to reach the Earth at any given (geomagnetic) latitude.

In the work of 1933 [Lemaitre1933] Lemaitre and Vallarta showed that the variations in intensity of the cosmic radiation with latitude could be fully explained if it was accepted that the radiation consisted, at least in part, of electrons—or protons—of energy from the order of 10 GeV ($10^{10}$ eV), arriving on Earth and coming from all directions.

Figure 3.5 shows the expected trend of the radiation intensity as a function of geomagnetic latitude, for different values of a parameter (from 0.1 to 1.0) which is related to the energy of the incident particle considered [Lemaitre1933]. As an example, a parameter value equal to 0.4 would correspond to 9.54 GeV in the case of electrons, and 8.61 GeV in the case of protons.

The problem of geomagnetic effects on the intensity of cosmic radiation was addressed in the 1930s by numerous other authors, as also reported in a review article of the period [Johnson1938].
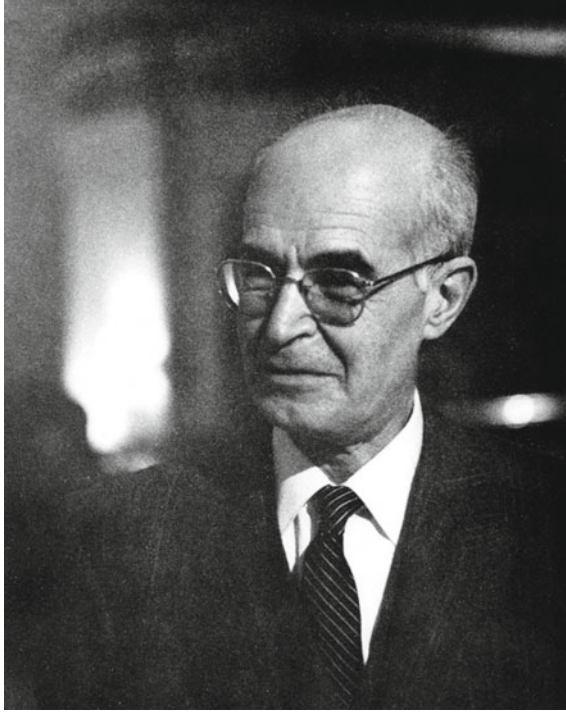
**Fig. 3.4** Sandoval Vallarta (1899–1977). *Source* American Institute of Physics (AIP), Emilio Segrè Visual Archives
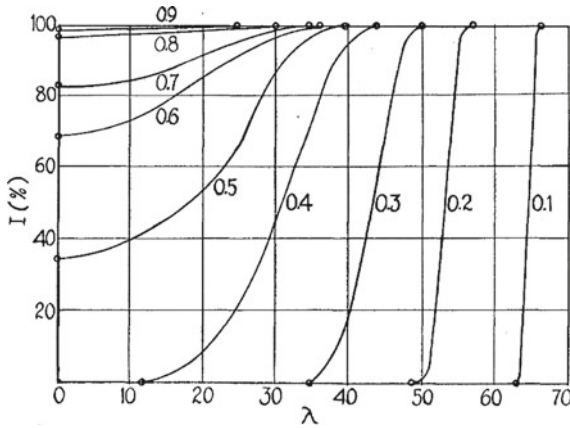


**Fig. 3.5** Trend predicted by Lemaitre and Vallarta [Lemaitre1933] of the intensity of the cosmic radiation as a function of geomagnetic latitude (see text). Figure reproduced from the work of G. Lemaitre and M. S. Vallarta, *On Compton's latitude effect of cosmic radiation*, Physical Review **43**(1933)87. Copyright (1933) by the American Physical Society, License No. RNP/22/MAY/054177

## 3.2  Campaigns for Measuring the Intensity of the Cosmic Radiation in Various Geographical Locations

The considerations made so far show how extremely important was to have a quantitative measure of the intensity of the cosmic radiation at different latitudes. This required measuring campaigns in the most disparate areas of the Earth, which in those years were indeed carried out, from latitudes close to the equator up to latitudes close to the poles. In the survey concerning the activity organized by his group of collaborators, which Compton published in 1933 [Compton1933] he recalls, quoting their works, how measurement campaigns of this kind had been carried out in previous years by the Dutch physicist Jacob Clay (1882–1955) (Fig. 3.6) [Clay1927, Clay1928] in a series of trips between Amsterdam and Batavia (Java), reporting lower intensity values near the equator, by Millikan and collaborators [Millikan1928a, Millikan1930b], who had measured the intensity of the radiation between California and Bolivia (observing very small variations) and between California and Churchill, a locality close to the magnetic North Pole (not observing any variation), from the Germans Bothe and Kolhörster [Bothe1930a], from Hamburg towards the North Pole, up to a latitude of 81° N (without observing any variation within the limits of experimental errors), from Kennedy and Grant [Grant1931] from Australia to Antarctica (still without appreciable observed changes) and by Corlin [Corlin1930] in Scandinavia, from latitude 50° N to 70° N (observing small variations, with a maximum around 55° N). Further measurement campaigns in various geographical locations had been organized in those years also by the French physicists Pierre Auger (1899–1993) and Louis Leprince-Ringuet (1901–2000), and by the Indian Piara Singh Gill (1911–2002) on the occasion of numerous ocean crossings between Vancouver and Tasmania.

Overall, the set of these observation campaigns seemed to indicate that the intensity of cosmic radiation was approximately constant in the various locations explored up to that moment, with the exception of the results obtained by Clay. If it had been shown that the intensity of the observed radiation was actually independent of the geographic location, in particular of the different Earth's magnetic field, this would have supported the hypothesis that the radiation was constituted by gamma (or possibly by charged particles with energy so high as to not be appreciably deflected by the Earth's magnetic field), thus denying the hypotheses that Bothe and Kolhörster had already made in 1929 [Bothe1929a] about the existence of a corpuscular radiation. On the contrary, the results obtained by Clay made it possible to observe with certainty the existence of considerable variations in the intensity of the cosmic radiation between these two explored latitudes, variations which were then estimated at around 15–20% in the observations obtained a few years later.

It was not clear, therefore, whether the intensity of the cosmic radiation really changed with latitude, because different experiments had given completely different answers. Although it may seem strange, all the different answers were reasonable, since, as it became clear later, the dependence of the flux on the geographical region

**Fig. 3.6**  Jacob Clay (1882–1955). *Source* Academictree.org

must be related more to the geomagnetic properties of the location (geomagnetic lati-
tude) than to the purely geographical location (see Appendix C). Clay's measurement
campaign had been conducted along geomagnetic paths that allowed more evident
variations to be observed, while the campaign by the German physicists had been
conducted along paths in which the expected variations were negligible.

Arthur Compton (1862–1962), former Nobel Prize winner in 1927 for the
discovery of the mechanisms of radiation-matter interaction (Fig. 3.7), decided to
enter the research field of cosmic radiation, not convinced by Millikan's arguments
regarding the nature and origin of this radiation. We will return again to the impor-
tant debate between Millikan and Compton about the corpuscular or photonic nature
of the cosmic radiation. Compton became interested in the nature of the cosmic
radiation only after the mid-1920s, perhaps following a trip to India for a series of
lectures delivered at the University of Punjab, which included a high-altitude scien-
tific expedition to measure the intensity of the cosmic radiation at different altitudes
[Johnston1967, Yodh2013]. In the early 1930s, Compton organized a campaign of

detailed measurements, the results of which were reported in a more systematic form in 1933 [Compton1933].

It extended over an enormous geographical area (Fig. 3.8). The campaign of measurements organized by Compton really represented a far-reaching enterprise in the panorama of the time. Several expeditions, with similar equipment, based on ionization chambers, travelled the globe, in the same period, in the most disparate geographical locations. Compton himself, who is portrayed aboard a ship playing on the deck in one of the archive photos, also participated in some of them.

Although preliminary results had been previously published by Compton himself and collaborators [Compton1931, Bennett1931, Compton 1932a, Bennett1932a, Bennett1932b, Compton1932b, Compton1932c], in the 1933 survey he summarizes the main results obtained from eight different expeditions, whose data were already available and which required—according to his statements—not to further delay their publication, probably because in the same period the publication of the results of another campaign of measures on a worldwide scale, organized by Millikan himself, was also underway, which will be discussed further on (Fig. 3.8).

In this review, published in Volume 43 of Physical Review, dated March 15, 1933 (but received by the Journal on January 30), Compton, after the description of the experimental procedures and the corrections necessary for the interpretation of the



**Fig. 3.7** Arthur Compton (1862–1962). *Source* American Institute of Physics (AIP), Emilio Segrè Visual Archives

**Fig. 3.8** Approximate location (blue dots) of the main stations for measuring the intensity of cosmic radiation, used during the measurement campaign organized by Compton [Compton1933]

results (for example those for the different atmospheric pressure due to the altitude, for the possible shielding effects offered by the buildings, …), summarizes in a long table all the results obtained, which are then reported in some of the famous graphs as a function of the geomagnetic latitude. The data reported by Compton, grouped into three ranges of altitudes (i.e., atmospheric pressure) and normalized to each other, are shown in Fig. 3.9. They show, according to Compton's interpretation, a clear difference between the intensity measured at geomagnetic latitudes close to the equator compared to that measured at geomagnetic latitudes above 50° N or S. This difference amounts to 14% at sea level, but it is greater at high altitudes, reaching 22% at an equivalent altitude of 2000 m and even 33% at an equivalent altitude of 4360 m.

The measured values, reported at an atmospheric pressure of 76 cm Hg, equivalent to sea level, are here also plotted in a more detailed figure (Fig. 3.10), together with the results obtained by Clay at different latitudes and with the value obtained by Millikan. In the original figure of Compton's article, some values had been averaged, while Fig. 3.10 shows the values reported in the original table. The agreement between the different data sets is good, so much that Compton concludes that "From a statistical standpoint, therefore, the probability of the existence of this latitude effect amounts practically to a certainty" [Compton1933].
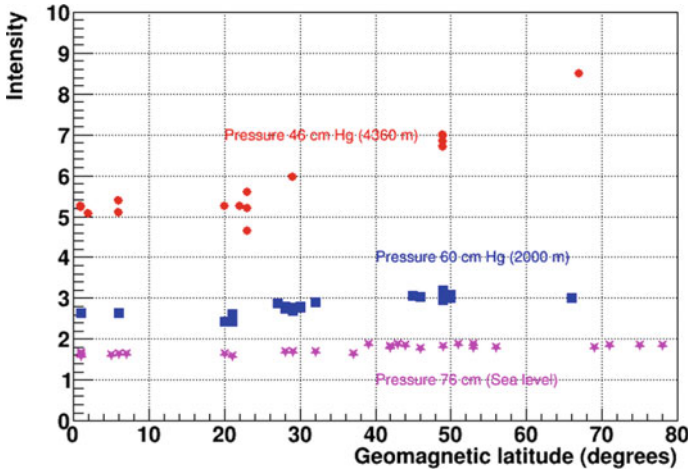
**Fig. 3.9** Radiation intensity measured as part of the expeditions organized by Compton [Compton1933] as a function of geomagnetic latitude, for three different altitude ranges, identified according to the value of the atmospheric pressure
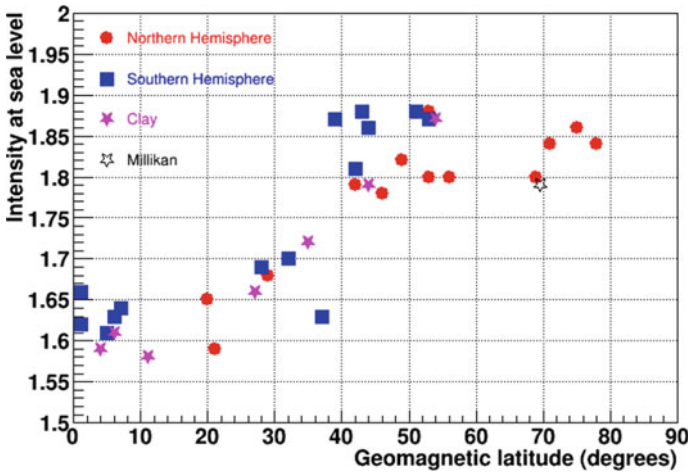


**Fig. 3.10** Radiation intensity at sea level, measured during the campaign organized by Compton [Compton1933] for different geomagnetic latitudes, and reported together with the values obtained by Clay and by Millikan. The values reported by Compton are distinct for the Northern and Southern hemisphere, with two different symbols

In Compton's original work, dashed curves are also shown, superimposed to the data, which represent calculations made on the basis of the theory of Lemaitre and Vallarta [Lemaitre1933], already cited, which hypothesized the arrival of high-energy electrons (5 and 13 GeV) in the vicinity of the Earth and their deflection following interaction with the Earth's magnetic field. Those of higher energy would be able to get to the poles, but not to latitudes below 50° N. The qualitative similarity of the curves with the trend of the measured data suggested to Compton that a substantial fraction of the particles could therefore be electrons of energy intermediate between these two values. Compton reports the data also as a function of the geographic latitude, observing an undefined trend, with a much greater dispersion of the data. The latitude effect, therefore, cannot be merely linked to the geographical latitude. Furthermore, if the same data are reported as a function of the local magnetic field (which extends for hundreds of km above the ground level), also in this case a not well defined distribution of values is observed, as instead occurs in the case of geomagnetic latitude.

This last result indicates something important, namely that the latitude effect cannot be due to a deflection of particles at low altitudes, in the Earth's atmosphere, but rather to phenomena that occur at much greater altitudes, hundreds of km, in the case of electrons with energy starting from some GeV. These considerations suggest that at least a significant fraction of the primary particles that reach the top of the atmosphere, coming from the outside, are charged particles.

The survey published by Compton was countered by another review of results, also obtained in various locations around the world, this time by Millikan and collaborators, published in April 1936 in Physical Review [Millikan1936], although some results had been published previously [Millikan1935b]. A striking aspect in this work by Millikan is the absolute lack of references to the work and results of both Compton and other authors. In fact, for the most part, the bibliographic references are self-citations of Millikan's previous works. This survey of results also required a massive organization: twelve different expeditions, by sea for the most part, with equivalent detection equipment, a variety of locations and routes explored that covered a substantial part of the globe, from the northern to the austral hemisphere, in a high range of geographical (and magnetic) latitudes. The result of this survey is first of all the confirmation of a latitude effect: the flux measured by the instruments shows a lower value at geomagnetic latitudes close to the equator, and an increasing value up to about 45° of geomagnetic latitude North, latitude at which the flux saturates without showing further increases at even greater latitudes. The observed variation is around 12%. The measurements also carried out at southern geomagnetic latitudes also allow us to observe an "equatorial dip", a valley in the flux values, between geomagnetic latitudes of about 40° S and 40° N, fairly symmetrical with respect to the geomagnetic equator.

Millikan's considerations on these results concern once again, as Compton had already done, the comparison with the analysis of Lemaitre and Vallarta, and therefore the conclusion that if we are dealing with primary electrons, they must have an energy around 6 GeV (within an uncertainty of 20%). The existence of a single geomagnetic latitude value at which the flux begins to decrease indicates, according to Millikan,

that there cannot be two classes of particles (such as protons and electrons) present at the same time, otherwise the intensity trend with the geomagnetic latitude should have shown evidence of a second decrease.

The abundance of results obtained at the different geomagnetic latitudes finally allows Millikan to draw a map of the intensity in the various regions of the globe, with lines that connect the locations where the intensity assumes the same value, therefore of the contour lines of the intensity of cosmic radiation (Fig. 3.11). This figure clearly shows that these contour lines generally follow a trend parallel to the geomagnetic equator, with an anomaly along the equator, and in particular in the area of South America.

Strangely enough, no discussion and interpretation of the results in relation to the nature of the primary cosmic radiation is present in this work, although in the Abstract of the article it is stated that these effects related to geomagnetic latitude derive from an asymmetry of the Earth's magnetic field, which extend up to large distances from the Earth, and that these effects are expected both in the case in which the primary radiation is of a corpuscular nature and in the case of photons. A marked difference, therefore, with respect to the clear interpretation of Compton, who saw in this effect linked to the geomagnetic latitude a consistent proof of the fact that the cosmic radiation was largely of a corpuscular type. This attachment of Millikan to the
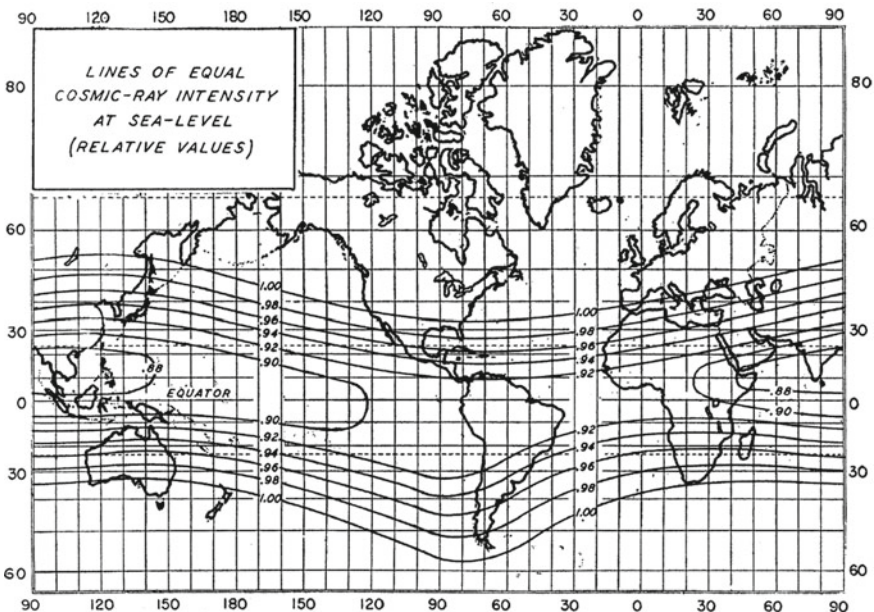


**Fig. 3.11** Map of the equal intensity curves of cosmic radiation, obtained from the survey by Millikan and collaborators [Millikan1936]. Figure obtained from the work of R. A. Millikan and H. Victor Neher, *A Precision World Survey of Sea-Level Cosmic-Ray Intensities*, Physical Review **50**(1936)15. Copyright (1936) by the American Physical Society, License No. RNP/22/MAY/053613

interpretation of radiation as essentially due to photons lasted a long time and gave rise to controversies between the two Nobel laureates, which the press emphasized, giving ample response to them.

## 3.3  The Debate on the Corpuscular or Radiative Nature of the Cosmic Radiation

Millikan's position on the nature of the cosmic radiation is also linked, according to the opinion of many historians of science, to the general vision of the world and of reality that Millikan professed, full of elements including those of religious nature, which led him to defend, even on principle, certain interpretations. It was also a period in which questions about the age of the universe, its dimensions, as well as its origin and evolution, were still in their initial phase. Millikan supported a cosmological hypothesis of a universe in continuous creation, while he did not look favourably an interpretation of a universe destined to a thermodynamic "death". In this context, the cosmic radiation had to play for Millikan the role of the "cry" of the new atoms forming in the interstellar space, a proof that the creative process was still in progress. "Millikan finds Creation still goes on while Creator directs the Universe", was the headline of the *New York Times*, after the communication made by Millikan to the Assembly of the American Association for the Advancement of Sciences (AAAS). According to this interpretation, the processes that led to the formation of new atoms had to produce gamma radiations as a result.

It was also these considerations that led Compton to enter the arena of cosmic ray physics, to verify for himself whether the corpuscular hypothesis, which he believed most, could be reflected in the observations of the intensity of the cosmic radiation at various latitudes. The first measurements made by Millikan in different locations seemed to indicate that the intensity was constant everywhere. Still in 1932, at the AAAS Annual Meeting, Millikan argued that there was no latitude effect, presenting his results in antagonism to those of Compton, discussed in the same Meeting. But after Compton's results, in 1933, the evidence seemed in favour of a corpuscular nature, which Compton announced, and which the press could not help but note, as it was the opinion of another Nobel laureate. That Millikan, despite his authority, was wrong? And if he was wrong about the nature of the cosmic radiation, what about the cosmological visions that were related to it?

The debate between Millikan and Compton also had a following in the non-specialist press, putting the question of science in the limelight of a broader cultural context, as the journalist Wolferton has recently described [Wolferton2019], but of course it was also played out in official contexts, conferences and scientific meetings, which even at that time were precious occasions for the presentation of one's results and for the exchange of opinions with researchers working in the same field.

Figure 3.12 shows one of the historical photos, taken on the occasion of the International Congress of Nuclear Physics, organized in Rome by Enrico Fermi

**Fig. 3.12** Participants in the International Congress of Nuclear Physics in Rome, October 1931. Among the scientists present on this occasion, Millikan and Compton are also recognizable, in the central part of the photo. *Source* Wikimedia Commons

in October 1931. Among the leading physicists participating in this Congress are present, among many others, also Millikan and Compton. It has often been noted that in this photo there is only one woman, Marie Curie, compared to about forty men, a proportion that fortunately has changed drastically in recent times, although many steps remain to be taken in this direction.

Coming back to the question of the origin of cosmic radiation, Millikan supported for many years hypotheses on which he then had to change his mind. Already in one of his articles of 1926 [Millikan1926b], Millikan had claimed that this radiation was emitted by nuclear transmutations, such as the capture of an electron by a light nucleus, the formation of Helium starting from Hydrogen or other processes such as the condensation of radiation into atoms, assuming that these cosmic radiations presumably took place not in stars, but in space and interstellar matter.

In a subsequent article [Millikan1928b], strictly dedicated to the origin of cosmic radiation, Millikan better clarifies his considerations about the nature of these processes capable of giving rise to the gamma radiation that he hypothesizes to constitute cosmic rays. Further precision measurements of the absorption of radiation in water, performed in the same Arrowhead Lake (1570 m) already used for previous measurements and in Gem Lake (2760 m), contributed to this vision. From these results Millikan had deduced three different absorption coefficients for the

cosmic radiation: one component with a coefficient of 0.35 per meter of water, one with a coefficient of 0.08 and finally a third one with a coefficient of 0.04.

The fact that the penetrating radiation had different values of the absorption coefficient was interpreted as due to the existence of different energy values of the gamma radiation, produced in nuclear processes with different energy values, such as quantum jumps. The enormous energy involved for these radiations implied, in Millikan's vision, processes of formation of heavier nuclei abundant in nature, such as helium, oxygen, silicon or iron, starting from the lightest nuclei (hydrogen or helium). There was also speculation about where these processes could take place, whether in the interior of stars or in the interstellar medium, concluding that it is the very low-density interstellar, or intergalactic medium, that is the natural candidate for the processes at the origin of the cosmic radiation.

In the years following 1933, therefore, even if evidence of a different type accumulated in favour of the corpuscular nature of cosmic radiation, Millikan continued to support the hypothesis of a highly penetrating gamma radiation, as evidenced by his works in the following years [Millikan1934, Millikan1936].

In 1936, however, Compton decided to definitely clarify the evidence supporting the corpuscular hypothesis, in a work published in Physical Review [Compton1936], summarizing this evidence in three different categories:

(a)  those related to the effects of latitude and directional asymmetry
(b)  those obtained from coincidence experiments
(c)  those coming from asymmetry effects due to the motion of the Earth in the Galaxy.

Note, once again, the Introduction section in this article, which reports not only the bibliographic references relating to the works that support the corpuscular hypothesis, but also, for correctness, those works, especially those of Millikan, which support a different hypothesis and an alternative interpretation.

Compton basically lists three arguments in favour of the corpuscular hypothesis.

The first concerns precisely the set of geographical variations observed in the intensity of the cosmic radiation. The fact that these variations follow the course of the Earth's magnetic field very closely suggests that the causes of these variations are of magnetic origin and that therefore at least a non-negligible fraction of the cosmic radiation observed at sea level must be produced by primary charged particles, since the effects are not reducible—according to the theory of Lemaitre and Vallarta as well as that of Størmer, already cited—to those produced by the magnetic field on secondary particles produced in the atmosphere. The measurement campaigns that made possible to observe these geomagnetic variations are those organized by Clay, by Compton himself and by Millikan. According to Clay's data, which Compton considers as a model, the reduction in radiation intensity is 17% between geomagnetic latitude 45° N and geomagnetic latitude 0°. At least this fraction of 17%, Compton concludes, must be charged, leaving the remaining 83% fraction to be interpreted.

But the experiments carried out with the first counters operated in coincidence as telescopes, therefore sensitive to the direction of arrival, also showed a further effect, namely that the intensity near the equator was greater from the West direction

than that measured from the East direction. These are the first evidence of what will be called "East–West Asymmetry", and which we will discuss in more detail in a later chapter. According to Rossi's results, for example, near the equator and at an inclination angle of 45°, the intensity from the East is 76% of that from the West. This means that at least 24% of the particles coming from the West (which correspond to about 12% of those incidents vertically) are charged. This further increases the minimum percentage of charged particles that must be present in the primary radiation. Further arguments, based on the energy distribution of the particles, are then used to establish an important feature, namely that the relevance of this latitude effect is limited simply by the strength of the Earth's magnetic field: if this were much higher, the fraction of particles able to reach the Earth near the equator would be practically null, demonstrating that almost all of the primary radiation must be charged.

The second argument concerns the results that had been obtained in those years with the use of counters operating in coincidence, also with the aid of cameras for viewing the tracks. The development of cosmic radiation detection techniques had made considerable progress in the previous decade compared to the use of the first electroscopes and will be the subject of a more detailed discussion in Chap. 5. We only recall here that by the date of 1936, in which Compton tries to defend his considerations about the corpuscular nature of the cosmic radiation, the first Geiger counters and the first cloud chambers had already been used, that the technique of coincidence between individual counters had been introduced, also to determine the direction of motion of the particles, and that in the meantime new particles had been observed, such as the positive electron (positron) and the neutron, which we will discuss later. The results of experiments conducted by several authors using counters operating in coincidence are considered by Compton perhaps the most striking evidence of the corpuscular nature of radiation, as they provide evidence of the passage of single high-energy particles.

With reference to Fig. 3.13, for example, which shows a typical experimental setup used in those years, the passage of a particle capable of giving a signal in coincidence in the detectors $C_1$, $C_2$ and $C_3$, allows to "trigger" the display (and the relative photographic recording) of any tracks in the "Chamber". In most cases (90%) these photographed tracks are single tracks, left by highly penetrating particles, capable of crossing 40–50 cm of lead along their path. Evidence of this kind had been obtained from Rossi [Rossi1932a, Rossi1933a], from Auger and Ehrenfest in 1934 [Auger1934] and from Street and collaborators in 1935 [Street1935].

The experiments of Rossi [Rossi1933a] and Hsiung [Hsiung1934], in particular, showed that these penetrating particles were not secondary particles generated near the counters, at sea level, but came from much greater heights. Compton admits that in principle they could be generated by gamma rays at high altitudes in the atmosphere; however, he excludes this possibility, as they are subject to the same latitude effect as the overall ionization due to cosmic radiation, and also show effects of directional asymmetry near the equator. They, therefore, in Compton's opinion, are generated by primary particles of high energy, or are even themselves the primary particles that make up the cosmic radiation.
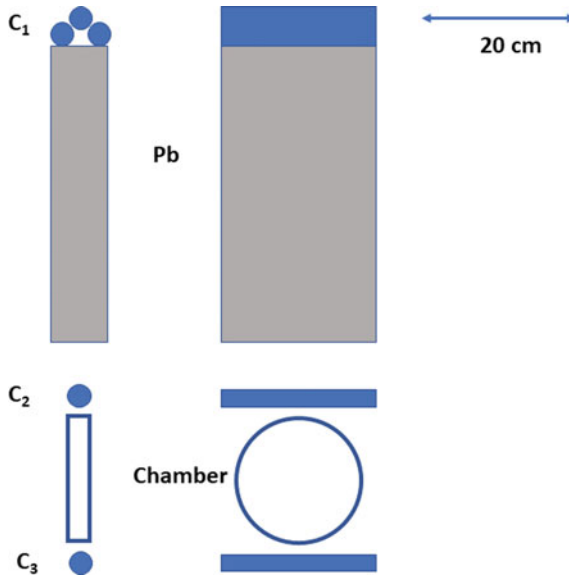
**Fig. 3.13** A typical experimental setup, used in the mid-1930s, for the display of tracks in a cloud chamber, triggered by the coincidence between several counters arranged vertically [Street1935]

These considerations show how long and tiring the path leading to the current visions of primary and secondary cosmic radiation has been. We are in a period in which many of the elementary particles, in terms of which we describe today the interactions that occur in the atmosphere due to the arrival of a primary, are still to be discovered, and therefore the statements about the very nature of cosmic radiation try to concatenate various experimentally observed elements, without yet knowing in detail many of the aspects involved in the different processes. To these arguments, Compton adds the consideration that in cloud chambers, in addition to the single tracks due to the passage of highly penetrating particles, a small "shower" is sometimes observed, produced by photons, but that these showers are also subject to the latitude effect, demonstrating that these photons in turn must also be produced by primary particles.

But there is another class of arguments, the third one, which Compton argues in favour of the corpuscular nature of the cosmic radiation, linked to the effect on the intensity of this radiation due to the motion of the Earth with the rotation of the Milky Way. According to the results provided by the astronomers, it had already been estimated that the rotation of our galaxy, the Milky Way, drags the Earth in the direction of the Constellation of Cygnus, with a speed that is about 0.001 c, that is, one thousandth of the speed of light. If the primary radiation consisted of photons, they would be subject to the Doppler effect, and a difference should be observed between those arriving from one side and those from the opposite side with respect to the motion of the Earth, an effect that had been actually studied and quantified by Compton and Getting [Compton1935]. The experimentally observed

effect indeed exists but is much less than what one would expect from a primary radiation made up of photons and it is instead compatible with the hypothesis of a radiation made up of charged particles, in which case the effect is very small, since they would be strongly deflected by the magnetic field. Two interesting aspects of these considerations should be noted: the first is that the presence of primary photons is not entirely excluded, admitting that they could be part of the primary radiation, but in an extremely small fraction of a few percent. The second aspect is that in this discussion the primary charged particles are once again hypothesized essentially as electrons or positrons.

As we said at the beginning of this section, Compton also intends to discuss the arguments raised so far in favour of the hypothesis that the primary radiation is constituted by gamma, arguments that were mainly supported by Millikan's group. According to these hypotheses, which Millikan had maintained up to that date, in 1936, it was possible to admit the presence of a small fraction, about 15%, of a charged component, while the remaining 85% must have been made up of gammas. In support of this hypothesis, Millikan cited some events observed in the cloud chamber by Anderson and collaborators, events that showed the production of electron and positron showers induced by gammas. However, these events were interpreted by Compton as due to gammas, also present in the secondary radiation, that is, produced in turn by the arrival of a primary in the upper part of the atmosphere. Further considerations about the different absorption of electrons and high-energy photons are also addressed and discussed, showing that on the basis of the knowledge already established at that time, the processes induced by both photons and high-energy electrons are substantially the same, as the high-energy electrons interact mainly through radiative processes, that is, with the emission of radiation. This means that the assertion that photons were 100 times more penetrating than electrons with the same energy was to be discarded on the basis of now commonly accepted knowledge.

Summarizing all the pros and cons of the hypotheses about the nature of primary radiation, Compton concludes that at the top of the atmosphere all observations seem to indicate that at least 75%, and probably 95% near the poles, of the primary radiation is made up of charged particles. At sea level, the evidence derived from the latitude effect, from the coincidence measurements and from the small daily variations observed, due to the motion of the Earth, indicate that no more than a few percent of the primary radiation can be made up of gamma.

Regarding the typology of these primary charged particles, Compton can only assume that they are electrons and positrons, although "*There is also some sugges-tion of the existence of protons. We cannot now discuss these interesting details*" [Compton1936a]. The crucial question, however, which according to Compton represents the most important feature of the last decade of research on cosmic radiation, is precisely its charged corpuscular nature.

Despite these considerations by Compton, which seem to establish with certainty the characteristic at least of charged particles as a source of the primary cosmic radiation, still in 1937–1938 Millikan moves in a totally independent way from these statements, practically never mentioning them, focusing attention on other aspects

but, on the other hand, then assuming at a certain point the "corpuscular" ideas as if they were his own.

In one of the works from this period [Millikan1938b], Millikan, using results relating to the intensity of ionization measured up to the top of the atmosphere by the launch of balloons, argues that the incident radiation consists of electrons or a combination of electrons and photons, since their ability to interact is not very different, and that these considerations arise from the analysis of their own results. Millikan even comes to extract an energy distribution of the incident electrons, which he believes may have energies between 1 and 17 GeV, distributed in different "bands", with a maximum around 6 GeV. In this work, the assertion that he himself demonstrated, in a previous work of a few months before [Millikan1938a], is almost taken for granted that the primary radiation is largely made up of electrons, and that they could not interact with matter before entering the Earth's atmosphere. This also indicates that they do not have their origin within the stars or in places of the universe where matter is present in abundance.

Regarding the origin of this radiation, Millikan still insists on a mechanism according to which it is the transformation into energy of the entire mass of atoms that is responsible for the production of this radiation, a sort of annihilation of the most abundant atoms in the universe. Since the mass of a hydrogen atom corresponds to approximately 1 GeV, the abundant elements $^{12}C$, $^{14}N$, … up to $^{56}Fe$, would correspond to energies of 12, 14, … 56 GeV. This annihilation should therefore produce, in most cases, an electron–positron pair, and, to a lesser extent, a gamma pair.

Thus, even if on the basis of arguments deriving from his own results and without making use of the arguments put forward in support of the corpuscular hypothesis by Compton, Millikan seems to have "converted" his mind to this hypothesis, or, better, seems to declare that he himself obtained the proof of these claims, an attitude not unlike from that taken over ten years earlier, when recognizing the very existence of radiation of extraterrestrial origin.

As for his previous work [Millikan1938a], the assertion that they are electrons relies on the absorption of these radiations at various altitudes, based on which Millikan excludes that they are protons. The real novelty lies in starting to consider that the tracks of the penetrating particles observed, both visually, in the cloud chamber, and through their passage in the particle counters operated in coincidence, are not electrons but other charged particles (positive and negative) with a different ionizing power, referring to the recent observation, just in 1937, by Neddermayer and Anderson [Neddermayer1937], of what will subsequently be called the μ meson. In the final part of the article, Millikan comes to discuss the "secondary" character of this penetrating component, that is, the fact that these particles cannot be present in the primary radiation but are rather the result of processes that take place in the Earth's atmosphere.

## 3.4  Further Contributions in Europe and Other Countries for Understanding the Nature of the Cosmic Radiation

Although the core of the activities related to the study of the cosmic radiation progressively shifted, starting from the end of the 1920s, towards the other side of the Atlantic, the contributions coming in that period from the environment of European research—and, to some extent, from other countries in the world—were certainly not negligible. Indeed, we have many examples of researchers who continued to work in European institutions, particularly in Germany, France, Italy, Great Britain, as many articles have pointed out [Sekido1982, Walter2012]. Significant contributions in the physics of cosmic rays gradually came also from other, non-European, countries, already during the 1930s. All these activities, which we will briefly mention in this section, certainly contributed to clarifying further aspects of the cosmic radiation and its nature, but above all they established, also through cultural exchanges and stages of many researchers among the various Institutions existing at the time, a common substrate in the study of this area of physics.

In Germany, the measurements aboard high-altitude balloons with a human crew continued in the following years, even by Kolhörster, who organized an ascent to an altitude of 12,000 m, using a balloon that was 26 m in diameter, filled with about 10,000 cubic meters of hydrogen. To reach these high altitudes, the crew needed an artificial breathing system with an oxygen cylinder, with an autonomy of several hours [Horandel2013]. Kolhörster himself in those years also actively contributed in the study of the intensity of the cosmic radiation in the subsoil, installing particle counters, also operating in coincidence, inside salt mines, up to a depth of about 1000 equivalent meters of water [Kolhörster1933, Kolhörster1934].

Measurements of the absorption of cosmic rays under a certain depth of water were also carried out by the German Erich Regener (1881–1955) (Fig. 3.14), in Lake Constance, up to a depth of 230 m below the surface of the water [Regener1932a], with an automatic apparatus which recorded the result of the ionization measurement on a photographic plate. Automatic recording devices were used by Regener in those years also aboard unmanned balloons [Regener1932b], up to altitudes of 30 km, thus extending the measurements previously carried out by Hess and Kolhörster. Regener also made significant experimental contributions for the improvement of automatic recording equipment, for the development of scintillation counters and in the use of the first rockets as a tool for high-altitude scientific investigations. Regener's pupil and collaborator was the physicist Georg Pfotzer (1909–1981), who contributed to many of the balloon ascents to evaluate the intensity of the radiation with altitude.

Still in those years, we may recall the flights of the Swiss physicist Auguste Piccard (1884–1962), together with his brother Jean Piccard (1884–1963), with a pressurized capsule, up to an altitude of over 15 km, for the study of various atmospheric phenomena and of the cosmic radiation. Auguste Piccard had already made balloon ascents since 1913. Subsequently, to reach even higher altitudes, in the stratosphere, he had designed balloons with an airtight cabin, reaching an altitude of 16,000 m in 1932. Two years later his brother Jean reached 17,500 m. Several members of the

**Fig. 3.14**  Erich Regener (1881–1955)

Piccard family, in addition to the two brothers Auguste and Jean, also contributed over the years to high-altitude explorations. In the following years Auguste Piccard dedicated himself to submarine exploration, reaching a depth of 11 km below the sea level, with the bathyscaphe Trieste, in the *Marianas Trench.* Figure 3.15 shows some of the members of the Piccard family with the pressurized capsule employed during one of the flights into the stratosphere.

First of all, it should be remembered that the cosmic radiation detection technique, initially based only on the use of electroscopes, had already undergone several improvements over the years. In particular, an enormous impulse to the study of cosmic rays came from the use of Geiger counters, widespread starting since 1928 [Geiger1928a, Geiger1928b] and which we will discuss in greater detail in a subsequent chapter, and from the possibility of evaluating—by means of coincidence circuits—whether two or more counters produced coincident signals over time, a

**Fig. 3.15** The photo shows William Swann (left), Jean Piccard (right), and Jeannette Ridlon-Piccard, wife of Jean, close to the capsule employed for stratospheric flights. *Source* AIP Emilio Segrè Visual Archives, Physics Today Collection

possibility that allowed the use of a telescope of counters, capable of signalling the passage of a single particle through the two counters and therefore defining its direction.

This possibility had been already exploited in 1929 by Bothe and Kolhörster in Germany, carrying out a series of measurements with two counters placed vertically on top of each other, laterally protected by a considerable thickness of lead absorbers and with an absorbent layer also placed between the two counters [Bothe1929a, Bothe1929b]. In this configuration (Fig. 3.16), it was possible to observe a relatively large number of coincidence events, which can be interpreted as the passage of a single penetrating particle through the two counters. The possibility that these events were due to electrons, emitted through the Compton effect by gamma rays interacting with the surrounding material, could be excluded, as these electrons have low energies and should have been stopped by the absorber interposed between the two counters, an effect not observed. Only considerable thicknesses, several cm, of heavy materials, such as gold, produced a small reduction in the number of observed coincidences. Gold has a density of 19.3 g/cm$^3$, higher than that of lead (11.3 g/cm$^3$) but of course it is not that easy or cheap to find, and Bothe and Kolhörster seem to have resorted to the National Bank of Germany to obtain loan of blocks of gold to be used during their measurements. Based on these results, the two German scientists had already concluded, perhaps overestimating the interpretation of their experiment, that the penetrating radiation observed was not made up of gamma rays but was rather of a corpuscular nature [Bothe1929b].
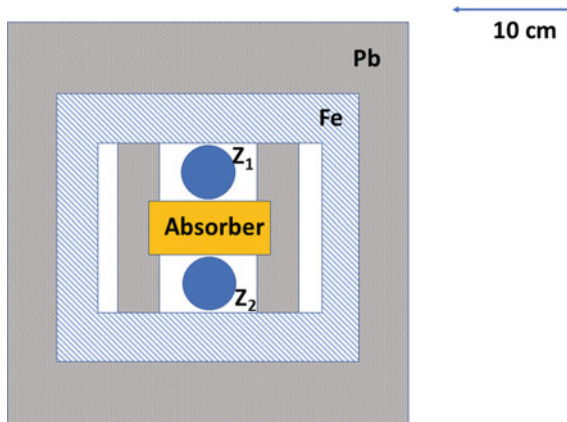
**Fig. 3.16** The arrangement used by Bothe and Kolhörster [Bothe1929a] for coincidence measurements between two counters ($Z_1$, $Z_2$) arranged one on top of the other vertically and laterally protected by absorbers, with an additional thickness of absorber material placed between the two counters

We will discuss later the contributions of Kolhörster related to the first evidence of the existence of correlated particles in the secondary cosmic radiation. Again in the 1930s we should remember the studies performed by means of nuclear emulsions by Marietta Blau, which we will recall later in connection with the phenomenon of the interaction of primary particles with the atmosphere. Moreover, a large impulse to cosmic ray investigations also came from the first permanent installations of cosmic detection equipment in the high mountains, for example on Mount Hafelekar, to which Hess himself contributed [Hess1932].

Other activities partly carried out in Germany concerned the first observations of the influence of atmospheric pressure on the intensity of cosmic radiation, by Myssowsky and Tuwim [Myssowsky1926], two Russian physicists who collaborated with Kolhörster. Tuwim, in particular, had also developed a numerical algorithm for the interpretation of coincidence data between two Geiger counters arranged in a telescopic configuration, based on their geometric properties. Additional studies on the influence of atmospheric pressure were done by Steinke [Steinke1930].

It should also be remembered that in the mid-1930s Heisenberg also dealt with the theory concerning the cosmic radiation, in particular by studying the processes that led to the formation of showers [Heisenberg1936] and the penetrating power of this radiation [Heisenberg1938].

The first Italian contributions to cosmic ray physics have been discussed in several texts mentioned in the bibliographic notes [Bonolis, Bertolotti, De Angelis, Marafatto] and in many articles [Scarsi2005, Peruzzi2007, DeAngelis2010, Bonolis2011a, Bonolis2011b, DeAngelis2012, Spillantini2013, Bonolis2014]. As far as Italy is concerned, one of the important contributions to the physics of cosmic rays, as it is universally known, is that of Bruno Rossi (1905–1993), whose work and results we will be able to use extensively in this review, and that we want to delimit

in this section to the more specific question of the nature of cosmic radiation. Bruno Rossi had started his scientific activity after graduating in Bologna in 1927. At the end of the 1920s he was already involved in activities concerning the study of the cosmic radiation, also intrigued by the availability of new working tools for the study of this radiation, such as the new Geiger counters and the associated coincidence techniques. The first results of coincidence measurements, carried out by Bothe and Kolhörster, had already been made available, as we have seen, in 1929, showing that the particles capable of crossing two counters vertically overlapping and separated by a thickness of a few cm of material with a high atomic number, like gold, could not be electrons produced by the Compton effect. Bothe and Kolhörster believed that these penetrating particles were already a component of the primary radiation, a hypothesis that later on turned out to be incorrect, but which allowed considerable progress to be made in understanding the overall components of radiation.

Starting from the knowledge of these first experiments by Bothe and Kolhörster, Rossi began in a few months his own research program dedicated to the study of the cosmic radiation in the laboratory, building and setting up new kinds of counters, improving the coincidence circuits, developing a series of geometric configurations with different counters and with different amount of shielding between the counters, using magnetic fields for the deflection of the particles, thus obtaining, in the course of a few years starting as early as 1930, a very remarkable series of results [Rossi1930a, Rossi1930b, Rossi1931a, Rossi1931b, Rossi1931c, Rossi1932a, Rossi1932b, Rossi1932c, Rossi1932d, Rossi1933a, Rossi1933b, Rossi1934a, Rossi1934b]. We are lucky to be able to learn his working method and the results obtained in this progressing activity not only from numerous comments on his work, already cited, but from the author's own words, through several textbooks and autobiographical papers that the Italian physicist published later during his career [Rossi1964, Rossi1981, Rossi1990] (Fig. 3.17).

It is interesting, for example, to read from Rossi's own story, that the ideas expressed by Millikan about the origin of cosmic radiation, as due to the fusion of hydrogen atoms to form heavier atoms, had not affected him positively [Rossi1981], but that at first, he too had shared the prevailing idea of a primary radiation consisting of high-energy gammas. The first results of Bothe and Kolhörster, therefore, which introduced an alternative experimental method for understanding the type of radiation observed, had particularly intrigued him. The introduction of an electronic coincidence circuit, which he designed [Rossi1930a], and which we will discuss in detail in Chap. 5, allowed to perform coincidence measurements even between more than two counters, making it possible to imagine and set up different kinds of geometric configurations, with a time resolution better than that of Bothe and Kolhörster's original apparatus, which was 0.01 s.

Among the first results of these experiments, performed by means of counters in coincidence, Rossi observed the first evidence of the effect resulting from placing a layer of material above the two counters arranged vertically on top of each other, rather than in the middle between the two: in the first case there was an increase in the coincidence rate between the two counters. In 1930 Rossi had spent a short time in Bothe's laboratory in Berlin, discussing both the experimental techniques used

**Fig. 3.17**   Bruno Rossi (1905–1993). *Source* AIP Emilio Segrè Visual Archives

and the first attempts to observe a dependence of the intensity of cosmic radiation on latitude, during an expedition to Northern Europe. Although the results of this first expedition had not been very significant, Rossi was aware of the importance of this type of measurements for the understanding of the corpuscular nature of the cosmic radiation, familiarizing himself with Størmer's results on the deflection of particles in the terrestrial magnetic field, and theoretically studying the effect of a possible East–West asymmetry [Rossi1930b], it too linked to the corpuscular nature of the radiation.

A first measurement to study the East–West asymmetry, carried out in Arcetri, did not initially give the desired results [Rossi1931c], but, carried out subsequently at latitudes close to the equator and at a higher altitude, in Eritrea, it clearly showed an excess in the intensity of the radiation coming from the West [Rossi1933b, Rossi1934a, Rossi1934b]. However, similar results had previously been published independently by Johnson [Johnson1933a, Johnson1933b] and by Alvarez and Compton [Alvarez1933]. These results once again proved the corpuscular hypothesis to be right, also showing—and this went against generally accepted ideas—that the primary particles were positively charged. We will be able to return to the East–West asymmetry later, as well as to the first evidence of coincidences between counters

placed on the same level at a certain relative distance, an effect which, although observed, was not investigated in detail by the Italian physicist.

In 1931, during the Conference on Nuclear Physics held in Rome, Rossi, at the invitation of Fermi, presented his results concerning cosmic rays, which denied Millikan's hypotheses about the nature of the cosmic radiation. We know from Rossi's own words that Millikan, who was also present at the Conference, along with most of the well-known physicists of the time, did not like his contribution very much, which he ignored even in the years to come, as he used to do. Rossi's contribution to this Conference was instead appreciated by Compton, who seems to have decided to deal more with the problem after hearing his presentation. According to Bruno Rossi, indeed, it was the Rome Conference that marked the beginning of the debate on the corpuscular or photonic nature of cosmic rays. As we saw, this debate took the form in the United States of a real conflict, which went beyond the strictly scientific aspect, and involved the personalities of two Nobel laureates, Millikan and Compton. In Europe, however, according to Rossi's opinion, the debate between the two positions had much more quiet tones and did not undermine respect, friendship and acceptance of the ideas of other colleagues.

Rossi's subsequent experiments, performed with a set of three counters in coincidence (to reduce the amount of spurious coincidences), separated by a considerable thickness of lead, highlighted the existence of particles so penetrating as to emerge even after a meter of lead. Moreover, in those years Kolhörster had also done experiments with counters placed in a salt mine, thus revealing coincidences originated by extremely penetrating particles.

Experiments of the same kind, with different configurations of three counters and lead absorber screens, arranged above and between the counters, were performed by Hsiung at the University of Chicago [Hsiung1934], in order to distinguish the coincidences due to showers and secondary particles produced in absorbers themselves from those due to primary ionizing particles passing through the counters. However, the current interpretation of these experiments still associated these highly penetrating particles with the primary radiation.

Among the other physicists who at that time carried out their activity, linked to the physics of cosmic rays, in Italy, even if they later moved to other countries, the name of Giuseppe (Beppo) Occhialini (1907–1993) is certainly worth mentioning. Occhialini, after graduating in Florence in 1929, began his career with Bruno Rossi, to move almost immediately to Great Britain, where he collaborated with Blackett on the experiments done with the use of a cloud chamber, coupled to a coincidence circuit, which will lead in 1933 to the observation of positrons in the cosmic radiation. Subsequently, in the second half of the 1930s, Occhialini moved to Brazil, at the University of Sao Paulo, an Institution that some European scientists had helped to found, moving and carrying out their activities there, to form a school of Brazilian physicists. Finally, after a further stay in Great Britain during the war years, Occhialini returned to Italy in the early 1950s.

We may also remember the expedition with the airship Italy, organized by Umberto Nobile in 1928, which brought on board a variety of scientific equipment, including electroscopes for measuring air ionization. Scientists of various nationalities also

participated in this expedition, which unfortunately ended tragically on its way back, including the Czechoslovakian František Běhounek (1898–1973), one of the few survivors of the expedition and a cosmic ray physicist, which he later described also in a book [Běhounek1929]. It is worth remembering that precision measurements of the intensity of cosmic radiation at latitudes close to the North Pole (66°–82° N) have been recently carried out by the EEE Collaboration [Abbrescia2020], using a scintillation detector telescope installed aboard of a sailboat, as part of the PolarquEEEst scientific expedition, as we will resume in a later chapter.

In Great Britain, in the second half of the 1930s, the Manchester school, with the contribution of Blackett and the numerous physicists, including foreign ones, who spent periods of study and research in that laboratory, made many significant contributions to the study of cosmic radiation [Sekido1982]. Contributing to this was the increasingly critical situation in Europe in the years leading up to the Second World War, which saw the transfer, escape or exile of many Central European scientists, in some cases to Great Britain, to stay there, or as an intermediate destination to the USA. Although Blackett was able to return personally to a full research activity only at the end of the conflict, his laboratory continued to be operative even in the previous years and during the same conflict, often by foreign physicists, one of which was the Hungarian physicist Janossy, whom we will mention later.

In France, the first studies of the cosmic radiation are associated with the names of Pierre Auger and Louis Leprince-Ringuet, pupils of Jean Perrin and Maurice de Broglie [Ravel2013, Degrange2013]. Among the first studies performed by the two French physicists, in the early 1930s, are the measurements of the intensity of the cosmic radiation during a two month voyage by ship, from Le Havre to Buenos Aires, results that had confirmed those obtained by Clay about the presence of a charged component in cosmic radiation, influenced by the Earth's magnetic field.

We will discuss later the contribution of Auger and collaborators, in the following years, which led to the observation of coincidence events between counters placed some distance apart and, therefore, to the evidence of extensive air showers, a result that will open a new path in the physics of cosmic rays. Subsequent studies were carried out with the creation by Leprince-Ringuet and Chanson of a laboratory located in the high mountains, at 3600 m of altitude (Aguille du Midi, Mont Blanc), equipped with a large cloud chamber and an intense magnetic field.

Lajos Janossy (1912–1978), Hungarian physicist, was one of Kolhörster's students in Potsdam, where he carried out many measurements with him in the early 1930s, using coincident Geiger counters in various geometric configurations [Kiraly2013]. Janossy later moved to Manchester, where he worked with Blackett's group and many other foreign physicists who spent time in that Institute, continuing to study different aspects of the cosmic radiation (directional asymmetries, magnetic field effect, properties of penetrating showers …). Janossy returned to Hungary a few years after the end of the Second World War, contributing to create a group dedicated to cosmic ray physics at the Physics Institute of the Academy of Sciences, of which he became director.

Experimental activities in Sweden were carried out as early as the mid-1920s by the astronomer Axel Corlin [Corlin1927, Corlin1928], who also participated in

the campaign to measure the intensity of cosmic radiation at latitudes close to the North Pole [Bartelt2018]. In the context of the activities related to the physics of cosmic rays in Northern Europe certainly it should be remembered, even if we will have the opportunity to further discuss this aspect, the figure of Hannes Alfvén (1908–1995), Swedish physicist, Nobel Prize in 1970, whose name is linked to magnetohydrodynamics, which has numerous connections with the problem of the transport of cosmic rays in interplanetary space.

Cultural exchanges between researchers from different countries, despite the difficulties both intrinsic (due to the scarcity of means of communication and transport), and linked to the particular post-war period, were of primary importance in determining the development of physical activities in cosmic rays also in non-European countries, as well as in the USA.

In Japan, the first studies of the cosmic radiation date back to the mid-1930s [Sekido1982, Nishimura2013], with the contributions of Y. Watase (1907–1978) and S. Kikuchi (1902–1974) at the University of Osaka, concerning the development of showers [Watase1937], and with the creation in Riken—by Yoshio Nishina (1890–1951)—of a Laboratory dedicated to various aspects of modern physics (Nuclear Physics, Cosmic Rays, …). The first group then directed its interests towards nuclear physics with accelerators while Nishina's group continued activities in cosmic ray physics. The first contributions in this area were obtained through the construction of a cloud chamber with a diameter of 40 cm—very large for that time—and a magnetic field of 1.7 T, to study the energy spectrum of cosmic rays and measure the mass of muons [Nishina1937]. Subsequent activities were also addressed to measurements of the cosmic radiation in the subsoil, for the study of the decay of the pion, and to the monitoring of the intensity of cosmic rays in different geographical locations, activities that suffered an abrupt halt due to the Second World War and were able to resume only several years after the war ended (Fig. 3.18).

An interest and some contributions related to cosmic ray physics are also present in India [Tonwar2013], with the figure of Debendra Mohan Bose (1885–1975), a physicist who had studied in Europe, in Great Britain, at the Cavendish Laboratory, and later, as a researcher, from 1914 to 1919 in Berlin, with Erich Regener. Bose organized several measurements in the late 1930s, with nuclear emulsions at large altitudes, in the Himalayas. Subsequent contributions were made by Bhaba (1909–1966), who had obtained his doctorate in Cambridge in 1933 on the absorption of cosmic rays and who conducted numerous measurements of the intensity of the radiation at high altitudes, with instrumentation mounted on board of balloons or by means of the use of an aircraft. Measurements of the intensity of cosmic rays at various latitudes were carried out in the years 1937–1938 by Piara Singh Gill (1911–2002), on the occasion of numerous ocean crossings between Vancouver and Tasmania, as part of the doctorate obtained with Compton in 1940. Returned to India, he continued his activity in cosmic ray physics, especially at high altitudes, also founding an observation laboratory in Kashmir at 2700 m above sea level. Finally, in the years immediately following the Second World War, Vikram Sarabhai (1919–1971) also made contributions, with activities concerning the effect of the Sun on cosmic radiation.

**Fig. 3.18** Japanese physicists from Yoshio Nishina's group in Tokyo in 1943, on the occasion of the awarding of a prize to Yukawa. *Source* AIP Emilio Segrè Visual Archives, Yukawa Collection

If the contributions of the German group of Bothe and Kolhörster, as well as those of Rossi, had made use above all of Geiger-Müller counters for the observation of penetrating particles, another instrument, the Wilson chamber, was at the origin of other experiments and gave rise to further experimental evidence regarding the nature of the highly penetrating radiation. We will describe Wilson's chamber in a later chapter. Here we may recall how the first and most important results regarding the observation of these penetrating particles, through the Wilson chamber, were obtained by the Soviet physicist Dmitry Skolbetsyn (1892–1990), who can be considered the founder of cosmic ray physics in Russia [Bazilevskaya2014], even if the first studies of cosmic radiation had already been carried out by Lev Myssovsky and Lev Tuwim, whom we have already mentioned for their collaboration with the German group of Kolhöster. Myssowsky and Tuwim had made numerous studies of the absorption of radiation in water and lead, they had studied the angular distribution of radiation and the effect of atmospheric pressure [Myssowsky1925, Myssowsky1926, Myssowsky1927, Myssowsky1928]. After the untimely death of both, however, it was Skolbetsyn who continued this activity for a long time.

As early as the mid-1920s Skobeltsyn had made observations with a Wilson chamber immersed in a magnetic field, initially for the study of electrons generated by the Compton effect. Among the tracks of these electrons, mainly of low energy, Skobeltsyn had however also observed tracks of highly energetic particles, over

20 meV, which could not be due to the radioactive source of RaC that he was using at that time [Skobeltsyn1927].

Skobeltsyn obtained hundreds of photos, even stereoscopic, of tracks observed through a Wilson's camera immersed in a magnetic field [Skobeltsyn1929]. Among these, some dozen showed evidence of tracks due to highly energetic particles, and some even evidence of the interaction of these particles with atoms, signalled by double or triple tracks that departed from the point of interaction. Skobeltsyn could perhaps have recognized in some of these tracks also the first evidence of the positron, but the magnetic field used was too low to allow this observation, which was then obtained by Anderson a few years later, using a higher magnetic field. It is true, however, that Anderson himself recognized Skobeltsyn's merit in having paved the way for the observation of these events linked to the cosmic radiation (Fig. 3.19).

Skobeltsyn also spent a period of research in France, where, together with Auger, he observed in 1929 some first evidence of correlated tracks. When the first systematic observations of coincidences between different counters were made, which we will



**Fig. 3.19**  Dmitry Skolbetsyn (1892–1990). *Source* Alchetron.com

discuss later, Skobeltsyn had returned to the Soviet Union, continuing to keep alive relations with foreign colleagues, so much so that in 1933 a conference was organized in Leningrad with the presence of many Western physicists.

In the second half of the 1930s, with positions of responsibility at the Academy of Sciences, he organized a series of activities in cosmic ray physics, including observations at high altitudes, in the mountains (Mount Elbrus, 3700 m, Pamir at 3760 m and then up to over 5000 m), as well as by means of balloons with radio data transmission. Skobeltsyn was also the author of the first textbook on cosmic rays in Russian, which served as the basis for the researchers of the following era and continued his research and organization until late in his life.

## 3.5   Protons as an Essential Component of Primary Radiation?

In the second half of the 1930s, the belief that the primary radiation could not be made by gammas became increasingly accepted, based on an accumulation of evidence related to geomagnetic effects, experiments with coincident counters, and understanding of the properties of the showers produced by the interaction of a gamma or a charged particle, as we have seen in the previous pages, also due to the diversified contribution of many researchers in different countries of the world.

Several works by William Francis Gray Swann (1884–1962), an English physicist who later moved to the United States and became director of the Bartol Foundation at the Franklin Institute, published around the mid-1930s, discuss in detail the aspects related to the nature of the primary radiation, progressively moving towards the increasingly convincing hypothesis that a good percentage of the primary radiation was made up of charged particles, and more specifically, of protons rather than electrons or positrons. In an educational article of 1961, Swann, at that time retired, summarizes some historical aspects of the physics of cosmic rays of that period [Swann1961], recalling how the hypothesis of the cosmic radiation as constituted by photons of high energy, however simple and capable to qualitatively reproduce the trend of absorption with the thickness of the atmosphere crossed, had not proved capable of interpreting in detail the various aspects observed. The existence of a more penetrating (hard) and a less penetrating (soft) component, observed from the beginning, with which to be able to interpret the absorption in terms of two exponential functions, with different slopes, had led Millikan to admit the existence of a multiplicity of components, those he had discussed in terms of the various nuclear processes capable of producing different ranges of energies.

The corpuscular hypothesis, however, had always been considered as a possible alternative. The difficulty in assuming the corpuscular hypothesis arose above all from the fact that charged particles do not follow an exponential or quasi-exponential law of absorption, as they are mostly associated with the concept of range (distance crossed by the particles before depositing all their energy). But if we hypothesize

these particles as electrons, the range of electrons emitted by radioactive substances is typically a few millimetres in solid materials, while it was evident that the hard component could also cross a lead thickness of several meters. Even assuming that the energy of the electrons present in the cosmic radiation was 1000 times greater than that present in beta decays, the Earth's magnetic field would have had to deflect these electrons in a very consistent way, producing large variations in intensity in different places on the Earth's surface.

The variations due to geomagnetic latitude had indeed been observed, but the amount of these variations was a few percent, at worst about 10% passing from the equator to the poles. While on the one hand this evidence confirmed the corpuscular nature of the primary radiation, on the other hand this was not compatible with the fact that a large part of the primary radiation was made up of electrons. In a review work of 1935, Swann summarizes in detail the status of the corpuscular theory of the primary cosmic radiation [Swann1935], without yet explicitly mentioning the hypothesis that primary particles are protons. A few months later, however, in an article of February 1936, Swann himself briefly discusses the "protonic" hypothesis [Swann1936] starting from recent considerations by Compton and Bethe [Compton1934, Compton1936b], and hinting at an experiment, just performed on his proposal, to evaluate the presence of protons at sea level.

In 1934, in fact, Compton and Bethe, in a short article in Nature [Compton1934], had discussed the existence of two different components (A and B) in the cosmic radiation capable of reaching the surface of the Earth, and of a third component (C), present in the upper part of the atmosphere, as evidenced by the results obtained aboard balloons launched into the stratosphere. Component A, of greatest importance at the top of the atmosphere, is associated with photons, while component B with electrons and positrons. Based on considerations about the loss of energy due to radiative processes of the different known particles, Compton and Bethe suggested that assuming that the component C consisted of protons was the most natural choice, able to provide a coherent explanation of most of the known phenomena.

The results of the experiment were indeed published in the same year, 1936 [Montgomery1936], but essentially concerned the possibility that the protons could also be found among the components present at sea level. The result is that the percentage of protons at sea level was established to be a small percentage, between 5 and 12%, depending on the assumptions made. These experiments, based on the conclusions drawn, however, do not exclude that protons are the primary particles, capable of giving rise to the various components then observed at sea level.

The hypothesis of a primary radiation as constituted by protons, able to correctly interpret most of the observed phenomena, is increasingly evident in a series of communications and works published around 1939–1941, for example those of Swann [Swann1939a, Swann1939b, Swann1940, Swann1941a, Swann1941b] and by Carlson and Schein [Carlson1941]. Swann summarizes the status of recent knowledge by stating that there is only one type of primary radiation, charged and predictably made up of protons; that this primary radiation has an energy distribution with a lower limit given by the possibility of penetrating the Earth's magnetic field; that protons—by means of mechanisms still unknown at the moment—are capable

of producing, upon their entry into the atmosphere, a certain number of mesotrons (μ mesons); that the mesons produced by low energy protons, being emitted almost at rest, given their very short average life, about 2 μs, as we will see later, will not have the possibility to penetrate into the atmosphere, but will travel only a few hundred meters and will be distributed on average in all directions; that the mesons produced by protons of higher energy will be able to penetrate deeper into the atmosphere, producing electrons and neutrinos, which will be emitted mainly in the direction of motion of the original particles. Similarly, Carlson and Schein [Carlson1941], recognizing that a model was still missing to describe the mechanisms of interaction of the primary protons, assumed that an "explosion" occurred in which the proton lost all its energy creating a certain number of mesons, multiplicity that increased with the energy of protons.

The hypothesis of protons as the main constituents of primary cosmic rays increasingly took shape as a natural choice. This despite the fact that the overall production mechanisms of the particles produced in the atmosphere were only clarified years later. Again in 1941, for example, Giuseppe Cocconi (1914–2008), an Italian physicist who worked in his country of origin before moving to the USA in 1947, in a short note in Physical Review [Cocconi1941], in confirming that the hypothesis of primary protons is the most reasonable to explain the generation of the different particles, including the "mesotrons" (μ mesons), as well as the gammas and electrons/positrons, admits that the mechanism of production is still unknown.

This was therefore the situation in the early 1940s: the acceptance of a proton nature of the primary radiation, more and more consistently accepted, even in the absence of a detailed description of the mechanisms by which the primary protons were able to ultimately produce all particles present in the atmosphere, down to the sea level.

# Chapter 4
# New Particles and Their Links with the Cosmic Radiation

**Abstract**  Since its beginning, the study of the cosmic radiation has been undoubtedly linked to that of the elementary particles. The discovery of new particles in this context and the understanding of their properties received a strong contribution from cosmic ray physics. This chapter briefly recalls the link between these two important areas, especially the discovery of the positive electrons in the cosmic radiation, made through the observation of their tracks in the cloud chambers, and the first evidence for the existence of particles with a mass intermediate between that of electrons and that of protons. Further observations of cosmic ray tracks by visual methods led in those years to the study and identification of the various mesons, and especially to the understanding of the properties and role of pions and muons in the cosmic radiation. A discussion concerned with first estimates of the muon mass by these experiments is further discussed in Appendix E.

## 4.1   The Discovery of New Particles and the Links with the Understanding of Cosmic Radiation

As Bruno Rossi pointed out [Rossi1964], the main problems related to the physics of cosmic rays, particularly between the 1930s and 1940s, were twofold: on the one hand, the attempt to understand the nature of the cosmic radiation, both primary and secondary; on the other hand, the classification of the particles existing in nature. The two issues were obviously closely linked to each other, and any progress made in one of the two areas would have greatly facilitated the understanding of the other. It was already established that the radiation capable of propagating in the Earth's atmosphere had at least two components, one "soft", being absorbed in a few cm of lead, the other more penetrating, or "hard", crossing even meters of lead. However, the nature of these two components was not established with certainty, in particular that of the more penetrating component, the other being predictably associated with electrons. The very existence of atmospheric showers, which we will discuss later, in a special chapter, had been highlighted in those years, but neither the mechanism by which the showers began nor their detailed composition, in terms of particles and energy distribution, had been clarified.

A partial answer to these questions came, as well known, from the discovery of new particles, which took place in the context of the study of the cosmic radiation, which at that time was the only high-energy physics laboratory able to provide information on the processes involved at energies significantly higher than those of radioactivity phenomena.

We mentioned the first observations of the tracks left by energetic particles, obtained by Skobeltsyn with the aid of cloud chambers, as early as 1929 [Skobeltsyn1929]. These observations were extended, by means of apparatus using more intense magnetic fields, in a series of experiments carried out since the 1930s by Anderson and Millikan. The results of these experiments were manifold.

In one of the first series of observations it was established that the particles present in the observed cosmic radiation had—almost all of them—the same elementary electric charge, as they produced the same ionization density as that produced by fast electrons [Anderson1932a]. In this first work Anderson, using a Wilson expansion chamber with a magnetic field up to a maximum value of 21,000 gauss, clearly observed the presence of tracks that curved in the opposite direction, and taking into account the fact that they came from above, it turned out to be possible to assign a negative or positive charge to each track. The evidence of these positively charged high-energy particles was interpreted in that work as being due to protons, while those negatively charged were identified as electrons. The analysis of these tracks also allowed to extract an angular distribution of the tracks themselves, which showed a prevalence for those emitted at small angles with respect to the vertical, with a dependence similar to $\cos^2 \theta$ (Fig. 4.1).
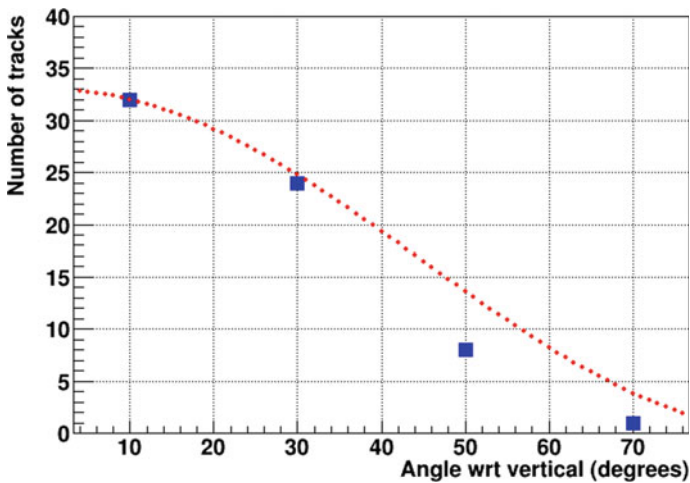


**Fig. 4.1** Angular distribution of the tracks measured by Anderson in one of his first works with the Wilson chamber. The data obtained, represented by the blue symbols, are compared with a $\cos^2\theta$ dependence (red points). Data extracted from [Anderson1932a]

Figure 4.2 shows one of the images, obtained with a magnetic field of 12,000 gauss, which Anderson interpreted as evidence of the passage of a 27 MeV negative electron and (probably) of a 450 MeV proton. The energies were estimated using the value of the magnetic field used and extracting the radius of curvature of the track from the photo. With a maximum magnetic field of 21,000 gauss, Anderson was able to measure even tracks that had a radius of curvature of 700 cm, and therefore a magnetic rigidity of $1.5 \times 10^7$ gauss cm, corresponding to kinetic energies of several GeV for both electrons and protons (See Appendix D).

These particles, therefore, had a wide distribution in energy, with values that far exceeded 1 GeV. In these first measurements it was possible to observe maximum energies of about 5 GeV, a limit which later, by other authors, was brought to 20 GeV.

However, the analysis of the ionization density of these positive tracks soon led to the exclusion of the fact that they were protons: the energy loss per unit length of these particles was compatible with a mass much smaller than that of the proton, for example with that, enormously smaller, of the electron. Anderson reached this conclusion in a very short time, so much so that both in the preliminary article published in *Science* at the end of 1932 [Anderson1932b] and in the more complete article published at the beginning of 1933 [Anderson1933a] the presence of these tracks of positive charge was associated with the first evidence of the existence of positive electrons, or positrons.
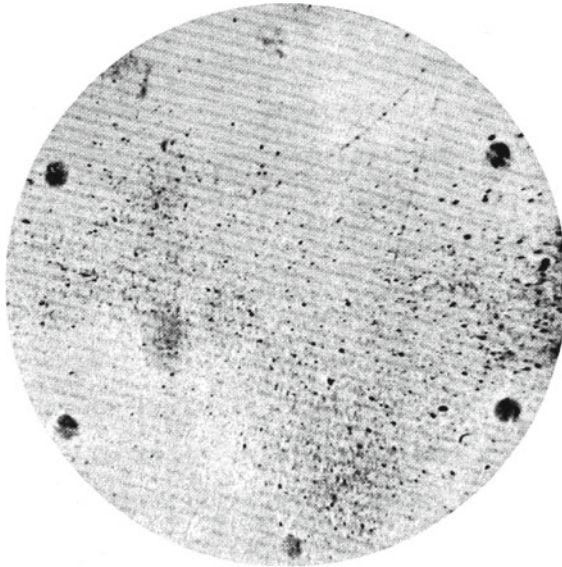


**Fig. 4.2**  One of the images obtained by Anderson in his early works [Anderson1932a], showing evidence of two tracks of opposite curvature, the first interpreted as a negative electron, the second as a high energy proton. Figure reproduced from the work of Carl D. Anderson, *Energies of cosmic ray particles*, Physical Review **41**(1932)405. Copyright (1932) by the American Physical Society, License No. RNP / 22 / MAY / 053614

This evidence was obtained by placing a lead plate in the middle of the observation chamber, in order to observe and measure the radius of curvature of the track before and after crossing the lead plate, which would have produced a loss of energy.

In some way, this arrangement also made it possible to establish whether the particles came from above or from below, in which case the sign of the curvature of the track had to be interpreted in the opposite way. While the results also highlighted the presence of tracks coming from below, it was possible to establish with certainty that the positive tracks could not be due to protons, but rather to positively charged electrons. A proton with the same magnetic rigidity, in fact, would have given rise to a much greater ionization density than that observed and would have had a much lower range (maximum distance travelled before completely losing its energy).

Anderson's observations were soon confirmed also by Blackett and Occhialini in England [Blackett1933a, Blackett1933b], who used a chamber controlled by two coincident Geiger counters to signal the passage of tracks [Blackett1932]. In a very short time, the idea of the existence of positive electrons was considered as completely "natural". Already in these works of 1933 Blackett argues almost for granted that low energy positrons are easily produced by gamma radioactive sources, when gammas interact with matter, or even emitted themselves as a result of nuclear transmutation processes. Blackett refers to works by Anderson and Neddermayer [Anderson1933b], by Curie and Joliot [Curie1933] and by Meitner and Philipp [Meitner1933], all published in 1933, which show that in a few months the observation of positrons in natural phenomena had become very common (Figs. 4.3 and 4.4).

The observation of the positive electron was related to Dirac's theoretical considerations, initially considered as difficult to understand, given the assumption of particles with states of negative mass and energy [Dirac1928]. Dirac's theory contemplated the existence of two states of charge of the electron, which the observations of Anderson and Blackett and Occhialini confirmed.

However, assuming the existence of these positive electrons allowed to explain in a more direct and natural way a variety of otherwise unclear phenomena; for example, the fact that an equal number of negative and positive electrons were produced in the showers, by the more energetic photons, or the fact that positrons had a very short life in matter, because once produced, they annihilated rapidly with electrons of negative sign, producing photons, based on the equivalence between mass and energy.

The process of producing electron–positron pairs, in which the energy of the incident photon was converted into the mass and kinetic energy of the pair, still needed to be understood in detail. However, already in Blackett's work [Blackett1933b], he discusses the number of pairs produced, in terms of the absorber material and of the gamma energy, observing that it grows as both quantities increase, and he refers to a work, by Oppenheimer and Plesset [Oppenheimer1933], in which the first estimates of what we can call the pair production cross section were reported.

A more complete theory of the interaction of gammas with matter, which also included the processes of creating $e^+e^-$ pairs was then formulated by Bethe and Heitler in 1934.

Before the formulation of this theory, it was already known that fast electrons, slowed down in matter, produced photons (*Bremsstrahlung* radiation), but that this
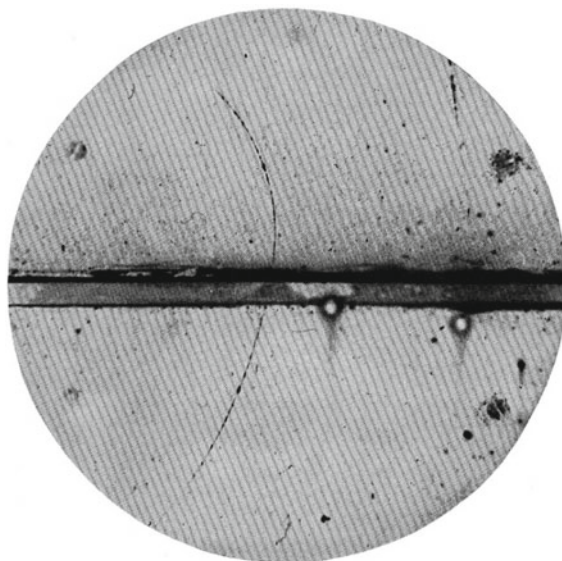
**Fig. 4.3** The historical image obtained by Anderson in 1933, showing evidence of a positive track, interpreted as a 63 MeV positron that loses energy as it passes through a 6 mm thick lead plate, positioned in the middle of the chamber, emerging as a 23 MeV positron [Anderson1933a]. The high range shown by this track is incompatible with that of the proton. Figure reproduced from the work of Carl D. Anderson, *The positive electron*, Physical Review **43**(1933)491. Copyright (1933) by the American Physical Society, License No. RNP/22/MAY/053615

radiative process represented only a small part of the overall process of energy loss for such electrons, considering that the collisional mechanism, the energy loss by ionization, was predominant. The new calculations by Bethe and Heitler, based on quantum and relativistic theory, instead predicted different results, in particular that these radiation losses increase with the energy of the particle, while those due to ionization processes decrease rapidly with the increase of energy. From a certain energy onwards, the loss of energy by radiation equals and finally exceeds that by ionization. This critical value is different for the different materials, amounting to about 10 MeV in lead, and to about 100 MeV in air. Furthermore, the theory of Bethe and Heitler predicted that the energy losses due to radiation were enormously greater for light particles, such as electrons, than those to which heavy particles, such as protons, were subject, due to a factor including the squared mass of the particle. These losses were also expected to be greater in materials containing high atomic number elements.

For the processes concerning the production of electron–positron pairs, the theory of Bethe and Heitler finally predicted that the cross section of this process increases with the atomic number of the element, and that starting from the threshold value (1.02 MeV) grew rapidly with the photon energy, until it reached an approximately constant value, while the cross sections of the other processes through which photons
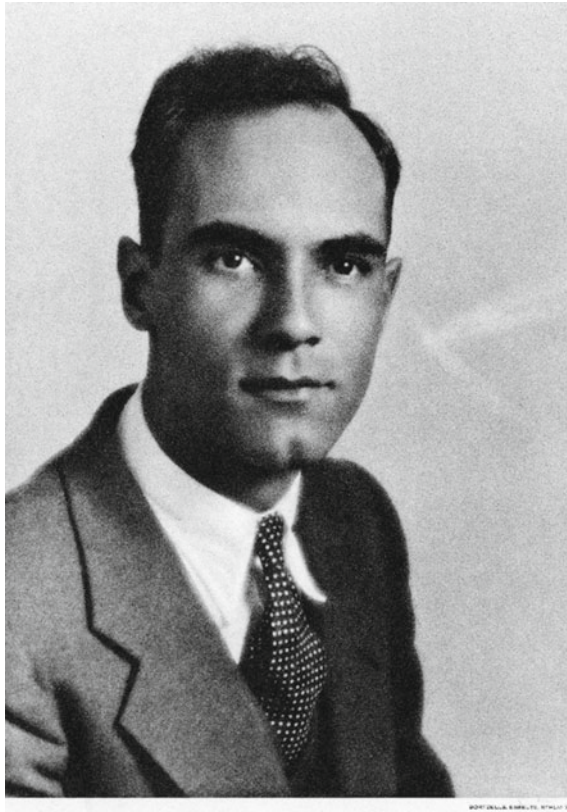
**Fig. 4.4** Carl D. Anderson (1905–1991). *Source* AIP Emilio Segrè Visual Archives, Weber Collection, W. F. Meggers Gallery of Nobel Laureates Collection

interact with matter—the photoelectric process and the Compton process—were characterized by a cross section that decreased with the energy of the photons. Following this theory, it appears that low-energy photons are mainly absorbed by the photoelectric and Compton effect and, subsequently, at higher energies, through pair-production processes. The energy at which the pair-production process begins to become more likely than the Compton process is about 5 MeV in lead, and about 20 MeV in air. Figure 4.5 shows a quantitative example of the cross sections for these processes, evaluated for air (assumed for simplicity as a mixture consisting of 80% Nitrogen and 20% Oxygen), as a function of the photon energy, from 10 keV to 1 GeV.

Now, the fact that high-energy electrons have to interact with high probability by means of radiative processes was in contradiction with the fact that the particles of cosmic radiation, imagined up to that moment as electrons or positrons, were capable of crossing even a lead thickness of one meter or more, so that Bethe and Heitler
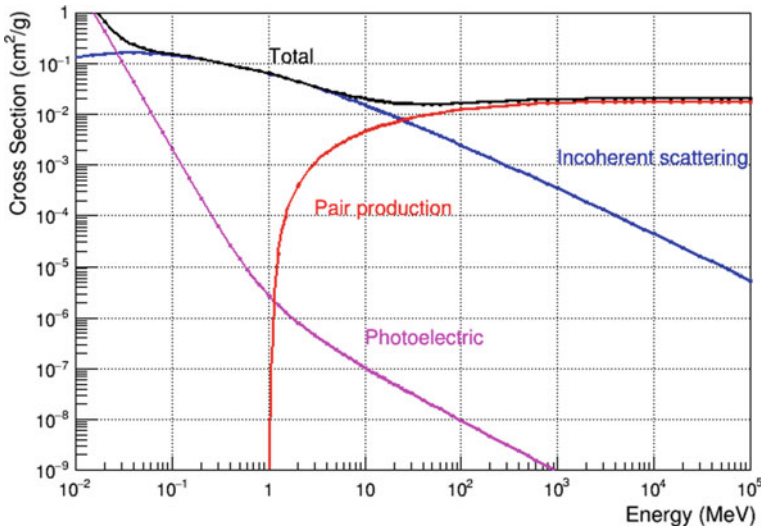
**Fig. 4.5**  Cross section of photoelectric effect, Compton scattering and creation of electron–positron pairs in the interaction of photons with air. Data extracted from the National Institute of Standards and Technology [NIST] database

themselves initially suspected that this theory and the same quantum hypotheses on which it was based, were not valid for very high-energy electrons.

However, it soon became clear, by analysing the structure of electromagnetic showers, created by high-energy photons by means of the different processes (creation of pairs, Compton effect, emission of bremsstrahlung radiation), that the theory was able to explain satisfactorily this phenomenon and that could be considered substantially correct. A major part of the secondary cosmic radiation present in the atmosphere could therefore be interpreted on the basis of this theory: in the cosmic radiation there were photons and electrons, even very energetic, which gave rise to these showers (cascade processes initiated by an electron or by a high-energy photon). This component represented the so-called "soft", or less penetrating, component of the cosmic radiation. However, it remained to explain the presence of a much more penetrating component, which could not be constituted by electrons.

The very discovery of the positron, as one of the constituents of the cosmic radiation observed at sea level, could not alone explain the set of observations and lead to a picture as complete as possible of the phenomena that occurred in the atmosphere due to cosmic rays. The other experimental evidence that made a great contribution to understanding the physics of cosmic rays was, as we know, that related to the existence of other charged particles, of intermediate mass between that of electrons and that of protons, the mesons.

Assuming, as it was initially done, that Bethe and Heitler's theory was not valid for large electron energies turned out to be an unreasonable choice. In those years already several physicists, such as Williams and von Weizsacker had confirmed that

this theory gave correct results even at energies well above some GeV, and moreover the strongly penetrating particles observed had energies both above and below the GeV. For a particle not to radiate it had to be a particle heavier than the electron, and at that time only protons were known as particles having a mass greater than the electron.

But the hypothesis that they were protons (both positive and negative, which although foreseen by Dirac's hypotheses, did not correspond to any observation made up to that moment) encountered difficulties, emerging from the observations of Anderson and Neddermayer [Neddermayer1937, Neddermayer1938]. The particles in question, in fact, as they ionized less than protons, should have a lower mass, but, on the other hand, not radiating as much as the electrons, their mass must have been larger than that of the electrons. From these results Anderson and Neddermayer concluded in 1937 that they had observed with certainty particles of intermediate mass between that of the electron and that of the proton.

Initially the measurements carried out by Anderson and Neddermayer were unable to accurately establish the mass of these particles, because the measurable ionization density in relation to the observed magnetic rigidity did not allow to distinguish masses of intermediate value between electrons and protons. However, in a short time, further observations by Street and Stevenson, in 1937 [Street1937], aimed at the possibility of detecting low-energy particles (therefore more distinguishable), made it possible to extract an estimate of the mass, around 200 times the mass of the electron (See Appendix E). These particles, as it is known, were initially given different names, including *yukon*, *mesotron* and *meson*. Later, with the discovery of other mesons, this specific class of particles was given the name of $\mu$ mesons. More precise measurements of the mass of these mesons were made by several groups in the following years, but still in 1950, the mass estimated by Brode's group was (206 $\pm$ 2) electron masses.

The chapter concerning the nature of these particles, constituting the penetrating part of the cosmic radiation, was destined, however, to remain complex for several years, for various reasons. On the one hand, an initial erroneous interpretation of the meaning of this particle, which was first identified with the particle theoretically hypothesized by the Japanese physicist Yukawa in 1935, on the other hand the need to understand the behaviour of these mesons and their decay.

Yukawa, in arguing that nuclear forces must be associated with some kind of particle, just as photons are associated with electromagnetic forces, foresaw the existence of particles associated with the nuclear field; because of the range of action of these forces they were supposed to have a mass equal to some hundreds of electronic masses. The discovery of $\mu$ mesons was therefore associated, as it seemed natural, with the theoretical prediction by Yukawa, who also hypothesized a decay for these particles, hence one of the assigned names, *yukons*.

## 4.2  **Properties of μ-Mesons**

The evidence of the existence of these particles was soon accompanied by numerous studies aimed at studying their properties, in particular their mass and their decay.

The number of particles detected at different heights can be used to get information on the possible decay of the mesons. Measurements of the number of particles present at various altitudes in the atmosphere had been carried out with accuracy by various groups in England, France, Germany and Italy around 1936–1937. Already from the first results it was understood that in comparing the paths crossed, corresponding to the same mass but to different materials, the absorption of cosmic rays was apparently different. This happens for example for air and water, in which case the same surface density correspond to a very different linear thickness. Still imagining that the particles were to be associated with the Yukawa particles, it was expected that these should decay spontaneously.

In 1938, the German physicist Helmut Kuhlenkampff (1895–1971) found that this property could naturally explain the anomalous absorption of cosmic rays in the air. If we consider for example a very small thickness of water and imagine that the mesons have an average life of the order of microseconds, none of these will decay in such a limited space. However, a large fraction of mesons will decay through an equivalent thickness of air of about 80 m instead of 10 cm of water; absorption is therefore also governed by the effect of spontaneous decay. Rossi also contributed to these studies, in the autumn of 1938 and in the spring of 1939, studying the instability of the meson through a direct comparison between the absorption of mesons in air and in a dense material. These experiments were mainly done after Rossi's move to the United States in 1939 at Compton's invitation.

The experimental apparatus used by Rossi consisted of a certain number of Geiger counters in coincidence, separated by a layer of lead and graphite sufficient to eliminate the soft component. With this apparatus, measurements were carried out at different altitudes, up to 4300 m, and Rossi understood that the absorption in the material was much lower than that observed in the air. The evident greater absorption was due to the decay of the mesons flying through the atmosphere.

This measurement also made it possible to extract a rough estimate of the average life of the mesons, which for low energies was estimated to be about two microseconds. The measured average life of these mesons due to relativistic effects is however greater than the average life of the mesons at rest. Taking into account the relativistic formulas for time dilation, it can be estimated, for example, that for mesons of kinetic energy 500 MeV the average life measured is almost 5 times greater than their average life at rest.

Measures of the average life for mesons of different momentum were reported by Rossi himself in 1941 [Rossi1941]. Similar experiments were carried out in the following years by various groups both in the United States and in Italy, despite the difficulties, in the Italian territory, during the war, to maintain research activities.

Figure 4.6, taken from the original work of Nereson and Rossi [Rossi1943] shows the disintegration curves of mesons in various materials (Pb, Al, brass) compared with the curve obtained in the absence of absorber material.

As to the mode of meson decay, this was established by the first photographs of the decay obtained by Williams and Roberts in England using condensation chambers [Williams1940]. One of these photos showed the track of a meson stopping in the gas of the chamber and a further track departing from the end of the previous track; this additional track was identified as that of a positive electron, and this showed, as expected, that the decay of the meson produced an electron.

Further experiments were carried out in 1941 by Franco Rasetti (1901–2001), an Italian physicist from the "Via Panisperna" group, who also emigrated, first to Canada and then to the USA, after 1939. Rasetti used a coincidence circuit with
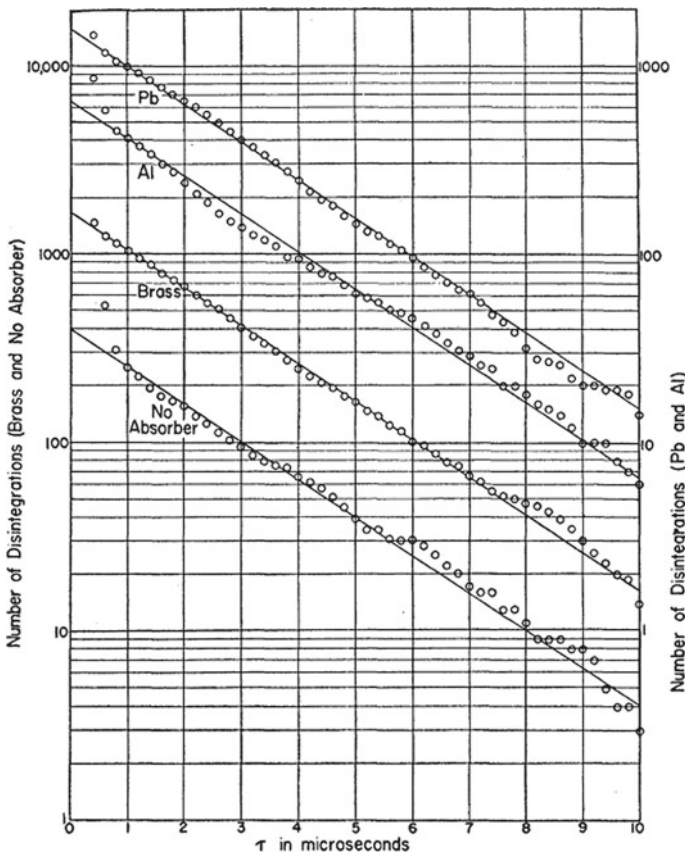


**Fig. 4.6** Disintegration curves of mesons in different materials [Rossi1943]. Figure reproduced from the work of N. Nereson and B. Rossi, *Further measurements on the disintegration curve of the mesotron*, Physical Review **64**(1943)199. Copyright (1943) by the American Physical Society, License No. RNP/22/MAY/053654

different time windows, to detect both the meson and the electron within a certain time interval [Rasetti1941]. With this apparatus, mean lifetimes of the mesons at rest equal to about 1.5 microseconds were measured. Finally, in 1942–1943, Rossi and Nereson [Rossi1942, Rossi1943] performed a very detailed experiment on the decay of mesons, using a set of Geiger counters and absorbers, using an electronic circuit to measure the delay between the arrival of mesons and the emission of electrons in a more accurate way. The result is a decay that follows an exponential law over time, exactly similar to that of the decay of nuclei. The trend of these data will also allow to extract a much more precise value of the average life of the mesons, equal to 2.15 microseconds, with an estimated uncertainty of 0.07 microseconds. More precise measurements were obtained only many years later, using particle accelerators.

## 4.3   The Discovery of the Pion

Although several years later, even the evidence of the existence of a further meson, the pion, which turned out to be the one predicted by Yukawa, was closely related to the issues discussed in the previous sections about the nature of the particles present in cosmic radiation and the processes that take place in the Earth's atmosphere.

One of the considerations that led to the evidence of the pions was the different behaviour of positive and negative muons. That they should behave differently in interacting with matter had already been discussed around 1940 by the Japanese physicists Tomonaga and Araki. The different hypothesized behaviour is linked to the fact that a positive meson, due to its electric charge, cannot get very close to an atomic nucleus, which is also positively charged. Therefore, the positive meson will be subject to spontaneous decay. In the case of negative mesons, however, the possibility of being captured by a nucleus before decaying represents a further way for the meson to "disappear", with an apparent decrease in their average life. The probability of capture of negative mesons, being linked to the electric charge, is expected to be greater for heavier nuclei, with a high atomic number.

A first demonstration of the correctness of this interpretation was obtained by Rasetti [Rasetti1941], with the same apparatus that had served to determine the average life of the muons. By evaluating the number of muons stopped in a block of iron and the number of decay electrons emitted, it was possible to estimate that only a fraction of the overall number of muons, about 50%, decayed into electrons, while the others presumably underwent a process of nuclear capture.

In the following years, experiments performed by Conversi, Pancini and Piccioni with an apparatus capable of separating the positive muons from the negative ones, a sort of magnetic lens, established that in the case of iron almost all the negative mesons underwent the capture process, while the decay electrons were emitted only by positive mesons. In the years around 1947–1948 these experiments were extended to various materials used as absorbers, showing that the percentage of negative muons that disappeared by nuclear capture was very small in elements with low atomic

numbers, while it became predominant in elements with high Z, such as reasonably expected, based on the charge of the mesons.

However, it was unclear why, even in light elements (for example carbon), the negative mesons in a certain (small) percentage decayed "normally", that is, without being captured by the nuclei, since the average lifetimes involved were of the order of microseconds, a time enormously greater than that typical of nuclear capture processes.

The conceptual difficulties arising from this experimental evidence were twofold. On the one hand, if muons were the particles predicted by Yukawa's theory, they would have to interact strongly with the nucleons (protons and neutrons) of the nuclei, while this interaction seemed to be weak, since muons could sometimes survive even for microseconds and then decay. On the other hand, if muons—as was still believed—were produced by the interaction of the primary particles of the cosmic radiation, therefore in nuclear processes with an extremely short duration ($10^{-22}$ s), why the inverse process, that is their absorption by the nuclei, did take such a long time?

The answer to these questions came from a series of experiments carried out with another experimental technique, which played an important role in the physics of cosmic rays, that of nuclear emulsions, photographic films capable of recording the passage of an ionizing particle and measuring the ionization density along the track. A more detailed discussion of this technique will be addressed in the next chapter, dedicated to the developments of the different experimental techniques that have contributed to this field of scientific knowledge.

These experiments were performed by the Brazilian physicist Cesare Lattes (1924–2005), by Giuseppe Occhialini, already mentioned, and Cecil Powell (1903–1969), in England, exposing some nuclear emulsions to the flux of cosmic rays in the high mountains. A series of introductory works, published in Nature in 1947, concerned the analysis of the different types of tracks observed, which had already shown evidence of the emission of mesons (understood as particles of intermediate mass between that of the electron and that of the proton). Soon after, a series of data collected on the Bolivian Andes, at 5500 m altitude, made it possible to establish in detail the existence of two different types of mesons, having different mass [Lattes1947a], and the fact that some of these mesons could be produced locally, through a sort of explosive disintegration of the nuclei [Lattes1947b]. Powell received the Nobel Prize in 1950 for the use of photographic techniques in the study of mesons (Fig. 4.7).

The observed tracks were compatible with the hypothesis that a meson of greater mass decayed into a meson of lesser mass, corresponding to the already known muon. The Yukawa particle, the π meson, or pion, was associated with this meson of greater mass. Such π mesons could be produced in abundance in the nuclear interactions of primary high-energy particles with the nuclei of matter. While in the original Yukawa framework these mesons had to decay into electrons, it was seen instead that the π mesons decay into μ mesons, and these in turn into electrons.

Because of their charge, either positive or negative, the same considerations also apply to pions, about the possible capture by the nuclei of negative pions. And in

**Fig. 4.7** Giuseppe Occhialini and Cecil Powell in a conversation on Como Lake. *Source* American Institute of Physics (AIP) Emilio Segrè Visual Archives

fact, for negative pions we do not observe the decay process in matter, but rather an interaction that produces a star of particles, following the disintegration of the nucleus.

If pions are not observed at sea level—or only a very small fraction of them - this means that they decay much faster than muons. The lifetime of pions, as well as their mass, were determined with great precision only later, with the first experiments performed with particle accelerators. As for their mode of decay, since they produce a muon, the conservation laws of energy and momentum allow to establish that another particle, of practically zero mass, should also be emitted in the process, which led to the hypothesis of a photon or a neutrino. The conclusion was that in the decay of the pion, together with the muon, a neutrino was also emitted, as no photon associated with this decay was observable. On the other hand, in the decay of muons into electrons, at least two "invisible" particles had to be emitted, since the energy of the decaying electrons was distributed over a wide range of values. These invisible particles were also neutrinos.

In summary, therefore, the decay patterns of the two types of mesons found in the cosmic radiation could be represented by the following processes:

$$\pi^+ \rightarrow \mu^+ + \upsilon_\mu$$

$$\pi^- \rightarrow \mu^- + \overline{\upsilon_\mu}$$

$$\mu^- \rightarrow e^- + \overline{\upsilon_e} + \upsilon_\mu$$

$$\mu^+ \rightarrow e^+ + \upsilon_e + \overline{\upsilon_\mu}$$

where the symbol $\overline{\upsilon}$ denotes the antineutrino. For the decay of muons, in addition to the electron, a neutrino and an antineutrino are produced. The average life of the charged pions was estimated, from results obtained with particle accelerators, to be about 26 ns.

From the first experiments carried out by means of particle accelerators, at the end of the 1940s, the existence of a neutral meson was also confirmed, which according to the mass could be classified as a $\pi$ meson, and which was produced in abundance in the same nuclear interactions that produced the charged pions. However, the latter decayed mainly into two photons, with an enormously shorter average life, about $10^8$ times shorter than that of charged pions.

Summarizing the situation, at the end of the 1940s, the essential components of the secondary cosmic radiation and the processes that produced these components were substantially defined. This period coincides with the beginning of the use of particle accelerators for the study of nuclear processes, which until that moment had only been investigate in nature through the processes generated by the cosmic radiation.

## 4.4  The Discovery of the Neutron

Starting from 1928 Bothe and Becker had carried out experiments in Berlin, using alpha particles emitted in the radioactive decay of Polonium to bombard samples of various materials (Lithium, Beryllium, Boron, Fluorine) and to observe the consequent production of a strongly penetrating radiation, emitted following this bombardment. They interpreted this phenomenon as due to the emission of gamma rays produced by the capture of alpha particles by these light nuclei, publishing the results in 1930 [Bothe1930b], and also presenting them at the 1931 Congress of Rome, already mentioned several times, where it raised further interest in Irène Curie (1897–1956) and Frédéric Joliot (1900–1958), who did similar experiments, finding that the penetrating power of this radiation was even greater than what Bothe hypothesized [Curie1930, Joliot1931]. Even in this case the radiation was interpreted as an extremely energetic gamma radiation. Subsequently, the same authors observed the emission of protons by hydrogenated materials bombarded by this penetrating radiation [Curie1932a]. However, further measurements showed that the characteristics of this radiation were incompatible with the assumption of gamma radiation [Curie1932b].

Shortly after, at the Cavendish Laboratory the English physicist James Chadwick (1891–1974) (Fig. 4.8) repeated similar experiments, clearly demonstrating [Chadwick1932a, Chadwick1932b] that it could not be a gamma radiation, but rather the emission of particles of unit mass (similar to that of protons) and zero charge,
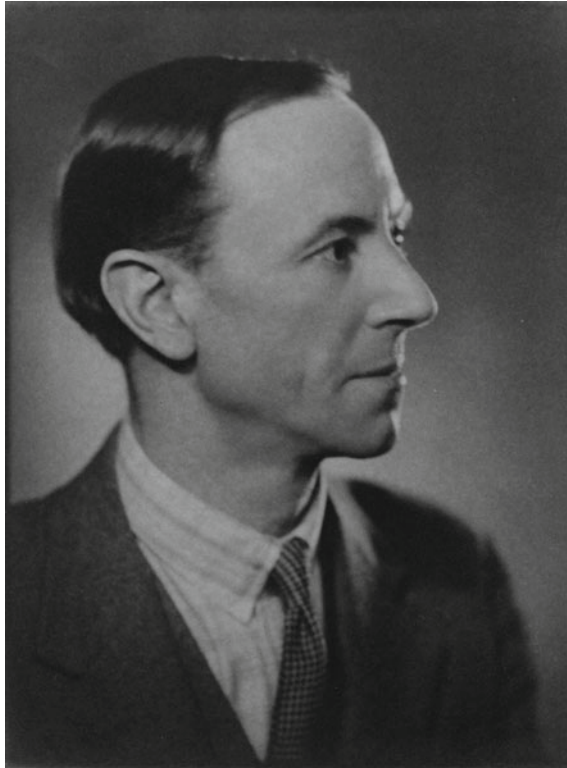
**Fig. 4.8** James Chadwick (1891–1974). Source: AIP Emilio Segre Visual Archives, W. F. Meggers Gallery of Nobel Laureates Collection

what could be indicated with a neutron. The same Joliot and Curie, after an initial skepticism, soon agreed with this hypothesis [Curie1932c].

Although Bothe, as well as Curie and Joliot, were not aware of the possible observation of a new particle, of zero charge, on the contrary this observation was within the expectations of other researchers. Chadwick in particular, following ideas already expressed previously by Rutherford, was strongly convinced of the possible existence of such a particle.

As it is well known, the discovery of the neutron contributed to rewriting much of the nuclear physics known at that time, from the internal structure of nuclei to beta decay phenomena. In this context we shall not deal with the consequences that the introduction of the neutron brought to nuclear physics, which are adequately dealt with in Nuclear Physics textbooks or in historical articles on the subject [Nesvizhevsky2017]. Let's just remember that while the proton appears to be stable, with a lower limit on its mean life enormously greater than the age of the universe, the neutron, on the other hand, is subject to decay, with an average life that was measured starting from 1948, but which is still the object of precision measurements, with a

recent estimate of (879.4 ± 0.6) s [PDG]. This value implies that neutrons cannot constitute a component of the primary radiation in the case of distant sources, since they would decay quickly compared to the time needed to travel distances between two close stellar systems. However, high-energy neutrons could in principle come to Earth from distances comparable to the size of the Solar System. For example, neutrons of the order of GeV would have free average paths of some astronomical units (Sun-Earth distance) and correspondingly greater for neutrons of higher energy. We will see later that neutrons also represent an important component of the cosmic radiation present in the atmosphere.

# Chapter 5
# Developments of the Techniques for the Detection of Cosmic Rays

**Abstract** This chapter is devoted to a review of the different techniques which were employed for the observation of the cosmic radiation. After the improvement and use of the electroscopes, even by means of automated systems of recording, strong developments in the observation techniques came both from Wilson cloud chambers, producing visual evidence of the passage of tracks, and from detectors based on single-event counting, allowing to observe the passage of even a single ionizing particle. Ionization chambers, proportional counters and Geiger-Muller counters played a leading role in this respect, pushing the study of the cosmic radiation to an unprecedented level of accuracy and allowing for new class of experiments, such as those provided by the coincidence technique, widely employed after its introduction at the end of 1920s. Nuclear emulsions and the early detectors based on scintillating materials also contributed to the technical developments of particle detectors. All these techniques are here discussed with ample references to the original papers which marked the history of such detectors.

## 5.1  Introduction

From the first evidence of the existence of cosmic radiation, in the first decade of the 1900s, up to the 1940s, the detection of high-energy particles found in the secondary cosmic radiation made use of different experimental techniques, mostly based on the phenomenon of ionization that charged particles produce by collision mechanisms.

In this Chapter we will briefly summarize the techniques mainly used in those decades, as they emerge from reading the original articles and results of the period. An important aspect to keep in mind when discussing the working principles and the overall performance of these detectors is their sensitivity, i.e., the capability to signal even a small number of ions produced in their volume in a certain time interval and therefore detect even the arrival of a few ionizing particles. From this point of view, a basic feature is related to the possibility of detecting individual events, that is, events due to the passage of a single particle, rather than the total number of particles arriving on the detector in a given time interval. While the first measuring devices were essentially detectors that integrated the flux of incoming particles over

long intervals of time, the use of the first "counters" made it possible to identify and count individual events, paving the way for the possibility of operating several counters in coincidence and therefore of highlighting also qualitatively new physical phenomena.

## 5.2   From Wulf's Electroscopes to Automatic Recording Equipment

As we discussed in Chap. 1, reporting the first observations of the cosmic radiation, most of the measurements carried out at the beginning of cosmic ray physics mostly involved the use of electroscopes, instruments capable of signalling the ionization of air, which in turn produced the discharge of the device.

As already mentioned, the simplest version of an electroscope consists of two thin metal sheets, electrically connected to an external conductor. The charge initially transferred, which causes the plates to diverge, is not maintained, but after some time it is neutralized, following the ionization phenomena in the air, caused inside the instrument by the passage of the ionizing radiation.

We have already seen how many experimenters in that period contributed to significant improvements to the basic idea of the electroscope, starting with Wulf, who replaced the original thin leaves with two metallized quartz fibres, placed in tension. The divergence of the fibres could be observed with greater precision using a small microscope. These were the electroscopes that Wulf brought with him during the well-known measurements at the top of the Eiffel Tower.

Further improvements were made by Kolhörster [Fick2014], to make the electroscopes used by Wulf (or rather the electrometers, since they allowed quantitative measurements) more suitable for balloon flights at high altitudes. In collaboration with the company Günther & Tegetmeier, a new design of these instruments had been introduced, with thicker walls, in order to withstand pressure differences of over 650 mbar (500 torr), expected at altitudes close to 9000 m. The mechanical assembly of the fibres and the microscope had been made less sensitive to changes in temperature, but, above all, the sensitivity of the instrument had been increased by reducing the electrostatic capacity. This last condition made it possible to take readings of the positions of the wires every minute, so that the reading was associated with a more precise altitude. On the contrary, Hess's previous measurements only allowed integrated measurements over an interval of 30 min, a time interval during which the altitude reached by the balloon changed considerably.

Climbing to such high altitudes to make measurements required considerable efforts and a dose of courage on the part of the experimenters. Already at that time the opportunity had been considered to equip the measuring instruments with automatic recording systems, which would allow the launch of unmanned balloons, to reach altitudes prohibitive for human crews.

Apart from rare exceptions, the possibility of using some automatic equipment made generally use of a setup including multiple balloons, which—once reached a certain altitude—had to return to the ground, by exploding one of the balloons. This solution proved to be competitive compared to the use of human crews. We have already mentioned previously that at the beginning of the 1930s manned flights at very high altitudes were carried out by Piccard [Piccard1932] up to 16 km above sea level, using a hermetically sealed cabin. However, during the first of these flights the crew ran into serious danger due to loss of cabin pressurization.

We know that Millikan and the group of US physicists were among the first, as early as 1926, to install recording equipment on board during scientific expeditions employing balloons [Millikan1926a], through photographs taken at intervals, which took up the reading of the electrometer and the altimeter. Figure 5.1 shows the structure of one of these devices used by Millikan in the first balloon flights [Millikan1926b]. The electroscope employed two quartz fibres, similar to those used in Wulf's electroscopes, which were charged by a 300 V battery.

Figure 5.2 shows a photo of this early instrument [Millikan1926b]. The sky light entering from aperture $S_1$ (a thin vertical collimator) produced a shadow on photographic film, through the aperture $S_2$. A second photographic film could record the reading of a thermometer and a barometer.



**Fig. 5.1** Sketch of the electroscope used by Millikan on the occasion of the first balloon flights with automatic recording of the measurements [Millikan1926b]. Figure reproduced from the work of R. A. Millikan and R. M. Otis, *High frequency rays of cosmic origin. II. Mountain peak and airplane observations*, Physical Review **27**(1926)645. Copyright (1926) by the American Physical Society, License No. RNP/22/MAY/053658
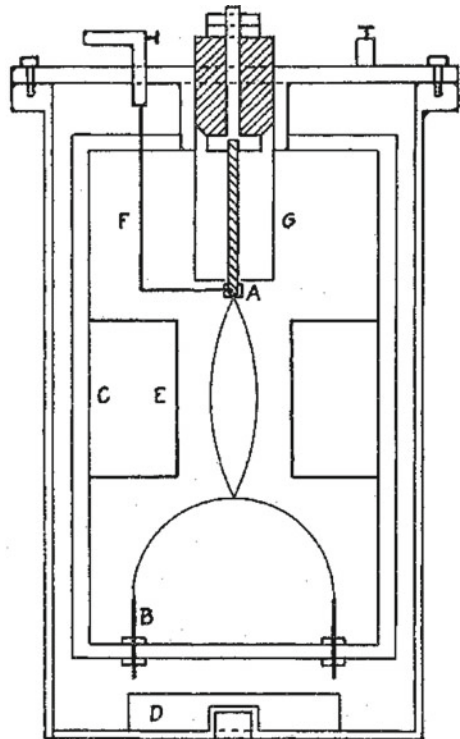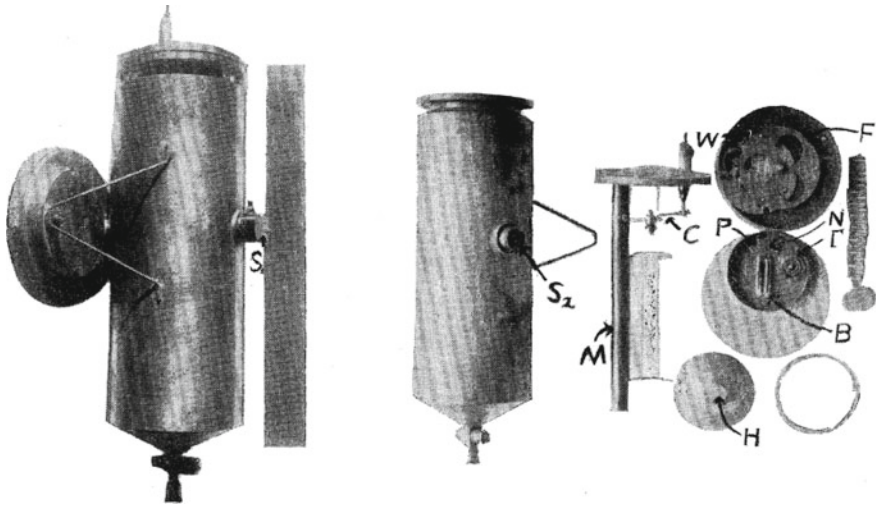
**Fig. 5.2** One of the electrometers with an automated reading system using photographic film, used by Millikan during the first measurements aboard of balloons in the second half of the 1920s [Millikan1926a]. Figure reproduced from the work of R. A. Millikan and I. S. Bowen, *High frequency rays of cosmic origin. Sounding balloon observations at extreme altitudes*, Physical Review **27**(1926)353. Copyright (1926) by the American Physical Society, License No. RNP/22/MAY/053657

These are among the first data loggers in history, perhaps together with the early chart recorders for environmental monitoring in use since the early 1900s: small devices capable of periodically monitoring the values of physical quantities in an automated way, for subsequent analysis. While the pioneering flights of Hess and Kolhörster suffer from a certain *artisan* approach, the American spirit was probably not foreign to this new approach, which enters the contest by bringing substantial innovations to the measurement procedures and designing the conditions in an almost *industrial* way. The electroscopes provided with recording devices, developed on the recommendation of Millikan, were in fact small jewels, having a mass of about 300 g, and therefore only required small balloons. Each electroscope was carried by two balloons, filled with hydrogen and having a diameter of about one meter. The purpose of the second balloon is to allow the instrumentation to return to the ground after the destruction of the other balloon, and also to signal the presence of the object to those who will find the instrumentation, with indications for its recovery. In fact, of the four devices used during one of the first flights, three will be recovered and two of them correctly recorded the data, reaching altitudes of 11.2 and 15.5 km, after moving to a distance of about 130 km.

For the measurements carried out in the high mountains, or under a certain depth of water, Millikan used different models of electrometers, whose construction details and method of operation are described in one of his works from 1926 [Millikan1926b].

**Fig. 5.3** Electrical circuit for the use of the electrometers employed by Millikan [Millikan1926b]. Figure reproduced from the work of R. A. Millikan and R. M. Otis, *High frequency rays of cosmic origin. II. Mountain peak and airplane observations*, Physical Review **27**(1926)645. Copyright (1926) by the American Physical Society, License No. RNP/22/MAY/053658
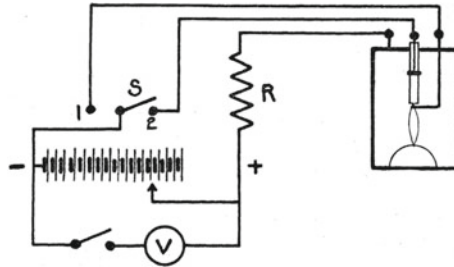
The way to operate an electrometer for quantitative measurements is to charge the electrometer with an external voltage source of known value and measure the change in the potential as a function of time as the electrometer discharges. With reference to Fig. 5.3, which describes the circuit used for these devices, the switches allow to apply a voltage to the fibres and, after a calibration phase, to read the values of the voltage over time. From these data, knowing the electrostatic capacity C and the volume $V_{air}$ of air contained in the instrument, the number $N$ of ions produced per unit of volume per second can be estimated by the relation

$$N = C \frac{\Delta V}{e \, \Delta t \, V_{air}}$$

where $\Delta V / \Delta t$ is the change in potential, expressed in Volts per second, and $e$ represents the electron charge.

In the case of measurements carried out under a certain depth of water, the electrometers were immersed appropriately protected, left under water for a long time (a few hours) and then recovered to be read, obtaining in this case only a few readings as a function of time, which is not particularly critical, since in this case it was necessary to measure what happened at a fixed depth, and not at a rapidly variable altitude with time.

Electrometers with automated reading by means of photographic film recordings were also used in more recent times by Millikan, for example for the geographic survey carried out in various parts of the world in 1936 [Millikan1936].

High altitude measurements with automated electrometers, up to 28 km of altitude (pressure of 22 mm of Mercury), were also reported in 1932–1933 by Regener [Regener1932a, Regener1932b, Regener1932c, Regener1933], with instruments whose reading was photographed at intervals of a few minutes.

## 5.3  Ionization Chambers

Devices that were widely used in Compton's measurement campaigns in the early 1930s, for example in expeditions to various parts of the world to study the dependence of ionization on geomagnetic latitude, were the ionization chambers filled with high pressure Argon. They are essentially instruments that integrate the flux of the detected ionizing particles, as they measure the total number of ion pairs created in a certain time interval within the volume of gas.

A description of such apparatus is reported for example in [Compton1933]. The following figure shows a sketch of the apparatus. It should be noted that in those years the Geiger counters already existed (see next section), but Compton believed that for this measurement campaign the ionization chambers were preferable, because of their greater reproducibility and lower statistical error.

Filling them with high-pressure Ar produced a high ionization, which was measured using an electrometer. The ions produced in the chamber were collected by a steel electrode that conducted the current to the electrometer needle. Spherical bronze and lead shells shielded the instrument from local gamma radiation, reducing it to about 5% of the ionization due to cosmic radiation. In order to calibrate the instrument, the readings were each time compared with ionization measurements produced by a radioactive radium capsule (Fig. 5.4).

Ionization chambers filled with high pressure gas were also used by Montgomery and collaborators in 1936 [Montgomery1936], using Nitrogen at a pressure of about 15 atmospheres. The chamber used in some experiments was segmented into two independent parts, each connected to an electrometer with automatic recording and operating in connection with Geiger counters whose reading was also recorded.

In general, in an ionization chamber there are two electrodes separated by a dielectric (the filling gas) and held at a certain potential difference. The electric field generated by the potential difference causes the ions to move along the lines of force of the field, following a motion that overlaps the random thermal motion. The average speed due to random motion is generally greater than the drift speed, due to the presence of the electric field. The ions, once formed in the gas, can not only diffuse, because of the thermal motion, or migrate with the electric field, but also recombine with particles of opposite sign before they can be collected at the electrodes. If the electric field reaches an adequately high value, most of the charges produced by ionization can be collected on the electrodes, and the measured current will be proportional to the total number of ion pairs produced.

How to read this current? If it were very high, it could be read by a galvanometer. However, in most of the measurements related to the detection of cosmic radiation, this very low current was read by electrometers. The variation over time of this potential difference could give a measure of the current, and therefore of the total number of ions formed, through the relation

$$I = C\frac{dV}{dt}$$

**Fig. 5.4** Ar-filled high
pressure ionization chamber,
used by Compton during the
measurement campaigns at
the various geomagnetic
latitudes [Compton1933].
Figure reproduced from the
work of A. H. Compton, *A
geographic study of cosmic
rays*, Physical Review
**43**(1933)387. Copyright
(1933) by the American
Physical Society, License
No. RNP/22/MAY/053659
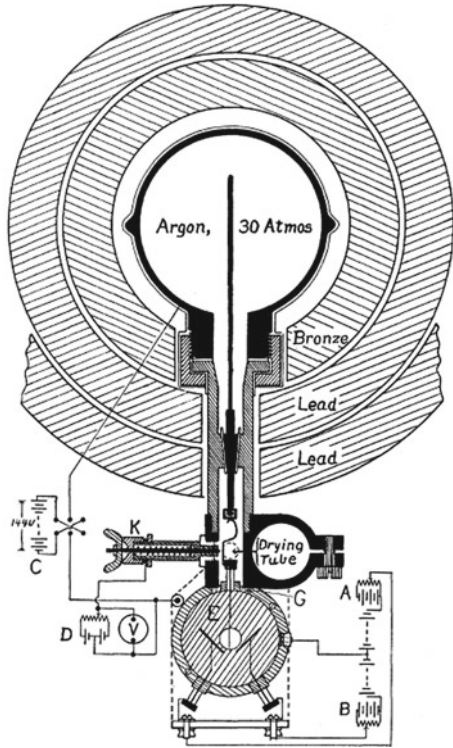


where C represents the capacity of the instrument. The integration time is given in this case by the subsequent time interval between two readings.

Of course, an ionization chamber can also be used to detect the passage of a single ionizing particle. However, it must be considered that in this case the voltage pulse that can be obtained at the electrodes is very small and requires an appropriate amplification system. Typically, for energies of some MeV, such as those deposited by particles emitted by a radioactive source, or by the passage of secondary cosmic radiation, the voltage pulses—for geometries typical of these chambers—are of the order of mV, therefore they certainly need to be amplified, which became possible in the following years with the progressive development of low-noise electronics.

Gas detectors based on ionization allow, by means of an appropriate choice of the electric field (in turn dependent on the geometry of the electrodes and the voltage applied to them), to choose an appropriate working point for the detector, also called operational regime. At relatively low voltage, the number of ion pairs produced by ionization may not be measured correctly, because the fraction of ions that will undergo recombination processes in the gas is still high. As the applied voltage is increased, the number of ions collected at the electrodes increases, until it saturates, a condition in which ideally all the ions are collected, and this number represents a measure of the total ionization produced in the integration interval. In case it is

possible to detect the passage of a single particle, the number of ions produced will give an estimate of the energy deposited by the particle in the sensitive volume, taking into account the average energy to produce a positive electron–ion pair in a gas, a few tens eV.

It is known that ionization-based gas detectors can operate in different regimes, depending on the electric field applied to the electrodes and the working pressure existing inside the detector. For a detailed description of the operation of gas detectors, reference can be made to one of the many modern textbooks existing in the literature [Leo1987, Knoll2000, Leroy2004, Grupen2008].

The different regimes are generally illustrated with reference to a qualitative plot which shows the number of ions produced as a function of the bias voltage, for a constant pressure (Fig. 5.5). The vertical scale is logarithmic, which implies a huge increase in the number of ions in passing from one regime to the next.

For low supply voltages (left part of the plot) the electric field is not sufficient to collect all the charges produced by primary ionization, which are partially recombined. The fraction of charges collected increases as the working voltage increases, until a first "plateau" is reached, where the number of charges collected does not increase further, even if the voltage is increased. This regime corresponds to the complete collection of the charges produced by primary ionization. Ionization chambers operate in this regime and produce, if used to detect single events, very low voltage pulses.
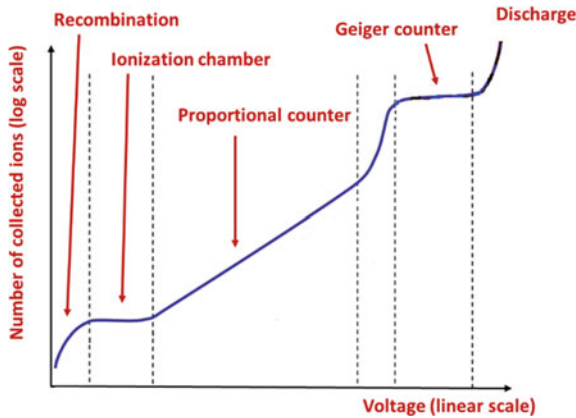


**Fig. 5.5** Operating regimes for a detector based on the ionization in a gas. The plot shows the number of ions collected (in logarithmic scale) as a function of the power supply voltage applied (at constant gas pressure). The two "plateau" (where the number of ions collected does not increase further, even by increasing the voltage) correspond to the operating modes of an ionization chamber and of a Geiger counter respectively

## 5.4  Proportional Counters

Since single particles, especially those with low ionizing power, produce a limited quantity of ions and the corresponding amplitude of the voltage pulse would be too small to be detected without adequate amplification, one of the possible strategies is to exploit the phenomenon of secondary ionization, according to which the number of ions initially produced by direct ionization can be multiplied, even by a very high factor, hundreds of times. The strategy is to use a cylindrical geometry and a much stronger electric field in a specific region of the sensitive volume. The cylindrical geometry makes use of a cylinder-shaped electrode, of radius $b$ (typically a few cm), and of a central wire, of radius $a$, stretched along the axis of the cylinder and of very small size. A potential difference $V$ is applied between the two electrodes, with the central wire at positive potential. Under these conditions the electric field has a radial symmetry, i.e., its value depends on the modulus of the distance $r$ with respect to the cylinder axis, and takes on a value given by

$$E = \frac{V}{r \ \log \frac{b}{a}}$$

The electric field is therefore very intense near the wire, and the electrons can be accelerated in that region until they take on an energy that is capable of ionizing in turn other atoms or molecules of the gas, multiplying the number of electrons initially produced. In the ionization process, photons are also emitted, which in turn can produce additional electrons. It can be shown that the total number of electrons reaching the central electrode is given by the series

$$n + \gamma n^2 + \gamma^2 n^3 + \cdots$$

where $n$ is the number of electrons produced initially and $\gamma$ is the proportionality constant. If the term $\gamma\, n < 1$, the series converges to a value given by

$$M = \frac{n}{1 - \gamma n}$$

which leads to a number of electrons $M$ approximately proportional to the number of electrons initially produced. Such are the conditions for the detectors usually called proportional counters. With reference to Fig. 5.5, the central area of the plot shows a trend in which the collected charge increases with the applied voltage, as $n$ increases with the voltage. Furthermore, different particles, having different ionizing power, would produce a different initial number of electrons and to some extent the total number of electrons produced could be used to distinguish the different detected particles. Proportional counters are capable of producing higher voltage pulses, which can be recorded with an appropriate electronic system, generally preceded by a further amplification of the signal. Proportional counters were used in subsequent years, for

example from the late 1940s, for various applications concerning radioactivity and the detection of cosmic rays.

## 5.5   Wilson Cloud Chamber

The cloud chamber is inextricably linked to the name of the Scottish physicist Charles Thomas Rees Wilson, already mentioned. Having first studied zoology and later physics, Wilson had received a temporary position as a meteorological observer in 1894. Impressed by the observation of numerous atmospheric phenomena, including cloud formation, Wilson realized that the ions existing within the gas could act as centres for the formation of water droplets.

It had already been established that solid particles (e.g. dust) could act as centres of condensation. Wilson, building his first cloud chambers at Cambridge, realized that dust grains were not necessary for condensation, as long as there was rapid expansion with a volume ratio, $V_1/V_2$, greater than a certain value. The first prototypes of these devices, built in glass, were very fragile, but after numerous attempts, Wilson was able, through a very rapid expansion, 1/100 of a second, to visualize some of the classic atmospheric phenomena. All this took place in 1895, and initially had no direct connection with the possibility of detecting the passage of particles contained in the cosmic radiation. But already in 1896, with the arrival in Cambridge of Rutherford and Townsend, and with the discovery of the phenomena of radioactivity and X-rays, it became clear that these devices could visualize phenomena produced by an ionizing radiation. At the beginning of 1896 X-rays sent on Wilson's devices were able to produce a dense mist, establishing the correlation between the condensation nuclei in the gas and the ions created by the ionization source. The formation of these droplets was due to the fact that the water vapor was supersaturated. The following years saw a number of detailed measures to assess the conditions under which droplet formation took place. It was established that for values of the expansion ratio below a certain limit the condensation centres were the negative charges; increasing the compression ratio the positive ions came into play, and finally the air molecules. It should be noted that this technique led to a first estimate of the electron charge by Thomson, evaluated as 2.2 $10^{-19}$ C. Millikan, as it is known, subsequently used the oil droplets to measure a more precise value of the electron charge.

Already in 1901, on the basis of measurements performed with his device also in underground tunnels, Wilson understood that the production of ions could be due to some external source of radiation [Wilson1901a, Wilson1901b]. It was only in 1910 that Wilson returned to dealing with these devices, after having investigated various problems related to atmospheric electricity, with the idea that they could be a tool for visualizing the passage of ionizing particles.

In 1910, Wilson's device already allowed to synchronize the expansion of the gas volume with the emission of the X-rays to be observed and with the lighting device to obtain the photograph [Wilson1912]. Figure 5.6 shows Wilson's original chamber

at the Cavendish Laboratory Museum. Finally, in 1911 Wilson was able to obtain the first detailed images of the passage of electrons and alpha particles (Fig. 5.7).

Subsequently, these chambers were used to visualize a remarkable variety of physical processes, including the observation of the positron, by Anderson, phenomena



**Fig. 5.6** Improved version of Wilson's chamber, 1911, exhibited at the Cavendish Museum. According to what Wilson himself reported, no other specimens of this chamber were built. *Source* Wikimedia Commons, Creative Commons Attribution-Share Alike 4.0 International License

**Fig. 5.7** Tracks of alpha particles, obtained in an expansion cloud chamber. Reproduced with permission from the Royal Society from C. T. R. Wilson, *On an expansion apparatus for making visible the tracks of ionising particles in gases and some results obtained by its use*, Proceedings of the Royal Society, London A **87**(1912)277
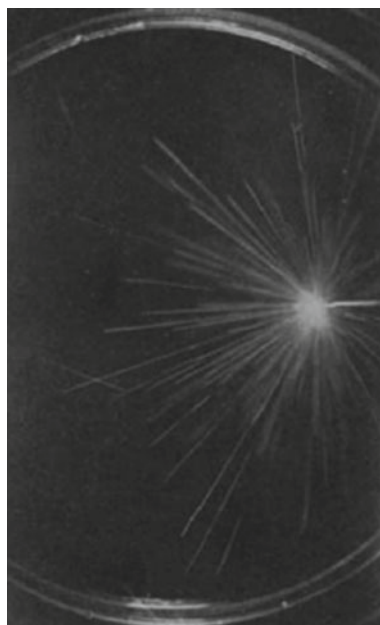
related to cosmic radiation, such as the passage of muons and their decay, the production of pairs, the production of showers, and, later, the observation of new particles, such as V0 or hyperons. In 1929, as we discussed, Skobeltsyn observed for the first time, by means of a Wilson chamber, tracks due to energetic particles in the cosmic radiation.

As we know, Wilson received the Nobel Prize in 1927, together with Compton, for having made it possible to observe the trajectories of charged particles through the condensation of vapor. A detailed historical analysis of the introduction of the cloud chamber in the 1930s has been reported, among others, by Leone [Leone2011].

Today, the use of small, manually operated, cloud chambers is an interesting educational tool for observing the tracks of particles emitted by radioactive preparations or particles of the cosmic radiation.

Demonstrative small cloud chambers, mainly for educational use, are available on the market at affordable prices from the major suppliers of teaching equipment for the study of physics. They can be of the expansion type, in which a compression and subsequent expansion performed manually on a small volume leads to a super-saturation of the mixture, making the passage of any tracks visible for a few seconds. Other models, for longer observations, are of the cold plate type, to be cooled by dry ice, or by Peltier cells, and make use of pure isopropyl alcohol. Once cooled, they allow observations of the tracks for several hours. Today it is also possible to build and operate this type of cloud chambers, according to the layout shown in Fig. 5.8. Many articles or educational sites report similar examples [Barradas2010, ESPER].
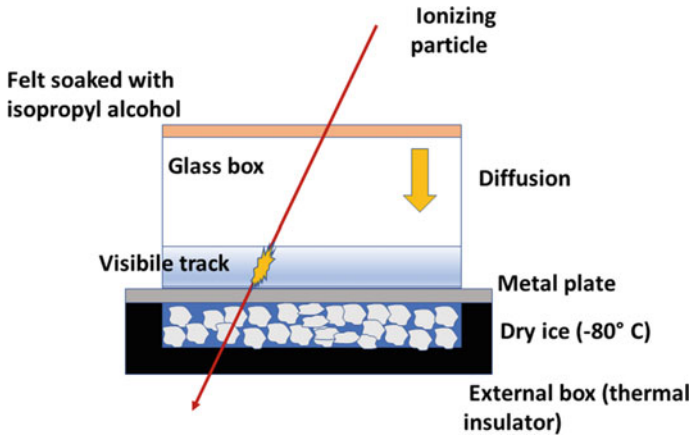


**Fig. 5.8** Operation diagram of a cloud chamber built for educational applications, based on the use of dry ice and isopropyl alcohol

## 5.6  Geiger-Müller Counters

If in a proportional counter with cylindrical geometry, such as those described above, the voltage difference between the central electrode and the outer cylinder is further increased, the number of electrons produced becomes greater than the number of initial electrons ($\gamma$ $n$ > 1). In this case, the mathematical series mentioned when discussing proportional counters, which estimates the total number of electrons produced for each primary pair, diverges. From a physical point of view there would be then a discharge. However, if the product $\gamma$ $n$ is not much greater than 1, the discharge fails to self-sustain, so it is extinguished after each single event. The counter is therefore capable of detecting every single ionizing particle that passes through it. It is in this regime, with reference to Fig. 5.5, that the Geiger-Müller counters work.

Geiger-Müller counters operate in correspondence to a second plateau, in which the increase in the supply voltage to a first approximation does not produce a further increase in the charges. In fact, this is not a strict plateau, as a few percent increase in charge can still be observed in this region. Geiger-Müller counters are characterized by a very high output voltage pulse, of the order of volts, and the amplitude of this pulse is independent of the primary charge. These detectors are therefore not able to distinguish between different ionizing particles or to evaluate the energy deposited in the sensitive volume.

Although the first counter prototypes had been developed by Hans Geiger (1889–1945) as early as 1908, under the supervision of Rutherford [Rutherford1908], to detect alpha particles, it was only in 1928 that Geiger and Walter Müller (1905–1979) made this type of counter usable also for the detection of electrons and gammas [Geiger1928a, Geiger1928b, Geiger1929a, Geiger1929b], in the form of a compact, robust, small size and low cost instrument.

The Geiger-Müller counter probably represents one of the best known tools, not only in the scientific field but also in a broader context, so much so that it was defined by Einstein as "The most sensitive organ of humanity" in addressing to Geiger in one of his letters. The history of the introduction of this type of detector and the significance it had in the field of experimental physics have been the subject of numerous historical and educational articles [Korff2013]. It represented one of the first examples of detectors capable of signalling the arrival of both alpha particles, electrons and gammas, as well as the muons from the cosmic radiation.

A Geiger-Müller counter essentially consists of a conducting cylindrical tube, which acts as a cathode and a thin wire, also conductor, arranged along the axis of the cylinder, which acts as an anode. The tube contains a suitable gas (Argon, …) or a gas mixture, in the most recent versions. Typical Geiger-Müller counters have diameters of a few centimetres and lengths of 5–10 cm, but they could also reach up to one meter in the larger models. Depending on the type of application, they can be equipped at one end with a thin entrance window, made of mica, which also allows the entry of alpha particles or low-energy electrons, which would otherwise be stopped in the constituent metal layer of the cylinder.

**Fig. 5.9** Basic circuit for powering and taking a signal from a Geiger counter
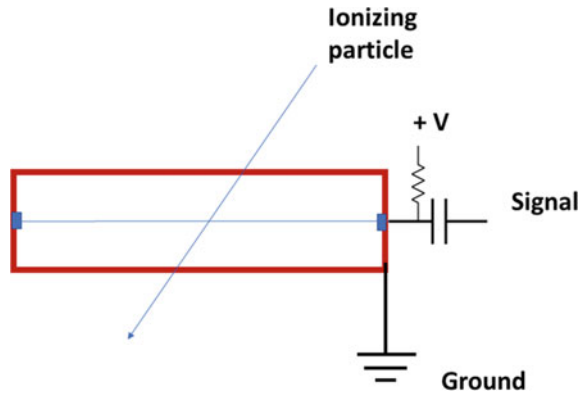
The basic power supply and signal pick-up circuit is sketched in Fig. 5.9. The central wire is connected to a positive potential + V by means of a high value resistor. The variation of the voltage produced by the collected charges is taken through a capacitor. Because of the cylindrical geometry of the electrodes, the electric field has a radial symmetry, as described for the proportional counter, and depends on the diameter of the external cylinder and that of the central wire which acts as anode. Typical potential differences of several hundred volts are applied between the two electrodes, depending on the size of the counter.

In the case of cosmic ray detection, due to the very high energies involved, the thickness of the outer cylinder does not have much influence on muons or high-energy electrons, which therefore can be detected without any problem. As for the gammas, they can be detected, albeit with a low probability (a few percent), since when interacting with the material constituting the outer cylinder (usually a metal with a high atomic number) they can produce electrons, which in turn interact in the fill gas, producing ionization. The detection efficiency is close to 100% for all the ionizing particles that are able to penetrate, directly or indirectly, into the internal gas volume. Figure 5.10 shows an example of a typical Geiger counter for educational activities.

In the first applications of Geiger-Müller counters, during the 1930s, various signal reading circuits were used, using vacuum tubes as amplifier circuits and various systems for counting the pulses [Curtiss1928, Libby1932].

After the first years of their discovery and their use in scientific research, Geiger counters were also successful as a tool also available to the general public. It is amazing to find how the diffusion of "kits" with numerous versions of Geiger counters, sold in particular in the US market from the 1940s to the 1960s [NRIC], was really impressive.

Geiger-Müller counters are now easily available on the market, also in a version accessible to the general public or for educational applications and constitute one of the most interesting tools for carrying out a variety of experiments and activities concerning the study of cosmic rays [Famoso2005, Blanco2006a, Blanco2006b, Blanco2008a, Blanco2008b, Blanco2009, Goldader2010, Maghrabi2021].

**Fig. 5.10** An educational Geiger counter (Photo by the author, from the collection of the Department of Physics and Astronomy of Catania)

In today's versions, the voltage difference is generally produced by a special electronic elevator circuit, which, starting from a voltage of a few volts, supplied by a battery, produces the required high voltage. These counters often contain also the electronics capable of providing a standard logic pulse at the output, for example of the TTL type (a transition from zero to a positive signal of 3–5 V), with a typical duration of about a hundred microseconds, and to signal the arrival of each particle by turning on an LED or producing a sound beep.

## 5.7  Electronics and Coincidence Techniques

The use of counters to detect the passage of ionizing radiations, especially the Geiger-Müller counters, opened the way to the possibility of operating two or more of these detectors "in coincidence", that is to signal the "simultaneous" passage of the same particle, or of two different particles, in the two counters. This possibility really represented a qualitative, as well as quantitative, novelty in the detection of particles, because it provided the possibility of highlighting new phenomena in cosmic ray physics, not observable by the use of a single counter. The coincidence technique, as it was named since its beginning, represents today a standard way for the selection of physical events of interest, not only in cosmic ray physics, but in general whenever

particles or ionizing radiation are detected in modern physics experiments, from astronomy to solid state physics.

The invention of the "coincidence" technique, that is the possibility of observing "simultaneous" phenomena in different detectors, dates back to 1924, when Bothe, in the context of the study of the Compton effect, developed a system to evaluate whether the scattered photon and the recoil electron detected in two different detectors were the result of a single physical process (with conservation of energy and impulse in the single event) or of a simple statistical correlation (with conservation of energy and impulse averaged over many events). As described by Bothe on the occasion of the Nobel Prize [Bothe1954], the prototype for reading each of the two detectors was done at first by recording with a writing needle on a moving paper roll, with consequent photographic recording. The analysis of the two rollers made it possible to establish, within a time interval of $10^{-4}$ s, that the two phenomena were simultaneous and that therefore it was a single physical process. The technique, according to Bothe himself, was rather rudimentary, and the consumption of film so high that the laboratory where the film was placed to dry resembled an "industrial laundry". The same technique had also been used in 1926, on the occasion of another experiment on the distribution of radiation, once again to establish whether the processes in which photons interacted were single processes.

It was in 1929 that this technique was used, by Bothe and Kolhöster, with Geiger counters, for the simultaneous detection of the passage of particles in different counters. A historical analysis of the valence and significance of the introduction of coincidence circuits in cosmic ray physics has been discussed by several authors [Pfotzer 1982, Bonolis2011b].

As an example, imagine having two cylindrical Geiger counters, represented as in Fig. 5.11, and placed with their parallel axes, at a certain distance vertically on each other. It is clear that each of these counters can be crossed by particles from the cosmic radiation (tracks A, B), but there will be tracks capable of crossing both counters if they come from certain directions (tracks C, D). If it were possible to select only those tracks that cross the two counters, this would automatically entail a selection of the incoming directions, within a certain angular interval defined by the dimensions of the counters and by their relative distance. In the configuration drawn in the figure, for example, the tracks that correspond to the passage of the particles in both counters are tracks with an orientation close to the vertical direction. The potential of this method is then clear, to select events in which the direction of the track is defined, even though within certain geometrical limits.

In fact, the first uses of coincident counters refer to experiments, such as those performed by Bothe and Kolhöster [Bothe1929a], in which it was useful to define the average direction of the particles, in order to select only those that had crossed a given thickness of interposed material between the two counters.

The technology for observing signals in coincidence was soon improved, and as early as 1930, instead of photographic recording, the first electronic circuits, based on vacuum tubes, coupled to mechanical recording systems, had been used. Bothe himself used one of these circuits, which made use of a vacuum tube with
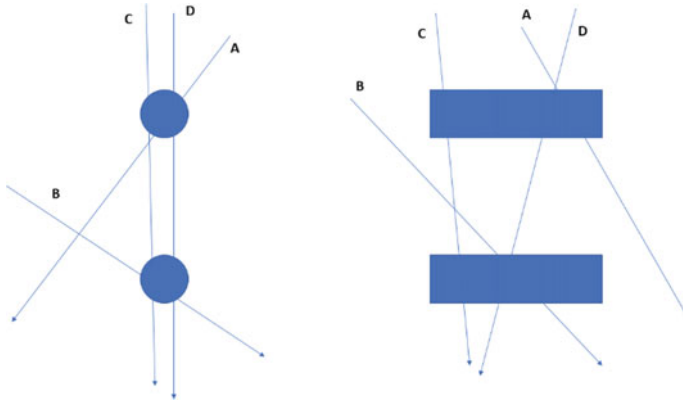
**Fig. 5.11** Geometric arrangement of two Geiger counters placed vertically, with parallel axes, seen on two orthogonal planes. Tracks A and B cross only one of the two counters, while tracks C and D cross both of them

multiple grids, to establish the coincidence between two detectors, improving the time resolution and therefore reducing the number of spurious or "random" coincidences.

The evaluation of possible random coincidences in a coincidence experiment is always an important aspect, in determining whether the number of events classified as "coincident" is partially or totally influenced by the possible occurrence of independent events within the same time window. This assessment can be made and is indeed reported in the same work by Bothe and Kolhöster of 1929 [Bothe1929a]. According to this evaluation, the rate $R_s$ of spurious coincidences (number of spurious coincidences per unit of time) is given by

$$R_s = 2 \, R_1 \, R_2 \Delta t$$

where $R_1$, $R_2$ are the counting rates of the two detectors individually and $\Delta t$ is the time coincidence window, i.e., the time interval within which the simultaneous arrival of the two signals can be evaluated. With the same counting rate of the two detectors ($R_1$, $R_2$), the rate of spurious coincidences can be decreased, therefore, by proportionally reducing the time coincidence window $\Delta t$, provided that possible events of interest are not lost (Fig. 5.12).

Electronic circuits based on the use of vacuum tubes were further improved by Bruno Rossi [Rossi1930a], and we can say that their principle is basically still used today. In the vacuum tube version used by Rossi, two or more triodes are used, which have the plate connected in common, while the grid of each triode receives, through a capacitive coupling, the signal from the Geiger counter. Only when the grid of each triode is simultaneously brought to a negative potential by the discharge of the corresponding Geiger counter, an output signal will be obtained. The advantage of Rossi's coincidence circuit is that this technique can also be used in the case
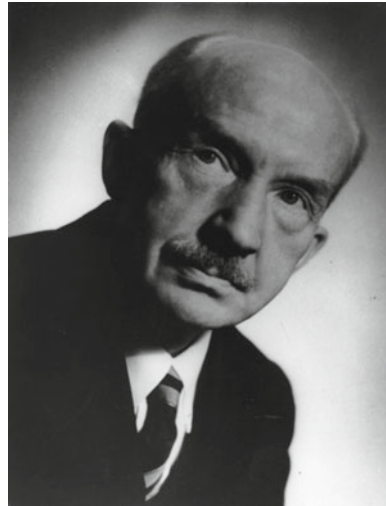
of multiple coincidences between more than two counters, while Bothe's use of a double-grid triode limited the possibility of coincidence to only two detectors.

In Rossi's coincidence circuit (Fig. 5.13) the output signal was initially detected by listening to the produced sound signal with a headset, which is impractical for long measurements. Subsequently, a galvanometer was used, the deviation of which was photographed, and later, a mechanical recorder capable of "counting" the coincidence events. It was with this instrumentation that Rossi contributed to the study and understanding of numerous aspects of the cosmic radiation, partly already described in the previous chapters.

We will later see another example of the use of coincidence circuits, this time not to signal the passage of the same particle through two distinct counters, but to detect the simultaneous arrival of different particles in detectors placed at a certain distance.

In the following years, with the development of nuclear physics and the first experiments carried out with particle accelerators, the use of coincidence circuits also became a common practice in nuclear and particle physics. As recalled by

**Fig. 5.13** Principle of
operation of Rossi's
coincidence circuit, based on
the use of two or more
triodes connected with the
common plate and with the
Geiger counters connected to
the grids of each triode
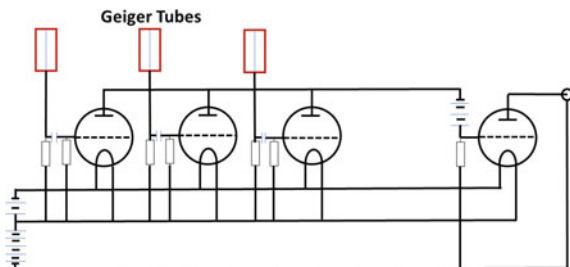
Bothe during his Nobel Lecture, "Many applications of the coincidence method will therefore be found in the large field of nuclear physics, and we can say without exaggeration that the method is one of the essential tools of the modern nuclear physicist" [Bothe1954].

The treatment of particle detector signals is today dominated by electronics and microelectronics. Referring to the history of cosmic ray physics, up to the Second World War, it is worth remembering that the first vacuum diodes were made by Fleming as early as 1897, and that the first triodes, tubes equipped with a grid, in addition to the cathode (filament) and to the anode, and used as the first amplifiers, were made in 1906 by De Forest, and used about ten years later, as common elements for radio sets.

## 5.8   Nuclear Emulsions

We also want to mention here another visual method for the detection of ionizing particles, which played an important role in the development of knowledge concerned with the physics of cosmic rays, especially in the period of the first decades of their history, but which still finds some application today for specific experiments. This is the use of nuclear emulsions, a special type of photographic plates coated with a gelatin emulsion containing fine grains of silver halide. Nuclear emulsions, so called because they can be used to record the passage of ionizing particles, must be developed, after being exposed to the particles to be detected, and finally observed under a microscope.

The track is geometrically defined with excellent precision (a few microns), comparable to the precision in the tracking of particles obtainable with current silicon detectors. Overlapping plates can be arranged to reconstruct the track of the particle even in 3D. As a visual detector, it does not require any electronics, cables, or power supplies for its operation, but of course the information is only available during the analysis phase—often long and tedious—and not in real time. Because of their characteristics, they have been used extensively for cosmic radiation measurements especially at high altitudes in the mountains or aboard in balloons, contributing to the discovery of some of the particles of modern physics.

There are extensive reviews, with historical notations, of the operating principles and applications of nuclear emulsions, including textbooks [Powell1959, Barkas1963] and review articles [Shapiro1941, Herz1966, Sime2013].

Since the early 1900s it was known that the silver halide grains in photographic emulsions could signal the passage of ionizing particles under certain conditions. Rutherford was one of the first to use photographic plates exposed to the radiation emitted by radioactive materials. The next step, investigating whether it was possible to detect the passage of a single particle, was taken by one of his collaborators, Sukeiti Kinoshita, who placed a photographic plate near a low-intensity alpha source, in order to calculate exactly the number of single tracks from which the plate would have been hit in a certain time interval, and subsequently verify that the corresponding points

of impact of the track could be found in the plate, once developed. It was thus demonstrated, in 1910, that photographic plates could detect single events, due to the passage of single particles [Kinoshita1910].

The real reconstruction of a single track, as an ordered set of grains that define its geometric characteristics, was made the following year, in 1911, by Maximilian Reinganum (1876–1914), professor of physics in Freiburg, who observed tracks of alpha particles arriving on the plate strongly inclined, therefore crossing a higher effective thickness, with a more consistent energy deposit [Reinganum1911]. In 1912 the Reinganum results were confirmed and extended by Michl [Michl1912], who was able to quantify some parameters of the observed tracks (length, number of grains corresponding to alpha particles of different energy). This technique was soon applied to a few experiments, such as the scattering of alpha particles from a thin sheet, detecting the scattered particles within concentric circular rings on the plane of the nuclear emulsion, and thus further verifying Rutherford's law of diffusion [Mayer1913], already experimentally studied by Geiger and Marsden [Geiger1909]. Kinoshita himself then observed "stars" of tracks due to numerous alpha particles that radiated from a point of the emulsion contaminated with a radioactive preparation [Kinoshita1915], as shown in Fig. 5.14 [Shapiro1941].

The detection of electrons, in addition to alpha particles, was another important step in the use of these first photographic plates, by Sahni [Sahni1915]. In this case the tracks, unlike the straight ones produced by alpha particles, were more irregular and tortuous, as were those produced by the gamma radiation, which in turn produced electrons.

It would therefore seem that already in the first decade of 1900 it was possible to detect by such tool the passage of ionizing particles, and, in principle, also those associated with the cosmic radiation. Indeed, it must be considered that particles of unitary charge, such as protons, or those that would have been identified later as mesons, have a much less specific energy loss than that of alpha particles, and would



**Fig. 5.14**  Tracks of alpha particles that radiate from a point of the emulsion, contaminated by a small amount of radioactive material (Polonium) [Shapiro1941]. Figure reproduced from the work of Maurice M. Shapiro, *Tracks of nuclear particles in photographic emulsions*, Review of Modern Physics **13**(1941)58. Copyright (1941) by the American Physical Society, License No. RNP/22/MAY/053805
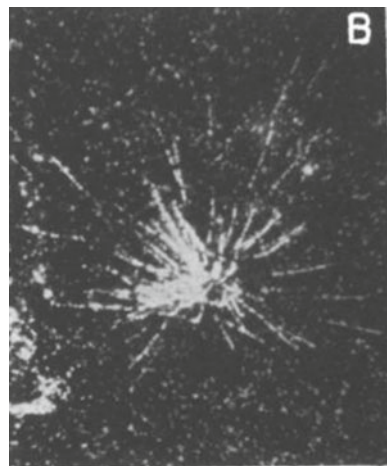
have been very difficult to detect them with the sensitivity of the first photographic plates, which became possible only a decade later.

The probability of observing the grains that make up the track depends in fact on the energy dissipated in that volume and, therefore, on the specific energy loss of the particle, in turn a function of the type of particle and its kinetic energy. The density of the grains along the track, i.e., the number of silver grains per unit of length, is given by the product

$$P \times A \times N$$

where P is the probability of producing a developable grain, A is the transverse area of the grains and N the number of grains per unit of volume. In photographic emulsions, however, following the development, a certain number of grains are always present, randomly distributed throughout the volume, forming a background. The possibility of distinguishing the track of a particle, that is an ordered set of grains that define a trajectory, depends on the average separation between the grains of the track and that between the background grains. A photographic emulsion, therefore, will not be able to detect charged particles that have a specific energy loss below a certain threshold.

One of the problems related to the use of nuclear emulsions is the time interval within which development must be carried out, starting from the date on which the emulsions were exposed to the passage of particles, before the image begins to "fade". This time was of the order of a month. The other problem was related to the need to observe the plates under a microscope to reconstruct the tracks of the particles, a work of patience and which took a long time; this procedure also generally produced a mosaic of several enlarged images, even to explore a small area of the emulsion.

The type of tracks observed through nuclear emulsions varies, depending on the type of particle and its energy. In some cases, the tracks are very thin and barely perceptible with respect to the background, while in other cases the lines are thick. The observed tracks can be straight lines or show large scattering effects. The detailed analysis of the tracks observed in nuclear emulsions can therefore lead to quantitative information about the density of the grains (extracting from this the specific energy loss), the range of the particle, whether it is stopped inside the emulsion, the mean scattering angle in the material, any deflection in the presence of a magnetic field. The combined measurement of different quantities can also lead to an effective identification of the particle.

Ordinary photographic films are not particularly suitable for use as nuclear emulsions, i.e., as track detectors, as they have a very small thickness (a few microns) and the particles would have to cross them with a considerable inclination to give rise to an appreciable loss of energy. Furthermore, the threshold value in dissipated energy is much higher than the value corresponding to the minimum of ionization, so much so that only strongly ionizing particles (for example heavy nuclei) could exceed it. In the following decades, however, photographic plates with a much larger thickness were produced and techniques were introduced to increase the sensitivity

**Fig. 5.15**   A few photographic emulsions used in the past (Photo by the author, from the collection of the Department of Physics and Astronomy of Catania)

of the plates (by increasing the number of grains per unit of length) and to improve the development of the plates by appropriate methods.

The possibility of using this technique for the detection of particles of cosmic origin was therefore only addressed a decade later. In particular, it was the Austrian physicist Marietta Blau (1894–1970), in Vienna, who investigated in the early 1920s the possibility of using different types of photographic plates to also detect protons. For this purpose, she used an alpha radioactive source, whose decay products, energetic alpha particles, were capable of producing the emission of protons (called H-rays in that context) from hydrogenated materials, such as paraffin. The first results demonstrating this possibility were published in the mid-1920s [Blau1925]. In the following years, Blau improved this method, using different types of support and changing the conditions of plate development, also managing to interest the English company that produced photographic material, ancestor of Ilford, to produce thicker supports more suitable for the detection of particles [Blau1932] (Fig. 5.15).

We will further discuss Marietta Blau's contribution to cosmic ray physics, with her measurements done in the second half of the 1930s, using nuclear emulsions at high altitudes, for the observation of nuclear interaction processes.

Because of this interest and the results achieved with this technique, from the end of the 1930s some models of photographic emulsions specifically produced to detect the passage of ionizing particles were made available by the major producers of photographic films (Kodak and Ilford). The first emulsions of Ilford allowed to trace protons of about 100 MeV of energy, while those produced by Kodak in the following years also allowed the detection of particles at the minimum of ionization. It should be noted that the development of these techniques and the realization of these commercial devices saw a close collaboration between the world of industry and that of research, represented in this context by Marietta Blau and subsequently by physicists such as Powell and Occhialini at the University of Bristol, who had heard of her first physics results at high altitude.

Although the Nobel Prize in Physics in 1950 was awarded to Powell "for his development of the photographic method of studying nuclear processes and his discoveries
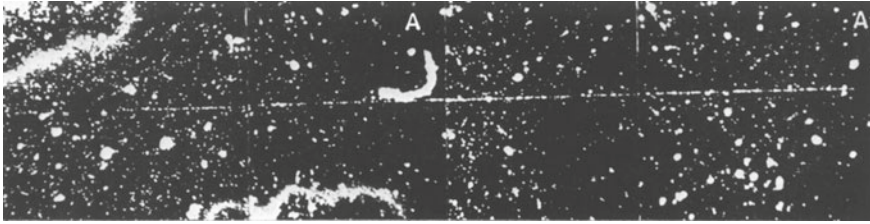
**Fig. 5.16** A plate installed aboard a stratospheric balloon shows the track of a cosmic radiation particle, probably a high-energy alpha particle. Overall length of the track 550 µm [Shapiro1941]. Figure reproduced from the work of Maurice M. Shapiro, *Tracks of nuclear particles in photographic emulsions*, Review of Modern Physics **13**(1941)58. Copyright (1941) by the American Physical Society, License No. RNP/22/MAY/053805

regarding mesons made with this method", the systematic use of nuclear emulsions for the quantitative observation of tracks produced by nuclear particles is undoubtedly linked to the name of Marietta Blau, who unfortunately had no recognition, and had a very troubled life, while continuing to carry out scientific activity until 1970, as we will see in the next chapter.

The use of nuclear emulsions, which in those years saw a period of great fortune for the physics of cosmic rays, decreased in the following decades, in favour of electronic detectors, even if they are still used today in particular experiments for the investigation of rare processes.

Figure 5.16 shows a track due to cosmic rays (probably an alpha particle), observed in one of the plates installed on board a stratospheric balloon [Shapiro1941].

## 5.9 Detectors Based on Scintillators

Although the period from the discovery of cosmic radiation up to the 1940s is characterized above all by the use of the detectors that we have discussed so far, it is worth mentioning in this context also the detectors based on the scintillation process, which began to be used only in the following decades, to the point of replacing in many cases most of the previous detectors. A historical review of the first uses of scintillation-based detectors was first reported by Krebs in 1955 [Krebs1955].

The origin of modern scintillators actually dates back to the scintillation process, studied and used in visual mode since the early 1900s. In 1903, for example, Crookes used a Zinc Sulfide (ZnS) screen to detect the fluorescence created by the emitted alpha radiation from a radioactive source. Observing the screen through a microscope, Crookes could see individual flashes of light created by the individual interactions of the alpha particles with the screen. The apparatus, called spintariscope, was used for some time, for example to study the diffusion of alpha particles. In more recent times, small spintariscopes were also used as scientific toys. Many historical models

**Fig. 5.17** Diagram of one of the first scintillation devices, based on the use of scintillating phosphors coupled to a special Geiger counter [Krebs1941]
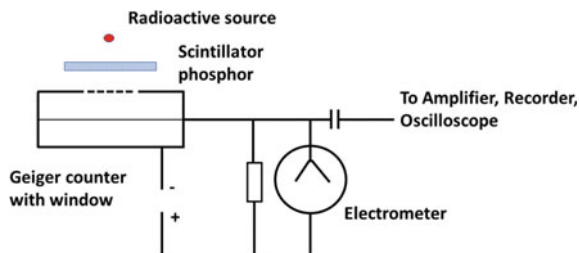
of spintariscopes are visible in museum collections, for example that of the Oak Ridge Associated Universities [ORAU].

The real beginning of the use of scintillators in research related to nuclear physics and cosmic ray physics, however, can be dated to the early 1940s. One of these devices, due to Krebs [Krebs1941], shown in Fig. 5.17, makes use of a Geiger counter with a special design, which allows the entry of scintillation photons produced in the scintillating material.

With these first devices, which were soon improved in the following years [Mandeville1950a, Mandeville1950b, Mandeville1950c, Mandeville1950d, Mandeville1950e], it was possible to detect alpha, beta and gamma radiation, up to the creation of commercial equipment within a few years [Daggs1952]. However, this configuration was soon replaced, in the mid-1940s, by devices based on photomultipliers, whose first prototypes had already been developed several years before. The first scintillation counters were thus made by Curran and Baker in 1944 [Curran1944], who showed how alpha particles with energies of the order of MeV could be detected. However, only a few years later, in 1947–1948, its potential and advantages for the detection of high-energy particles were fully recognized [Marshall1947a, Marshall1947b, Coltman1947].

In 1947 Marshall, Coltman and collaborators demonstrated the possibility of detecting single events due to alpha particles, electrons or gammas. These detectors also proved capable of detecting X-rays, protons and neutrons. Further improvements of these first detectors were proposed by these researchers, concerning the possibility of using different scintillating materials, a different shape or volume of the scintillator, improvements in the collection of light and in general in the optical system and associated electronics. Similar results on the detection of alpha particles were also obtained in the same year by Broser and Kallmann [Broser1947a]. Soon after the same authors published another work, referring to other possible scintillating materials, such as $CaWO_4$, $Zn_2SO_4$ [Broser1947b]. The following years, around the end of the 1940s, saw further improvements and uses of these detectors in different areas of research, from nuclear physics to cosmic ray physics, from medical applications to dating techniques [Bell1948, Hofstadter1948, Morton1949, Mayneord1950, Pringle1950]. It was soon recognized that scintillator-based detectors actually constituted a new radiation observation tool, representing a breakthrough equal to that of the introduction of the Geiger counter at the end of the 1920s (Fig. 5.18).
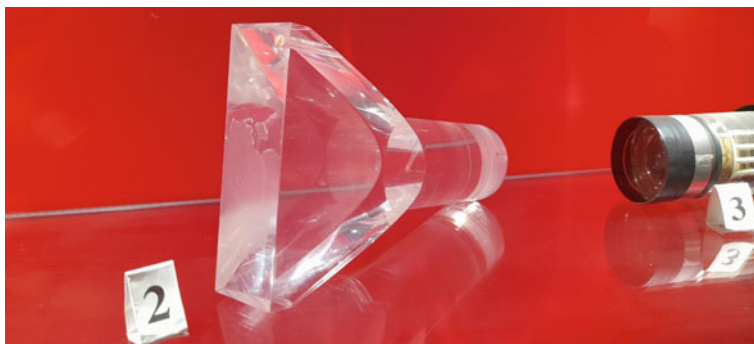
**Fig. 5.18** A scintillator coupled to a light guide to direct the scintillation light towards a photo-multiplier (Photo by the author, from the collection of the Department of Physics and Astronomy of Catania)

The use of liquid organic scintillators to build cosmic ray detectors with a large area (of the order of a square meter) had some disadvantages, including high flammability, volatility, and toxicity. Other types of scintillators, free from these defects, had a high cost. For this reason, low-cost plastic scintillators were developed in the 1950s. In a work of 1957 [Clark1957a], for example, the preparation technique of this type of scintillators is discussed, in view of the realization of a large number of devices to be used for the detection of cosmic rays for a surface array.

Detectors based on scintillators of different compositions, both organic and inorganic, with reading of the scintillation light carried out by means of photomultipliers or more compact photosensors (Avalanche Photo Diodes, Silicon Photomultipliers …), sometimes in connection with the use of special optical fibres (WaveLenght Shifter fibres, WLS) have become common in recent decades and are also widely used for the detection of particles associated with cosmic radiation. We refer to one of the specialized textbooks [Leo1987, Knoll2000, Leroy2004, Grupen2008] for a detailed description of the use of scintillation counters.

# Chapter 6
# The Interaction of Primary Cosmic Rays in the Atmosphere

**Abstract** The chapter focuses on the interaction of the primary particles with the Earth atmosphere. This aspect played an important role up to 1950s since it was the only mean of observing high energy nuclear processes, before the advent of particle accelerators. The first evidence of nuclear disintegration processes producing secondary tracks came from the early observations by Marietta Blau, who employed nuclear emulsions at the end of 1930s. Nuclear interaction events occurring at high altitude were studied in the following years by different methods, confirming the role and the importance of high-altitude laboratories, where most of these investigations were carried out. An extended list of these laboratories is also reported in Appendix F. The study of high energy particle interactions in the atmosphere gave also the first evidence for a complex primary radiation, as well as for the production of a variety of secondary particles, whose properties were extensively studied from 1940s on.

## 6.1 The First Evidence of Nuclear Interactions of Cosmic Rays

When the nature of the primary cosmic radiation, as essentially consisting of high-energy protons, was more and more accepted, it became important to understand how they interacted with the nuclei of the Earth's atmosphere and by which mechanisms the different particles present in the secondary component were created, some of which are able to reach the ground level.

The first experimental evidence of nuclear interaction processes capable of producing a multiplicity of particles (nuclear disintegrations) came from the observations of the so-called "cosmic ray stars" (or disintegration stars), obtained by Marietta Blau and Hertha Wambacher, in 1932, by the use of nuclear emulsions exposed on the mountains, at an altitude of 2300 m, and which we have mentioned when discussing the use of this method for the observation of particle tracks.

Some results on the nuclear interactions produced by particles of the cosmic radiation had been obtained in those years also through measurements performed with cloud chambers. For example, Anderson and Neddermayer reported several results [Anderson1936] from a series of measurements conducted on Pike's Peak

(4300 m), while Brode and collaborators [Brode1936] also obtained at sea level some evidence of the existence of processes due to particles heavier than protons.

Marietta Blau, an Austrian physicist, had contributed since 1923 to the study of the tracks of charged particles, firstly using commercial photographic emulsions and managing to identify the tracks of protons and alpha particles. Subsequently, using photographic emulsions produced specifically by Ilford, Blau significantly improved the visibility of these tracks, also determining the energy of fast protons observed in the emulsions, as well as that of neutrons, based on the recoil protons. By exposing a certain number of these emulsions for several months at an altitude of 2300 m, in addition to the observation of normal proton tracks, Blau and Hertha Wambacher, her assistant, realized the existence of specific events, in which the observed tracks (sometimes even a dozen) came from a single point. These events were interpreted as the disintegration of a heavy nucleus present in the emulsion, due to the interaction with the primary track [Blau1937].

Figure 6.1 shows the diagram of an event reconstructed by Blau and Wambacher [Blau1937], with the presence of several tracks, some of which are drawn with a more or less thick line, indicating a greater or lesser ionization along the path.

Blau's contribution in the use of nuclear emulsions and in the observation of nuclear interaction processes induced by primary cosmic rays was of great importance, even if her work has often been overlooked or not properly considered. Powell himself had begun to use nuclear emulsions for the observation of nuclear interaction processes only in 1938, after having recognized their usefulness following the work of Blau (Fig. 6.2).

The events of the Second World War and the Nazi occupation of Austria also played a part in Marietta Blau's personal life. Blau, as a Jew, was forced to leave
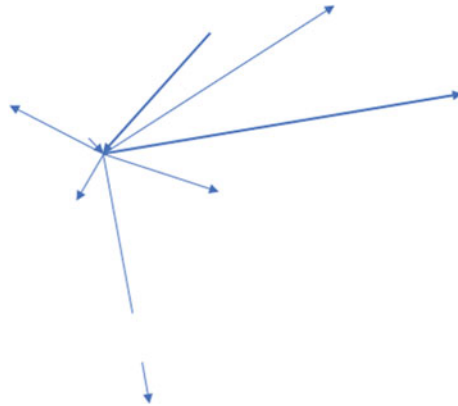


**Fig. 6.1** Schematic diagram of the first observations, by Blau and Wambacher [Blau1937] of the existence of disintegration stars, produced by the interaction of a primary particle with a nucleus present in the nuclear emulsion. The thickness of the line indicates a greater or lesser density of grains in the emulsion, while the arrow indicates the direction of the track, from the emulsion towards the glass. The bottom interrupted track shows a longer track (not to scale)

**Fig. 6.2** Marietta Blau in 1937, at the time when she obtained the first images of "disintegration stars" by means of nuclear emulsions taken to high mountain. *Source* AIP Emilio Segrè Visual Archives, Gift of Eva Connors

Austria in 1938 and to live in Norway, Mexico and then in the United States, without being able to fully continue her research activity, which in the meantime her colleagues in Austria—loyal to the regime—had appropriate. Her contribution was often omitted, for example from the list of possible Nobel candidates, which initially also contained her name, proposed by Schrodinger; Powell himself, in his speech on the occasion of the Nobel award, did not even mention her papers and her contribution [Strohmayer2006].

The tracks observed were initially attributed by Blau to particles with a high ionization capacity, such as low-energy protons or alpha particles. Once the possibility that these stars could be produced by small quantities of radioactive substances present in the emulsions was excluded, their origin was recognized as due to cosmic rays. This hypothesis was later confirmed by the fact that the probability of observing these events increased if the emulsions were exposed at high altitudes, where the intensity of the cosmic radiation is greater [Setter1939]. The discovery of mesons in those years also suggested that they were produced precisely because of these interactions, as secondary products in the atmosphere, excluding the possibility of processes in which pairs of mesons were produced directly by photons, in analogy to the creation of electron–positron pairs.

Experiments aimed at detecting penetrating mesons created as a result of nuclear interactions in materials were carried out by Wataghin and Janossy around 1940, using configurations of Geiger counters arranged under a layer of lead, or with additional layers of lead placed between the counters. Because of the thickness of lead involved, the energy of the particles capable of producing these secondary particles had to be of the order of some GeV. Such events were also observed by means of condensation chambers.

The characterization of these nuclear interactions went through a systematic series of measurements made at different altitudes and on different materials. It immediately became clear that the particles capable of producing these interactions could not be photons or electrons, because these processes took place even after crossing a considerable thickness of lead, capable of absorbing photons and electrons.

To evaluate whether the interactions were produced by the same μ mesons present in the cosmic radiation, the measurements carried out at various altitudes were decisive. These showed that the number of particles which produced these nuclear processes, with the creation of penetrating showers, increased with altitude much more rapidly (about a factor of 10) than the increase with the altitude of the μ mesons. It was therefore demonstrated that neither photons, nor electrons, nor muons had an appreciable probability of interacting with atomic nuclei, producing secondary particles through nuclear processes. The possible candidates as probes capable of producing these interactions were therefore protons, neutrons and π mesons, a hypothesis that was further confirmed by the activity carried out in the following years using detectors brought to high altitudes, both in laboratories in the high mountains and by equipment launched aboard balloons at very high altitudes.

In summary, these nuclear interactions induced by particles present in the cosmic radiation are capable of producing a great variety of reaction products, from charged particles to neutrons, which then follow a different fate, depending on their nature and the materials with which they interact: first of all the air in the terrestrial atmosphere, where the first interaction of the particles coming from outside the Earth takes place, and subsequently also the interactions of the secondary products.

## 6.2   Interactions in the Atmosphere and First Evidence of a Complex Primary Radiation

The phenomenology based on the observation of the tracks produced in high-altitude nuclear emulsions confirmed the hypothesis about the nature of primary cosmic rays, mostly identified as composed by high-energy protons. Although in principle even neutrons and pions were capable of producing nuclear interactions, both are subject to spontaneous decay—neutrons with a lifetime of about 14 min, pions with an enormously shorter lifetime of tens of nanoseconds—and therefore they could not travel long in space before reaching the Earth. It was therefore more reasonable to assume that the primary particles were protons, stable particles. As for their energy, it was already clear that it had to be higher than some GeV.

Although some evidence of primary tracks due to nuclei heavier than protons had been obtained, as we have seen, as early as 1940, it was only in the late 1940s, however, that further measurements with nuclear emulsions performed by Bradt, Peters and others collaborators of the Rochester group, at great height in the atmosphere, about 30 km, using sounding balloons, showed more systematically events in which the primary interaction was produced by very dense tracks, typical of nuclei

heavier than protons [Freier1948a, Freier1948b, Bradt1948]. A systematic work on the abundance of such nuclei in the primary radiation was published by Bradt and Peters in 1950 [Bradt1950]. A spectacular image of one of these events, taken from their work, is shown in Fig. 6.3. In this picture we can see the interaction of a heavy nucleus, identified as a Calcium nucleus (estimated atomic number $Z = 20 \pm 1$), which interacts with one of the nuclei present in the nuclear emulsion employed (Silver or Bromine), producing a star with 42 outgoing tracks of charged particles. Some of them are low ionization tracks, barely visible in the figure, and identified as probable tracks of mesons created as a result of local showers, while other tracks, with a high ionization density, show evidence of secondary particles produced in the process. One of them produces a further nuclear interaction in the same emulsion, less than 100 μm away from the first interaction. The energy of the primary particle, in this event, was estimated to be greater than 100 GeV.
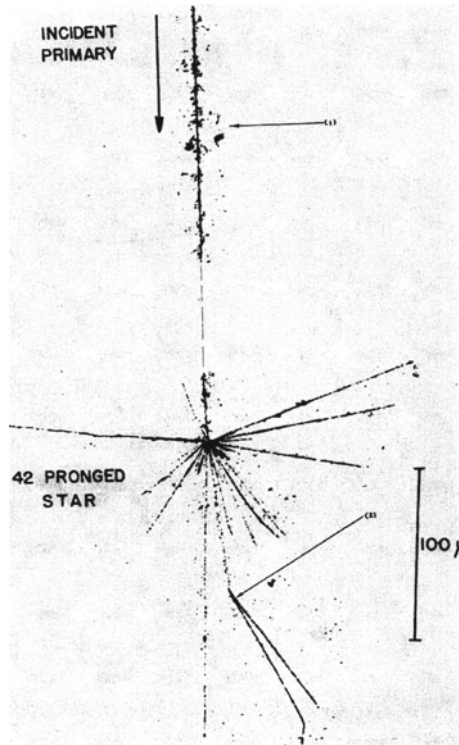


**Fig. 6.3** A nuclear interaction event, produced at high altitude by a heavy primary, identified as a high energy (> 100 GeV) Calcium nucleus, with one of the nuclei present in the emulsion. The interaction produces dozens of secondary particles, one of which is capable of giving rise to a further nuclear interaction a few tens of microns away [Bradt1950]. Figure reproduced from the work of H. L. Bradt and B. Peters, *The heavy nuclei of the primary cosmic radiation*, Physical Review **77**(1950)54. Copyright (1950) by the American Physical Society, License No. RNP/22/JUN/054397

Postponing for the moment a detailed analysis of the composition of the primary radiation, which will be resumed later, we are here faced with the first quantitative evidence of the fact that the primary radiation is not constituted only by protons, although these are the most abundant component: in the primary radiation it is also possible to find the presence of nuclei much heavier than protons, with mass greater than that of oxygen, which raises further questions about the origin and nature of the primary radiation. In this same work of 1950, in fact, Bradt and Peters discussed the significance of the presence of these nuclei in the primary radiation in connection to their origin (whether deriving from the Sun or the Galaxy) and the acceleration mechanisms that can justify the observed energies.

If not only protons but also other complex nuclei were present in the primary radiation, the question arose whether other stable components, such as photons and electrons, could also be present. The search for these additional components in the primary radiation occupied an important role in the activity of researchers in the following decade. Research groups from MIT and the University of Minnesota in the USA initially obtained negative results, until, about ten years later, the first evidence was also obtained of the presence of electrons [Earl1961, Meyer1961] and high-energy primary photons [Kraushaar1962].

A more complete quantitative discussion of the composition of the primary cosmic radiation will be dealt with later, also referring to the most recent results obtained in this field. However, we can now mention the fact that the other components represent a total of less than 10% of the most abundant component, consisting of protons, and that among these the greatest abundance belongs to the nuclei of Helium. The most probable interactions that occur in the upper part of the atmosphere, and which produce secondary particles capable of reaching even sea level, therefore originate to a large extent from these light nuclei.

## 6.3   Production of Other Particles in Nuclear Interactions

It should be remembered that in those years the study of these first high-energy nuclear interactions were the only means of investigating the interaction process between two nuclei, with the exception of the known processes at much lower energies, typical of radioactivity. For many years, therefore, before the advent of accelerators, the only interaction processes that could be investigated, even at energies of the order of a hundred MeV or GeV, were those that gave rise to these "stars" with multiple tracks leaving the point of interaction.

These experiments also gave rise to the observation, during the 1940s, of entire classes of new particles, as secondary products of these interactions, and on which we will not go into many details. It will be enough to mention, for example, the evidence of the existence of the neutral pion, which decays in very short times, mainly into two gammas, observed in cosmic rays [Powell1950] and also in the first experiments carried out with accelerators [Bjorklund1950], of the lambda neutral particle ($\Lambda_0$), which can decay into a proton and a negative pion, of the positive Sigma particle

($\Sigma^+$), which decays into a neutron and a positive pion, and of the charged mesons $K^\pm$, which decay into a considerable variety of different channels. Over the years, the possible rules were also enunciated that allowed to establish allowed and forbidden modes of the various decay channels, based on the conservation of certain variables.

Furthermore, following these observations, the class of antiparticles expanded enormously, consistently with Dirac's theory. The first observations of events compatible with the existence of antiprotons and antineutrons, related to cosmic ray physics experiments, were then confirmed by high statistics experiments performed with particle accelerators in the 1950s.

## 6.4  The Role of High-Altitude Laboratories

We have already seen how, from the very beginning of the study of the cosmic radiation, the possibility to carry out measurements at high altitudes was considered an important aspect, initially to understand the basic question of the extraterrestrial origin of this radiation, later to characterize the intensity of the radiation as a function of altitude, finally to study the nuclear interaction processes by which primary particles were able to generate secondary particles.

Although many measurement campaigns were organized using airplanes or by means of balloons (firstly handled by human crews, later on by automatic devices), the role of the laboratories located over the top of high mountains has always been central to the studies of the cosmic radiation, as it offered the possibility of installing detection devices larger and heavier than those that can be carried on board of balloons or airplanes, and above all for the possibility of operating these devices for long periods, in order to monitor the flux of cosmic rays over time or measure rare events. The history of many of these laboratories and the role they played in the research activity in cosmic ray physics, in the training of new scientists, in cultural exchanges and in international collaborations is itself a topic of considerable interest [Korff1982, Zanini2009].

Already in the early years after the discovery of the cosmic radiation, measurements had been carried out in the mountains, creating small permanent observation structures. Victor Hess himself had installed measuring equipment in 1913 on Hochobir, in Carinthia, at an altitude of 2040 m. After returning from the United States, Hess organized a series of observations on the Sonnblick, at 3100 m, with ionization chambers, which had to be recharged every 4 h and therefore required continuous work shifts. The transport of materials, in particular of the iron shielding of the equipment, required considerable manpower, due to the lack of suitable means of transport that reached that altitude. Later, taking advantage of the construction of a cable car on Mount Hafelekar (2334 m), Hess then built an Observatory on this mountain [Hess1932], which was put into operation in 1931, and which over the years became a reference point also for many other foreign researchers, as evidenced by the messages left in the GuestBook of the Laboratory [Steinmaurer1982] (Fig. 6.4).
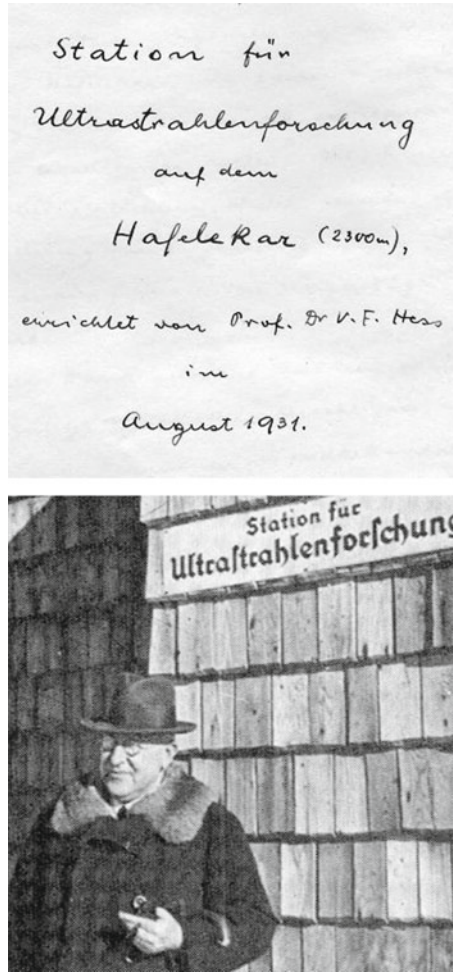
**Fig. 6.4** Top, fragment of the GuestBook of the Laboratory on Mount Hafelekar. On the bottom Victor Hess at the Laboratory, in November 1936, the period of the awarding of the Nobel Prize. *Source* V. F. Hess home page, University of Innsbruck (http://physik.uibk.ac.at/hephy/Hess/homepage/)

Starting from the 1920s, many observation stations were built in various parts of the world, as evidenced by a Report prepared in the mid-1950s [Korff1952, Korff1982], which in its original version included many other details on the characteristics and the organization of each station.

One of the first stations in North America for the study of cosmic rays was the station located on Mount Evans, at 4350 m. In 1928 Millikan and Compton began high altitude experiments in Peru, on Mount Huancayo (3350 m), near the geomagnetic equator. Also in South America, on Mount Chacaltaya in Bolivia, one of the

**Fig. 6.5** View of the high-altitude laboratory of Chacaltaya, in the Bolivian Andes. *Source* American Institute of Physics, Emilio Segrè Visual Archives

highest stations (5200 m) for observing cosmic radiation was built. In Europe, several observation stations were installed both in the Alps and the Pyrénées. One of these stations was on the Jungfraujoch, reachable by a railway, at 3570 m, and from the very beginning it had an international character, with contributions from Austria, Belgium, France, Germany, Great Britain and Switzerland. Other observing sites in Europe were that of the Aiguille du Midi (3600 m), in France, the Italian site Testa Grigia (3380 m), that of the Pic du Midi, in the Pyrénées (2860 m), originally an astronomical observatory but with equipment also for the detection of cosmic rays. Survey stations were also built on the Asian continent, for example in Gulmarg, India, as well as in the Hawaii. Appendix F reports a list of the main high-altitude stations existing in the mid 50s (Fig. 6.5).

Of course, one of the problems of high-altitude installations, especially in that period, was the accessibility of the site, in particular whether it could be reached by suitable means of transport through roads, in which case the shipment of equipment, even heavy, was relatively smoother. Other means of reaching the site, such as the cable car, or manual transport, at least for critical parts of the path, greatly limited the equipment that could be transported and the maintenance of the site itself. In principle, altitudes of 5000–6000 m represent the upper limit for a reasonable access to an observation site. These altitudes correspond approximately to half the thickness of the Earth's atmosphere.

High-altitude installations have been, and still are, useful even for other disciplines, such as meteorology, geology, and also biology, in addition of course to astronomy.

# Chapter 7
# Extensive Air Showers

**Abstract**  A new and important step to understand the properties of the cosmic radiation came with the observation of time- and space-correlated particles, originating from the interaction of a high energy primary particle at the top of the atmosphere. The existence of extensive air showers dates back to the observations made by Pierre Auger in the Alps, with counters separated up to 300 m, although some evidence had been observed by Rossi a few years before. The study of the properties of extensive air showers opened an entire new area in the history of cosmic ray physics. Early evidence of this phenomenon is discussed with reference to the original papers and results, including the first measurements of the decoherence curve, i.e., the probability to observe coincidences as a function of the separation distance between the counters. The chapter then presents in a quantitative way some of the main features concerning atmospheric showers: their intensity profile, the longitudinal and transverse development, their time properties, and the density distribution of the associated secondary particles. Results from modern simulations of extensive air showers based on the Corsika package are also included in the chapter and further discussed in Appendix G and I.

## 7.1  Secondary Processes and Local Showers

We have already mentioned the observations of individual tracks of particles by means of the condensation chambers. Looking at the pictures of these tracks, it had been sometimes noted the simultaneous presence of several tracks close to each other. Such observations had been made for example by Skobeltsyn in 1928. From the observation of these tracks Skobeltsyn had deduced that the tracks came from regions close to the observation area, even if it was not clear whether they came from a single point (vertex). In any case, this was evidence of processes in which other secondary particles were produced. These secondary particles were most likely electrons produced by the Compton effect in the material overlying the detectors.

A consequence of these processes is that the number of the secondary particles depends on the thickness of the material, according to a "transition" effect: electrons or photons of high energy, interacting with a material, especially materials with a high

atomic number, produce in turn photons or secondary electrons. The number of these by-products initially increases with the thickness of the material, as new electrons are produced; however, by further increasing the thickness, the electrons produced start to be absorbed into the material itself. Detailed measurements of this kind were carried out by Rossi with different configurations of Geiger counters operating in coincidence and displaced according to geometries that made it possible to highlight these effects [Rossi1933a].

Figure 7.1 shows possible configurations of Geiger counters. In configuration A, in which 3 counters are superimposed vertically, they can detect tracks of a single particle which cross all the counters at the same time; configuration B is instead made up of 3 counters arranged in such a way that a single particle cannot cross them all, for example if the centres of their circular sections occupy the vertices of an equilateral triangle. A possible coincidence between these 3 counters would therefore give evidence of the passage of at least two independent particles, represented by the dashed tracks. By analogy, a configuration of 4 detectors, if they are arranged with a suitable geometry (C), would indicate the passage of at least 3 independent particles. The appropriate configuration to be used can be optimized if the approximate point at which these secondary processes can occur is known.

To study how the number of such secondary processes depends on the thickness of the material placed above the detectors, Rossi studied the number of coincidences between two or more detectors appropriately arranged, as the thickness of the material placed above the detectors was varied, for example with lead plates of increasing thickness, placing this amount of material at different vertical distances from the counters. Figure 7.2 shows the data obtained by Rossi with a lead layer placed at a distance of 14.6 cm from the counters.

As it can be seen, the insertion of a thin layer of lead above the detectors (1– 2 cm, corresponding approximately to 10–20 g/cm$^2$) produces a notable increase in the number of coincidences, while a further increase in the material thickness leads to a slow decrease in the number of observed coincidences, due to the progressive absorption in the lead itself of the particles produced, until reaching an almost constant value. This is the so-called Rossi transition curve [Rossi1933a], an effect
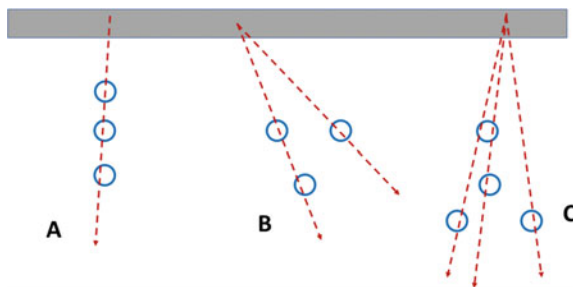


**Fig. 7.1** Geometric configurations of cylindrical Geiger counters (seen in section) operating in coincidence, which allow to observe events due to the passage of a single particle (**A**), or of several individual particles (**B**, **C**)
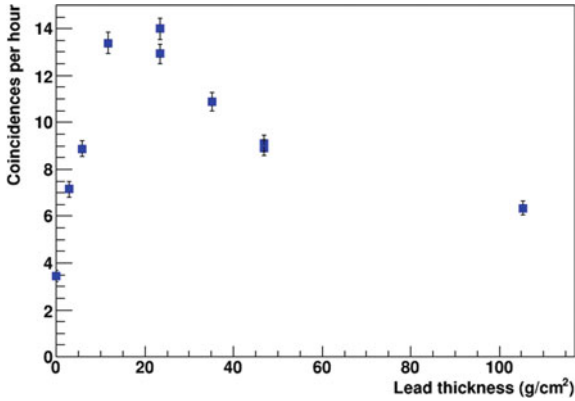
**Fig. 7.2** Rossi transition curve, represented by the number of hourly coincidences between several detectors placed below a lead layer and operated in coincidence, as the interposed thickness of lead varies. Data extracted from [Rossi1933a]

which has been also reproduced in many educational experiments in cosmic ray physics [Blanco2008a].

The fact that the coincidence rate between the counters did not decrease to exactly zero, even with a very large amount of lead, was for some time an incomprehensible aspect of the phenomena related to the cosmic radiation. In fact, one would expect that the increase in the thickness of material leads to a complete absorption of the secondary particles produced by these "local" showers, due to the interaction of a single photon or high-energy electron in the material, with the production of secondary electrons. The coincidences, although rare, observed even with a large thickness of lead, could not therefore be due to electrons, but to more penetrating particles, the nature of which was later clarified. At the same time, the observation of coincidence events even between counters placed at large relative distances helped to clarify the nature of one of the most striking phenomena in the physics of cosmic rays, namely the existence of atmospheric showers of enormous transverse size, able of develop along the longitudinal direction in the various layers of the atmosphere.

## 7.2 First Evidence of the Existence of Atmospheric Showers

The evidence of correlated particles in the cosmic radiation present in the atmosphere is generally associated with the measurements of Pierre Auger and collaborators, published in 1938–1939 [Auger1938a, Auger1938b, Auger1939a, Auger1939b, Auger1939c]. In summarizing the results of these measurements [Auger1939c] Pierre Auger recalls how, in addition to the soft particles deriving from the decay of mesons, there must be other spatially and temporally correlated components associated with the showers created by the interaction of the primary particle. This coherence effect

between different particles can be somehow highlighted by coincidence measurements between individual detectors, placed at a certain relative distance and able to detect their arrival. Auger refers to a series of measurements, performed both at sea level and at high altitude, on the Jungfraujoch (3500 m) and Pic du Midi (2900 m), using Wilson chambers and counters, which had shown evidence of those that will be immediately called Extensive Air Showers.

Some preliminary evidence of coincidence events between distant counters had actually already been obtained by Bruno Rossi in 1933, while performing coincidence measurements between two Geiger counters, in particular to study the dependence of the number of observed coincidences on the orientation of the detector telescope, for the study of the so-called East-West effect. Occasionally Rossi had noticed how some coincidence events also occurred with counters arranged at a large distance between them [Rossi1934b], in which case the number of observed coincidences had to simply correspond to the expected number of spurious coincidences. Strangely, however, the number of observed coincidences always exceeded the estimated number of spurious coincidences, a phenomenon that Rossi describes as if from time to time showers of particles arrived close to the detectors, producing coincidences. Rossi, as he himself writes, did not have the time to investigate the phenomenon further, but certainly what he observed was due to physical coincidences between particles of an extensive air shower, which somehow represents first evidence of this phenomenology.

Bothe and Kolhöster at the same time that Auger's results were published had also observed similar phenomena [Bothe 1937; Schmeiser1938; Kolhöster1938], placing Geiger counters at some distance. The data obtained by Schmeiser concerned coincidences between relatively close counters, up to about one meter away, while those obtained by Kolhöster reported the coincidence rate between two detectors up to about 75 m apart [Kampert2012]. Both these datasets were obtained at sea level. The trend of the number of coincidences observed as a function of the distance represents what is usually called decoherence curve, and is linked, as we will see later, to the characteristics of the shower, in particular to its transverse profile.

From the knowledge of electromagnetic showers (cascades) it was expected that electrons and photons, components of these showers, should arrive at sea level separated by small distances. For example, it was possible to calculate that the average distance between two electrons belonging to a shower created at a height of 10 km by an electron of energy equal to 10 GeV should be of the order of a few meters. Such considerations had been made, among others, by Clay and Blackett. As just mentioned, however, these observations by both Auger and the aforementioned authors showed evidence of correlations between particles of the same shower up to much greater distances than could be expected (Fig. 7.3).

By placing two or more counters in the air, at a certain distance, Auger had in fact observed a certain number of coincidences, a number that decreased as the relative distance between the counters increased. While the measurements reported by the other authors had been carried out for relatively small distances, up to a few tens of meters, Auger had carried out measurements up to much greater distances, of hundreds of meters, still observing a small effect. It must be said that the possibility of observing "true" coincidences is determined by the amount of "spurious", or random,

**Fig. 7.3** Pierre Auger (1899–1993) in 1978. *Source* Fonte: American Institute of Physics Emilio Segrè Visual Archives
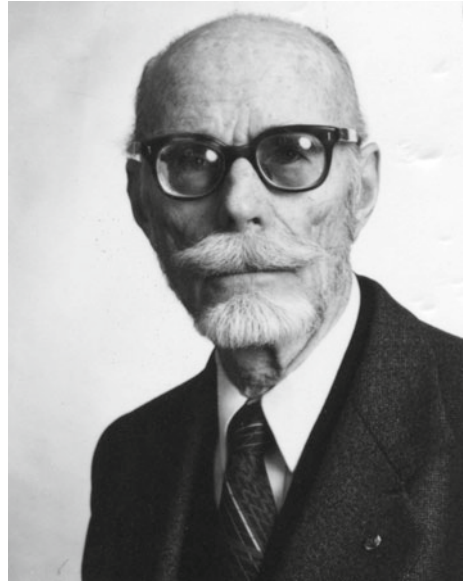
coincidences, which always occur in a coincidence experiment between two or more detectors, as discussed in detail in Chap. 5. The quantity of random coincidences per unit of time, as we have seen, depends on the counting rate of the individual detectors and on the coincidence "window", that is, on the time interval within which the signals produced by the two detectors are considered as simultaneous. In Auger measurements, this coincidence interval was reduced, following the development of the coincidence circuits by Roland Maze [Maze1938], to less than 5 µs. In the detector configuration used by Auger, it could be estimated that with two counters of area equal to 200 cm² each, the expected random coincidence rate, for measurements done at high altitude, was about 1 per hour.

With an apparatus consisting of two counters placed horizontally, the number of coincidences was measured by Auger at various distances, up to about 300 m, as shown in Fig. 7.4. As can be seen, the probability of observing such coincidences rapidly decreases with increasing distance and can be related to the theoretical description of the interaction processes of cosmic rays in the atmosphere, in particular with the resulting lateral profile of the shower. In the original figure by Auger the experimental results were compared with the predictions of a model describing the development of the "standard" cascades [Euler1940]; consistent deviations were observed for distances of more than about ten meters, testifying to the fact that different processes intervened with respect to the electromagnetic showers produced by individual electrons and photons. According to these processes, the probability of having coincidences should have been reduced to practically zero for distances beyond a certain value—about ten meters—while true coincidences could
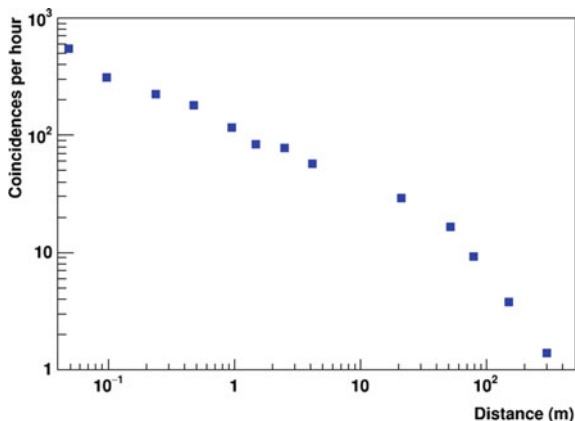
**Fig. 7.4** Number of hourly coincidences observed between two horizontal counters, as a function of their relative distance, obtained from the first Auger experiments

be still observed, albeit in a limited number, up to enormous distances, of hundreds of meters.

The observation of coincidences even between very distant detectors, at distances greater than those that can be expected from the separation between electrons in a local shower, led to the conclusion that extensive showers of enormous size existed, caused by processes other than the standard electromagnetic processes that produced local showers. The comparison between measurements made at low altitudes and those made at high altitudes, in which the number of coincidences at great distances was significant, more than at low altitudes, naturally led to the idea of a shower that developed throughout the atmosphere, originated from a single primary particle, with a particle density of even several tens per square meter and distributed, at sea level, over an area of enormous dimensions. Further evidence of the existence of correlated particles associated with extensive air showers was also obtained in those years by Lovell [Lovell1939] by means of cloud chambers triggered by Geiger counters.

In the years after the first evidence of these extensive air showers, a detailed work to characterize their properties and behaviour was started, in a similar way to what had been done for the individual particles of the cosmic radiation in the previous decade. Thus, for example, Neher and Pickering [Neher1940] investigated, by means of a certain number of Geiger counters operating in coincidence, the possible dependence of the number of extensive air showers on varying latitude, finding no effect within the limits of the statistical uncertainty associated with their measures. Auger himself, with Jean Dadin, published in 1940 a short note [Auger1940] concerning the possible diurnal variations in the number of showers observed. No striking effect was observed in these measurements, with the exception of a slight increase in correspondence with solar noon, which was presumably attributed to thermal causes.

A few years later, in 1942 [Auger1942], Auger also investigated the influence of atmospheric pressure (therefore of particle absorption) on the number of showers,

identified through the coincidence between two detectors placed at a certain separation distance, 3 m and 13 m in the case of these observations. The measurements were carried out both at sea level and at an altitude of 2900 m. At sea level, the dependence of the number of hourly coincidences between two detectors placed at a distance of 3 m, on the atmospheric pressure, made it possible to obtain, albeit with high errors, a barometric coefficient equal to 9% increase for a decrease in pressure equal to 1 cm Hg. Another series of measurements, performed for two different relative distances between the counters, led to a coefficient of $(23 \pm 5)\%$ per cm Hg for a separation of 13 m and of $(9 \pm 2)\%$ per cm Hg for a separation of 3 m. The different value of the barometric coefficient reflects the different nature of the coincidences observed in the two cases, being those measured at a short relative distance strongly influenced by local showers, mainly composed of electrons and photons, while those measured at greater distances are indicative of extensive air showers, with prevalence of muons. Preliminary measurements of this kind had also been reported by Cosyns in 1940 [Cosyins1940], who had observed some evidence that the barometric coefficient was higher for showers extending farther away. Additional considerations about the effect of atmospheric pressure on the detection of secondary particles will be discussed in Chap. 11.

Further measurements at different altitudes and on board aircraft had been already carried out during the 1940s, also by Auger and collaborators. Within a few years, the first models were also formulated to try to interpret the existence of these showers and their properties, including the presence of high-energy mesons within the showers.

At the end of the 1940s, about a decade after their discovery, the knowledge of extensive air showers nevertheless presented several problematic aspects. A reading of the scientific papers of that period by the physicists most directly involved in this activity, including Janossy and Auger himself, shows some of these problems.

In the work of Janossy [Janossy1949] it is recognized, for example, that extensive air showers are mainly made up of electrons and photons but contain a certain percentage of particles that are more penetrating than electrons. The nature of these particles—as discussed in this work, also quoting the work of Auger and his group [Auger1949]—seems to be unable to be traced back to that of ordinary mesons, but rather to that of $\Lambda$ mesons, or heavy electrons: particles with a mass equal to 3–10 times the mass of electrons. Experimental evidence had also been cited of the existence of these hypothetical particles, obtained by Cowan [Cowan1948] through the observation of a track in a cloud chamber operated at high altitude. We recall that only around the end of the 1940s was the role of mesons clarified, with the observation of the pion and its possible decay, so a unitary framework about the structure of the showers was still being defined at the time.

## 7.3   An "Operational" Definition and the First Properties of Extensive Air Showers

An excellent review of the situation concerning the results and problems concerned with the extensive air showers at the end of the 1940s is that carried out by Giuseppe Cocconi (1914–2008) in 1949 [Cocconi1949a]. Cocconi starts from the consideration that extensive air showers are the only known phenomenon in nature in which enormous energies are at play, between $10^{15}$ and $10^{18}$ eV (later, even larger energies will be measured, to about $10^{20}$ eV), and believes that, after a decade since their discovery, the results and interpretations are sufficiently developed to allow a clear picture of the situation.

What is meant by an extensive air shower? To clear the picture of possible confusions about the experimental description of what an extensive air shower is, Cocconi provides a sort of operational definition: an event is to be interpreted as due to an extensive air shower when we observe the simultaneous arrival in n (> 1) horizontally placed detectors of at least one ionizing particle due to cosmic radiation, with the condition that the horizontal distance between the detectors is at least 10/n–20/n times greater than the average size of the detectors used, and in any case not less than 2–4 m. While this operational definition of an extensive air shower can eliminate some showers of small size or made up by only a few particles, it certainly helps to eliminate events that could be improperly considered to be extensive air showers, for example single particles arriving to a detector and accompanied by some secondaries generated in the air or locally produced. A set of Geiger counters (or ionization chambers) placed at a certain relative distance can therefore be used to signal the arrival of a shower by meeting the requirements described above. The coincidence events between sets of detectors operating in these conditions will therefore be indicative of the detection of an extensive shower, with the presence of a large number of particles scattered over a very large area, hundreds or thousands of square meters.

Cocconi then recalls that the detection of these showers has highlighted up to that moment the existence of three components: a "soft" component, a highly penetrating component, and a neutron component, even if the understanding of these different components, especially for the last two, is not yet complete.

With regard to the soft component, it can be said that coincidence events between small unshielded detectors (Geiger counters or ionization chambers) placed outdoors, basically are coincidences due to electrons, which make up the vast majority of the particles present in the shower.

An experimental characterization of the number of coincidences observed between detectors is provided by the measurement of the so-called "decoherence curve", i.e., the probability of observing coincidences between two detectors as a function of their distance d. The first Auger measurements around 1938, already discussed (see Fig. 7.4), had shown evidence of coincidence events even between detectors located 300 m away. In subsequent years, coincidence measurements between distant detectors were carried out by Skobeltsyn, Zatsepin and Miller [Skobeltsyn1947], obtaining evidence of events up to a distance of 1000 m.
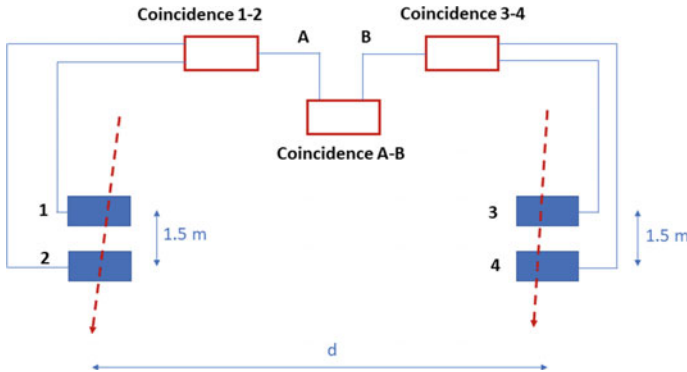
**Fig. 7.5** Arrangement of detectors used by Skobeltsyn and collaborators to measure coincidences between pairs of detectors placed at large distances [Skobeltsyn1947]
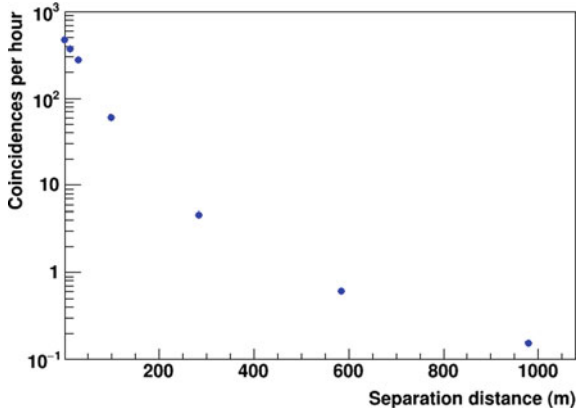
The technique used by Skobeltsyn and collaborators consisted in arranging the pairs of counters (1–2) and (3–4) superimposed at a small relative distance (1.5 m), making a "local" coincidence between the two counters of each pair, and then look for coincidences between pairs of distant detectors (Fig. 7.5). In doing so, the number of spurious coincidences could be greatly decreased, as it involved quadruple rather than double coincidences.

Taking advantage of this arrangement, Skobeltsyn and collaborators were able to measure the decoherence curve represented in Fig. 7.6, using 4 sets of Geiger counters, each with a relatively large sensitive area, equal to 1840 cm². The coincidence time between the two counter pairs was about 4 μs, which allowed a spurious coincidence rate of 0.03 per hour, against a measured coincidence rate, at a distance of 600 m, equal to 0.6 per hour. The measurements shown in Fig. 7.6 were carried out at a rather high altitude, at 3860 m, on Mount Pamir.

Another important property of extensive air showers concerns the density $\Delta$ of particles (number of particles in the shower per unit area). Measurements aimed at studying the density of particles were carried out by Cocconi and collaborators [Cocconi1944a, Cocconi1946a] both at altitudes close to sea level and at about 2000 m above sea level, obtaining results that could be parameterized with a power law of the type

$$N(\Delta) = k\Delta^{-\gamma}$$

where $N(\Delta)$ represents the rate of showers with density $> \Delta$, and $\gamma$ represents an exponent whose value depends on the observation altitude. The technique for extracting the particle density in the shower consists in comparing the number of coincidences obtained between n counters and $(n - 1)$ counters in the same area and is described in Appendix G. In the measurements carried out by Cocconi and collaborators, particle density were estimated from about 10 to over 200 particles/m².

**Fig. 7.6** Decoherence curve measured by Skobeltsyn and collaborators with the arrangement of counters shown in the previous figure, up to relative distances of about 1 km [Skobeltsyn1947]

An important feature to be evaluated for extensive air showers is their abundance at different altitudes: the first studies of the dependence of the rate of extensive air showers on altitude date back to the early 1940s. Hilberry, for example, investigated the variation in the number of showers observed, from sea level up to 4300 m on Mount Evans [Hilberry1941]. The detection apparatus consisted of a set of 4 Geiger counters, two placed in a telescopic configuration on each other and the other two positioned at a distance of 1.25 m symmetrically with respect to the telescope. The detectors were simply placed in a car (a station wagon of the time), which made several stops between sea level and the maximum altitude reached. The number of quadruple coincidences between the different counters, which can be interpreted as the measured number of showers, is shown in Fig. 7.7.
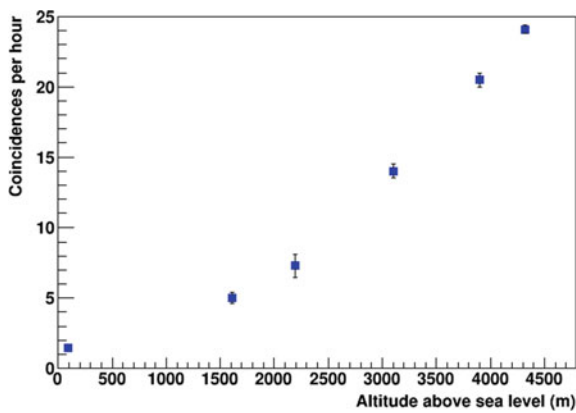


**Fig. 7.7** Number of hourly coincidences measured between different Geiger counters, as a function of the altitude of the observation site [Hilberry1941]

As it can be seen from these results, the intensity of the showers increases a lot with altitude, such that at an altitude of 4000 m the number of showers observed is about 15 times higher than at sea level. Already in this work the results were compared with a trend obtained by the assumption of a power law for the primary energy distribution, with an exponent of the order of 2.6–2.8, which starting from a certain altitude gave a good representation of the results.

Measurements at higher altitudes were carried out a few years later, using detection equipment installed on board airplanes, up to an altitude of 12,000 m [Kraybill1948, Kraybill1949]. The detection apparatus, consisting of nine Geiger counters of 75 cm$^2$ active area, had been mounted for these measurements on board a B29 aircraft, flying between the altitude of 6000 m and 12,000 m. The counters arranged in the same line along the longitudinal part of the aircraft, at various relative distances, were operated selecting different combinations of triple coincidences; under these conditions the number of spurious coincidences was in the order of 0.03/h, while the rate of measured coincidences was in the order of 10 coincidences/hour. A first set of results was obtained by flying at a constant altitude (or rather at a constant atmospheric pressure), as a function of the geomagnetic latitude, observing negligible variations in passing from latitudes 0°–30° N to the interval 30°–63° N.

The number of triple coincidences as a function of altitude is shown in Fig. 7.8. Compared to the data shown in the previous figure, these data, also measured at higher altitudes, suggest the achievement of a maximum, or plateau, around the altitude of 7000–8000 m, followed by a subsequent decrease.

These characteristics, observed in extensive air showers, suggested that the soft component present in the showers was made up of electrons and photons, generated through electromagnetic cascade processes induced by very high-energy primary electrons ($> 10^{14}$ eV) in the upper part of the Earth's atmosphere. This assumption about the existence of very high-energy primary electrons is not necessary, something
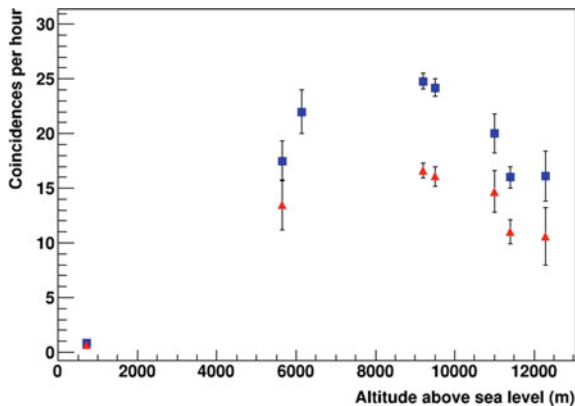


**Fig. 7.8** Rate of atmospheric showers (triple coincidences between Geiger counters located on board an aircraft) as a function of the altitude [Kraybill1949]. The two datasets, with different symbols, refer to different distances between the counters

of which Cocconi himself was aware, admitting that other primary particles can also generate the same electromagnetic cascade, with the presence of electrons and photons. This means that looking at the soft component of the showers is not the best strategy to understand their nature, even if this component is predominant. Rather, it is necessary to investigate the other components, though they have very small abundances: the penetrating component and the neutron component.

For the study of the penetrating component, the detection devices can be similar to those used for the soft component, i.e., combinations of counters arranged into appropriate geometric configurations and operating in coincidence, with the condition that they are effectively shielded with an adequate amount of lead, at least 20 cm, above the detectors and along their sides. Under these conditions, several observable aspects proved effective in elucidating the main properties of atmospheric showers.

A first aspect concerns the contemporary existence of the soft component and the penetrating one. In fact, measurements of the penetrating component in the showers showed that a soft component was always associated with it and vice versa; in other words, the two components were always present, so that it was not possible to explain the soft component in the showers with the existence of a single process, such as a pure electromagnetic cascade. Conclusions of this kind were reached following the measurements carried out by Cocconi and collaborators [Cocconi1946b], and by Treat and Greisen [Treat1948], through the use of shielded (for the penetrating component) and unshielded (for the soft component) counters. Similar conclusions were also obtained by Fretter [Fretter1948] by observations of events in cloud chambers.

A second aspect concerned the relative abundance of the two components, soft and penetrating. At sea level the penetrating component was about 2% compared to the soft one, while this proportion increased with altitude, resulting in 3% and 4% at altitudes of 3200 m and 4300 m respectively, as obtained from the measurements reported by Treat and Greisen [Treat1948]. These values, however, are only indicative, as the abundance of the measured soft component strongly depends on the thickness of the absorber surrounding the detectors. Furthermore, as it soon became evident, this proportion between the two components is different in the different regions of the shower. In fact, electrons and penetrating particles are created with different mechanisms, which may result in a different angular distribution for the two. The study of this proportion between the components can therefore effectively help to understand the nature of the processes involved in their production, in particular to understand if the structure of the extensive air shower includes a single "core" or can have a "multiple core" structure, as some theories predicted at the time [Lewis1948].

As regards the neutron component, evidence of the existence of neutrons associated with extensive air showers had already been obtained in those years [Tongiorgi1948a, Tongiorgi1948b], by means of $BF_3$ proportional counters, estimating an abundance of this component (at least for low energy) similar to that of the penetrating component—about 1–2% at sea level. Although at that time the experimental data on the production of neutrons were still scarce, it seemed evident that they were produced not by the soft component, but by a more penetrating component,

and that therefore a non-negligible fraction of this component was also constituted by nucleons.

These and other arguments supported the hypothesis that the two components, soft and penetrating, were the result of a unique process, which starts from the interaction of a primary, most likely a very high-energy proton. Unified descriptions of such processes had already been proposed at that time by Greisen [Greisen1948].

## 7.4  Towards a More Complete Description of the Formation of Extensive Air Showers

In the aforementioned article by Greisen [Greisen1948] we can find a concise but clear description of the generation of an extensive atmospheric shower, which revolves around the existence of the neutral meson. By reviewing experimental evidence of various kinds, from the first evidence of the existence of a neutral meson, to the absorption of mesons in the subsoil, to the dependence on the altitude of the number of local showers created for a different thickness of material positioned above the detectors, Greisen concludes that a unitary description of these processes can be made by assuming that a primary proton—or a heavy meson—interacts, by nuclear interaction, with a nucleus of the atmosphere, producing groups of mesons, which contain both charged mesons (of both signs) and neutral mesons, as well as nucleons.

Neutral mesons almost instantly decay into two gammas, thus initiating an electromagnetic cascade. A further contribution to the production of electrons and positrons comes from the decay of charged pions into muons and from the decay of the latter into electrons or positrons. The electrons in turn produce gammas through the mechanism of the emission of bremsstrahlung radiation and the positrons can annihilate themselves with the electrons of ordinary matter giving rise to gammas. Due to the very high energies, the particles of the electromagnetic cascade are emitted along directions little different from that of the primary particle. Even the charged pions emitted in these nuclear collisions are characterized by high energies, and therefore are emitted mainly within a cone with a small aperture with respect to the initial direction of motion. Through successive inelastic collisions with the nuclei of the atmosphere, the charged pions can in turn produce a cascade consisting of mesons and nucleons.

A typical structure of an extensive air shower is shown in Fig. 7.9. The most penetrating components of this shower, apart from the weakly interacting neutrinos, are represented by muons, capable of reaching the sea level, despite their average life at rest, due to the relativistic dilation of time. The more energetic muons are also capable of crossing a considerable thickness of solid material, such as terrestrial rock, and therefore of being detected even at great depths in the subsoil, while the electromagnetic component is absorbed much more easily even by a very small amount of material.
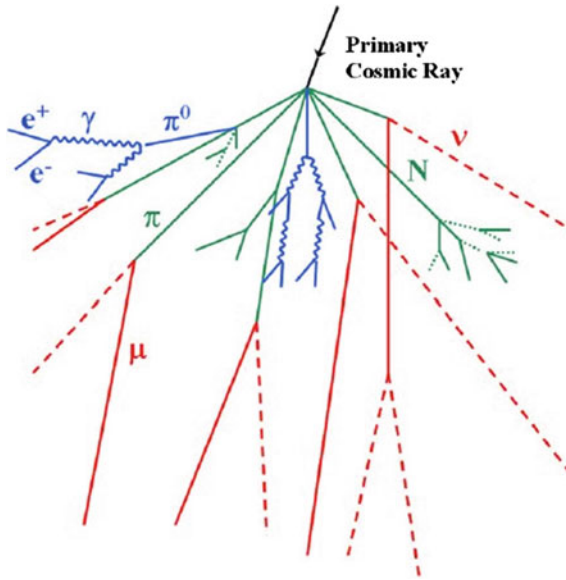
**Fig. 7.9** A qualitative representation of a typical atmospheric shower, with its main components. The interaction of a primary particle gives rise to a nuclear interaction in which nucleons and pions (charged and neutral) can be produced. The decay of the neutral pions into two gammas gives rise to the electromagnetic component, with processes of creation of electron–positron pairs. The charged pions can decay, producing muons, or further nuclear interactions. Muons and neutrinos represent the most penetrating component of the shower

Much progress has been made since the 1950s, about the experimental study and understanding of extensive air showers, up to the present time, in which some of the most relevant problems concerning modern physics are strictly related to the study of showers of extreme energy. Without going into too much detail of all the mechanisms of interaction that contribute to determining the detailed structure of a shower, we will briefly review some of their main properties, as they emerged from the experimental activity carried out since 1950s.

## 7.5   The Study of Atmospheric Showers Since the 1940s

We know today that most of the atmospheric showers are created as a result of the interaction of extremely energetic hadrons, which arrive isotropically on the Earth's atmosphere, coming from the outer space and giving rise to subsequent nuclear collisions with the nuclei of the atmosphere, as a result of which a huge number of secondary products are produced, which in turn can decay or interact to produce new particles.

As the shower propagates longitudinally in the atmosphere, along the initial direction of motion of the primary particle, it also spreads transversally. The shower includes a hadronic component, in which, however, a significant part of the energy is converted into electrons and high-energy photons, through the decay of the neutral pions, thus contributing to the electromagnetic component. The proportion between the abundance of the various particles that make up the shower changes along the direction of propagation and is therefore different at different altitudes. Muons and neutrinos represent the most penetrating component of the shower.

The development of the extensive air shower along the atmosphere is accompanied by further physical processes (Cherenkov emission, fluorescence radiation, radio waves) that have been used in more recent years as an additional tool to understand the properties of the showers.

The longitudinal and transverse extensions of a shower essentially depend on the energy of the primary. For low-energy primaries, the development of the shower stops in the upper atmosphere, and many of the secondary products, with the exception of muons and neutrinos, are unable to penetrate to sea level. On the contrary, for extremely high energies, the development occurs down to altitudes close to sea level, with the presence of the other components as well. The electromagnetic component of the shower is in any case absorbed even by a modest layer of material, while energetic muons are able of penetrating even into the subsoil down to great depths. Furthermore, neutrinos, due to their reduced interaction cross section, can cross an enormous thickness of rock—even the entire Earth—without being appreciably reduced in number. In fact, their detection is extremely difficult and requires huge detectors to reach a reasonable probability of interacting within their volume.

## 7.6 The Longitudinal Development of an Extensive Air Shower

After the discovery of the existence of extensive air showers, one of the basic characteristics that was investigated was the study of these showers at different altitudes, both in terms of their abundance and their composition. A large number of measurements were made using detectors positioned at different altitudes, from the sea level to accessible mountains. For higher altitudes, up to about 12,000 m in height, balloons and, above all, airplanes were used, capable of carrying a certain number of small detectors operating in coincidence [Kraybill1948, Kraybill1949]. However, due to the limited transverse dimensions of these arrays of detectors, it was possible to characterize only showers with a small size.

One of the main properties of an extensive air shower is the number of particles it contains, or shower size. The shower size is often expressed in terms of the number of charged particles present, since gammas and neutrinos require different detection techniques, or even in terms of the number of electrons/positrons only, since they are the most abundant component at sea level. The shower size essentially depends on

the energy of the primary particle, as well as on the angle of inclination with which it arrives in the atmosphere, and on the height at which the first interaction occurs. The shower size grows with the energy E of the primary almost in proportion to it, following a law of the type

$$N_e = \alpha E^n$$

where the exponent n is of the order of 0.9.

The longitudinal development of the shower—therefore the shower size at various atmospheric depths—can be experimentally evaluated by observing the fluorescence light in the air, produced by the passage of charged particles, or by the light produced by the Cherenkov effect.

It has a characteristic trend, which starts from low values near the point of first interaction, reaches a maximum at a certain atmospheric depth and then decreases again near the ground (atmospheric depth of about 1000 g/cm$^2$). The relationship between altitude and atmospheric depth is discussed in Appendix H.

The position of the maximum of the shower, $X_{max}$ (atmospheric depth at which the number of particles is maximum), progressively moves towards greater atmospheric depths (lower altitudes) for greater primary energies, as can be seen in Fig. 7.10, which reports one of the first detailed simulation calculations made by Grieder in the late 1970s [Grieder1979].

In the first measurements, the uncertainty in the longitudinal profile was so high as to allow only the estimate of the average value of the distribution and not the distribution itself. A comparison between the experimentally obtained distributions and simulation calculations of the development of the showers allows today to evaluate the goodness of the hadronic interaction models and other aspects of the overall development of the extensive air showers. Usually, the statistical fluctuations from
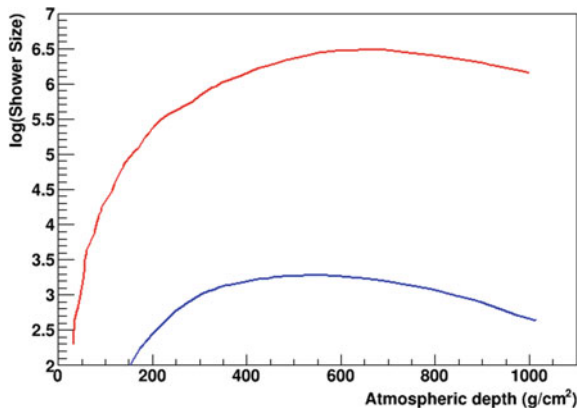


**Fig. 7.10** Shower size of extensive air showers, induced by primary protons of energy $10^{13}$ eV (lower curve) and $10^{16}$ eV (upper curve), at different atmospheric depths, highlighting the longitudinal development of the showers. Data adapted from [Grieder1979]

shower to shower, with the same energy and orientation of the primary, are high, so it is necessary to consider the average information extracted from a large number of individual shower events.

The longitudinal profile ultimately depends on the physical processes that govern the development of the shower, both of the hadronic and the electromagnetic type, therefore on the cross sections (probability) of these processes, on the multiplicity of particles created in each interaction and on the proportion between the different particles, as well as by the kinematical constraints which govern the production of each individual particle species.

Profiles of this kind can be fitted with semi-empirical functions to parameterize their behaviour. One of the widely used functions was introduced by Gaisser and Hillas [Gaisser1977]:

$$N(X) = N_{\text{max}} \left( \frac{X}{X_{\text{max}}} \right)^{\frac{X_{\text{max}}}{\lambda}} e^{(X_{\text{max}} - X)/\lambda}$$

where X represents the atmospheric depth (expressed in g/cm$^2$), $N_{\text{max}}$ is the number of particles corresponding to the maximum $X_{\text{max}}$, while $\lambda$ represents a characteristic depth (usually assumed to be 70 g/cm$^2$). Figure 7.11 shows as an example a typical longitudinal profile (apart from the multiplicative factor $N_{\text{max}}$), which can be described by the previous parameterization, assuming a value of $X_{\text{max}}$ equal to 300 g/cm$^2$ and a value of $\lambda$ equal to 70 g/cm$^2$. Appendix I reports additional examples of longitudinal profiles evaluated from parameterizations of this type.

In this relation it is assumed that the first interaction takes place exactly at an atmospheric depth $X = 0$. However, it is possible to generalize this relationship by
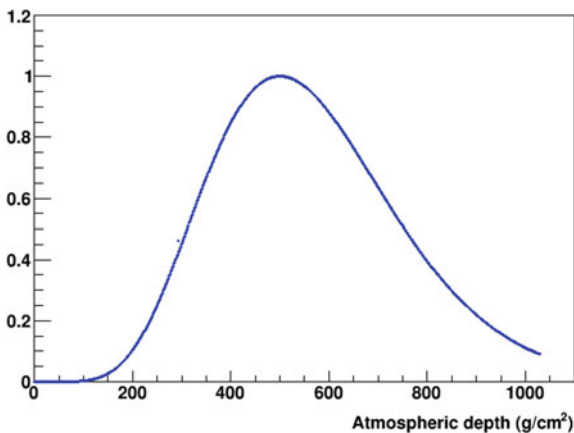


**Fig. 7.11** Typical shape of a longitudinal profile of an extensive air shower, as a function of the atmospheric depth, according to the parameterization of Gaisser and Hillas, with $X_{\text{max}} = 500$ and $\lambda = 70$ (in g/cm$^2$)

introducing a further parameter $X_0$, which denotes the atmospheric depth at which the first interaction occurs [Pryke2001].

The dependence of the position of the shower maximum on the energy of the primary is characterized by a quantity which is called the elongation rate. This quantity, introduced by Linsley [Linsley1977] is defined by the variation of the quantity $X_{max}$ per decade of energy:

$$ER = \frac{dX_{max}}{d \log_{10} E}$$

It therefore represents a measure of the displacement of the maximum of the shower when the energy of the primary varies by a factor of 10. As an example, in the range of energies between about $10^{17}$ and $10^{20}$ eV, the elongation rate extracted from the data is of the order of 70 g/cm$^2$ per energy decade [Walker1981].

Simulation calculations carried out using codes that make use of the most common hadronic interaction models show that the atmospheric depth at which the maximum of the shower occurs depends not only on the energy but also on the nature of the primary, i.e., whether it is a proton, or an electron, a gamma or a heavy nucleus, as well as on the angle of inclination with respect to the vertical.

The attenuation of an extensive air shower in crossing the thickness of air that constitutes the Earth's atmosphere can be discussed both in terms of the attenuation of the rate of these showers at different altitudes, and in terms of the absorption of the number of particles which constitute it. Although a complete description of the development of a shower occurred in more recent years, the concepts of attenuation length for the rate (rate attenuation length), $\Lambda_{att}$ (expressed in g/cm$^2$), and length of absorption for the number of particles (particle number absorption length), $\lambda_{abs}$ (also in g/cm$^2$), are still used today, together with their inverse quantities $\mu_{att}$ (cm$^2$/g) and $\mu_{abs}$ (cm$^2$/g), i.e. the attenuation and absorption coefficients.

The attenuation of the rate, that is the frequency of showers with a given shower size, as found in many experiments, follows, to a first approximation, an exponential law with the atmospheric depth X measured along the axis of the shower:

$$I(X) = I(X_0)e^{-\frac{X}{\Lambda_{att}}} = I(X_0)e^{-\mu_{att} X}$$

so, the variation with the atmospheric depth X will be

$$-\frac{d \ln I(X)}{dX} = \mu_{att} = \frac{1}{\Lambda_{att}}$$

The absorption of the particles of the shower can be evaluated by assuming that the shower size has a distribution represented by a power law

$$I(N) = kN^{-(\gamma+1)}$$

where $\gamma$ is the spectral index, approximately equal to 1.7. It can be shown that the variation with atmospheric depth will be given by

$$-\frac{d \ln N}{d X} = \mu_{abs} = \frac{1}{\Lambda_{abs}} = \frac{1}{\gamma \Lambda_{att}}$$

For inclined showers, it is necessary to consider the actual atmospheric depth crossed, based on the angle of inclination. At a given altitude, or atmospheric depth, an inclined shower will need to be more energetic than a vertical shower to produce the same shower size. In other words, at the same atmospheric depth, the rate of showers with a given shower size will decrease with the increase in the polar angle of inclination according to the relationship

$$I(X, \vartheta) \sim (\cos \vartheta)^{X/\Lambda_{att}}$$

Measures to determine the attenuation and absorption coefficients (or the corresponding attenuation or absorption lengths) were carried out starting from the early 1940s using small arrays of detectors at various altitudes or mounted on board aircraft. Ground measurements at various altitudes were carried out, among others, by Auger [Auger1939a, Auger1939b, Auger1945], Cocconi and collaborators [Cocconi1946a, Cocconi1949a, Cocconi1949b, Cocconi1949c, Cocconi1949d], Broadbent [Broadbent1950], Hilberry [Hilberry1941], Treat and Greisen [Treat1948], and Antonov and collaborators [Antonov1957], some of which have already been cited. These measurements, as well as the first obtained on board airplanes, used very small detector arrays (a few meters in size). Among the first measurements carried out on board airplanes, we should mention those made by Maze [Maze1948], Biehl [Biehl1949], Kraybill [Kraybill1948, Kraybill1949, Kraybill1954a, Kraybill1954b], Hodson [Hodson1952, Hodson1953a, Hodson1953b], and above all, an extensive series of investigations organized by Antonov and collaborators in the years from 1960 to the mid-1980s [Antonov1960, Antonov1964a, Antonov1964b, Antonov1971, Antonov1975, Antonov1983], by means of detectors distributed over larger areas (about $30 \times 30$ m$^2$), making use of space located not only in the fuselage but also along the wings of the aircraft.

The dependence on the zenith angle $\vartheta$ corresponding to the axis of the shower is a further information that allows us to better understand the properties of the shower, since the amount of atmosphere that the particles must cross to reach a given altitude h is equal to $X(h, \vartheta = 0)\sec(\vartheta)$. For large zenith angles (shower axis close to the horizontal direction) it is necessary to take into account the curvature of the Earth to evaluate the thickness of air crossed, as it was done for the individual particles (see Appendix J). The numerous measurements carried out already in those years made it possible to establish that the angular dependence of the rate of the showers roughly follows a relationship of the type

$$I(\vartheta) = I(\vartheta = 0)(\cos \vartheta)^n$$

where the exponent n depends on the shower size (for example it is of the order of 8 for a particle density of about 20/m$^2$ and increases up to n = 10 for a density of 250/m$^2$). The exponent also decreases with altitude.

Historical measurements of the dependence on the zenith angle were carried out in the 1940s by Hilberry [Hilberry1941], Cocconi and Tongiorgi [Cocconi1946c, Cocconi1949e], Deutschmann [Deutschmann1947], Williams [Williams1948] at altitudes between sea level and about 3000 m, and by Biehl [Biehl1949] and Kraybill [Kraybill1954b] at higher altitudes, up to about 9 km, by means of instrumentation on board aircraft. Further measurements, in different locations around the world and at different altitudes, were also made in the following decades. As an example, Fig. 7.12 shows an angular distribution (dependence of the shower rate on the zenith angle) obtained at sea level by Bassi and collaborators [Bassi1953], for shower sizes of the order of $10^5$–$10^6$, by means of the time correlation between 3 detectors (liquid scintillators, with a sensitive area of 600 cm$^2$) placed at a relative distance of a few tens of meters, in a right-angled triangle configuration. The distribution obtained shows a strong dependence on the cosine of the zenith angle, compatible with a very high exponent.

The measurement of the direction of arrival of the shower (in polar coordinates θ, φ) allows not only to determine the dependence of the rate on the amount of matter crossed, but also to carry out studies on the influence of the geomagnetic field and look for possible effects of anisotropy, as we will see later. The direction of arrival of an extensive air shower can be estimated by reconstruction of the individual shower particle with tracking detectors or by the use of an array, observing the difference in the time of arrival of the particles in the individual detectors of the array (Appendix K).

We can define an "age" parameter s of a shower, which characterizes the stage of development of the shower in the atmosphere. This concept derives from the treatment of electromagnetic showers, but it can also be applied to hadronic showers
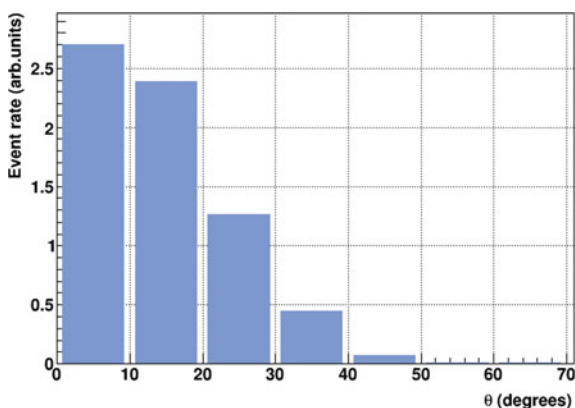


**Fig. 7.12** Angular distribution (shower rates as a function of the zenith angle), obtained by Bassi and collaborators [Bassi1953] at sea level. Data adapted from their work

[Kamata1958]. In the case of an electromagnetic shower, the "age" parameter is linked to the atmospheric depth X by the relation

$$s = \frac{3t}{(t + 2\beta)}$$

where t indicates the ratio between X and $X_0$ (= 1030 g/cm$^2$), and $\beta = \ln(E/E_c)$, being E the energy of the primary, $E_c$ the critical energy for the production of secondary particles. Referring to the longitudinal development, as represented for example in Fig. 7.11 or in the plots shown in Appendix I, the first part of the shower is characterized by a parameter s < 1, while the second part, after the maximum, is characterized by s > 1.

Showers generated in the upper part of the atmosphere are called "old" and have a high value of the s parameter. They are generally produced by lower energy primaries or heavier nuclei. On the contrary, "young" showers have a limited value of s, being produced in the lower part of the atmosphere, and are generally associated with more energetic showers or created by light nuclei.

## 7.7   The Transverse Development of an Extensive Air Shower

An important property of extensive air showers is given by the spatial distribution of the associated particles. In the case of electron-generated showers, the particles produced are expected to be more concentrated around the axis of the shower, with a lateral (transverse) profile governed by the Molière distribution, while in the case of hadron-generated showers, we may expect a larger spread of the particles around its axis. Quantitative measurements of the transverse development of extensive air showers were first obtained in the late 1940s, for example by Williams [Williams1948] and Cocconi [Cocconi1949f].

In the experiment carried out by Cocconi and collaborators, for example, a few detectors were used (each of them based on a multiple coincidence between different counters, partly shielded by lead), to determine the "core" of the shower, while additional, segmented, detectors, located in various positions, were employed to measure the density of particles (both of the electrons and of the penetrating component) at various distances from the core itself. In this work we may find also the first examples of "pictures" of the shower distribution, obtained from the lighting of neon tubes arranged geometrically in the array, which give an idea, albeit approximate, of the presence of particles at various distances from the core.

The experiment, for that time, had a certain complexity, both in terms of the number and type of detectors to be used (including a cloud chamber), and for the location and management of the experiment itself. The detectors, in fact, installed at an altitude of 3260 m, were positioned inside tents, and interconnected by long

cables, up to a length of about 200 m, which represented the maximum separation between the detectors. The electronics required for the various detectors, as well as multiple coincidence circuits, with resolution times of 25 μs, included a sort of "trigger" capable of controlling data acquisition by the other detectors and also taking photographs from the cloud chamber. The heavy materials that acted as screens had masses of the order of tons and had to be moved together with the detectors. Although the article is signed by only three authors, they explicitly acknowledge that the management of this experiment, which lasted over two months, had required the contribution of many other collaborators, both in the construction and management phases.

The results of this experiment made it possible to quantitatively evaluate the density of electrons at various distances from the core of the shower and to compare the observed shape with the standard theory of electromagnetic cascades. This result, deduced from the cited article [Cocconi1949f], is shown in Fig. 7.13.

In the original figure [Cocconi1949f], the data are well reproduced by the curve, based on Molière's theory, which at that point could be used to evaluate the overall number of particles (shower size). As an example, Cocconi and collaborators cite the characteristics of the largest observed shower, with a density of up to 500 particles/m$^2$
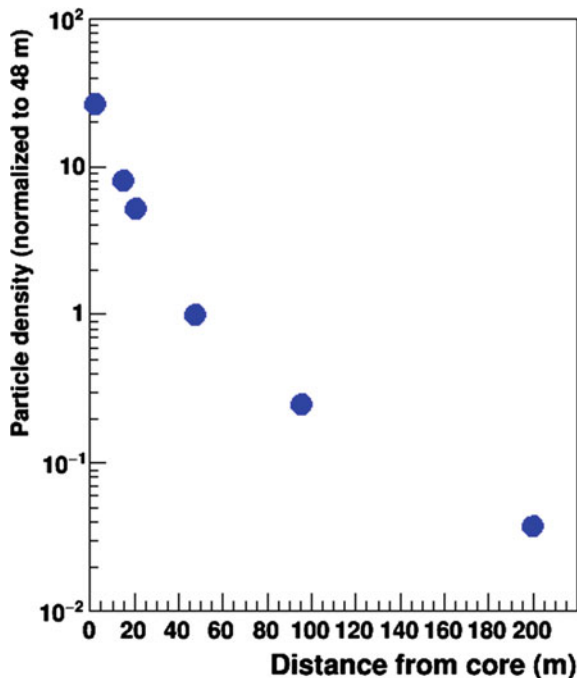


**Fig. 7.13** Particle density (soft component) estimated at various distances from the core, normalized to that measured at a distance of 48 m, obtained by Cocconi and collaborators [Cocconi1949f]. The data are adapted from their work

at a distance of 100 m from the core, corresponding to a total number of particles in the shower equal to $10^8$. Although with various limitations regarding the knowledge of the primary interaction point in the atmosphere, from these data it could be estimated a minimum energy of the primary equal to $10^{17}$ eV. By contrast, events originating from showers with very small size, with a density of about 4 particles/m$^2$ at a distance of about 3 m from the core, corresponded to a total number of particles of the order of 4000.

As for the penetrating component, this was estimated to be only 1–2% compared to the soft component, therefore not easily measurable in single showers. It was possible, however, to statistically estimate that the fraction of the penetrating component compared to the soft one increased with distance from the core (e.g., 1.5% at 48 m and 2.5% at 96 m). The distribution of the penetrating component is therefore "flatter", extending up to large distances from the core, where it is more abundant than the soft one, while the latter is more concentrated around the core.

The lateral widening of a shower at altitudes close to sea level can give rise to very large dimensions for high-energy showers, which can cover areas of several km$^2$, depending on the shower size. For example, it is illustrative to see maps of the coordinates (X, Y) of the impact points of the individual particles of an extensive air shower, to realize the number and distribution of these particles at a given observation level. Experimentally reconstructing such a map would involve using a detector with continuous coverage, sensitive to position and of enormous area, equal to the typical size of a shower with that energy, which of course is not possible for large showers. However, we can have a fairly precise idea of these distributions looking at the shape of simulated showers, employing one of the simulation codes existing today, which take into account the possible physical processes not only of the primary cosmic, but also of the secondary particles generated during the various steps.

Figure 7.14 gives an example of these maps, showing the position (X, Y) of the impact point in the horizontal plane, at the sea level, of the most abundant charged particles in the shower (electrons and muons), assuming a shower produced in the atmosphere by a vertical primary proton of energy equal to $10^{13}$ eV (10 TeV), whose axis intersects the origin (0, 0). The simulations were carried out with the CORSIKA code, one of the most used in the field of cosmic ray physics [Heck1998].

As can be seen, the particles—in this case several hundred—are distributed over a very large area, although the majority is concentrated in a smaller area around the origin. The number of secondary particles and the extension of the shower of course increase with the energy of the primary particle.

The lateral profile of a shower can be quantitatively represented through the radial distribution of the density of particles, which expresses the number of particles per m$^2$ existing at a certain radial distance r from the axis of the shower. These distributions are generally different for the different particle species contained in the shower. Figure 7.15 shows a typical radial distribution for electrons and muons in showers originating from primary protons of energy equal to $10^{12}$ eV, calculated on the basis of air shower simulation codes.
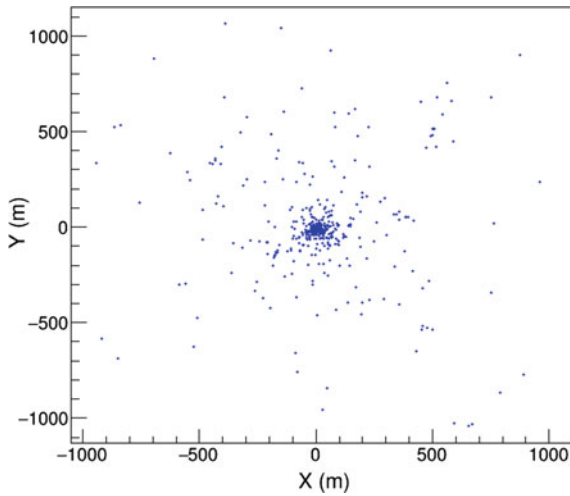
**Fig. 7.14** Map (X, Y) of the impact points at sea level of charged secondary particles (electrons and muons) generated during the development of an extensive air shower created by the interaction of a primary proton, of energy $10^{13}$ eV, incident vertically. Simulations produced with the CORSIKA code [Heck1998]
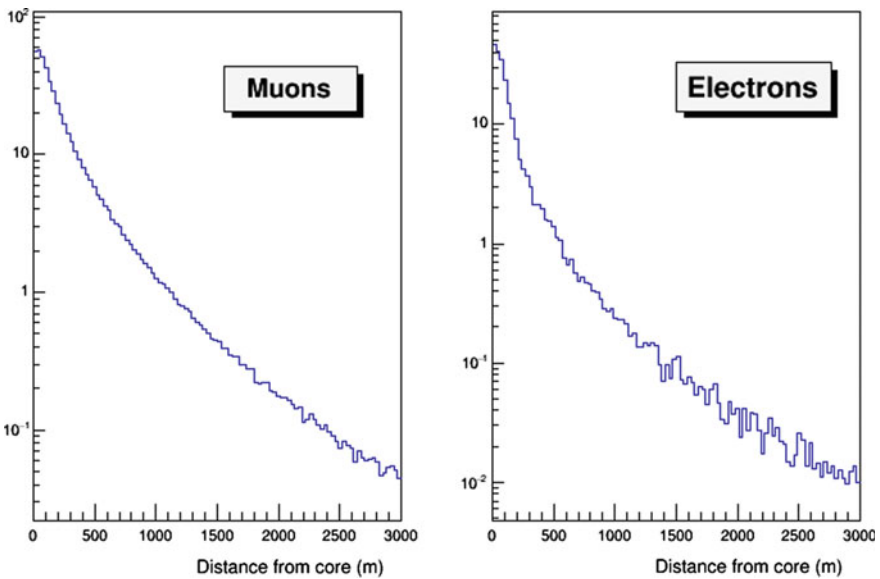


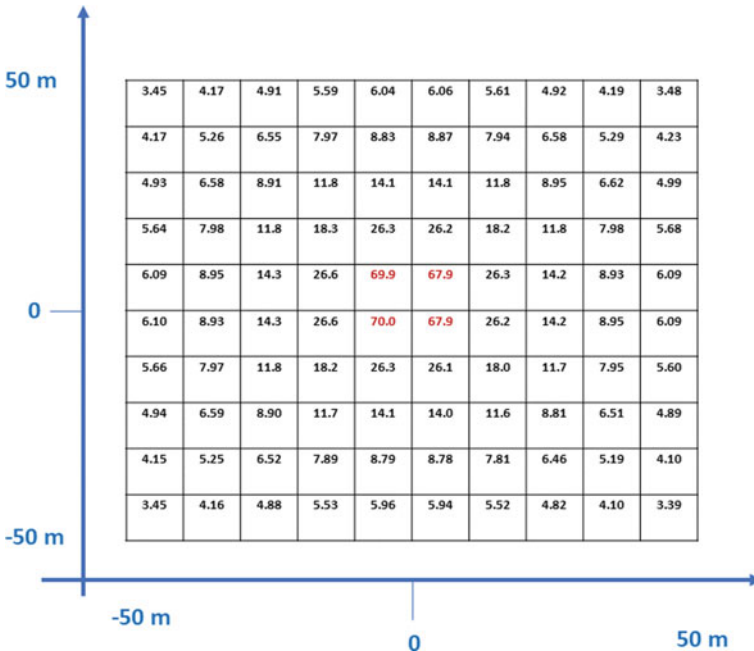**Fig. 7.15** Average radial distribution of charged particles (electrons and muons) in showers generated by protons of energy equal to $10^{12}$ eV. A lower threshold in energy, equal to 10 MeV and 1 GeV respectively, was assumed for electrons and muons. Simulations produced with the CORSIKA code [Heck1998]

These distributions are in principle symmetrical with respect to the axis of the shower; however, the effect of the Earth's magnetic field can deflect charged low-energy particles in different ways, creating asymmetry effects, which are generally negligible for higher-energy particles.

The experimental measurement of the density of particles in different positions, using detectors located on an appropriate area, can be used to estimate the position of the core and the direction of the axis of the shower (initial direction of flight of the primary particle). As an example, Figure 7.16 shows a two-dimensional map of density values (number of particles per m$^2$), calculated according to the CORSIKA simulation code for extensive air showers [Heck1998].

The density values refer in this case to showers generated by protons of energy equal to $10^{15}$ eV, with the axis at the origin ($X = 0$, $Y = 0$). The particles considered are muons and electrons, with a minimum threshold in energy. The numerical values show the average density in each cell ($10 \times 10$ m$^2$ in size), evaluated in the range from $X = -50$ m to $X = +50$ m, and from $Y = -50$ m to $Y = +50$ m. As it appears from the map, in the vicinity of the central cells, corresponding to the position of the core, a density of about 70 particles/m$^2$ may be estimated, which gradually decreases moving progressively away from the core.



| 50 m | | | | | | | | | | |
|---|---|---|---|---|---|---|---|---|---|---|
| | 3.45 | 4.17 | 4.91 | 5.59 | 6.04 | 6.06 | 5.61 | 4.92 | 4.19 | 3.48 |
| | 4.17 | 5.26 | 6.55 | 7.97 | 8.83 | 8.87 | 7.94 | 6.58 | 5.29 | 4.23 |
| | 4.93 | 6.58 | 8.91 | 11.8 | 14.1 | 14.1 | 11.8 | 8.95 | 6.62 | 4.99 |
| | 5.64 | 7.98 | 11.8 | 18.3 | 26.3 | 26.2 | 18.2 | 11.8 | 7.98 | 5.68 |
| | 6.09 | 8.95 | 14.3 | 26.6 | 69.9 | 67.9 | 26.3 | 14.2 | 8.93 | 6.09 |
| 0 | 6.10 | 8.93 | 14.3 | 26.6 | 70.0 | 67.9 | 26.2 | 14.2 | 8.95 | 6.09 |
| | 5.66 | 7.97 | 11.8 | 18.2 | 26.3 | 26.1 | 18.0 | 11.7 | 7.95 | 5.60 |
| | 4.94 | 6.59 | 8.90 | 11.7 | 14.1 | 14.0 | 11.6 | 8.81 | 6.51 | 4.89 |
| | 4.15 | 5.25 | 6.52 | 7.89 | 8.79 | 8.78 | 7.81 | 6.46 | 5.19 | 4.10 |
| -50 m | 3.45 | 4.16 | 4.88 | 5.53 | 5.96 | 5.94 | 5.52 | 4.82 | 4.10 | 3.39 |

-50 m          0          50 m

**Fig. 7.16** Average density of particles (muons and electrons) evaluated in a $10 \times 10$ m$^2$ grid, around the axis of the shower, located at the origin. Showers generated by vertical primary protons of $10^{15}$ eV energy. Simulations produced with the CORSIKA code [Heck1998]

Particle densities near the core can be very high, even thousands of particles per m$^2$, in the case of very energetic showers, but they rapidly decrease with radial distance. Their trend, in the case of purely electromagnetic cascades, was calculated by Nishimura and Kamata [Kamata1958]. In the range of values of the age parameter s between 0.5 and 1.5 this distribution can be written in an approximate form as a function of s, using the dimensionless variable x = r/r$_M$ (ratio between the radial distance perpendicular to the axis of the shower and the radius of Molière r$_M$) as

$$f(s, x) = x^{s-2}(1 + x)^{s-4.5} \frac{\Gamma(4.5 - s)}{2\pi\Gamma(s)\Gamma(4.5 - 2s)}$$

where $\Gamma$ represents the Gamma function. More complex functions to describe these distributions have been reported recently [Morales2019; Fadhel2021].

## 7.8  The Time Profile of an Extensive Air Shower

During the longitudinal and transverse development of an extensive air shower, due to the differences in speed of the various particles, and especially because of the different paths they follow because of the interaction processes and the various decays, not all particles arrive at the ground simultaneously. In particular, those far from the shower axis have on average a certain delay compared to the more central ones. We can then imagine the front of the shower as having the shape of a disc with a slight curvature, as shown in Fig. 7.17, which reports the results of a simulation for a shower induced by a proton of $10^{15}$ eV energy. Each point in the plot represents the arrival time of each single particle in the shower, associated with the distance X from the core. As it is seen, on average the particles farthest from the core, at a distance of a few hundred meters, have slightly longer times than those arriving in the vicinity of the core.

Due to the very high speed of the particles in the shower (close to the speed of light), all the particles of the shower reach the ground within a very short time interval, of a few nanoseconds near the axis of the shower, and slightly greater at the ends of the disc. We can imagine this curved disc as having a certain thickness, which increases with the distance from the axis, due to greater paths by the particles and corresponding larger statistical fluctuations. The time profile of the shower represents the distribution of the arrival times of the particles at sea level, with respect to the arrival of the first particle. Although most of the particles are concentrated in times of a few tens of ns, there may be a very long tail (hundreds of ns, up to a few microseconds), produced by the slowest particles in the shower (low-energy muons and nucleons, for example neutrons), while energetic muons, pions and kaons are concentrated in the region with very short arrival times, also due to their short average life. Figure 7.18 shows a typical temporal profile of a shower, obtained from Corsika simulations, in the case of vertical protons with energy $10^{13}$ eV.

Relative timing measurements between detectors were first introduced by Bassi, Clark and Rossi in the early 1950s [Bassi1953], using detectors based on liquid
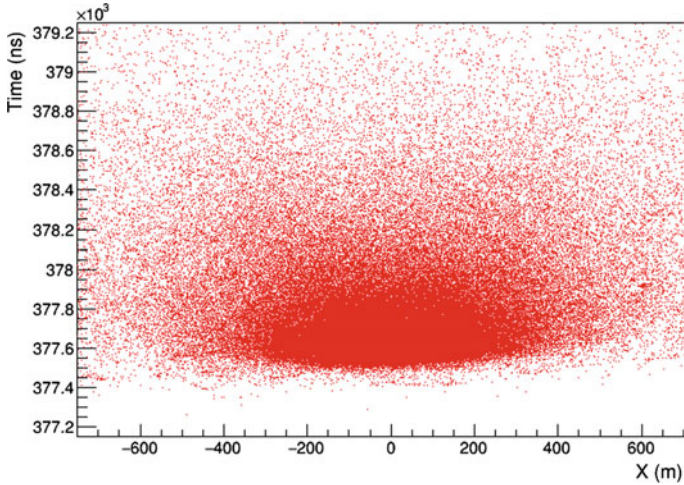
**Fig. 7.17** Characteristic shape of the wave front of a shower, generated by a proton of energy equal to $10^{15}$ eV. Results obtained from CORSIKA simulations [Heck1998]. Each point in the figure reports the arrival time (expressed in ns) of the individual particles in the shower, and the corresponding distance X from the position of the core
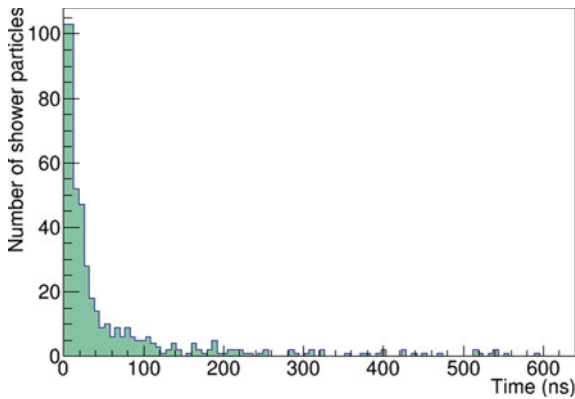


**Fig. 7.18** Distribution of the arrival times of charged particles (muons and electrons) in a shower generated by a vertical proton of energy equal to $10^{13}$ eV. Times are measured with respect to the first arrived particle. Results obtained from CORSIKA simulations [Heck1998]

scintillators, placed at distances between 3 and 30 m. They also made it possible to investigate the spatial (or temporal) thickness of the disk representing the wave front of the shower, and to extract, as already mentioned above, an angular distribution of the shower with a certain shower size.

The temporal information on the arrival of the particles from a shower in several detectors (at least three) placed at a certain relative distance, in fact, allows to evaluate,

on the basis of the sequence of arrival times, the direction of the shower axis by triangulation methods (See Appendix K). Subsequently, in the 1960s, the technique of relative timing between distant detectors was improved to the point of being able to reconstruct the direction of the shower axis, therefore the direction of arrival of the primary, with excellent precision. Arrays of detectors with good time resolutions allows to determine this direction even with resolutions of the order of 0.1° if the detectors are properly arranged.

# Chapter 8
# The Detection of Extensive Air Showers

**Abstract** The main experimental methods employed in the detection and reconstruction of extensive air showers are here discussed and commented, with wide examples of the techniques and analysis procedures originally employed for this task. The structure and performance of the ground particle arrays, collection of detectors to identify and reconstruct the arrival of a shower, are here discussed and a description is given of the main detection facilities which were used from mid-1940s. The chapter also discusses the detectors arrays based on the Cherenkov effect, the fluorescence detectors and the radio wave detection technique. A brief description of modern arrays, even those built with educational purposes is also presented. Details on how to reconstruct the shower direction by the relative timing associated to several detectors is discussed in Appendix K.

## 8.1 Direct and Indirect Methods

From what has been said so far about the nature and main properties of an extensive air shower, created by the interaction of a high-energy primary particle in the upper part of the atmosphere, it is clear that the primary particle could in principle be detected directly, by means of suitable detectors placed at very high altitudes, or, even better, on sounding balloons or satellites, even outside the Earth's atmosphere. Such detectors would have the advantage of directly detecting the primary particle, to try to determine its mass and energy. Such methods, called direct methods, however, have several limitations. First of all, the dimensions and the maximum weight of the detectors are strongly influenced by the fact that neither aboard balloons launched at stratospheric heights, nor aboard satellites (or as happens today, aboard the International Space Station) it is possible to install detectors of huge size. Since the flux of primary particles is greatly reduced as their energy increases, direct detection is realistically possible only up to certain energies of the primaries, of the order of $10^{14}$–$10^{15}$ eV.

Beyond these energies, indirect methods must be used, in which the information on the primary is obtained from the properties of the shower created in the atmosphere, by means of sets of detectors placed on the ground. In most cases, detector arrays, based on solid or liquid scintillators, are used for the detection of the secondary

particles contained in the shower. However, showers also produce other effects in the atmosphere that can be used for indirect detection, such as Cherenkov radiation, emission of radio waves and fluorescence light. Each of these components has given rise to specific techniques to detect the arrival of an extensive air shower and to measure some of its properties. More recently, the possibility of using acoustic effects, created by energetic and compact showers in dense media, such as water, has also been explored. In this chapter we will briefly mention each of these techniques, with particular reference to the use of particle detector arrays, due to its historical importance and the wide diffusion of this method. A recent review, very extensive and complete, of the characteristics of extensive air showers and their detection methods is that of Grieder [Grieder2009].

## 8.2    Arrays of Particle Detectors

The most common method for the detection of extensive air showers and for the reconstruction of their properties is to make use of suitable groups of detectors installed on the ground—either at sea level or at higher altitudes—which can operate in coincidence, indicating the simultaneous passage of individual particles belonging to the same shower. As we have seen, the number of particles present in a shower, even of not too high energy, is considerable and, for very high-energy showers, it can reach values higher than a million particles. It is therefore clear, especially for high-energy showers, that the detectors will only be able to detect a small fraction of these particles, based on the number of devices used, their size and geometric configuration. It is therefore a sampling of the shower, which is done in the positions occupied by the detectors, trying to deduce from this sampling some of the general properties of the shower itself. If the individual detectors are able to provide an estimate of the particle density detected in different positions, these values can be used to evaluate the position of the core (axis of the shower), the overall size of the shower and the shape of the particle density at various distances from the core, i.e., its lateral profile. This requires that the detectors not only signal the passage of the particles but also provide a response proportional to the energy deposited in their volume.

In terms of the energy released by a single particle at the minimum of ionization (for example a vertical muon), and assuming that this quantity is known for the detector, the deposited energy may be used to give a signal proportional to the number of equivalent vertical muons passed through its sensitive surface, and therefore to the density of particles in that position. This (analog) information can be extracted from scintillators, either liquid or solid, after an appropriate calibration phase. The temporal information associated with the arrival time of the particles in independent detectors can instead give information on the incoming direction of the particles and therefore on the axis of the shower, as discussed in Appendix K.

The reconstruction procedures for extensive air showers however are not trivial, as it is necessary to take into account different aspects which may distort the information.

For showers induced by vertical or almost vertical primary particles, the pattern of the distribution of the particles in the plane in which the detectors are arranged is symmetrical with respect to the axis, within the inevitable statistical fluctuations, and assumes a circular shape. However, for low-energy showers, the influence of the Earth's magnetic field can induce significant deviations from the original direction of motion, and different effects can even be observed for positively charged particles compared to negatively charged ones (separation of charges). Finally, for inclined showers the pattern of the distribution of the particles on the ground no longer has a circular shape, but rather an elliptical shape (Fig. 8.1), for obvious geometrical considerations. Additional aspects can further distort the shape of the distribution by producing asymmetries.

An array is therefore a set of N detectors arranged on a plane (although this is not a completely necessary condition) in certain geometrical positions $(x_i, y_i)$, $i =$ 1,... N. The geometrical arrangement and the number N of detectors determine the topology of the array. For example, imagine a geometrical configuration in which the detectors are located in a "hexagonal" geometry (Fig. 8.2). This has the advantage of arranging the detectors with equal relative distances between each detector and the six detectors surrounding it, with a repetitive arrangement of this pattern, which can be replicated to include a very large number of similar detectors.



**Fig. 8.1** Pattern of the particle distribution of a shower, in the case of vertical (left) and inclined (right) primaries. In the latter case, the pattern takes on an elliptical shape
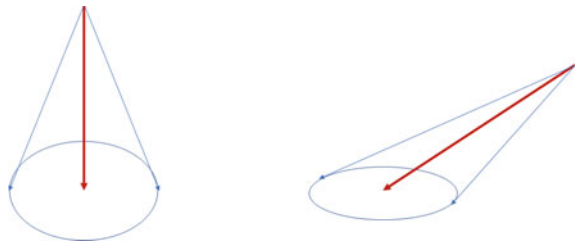


**Fig. 8.2** Typical hexagonal arrangement of detectors in an array for the detection of extensive air showers. Topologies of this kind have been widely used to build detector arrays, even with a very large number of similar detectors
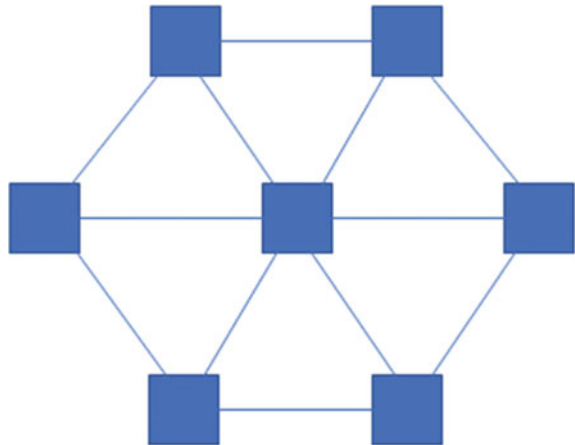
This configuration has been, and still is, widely used even in large experiments for the detection of extensive high-energy air showers. In other cases, it is preferred to use a more compact structure (with shorter distances between the individual detectors) in the central part of the array, and a more "looser" structure in the periphery of the array, possibly with detectors with a larger sensitive area, to compensate for the lower particle density.

The scale of the relative distances between the individual detectors and the overall dimension of the array determine the ability of the array to be sensitive to showers of lower or higher energy. More rigorously, generally on the basis of simulations, a quantity called the acceptance of the array is evaluated, commonly expressed as a function of the energy, or as a function of other parameters of the shower, such as the shower size, zenith angle of arrival, location of the core, ... [Grieder2009].

Another important parameter to establish the operating conditions of a detector array is represented by the choice of the event acquisition condition, what in the language of experiments is called "trigger". This is an arithmetic-logical condition established on the basis of the information provided by the detectors, to determine which are the "good" events to be acquired and which are to be discarded. The choice of a trigger is essential, as it is rarely possible to acquire and store data from all possible events, especially if there are many detectors in the array, and the rate of events by each detector is high. As an example, if we had 50 detectors and each had a single event rate of 100 per second, we would have 5000 events per second to consider. However, these events would be of little significance in this context, if the purpose is to detect the arrival of showers of a certain minimum energy. In this case, a more appropriate trigger condition could be the coincidence—within a certain time window—between at least k distinct detectors (for example k = 3 or 4, ...), a condition that greatly reduces the possible events to be acquired, preferentially selecting showers of energy higher than a certain value. A further condition to be defined in the trigger can be that of imposing a certain minimum energy deposited in each detector, which corresponds to a density of particles above a given threshold. In complex experiments even more elaborate triggers are used, based on the geometrical arrangement and the type of detectors employed.

The time coincidence window within which to search for signals from multiple detectors depends on the relative distance between the different detectors. If we assume that most of the particles in a shower travel at the speed of light, and we also want to detect showers with a direction of arrival close to the horizontal, we must consider the time for the shower front to arrive from one detector to another. Thus, with detectors 100 m apart, the time required for a particle moving at speed c, to propagate from one detector to another, is of the order of 300 ns. In this case, adequate time windows (at least $2 \times 300$ ns) must be chosen, in order to allow the detection of coincident particles from any arrival direction.

## 8.3   Detector Arrays Based on the Cherenkov Effect

For the detection of the Cherenkov light produced during the development of an extensive air shower in the atmosphere, photon detectors can be used, with a wide angular aperture, therefore with a considerable portion of the sky in their field of view.

Cherenkov light is produced by the passage of particles that have a speed higher than the speed of light in that medium. The Cherenkov effect was observed in the mid-1930s by Pavel Cherenkov and theoretically studied by Franck and Tamm. These, together with Cherenkov, obtained the Nobel Prize in 1958. A presentation of this phenomenon in connection with the technique of observation of extensive air showers has been reported, among others, by Watson [Watson2010]. Reminiscences of the period in which this technique was first used are reported by Jelley [Jelley1981] and by Thompson [Thompson2012]. Cherenkov himself was aware of the fact that the emission of this radiation could be used for the detection of particles. The production of Cherenkov light in the air was instead proposed by Blackett in 1948 as a technique for the detection of extensive air showers [Blackett1948]. Blackett had estimated that the intensity of this radiation should be very low, of the order of 0.01% of the total, and therefore difficult to observe.

Galbraith and Jelley, following Blackett's considerations, however, believed that a large shower, containing a large number of particles, could produce enough Cherenkov light to be detected. In 1953, making use of simple equipment (a metal cylinder, a surplus WWII parabolic reflector and a 5 cm-diameter photomultiplier, positioned in the focus of the reflector), they were able to observe signals associated with cosmic rays for the first time [Galbraith1953], as they were coincident with those produced in an array of large area Geiger counters by which the arrival of a shower was detected. Measurements carried out in the high mountains during the following years, in more specific conditions (for example with polarizing filters, to verify if the light was really polarized, as expected for the Cherenkov radiation) gave more significant and definitive results [Jelley1955].

In the case of air under standard conditions, the refractive index n is equal to 1.0003, only slightly different from that of vacuum; the minimum velocity that the particles must have to produce the Cherenkov effect is therefore given by c/n = 0.9997 c. Cherenkov light is produced largely in the ultraviolet, within a small cone around the direction of motion of the particle [Cerenkov1937], of angular aperture $\theta$ governed by the relation cos $\theta$ = 1/$\beta$n, where $\beta$ = v/c. A typical particle of a shower can also produce 10–20 photons per meter of path, so the total number of photons produced, taking into account the high number of particles present in a high-energy shower, is enormous. One of the problems related to the use of this technique is that the observational conditions of the sky must be more than good: a low level of background brightness (light pollution), absence of clouds, atmosphere free from dust and aerosols, low rainfall. Also, observations should generally be limited to those nights when the moon is not visible. Overall, therefore, the fraction of observing time (duty cycle) is quite limited. Each detector can determine the

number of photons and the time of arrival. The reconstruction of each event can be done with the same method used for the charged particle detector arrays, once the positions $(x_i, y_i)$ of each detector in the array are known. The substantial difference with respect to charged particle detectors is that Cherenkov light detectors measure the photons produced along the entire path of the shower, while the former detect particles that have reached the ground.

It should be remembered that the same charged particles that reach the ground can produce Cherenkov light inside the detectors, especially if they have an adequate volume. A typical example are the water Cherenkov detectors, containers (tanks) of suitable volume, filled with pure water, through which the charged particles can produce photons, subsequently collected by photosensors, for example large area photomultipliers. In the case of water, the refractive index is such that the threshold for the Cherenkov effect is much lower (about 0.77 c). This technique was introduced by Porter and collaborators in 1958 [Porter1958], using square section vessels, measuring 1.20 m $\times$ 1.20 m, about 0.9 m deep, filled with demineralized water. The internal surface of the containers was coated with a reflective material, and the photons produced in the water were collected by a single large photomultiplier (5″), mounted vertically and in contact with the water. With this technique, the energy density was measured as a function of the distance from the axis of the shower, up to distances of about 500 m. This technique is practically the basis for the large detector arrays that were built in the following years, such as that of Haverah Park [Tennent1967] and the Pierre Auger Observatory in Argentina [AUGER_OBS].

## 8.4  Fluorescence Detectors

The development of an extensive air shower also produces the emission of fluorescence radiation into the atmosphere. This is due to the de-excitation of the nitrogen ions and molecules and is mainly concentrated in the band between 300 and 400 nm, with an isotropic emission. Because of the isotropic angular distribution of this radiation, it can be observed in principle from any direction (as opposed to the highly directional Cherenkov radiation), using suitable optical photosensors. The first prototypes of fluorescence detectors for observing atmospheric showers were developed by Bunner [Bunner1967], as part of the activities carried out by the Greisen's group at Cornell University around the end of the 1960s. In these prototypes, a number of photomultipliers were used that looked at the sky through a Fresnel lens (Fig. 8.3).

Despite the high number of photomultipliers (500, divided into 10 groups), with a Fresnel lens of 0.1 m$^2$ area in each module, this apparatus, operated for a long time, was not able to adequately detect the associated fluorescence light upon the arrival of a shower, also because of the high light pollution of the area where the apparatus was installed.

A different design, based on large diameter mirrors (1.5 m), with a limited number of photomultipliers placed in the focal plane of the mirror, was used with better results in the mid-1970s [Bergeson1975], both because this design allowed a collection of

**Fig. 8.3** One of the modules of the apparatus used by Bunner [Bunner1967] for the detection of fluorescence light, using photomultipliers that looked at the sky through a Fresnel lens
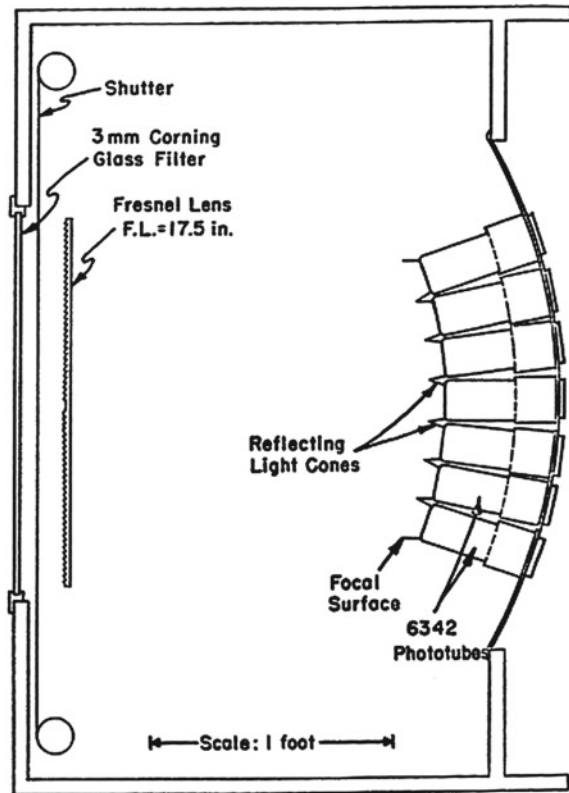
light approximately a factor of 20 higher than in the previous design, and because the apparatus was installed at Volcano Ranch, New Mexico, where a surface array also operated, in an area with much clearer air. This is the apparatus that was later called Fly's Eye, made up of 79 modules, each including the mirror and a set of 12 photo-multipliers. Detectors based on this design have proved suitable for the detection of very high-energy showers, in particular for studies related to the determination of $X_{max}$, mass composition and estimation of the energy of the shower. Their use is in any case affected by the particular atmospheric conditions (light pollution, air purity ...). In more recent times, the combined use of several such detectors has made it possible to obtain stereo images, or, in coincidence with surface arrays, to use hybrid shower reconstruction techniques.

## 8.5   Detection of Radio Waves Associated with Extensive Air Showers

The possibility of associating the formation of an extensive air shower with electromagnetic waves emitted in the radio wave frequency band has been investigated for at least 50 years, with mixed results.

On the one hand, the mechanism itself that should contribute to generating electromagnetic signals in appropriate radio frequency bands was not, especially at the beginning, fully understood. On the other hand, it must be realized that any detection technique based on radio waves must take into account the enormous "noise" existing in this part of the spectrum of electromagnetic waves, due to the presence of natural and artificial sources (radio, TV, communication systems, …). This made very difficult to consider the "inclusive" observation of showers, using the information extracted from radio signals alone, while the possibility of observing these signals in coincidence with those produced by conventional detectors, sensitive to the passage of particles, appeared more promising.

A review of the experiments performed in the early period of this activity was published by Allan [Allan1971], while a recent review of the status of this technique was made available by Schröder [Schröder2017]. The first predictions of the emission of radio signals from particles of an extensive air shower date back to the 1960s [Askaryan1962], and the first experimental evidence came shortly after [Jelley1965; Allan1966; Vernov1967].

In the work of Jelley and collaborators, for example [Jelley1965], the arrival of the showers was signalled by a set of Geiger counters operating in coincidence, while for the reception of radio signals, an antenna system consisting of 72 oriented dipoles was used along the East–West direction, operating at a frequency of 44 MHz, with a bandwidth of 4 MHz. The simultaneous observation of radio signals and showers was observed with an oscilloscope, triggered by the arrival of a shower. Similar systems, even if operating at different frequencies, were also used by Allan and collaborators [Allan1966], in the context of the Haverah Park array, which already allowed a "traditional" study of the showers, as the reconstruction of the shower size and of the direction, by the use of particle detectors. The antennas used in this study consisted of eight dipoles, arranged a hundred meters away from the particle detectors. Over a period of about two months of observation, an analysis of radio signals synchronized with showers showed evidence of 28 events compared to 625 showers detected. Measurements of this type were then carried out in the following years by many experiments capable of detecting the arrival of extensive air showers. In this first investigative phase, the frequencies used were typically tens of MHz (frequency range still used today), but in some cases both higher (hundreds of MHz) and lower (of the order of MHz or lower) frequencies were also exploited.

As a result of this first exploratory phase, qualitative evidence of the emission of radio signals synchronized with the propagation of a shower in the atmosphere was clearly established. From a quantitative point of view the information was not very significant and above all it was not able to provide reliable information on the

properties of the showers observed, so much so that interest in the 1970s towards the use of this technique as a quantitative means of investigation slightly decayed.

However, a greater interest in radio technology has resumed in recent decades, with a better understanding of the mechanisms of production of radio signals, with the advent of digital technologies and with the use of large observational installations, which now make the technique mature also for quantitative characterizations of extensive air showers. It can be said that today almost all the large detection facilities for the physics of cosmic rays have created an appropriate system for detecting radio signals in coincidence with the other detectors of the array. From the point of view of the performance of this technique, in a few decades we have gone from a situation in which the observation of radio signals associated with cosmic rays was little more than qualitative evidence of the existence of the phenomenon to a situation in which the possibility exists that in some respects this technique could supplant traditional detection techniques. Observations in the radio frequency band can also be done in principle with a duty cycle of 100%, as they are not subject to limitations related to light or the day/night cycle. Although traditional techniques will likely not be supplanted, the combined use of radio techniques together with those based on particle detectors, on the detection of Cherenkov radiation or fluorescence light, seems the most promising way for the near future.

## 8.6   An Example of Reconstruction of Extensive Air Showers in the 1950s

We have already mentioned the procedures for reconstructing the essential parameters of a shower, based on the information produced by a set of detectors located over a certain area. Many of these procedures are independent of the particular detection technology used and were formulated as early as the late 1940s. They are basically based on the measurement of the differences in the arrival times of the particles in the different detectors [Bassi1953] and on the density sampling measured in different positions [Williams1948]. In the works of the MIT group [Clark1957b, Clark1961], for example, where Bruno Rossi also worked, reference is made to the procedures used for the analysis of the data obtained from a small array of detectors, including 11 large area scintillators (diameter 1.05 m), positioned along two concentric circles (5 detectors for each ring and a central detector), the largest of which had a diameter of 460 m. In some periods a further group of 4 detectors was positioned along an innermost ring, to detect even lower energy showers. We can refer to this detection apparatus to understand some of the issues related to the reconstruction of showers (Fig. 8.4).

The trigger condition in this experiment was given by the coincidence between at least three detectors, with a signal of such amplitude as to indicate the passage of at least 10 particles of the shower in each detector.
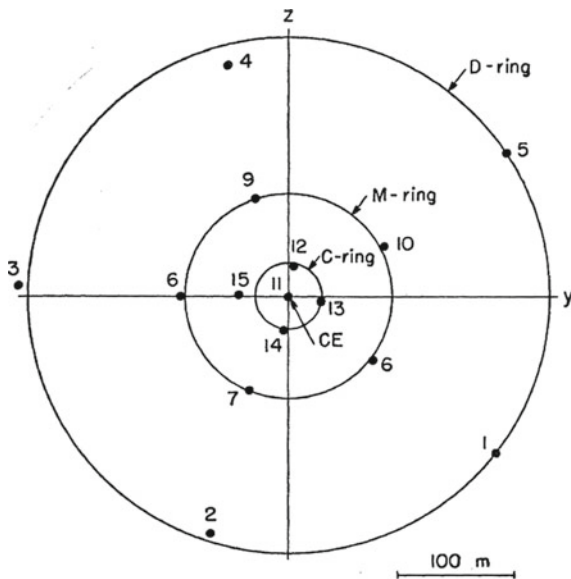
**Fig. 8.4** Geometrical arrangement of the detectors in the array used by Clark and collaborators in the 1950s [Clark1961]. The innermost ring (C) was used in some periods to detect showers of small energy, while for most of the measurements the outermost rings (M, D) were used, which included 5 detectors each, in addition to the central detector. Figure reproduced from the work of G. W. Clark et al., *Cosmic-ray air showers at sea level*, Physical Review **122**(1961)637. Copyright (1961) by the American Physical Society, License No. RNP/22/JUN/054686

The system used to simultaneously measure the amplitude of the signals produced in each detector is of historical interest. We must remember that there were no analog-to-digital converters at that time (the first prototypes of which were developed precisely in the period of the Second World War and initially covered by military secret). The signals produced by each photomultiplier, after an appropriate amplification, were sent to a corresponding number of oscilloscopes, whose screens, placed side by side, could be photographed by a single camera at the arrival of an event, in order to evaluate the amplitude (and therefore the particle density) measured in each detector. Figure 8.5 shows the schematic photographic recording of a very high-energy event measured with this system [Clark1961].

The direction of the shower axis was obtained by comparing the arrival times of the particles in the individual detectors by means of a minimization procedure (see Appendix K), with an uncertainty of the order of 5 degrees.

The lateral profile could also be determined for each shower, using different possible parametrizations of the radial density of particles f(r). Initially the following shape was used:

$$f(r) = \frac{N}{2\pi r_0} \frac{e^{-r/r_0}}{r}$$
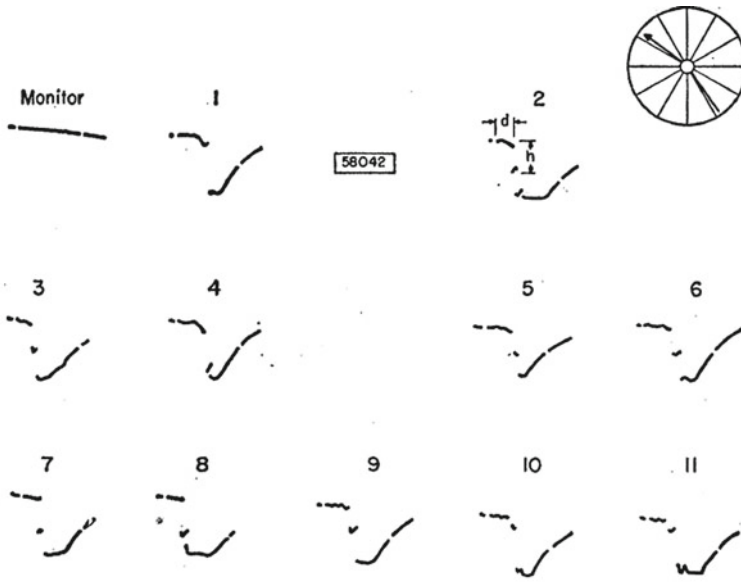
**Fig. 8.5** Photographic recording of the coincident signals observed in the oscilloscopes associated to each detector, in the measurements performed by Clark et al. in the 1950s [Clark1961] for the measurement of high energy showers with an array of scintillators. Figure reproduced from the work of G. W. Clark et al., *Cosmic-ray air showers at sea level*, Physical Review **122**(1961)637. Copyright (1961) by the American Physical Society, License No. RNP/22/JUN/054686

where $r_0$ is a free parameter, and r the radial distance from the centre, with coordinates (X, Y). The parameters N (total number of particles in the shower), $r_0$ and the position (X, Y) of the shower centre were determined by a procedure which minimized the deviations between the measured densities and those predicted by the previous relationship. Later, other parameterizations were also used [Clark1961].

Based on these procedures, one of the first maps in equatorial coordinates (right ascension, declination) of the directions of arrival of the reconstructed showers was reported, for different classes of the total number of particles in the shower [Clark1961]. This work summarizes the results obtained over a few years of measurement with this apparatus, with the dual purpose of studying the energy spectrum and the distribution of the arrival directions of the high-energy showers and at the same time of investigating the detailed structure of these showers. Figure 8.6 shows one of these maps, for shower sizes larger than $10^8$.
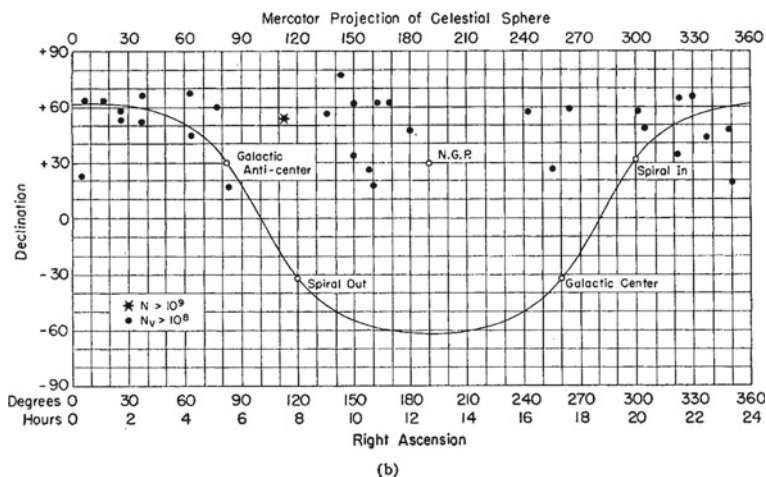
**Fig. 8.6** Map in equatorial coordinates (right ascension, declination) of the arrival direction of extensive air showers reconstructed with the procedure described by Clark et al. [Clark1961]. Figure reproduced from the work of G. W. Clark et al., *Cosmic-ray air showers at sea level*, Physical Review **122**(1961)637. Copyright (1961) by the American Physical Society, License No. RNP/22/JUN/054686

## 8.7  Arrays for the Reconstruction of Extensive Air Showers

The construction of effective arrays for the detection of extensive air showers began, as we have seen, in the period following the Second World War, in the early 1950s. Measurements with small detector arrays had in fact been carried out already in the mid-1940s, for example by Cocconi [Cocconi1944a, Cocconi1944b, Cocconi1946b] (Fig. 8.7), with configurations (see Appendix G) that allowed to estimate the average density of particles in an extensive air shower. Slightly more complex configurations were used by Cocconi himself in the following years [Cocconi1949f], at an altitude of 3260 m (Echo Lake), with several detectors deployed up to relative distances of about 200 m, and by Bassi [Bassi1953], which we already have quoted in connection with the reconstruction of some properties of the showers.

That atmospheric showers could have an enormous transverse dimension, even of the order of km, had already been ascertained from various measurements carried out at the end of the 1940s [Williams1948], in which it was possible to detect showers with an estimated energy around $10^{15}$ eV, and in some cases, even greater. This gave rise to the creation of arrays with a gradually increasing size, with a greater number of independent detectors positioned within a larger area. In the mid-1950s the MIT group, with Bruno Rossi and collaborators, used the array already described in the previous section, with about fifteen detectors, each with a sensitive surface of about one square meter, based on plastic scintillators, and displaced within a diameter of 460 m, replacing previous detectors that had been made with liquid scintillators.

**Fig. 8.7** Giuseppe Cocconi (1914–2008). *Source* alchet ron.com

The same group, with Clark, developed and operated in those years several medium-sized arrays also in other locations in the world, partly moving the detectors already made at MIT also in India and Bolivia, above all to look for evidence of possible anisotropies or cutoff in the energy spectrum.

The era of large arrays began in the 1960s, with the proposals of John Lisley, Livio Scarsi and Bruno Rossi, and the construction of the array of Volcano Ranch [Lisley1961], near Albuquerque, in the New Desert Mexico: a set of 19 detectors each with an area of 3.3 m$^2$, located 442 m away from each other, in a "hexagonal" configuration with a maximum diameter of 1.8 km (Fig. 8.8).

This array was further magnified to an outer ring radius of about 3 km [Linsley1963], observing events with an energy around $10^{20}$ eV for the first time.

In the same period, the BASJE array (Bolivian Air Shower Joint Experiment) was built in Bolivia, at 5200 m altitude, in connection with a large area muon detector (60 m$^2$), particularly intended to observe possible showers poor in muons, which could be indicative of high-energy gamma-induced showers [Suga1962]. The acceptance of the array, as it later proved, was however too small to reveal extremely rare events such as those searched for.

The following years, from the second half of the 1960s onwards, saw the creation of increasingly gigantic arrays, some of which are still in operation today. A complete list of existing devices or those that have worked in the past can be found in the excellent review by Grieder [Grieder2009] or by using resources available on the Web, which summarize the status of existing facilities, for example [MPI]. In addition to those mentioned, we cite below only some other examples of arrays that historically represented a reference point in the first years dedicated to the measurement of extensive air showers.

The Haverah Park facility, in Great Britain, was developed starting in 1967, on the initiative of Alan Watson and collaborators, to measure high-energy showers, from $4 \times 10^{17}$ eV to $10^{20}$ eV. A complete summary of the activities conducted with
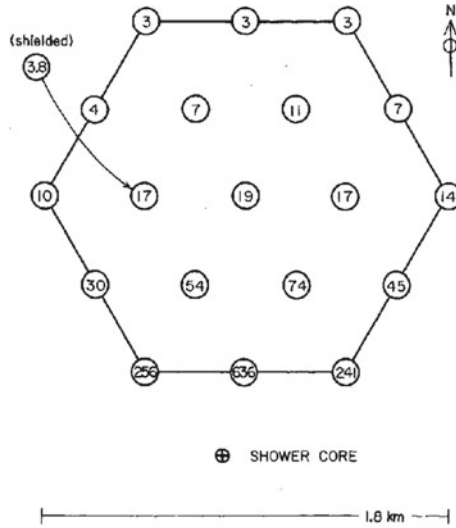
**Fig. 8.8** Topological configuration of the Volcano Ranch array [Linsley1961], a set of 19 large area detectors spread over an area of approximately 2 km$^2$. The figure shows, for the particular event measured, with an estimated energy around 10$^{19}$ eV, the reconstructed position of the shower core and the density of particles/m$^2$ measured in each detector. Figure reproduced from the work of J. Linsley et al., *Extremely energetic cosmic ray event*, Physical Review Letters **6**(1961)485. Copyright (1961) by the American Physical Society, License No. RNP/22/JUN/054761

the Haverah Park array from 1968 until 1987, when data taking was interrupted, is reported by Lawrence, Reid and Watson [Lawrence1991]. The Haverah Park array, located at low altitude (220 m above sea level), consisted of a number of tank-based detection units filled with water, with Cherenkov light-sensitive photomultipliers. Four detectors, each with an area of 34 m$^2$, placed at the vertices of a triangle, with the fourth detector in the centre, acted as triggers for the detection of events. Other detectors, grouped into 6 sets of 4 detectors each, with an area of 13.5 m$^2$, were arranged approximately along a ring about 1.5 km away, around the trigger detectors. Further detectors, singly or in groups, were arranged in the intermediate space. The entire array occupied an area of about 12 km$^2$.

Given the complexity, type and number of detectors that made up these large arrays, it should be remembered that these installations generally undergo an evolution over time, taking into account that the period of operation of these detection facilities is measured on the scale of decades, during which new detectors are added or replaced, the technology of detection, signal transmission and data acquisition evolves, and various upgrades and improvements of the equipment take place.

In the years between 1968 and 1979 an array (Sydney University Giant Air shower Recorder, SUGAR) remained in operation, located in Narrabri in Australia, at an altitude of about 250 m above sea level. The array covered a total area of about 70 km$^2$, and was equipped with 54 underground detection stations, each of which included two liquid scintillator tanks 50 m apart and with an area of 6 m$^2$. The detectors

were placed at a depth of about 1.5 m underground, corresponding to a threshold of 0.75 GeV for vertical muons [Brownlee1968]. Energy region measurements above $10^{17}$ eV were reported in later years [Winn1986].

Another array was built in the 1970s in Yakutsk (Siberia), with 58 surface detectors and 6 underground detectors as well as 48 detectors for the Cherenkov radiation produced in the atmosphere, reconfigured several times over the decades, with stations spaced between 100 and 500 m, spread over a total area which over the years was increased up to 17 $km^2$ [Ivanov2009].

The AGASA (Akeno Giant Air Shower Array) was built in Akeno, 120 km from Tokyo, on an area of about 100 $km^2$, between 1987 and 1991, with 111 scintillators of 2.2 $m^2$ area and 27 muon detectors of various surface [Chiba1992]. A previous 1 $km^2$—array, totalling 156 detectors with 1 $m^2$ area, and 11 muon detectors, had already been in operation since 1979.

In Australia, the Buckland Park Air Shower Array was operated in the early 1970s and included about 40 scintillators to detect showers with energy of the order of $10^{14}$ eV [Clay1984]. A second array in the same area was built in the 90s, also employed as a teaching tool for cosmic rays.

From the end of the '80s the GRAND array was operated at the University of Notre Dame, made with a grid of 8 × 8 detectors, each of which equipped with several floors of proportional wire chambers of about 1.3 $m^2$, which contributed up to recent years to numerous aspects of physics [GRAND].

The Chicago Air Shower Array (CASA) was a large array, operated in the 1990s in Utah (USA) [Gibbs1988]. It consisted of 1089 detectors, located on a square grid of 33 × 33 detectors spaced 15 m apart. Each detector was based on 4 scintillators of $60 \times 60 \, cm^2$ sensitive area. It was operated together with a second group of detectors (MIA, Michigan Muon Array), consisting of 1024 scintillators with an area of $1.9 \times 1.3 \, m^2$, installed underground, at a depth of 3 m, for the measurement of muons. The set of these detectors (CASA-MIA) was able to detect showers above $10^{14}$ eV with good efficiency and operated continuously until the end of the '90s.

The ARGO-YBJ array was built starting from 1996 in Tibet, at an altitude of 4300 m, with a layer of RPC (Resistive Plate Chambers) type detectors with a total area of 6700 $m^2$, sensitive to position, and is particularly dedicated to the study of high-energy gamma radiation.

A large array created in the following years was the KArlsruhe Shower Core and Array DEtector (KASCADE) [Antoni2003], developed in Karlsruhe, Germany in the 1990s, and later extended as KASCADE-Grande [Apel2010]. These are large facilities made with different types of detectors. The original KASCADE setup included an array of 252 scintillator-based detection stations, located along a rectangular grid with 13 m spacing, over a total area of $200 \times 200 \, m^2$, coupled to a central detector (hadron calorimeter) and tracking detectors for muons. The KASCADE-Grande extension, built later, included an additional 37 scintillator detector stations (10 $m^2$), located at a distance of about 130 m over an area of 0.5 $km^2$. This array was operationally decommissioned in 2009.

Facilities of enormous size dedicated to the detection and study of very high-energy cosmic rays are currently in operation, including the Telescope Array in

the USA, the GRAPES-3 observatory in India and the Pierre Auger Observatory in Argentina [AUGER_OBS].

The Telescope Array is a hybrid detection system based on a surface array with over 500 scintillators, spread over an area of over 700 km$^2$, with a distance of 1.2 km between them, located in Utah at about 1400 m above the sea level [TA].

The GRAPES-3 experiment is an extension of previous facilities built in India. Located in Ooty, it currently includes about 400 scintillation detectors and a huge (560 m$^2$) muon tracking apparatus [GRAPES-3].

The Pierre Auger Observatory is a hybrid detection system, which has undergone a continuous evolution over time, reaching a total area of about 3000 km$^2$. Currently it includes 1660 surface detectors, each consisting of a tank of 12 m$^3$ volume, located at about 1500 m relative distance, to read the Cherenkov light produced in the tank, 27 fluorescence detectors grouped in 4 stations, to detect the light produced in the atmosphere, and further detectors of various nature to complement the information provided by the main detection systems [AUGER_OBS].

Because of the complexity of these detection facilities and of their continuous evolution, we refer to their website or specific publications for a detailed description of their structure and the physics problems to which they are dedicated.

We also want to mention in this context the fact that in the last decades, a variety of detector networks have been created for the detection of extensive air showers, with mainly educational purposes, but also able to contribute to scientific investigations. These arrays differ from each other for the characteristics of the detectors used, for their topology and location, and for the associated educational and scientific activities around them. A review of a variety of educational experiments on cosmic rays, updated to 2008, is reported in [Blanco2008a]. As far as the organization of detector networks is concerned, the following should be mentioned in this context:

- The NALTA consortium (North American Large area Time coincidence Arrays) which groups together several arrays located in the North American and Canadian territory (ALTA, CHICOS, CROP, WALTA, SALTA), which have often operated jointly, based on small scintillation detectors installed at educational establishments [NALTA].
- The HISPARC project (High School Project on Astro-Physics Research with Cosmics) [HISPARC] in the Netherlands, also based on a large number of scintillation detectors, distributed in as many upper secondary schools.
- The LAAS (Large Area Air Shower) project, created in 1996 and consisting of a dozen stations—each with a certain number (4–12) of scintillators operating in coincidence—located at a great relative distance, in order to also search for coincidences among distant showers [Ochi2003].
- The Extreme Energy Events [EEE] project, which exploits the peculiarities provided by large area telescopes based on Multigap Resistive Plate Chambers, capable of reconstructing the trajectories of individual muons with excellent efficiency and resolution. The telescopes of the EEE project have

been distributed since 2007 in almost a hundred schools in the Italian territory and have been operational since that date, also searching for long-distance correlations (hundreds/thousands of km), and contributing to a wide range of educational and scientific activities [Abbrescia2011, Abbrescia2013, Abbrescia2015, Abbrescia2016, Abbrescia2018, Abbrescia2021; Riggi2017; LaRocca2019, LaRocca2020a, LaRocca2020b].

Other small local arrays, mainly for educational use, have been built and are operating in various parts of Europe, from Portugal to Poland, Greece and Sweden. The use of very small detector arrays, located within a restricted area, with easily modifiable configurations, has also proved to be a useful tool for carrying out a variety of educational activities [Pinto2020a; LaRocca2020c; Riggi2021a].

# Chapter 9
# The Primary Cosmic Radiation

**Abstract** A more detailed presentation of the nature of the primary cosmic radiation is reported in this chapter. The all-particle energy spectrum of the primary radiation, which extends over a huge number of orders of magnitude, both in energy and in intensity, is commented, together with the most recent findings from modern experiments, up to the still open problem of the highest energy part of the spectrum and the possible existence of an energy cutoff. The composition of the hadronic component and the abundance of light nuclei in the primary radiation, as compared with the natural abundance of elements in the solar system is discussed. A detailed presentation is also made of the electron/positron and of the gamma components, as well as a discussion of the intensity of the primary radiation at different heights in the Earth atmosphere.

## 9.1 Introduction

We have seen how understanding the nature of the primary radiation played a central role during the first decades of the history of cosmic ray physics. In some ways we can say that it still occupies an eminent role today, long after the first insights into its composition, although the problems have shifted to other fronts or to more specific details. It is known, in fact, that what we call primary cosmic radiation consists of particles and radiations that cover an enormous range of energy. Among the most important components recognized today, in particular those which produce extensive air showers in the atmosphere, we certainly have hadrons, gamma rays and neutrinos, as well as electrons, even if the latter do not contribute predominantly to the formation of extensive showers. The detailed composition of the primary radiation, in the different energy ranges, is however still being investigated today, as is the energy spectrum in its most energetic component. Other open problems are obviously those related to the origin and production mechanisms of the different components, as well as the possible effects of anisotropy or the existence of point sources.

As previously remarked, up to a certain energy it is possible to investigate the different components by means of direct measurements, carried out on board sounding balloons or satellites. At higher energies, however, the flux of the primary

cosmic radiation is reduced to such an extent that it is impossible in practical terms to obtain meaningful measurements by direct methods. The energy border between direct and indirect measurements is around an energy of $10^{14}$ eV for protons, but at significantly lower values for electrons, around $10^{12}$ eV, and even less for gamma rays, a few tens of GeV.

In the past, one of the problems concerned with the measurement of the energy spectrum of the various components was the gap existing between the range exploitable by direct measurements and that by indirect measurements. The more energetic particles that could be measured directly, in fact, produced showers that the large detector arrays found difficult to measure, as their design was oriented towards the detection of those of even higher energy. In more recent times, the possibility of extending direct measurements to higher energies (using sounding balloons and longer measurement times), combined with the possibility of extending indirect measurements to lower shower energies, have made it possible to fill this gap.

Beyond the usual distinction between primary and secondary radiation, which is made in connection to the peculiar phenomena that occur in the Earth's atmosphere, we can somehow say that the "primary" radiation, which affects the top of the Earth's atmosphere, includes stable particles and nuclei with a sufficiently long average life. From the astrophysical point of view, this primary radiation is associated with particles or radiations emitted "directly" by astrophysical sources, while we may consider as "secondary" in this context the particles, or the radiations emitted in the interaction of the primary particles with the interstellar medium. From this point of view, protons and other light nuclei synthesized in stars, in addition to electrons, can be considered as a true primary component, while other nuclei that do not derive from stellar nucleosynthesis and are rather the product of successive interactions with the interstellar medium, can be considered as secondary.

## 9.2   The Hadronic Component and the Energy Spectrum

As regards the hadronic composition, we have already mentioned that the large majority are protons, which make up approximately 90% of the primary radiation. Particles such as neutrons and mesons cannot be constituents of the primary radiation, due to their instability, which would not allow to travel long paths, though in the case of neutrons a local component could exist. A certain fraction of the primary component is instead made up of light nuclei or nuclei of intermediate mass. This composition, and the ratio between the different components, however, depends on the energy range considered.

The hadronic component covers a very high energy range, from values below 1 GeV up to energies in excess of $10^{20}$ eV, limited to low energy by the existence of a geomagnetic cut-off, at least if it refers to measurements performed near the Earth. The flux of low-energy hadrons is subject to large temporal variations, both periodic and aperiodic, due to the influence of the Sun. Such variations, on the other hand, become negligible as the energy of the primaries increases. The (chemical)

composition depends in detail on the energetic region considered, but it can be said that in general it includes from protons to heavier elements. Direct measurements of this component were carried out up to energies of the order of $10^{14}$ eV, using various types of instrumentation placed on board balloons, satellites and more recently also in space stations. For example, the JACEE [JACEE1999] mission, based on emulsion chambers launched aboard balloons into the stratosphere, with a series of launches between 1979 and 1996, investigated the composition and energy spectra of the primary components at the top of the atmosphere. The typical detection configuration included a set of nuclear emulsions, alternating with layers of plastic or lead material, and grouped into various sections that performed the different necessary roles: a primary charged particle detector, a target volume (in which the shower was generated), and a calorimeter for measuring the energy of the shower produced. We should once more remember that such measurements were at that time the only possibility—before the advent of very high-energy accelerators, such as the Large Hadron Collider—to study nuclear interactions in that energy range.

High-altitude balloon launches have been and continue to be a powerful means of investigating the cosmic radiation—as well as other physical quantities of interest—and have a long history in research. A fairly detailed list of the launches made from the mid-1940s to today is shown on the [STRATOCAT] website.

In addition to nuclear emulsions, to be recovered and analysed by visual observation after they have been exposed to cosmic rays, the instrumentation used on board satellites, especially in more recent times, has also made use of magnetic spectrometers and electronic detectors, to determine charge and energy, or mass and impulse of the primary particles.

At higher energies, over $10^{14}$ eV, apart from the measurements still making use of nuclear emulsions in the high mountains, up to 5450 m, most of the data were obtained from detector arrays, from the sea level up to altitudes of 5000 m. The use of these arrays, as we have seen, is not in itself able to determine the mass of the primary particle, but only the energy. However, the combined use of particle detector arrays with Cherenkov light observation or other hybrid techniques has also allowed in many cases an approximate estimate of the mass of the primary, allowing at least the selection of events generated by protons, by light and by heavy nuclei.

From a huge number of different experiments and measurements, it has been possible to obtain an inclusive energy spectrum (unidentified particles) in a wide energy range. Figure 9.1 shows a collection of data from several experiments; the plot shows the flux of particles in the range from 1 GeV to $10^{20}$ eV, expressed in number of particles per ($m^2$ s sr GeV). Data below 1 GeV, which typically show a decrease (dip) around 10 MeV and then a further rise at even lower energies, are strongly dependent on temporal variations and cannot be considered—in absolute value—as significant. An interactive database for the extraction of cosmic ray data has been reported in recent years by Maurin et al. [Maurin2014].

This plot, reproduced in various forms, is one of the most important classical results of today's cosmic ray physics, and it is worth commenting on several of its aspects. It covers a huge number of orders of magnitude (12 in energy and 32 in flux). To get an idea of the measurable flux in practical conditions, it is usual
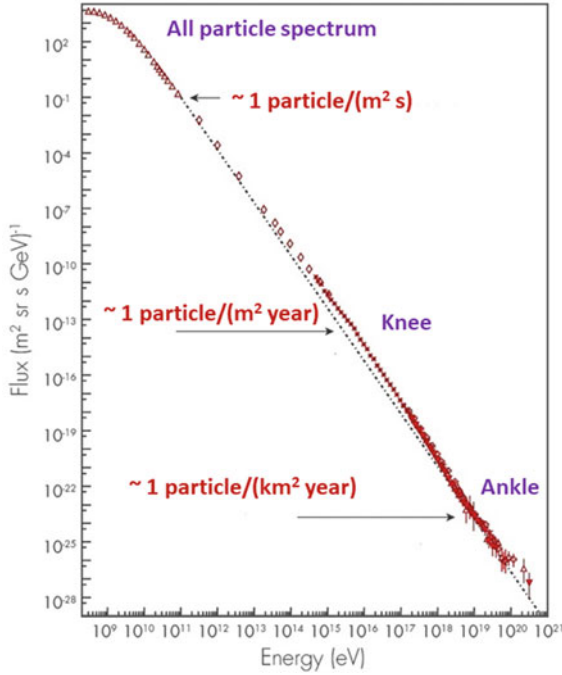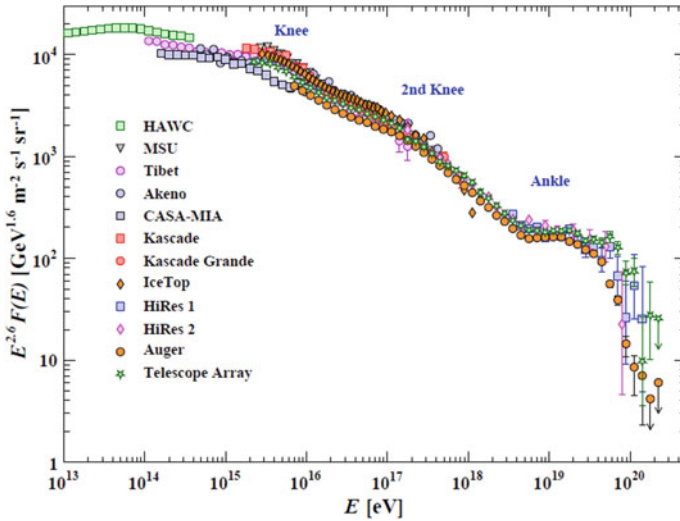
**Fig. 9.1** Energy spectrum of primary particles (All particle spectrum), starting from the energy of 1 GeV, up to about $10^{20}$ eV

to report in various areas of the plot how many primary particles per unit of time and surface correspond to the flux shown. Thus, for example, at an energy around $10^{11}$ eV (100 GeV), the flux corresponds to about 1 particle per m$^2$ per second, a relatively high value. However, the flux is greatly reduced by going to higher and higher energies, reaching values of 1 particle per m$^2$ per year around $10^{15}$ eV, and 1 particle per km$^2$ per year around $10^{19}$ eV.

The shape of this spectrum is well represented by a power law, of the $E^{-\gamma}$ type, where the exponent $\gamma$ assumes slightly different values in the first energy region, up to $10^{15}$ eV, where $\gamma$ is approximately 2.7, and in the subsequent region, up to about $10^{19}$ eV, where $\gamma$ is about 3.15. The intersection between these two regions, around an energy of $3 \times 10^{15}$ eV, has traditionally been called *knee*, and the first evidence of a change in the spectrum shape in this region dates back to the late 1950s [Kulikov1958]. A slope parameter $\gamma$ of 2.7 implies a reduction of a factor of 500 in the flux for each decade in energy, which explains the extremely low values of flux at very high energies. Around $10^{19}$ eV a further change in the slope of the spectrum is observed, with a parameter $\gamma$ coming back to a value of about 2.7. This region is traditionally called *ankle*.

The trend of the energy spectrum of the primary component, well represented by a power law, albeit with a slightly different exponent in the lower and intermediate

**Fig. 9.2** Energy spectrum of primary particles (All particle spectrum), scaled by the factor $E^{2.6}$ [PDG]. The different symbols show the results obtained from different experiments. Figure reproduced with permission from R. L. Workman et al. (Particle Data Group), Prog. Theor. Exp. Phys. 2022, 083C01 (2022)

energy regions, suggests representing the flux values multiplied by $E^\gamma$, choosing an appropriate value of the exponent $\gamma$ (between 2.5 and 3). With this representation, it becomes easier from a graphical point of view to verify whether the trend of the data actually follows that law, as the values should ideally be arranged along a horizontal line. The current knowledge of the spectrum of primary particles in the energy region from $10^{13}$ eV upwards is shown in Fig. 9.2, taken from the documentation reported by the Particle Data Group [PDG], in which an exponent equal to 2.6 has been used.

In this representation we see how in the interval between $10^{13}$ eV and about $3 \times 10^{15}$ eV, the spectrum shows a much smaller variation, due to the multiplication factor with energy, compared to the original spectrum. This type of representation also has the advantage of better highlighting from a graphical point of view the regions where it is possible to notice a change in the slope.

Regarding the characteristics of this change in the slope of the spectrum in the energy region of the "knee", several problems are still open, in particular whether this change in slope is discontinuous or occurs continuously in a certain energy range, and what is the detailed cause of the change, whether it is due to the superposition of the spectra of the different particles, which have slightly different trends, or to differences already in the mechanisms of production at the origin. In the energy region of the "knee" an enormous amount of experimental data is now available [Grieder2001, Grieder2009], obtained in particular in the '80s and '90s, with different techniques and from dozens of different experiments, making use of detector arrays with dimensions intermediate between the first arrays used in the past and the current huge arrays.

The region of the spectrum at higher energies, from $10^{18}$ eV onwards, is obviously characterized by an enormously reduced flux, which required huge arrays (thousands of km$^2$), and data taking times of the order of years, for its study. One of the main problems related to the study of extreme energy cosmic rays is, as it is known, the existence of a limiting value in the energy (cutoff). The idea of a limiting energy for the primary particles capable of arriving on Earth was introduced in the 1950s by Zatsepin [Zatsepin1951] and revived in the 1960s by Greisen [Greisen1966], and by Zatsepin and Kuzmin [Zatsepin1966, Kuzmin1968] and is commonly referred to as the GZK (Greisen-Zatsepin-Kuzmin) cutoff. This limit would be introduced by the interaction of primary cosmic rays with the microwave radiation background, discovered by Penzias and Wilson in 1965 [Penzias1965]. Protons of very high energy, starting from $10^{20}$ eV, would in fact interact with the photons of the microwave background, resulting in the photoproduction of pions, which becomes the dominant process, degrading their initial energy and effectively eliminating the higher energy component of these particles over large distances. Estimates of the mean time required for this loss of primary proton energy to occur were made by Stecker in 1968 [Stecker1968].

Figure 9.3 shows the effect of this interaction for cosmic rays of energy equal to or greater than $10^{20}$ eV, as a function of the distance crossed [Anchordoqui2019]. Unless we admit the existence of very high-energy cosmic sources within relatively small distances (50–100 Mpc, against the size of the order of 5000 Mpc for the entire universe), this would prohibit the arrival of protons with energy higher than a certain limit.

From an experimental point of view, only the huge arrays such as AGASA, HiRes, the Pierre Auger Observatory and the Telescope Array have the potential to observe very high-energy events, albeit with different techniques, which makes the comparison between the data obtained critical. The results obtained by Auger so far seem to indicate the existence of a cutoff, with the observation of very few events beyond the cutoff, interpreted as due to heavy nuclei rather than protons. In contrast, the AGASA results initially seemed to indicate many more events in that region, with the predominance of protons, which would suggest a violation of the GZK effect. A recent comparison between the results reported by the Auger and Telescope Array



**Fig. 9.3** Effect of the interaction of primary cosmic rays with microwave background radiation, with consequent photoproduction of pions, as a function of the distance crossed
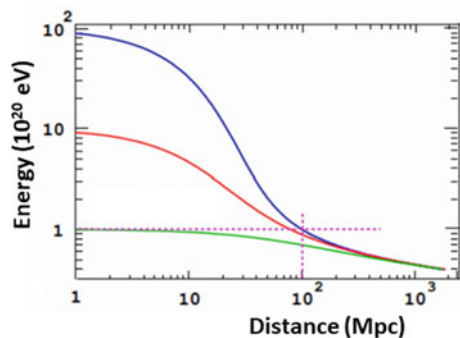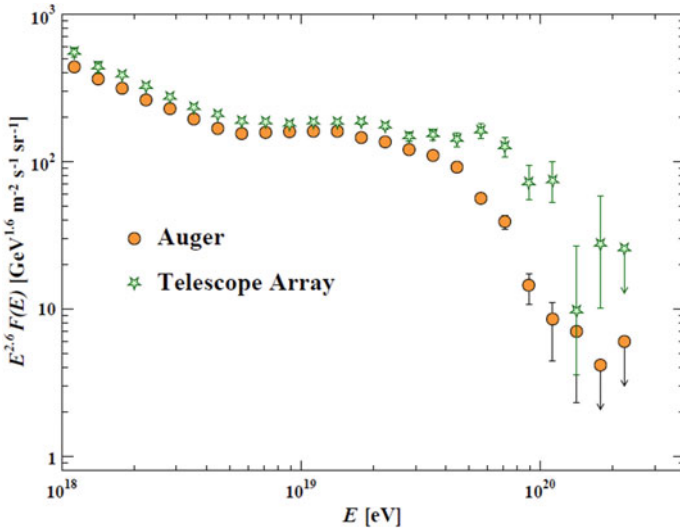
**Fig. 9.4** Spectrum of the primary cosmic radiation, in the region from $10^{18}$ eV upwards, scaled by the factor $E^{2.6}$, measured by the Auger and Telescope Array experiments [PDG]. Figure reproduced with permission from R. L. Workman et al. (Particle Data Group), Prog. Theor. Exp. Phys. 2022, 083C01 (2022)

Collaborations again shows (Fig. 9.4) a discrepancy in the spectrum measured by the two experiments at energies greater than $10^{19}$ eV [PDG].

## 9.3   Composition of the Hadronic Component

In a complementary way to the study of the inclusive spectrum in energy, it is of interest to know a more detailed composition of the primary radiation, while limiting itself to the hadronic component. Measures of this kind, aimed at establishing the abundance of the various nuclei, the energy spectrum of the individual components, or even the isotopic composition (ratio between the various isotopes of the same chemical species), were carried out as early as the late 1940s, although more significant results were obtained only many years later. More precise results on these aspects have obviously been obtained in the region with lower energies or in the case of light nuclei (H, He …), since the flux at higher energies or for heavier nuclei decreases rapidly, making observations with high statistics difficult to achieve. For this reason, the different nuclei found in the primary radiation are often grouped together into mass regions, for example light elements (Z = 3–5), medium mass elements (Z = 6–9), and so on.

Once again, the first answers to these questions came from measurements carried out with nuclear emulsions aboard sounding balloons, in the late 1940s [Freier1948a,

Freier1948b, Bradt1948], a period in which the existence of nuclei significantly heavier than protons was established in the primary radiation. Subsequent measurements were then carried out by the use of satellites, at much greater distances from the Earth, where the influence of the Earth's atmosphere was negligible. Review papers discussing the nuclear composition of the primary radiation, dating back to the 1970s, are for example that of Shapiro and Silberberg [Shapiro1970] and that of Webber [Webber1974]. More recent reviews can be found in [Grieder2001]. A recent review, also available in interactive mode, of data relating to the abundance of the different nuclei is that of Maurin [Maurin2014], in addition to the documentation provided by the Particle Data Group [PDG], which is constantly updated. Figure 9.5 shows a recent status regarding the energy spectrum and the abundance of the various species of nuclei, as reported by [PDG], summarizing a series of experimental data obtained in recent times and by different experiments.

The low energy region (below some GeV/nucleon) is strongly influenced by the measurement conditions, in particular by the solar period in which the measurements are made, and this explains why different experiments, performed in different periods, obtain values of the absolute flux that can differ even by an order of magnitude. Above some GeV/nucleon, however, the spectra have a well-defined behaviour, regardless of solar conditions. As regards the abundance of the various species, it can be seen how protons dominate the yield compared to other nuclei, especially those heavier than He. However, the abundance of the latter is not negligible, amounting to about 20% of the proton component at low energies (about 1 GeV/nucleon), but decreasing to a few percent of the protons at much higher energies.

The integrated abundance of the individual components in the primary radiation, from light nuclei up to Fe (Z = 26) is shown in Fig. 9.6, introducing a threshold of 5 GeV to exclude the effects due to the modulation produced by the Sun [Grieder2001]. As it can be seen, the nuclei beyond Helium have abundances between 2 and 4 orders of magnitude lower than the dominant component, the protons.

Beyond Iron (Z > 26) the presence of nuclei in the primary cosmic radiation, although highlighted by more recent measurements, is very small, and, in particular for elements with Z > 30, it is about 6 orders of magnitude smaller. This causes the Iron to represent in some way the upper extreme of the chemical composition of the primary radiation. Of particular interest is also the comparison between the abundance of these nuclei in the cosmic radiation and the natural abundance of elements in the Solar System, as determined to a large extent by the study of meteorites.

Figure 9.7 shows the relationship between the abundances of the various species found in the primary cosmic radiation—assuming a minimum threshold in energy equal to 5 GeV—and those of the elements present in the Solar System. As can be seen, for some species the ratio is close to 1 (in other words the abundance in the cosmic radiation roughly follows the distribution of the elements in the Solar System), while for some of them the abundance found in the cosmic radiation is much greater than what is present in the Solar System. It can be seen in particular that the elements with Z = 3 (Lithium), Z = 4 (Beryllium) and Z = 5 (Boron) are enormously more present in the cosmic radiation (from 10,000 times to a million times more abundant). This phenomenon is interpreted as due to nuclear spallation
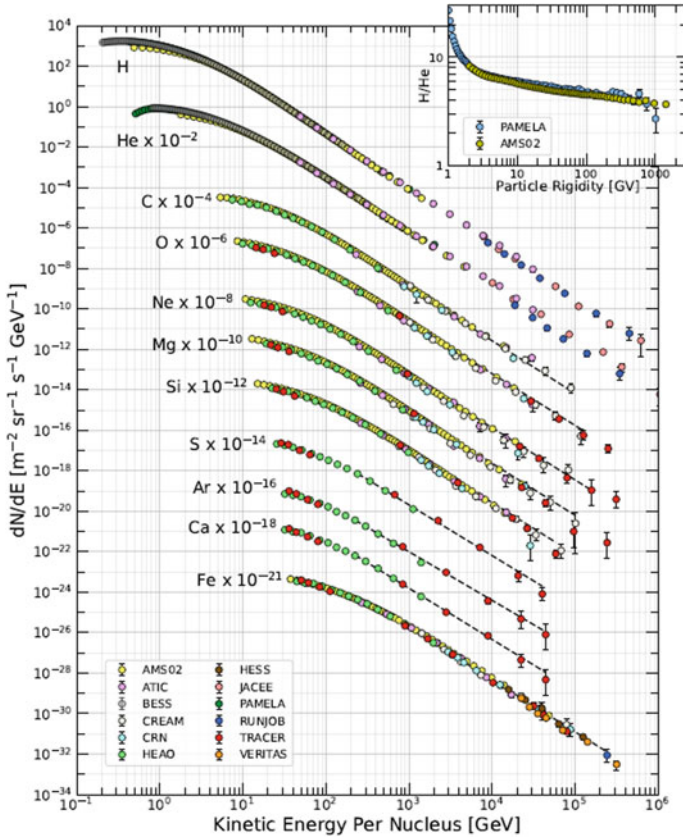
**Fig. 9.5** Review of recent experimental results concerning the abundance and energy spectrum of the different species of nuclei present in the primary cosmic radiation. The insert also shows the relationship between the abundance of hydrogen and that of helium, as a function of the particle rigidity [PDG]. Figure reproduced with permission from R. L. Workman et al. (Particle Data Group), Prog. Theor. Exp. Phys. 2022, 083C01 (2022)

reactions of the original primary nuclei when crossing the interstellar space. The same phenomenon, albeit with smaller factors, also occurs for elements with $Z = 21$–$25$. In other words, the particles arriving on Earth are not necessarily "primary" but can also derive from these secondary processes that occur along the enormous journey they make.

The flux of the primary nucleons, which to a large extent are protons or nucleons belonging to the nuclei of Helium, can be parameterized, in a wide range of energy (from some GeV to over 100 TeV) by the following relationship

$$I_N(E) = 1.8 \times 10^4 \, E^{-\alpha} (GeV) \text{particles}/(m^2 \text{ s sr GeV})$$

where E represents the energy per nucleon, and $\alpha$ is approximately 2.7.
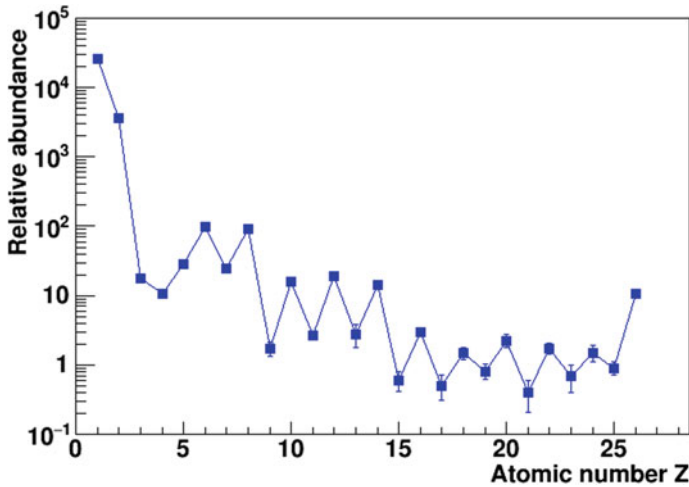
**Fig. 9.6** Relative abundance of the various species present in the primary cosmic radiation, normalized to the abundance of Carbon (Z = 6), assumed to be 100. Data extracted from [Grieder2001]
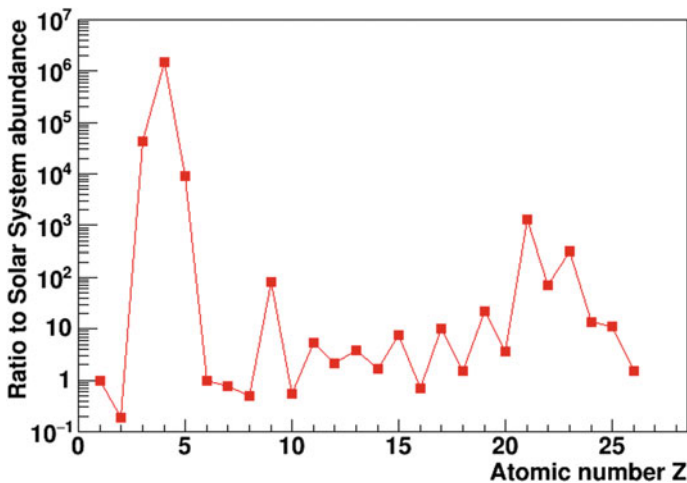


**Fig. 9.7** Ratio between the abundance of the various species present in the primary cosmic radiation, compared to that present in the Solar System, assuming a threshold equal to 5 GeV. Data extracted from [Grieder2001]

The mass composition of the higher energy primary cosmic rays cannot be investigated by directly detecting primary particles, due to the very low flux, and must be studied through the development of the extensive air showers produced by them, generally employing hybrid techniques, as discussed. In the knee region, many measurements were made in the 1980s and 1990s, although in most cases it was

only possible to determine an average mass of the primaries, or to distinguish simply between protons and much heavier nuclei, such as Iron. In particular, data obtained for primary energies between $10^{11}$ and $10^{15}$ eV, up to the '90s, indicated an increase with the energy of the fraction of nuclei such as Iron, while the component due to protons remained approximately constant [Ichimura1993]. At the end of the 1990s it was however quite clear that up to energies of $10^{15}$ eV the mean value of the mass of the primary particles was quite low (about 7), while a sharp variation could be observed beyond $10^{16}$ eV, where the average mass value reached roughly a value of 30. Results obtained in recent decades, especially by large detector arrays coupled to hybrid techniques, have allowed to establish that the average mass value decreases again for energies around $10^{18}$–$10^{19}$ eV. The study of the mass composition for the higher energy cosmic rays, from $10^{19}$ eV upwards, is still under investigation [Aab2017a].

## 9.4 Electrons and Positrons

Apart from the initial hypotheses on the nature of the primary cosmic radiation as constituted by electrons, already discussed in relation to the events around the mid-1930s, after the general acceptance that it consisted largely of protons and other light nuclei, the attempts to establish the quantitative existence of an "electronic" component in the primary radiation continued, but unsuccessfully, until about 1960. Measurements carried out, for example, in the early 1950s by Critchfield et al. [Critchfield1951], using cloud chambers carried at high altitudes by sounding balloons, had allowed to establish only a maximum limit to the presence of electrons, of the order of 0.6% of the total flux. Only in 1961, by Earl [Earl1961] and by Meyer and Vogt [Meyer1961], in two different experiments with measurements always carried out on board balloons, could the existence of a primary component due to electrons be confirmed.

Earl's work justifies the possibility of making new measurements—about 10 years after Critchfield's previous experiments—due to the fact that the experimental techniques making use of cloud chambers, in particular keeping them on board balloons at high altitudes have in the meantime improved significantly. The existence of electrons and gammas could be identified based on the electromagnetic showers generated in the lead plates overlying the different sections of the (multiplate) cloud chamber and discriminated against nuclear interaction events. Figure 9.8 shows one of the events in which the track of an ionizing particle at the minimum of ionization coincides with the axis of a shower that develops in the following sectors, taken from the work of Earl [Earl1961].

The result of Earl's work led to an unambiguous, albeit with low statistics, evaluation of the number of events due to the arrival of primary electrons, with an estimate equal to $(3 \pm 1)$ % with respect to the proton flux, against the upper limit of 0.6% set by the Critchfield measurements carried out about 10 years earlier. This discrepancy was interpreted as due to several factors: the different threshold in energy, the

**Fig. 9.8** An event identified as being produced by a primary electron in a "multiplate" cloud chamber [Earl1961]. Figure reproduced from the work of J. A. Earl, *Cloud chamber observations of primary cosmic ray electrons*, Physical Review Letters **6** (1961)125. Copyright (1961) by the American Physical Society, License No. RNP/22/JUN/054867

different absolute flux of cosmic rays between 1949 and 1960 and the different altitude. From this measurement a first rough energy spectrum of the primary electrons was also extracted, within 3 GeV, with a preponderance for those of lower energy, between 0.5 and 1 GeV.

In another work, by Meyer and Vogt, practically contemporary to that of Earl— since it was received and published by the same Journal about a month after—the data obtained from three different balloon flights, carried out in 1960, were used with a different experimental setup [Meyer1961]. The latter was based on scintillators read by photomultipliers, arranged in a vertical telescopic configuration, with further plastic scintillators arranged laterally and operating in anti-coincidence with the

others. This apparatus made it possible to easily identify the primary protons, and therefore to search for events that were not due to these particles.

Measurements performed at various altitudes, from about 2 to 300 g/cm$^2$ of atmospheric depth, made it possible to observe how the flux of these events as a function of atmospheric depth followed closely the behaviour of secondary electrons up to the altitude corresponding to the maximum point, at about 100 g/cm$^2$. At higher altitudes, where the contribution of secondary electrons should have decreased, a significant residual contribution was instead observed, which even increased at the top of the atmosphere, as shown in Fig. 9.9.

Even in this case a rough energy distribution of these events was estimated, observing how the major fraction of events corresponded to electrons of relatively low energies (some hundreds of MeV).

As regards the energy spectrum of the primary electronic component, a review of measurements made with different techniques in the second half of the 1960s has been reported by [Fanselow1969]. A review of the data currently available can be found through the documentation offered by the Particle Data Group [PDG]. As an example, Fig. 9.10 shows the spectrum of electrons and positrons, multiplied
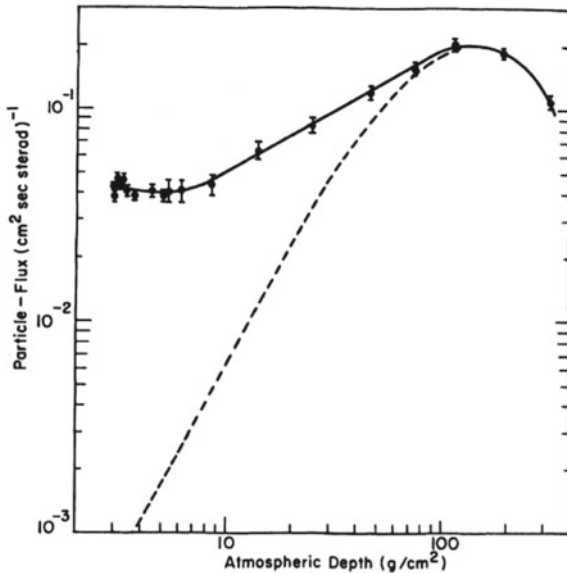


**Fig. 9.9** The flux of events measured at high altitudes, between about 2 and 300 g/cm$^2$ of atmospheric depth, not attributable to events generated by primary protons, measured during balloon flights by Meyer and Vogt [Meyer1961]. The dotted line describes the expected contribution for secondary electrons, which at high altitudes (small atmospheric depths) should be negligible compared to that observed. Figure reproduced from the work of P. Meyer and R. Vogt, *Electrons in the primary cosmic radiation*, Physical Review Letters **6**(1961)193. Copyright (1961) by the American Physical Society, License No. RNP/22/JUN/054868
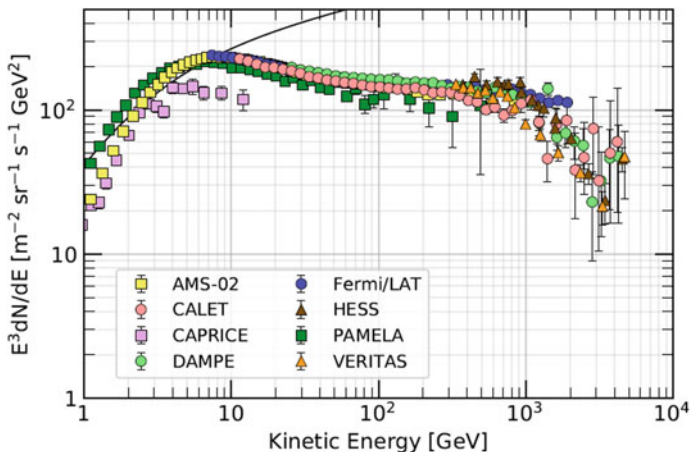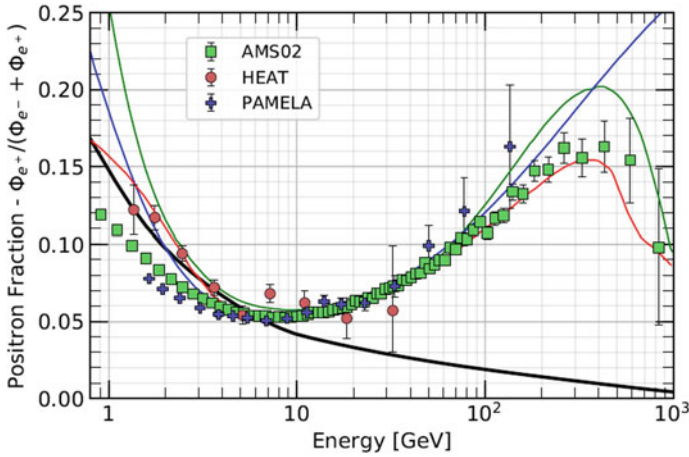
**Fig. 9.10** Recent results about the energy spectrum of primary electrons, obtained from a variety of experiments [PDG]. Figure reproduced with permission from R. L. Workman et al. (Particle Data Group), Prog. Theor. Exp. Phys. 2022, 083C01 (2022)

by the factor $E^3$, known today, following the observations produced by a variety of experiments.

As for the sign of the charge of these electrons, i.e., the fraction of negative electrons and positive electrons (positrons) in the primary radiation, the first estimates were made in 1964 [DeShong1964] by means of a magnetic spectrometer, capable of separating particles with different charge states. The results gave different values, albeit with large statistical uncertainties, depending on the energy: in particular a fraction of the positrons with respect to the total (electrons + positron) of 31%, 38% and 16% for the energy intervals 50–100 MeV, 100–300 MeV and 300–1000 MeV respectively. Positrons therefore have a lower abundance than electrons. More sophisticated measurements date back to more recent times, from the 1990s onwards, confirming that the positron fraction, especially at high energies (> 1 GeV), is less than 10% of the total, reaching values slightly higher (about 20%) for lower energies [Grieder2001].

Today the ratio between positrons and electrons is known with excellent precision over a wide range of energy, up to TeV, and shows that the positrons fraction reaches a minimum around the energy of 10 GeV (about 5%), and then rises again up to about 15% in the energy range between 100 GeV and 1 TeV. Figure 9.11 shows the current situation, as available from the Particle Data Group documentation [PDG]. The black line shows the prediction of positron abundance based on a pure secondary production mechanism, which largely underestimates the observed contribution at energies above 10 GeV, while the other lines indicate the prediction of different models, based on more complex mechanisms of astrophysical interest.

**Fig. 9.11** Recent results about the fraction of positrons with respect to the total of (electrons + positrons), obtained from different experiments [PDG]. Figure reproduced with permission from R. L. Workman et al. (Particle Data Group), Prog. Theor. Exp. Phys. 2022, 083C01 (2022)

## 9.5   Other Components in the Primary Radiation

In this context we will not discuss, if not for a very brief mention, the other components found as part of the primary radiation. Although they represent an enormously smaller fraction from the point of view of the flux, with respect to the hadronic and electronic fractions, they are nevertheless the subject of current investigations, also in relation to other important aspects of astroparticle physics.

Among these components we must certainly include gamma rays, which at the beginning of the history of cosmic rays seemed to made up most of the primary radiation.

Experiments aimed at studying the characteristics of gamma radiation in primary cosmic rays have usually been carried out using instrumentation aboard satellites in space, but also aboard balloons, or even from the ground, using different tools and methodologies, also suitable for the specific energy range of gammas and for the expected flux. The lower energy component, up to energies of a few tens of GeV, is in fact studied mainly in space or aboard balloons at the top of the atmosphere, due to the absorption in the Earth's atmosphere, which precludes its detection by experiments on the ground. The latter are mainly dedicated to the detection of high-energy gammas, from 100 GeV upwards. Recent reviews concerning the contribution of gammas to the primary radiation have been reported for example by Lorenz and Wagner [Lorenz2012] and by De Angelis and Mallamaci [DeAngelis2018b]. The gamma radiation as a component of the primary cosmic rays is also important because to some extent it retains the original imprint of its origin, from the point of view of direction and energy spectrum.

Of particular interest, for experiments in space, is the study of the distribution of the arrival directions (gamma rays maps), in order to look for evidence of point sources or possible anisotropies. In fact, it should be considered that, unlike charged particles, deflected by magnetic fields, gamma rays can in principle keep information on their original incoming direction, even if after a more or less long path, they can interact with interstellar matter and with the existing photon field.

At lower energies, in the X-ray region, evidence of this radiation from the Sun had already been discovered in the 1940s. In much more recent years, it has been seen that the Sun is also a source of gamma radiations, at energies of the order of MeV, emitted in the context of nuclear processes. Only in the early 1960s, however, there was evidence of X-radiations coming from outside the Solar System, by Roberto Giacconi, Nobel laureate in 2002 for this discovery [Giacconi1962]. The first X-ray sources highlighted, by X-ray instrumentation mounted on board a rocket, were well-defined sources, such as Scorpius X-1, a low-mass binary star (one of which is a neutron star), known as the strongest X-ray source visible in the sky. The X-ray emission of this source is about $10^4$ times more intense than that in the visible region, and greatly exceeds the emission by the Sun in all other wavelengths. In the following years, in 1964, the emission of X-rays was also observed by other objects, such as the Crab Nebula. In addition to the emission from defined sources, a diffuse background of X-radiation is also observed, which appears to be isotropic.

In the gamma-ray region, the first observations of photons with energies of the order of 100 MeV of extrasolar origin occurred in the late 1960s, with satellite observations (OSO-III in 1968, SAS-2 in 1972 and, above all, COS-B in the years 1975–1982 [Swanenburg1981]). The gamma radiation detected by COS-B had energies between a few tens of MeV and 5 GeV, and it was possible to distinguish between the diffuse component and the localized ones.

One of the first gamma ray maps of the Milky Way was provided by the COS-B mission in the second half of the 1970s. Other elements of interest for gamma astronomy, in addition to the study of point, or well-defined, sources, are represented by gamma-ray bursts, as well as by the study of gamma rays with specific energies, related to the nucleosynthesis of the elements.

Diffuse gamma radiation of galactic origin is mainly due to the interaction of the primary nuclei of the cosmic radiation with interstellar matter, through three main mechanisms: the decay of the neutral pions produced in the nuclear interactions of the primary nuclei with the interstellar medium, the bremsstrahlung processes of the electrons, or the reverse Compton scattering of electrons with photons of the galactic radiation field. The energy spectrum of the gamma radiation diffused in the low energy range, through measurements obtained on board of balloons, up to 20 MeV, is shown in Fig. 9.12 [Schönfelder1980]. A review of the results obtained from various experiments in the 1970s up to energies of about 100 MeV is reported in [Fichtel1978].

Today, gamma astronomy has become one of the most promising fields of investigation for the study of numerous celestial objects, either within the Milky Way or in extragalactic regions, and is accompanied by other probes (cosmic rays, neutrinos,
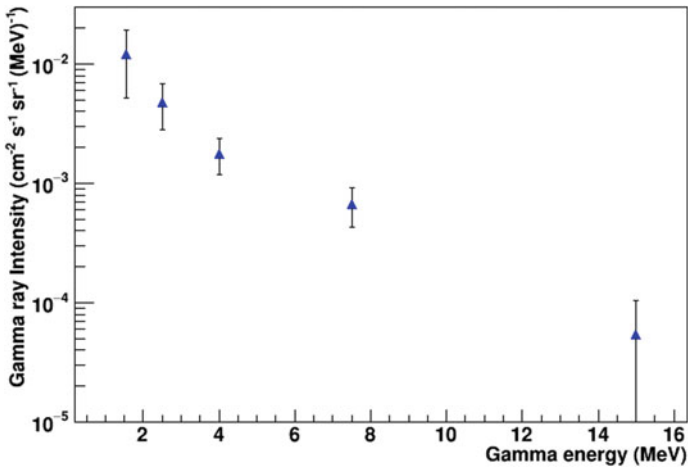
**Fig. 9.12** Diffuse flux of primary photons up to energies of about 20 MeV. The energy value reported refers to the average value of each measured energy interval. Data extracted from [Schönfelder1980]

gravitational waves) in approaches that make more and more use of the concept of multi-messenger astronomy.

As far as the contribution of neutrinos is concerned, a component of which in this context we will limit ourselves only to mentioning the existence, if we neglect the continuous flux of low-energy neutrinos coming from the Sun and deriving from the reactions that take place in it, high-energy neutrinos can be produced in a variety of objects of astrophysical interest, and their study represents one of the leading aspects of modern, rapidly evolving, astroparticle physics experiments. Neutrinos can be produced in general by thermonuclear processes within stars, during their lifetime, as well as in the collapse of stars that can lead to the formation of supernovae. From this point of view, the observation, for the first time, of a neutrino burst associated with the explosion of the supernova SN1987a, has aroused enormous interest in the study of this type of processes.

As they interact weakly with matter, neutrinos carry direct information on the processes that generated them and on their location. Of course, just because of the very low probability of interaction, the possibility of detecting them is linked to the availability of detectors of enormous volume, which has become possible in recent times, also taking advantage of the possibility that they produce events of interest for their detection in enormous quantities of "natural" matter, such as ice and sea water, environments in which different types of equipment have been installed in recent decades for the detection of neutrinos. For a review of the recent historical steps regarding the creation of a true neutrino astronomy, a recent contribution has been made available by Spiering [Spiering2012].

One of the other issues of considerable interest about the components present in primary cosmic radiation concerns the presence of antinuclei, such as antiprotons and

antideutons. The first laboratory observations of antiprotons, using particle acceler-
ators, date back to 1955, by Chamberlain and collaborators [Chamberlain1955]. In
the same period, the hypothesis that such antiparticles could also be present in the
primary cosmic radiation was also discussed [Fradkin1956]. It is believed that such
antiparticles can be produced by energetic collisions of the primary radiation with
the interstellar medium; in this sense they would not really be "primary". A possible
primordial origin for such antiparticles, for example as deriving from relevant
portions of antimatter present in the universe, are currently highly speculative. After
several unsuccessful attempts, between the end of the 1950s and the beginning of
the 1970s [Haskin1959, Aizu1959, Aizu1961, Grigorov1961, Apparao1967], using
nuclear emulsions, or with the aid of a permanent magnet [Bogomolov1971], the
first evidence was reported by Golden and collaborators [Golden1978, Golden1979a,
Golden1979b] and by Bogomolov and collaborators [Bogomolov1979], by means
of measurements carried out aboard stratospheric balloons, capable of reaching alti-
tudes corresponding to a few $g/cm^2$ of residual atmosphere. In the measurement
reported by Golden [Golden1979a, Golden1979b], carried out with a magnetic spec-
trometer and a Cherenkov detector, some dozen events attributable to antiprotons
were observed, estimating a ratio between antiprotons and protons of $(5.2 \pm 1.5) \times 10^{-4}$. The first Bogomolov measurements with evidence of events due to antiprotons
[Bogomolov1979] reported a ratio of $(6 \pm 4) \times 10^{-4}$ in the energy range between 2
and 5 GeV. Values of the same order of magnitude, depending on the energy range
explored, from 0.1 GeV to over 10 GeV, were obtained in the '80s and '90s by the
same authors. In general, it was established that this ratio is slightly greater for higher
energies.

Today, modern experiments dedicated to the search for antimatter in cosmic radi-
ation use sophisticated equipment, in some cases with superconducting magnetic
spectrometers mounted on board satellites or the International Space Station (ISS).
Figure 9.13 summarizes recent results about the relationship between antiprotons
and protons, as well as between antiprotons and positrons, obtained by the AMS
Collaboration, which uses an apparatus mounted on board the ISS [Aguilar2016].

## 9.6   The Intensity of the Primary Radiation at Different Altitudes

We have already mentioned in Chap. 7 the experimental studies to measure the
abundance of extensive air showers at various altitudes. This is somehow related to
the flux of primary radiation. More specific and direct measurements of the intensity
of primary radiation as a function of altitude were made as early as the second half
of the 1930s [Pfotzer1936, Schein1941].

In the work of Schein and collaborators [Schein1941], the result of which is
shown in Fig. 9.14, the intensity of the vertical radiation capable of passing through
a considerable thickness of lead, without however producing showers (curve A in the
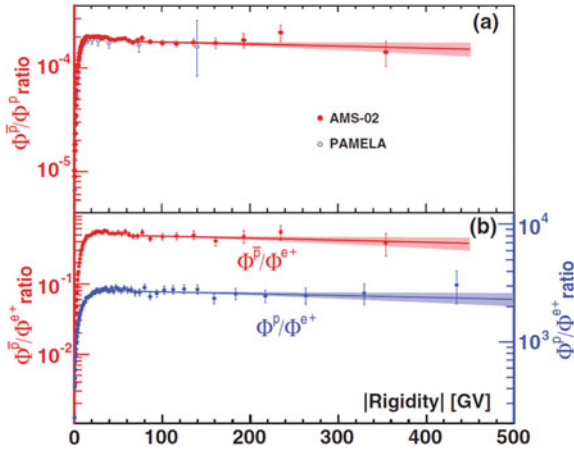
**Fig. 9.13** Values of the antiproton/proton ratio as a function of rigidity. The antiproton/positron and proton/positron ratios are also shown below. Figure reproduced from the work of M. Aguilar et al. (AMS Collaboration) [Aguilar2016] (Creative Commons Attribution 3.0 License)

figure) showed that this radiation could not be constituted by electrons and not even by mesons (due to their decay) but rather by protons, and that this intensity increased continuously with altitude, unlike the trend of the total intensity—essentially electrons and gamma—of the secondary radiation measured without absorbers (curve B, by Pfotzer).

The flux of vertical protons decreases with atmospheric depth, following an exponential attenuation law, with the consequence that the abundance of protons at sea level, which represents the residue of primary radiation, is very small, with an integrated intensity, for energies above 1 GeV, of the order of 0.9/(m$^2$ s sr) [PDG].

The point where the interaction of primary cosmic rays first occurs in the Earth's atmosphere (first interaction point) assumes a distribution as a function of the atmospheric depth X of the type:

$$\frac{dN}{dX} = \frac{1}{\Lambda_{p-air}} e^{-X/\Lambda_{p-air}}$$

where $\Lambda_{p\text{-air}}$ represents the free average path of interaction of protons in the air, linked to the cross section of interaction of protons with the nuclei of the Earth's atmosphere. Measurements of these cross sections were obtained from experiments carried out with accelerators of gradually increasing energy, up to the current maximum energy range covered by the Large Hadron Collider at CERN, which corresponds to energies of the primary protons of the order of 10$^{17}$ eV. On the other hand, at energies higher than those obtainable in the laboratory, are rather the data from cosmic ray physics to suggest the values of the interaction cross sections.
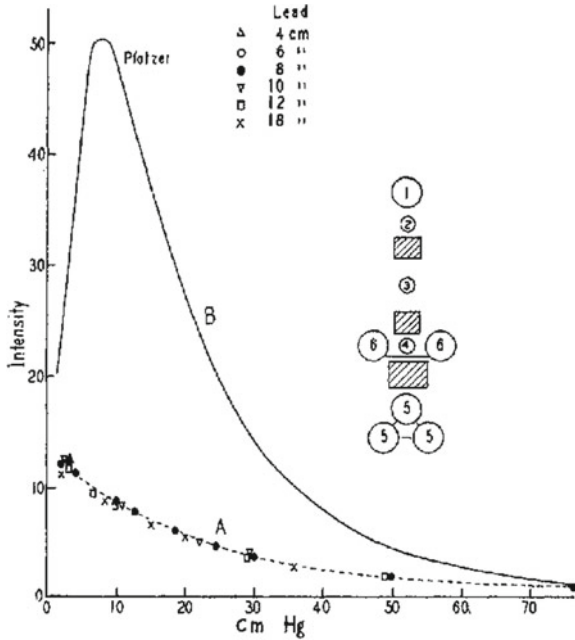
**Fig. 9.14** Intensity of the penetrating radiation (identified mainly as consisting of primary protons, curve A), compared with the intensity of the secondary radiation (curve B). Figure reproduced from the work of M. Schein et al., *The nature of the primary cosmic radiation and the origin of the mesotron*, Physical Review **59**(1941)615. Copyright (1941) American Physical Society, License RNP/22/JUN/054914

## 9.7   Possible Anisotropy Effects in the Primary Radiation

The primary high-energy cosmic rays, coming from outside the Solar System, have a fairly isotropic distribution of the arrival directions, reflecting the diffuse propagation in the galactic magnetic field along very long paths. At slightly lower energies, some small effect of anisotropy can be expected, due to local irregularities of the magnetic field or to other factors. The so-called Compton-Getting effect, introduced in 1935 [Compton1935] provides for a dipolar component in the distribution of the arrival directions, due to the motion of the observer with respect to a reference system based on an isotropic plasma of cosmic rays. For example, the anisotropy resulting from the motion of the Earth around the Sun, predicted to be of the order of $10^{-4}$, has been observed in recent times [Aglietta1996, Amenomori2004].

Precision measurements of primary cosmic rays, in the energy range from a few tens of GeV up to PeV ($10^{15}$ eV), revealed small but measurable anisotropies in the distribution of cosmic arrival directions, at the level of $10^{-5}$–$10^{-3}$ [Amenomori2006, Guillian2007, Abdo2009, Abbasi2010]. As easily understood, such a small value of anisotropy (1 part in 1000, or one part in 100,000) requires very high-statistics measurements, in order to reduce the statistical fluctuations below the desired effects.

Just as an example, with 10,000 events measured in a certain angular interval, there would be a statistical accuracy of 1%, and therefore only effects much more consistent than 1% could be highlighted. Assuming that statistical accuracy improves with the square root of the number of events measured, according to the Poisson distribution, it is easy to understand that looking for variations of 0.1% ($10^{-3}$) would require a measurement with several million events in any given angular interval, and so on. If one wants to obtain a two-dimensional map in equatorial (or galactic) coordinates of the intensity of cosmic radiation, the same statistical reasoning must be repeated for each angular interval in two dimensions, making this type of measurements extremely long and difficult, with a statistic that can only be reached after years of data taking by large area experiments. However, this is the case of some large current experiments [Amenomori2010, Abbasi2010, Aartsen2016, Amenomori2017, Abeysekara2019], which are capable of measuring $10^{10}$–$10^{11}$ events/year, with the possibility of exploring anisotropies between $10^{-5}$ and $10^{-3}$.

In the context of the search for deviations from the isotropic distribution, it is then necessary to distinguish between the search for point sources, with an excess of events coming from the same direction, and the search for widespread anisotropies on a large scale, involving large regions of the sky. This issue has become particularly relevant in recent years for extreme energy events, where some results have already been obtained [Aab2017b].

# Chapter 10
# The Secondary Cosmic Radiation

**Abstract** The interaction of a primary particle at the top of the atmosphere produces a complex secondary radiation, whose composition and properties are discussed in this chapter. Electrons and positrons, gammas, muons, charged hadrons and neutrons are the main components of the secondary cosmic ray radiation. The relative abundance of these species at the various altitudes along the atmosphere, their intensity profile, as well as the energy and angular distribution of each component constitute an important part of the cosmic ray physics on Earth. A collection of experimental data originating from pioneer measurements of these quantities, compared to most recent findings is presented along the chapter. Different parameterizations of the muon flux at the sea level are also discussed and compared in Appendix L.

## 10.1  Composition of the Secondary Radiation

As we have discussed, the development of extensive air showers in the Earth's atmosphere, generated by the interaction of primary high-energy particles (mostly protons or light nuclei), determines the composition and properties of the secondary radiation, i.e., the set of particles and electromagnetic radiation present at any given altitude above the sea level, together with their energy and angular distributions. The development of the shower is in turn determined not only by the possible interactions of the secondary particles during their propagation in the atmosphere, but also by their possible decays. It is therefore clear that the composition of the secondary radiation itself and its properties will be different at the different altitudes with respect to the sea level. We know, for example, that muons are subject to decay, with a lifetime at rest of about $2.2\,\mu s$. Despite their speed, close to that of light, which allows them to reach the sea level, due to the relativistic dilation of time, a certain fraction of muons decay along their path in the atmosphere, altering the proportion between muons and electrons at the various altitudes. Particles that have significantly shorter lifetimes than muons have a negligible probability of crossing the atmosphere to reach sea level.

Of particular interest for the physics of cosmic rays are the properties of the cosmic radiation observable at sea level or at moderate altitudes, where most of the

experiments capable of detecting the secondary products of an extensive air shower take place.

## 10.2  Muons

Cosmic muons mainly originate from the decay process of charged pions, and, to a much lesser extent, from that of charged kaons, processes that occur in the atmosphere during the development of an extensive air shower. Only very high-energy muons (larger than TeV) can originate in processes involving other particles. The main results concerning the muonic component in the atmosphere and at the sea level concern the dependence of their intensity on the altitude, the abundance of the two charge states, hence the ratio between positive and negative muons, their energy, or momentum, spectrum and their angular distribution.

Measures aimed at investigating these properties have already been carried out since a long time, as we have partially discussed in previous chapters, using counter telescopes, magnetic spectrometers and other kind of detectors.

Referring first to the study of this component in the atmosphere, i.e., at altitudes significantly above the sea level, we can divide the experiments into two broad categories: those carried out with the experimental setup fixed to the ground—even if at high altitudes—and those carried out with some apparatus aboard balloons. Measurements of the first type are for example those reported by Blokh and collaborators in the 1970s [Blokh1977] at various altitudes (atmospheric pressures between 650 and 950 mbar, corresponding to altitudes between just over 500 and 3600 m), where an intensity equal to about 1.8 cm$^{-2}$ min$^{-1}$ sr$^{-1}$ at the highest altitude and about 0.3 cm$^{-2}$ min$^{-1}$ sr$^{-1}$ at an altitude of 500 m was measured. In more recent years high altitude measurements have been obtained by means of detectors placed on board stratospheric balloons (MASS, IMAX, CAPRICE experiments in the '90s), able to obtain the intensity profile of the muonic component in the atmosphere, from an atmospheric depth of a few g/cm$^2$ to the sea level, also separating the two charge states.

The trend of the intensity vs atmospheric depth has shown that the profile grows starting from low values at the top of the atmosphere to reach a maximum at atmospheric depths around 200 g/cm$^2$ (altitudes of 12 km), although with some differences depending on the selected muon energy range. Figure 10.1 shows as an example the intensity profile reported by Bellotti and collaborators [Bellotti1999] for negative muons in the overall momentum range from 0.3 to 40 GeV/c.

High altitude measurements, at about 3000 m, of the muon energy spectrum were carried out from the second half of the 1950s [Kocharian1956, Kocharian1959, Allkofer1964], and in the following years also at an altitude of 5260 m [Allkofer1965]. At even higher altitudes, measurements of the energy spectrum were obtained, again in those years, by means of sounding balloons and on board airplanes [Baradzei1959]. More recent measurements were obviously carried out in the '90s and beyond, with instrumentation installed on board stratospheric
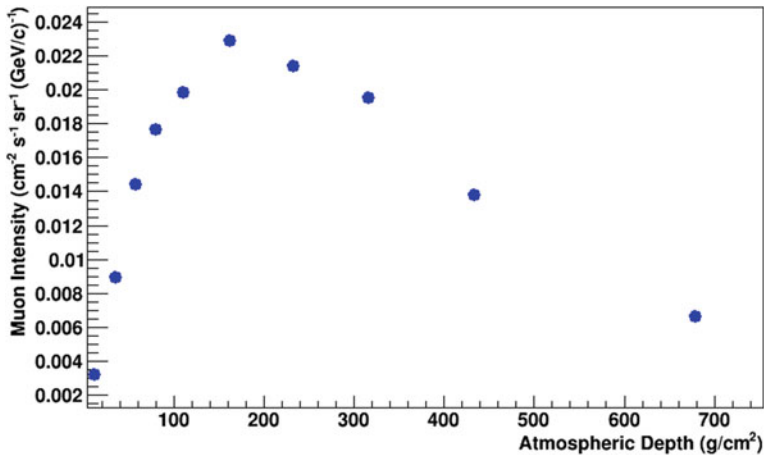
**Fig. 10.1** Intensity of the muon component at different atmospheric depths. Data extracted from [Bellotti1999]

balloons up to an altitude of 36 km. In some of the measures mentioned, the charge state of the muons was identified, obtaining a value of the ratio between positive and negative muons, which, although with large fluctuations, also depending on the muon momentum range, is close to the value of 1.3.

If we exclude low-energy particles, considering an energy threshold of the order of GeV, muons are the most abundant charged component observed at sea level. Most muons are produced in the upper part of the atmosphere (10–15 km of altitude) following the processes already described. The muons produced continue their travel in the atmosphere, losing part of their energy through ionization processes, or possibly decaying. The energy lost by a muon in crossing the atmosphere can be estimated at about 2 GeV, since they behave as particles at their minimum ionization [with a specific energy loss of about 2 MeV/(g cm$^2$)] and must pass through an atmospheric thickness of about 1000 g/cm$^2$. As a consequence of the different processes (production, energy loss, decay) the muons have an energy distribution at sea level, with an average value, for the vertical ones, around 3–4 GeV, and an angular distribution that can be represented to a first approximation by a dependence of the type $\cos^n\theta$, where the exponent n is close to 2. The distribution in energy (or momentum p) is however very different depending on the zenithal angle of arrival, as shown in Fig. 10.2, which shows a comparison between the momentum spectra (multiplied by $p^{2.7}$) of the approximately vertical and highly inclined muons (zenithal angle 75°).

As can be seen from Fig. 10.2, which reports the results of a series of measurements carried out by different experiments [PDG], the spectrum of highly inclined muons, i.e., close to the horizontal, is shifted towards higher momenta. The path of these muons, in fact, involves crossing a greater thickness of the atmosphere, with significant differences in terms of the loss of energy suffered and decays.
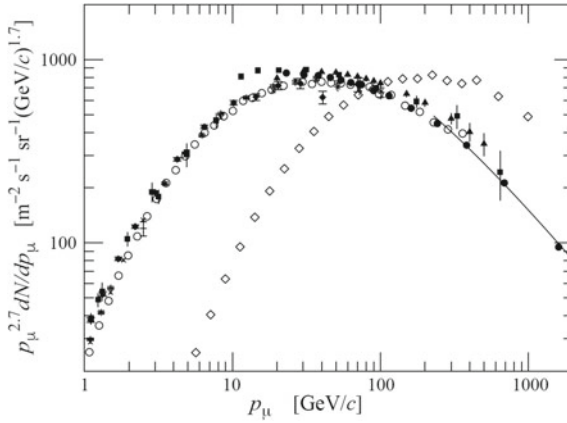
**Fig. 10.2** Momentum spectra of secondary muons observed at sea level, multiplied by the factor p$^{2.7}$, in the case of vertical muons (solid symbols) and with a zenithal angle of 75° (empty symbols) [PDG]. Figure reproduced with permission from R. L. Workman et al. (Particle Data Group), Prog. Theor. Exp. Phys. 2022, 083C01 (2022)

The absolute value of the intensity of vertical muons at sea level is shown in Fig. 10.3 in a wide momentum interval, from 0.2 GeV/c up to about 1000 GeV/c, as reported by Allkofer and collaborators [Allkofer1971] from various measurements carried out between the end of the '60s and the beginning of the '70s, also in order to evaluate possible discrepancies with the data available in that period. As it is seen, the spectrum presents a maximum for momenta slightly lower than 1 GeV/c and a trend that to a first approximation, starting from a few GeV/c, follows a relationship similar to E$^{-\gamma}$, even if in Allkofer's work the spectrum was parameterized with slightly more complex functions, having different parameters obtained from the fit of the data. Detailed measurements up to zenithal angles close to the horizontal have also been reported by Crookes and Rastin [Crookes1972] in the same years.

Due to the enormous variety of experimental data concerning the muon spectrum, it is useful in many cases to use simple analytical forms (parameterizations) that best represent the trend of the data and can be used in calculations, for example in simulation procedures, or for the evaluation of the response of the detectors. There are different parameterizations of the muon spectrum, depending on their energy (or momentum) and their zenithal angle. One of the most used, valid at high energies and for zenithal angle not too large, so as to neglect the effect of the curvature of the Earth, is the following, due to Gaisser [Gaisser1990], in which the energy of muons is expressed in GeV:

$$\frac{dN}{dEd\Omega} = 0.14E^{-2.7}\left(\frac{1}{1+\frac{1.1E\cos\theta}{115\,\text{GeV}}} - \frac{0.054}{1+\frac{1.1E\cos\theta}{850\,\text{GeV}}}\right)\text{cm}^{-2}\,\text{s}^{-1}\,\text{sr}^{-1}\,\text{GeV}^{-1}$$
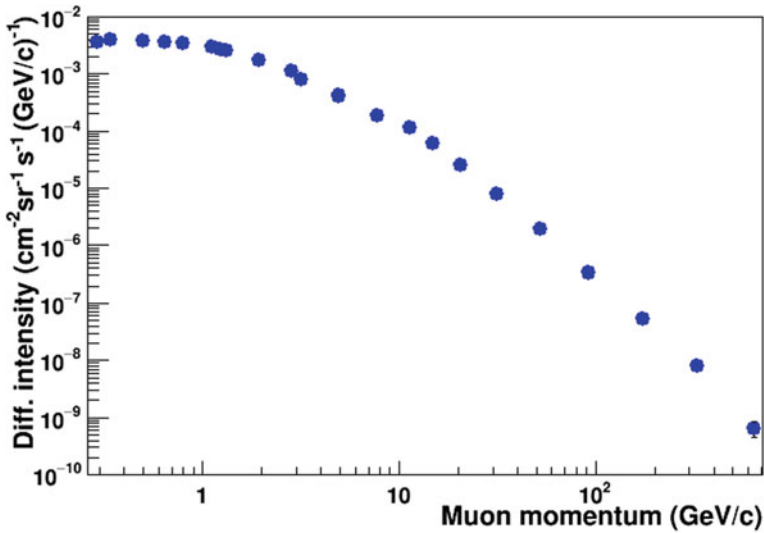
**Fig. 10.3** Vertical intensity of muons, extracted from various experiments reported by Allkofer and collaborators between the end of the '60s and the beginning of the '70s. Data extracted from [Allkofer1971]

Figure 10.4 shows a typical plot of the Gaisser parametrization, for vertical muons, in which the vertical scale is multiplied by the factor $E^{2.7}$.
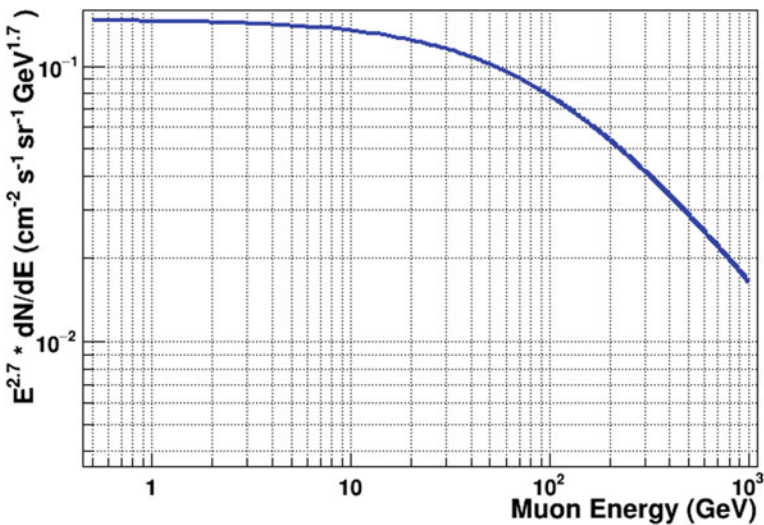


**Fig. 10.4** Spectrum of vertical muons, multiplied by the factor $E^{2.7}$, according to the Gaisser parameterization described in the text

Various other parameterizations have been proposed in more recent years, also
to extend the range of applicability of the Gaisser formula. Appendix L discusses
some of them and shows numerical examples of spectra calculated from these
parameterizations.

Measurements of the muon flux as a function of the zenithal angle, extended
to values close to the horizontal [Crookes1972] in the 1970s, made it possible to
establish that the intensity can be represented by a relationship of the type

$$I(\theta) = I(\theta = 0) \cos^n \theta$$

with an exponent $n$ slightly dependent on the momentum range considered, with an
average value around 1.85. Table 10.1 shows a summary of the values of the exponent
$n$ extracted from different experiments [Riggi2020].

While the primary radiation is made up almost exclusively of positively charged
particles, in the secondary muon component it is possible to find both positive and
negative muons, with an excess in favour of the positive ones. The ratio between
positive muons and negative muons is of the order of 1.3–1.5 and depends not only
on the energy of the muons, but also—particularly for low-momentum muons—
on the geomagnetic latitude of the observation site and on the angle of inclination
of muons. Measurements of the charge ratio of muons had been made as early as

**Table 10.1** Values of the exponent n relating to the relation $I(\theta) = I(\theta = 0)\cos^n\theta$ which describes
the trend of the angular distribution of muons at sea level or at moderate altitudes [Riggi2020]

| Exponent $n$ | Experimental conditions | References |
|---|---|---|
| 2.1 | $> 0.33$ GeV/c, sea level, 50° N | [Greisen1942] |
| $1.6 \pm 0.1$ | $> \sim 10$ GeV/c, underground, 38.3° N | [Sheldon1963] |
| $1.96 \pm 0.22$ | $> 0.7$ GeV/c, sea level, 53° N | [Judge1965] |
| $2.16 \pm 0.01$ | $> 0.35$ GeV/c, sea level, 53° N | [Crookes1972] |
| 2.2 | $> 0.35$ GeV/c, 120 m a.s.l., 16° N | [Karmakar1973] |
| $1.91 \pm 0.1$ | $> 0.4$ GeV/c, sea level, 12° N | [Bhattacharyya1974] |
| $1.85 \pm 0.11$ | $> 1$ GeV/c, sea level, 12° N | [Bhattacharyya1974] |
| $1.75 \pm 0.11$ | $> 2$ GeV/c, sea level, 12° N | [Bhattacharyya1974] |
| $2.23 \pm 0.33$ | 417 hg cm$^{-2}$ underground, 13.0° N | [Bhat1978] |
| $1.95 \pm 0.13$ | 1200 m a.s.l., 35.4° N | [Bahmanabadi2005] |
| $1.884 \pm 0.005$ | 1.5 GeV, $\sim 150$ m a.s.l., 55.6° N | [Dmietreva2006] |
| $2.15 \pm 0.01$ | $> 0.28$ GeV/c, sea level, 19° N | [Pal2012] |
| $1.91 \pm 0.07$ | 1200 m a.s.l., 35.4° N | [Abdhollai2013] |
| $2.00 \pm 0.14$ (syst) | $> 0.11$ GeV/c, 160 m a.s.l., 9.9° N | [Pethurai2017] |
| $2.33 \pm 0.11$ | 1200 m a.s.l., 35.4° N | [Bahmanabadi2019] |
| $1.91 \pm 0.15$ (syst) | Sea level, 24.5° N | [Arneodo2019] |
| $1.83 \pm 0.13$ | $> \sim 0.2$ GeV/c, 3100 m a.s.l., 37.7° N | [Riggi2020] |

the 1950s and over time they were extended to wider energy intervals, with greater precision, in different locations (geomagnetic latitudes) and for inclination angles even close to the horizontal. A large amount of data is now available, obtained under various conditions. For vertical muons the $N_{\mu+}/N_{\mu-}$ ratio stands at values around 1.3, although with large fluctuations between different experiments, in a wide muon momentum interval, from about 5 GeV/c up to 1000 GeV/c, with slightly lower values for low momentum muons (< 5 GeV/c). For muons close to the horizontal (inclination angles from about 80° upwards) the charge ratio $N_{\mu+}/N_{\mu-}$ increases enormously, until it reaches values of the order of 10–20 for low momentum muons close to the horizontal [Allkofer1979]. Finally, due to the East-West asymmetry, for a given intermediate value of the zenithal angle (for example 45°) and for muons of low momentum, below a few GeV/c, the ratio $N_{\mu+}/N_{\mu-}$ differs, showing values even lower than 1 along the East direction, and values up to 1.5 along the West direction [Allkofer1967].

## 10.3  Electrons

As already discussed, the secondary cosmic radiation also includes a "soft" component, which unlike the "hard" one, made up of muons, is absorbed by even relatively small thicknesses of solid material. Generally, by convention, a lead layer of 15 cm ($167 \text{ g/cm}^2$) is assumed to define the demarcation threshold between the radiation capable of penetrating through this thickness (hard component) and that which is instead arrested (soft component). The soft component actually consists not only of electrons and positrons, but also of gammas, whose properties are described in more detail in the next section. The abundance of the soft component, or, more specifically, that of electrons/positrons, with respect to the muonic component, strongly depends on the selected energy range.

In the atmosphere, the electronic component is also partially affected by the presence of primary electrons. Primary electrons, however, constitute a non-negligible fraction of the total electrons present only at very high energies and at the top of the atmosphere (atmospheric depths up to a few tens of $\text{g/cm}^2$). As an example, in the energy range between about 50 and 100 MeV the primary electrons represent about 10% of the total electrons present up to atmospheric depths of 100–200 $\text{g/cm}^2$, while they are negligible at greater atmospheric depths (lower altitudes). Only in the energy range of the order of GeV the primary electrons are comparable in abundance with the secondary ones. A review of numerous results obtained from various experiments in the 1970s using high-altitude balloons, is reported by Grieder [Grieder2001].

The intensity profile of secondary electrons in the atmosphere also has a behaviour to a first approximation similar to that of muons. At high altitudes in the atmosphere (atmospheric depths starting from a few $\text{g/cm}^2$) the intensity gradually increases with the atmospheric depth, up to about 100–200 $\text{g/cm}^2$, where the intensity reaches a maximum, then decrease again going towards the sea level. Figure 10.5 shows a typical behaviour, measured by Fulks and Mayer in the 1970s [Fulks1974] by
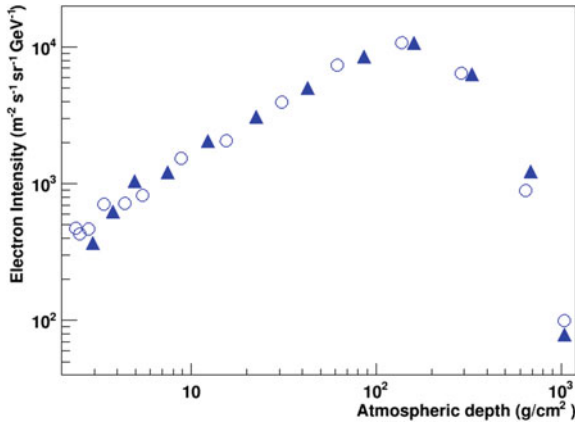
**Fig. 10.5** Intensity profile of secondary electrons in the energy range (54–85) MeV. Data extracted from [Fulks1974]. The different symbols refer to different balloon ascents

instrumentation aboard balloons, for energies in the range (54–85) MeV, in which the contribution of secondary electrons is preponderant with respect to that of the primary. For gradually increasing energies, at the top of the atmosphere and up to a depth of about 100 g/cm$^2$, the contribution of the secondaries gradually becomes less significant than that of the primary ones.

The energy spectrum of electrons in the atmosphere, also measured in numerous experiments in the 1970s at various atmospheric depths [Fulks1974], generally shows a pattern of the $E^{-\gamma}$ type, where the exponent $\gamma$ is approximately equal to 2 at low atmospheric depths and assumes higher values going towards the sea level. A large fraction of the electrons therefore has very low energies, below 100 MeV, even at high altitudes in the atmosphere. Figure 10.6 shows the energy spectrum of electrons, at two different atmospheric depths (291 and 637 g/cm$^2$) [Fulks1974].

At sea level, comparative measurements of the soft and hard components had been already carried out in the 1940s, for example by Greisen [Greisen1942], using a telescope—orientable in the zenithal angle—with several Geiger counters in coincidence, even separated by lead layers. The comparison between the number of coincidences obtained with and without the interposed lead layers made it possible to evaluate the proportion between the two components.

At an altitude close to sea level, in the case of vertical particles, the relative intensities measured for the hard and soft components were respectively 2.27 and 0.59, thus corresponding to a fraction of the soft component of about 26% compared to that of the hard component. Under the Greisen measurement conditions, the so-called soft component included electrons with an energy greater than about 20 MeV. This same apparatus had been used to carry out similar measurements, at altitudes of 1600 m, 3200 m and 4300 m, obtaining in this case fractions equal to 38%, 58% and 77% respectively. It is clear, therefore, that the abundance of electrons compared to muons is lower at sea level, compared to what occurs at higher altitudes.
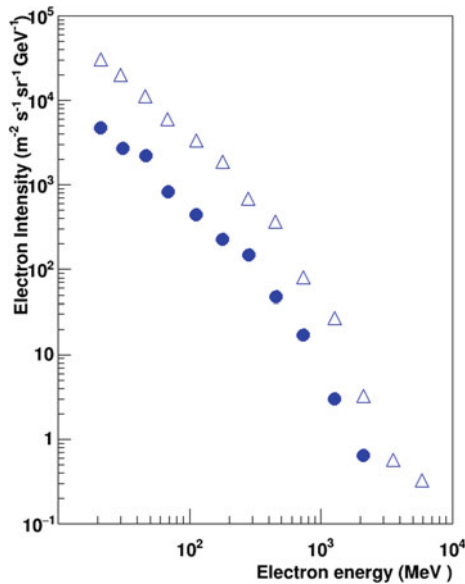
**Fig. 10.6**  Energy spectrum of secondary electrons at two different atmospheric depths: 291 g/cm$^2$ (empty triangles) and 637 g/cm$^2$ (solid symbols). Data extracted from [Fulks1974]

The energy spectrum of secondary electrons, even at sea level, is highly concentrated at low energies compared to that of muons. Measurements of the energy spectrum of electrons were obtained in the 1960s and 1970s by various authors [Wibberenz1962; Allkofer1970]. Figure 10.7 shows a series of data reporting the vertical intensity of electrons (positive and negative) obtained from various measurements made at sea level [Grieder2001].

## 10.4  Gammas

The presence of gammas in extensive air showers is linked to a variety of physical processes, including mainly the decay of neutral pions and other unstable particles, the bremsstrahlung processes of electrons and positrons and their annihilation.

Although high-energy gamma rays have also been measured, beyond TeV, most of the gamma radiation has a low energy, and the energy distribution follows a power law of the E$^{-\gamma}$ type, with an exponent close to 1.8. The gamma intensity profile increases with atmospheric depth, reaching—for ranges close to the vertical—a maximum at atmospheric depths around 100–200 g/cm$^2$, and then decreasing as it goes towards high atmospheric depths, close to sea level, as shown in Fig. 10.8, which reports Thompson's results obtained in the mid-1970s [Thompson1974].
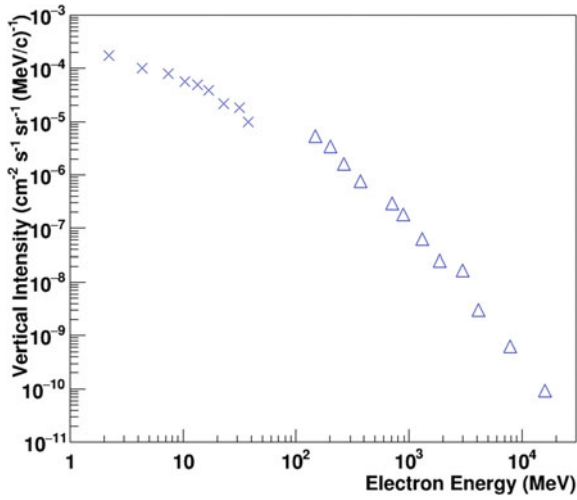
**Fig. 10.7** Vertical electron intensity, obtained from measurements made at sea level by Beedle and Webber [Beedle1970] (crosses) and by Beuermann and Wibberenz [Beuermann1968] (triangles)
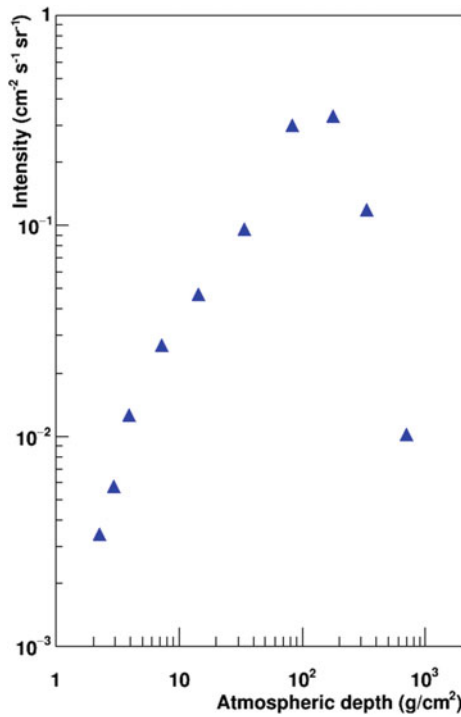


**Fig. 10.8** Intensity profile of the gamma (with energy E > 30 MeV and inclination close to the vertical), as a function of atmospheric depth. Data extracted from [Thompson1974]

At sea level, the gamma spectrum has often been measured together with that of electrons and positrons, without discriminating between the different components of the soft radiation. Figure 10.9 shows an example of a gamma spectrum separated from the electronic component [Beuermann1968], obtained at an atmospheric depth of 760 g/cm$^2$, for energies from 100 MeV upwards.

At lower energies, from a few MeV to tens of MeV, gamma spectra measured at different atmospheric depths have been reported by Ryan [Ryan1979], as shown in Fig. 10.10, which reports some of these data.
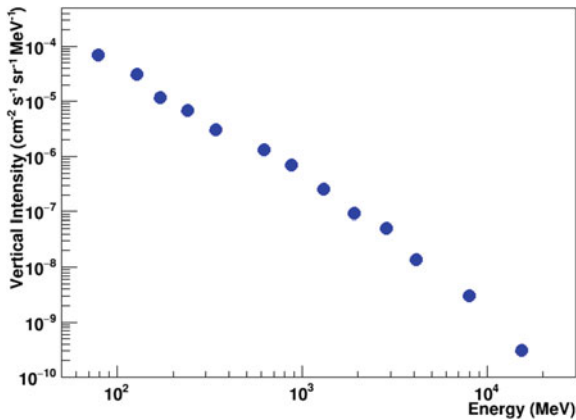


**Fig. 10.9** Gamma spectrum measured at atmospheric depth of 760 g/cm$^2$. Data extracted from [Beuermann1968]
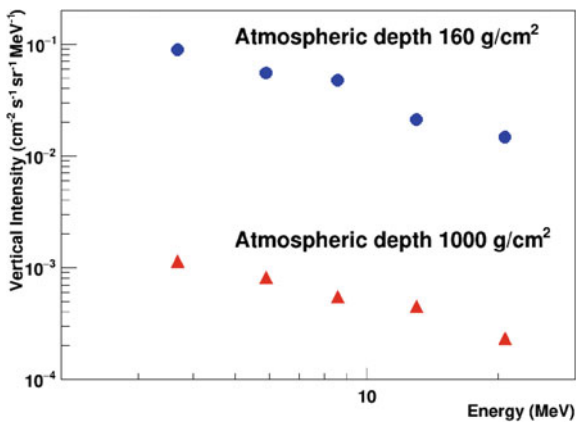


**Fig. 10.10** Gamma spectrum at sea level and at atmospheric depth of 160 g/cm$^2$. Data extracted from [Ryan1979]

Therefore, the measurable gammas at the sea level, even if abundant, have an energy distribution mainly below 10 MeV, so that even a moderate shielding is able to greatly reduce their contribution compared to that of muons.

## 10.5   Charged Hadrons

The flux of secondary charged hadrons, in particular protons and pions, and the corresponding energy spectrum, has been measured in a variety of experiments carried out at high altitudes, in the mountains, and with instrumentation aboard aircraft or balloons. The first results were obtained by nuclear emulsions, while more complex experiments, also with the aim of separating protons from pions—the two most abundant components—performed in more recent years, used combinations of magnetic spectrometers, calorimeters and time of flight measurements.

The dependence of the proton flux (of energy greater than 1 GeV) on atmospheric depth, as emerges from a series of measures summarized by the work of Shopper and collaborators [Schopper1967], is shown in Fig. 10.11.

As it can be seen, the flux decreases by several orders of magnitude going from the top of the atmosphere towards sea level, where this component is practically negligible compared to the penetrating component.

Although the spectrum in energy extends up to very high values (TeV), as evidenced by recent experiments, most protons have relatively low energies, with
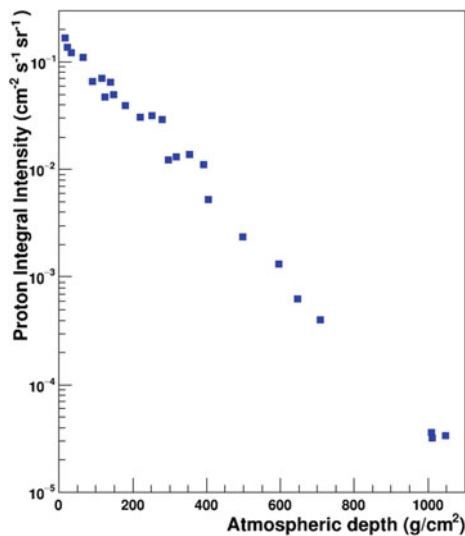


**Fig. 10.11** Profile of the flux of vertical protons (energy E > 1 GeV) as a function of atmospheric depth, from different experiments carried out between 1948 and 1955. Data extracted from [Schopper1967]
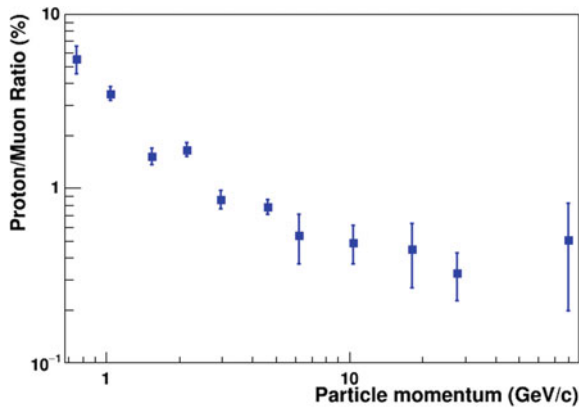
**Fig. 10.12** Energy spectrum of vertical protons, measured at an altitude of 3200 m. The different symbols refer to different datasets. Data extracted from [Kocharian1956, Kocharian1959]

a maximum around a hundred MeV and a sharp decrease in flux going towards the higher energies. Measurements of the flux of vertical protons, already carried out around the end of the 1950s, had made it possible to extract the energy spectrum of the protons, as for example represented in Fig. 10.12, which reports some data from the measurements obtained by Kocharian and collaborators [Kocharian1956, Kocharian1959] by the use of magnetic spectrometers combined with calorimeters. Further sets of measures of the energy spectrum of protons, measured under various conditions, are available in the Grieder review [Grieder2001].
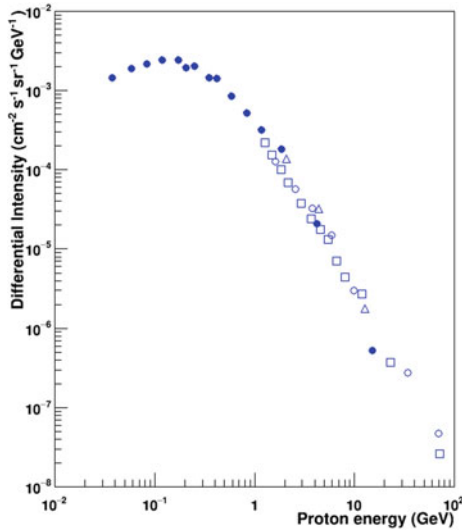
At sea level the abundance of protons is very low compared to that of muons, of the order of percent, especially at energies higher than GeV [Brooke1964]. Figure 10.13 shows the value of the proton to muon ratio in the momentum interval between about 1 and 80 GeV/c. Only for very low energies, less than about GeV, the abundance of protons exceeds a few percent compared to that of muons.

From the same work by Brooke and Wolfendale [Brooke1964] it is also possible to extract the spectrum of protons at sea level, which is shown in Fig. 10.14.

## 10.6  Neutrons

Neutrons represent an important component of the secondary cosmic radiation present in the atmosphere and also at sea level. They can be generated as evaporation products from the de-excitation of nuclei in the atmosphere, with low energies, typically below 10 MeV, or as a result of high-energy nuclear collisions, in which case they also have high energies. Low-energy neutrons, in particular, are affected by solar events, both in terms of periodic variations due to solar cycles and catastrophic events, such as solar flares, which we will discuss in a later chapter.

**Fig. 10.13** Percentage abundance of protons compared to that of muons, evaluated at sea level, as a function of the momentum of the particle. Data extracted from [Brooke1964]
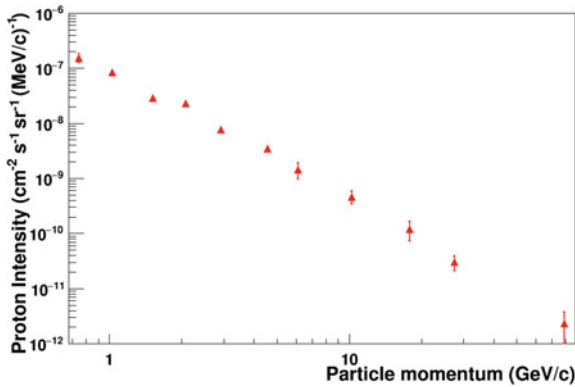


**Fig. 10.14** Intensity of protons at sea level, as a function of their momentum. Data extracted from [Brooke1964]

The intensity profile of neutrons at different atmospheric depths, reported by Armstrong and collaborators in the 1970s [Armstrong1973] is shown in Fig. 10.15, between thermal energies and 20 MeV.

As it can be seen from the figure, the maximum intensity is reached around atmospheric depths of about 100 g/cm$^2$, then decreasing by over two orders of magnitude at sea level.

The energy spectrum of neutrons, measured at different altitudes and with different techniques, shows that most neutrons have very low energies, from thermal neutrons
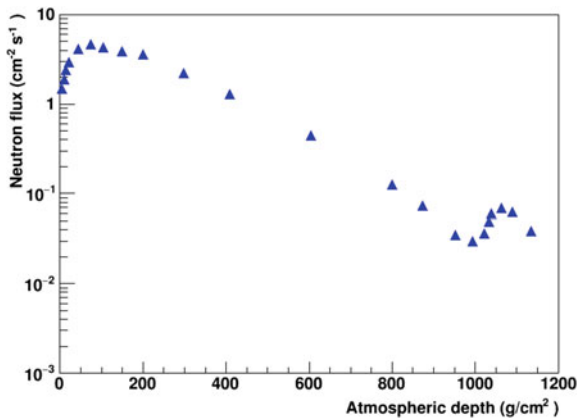
**Fig. 10.15** Neutron intensity profile (from thermal energies to 20 MeV) at different atmospheric depths [Armstrong1973]

(energies of the order of eV) up to energies of several GeV, with a shape that from about 10 MeV can be represented with a power law, of the $E^{-\gamma}$ type. A detailed measurement of the neutron spectrum in the upper atmosphere, at 12.5 km latitude, in a wide energy range, from 0.01 eV up to GeV, was reported at the conclusion of a series of aerial flights with instrumentation on board, by Hewitt and collaborators [Hewitt1978], and is shown in Fig. 10.16.

In more recent times, studies of the flux of cosmic neutrons at various altitudes and under different conditions have been carried out, even by the use of passive detectors, mainly for the purpose of evaluating the possible effects on the absorbed dose [Zanini2001].
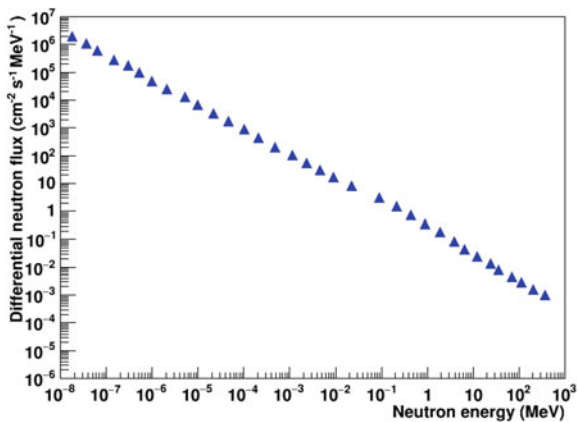


**Fig. 10.16** Energy spectrum of neutrons, measured at high altitude (12.5 km), in a wide range, from about 0.01 eV up to about 1 GeV. Data extracted from [Hewitt1978]
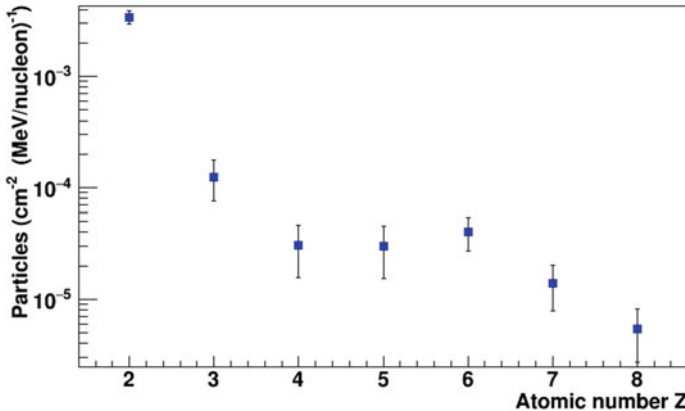
**Fig. 10.17** Abundance of light nuclei in measurements obtained during a series of Concorde flights at high altitude (13–17 km) [Zhou1999]

## 10.7  Nuclei

Although in the primary radiation we have the presence of light and medium mass nuclei, as seen in the previous chapter, the probability that such nuclei can propagate intact in the atmosphere is enormously small, due to nuclear interactions. This is also generally true for any secondary nuclei created in these interactions. The average free path for nuclear interaction in air is in fact a few tens of $g/cm^2$ (from 75 $g/cm^2$ for protons to 14 $g/cm^2$ for heavier nuclei, such as Iron), so the flux, even for light nuclei such as Helium, practically reduces to zero after about 100 $g/cm^2$ of atmospheric depth.

Measurements of the yield of light nuclei in the atmosphere were, for example, carried out using instrumentation installed on board the Concorde during a series of high-altitude flights (between 13 and 17 km) in the 1990s [Zhou1999]. Figure 10.17 shows the yield of light nuclei, (from Z = 2 to Z = 8) at these altitudes, obtained from an observation period of several hundred hours of high-altitude flight.

As expected, based on the previous considerations about the probability of nuclear interaction during their path in the atmosphere, the presence of nuclei, even the light ones, at sea level, is practically negligible. Measurements aimed at establishing the presence of nuclei associated with cosmic radiation, or at establishing an upper limit for their flux, have been carried out in recent decades. In Yock's work [Yock1986], for example, only some events due to nuclei heavier than protons (d, t, $^3$He), were observed, using a range telescope and a measurement time of about 5000 h, establishing an upper limit on the presence of $^4$He.

# Chapter 11
# The Influence of the Earth

**Abstract** The atmosphere and the magnetic field of the Earth exert an important influence on the flux of primary and secondary cosmic rays. These effects have been observed since the early history of cosmic rays and were an important part of the understanding the general properties of the cosmic radiation. Meteorological effects due to the presence of the atmosphere, in particular the temperature effect and the anticorrelation between the cosmic ray flux and the atmospheric pressure, resulting in a barometric coefficient to be determined for any specific component are discussed, with various quantitative examples. The influence of the Earth magnetic field and the associated latitude and East–West effect are also presented. The latter had an important role since the early investigations of the cosmic ray flux in the mid-1930s and still gives an opportunity to carry out educational experiments in cosmic ray physics.

## 11.1 Introduction

The Earth, with its atmosphere and its magnetic field, influences in various ways the properties of the cosmic radiation, both primary and secondary, existing in the vicinity of our planet. The Earth's magnetic field, whose effects are important even at large distances from the Earth's surface, in fact strongly modify the propagation of charged particles that are part of the primary cosmic radiation. These effects are also important on the secondary particles produced in the atmosphere by the development of extensive air showers. The first evidence of these effects, which lead to a different flux of cosmic rays over different geomagnetic coordinates (geomagnetic latitude and longitude of the observation point), dates back, as we have already seen, to the first decades of the history of cosmic ray physics. Another important aspect through which the Earth influences the propagation of the secondary cosmic radiation is obviously the existence of the Earth's atmosphere itself, with its composition and the variations that characterize it, in terms of temperature and pressure. The presence of the Earth's atmosphere and its variations, together with the presence of the magnetic field, result in an intensity which depends on the orientation (zenithal and azimuthal angles) for the various secondary components. Variations in pressure and temperature

also determine variations in the secondary flux observed locally, with the need to make corrections to this, which then allow for further analyses of other physical phenomena, for example those related to the Sun or to the properties of the primary radiation.

We shall discuss some of these aspects throughout this chapter. On the other hand, we have already discussed, both in relation to the properties of the primary radiation and of the various secondary components, the effect of altitude with respect to sea level on the measured intensity, which is largely determined by the presence of the atmosphere and by the processes that take place in it. Measurements of the intensity of the cosmic radiation in the Earth's subsoil, under the ice or underwater, will be discussed separately in a specific chapter.

## 11.2   The Interaction with the Atmosphere and Meteorological Effects

Meteorological effects on cosmic rays are of interest both because their study makes it possible to evaluate the corresponding corrections that must be introduced in the experimental data in order to subsequently proceed with the study of extra-atmospheric effects, and because the observed effects can contribute in themselves to a better understanding of the changes taking place in the Earth's atmosphere.

Basically, there are two effects on the variations in the observed flux of cosmic rays, related to atmospheric causes: the barometric effect and the temperature effect. A very complete treatment of these effects, in the context of the different sources of variation of the cosmic ray flux, is reported in a comprehensive textbook by Dorman [Dorman1974].

The atmospheric pressure is subject to temporal variations of various kinds, both periodic and aperiodic. Periodic variations are those related, for instance, to the day/night cycle (daily variations) and those on an annual basis.

The daily variations, basically linked to the atmospheric tidal phenomena and the expansion of the air that accompanies the increase in temperature caused by the solar radiation, have two maxima within 24 h, one around 10 o'clock in the morning, more pronounced, and a second one around 10 p.m., and two minima, the first around 4 a.m., the second, more pronounced, around 4 p.m. In these considerations the times are expressed in local time. The amplitude of these variations is greater during the day than during the night. The difference between the high value in the morning and the low value in the afternoon can therefore be taken as an estimate of the maximum daily variation. The amplitude of these variations is of the order of at most a few mbar, however it depends on the season and on the location of the observation site. It is also known that planetary waves (Rossby waves), naturally occurring in rotating fluids, may also be observed in the atmosphere of a planet, due to its rotation. These waves are characterized by a low-pressure amplitude, and by a period in the order of a few days.

In addition to regular (periodic) variations, the atmospheric pressure is also subject, as we know, to aperiodic variations, linked to the overall weather conditions of that location. These variations can have a much greater amplitude, even 10–20 mbar, and may last even several days, so that their effect is able sometimes to mask the regular variations.

By an example, Fig. 11.1 shows the trend of atmospheric pressure, expressed in mm Hg, monitored with a pressure sensor connected to a data logger system during a period of approximately 3 months, at intervals of 30′, except for some short breaks.

An expanded region of the previous graph is shown in Fig. 11.2, in a time interval during which the overall weather conditions were sufficiently stable (average pressure value only slightly increasing over a week). It is possible to see the daily variations, with a period of 24 h, while the second daily maximum is hardly seen.
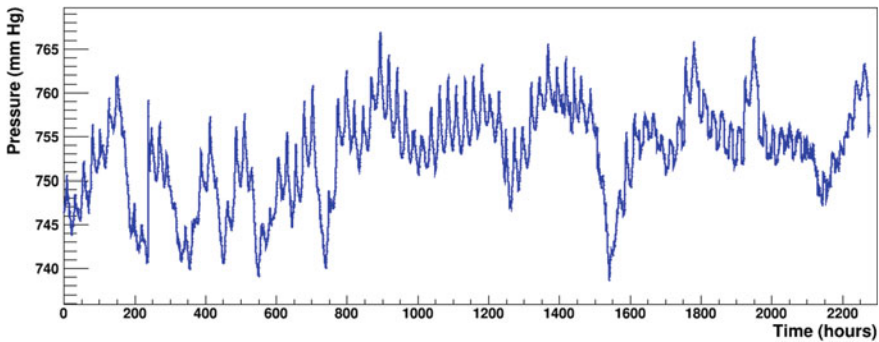


**Fig. 11.1** Atmospheric pressure trend, monitored over a period of about 3 months, at regular intervals of 30′. Both the daily variations, of a periodic nature, and the aperiodic ones, of greater amplitude, linked to the overall weather conditions, are visible
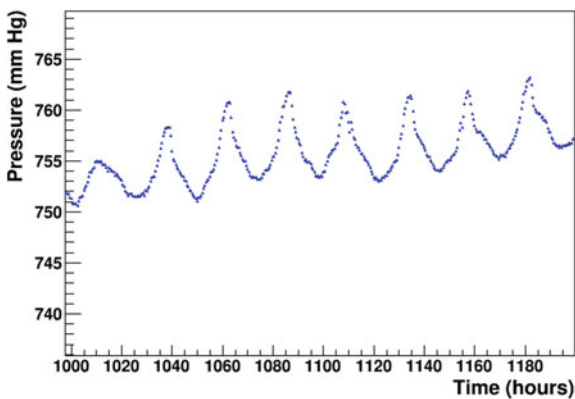


**Fig. 11.2** Expanded region of the previous graph, in a time interval of about a week, with the presence of the daily maxima, and an average pressure trend only slightly increasing over time, due to the overall weather conditions

The position of the maxima in the daily cycle is however strongly influenced by the geographical location of the observation site, by its altitude and the overall climate of that region (e.g., continental or desert climate). Depending on these specific conditions, displacements of several hours in the time of the maximum and minimum pressure have also been observed.

Quantitative analyses of these pressure data, measured as a function of time for long periods, can be performed with methods used in general for the analysis of time series. The use of correlograms, in particular, allows to accurately establish the period of the main cycles and the existence of secondary periodicities. The existence of a second daily maximum in the pressure trend has been, still in recent times, the subject of discussion and detailed interpretations (resonance phenomena, absorption of UV radiation by ozone, periodic wind trend) [Janeselli1968].

On an annual scale, further small variations in atmospheric pressure are observed, linked to the cycle of the seasons and to the effects of heating and cooling of the soil. They are smaller in amplitude, and strongly dependent on the particular geographical area of observation.

The aperiodic variations in pressure are instead linked to the overall trend of atmospheric weather, which in turn depends on numerous parameters, such as the temperature of the air layers, humidity conditions and winds. The pressure conditions are different from area to area, and determine, together with many other parameters, the weather conditions also in the following days. In this context, the maps of isobars (lines that connect geographical points with the same pressure value), frequently shown during weather forecasts, are of considerable importance as a tool for understanding the evolution of atmospheric weather in the following days.

Catastrophic events, such as large volcano explosions, are also able to produce shock waves in the Earth's atmosphere, which can be observed even at large distance from the explosion. Sometimes these waves, which may produce local pressure variations up to a few mbar, are able to go around the Earth even two or more times. A recent example was offered by the explosion of the Hunga-Tonga volcano in 2022, whose shock waves were observed in different parts of the Earth, and also monitored by one of the EEE stations located in the Svalbard archipelago [Abbrescia2022].

Considering the effect of the pressure $p$ at sea level, the variation $dI$ in the intensity of a specific component of the secondary cosmic radiation can be expressed as

$$dI = -\mu I dp$$

where $\mu$ is the absorption coefficient for that specific component. In the hypothesis that this coefficient is constant, the previous equation admits a solution of the type

$$I = I_0 e^{-\mu(P-P_0)}$$

where $I_0$ is the intensity at pressure $P_0$. If the pressure variations $(P - P_0)$ are small enough, the intensity variation can be expressed, in the approximation to the first order, as a linear function of the pressure variation:

$$\Delta I = \beta I \Delta p$$

where β represents a barometric coefficient, usually expressed in %/mbar. The sign of this coefficient is negative, as the pressure variation is anti-correlated with the intensity variation. In other words, the higher the pressure, the lower the intensity of that specific component. Generally, for the muonic component the barometric coefficient values are in the order of 0.1–0.2%/mbar and the linear approximation is quite reasonable. For the neutron component, however, the observed variations are much greater, with coefficients of the order of 0.7–0.9%/mbar, and therefore using a linear approximation is not correct, requiring in this case to use the original exponential dependence.

Having clarified this in a synthetic way, it must however be remembered that the barometric coefficient, as it is linked to the absorption of a given component of the secondary radiation in the atmosphere, depends on many factors, in particular on the energy composition of that given component, which in turn is different depending on the geographical position and altitude of the place of observation. It also depends on the characteristics of the detector (for example its geometrical acceptance and its efficiency at different energies). These considerations therefore suggest that each detection apparatus is characterized by its own barometric coefficient, which should be determined experimentally and subsequently used to correct the data measured with that apparatus.

As an example, Fig. 11.3 shows the trend of atmospheric pressure (top) and the corresponding counting rate (bottom) in a cosmic ray detector (telescope based on MRPC chambers of the EEE Project) over a period of time of about 20 days. As it can be seen, in correspondence with a strong decrease in the atmospheric pressure, determined by the overall weather conditions, an increase in the event rate is observed.

Figure 11.4 shows the correlation plot between the two quantities, which shows an almost linear trend.

To quantitatively obtain the value of the barometric coefficient, using in this case a linear approximation, a linear fit of the pairs of values (pressure, event rate) can be performed, obtaining the angular coefficient of the best-fit line. This coefficient expresses the variation in the number of counts per second with respect to a unitary variation in pressure (for example one millibar). To obtain the percentage change, the angular coefficient determined by the fit can be divided by the average value of the count rate in the data set considered.

The determination of the barometric coefficient for each particular experimental apparatus presents however some critical aspects, as in the considered period all the other effects that may lead to a variation in the observed flux must be regarded as negligible. For this reason, the barometric coefficients are generally extracted from limited data collection periods (for example a few weeks), possibly by averaging the values obtained over different but compatible periods.

Depending on the specific secondary component (muons, electrons, neutrons), and the energy range considered for these particles, the values of the barometric coefficients can be quite different, as already mentioned.
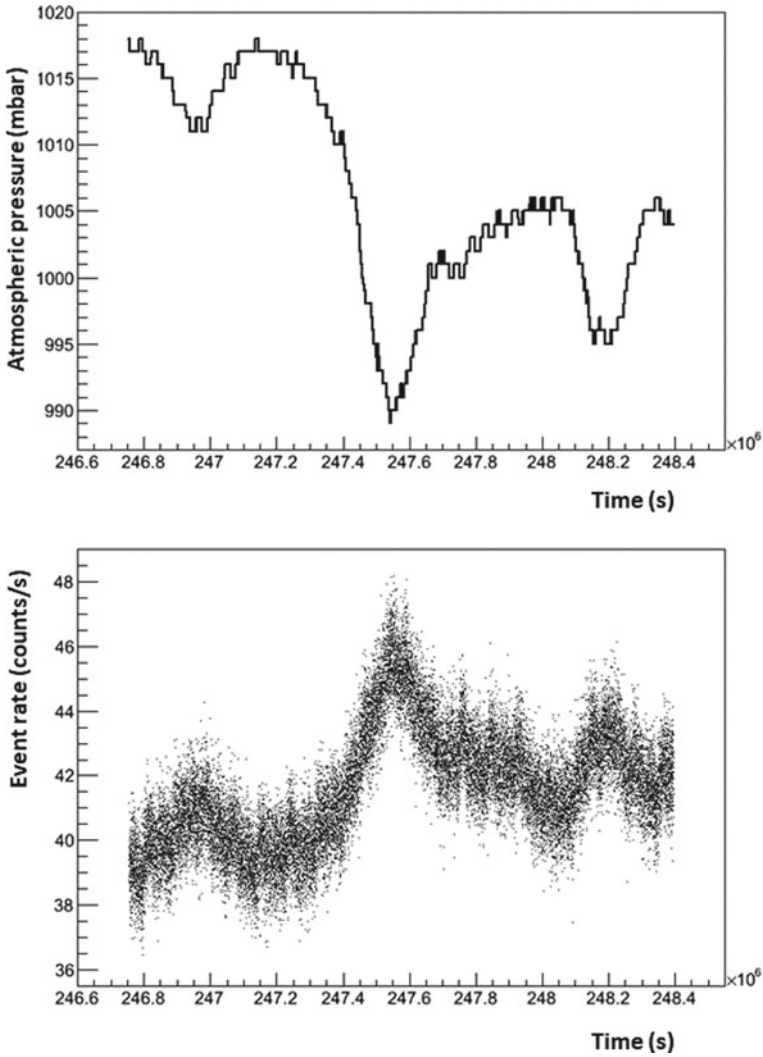
**Fig. 11.3** Atmospheric pressure trend (top) and the corresponding event rate measured in one of the MRPC telescopes of the EEE project

For the muonic component, detailed measurements were made starting from the 1950s, with different types of detectors and different amounts of shielding material placed above the detectors, observing values between 0.13 and 0.2%/mbar. As expected, the muon flux observed in the subsoil, therefore with a considerable amount of rock absorber material, has a much lower barometric coefficient than that observed on the surface. Typical values deduced from measurements performed at equivalent
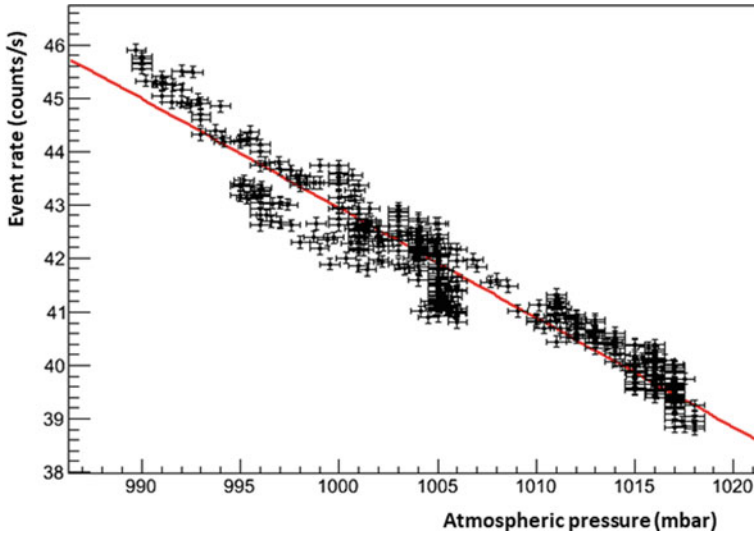
**Fig. 11.4** Correlation plot between atmospheric pressure and event rate measured in an MRPC telescope of the EEE project, over a period of about 20 days. The solid line in the plot shows the result of a linear fit to the data

water depths of 40–60 m show barometric coefficients between 0.03 and 0.06%/mbar [Dorman1974].

Reviews of recent data relating to the muonic component, measured by detectors located in different locations around the world [Mendonca2019] have made it possible to study the barometric coefficients and the temperature effect as a function of the geomagnetic cutoff and the muon arrival angle. For example, it is observed that the barometric coefficient for such detectors is lower in areas of low geomagnetic cutoff, increasing towards the higher cutoff values.

For the soft component of the secondary cosmic radiation, generally higher values are observed, of the order of 0.3%/mbar, although these values strongly depend, as expected, on the amount of the absorber thickness placed above the detector. Measurements carried out with an ionization chamber surmounted by various amounts of material [Shamos1966] have shown for example values of the barometric coefficient decreasing from 0.3%/mbar (in the absence of external absorbers) down to values of 0.04%/mbar with absorbers larger than 2000 g/cm$^2$.

In the case of the neutron component, the barometric coefficient values are around 0.7–0.9%/mbar, also depending on the geomagnetic latitude.

If we consider instead the effect of atmospheric pressure on extensive air showers as a whole, the dependence of the observed shower rate on atmospheric pressure shows coefficients varying between 0.5 and 1%/mbar, depending on the energy of the shower and the altitude of the observation site [Dorman1974]. Measurements of the coincidence rate between individual detectors (therefore signalling the arrival of simultaneous particles associated with a shower) were already made in the second half
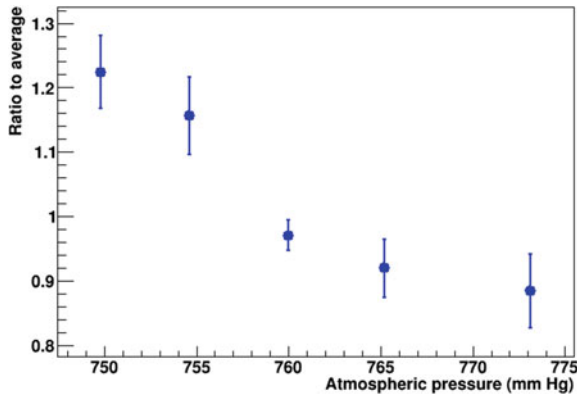
**Fig. 11.5** Dependence of the number of showers observed (ratio with respect to the average value of the shower rate) on varying atmospheric pressure. Data reproduced from [Cosyns1940]. The showers were identified in this context by the triple coincidence between detectors placed within a distance of 18 m

of the 1930s, using for example three Geiger counters operated in coincidence and observing how the number of these coincidences varied in an anti-correlated way with the atmospheric pressure, with a significantly higher correlation coefficient than that associated with the detection of individual particles in the shower [Stevenson1935, Cosyns1940].

An example of the dependence of the number of showers observed on the atmospheric pressure is shown in Fig. 11.5 [Cosyns1940], which shows the ratio between the observed shower rate and its average value, for different pressure values. In this context, to evaluate the number of showers, the coincidence between three detectors positioned within a distance of 18 m was employed.

Using a set of detectors located at a certain distance, in other words a small array, it is possible to determine how the barometric coefficient depends qualitatively on the energy of the shower, selecting the events with a gradually increasing particle density in each detector of the array. An example of such a measurement, carried out in the 1960s by Jones [Jones1965] shows that as the density of particles increases, the barometric coefficient also increases, from values of about 0.2%/mbar to values of about 0.6%/mbar.

Even in the absence of variations in the atmospheric pressure at ground level, variations in the local density of the air column above the observation site can also determine an effect on the flux of secondary cosmic rays measured. This effect, due to temperature, is the result of two causes, one due to interactions and one due to the decays of secondary particles (pions and kaons) through the atmosphere, capable of producing muons. An increase in temperature reduces the density, while at the same time slightly varying the probability of interaction. On the other hand, the effects due to decay increase, and the net result is an increase in the rate as the temperature increases (positive correlation between temperature and observed rate). The other effect (with negative correlation between temperature and observed rate) is linked

to the phenomenon of the decay of the muons themselves. With the increase in temperature and the consequent reduction in density, muons must travel longer paths before decaying, thus producing a greater flux of muons observed at ground level. Which of the two effects, that of positive correlation or that of negative correlation with temperature, is preponderant? It turns out that everything depends on the energy of the particles. In the case of high-energy particles, the positive correlation effect is dominant, while the opposite happens for low-energy particles.

The variations related to the temperature effects of the atmosphere are however different from those related to pressure and are approximately an order of magnitude smaller.

Furthermore, while the variations related to pressure are interpreted in relation to the atmospheric pressure measured on the ground, those related to temperature require the knowledge of the temperature profile $T_i$ along the different layers $i = 1$, 2, … N of the atmosphere itself.

Data of this kind, which are more difficult to obtain, generally require the use of sounding balloons launched regularly. From these it is however possible to obtain a single variable, an effective temperature $T_{eff}$, averaged over the mass, in terms of which to report the variations in intensity corresponding to a unit variation of this temperature [Dorman1974, Riadigos2020]:

$$\Delta I = \alpha I \Delta T_{eff}$$

where α represents a temperature coefficient, with values of the order of 0.2–0.3%/K.

## 11.3   The Influence of the Earth Magnetic Field

The Earth affects the flux of cosmic rays, even before the phenomena that occur in the atmosphere, already at a large distance, through the magnetic field it generates. Terrestrial magnetism, or geomagnetism, is one of the phenomena intimately linked to cosmic radiation. We have already discussed how the hypotheses on the corpuscular or radiative nature of the primary cosmic radiation could be verified precisely on the basis of measurements performed at different geomagnetic latitudes. Even more deeply, the flux of primary charged particles is strongly influenced by the Earth's magnetic field, which acts in some way as a screen for a large fraction of them, with consequences of primary importance also on the very existence of life on Earth.

The Earth's magnetic field extends from the inside of the Earth to very large distances from the Earth's surface and is generated by electric currents due to the convective motions of the components present in the liquid state in the central part of the planet, in turn caused by the flow of heat towards the outermost layers. The intensity of the magnetic field at the Earth's surface varies between about 30 and 60 μT (0.3–0.6 gauss), and as a first approximation it can be represented as the field produced by a simple dipole inclined with respect to the Earth's rotation axis. This

leads to a difference between the geographic coordinate system (latitude and longitude), based on the rotation axis and the geographic equator, and the geomagnetic coordinate system, as described in more detail in Appendix C. On a time scale of the order of years, the position of the magnetic poles moves over the Earth's surface (with displacements of up to 40 km per year), while—but on a time scale of hundreds of thousands of years—the whole Earth's magnetic field reverses, as evidenced by paleomagnetic studies on rocks. Paleomagnetism is precisely the study of the Earth's magnetic field in the past, which provides evidence of the movement of continents.

The effect of the Earth's magnetic field extends up to distances of tens of thousands of km with respect to the Earth's surface (several times the Earth's radius), where the presence of the atmosphere is already negligible. Although of low intensity at these large distances, the existence of a magnetic field extended over a very large region makes the effect exerted on the motion of the charged particles in this region important. In particular, this effect is noticeable on lower energy charged particles, such as the so-called "solar wind", a stream of particles released from the outermost part of the Sun, the solar corona. Although during solar flares high-energy—even GeV—particles may be emitted, for the most part these particles (mainly electrons, protons and alpha particles, together with small percentages of heavier nuclei) have very low energies—of the order of keV—but sufficient to escape the gravitational pull of the Sun. We will discuss further aspects of cosmic rays due to the Sun in the next chapter, while we are concerned here with understanding how the Earth, with its magnetic field, can act as a screen against these particles.

The magnetosphere, or region in which the Earth's magnetic field exerts its influence, has a complex structure. The ideal dipolar form that it would have is in fact distorted by the presence of the solar wind, which itself shapes the outer solar field in the interplanetary magnetic field. The magnetosphere is therefore asymmetrical, with dimensions of the order of 10 times the Earth's radius on the side of the Sun, but with much larger dimensions, of the order of 100 times the Earth's radius, on the opposite side. Within the magnetosphere, a region—extending from 60 km above the ground up to a few times the Earth's radius—contains low energy ionized particles. In this region there is also the ionosphere and the Van Allen belts, discovered following explorations with the first satellites in the late 1950s, which contain particles of higher energy, even of several MeV. The first of these bands is located at a distance from the Earth equal to 1–2 terrestrial radii, the second at greater distances, between 4 and 7 terrestrial radii. Figure 11.6 shows a sketch of the structure of the Earth's magnetosphere.

It must be remembered that many other objects in the solar system—but not all of them—have a magnetosphere. Among these the planets Jupiter and Saturn, while for example Venus and Mars do not have a magnetic field. The magnetic field of Jupiter is greater than that of the Earth and enormously more extended, about 7 million km on the side of the Sun and up to the orbit of Saturn on the opposite side.

The existence or absence of a magnetic field also implies a different geological history for each planet, as well as the existence of certain conditions (such as, for example, the presence of water or the atmosphere itself), which can make life possible.
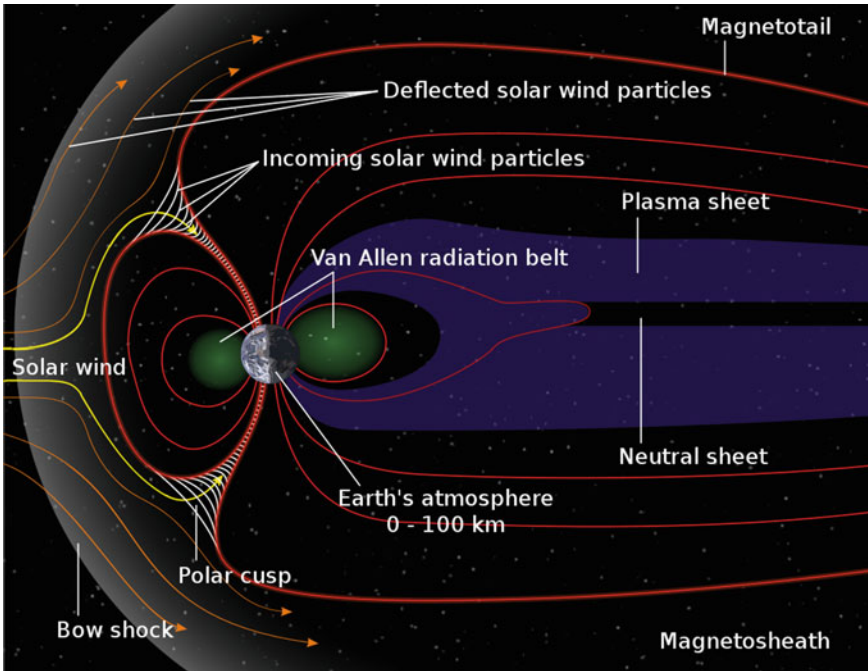
**Fig. 11.6**   Sketch of the Earth's magnetosphere. *Source* Wikimedia Commons, Creative Commons Attribution-Share Alike 4.0 International License

This is an important condition for the Earth, in which the existence of the Earth's magnetic field largely protects it from radiations. In addition to deflecting low energy particles that make up the solar wind, the Earth's magnetic field also acts on high-energy particles, cosmic rays that come from outside the solar system. A previous action on these cosmic rays is already exerted by the Sun with its magnetic field, as we will see in the next chapter. As for the Earth, the trajectories of particles, even of relatively high energy, and above all the possibility that they actually arrive in the atmosphere, is strongly influenced by the geomagnetic field. In turn, the overall conditions of the magnetosphere undergo changes due to solar conditions, particularly in connection with catastrophic events, such as flares or coronal mass ejections (CMEs). A recent example of a change in the conditions of the magnetosphere occurred in June 2015, causing a sudden increase in the observed flux of muons [Mohanty2016], which correlated with a large variation in the interplanetary magnetic field.

The overall effect of the Earth's magnetic field, in terms of shielding with respect to the primary cosmic radiation, in particular for high-energy particles of extrasolar origin, is to deflect the particles below a certain threshold (geomagnetic cutoff) which therefore cannot reach the Earth. Variations of this cutoff during a magnetic storm can produce an increase in the observed flux of cosmic rays.

The geomagnetic cutoff can be calculated in principle from the detailed knowledge of the magnetic field map. The general method consists in solving the equations of

motion of the particles, tracing the possible trajectories in the magnetosphere of each particle of given energy or momentum, a complex problem from the point of view of calculation.

In a simplified approach, the basic equations that regulate the motion of a charged particle in a dipolar magnetic field allow us to understand the behaviour of a charged particle approaching the Earth with its magnetosphere. Imagining the trajectory seen by an observer located above the North Pole, if the particle has a very high energy, it will not be appreciably deflected by the magnetic field and will be able to reach the top of the Earth's atmosphere. Particles with low energy, below a certain threshold value, will be deflected backwards in interplanetary space, failing to penetrate the Earth's atmosphere. Particles of intermediate energy, higher than the threshold value, will be curved more or less strongly by the magnetic field, penetrating the atmosphere along a curvilinear path. However, what happens depends on the latitude of the place and on the inclination of the arrival direction of the particle with respect to the magnetosphere. Around the poles, the magnetic field lines are radial in first approximation and the particles arriving radially will have easier access to the atmosphere; in the equatorial region the shielding effect of the magnetic field is greater and the threshold value higher. Particles that have an energy just above the threshold can follow very complicated trajectories.

The Norwegian mathematician and astrophysicist Carl Størmer was the first to tackle this problem analytically, as early as at the beginning of 1900s, starting from the observation of the northern lights. Størmer's theory starts from the first calculations, carried out in 1907 and related to the motion of charged particles in a dipolar magnetic field, in order to understand under which conditions electrons coming from the Sun could reach the Earth, producing those phenomena known as Northern Lights [Størmer1907]. Only in the 1930s did Størmer apply this method to the treatment of the motion of particles of much higher energy, the cosmic rays of extrasolar origin [Størmer1930]. Without going into the complex treatment of this theory, the main consequence that follows is that the trajectories of the particles are confined in permitted regions, while other (forbidden) regions are not compatible with trajectories that satisfy the equations of motion. Using Størmer's theory it became possible to understand the dependence of the observed flux of particles on latitude, as well as the effects of East–West asymmetry. Subsequently, the possibility that charged particles remained trapped in the Earth's magnetic field was also studied on the basis of developments in this theory, a possibility that was confirmed in 1958 with the observation of the Van Allen belts. Given the complexity of the calculations involved, even with modern computing resources, numerical solutions of the equations are often used to evaluate the geomagnetic cutoff at any given point, especially to estimate the dose of radiation absorbed in space (for example in the International Space Station) [Smart2005].

Figure 11.7 shows a sketch of some possible trajectories of charged particles of different energy (magnetic rigidities) [Smart2005, Copeland2020]. Cosmic rays with a high magnetic rigidity are less affected by the influence of the magnetic field and follow relatively simple orbits (trajectory 1). For particles that have gradually lower magnetic rigidity, the trajectories are curved more by the action of the field and are

more complex (trajectories with increasing numbers, 2, 3 … up to 15), even with the presence of loops.

The distribution of the geomagnetic cutoff values can be obtained in any given historical period by means of a numerical calculation of the possible trajectories based
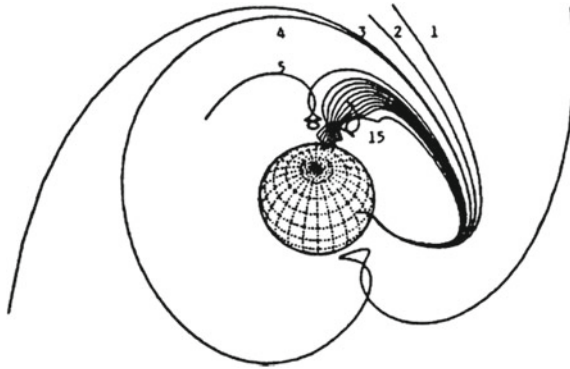


**Fig. 11.7** Possible trajectories of charged particles with different magnetic rigidity in the geomagnetic field [Smart2005, Copeland2020]. The trajectories from "1" to "15" correspond respectively to rigidities from the largest ones (more "resistant" to geomagnetic deflection) to the smallest ones
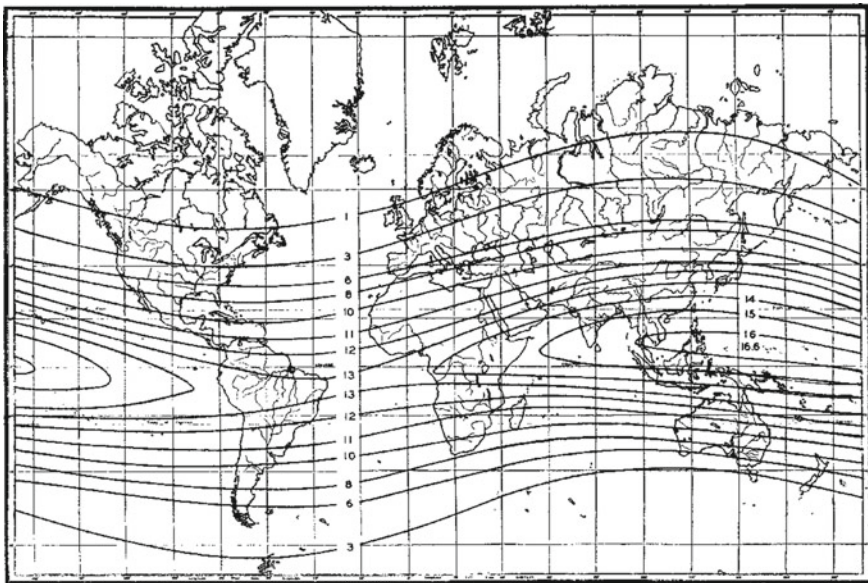


**Fig. 11.8** Geomagnetic cutoff map [Johnson1938], with the level curves connecting the zones with equal cutoff value. Figure reproduced by T. H. Johnson, *Cosmic ray intensity and geomagnetic effects*, Review of Modern Physics **10**(1938)194. Copyright (1938) by the American Physical Society, License No. RNP/22/JUN/055239

on a given model of the geomagnetic field. Figure 11.8 shows a historical example, dating back to the late 1930s of the geomagnetic cutoff map, with the level curves that connect the areas of equal value to the cutoff. Recent data on the distribution of vertical geomagnetic cutoff values are for example reported in [Gerontidou2021]. As it can be seen, at high latitudes the geomagnetic cutoff is lower, which means that even protons with relatively low energy can reach the top of the atmosphere, producing extensive atmospheric showers. Going towards the equator, the geomagnetic cutoff increases, and in the equatorial regions minimum energies up to about 15 GeV are required for a vertical proton to penetrate the atmosphere. The contours of the regions with the same cutoff are curved since the axis of the magnetic field does not coincide with the axis of rotation of the Earth.

A very detailed report on geomagnetic cutoff calculations, with tables and graphs for the period 1965–2010 is the one edited by Copeland [Copeland2020].

## 11.4   Angular Distribution of Muons and the East–West Effect

Although we have already discussed some of these aspects as they were first observed, it is worth mentioning explicitly in this context how some characteristics of the secondary cosmic radiation are attributable to the influence of the Earth system. In this section in particular we will examine the phenomenology concerning the East–West effect.

While the angular distribution in the zenithal angle of the particles of the secondary radiation is determined to a large extent by the influence of the Earth's atmosphere, based on the actual path that these particles take to reach the place of observation and the processes (loss of energy, decays) that occur along this path, the dependence on the azimuth angle in a given place is strongly linked to the charge of the particles and to the effect of the magnetic field.

As far as the dependence on the azimuthal angle $\varphi$ is concerned, anisotropic effects between the flux of particles coming from the East compared to that of the particles coming from the West, the so-called East–West effect, had been observed, since 1930s by Johnson and Street [Johnson1933a, Johnson1933b] and by Rossi [Rossi1934a]. In the work that reports the main results of the study by Johnson and Street [Johnson1933b], reference is made to sets of measurements obtained with Geiger counter telescopes, operated in such a way as to be able to observe, for the same interval of zenithal angles, the number of associated events to cosmic rays from the East and West directions. The measurements were carried out for different zenithal angles, from 25 to 75°, with measurement periods of the order of ten hours for each measurement, which made it possible to record a number of events of a few thousand in each condition. The location of the experiment was in Mexico City, at an altitude of 2250 m and a geomagnetic latitude of 29°.
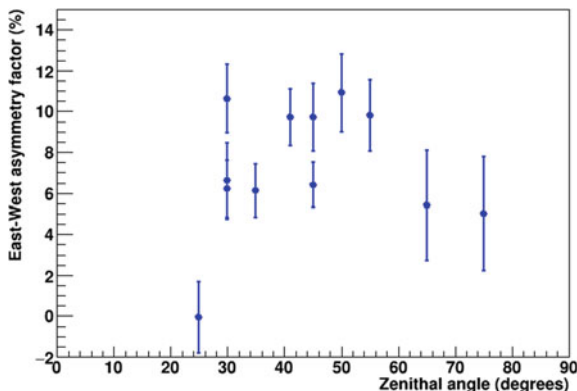
**Fig. 11.9**  East–West asymmetry ratio observed by Johnson and Street in a series of measurements obtained in the early 1930s at different zenithal angles and at an altitude of 2250 m. Data reproduced from [Johnson1933b]

Figure 11.9 shows the results of these measurements, in particular the value of the asymmetry ratio

$$R = 2\frac{I_W - I_E}{I_W + I_E}$$

where the quantities $I_W$, $I_E$ represent the intensity relative to the two directions of origin of the particles. This ratio therefore expresses the percentage difference between the two intensities with respect to their average value.

As it can be seen from the previous figure, the percentage difference between the intensities measured along the East and West directions amounts in these conditions to about 10% for the intermediate zenithal angles, where it has a maximum around 40–50°, while the asymmetry decreases for inclinations close to the horizontal or to the vertical.

In Rossi's measurements [Rossi1934a], carried out in Africa, at a geomagnetic latitude around 11° and at an altitude of 2370 m, it was found, for example, that the W/E ratio between the flux of particles coming from the West (W) with respect to those coming from East (E), was around 1.11 for $\theta = 15°$, 1.16 for $\theta = 30°$, and about 1.19 at $\theta = 45°$.

The measurements done in that period typically used Geiger counters and were not always able to discriminate—based on the amount of shielding provided above the detectors—between the soft and hard component of the secondary cosmic radiation. As we discussed in the introductory chapters, such experiments were the basis for considerations about the nature of the detected particles, as being charged, long before the specific characteristics of these particles were clarified.

More detailed measurements, carried out in the following years [Johnson1934, Johnson1935, Johnson1941], also showed that the amount of this effect depends on the latitude and altitude of the observation site. The result of this campaign of

measurements, carried out using an apparatus with many Geiger counters arranged on two concentric crowns, which could rotate around an axis, and a system of multiple coincidences between the different counters, gave rise in those years to measurements in different locations, at various altitudes (at sea level, between 2000 and 3000 m and at the maximum altitude of 4300 m) and at different geomagnetic latitudes.

Since that period, East–West asymmetry measurements have been carried out by many experiments capable of measuring the directions of arrival of cosmic particles, in various locations around the world, at different geomagnetic altitudes and latitudes. We cite as an example those carried out by Barber in 1949, at high altitude, using airplanes [Barber1949], a review of the 1950s [Winckler1950] and many other works.

Measurements of the East–West effect today also represent a classic example of possible educational activities in cosmic ray physics, which can also be carried out with relatively simple equipment. An example of such activity is reported in [Blanco2008c], which discusses some measurements made with a telescope of small scintillators that can be oriented both in azimuth and zenithal angle.

## 11.5   The Latitude Effect

As we have already discussed with regard to the first worldwide measurement campaigns conducted in the 1930s by Compton and Millikan, as well as by other authors, the dependence of the cosmic ray flux on latitude, in particular on geomagnetic latitude, was of great help for establishing the corpuscular nature of the radiation. These campaigns in fact showed, as we saw in detail in Chap. 3, a dependence of the observed flux on geomagnetic latitude, with an increase in intensity going from the equator towards the poles, up to a certain latitude, around 50° N, beyond which the intensity remained almost constant. The interpretation of these measurements, as well as being based on the nature of the primary radiation as essentially constituted by charged particles, was related to the characteristics of the Earth's magnetic field, capable of introducing a geomagnetic cutoff, i.e., a minimum energy that the primary particles (vertical) must possess in order to penetrate into the Earth's atmosphere and therefore give rise to the creation of extensive atmospheric showers. This geomagnetic cutoff is dependent on the particular geographic location (geomagnetic latitude and longitude), according to some maps, examples of which we reported in Chap. 3.

Although further measurement campaigns—following those dating back to the 1930s—were organized sporadically in the following years, detailed and organized measurements of the flux of cosmic rays in geographic locations spread out on a large scale on the surface of the Earth have not apparently received the same attention over the following decades, with the exception of the use of neutron detection stations, which are in any case located in fixed positions. In particular, it is difficult to find examples of measurement campaigns carried out with the same detector transported over long distances, thus avoiding problems of comparison and normalization between detectors having different characteristics.

Only in very recent years have some measurement campaigns based on exploiting the cosmic ray flux over different latitudes been organized by various Institutions, quite often in the context of large-scale educational and scientific projects. An example is represented by the measurement campaign carried out with a neutron detector based on $^3$He [Pyle1999]. Another example is the recent campaign of measurements done on board an oceanographic vessel equipped with an MRPC camera telescope, the TRISTAN detector [Saraiva2020], traveling between Spain and Chile. A further recent example is the campaign of measurements undertaken within the scope of the scientific and educational activities of the EEE project, which used a scintillator telescope, the POLA detector, installed on board a boat on a voyage between Iceland and the Svalbard Archipelago, up to a latitude of 82° N [Abbrescia2020]. The same telescope was also used for a further campaign of measurements of the cosmic ray flux from latitude 35° N, thus covering a large part of the entire range between 35 and 82° N [Abbrescia2023].

## 11.6 Other Influences on the Cosmic Ray Flux Due to the Earth Environment

Due to the close connection between the observed flux of cosmic rays and the geomagnetic field, it is reasonable to expect that variations in the Earth's magnetic field will produce variations in the measured flux of cosmic rays. Variations in the geomagnetic field may be due to processes occurring inside the Earth, to processes in the ionosphere or in the radiation belts around the Earth, or to processes in interplanetary space near the Earth.

As already mentioned, long-term variations of the Earth's magnetic field due to internal causes have been highlighted by paleomagnetism studies, which have also shown the polarity changes of the magnetic field on scales of hundreds of thousands of years. It is plausible that in correspondence to these polarity inversions the magnetic field undergoes considerable variations, leading to corresponding variations in the cosmic flux, for example to an increase in flux at the polarity inversion. The characteristics of these polarity reversals are still the subject of experimental studies and theoretical considerations, in particular as regards the duration of the reversal periods, with some estimate between 1000 and 10,000 years, although there are estimates of much shorter duration, about 100 years, compatible with the average life span of people. It is known that the last reversal of the Earth's magnetic field occurred 780,000 years ago, with a duration of about 22,000 years. Inversions generally occur randomly, governed—according to some scientists—by Poisson processes, by more complex statistical distributions or with chaotic characteristics. The average interval between successive reversals of the polarity has however been estimated at 450,000 years, based on the reversals that have occurred in the last 83 million years.

As for the variations due to magnetic storms, these were highlighted in the late 1950s [Yoshida1959]. Magnetic storms are sudden variations in the magnetic field,

generally distributed throughout the planet, with a duration that can range from a few hours to a few days.

Other aspects related to the structure of the magnetosphere are related to the "tail" on the opposite side of the Sun, which also extends to very large distances, greater than the radius of the Moon's orbit. It has been shown that if the extension of this tail is large enough, low energy particles can penetrate by diffusion inside it and reach the polar caps, decreasing the value of the geomagnetic cutoff. The effect of this tail was also evaluated for particles with slightly higher energy, for example protons with energy around 1 MeV, to explain the (anomalous) fact that they can reach locations at low latitudes.

It should also be remembered that to evaluate the variations in the measured flux of cosmic rays due to extraterrestrial origin, it is necessary to take into account the conditions under which the flux is measured, depending on the motion of the Earth around the Sun, on the inclination of its rotation axis with respect to the ecliptic plane and on the distance from the Sun. These aspects require the evaluation of appropriate geometrical correction factors, which must be applied to the observed flux, in addition to those due to the influence of the pressure and temperature of the atmosphere, before investigating other causes of variation. A detailed treatment of these aspects has been reported by Dorman [Dorman1974].

# Chapter 12
# The Secondary Cosmic Radiation and the Influence of the Sun

**Abstract** The influence of the Sun, especially on the secondary components of the cosmic ray flux, is discussed in this chapter. The Sun is subject to periodic phenomena, among which the 11-years cycles and the 27-days periodicity related to its rotation, and to aperiodic, catastrophic effects, such as the solar flares and coronal mass ejections. Both have an effect on the observed flux of cosmic rays on Earth. The modulation of the cosmic ray flux as determined by the solar cycle is presented, with quantitative plots showing the number of sunspots and the corresponding cosmic ray flux. An important aspect of the influence of solar events on the cosmic ray flux is provided by the Forbush variations, discovered in the mid-1930s, sudden decreases of the cosmic ray intensity followed by a slower recovery to its average value. Historical data are provided about Forbush events, together with more recent data showing examples of such effects on the neutron and muon flux. A brief mention is also given on other solar effects, including ground level enhancements in the intensity of the cosmic ray flux.

## 12.1 Introduction

The Sun exerts its influence on the surrounding environment through various physical processes, the study of which exceeds the topics most closely related to the physics of cosmic rays. The region in which these phenomena are mainly localized is called the heliosphere, and extends to a large distance from the Sun, exceeding 100 astronomical units, therefore well beyond the orbit of the outer planets. One of the main characteristics is represented by the magnetic field present in the heliosphere, by which cosmic rays of extra-solar origin are affected when passing through this region. Depending on their point of arrival with respect to the heliosphere and on their energy, the flux of particles of the cosmic radiation can undergo temporal variations, thus encountering a modulation of solar origin.

Solar activity mainly affects particles with an energy lower than about 10 GeV/nucleon. This activity has periodic components, such as those represented by the 11-year cycle of sunspots, and by the rotation of the Sun, with a period of 27 days. However, there are also aperiodic phenomena, such as solar flares and

coronal mass ejections that occur without a fixed periodicity, but are in some way
related to the number of sunspots, therefore to the eleven-year cycle of the Sun. These
local disturbances cause irregularities in the solar wind and associated magnetic
field. The Sun's magnetic field reverses its polarity every 11 years, with effects on
the phenomena related to the transit of cosmic rays in the heliosphere. The geom-
etry and intensity of the magnetic field in the heliosphere have been modelled by
numerous authors (see for example [Gray1980]) based on four different components
("dynamo", "sunspot", "dipole" and "ring"). The solar and terrestrial magnetic fields,
discussed in the previous chapter, together with the solar wind, constitute a complex
environment, subject to temporal variations, which also determine the flux of cosmic
rays observed on Earth.

## 12.2   Periodic Phenomena in the Sun and Solar Cycles

The solar cycle, or cycle of the magnetic activity of the Sun, is a cycle with a period
equal to 11 years, the main characteristic of which is highlighted in the number
of sunspots observed on the surface of the Sun. The phenomenon of sunspots was
observed quantitatively already at the beginning of 1600, with Galilei and Scheiner.
Starting from the second half of the 1700s, a periodicity in the average number of
observed spots was then noted. A more detailed study and a historical reconstruction
of the sunspots and observed periodicities were carried out by the Swiss astronomer
Wolf, around the mid-nineteenth century, who also introduced a quantitative index
for measuring the number of sunspots as well as the names of the various cycles,
starting from that relating to the period 1755–1766, conventionally called cycle 1.
The cycle in progress at the date of 2022 is cycle 25, which began at the end of 2019.

At the beginning of 1900 the deep link between the spots present in the Sun and
the phenomena of solar magnetism was recognized, establishing that within the 11-
year cycle the polarity remains unchanged, changing instead from one cycle to the
next, and returning to the value of departure after 22 years. Although the basic cycle
is considered to have a period of 11 years (and not the 22 years required by a full
magnetic cycle), the two halves of the 22-year period are not exactly equivalent in
terms of the number of spots.

Today the Sun's activity is constantly monitored from many points of view,
with data available online for the various parameters that describe its activity
[SPACEWEATHER]. Figure 12.1 shows a recent image of the Sun, with some group
of sunspots in evidence.

Figure 12.2 shows instead the periodicity in the number of sunspots observed over
the last few centuries, from about 1750, the period from which the monthly averages
of the number of observed spots were recorded in a quantitative way. The inversion
of the solar magnetic field occurs in correspondence with the periods of maximum
number of sunspots.

The detailed trend for the last cycles is further shown in Fig. 12.3.
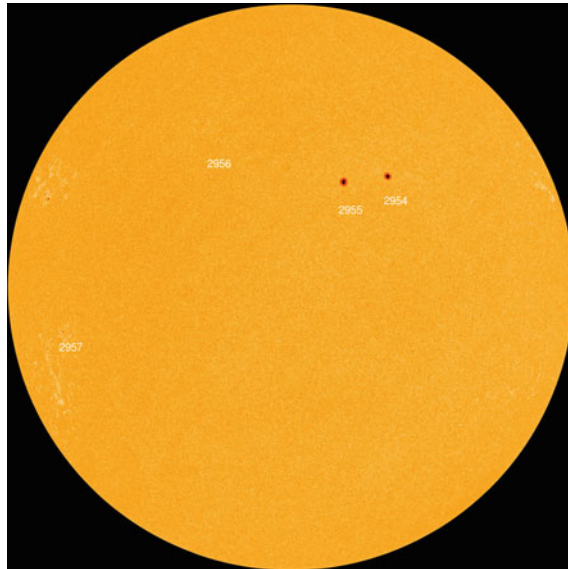
**Fig. 12.1** A recent image (February 28, 2022) of the Sun, showing several groups of spots [SPACEWEATHER]. Also seen close to the borders of the image are photospheric faculae, bright extended structures
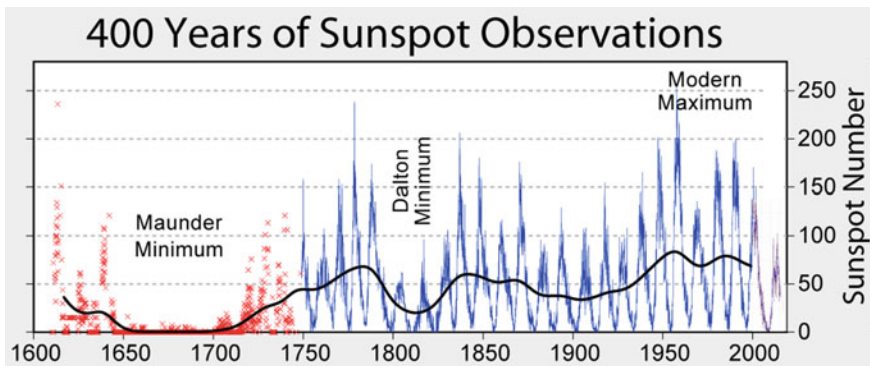


**Fig. 12.2** The number of sunspots observed over the last few centuries, since around 1750. *Source* Wikimedia Commons

## 12.3 Modulation of the Cosmic Ray Flux Due to the Sun

When a greater number of spots are observed on the surface of the Sun, it exhibits a phase of greater activity and emits more energy into the surrounding space. In the minimum periods, even for intervals of the order of weeks, the presence of any spot is not noticed; on the contrary, in peak periods, the simultaneous presence of several
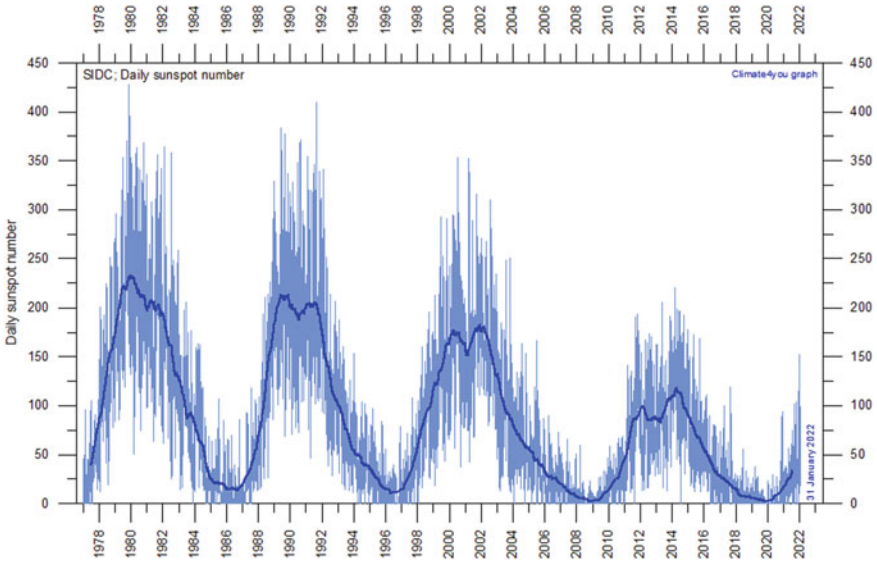
**Fig. 12.3** The number of sunspots observed over the last four cycles. *Source* [CLIMATE]

groups of spots can be observed. Although other phenomena, such as solar flares and coronal mass ejections, are not exactly periodic phenomena, their average frequency is somehow correlated with the 11-year cycle.

Without going into the detail, it can certainly be said that variations in the solar activity affect many aspects of the conditions observed on Earth, such as the structure of the geomagnetic field, the Northern Lights, and, in some ways, also the climate. In this context we will mainly discuss the effect on the flux of cosmic rays.

When solar activity increases, so does the intensity of the solar wind, the flux of particles that propagate in space and the associated magnetic field. This in turn deflects the energetic particles arriving from outer space, resulting in a reduction in the observed flux of cosmic rays to Earth.

Figure 12.4 shows the anti-correlated trend of solar activity and the flux of cosmic rays, monitored through neutron monitoring stations, particularly sensitive to the effects of solar variations. The observation period shown in this figure includes an interval of about 50 years, in which, for five consecutive solar cycles, the anticorrelated trends of these two quantities, albeit slightly different from cycle to cycle, are clearly visible.
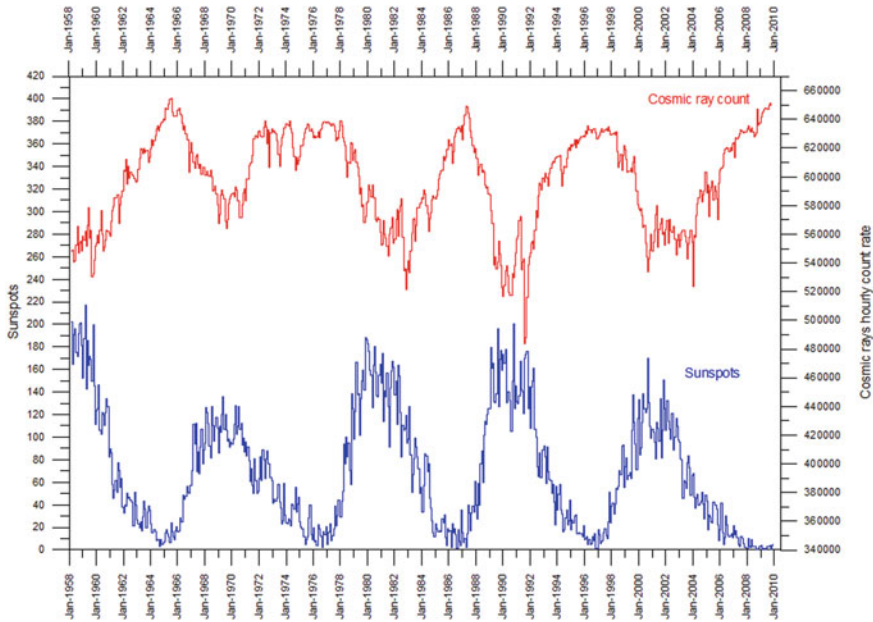
**Fig. 12.4**  Number of observed sunspots and the corresponding cosmic ray flux, measured at the Kiel neutron monitoring station. *Source* [CLIMATE]

## 12.4   Forbush Variations

The effect of solar phenomena on the observed flux of cosmic rays in the Earth manifests itself not only in the periodic behaviour of sunspots, but also in aperiodic events, during which abrupt changes in the intensity of cosmic rays can be observed.

One type of such events is the so-called Forbush variations, which were highlighted by the American physicist and geophysicist Scott Ellsworth Forbush (1904–1984) in the mid-1930s [Forbush1937, Forbush1938]. Since that period, a few hundred events of this type have been observed so far, in most cases by measurements performed at ground, although in more recent times also by observations carried out on board satellites (Fig. 12.5).

Forbush's observations fall within the framework of continuous monitoring of the intensity of secondary cosmic radiation. Already in the early 1930s, some stations for detecting cosmic radiation had been equipped, in various locations, for the continued observation of the intensity of this radiation, also on the proposal of Millikan and Compton. The first examples were the survey stations built in Cheltenham (Maryland, USA), Huancayo (Peru) and Christchurch (New Zealand), which were followed by many others. It was precisely by observing and analysing the data obtained from these stations, using a detection apparatus based on a special type of ionization chamber made by Compton, Wollan and Bennett in 1934, that Forbush found evidence of a significant variation in the intensity, visible in a correlated way by two distant stations,

**Fig. 12.5** Scott Ellsworth
Forbush (1904–1984).
*Source* American Institute of
Physics, Emilio Segre Visual
Archive



the one located in Cheltenham and the one located in Huancayo [Forbush1937]. The (negative) variation observed in the two stations had occurred rapidly, within a few hours, on April 25, 1937, with a slower recovery phase, over a few days, to the previous intensity values, as shown in Fig. 12.6, taken from the original work by Forbush. The data in the figure show, with two different symbols, the intensity measured at the two stations. As clearly seen, the trend is very similar in the two cases, and since the two stations are enormously distant, the effect could not be due to a local cause, but evidently involved a cause at least at a planetary level. The other important aspect of this observation is the correlation of this trend in the intensity of cosmic radiation, measured at the two stations, with the values of the horizontal component of the Earth's magnetic field, also shown in the same figure. Both the intensity and the magnetic field values are averaged in these results using intervals equal to 2 h, intervals that allow at the same time to have sufficient statistical precision and allow for the observation of any variations, even on a relatively short time scale.

The intensities measured by the two stations during this period, from 23 to 30 April 1937, showed—after correcting for the effect of atmospheric pressure—successive variations, up to a maximum of about 4% of the intensity observed in the previous days.

Already in this work Forbush identified what would become the salient features of these variations: a sudden increase (SC, Sudden Commencement) for a period of a few hours, followed by a rapid decrease and a phase of slow recovery of the initial conditions, lasting a few days.

Subsequent observations, with data from additional survey stations [Forbush1938] showed that the intensities observed in any two of the distant stations, after correcting for local barometric effects, were in general highly correlated with each other over time. In other words, the most significant variations in the intensity of the cosmic radiation were phenomena of a planetary nature, and this was true not only for long time-scale variations, such as seasonal variations, but also for sudden variations, such
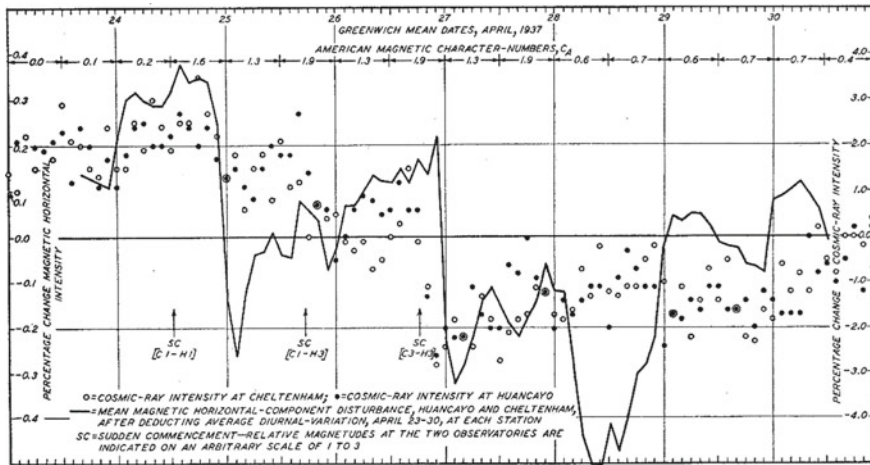
**Fig. 12.6** Trend of the intensity of cosmic radiation measured continuously at two distant survey stations (Cheltenham in USA and Huancayo in Peru, data indicated by empty and solid symbols respectively), compared with the trend of the horizontal component of the Earth's magnetic field (solid line). Figure reproduced by S. E. Forbush, *On the Effects in Cosmic-Ray Intensity Observed During the Recent Magnetic Storm*, Physical Review **51**(1937)1108. Copyright (1937) American Physical Society, License RNP/22/JUL/055430

as those observed in correlation with large variations in the magnetic field. Similar observations and considerations were also made in the same period by Hess and collaborators [Hess1937, Hess1938].

At that time, considerations about the cause of these variations in the intensity of the radiation were limited to the existence of a magnetic storm, the extent of which was estimated by Forbush to be at least twice the Earth's radius.

Forbush variations are now constantly monitored through the many neutron component detection stations distributed worldwide.

Figure 12.7 shows the trend of the intensity measured by one of the neutron monitoring stations, the Moscow Neutron Monitor Station, located near Moscow [IZMIRAN], during the month of November 2004, during which a typical Forbush decrease of high amplitude and duration is clearly observed. As an evidence that these phenomena occur on a planetary scale, it is possible to see a comparison, Fig. 12.8 [LaRocca2005], between the data measured by this station and those reported by another station, the Oulu Neutron Station, in Finland [OULU].

Forbush variations can also be observed for the muon component, as shown in Fig. 12.9, which shows the temporal correlation observed between the data obtained during the month of November 2004 from the Moscow Neutron Station and from a muon detector operating at the time in Adelaide (Australia).

According to some authors, the exact definition of what is meant by Forbush variation presents some ambiguity. Just to assume that these are a change in the
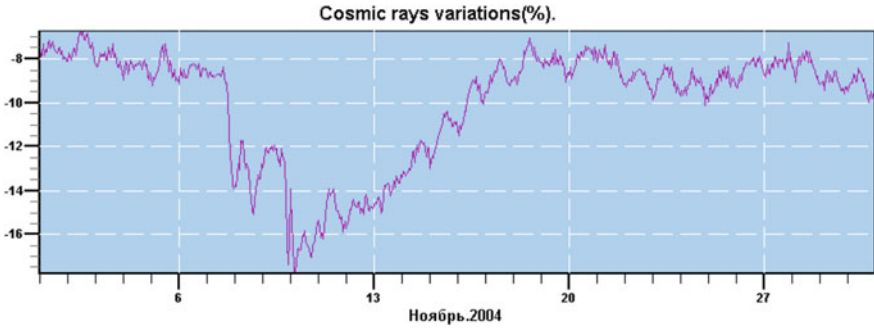
**Fig. 12.7** Percentage change in cosmic ray flux, measured by the Moscow Neutron Monitor Station [IZMIRAN], during November 2004
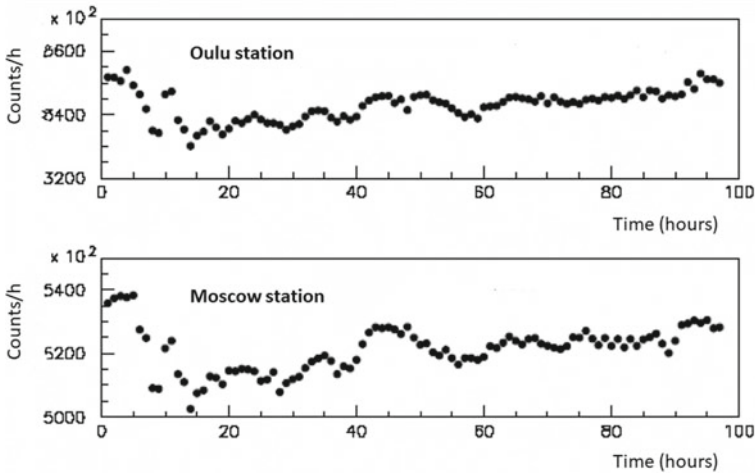


**Fig. 12.8** Comparison between the intensity measured by two different neutron monitor stations, located in Moscow and Oulu (Finland) for a few days, starting on November 9, 2004 [LaRocca2005]

flux of cosmic rays during a geomagnetic storm—as mentioned in some classical textbooks—or sudden changes (a few hours), at least 10%, in the intensity of galactic cosmic rays, observed by neutron monitor stations, as defined by other sites, overlooks notable aspects of these variations, as observed in more recent times.

Forbush variations are not necessarily sudden, as in some cases they have been observed to occur gradually. The amount of these variations can reach 10%, but these are very rare events, and in most cases the variation is only a few percent. Forbush variations in cosmic flux have been observed not only through neutron monitor stations, but also through muon-sensitive detectors, both at sea level and underground or at high altitudes. Finally, the variations were observed not only for the galactic component of cosmic rays, but also for that of solar origin.
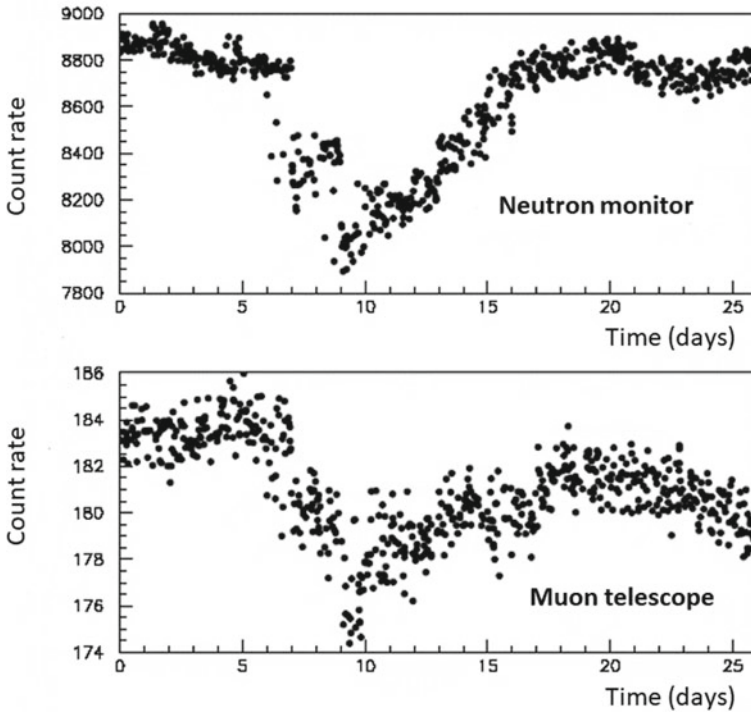
**Fig. 12.9** Comparison between the intensity measured by a neutron monitor station located in Moscow and a muon detector operating in Adelaide (Australia), during the month of November 2004 [LaRocca2005]

Forbush variations are the net result on the intensity of cosmic rays of solar flares or coronal mass ejections and/or of solar wind particle flow. Solar flares are intense bursts of radiation connected to the release of energy stored into solar magnetic fields. The emission of radiation from a solar flare involves all wavelengths of electromagnetic radiation, even in the X-ray band, and therefore appears as a flow of energy that propagates at the speed of light, and—if it occurs in the part of the Sun looking to the Earth—it can reach our planet in about 8 min. Coronal mass ejections produce the emission of material in the form of plasma, consisting mainly of electrons and protons, by the solar corona, the outermost part of the solar atmosphere. A coronal mass ejection can produce up to a billion tons of matter, emitted at speeds of millions of km/h, which can reach our planet after a period of a few days. Although these are two distinct types of events, solar flares and coronal mass ejections can also occur together.

The topology of the Forbush variations is multiple: the time scale can be faster or slower, the amplitude can vary within wide limits, the time profile can be simple, with a single decrease followed by a recovery phase, or multiple, with several minima.

**Fig. 12.10** Annual number of Forbush decreases, exceeding a certain magnitude (3%), over the years (data extracted from [Belov2009])
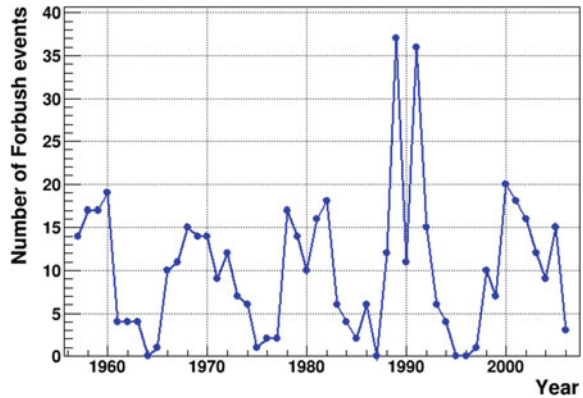


These characteristics can also be different, depending on the place of observation on Earth.

Most of the Forbush variations are sporadic and related to coronal mass ejections. In these cases, the variation in the intensity of the cosmic rays is linked to a region of the solar wind perturbed by strong magnetic fields. Often the decrease in intensity is preceded by a slight increase. The actual Forbush decrease begins when the coronal mass ejection impacts the Earth magnetosphere. Finally, there is a recovery phase when the CME propagates beyond the orbit of the Earth.

Although Forbush events occur sporadically, there is a certain correlation between the amplitude of Forbush decreases or the number of events greater than a certain amplitude and the eleven-year cycle of the Sun, as shown in Fig. 12.10 [Belov2009].

In general, much statistical information is now available on Forbush variations observed over the past 70 years by continuously operating neutron monitor stations. Some of these stations make their data available through their respective websites which can be addressed for further analysis. The possibility of correlating these events with additional databases containing information related to solar parameters and geomagnetic disturbances makes these analyses an important tool for understanding the properties of these events.

An analysis of several Forbush events between 1957 and 2006, reported by [Belov2009] showed for example that the distribution of the amplitudes A of these variations, starting from amplitudes greater than $(1–1.5)\%$, follows a power law $dN/dA \sim A^{-k}$, with $k = 3.1$. Variations with amplitudes greater than 3% correspond to intense geomagnetic storms.

Finally, it should be noted that Forbush decreases have been observed in recent times also in the space around the Earth, for example on the International Space Station, through the instrumentation of the AMS Collaboration, on the planet Mars [Forstner2018] and also at the borders of the Solar System, through the Voyager 1 and 2 probes.
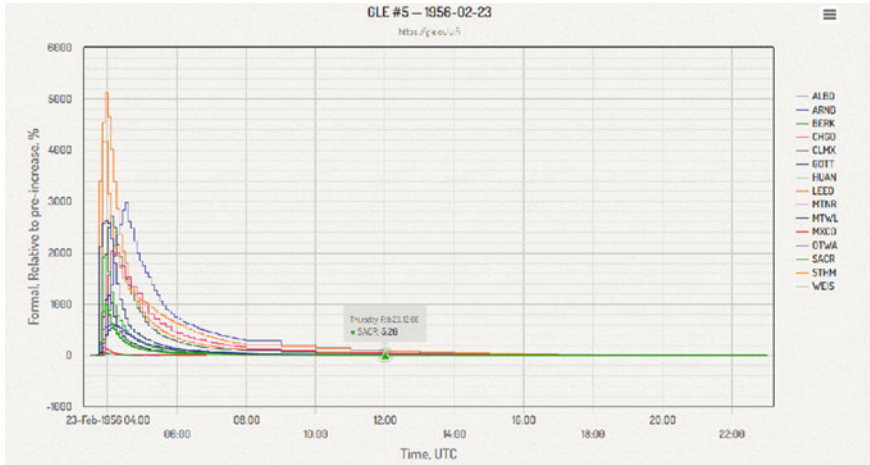
**Fig. 12.11**  Increased intensity observed at ground by different neutron monitoring stations, corresponding to the GLE event of 23 February 1956. Figure reproduced from the GLE database of the Oulu Cosmic Ray Station [OULU]

## 12.5   Other Effects Related to Solar Activity

Another phenomenon particularly linked to solar activity is represented by Ground Level Enhancements (GLE), sudden increases in the intensity of cosmic radiation measured at ground, in particular by neutron monitors. They are linked to the occurrence of solar flares, although the mechanism by which highly energetic particles of the order of GeV can be produced on these occasions is not fully known. Although the average number of these events is typically of the order of one per year, in some periods of intense solar activity, several of these events have occurred. The increase in the observed intensity ranges from a few percent up to the extremely high value of 45 times the average intensity, in the case of the event observed on February 23, 1956 [Belov2005], as shown in Fig. 12.11, which reports the data obtained for this event from different stations far from each other.

A currently accepted formal definition for a GLE-type event is the occurrence of a statistically significant and simultaneous increase in at least two distant neutron monitoring stations, of which at least one is located at altitudes close to sea level, and a corresponding increase in proton flux measured by instrumentation in space [Poluianov2017].

# Chapter 13
# Interaction of Muons with Matter

**Abstract** This chapter briefly recalls the most important aspects of the muon inter-action in matter, since they have a crucial role in understanding various basic and applied phenomena concerned with the physics of cosmic rays. The various mechanisms contributing to the energy loss of muons are considered, also providing the reader with quantitative plots describing the specific energy loss and the muon range in a solid material. Effects due to the multiple scattering of these particles in various elements are also discussed in the chapter.

## 13.1 Introduction

The interaction of the particles that make up the cosmic radiation with matter is an important aspect in the study of the properties of this radiation and its possible applications. In general, the interaction of electrons, of "heavy" charged particles, those having a mass significantly greater than that of electrons, as well as the interaction of photons, are all aspects commonly and extensively treated in several specific textbooks on the subject [Leo1987, Knoll2000, Leroy2004, Grupen2008], to which we refer. In this chapter we only recall some brief considerations that specifically concern the interaction of muons with matter. The soft component of the secondary radiation, as we have discussed in previous chapters, can in fact be absorbed by a relatively limited layer thickness of solid material, while the more penetrating charged component, muons, is capable of going deep inside a solid material, even crossing layers of considerable thickness. For this reason, the possible interactions of muons with matter, in particular with solid rocks, constitute an important aspect of cosmic ray physics, especially for the evaluation of shielding effects and for the application aspects in which muons play a significant role that we will examine in a specific chapter.

In propagating inside a material, muons are subject to different mechanisms: the main ones concern the phenomena of ionization and atomic excitation, production of $e^+e^-$ pairs, bremsstrahlung and nuclear interactions.

## 13.2  Energy Loss of Muons

The average energy loss per unit of path can generally be written in the case of muons as the sum of two terms:

$$\frac{dE}{dx} = a(E) + b(E)E$$

where the first term, a(E), represents the contribution of the ionization and atomic excitation processes, usually described, for not too high energies, by the Bethe-Bloch relation used for heavy charged particles:

$$-\frac{dE}{dx} = 4\pi N_A r_e^2 m_e c^2 z^2 \frac{Z}{A} \frac{1}{\beta^2} \left[ \ln\left(\frac{2m_e c^2 \gamma^2 \beta^2}{I}\right) - \beta^2 - \frac{\delta}{2} \right]$$

where $N_A$ is the Avogadro number, r the classical radius of the electron, m its mass at rest, c the speed of light in vacuum, z the electric charge of the particle, Z/A the ratio between the atomic number and the atomic mass of the medium in which the muon propagates, $\beta = v/c$ (v being the velocity of the particle), $\gamma = 1/\sqrt{1-\beta^2}$ is the Lorentz factor and $I$ (in eV) represents the ionization potential. The last term in the previous formula represents a correction factor due to the density, often approximated with $2\ln\gamma + k$, with k constant. The traversed thickness x is expressed in terms of the surface density (g/cm$^2$). In energy units, the constant quantities in the previous relation are equivalent to a factor

$$4\pi N_A r_e^2 m_e c^2 = 0.3071 \text{ MeV g/cm}^2$$

The ionization potential can be parameterized in different ways, either by the choice of using a value common to all the elements, by a simple proportionality between $I$ and Z (or a power of Z with exponent close to 1), by semi-empirical formulae which link $I$ and Z or even by customized tables of values for each element. Further details on the various terms are available in general textbooks on the interaction of radiation with matter, already quoted, or in specialized reports [Groom2001].

The second term, b(E), includes the contribution to energy loss resulting from bremsstrahlung processes, pair production and nuclear interactions. Each of these processes depends on the energy of the muons, and this dependence, complex from a mathematical point of view, can be expressed in graphical form as in Fig. 13.1, taken from the Particle Data Group [PDG]. To evaluate these values, the so-called "standard rock" was considered, in which an average density of 2.65 g/cm$^3$ is assumed, and an average atomic number of 11, with Z/A = 0.5 and an average value of $Z^2/A$ equal to 5.5. It is also assumed that the average ionization energy and the parameters describing the density effects correspond to those of calcium carbonate [Groom2001].

The overall energy loss of muons in standard rock, together with the contribution due to ionization alone, is shown in Fig. 13.2. As can be seen, up to energies of the
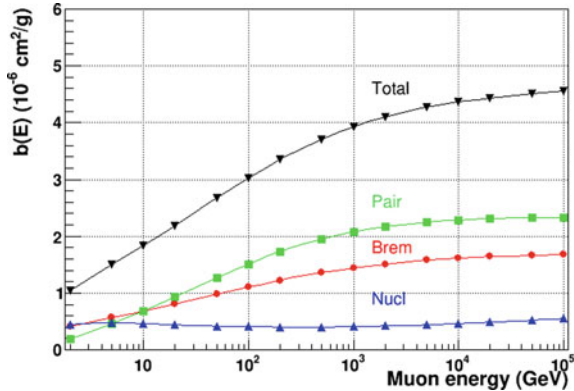
**Fig. 13.1**  Trend of individual contributions due to bremsstrahlung, production of pairs and nuclear interactions in the factor b(E) which expresses the energy loss of muons in standard rock (Z/A = 0.5, density 2.65 g/cm$^3$). Data extracted from the Particle Data Group [PDG]

order of 10 GeV, the mechanism of energy loss is essentially that due to ionization, while above 100 GeV the contribution due to the other mechanisms begins to become relevant. It can also be noted that the contribution due to ionization does not vary much over a wide range of values of the incident energy.

Quantitative data on the interaction of muons in different materials, including water, different chemical elements, and the most commonly used materials, can also be extracted interactively from the Particle Data Group Web site [PDG] for practical purposes or to evaluate the absorption of these particles.
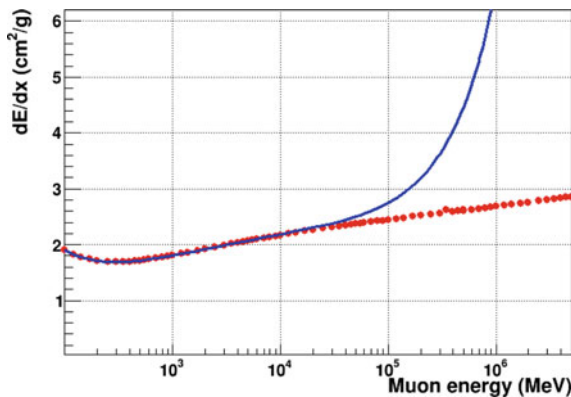


**Fig. 13.2**  Total energy loss of muons in the standard rock (upper blue line), together with the contribution due to ionization alone (lower red symbols), plotted as a function of the muon energy

## 13.3   Range of Muons in Matter

Of particular interest, also for the purposes of possible applications, is the evaluation of the muon range in a given material, that is, the path that muons of a given energy can travel within a material before being stopped. The mean range R(E) can be expressed in g/cm$^2$ and is related to the specific energy loss by the general relation:

$$R(E_\mu) = \int_{E_\mu}^{0} \left(\frac{dE}{dx}\right)^{-1} dE$$

For very high energies it can be assumed as a first approximation that the terms a(E) and b(E) in the relation dE/dx = a(E) + b(E)E are constant (not strongly dependent on E); we can then write:

$$R(E_\mu) = \int_{E_\mu}^{0} \frac{1}{a + bE} dE = \frac{1}{b} \ln \frac{a + bE_\mu}{a} = \frac{1}{b} \ln\left(1 + \frac{E_\mu}{E_c}\right)$$

where $E_c$ = a/b represents the critical energy, that is, the energy at which the loss of energy due to electronic processes (ionization and excitation) becomes equal to the loss of energy due to radiative effects. From the previous equation it is also possible to derive the relationship between the muon energy $E_\mu$ and its range:

$$E_\mu = \frac{a}{b}\left(e^{bR} - 1\right)$$

Figure 13.3 shows the expected range values, expressed in g/cm$^2$, corresponding to a given muon energy, in the interval between a few hundred MeV and some TeV. As can be seen from this figure, muons with energy 2–4 GeV, equal to the average energy that these particles have at sea level, are able to cross a thickness between 1000 and 2000 g/cm$^2$ of standard rock, equal to linear paths approximately between 3.5 and 7 m.

## 13.4   Multiple Scattering

Muons, like other charged particles, in addition to losing energy when crossing a medium, can undergo scattering effects due to the Coulomb interaction. In the case of a single process, diffusion can be described by Rutherford's formula. This relationship had, as it is known, a decisive role in the understanding of the phenomenon of diffusion of alpha particles by thin sheets of gold, leading to the formulation of

**Fig. 13.3** Expected range of muons, in g/cm$^2$, in standard rock, as a function of the muon energy
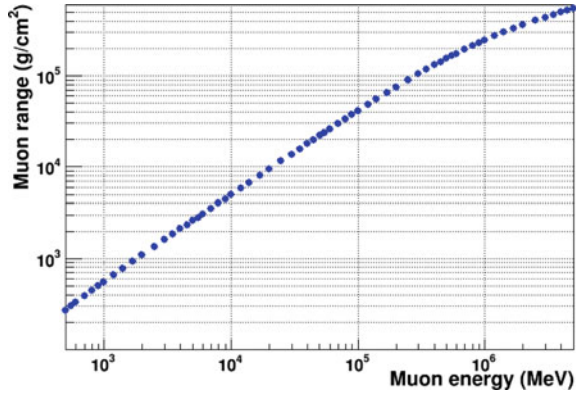
atomic models based on the existence of a massive central core. Since the probability of having a deflection of an angle $\theta$, in Rutherford's formula, is proportional to $1/\sin^4(\theta/2)$, it is expected that in most cases, the angular deflection will be very small. The path of the charged particle in the medium will therefore follow a "jagged" trajectory, with small changes of direction in each interaction. However, the possibility that a particle undergoes a large number of individual scattering processes in crossing a considerable thickness of material can lead to a non-negligible value of the overall deflection (Fig. 13.4).

In the treatment of these processes a distinction is generally made between three different possibilities, depending on the thickness crossed and therefore on the average number of individual scattering processes expected.

(a) If the thickness is very small, and therefore the probability that the particle undergoes more than a single scattering process along its path in the material is negligible, the phenomenon can be described as due to a single Rutherford deflection (single scattering).



**Fig. 13.4** Schematic description of the multiple scattering phenomenon. A charged particle of momentum p can undergo, in crossing a certain thickness X of matter, a series of small deflections that lead to a finite deviation from the initial direction of motion
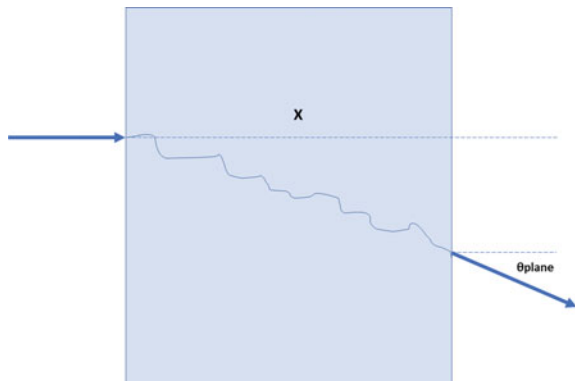
(b) If the thickness is very large, so much that the number of single scattering processes is very high, greater than a few tens, and the overall energy loss is still small, the phenomenology can be treated with statistical methods, to obtain, according to various approximations, the probability of having a given overall deflection. In this case we speak of multiple scattering, and it is the most commonly treated case, even in practical applications.

(c) If the thickness has an intermediate value, such that the number of individual scattering processes is of the order of ten, we speak of plural scattering. This is a difficult situation to deal with, since the process cannot be described neither by a single interaction nor by the combined effect of many interactions. A treatments of this kind of situation has been reported for example by Keil and collaborators [Keil1960].

However, even in the case of multiple scattering it is possible to find different approximations to the general solution, which is very complex. Among the most used approximations are those provided by Molière [Bethe1953] and by Snyder and Scott [Snyder1949], equivalent to each other and valid for values of the deflection angle that are not too high.

For small scattering angles a Gaussian approximation to the probability distribution can be used, with a zero mean value and a standard deviation (in the plane) $\theta_0$ given by

$$\theta_0 = \frac{13.6\text{MeV}}{\beta cp} \sqrt{\frac{X}{X_0}} \left[ 1 + 0.0038 \ln \frac{X}{X_0} \right]$$

where $\beta c$ is the speed of the particle, p its momentum, X is the thickness crossed and $X_0$ the radiation length of the material. The latter is a characteristic quantity of the material, also linked to the development of electromagnetic showers, and which can be expressed in terms of the chemical properties (Z, A) of the material according to various parameterizations, for example [Grupen2008]:

$$X_0 = \frac{A}{4\alpha N_A Z^2 r_e^2 \ln\left(183 Z^{-\frac{1}{3}}\right)}$$

The standard deviations of the scattering angle in the plane and in space are linked by the relationship:

$$\theta_0 = \frac{1}{\sqrt{2}} \theta_{space}$$

As it can be seen from the previous relations, the scattering angle depends on the momentum of the particle, being smaller for higher momenta, and it depends a lot on the atomic number of the material. What has been said so far also applies to cosmic muons and electrons, as charged particles of high energy. The phenomenon

**Fig. 13.5** Standard deviation in the scattering angle of muons of various momentum, in the case of crossing a standard 10 cm thick solid rock
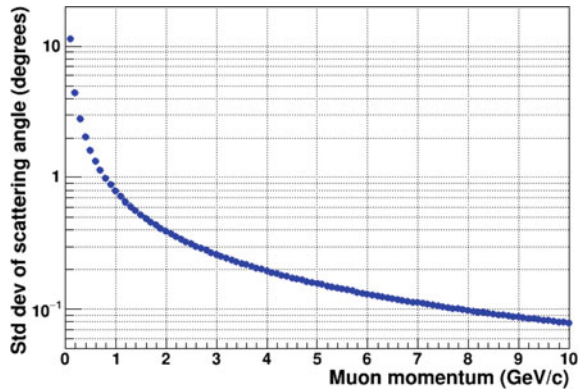


**Table 13.1** Standard deviation of the multiple scattering angle distribution, for muons of 3 GeV/c traversing a linear thickness of 10 cm in various materials

| Element | Air | Rock | Aluminum | Iron | Lead | Uranium |
|---|---|---|---|---|---|---|
| Std. Dev. (°) | 0.005 | 0.26 | 0.28 | 0.62 | 1.11 | 1.48 |

of multiple scattering must be appropriately taken into account in various aspects concerning the physics of cosmic rays and its applications. The tracking accuracy of charged particles, including muons and electrons present in the secondary radiation, is sometimes limited just by the amount of multiple scattering that the particles undergo in passing through any material placed above the detection apparatus (absorbers, roof or floors of the building, …). Particularly underground experiments can be influenced by this aspect, although in general the particles of lower energy are absorbed and for those of high energy the effect of multiple scattering is reduced.

Figure 13.5 shows as a practical example the value of the standard deviation $\theta_0$ as a function of the muon momentum, assuming a standard rock thickness equal to 10 cm.

For different materials, in particular those with a high atomic number, the scattering angle can be significantly higher, as can be seen from Table 13.1, which reports the values of the standard deviation ($\theta_0$) of the distribution of the scattering angles for various materials, with the same thickness of 10 cm. This constitutes the basis, as we shall see, also for possible applications in the field of muon tomography, which will be discussed in Chap. 16.

# Chapter 14
# Cosmic Radiations Underground, Under Water and Under the Ice

**Abstract** This chapter is concerned with measurements of the cosmic ray intensity underground, under water and under the ice. Both historical experiments providing the first measurements of this type, and more recent results obtained to large depths are presented and discussed, with quantitative plots showing the absolute value of the muon flux under a large thickness of material, together with different parameterizations which summarize the results. Possible parameterizations of the muon flux underground are further discussed in Appendix M.

## 14.1   Introduction

The particles of the secondary cosmic radiation that manage to reach the ground can further interact with the soil (or with water), according to the same mechanisms with which they interacted with the air of the atmosphere. In a solid or liquid material, however, which has a density much greater than that of air, unstable particles are subject to a higher probability of interaction than the probability of decaying, contrary to what happens in air. As for the type of particles, while electrons and hadrons are easily absorbed because of these interaction processes, the most penetrating components—muons and neutrinos—can also reach great depths in the underground rock, in the sea or in the ice. The interaction of muons with materials can also produce additional secondary particles of various kinds. We will not discuss in this context neutrinos, which, due to their interaction cross section, have a very low probability of interacting with even a considerable amount of solid material, most of them managing to cross the entire Earth. The detection of neutrinos is today of considerable importance in astroparticle physics, but it requires enormous detection volumes to compensate for the very low probability of interaction and to collect, despite this, a significant number of events. On the contrary, muons, as charged particles, easily interact with rock, sea water or ice, according to the mechanisms described in the previous chapter, and their flux progressively attenuates in the subsoil, making their detection possible basically with the same equipment and the same techniques used on the surface.

Measurements of the muon flux at different depths in the Earth's subsoil, or underwater, have been carried out in various conditions, up to great depths, in excess of $10^6$ g/cm$^2$ (10 km.w.e.), depths at which the atmospheric muon flux becomes comparable with the background value of muons created by neutrinos. Recall that the entire thickness of the atmosphere corresponds to about 1000 g/cm$^2$; therefore, the depths involved in these measurements are up to 1000 times greater. In the case of measurements carried out under water, the composition of the liquid is quite known, apart from small variations in density or the presence of dissolved substances, while in the case of solid materials such as rocks, consistent variations in the composition and density of the rocks, as muons penetrate deeply, make data analysis more complex.

The measurement of the intensity of muons underground has numerous aspects of interest, due to the possibility of studying in detail the interaction mechanisms of high-energy particles, as well as from an application point of view, either in the design of underground laboratories with a low cosmic background noise, such as many of the astroparticle physics experiments require, or in those applications that use cosmic muons for the tomography of large natural structures, such as volcanoes.

## 14.2    Underground Measurements

The first measurements of the intensity of the cosmic radiation in the subsoil, or under a certain depth of water, date back to the history of the discovery of cosmic radiation, as we discussed at the beginning of this text. In that case, it was a question of establishing the very nature of the radiation, whether it came from the outside or from the radioactivity of terrestrial rocks. We now turn instead to the more systematic measurements, carried out in the following years, once the nature of these radiations had been clarified, and in particular of the measurements concerned with the most penetrating component, the muons. A review of the main results and interpretations of these first measurements, carried out up to the 1950s, can be found, for example, in a work of 1952 by Barrett and collaborators [Barrett1952], which in addition to reporting their original measurements, carried out in a mine located at the depth of 1574 m.w.e. ($1.574 \times 10^5$ g/cm$^2$), reviewed experiments performed up to that time by other authors.

At that time it was already well established—from measurements carried out in previous years at various depths in the subsoil—that the penetrating particles, capable of propagating and being detected even under a consistent amount of rock, were muons; however, it was precisely the underground measurements that were seen as a precious investigative tool to test the overall representation of extensive air showers, with their fraction of penetrating particles, as well as the mechanisms of interaction of these particles, including the secondary reactions to which muons could give rise. At the end of the 1930s, different types of measurements were already available, organized inside mines, with detectors of various kinds (including Geiger counters operating in coincidence). Examples of such experiments are reported, among others,
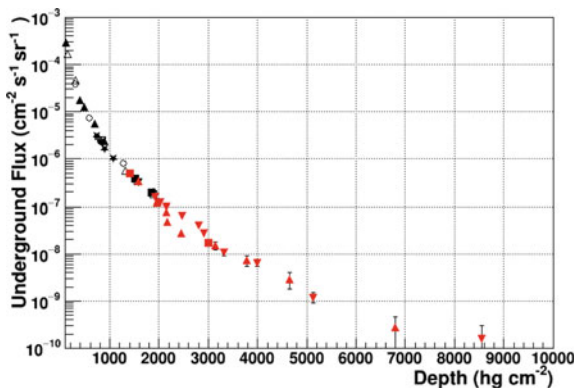
**Fig. 14.1** Vertical intensity of muons, obtained from various experiments, each with a different symbol. The values indicated with the symbols in red, corresponding for the most part to greater depths crossed, indicate the measurements extrapolated from inclined trajectories of the muons. Data extracted from [Grieder2001]

by Barnóthy and Forró [Barnóthy1939], by Clay [Clay1939], Wilson and Highes [Wilson1943], Nishina [Nishina1941] and Miyazaki [Miyazaki1949].

A review of the vertical intensity measurements of muons at various depths, as reported by different experiments (each shown with a different symbol) [Grieder2001] is shown in Fig. 14.1. The corresponding measurements at higher depths, indicated with red triangles in the figure, were obtained from experiments in which muons with inclined trajectories were also detected, evaluating the thickness of the rock actually crossed.

As can be seen from these results, the flux of vertical muons in the subsoil decreases by a factor of 10 after a depth of approximately 250 hg/cm$^2$, equivalent to 25 m.w.e. In the measurements of Barrett et al. [Barrett1952], the flux measured at a depth of 1574 m.w.e. was approximately a factor 1000 smaller than that measured at the surface, as can also be seen from the overall set of results in Fig. 14.1. Going further in depth, as it has been done in more recent times, in order to evaluate the flux of muons in sites dedicated to the installation of astroparticle physics experiments, which require environments with a much reduced background of cosmic muons, they have shown a further decrease of 3 orders of magnitude from a depth of 1500 m.w.e. to a depth of about 8500 m.w.e., like that corresponding to the LVD experiment at the Gran Sasso underground laboratories. We therefore understand the growing difficulty in measuring the muon flux at ever greater depths, in terms of the measurement times required or the geometric dimensions of the detectors, in order to have a significant number of events. For a review of recent results on underground muon flux, see the section provided by the Particle Data Group [PDG] on this topic.

The relationship between cosmic muon flux and depth in the subsoil—expressed by the results shown in Fig. 14.1—has been parameterized according to various semi-empirical formulas. A frequently used relation has been for example proposed by Miyake [Miyake1963], which expresses the vertical intensity I(X) as a function

of the depth X as

$$I(X) = (X + a)^{-\alpha} \frac{K}{X + H} e^{-\beta X}$$

where the parameters a, K, H, $\alpha$ and $\beta$ are obtained from a fit of the experimental data and the depth X is expressed in m.w.e. (or hg/cm$^2$). Appendix M shows the intensity as a function of depth X, with a series of numerical parameters used to reproduce the first measurements available at the time, together with a simplified formula that was sometimes used instead of the previous equation. At very large depths, the behaviour of intensity as a function of depth can be represented by a simple exponential relationship, such as

$$I(X) = A e^{-X/\Lambda}$$

where the two parameters A and $\Lambda$, obtained from the data, vary according to the range of depths explored. As an example, measurements carried out by Meyer [Meyer1970] between 4000 and 9000 hg/cm$^2$, can be represented by the previous relation, assuming $A = 1.04 \times 10^{-6}$ and $\Lambda = 804$ hg/cm$^2$.

A more detailed list of the intensity measurements of muons, carried out underground since the 1950s by various experiments, is reported by Grieder [Grieder2001]. It should be noted that some experiments directly measure the flux of vertical muons, while others, also sensitive to muons with inclined trajectories, make corrections to the data in order to obtain the vertical flux. The detection apparatus in these measurements used sets of Geiger counters operating in coincidence, photographic emulsions or telescopes of plastic scintillators.

The results of the first underground measurements had allowed, among other things, to extract not only the intensity of the vertical component, but also the angular distribution of muons in the subsoil, a trend of the $\cos^n \theta$ type, with an exponent $n$ whose value was however different at various depths. In Barrett's work [Barrett1952], for example, with measurements made at 1574 m.w.e. the shape of the angular distribution of muons, shown in Fig. 14.2, could be represented using a value of $n$ equal to 3.

Neglecting the Earth's curvature, at least for inclination angles not too far from the vertical, a vertical depth X corresponds, for muons arriving with a zenith angle $\theta$, to an effective depth (slant depth) equal to $X_S = X \sec(\theta)$. If we assume an exponential attenuation law for the muon flux, they will be attenuated by a factor $e^{-X \sec \theta/\Lambda}$ as they penetrate to a vertical depth X with an inclination angle $\theta$. For greater zenith angles, the approximation of a "flat" Earth surface is no longer valid, and the effect of the Earth's curvature on the distances actually crossed must be considered.

Even in more recent times, the zenithal angular distribution of underground muons has been represented with a dependence of the $\cos^n \theta$ type, with an exponent $n$ varying with the depth, roughly like [Miyake1973]:

$$n = 1.53 + 8 \times 10^{-4} X$$
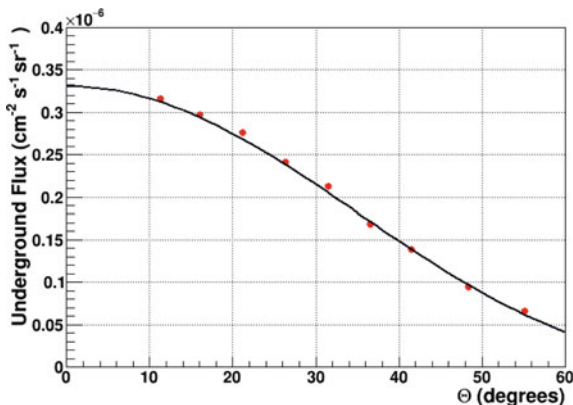
**Fig. 14.2** Angular distribution of muons measured at a depth of 1574 m.w.e. Data extracted from [Barrett1952]. The solid line shows the shape of the $\cos^n \theta$ function that fits the data, with a value of the coefficient $n = 3$

where X is the depth expressed in $hg/cm^2$. At large depths the exponent $n$ increases significantly, and this makes the zenithal angular distribution more pronounced in correspondence with the vertical, with a gradually more negligible contribution from the inclined muons. In Miyake's work [Miyake1973], more sophisticated parameterizations are also proposed to describe the zenithal angular distribution at large depths. The distribution of the azimuth angle, on the other hand, is uniform, since the East–West effects perceived on the surface are mainly due to the lower energy muons, sensitive to the magnetic field, while at large depths only highly energetic muons are able to penetrate, on which the geomagnetic effect is negligible (Fig. 14.3).
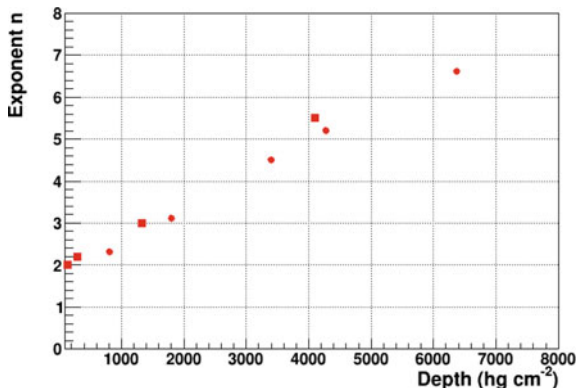


**Fig. 14.3** Values of the exponent $n$ in the relationship that expresses the intensity of underground muons as $\cos^n \theta$, obtained from experiments performed at various depths in the subsoil. Values extracted from [Grieder2001]
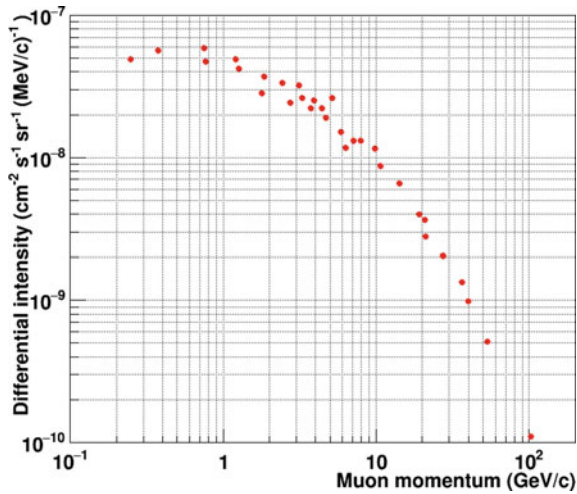
**Fig. 14.4** Differential intensity of muons, in an underground experiment carried out at a depth of 70 hg/cm$^2$ of rock by means of a magnetic spectrometer [Murdoch1960]

The first attempts to measure the energy distribution of muons at a certain depth in the subsoil date back to the 1950s and 1960s, with measurements made with nuclear emulsions [George1956], cloud chambers [Nash1956] and magnetic spectrometers [Daion1959, Ashton1960, Murdoch1960], at a depth of a few tens of m.w.e. below ground level. Measurements at greater depths (850 hg/cm$^2$) were carried out in the 1970s, with emulsion chambers, up to energies of several TeV [Mizutani1979]. The result of the measurements carried out at the end of the 1950s had already made it possible to obtain the spectrum of the differential intensity of muons up to energies of the order of 100 GeV (Fig. 14.4).

From the analysis of these first measurements, a power law was suggested for the relationship between flux and energy, of the type $E^{-w}$, with w = 1.8 for energies greater than $10^{10}$ eV.

By increasing the depth, the amount of the rock above acts as a filter, gradually selecting muons of increasingly higher average energy, as shown in Fig. 14.5, which summarizes data obtained in the course of various experiments.

Carrying out measurements at a certain depth therefore means selecting muons with a given average energy, depending on the depth. Assuming an approximately constant rate of muon energy loss, equal to 200 MeV per meter of water equivalent (m.w.e.), the average muon energy at a depth h (expressed in m.w.e.) is equal to 200 h/(w − 1) in MeV. For example, at a depth h equal to 1000 m.w.e., the average energy would be $2.5 \times 10^{11}$ eV, or 250 GeV.

The main characteristics of the energy and angular distributions of muons measured in depth have already been extracted from the experiments performed several decades ago. In more recent times, starting from the late 1970s, several experiments in astroparticle physics, dedicated to neutrino physics, looking for
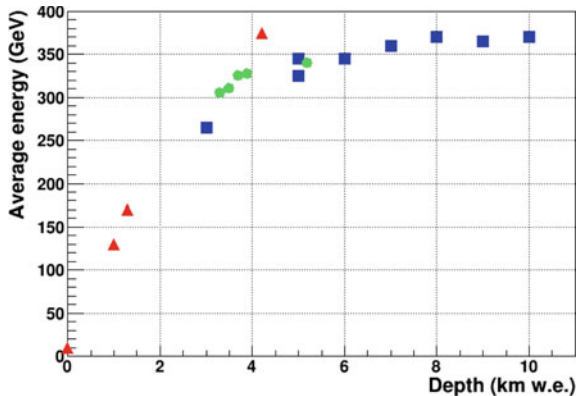
**Fig. 14.5** Average energy of vertical muons measured at a certain depth in the subsoil, as a function of depth, expressed in equivalent km of water (km w.e.). Data reproduced by [Alexeev1973] (red triangles), by [Castagnoli1997] (blue squares), and by [Ambrosio1999] (green dots)

possible proton decays or for dark matter, have installed large underground detectors, with good detection capabilities for muons, which allowed to obtain more detailed information on the distribution of muons at large depths.

## 14.3  Measurements Underwater and Under the Ice

Apart from the first measurements of historical interest carried out at the beginning of the history of cosmic rays, such as the measurements made by Pacini, and already mentioned in Chap. 1, measurements at great depths underwater in the marine environment were carried out starting from the 1960s by Higashi and collaborators [Higashi1966] up to a depth of 1380 m, and subsequently, by Davitaev and collaborators [Davitaev1970] up to 3190 m, by Vavilov and collaborators [Vavilov1970] up to 3190 m, by Fyodorov and collaborators [Fyodorov1986] up to about 5000 m, from Babson et al. [Babson1990] up to 4150 m. Figure 14.6 shows the set of these results, which show a well-defined behaviour, similar to that obtained under a certain thickness of rock and already shown in Fig. 14.1.

Measurements in a lake environment (pure water instead of salt water, as in the seas) were also carried out in subsequent years, obviously at shallower depths. For example, Rogers and Tristam [Rogers1984] used, up to a depth of 175 m, in the Geneva Lake, a cylindrical scintillator telescope read by photomultipliers, completely autonomous (from the point of view of power supply, control and data saving), placed inside a suitable sealed container. Their results are shown in Fig. 14.7. Measurements in Lake Baikal, at larger depths (1170 m) were carried out in the 1990s.

**Fig. 14.6** Vertical intensity of muons, obtained from various experiments organized underwater in the sea, each shown with a different symbol. Data extracted from several experiments and summarized in Grieder's review work [Grieder2001]
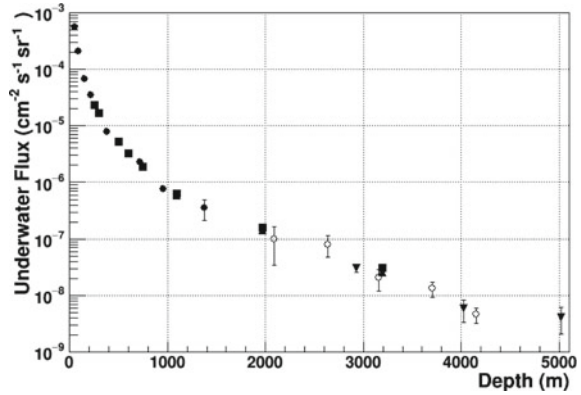
**Fig. 14.7** Vertical intensity of muons, obtained from measurements made by Rogers and Tristam [Rogers1984] in the Geneva Lake, up to a depth of 175 m
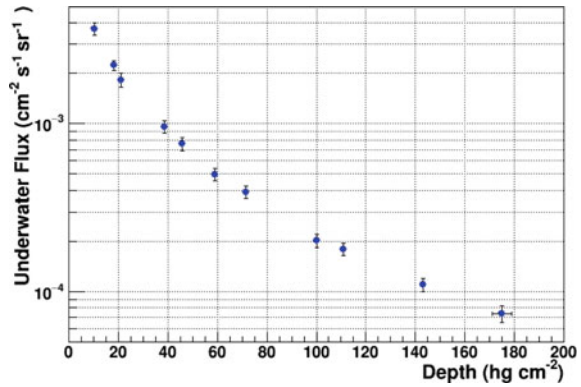
In even more recent years, large-scale experiments for neutrino physics have been set up or are being set up underwater or under the ice, providing new experimental data regarding muons at very large depths, particularly for the high-energy component.

Measurements carried out at large depths under water or under the ice have the advantage of being able to know more precisely the thickness of the material traversed than those performed under rock thicknesses whose composition is never known in detail along the entire path of the muons. Such measurements can therefore be used for more quantitative tests of particle propagation and energy loss.

As regards the flux of muons under a given thickness of ice, the first measurements under the ice were carried out in Greenland, at a depth of about 200 m, by the AMANDA Collaboration [Lowder1991]. Recent measurements, at depths of up to about 2 km under the ice of Antarctica, have been carried out very recently as part of the activities of the IceCube Collaboration.

# Chapter 15
# The Origin of Cosmic Rays

**Abstract** The question of the origin of the cosmic radiation has been raised since the early evidence of the existence of this radiation and it is still an important aspect addressed by several recent investigations. A few historical considerations about the acceleration mechanisms and the origin of cosmic rays are provided along the chapter, with a brief discussion of the Fermi acceleration mechanism. The role of the supernovae in the understanding high energy cosmic rays is also presented, together with a brief mention concerned with the extra-galactic high energy components.

## 15.1 Introduction

Although the question of the origin of cosmic rays has been raised since the earliest evidence of the existence of an extraterrestrial radiation, after more than a century the problem still has a number of open aspects, despite significant progress has been made in its understanding. Although these pages are not expressly dedicated to presenting the astroparticle issues inherent in the question of the origin of cosmic radiation, we cannot avoid mentioning at least some historical steps, the general problem and some recent results. General considerations of historical interest about the origin of cosmic rays can be found not only in the original papers by various authors, but also in textbooks dating back to the '60s [Ginzburg1964, Sandström1965].

Meanwhile, we mention that the energy spectrum of the primary cosmic radiation, which we discussed in one of the previous chapters, does not show evident discontinuities, except for a slight change in the slope, along an enormous energy interval, which covers from a few MeV to over $10^{20}$ eV. This, however, does not mean that the particles of such different energies all have the same origin, or are accelerated by the same mechanisms. Already a few decades after the first evidence of the extraterrestrial origin of this radiation it was considered reasonable that the processes that gave rise to the primary particles took place in different environments of space, from regions close to our solar system to regions outside the Milky Way. The considerations about the origin of the primary cosmic radiation generally refer, in fact, to a "local" origin (in which it is assumed that this is produced—if not within the Solar System—in a region of negligible dimensions compared to those of our Galaxy), to

a "galactic" origin (to denote those components that are produced and accelerated in regions comparable to the size of the Milky Way) and finally to an "extragalactic" origin (to indicate the components originating from outside our Galaxy).

The phenomena of the production of particles and their subsequent acceleration cannot be completely unrelated, and the question of where the particles in question originate is also dependent on the possible mechanism hypothesized for their acceleration. The evidence that in a first approximation the primary cosmic radiation is isotropic, that is the flux is independent of the incoming orientation, would lead to hypothesize either a large number of "local" sources uniformly distributed throughout the space, or a "storage" mechanism of very long duration, through which the particles reach a sort of equilibrium that causes them to come from all directions. As was recognized many decades ago, discussions about the origin of cosmic radiation include at least four different types of problems: the production (injection), acceleration, localization and storage of particles.

In general, observational evidence should be used to answer such questions. However, there has not been much evidence from the past capable of directly telling us something about the origin of the radiation and providing an answer to the type of problems listed. Most of the characteristics of the primary cosmic radiation, for many decades, have been obtained from measurements performed on Earth or in the Earth's atmosphere. Only since the 1960s has a considerable amount of data been obtained, also through observations by satellites, first in orbit around the Earth, and, subsequently, in interplanetary space. The probes which are at the largest distance from Earth, such as Voyager 1, have only recently passed what can be qualitatively defined the boundaries of the Solar System, giving in principle experimental information on what is happening in the interstellar space. It should also be remembered that in recent decades it has been possible to extend the observation of the universe beyond the visible band, both in infrared and radio waves and in the X and gamma ray regions. This has enormously increased the amount of observational data, some of which can also give valuable information about the origin and distribution of cosmic radiation.

If we were to say which experimental evidence of the past could give direct information on some of the problems listed above, they mainly concern the variations related to solar phenomena, as discussed in one of the previous chapters. In this case, for example for solar flares, the question of origin is well defined, but it concerns only a small component of the energy spectrum of primary radiation, usually the low energy region. However, it is not known exactly what the upper limit of the component of cosmic radiation associated with the Sun may be, because there is also evidence of protons with an energy equal to a few tens of GeV associated with the Sun or with interplanetary space in the Solar System, without a clear identification of acceleration mechanisms.

The energy spectrum of this radiation shows, as we have discussed, a variation in the exponent of the power law depending on the specific energy region. However, it is not easy to separate this spectrum into separate individual components, corresponding to different origins and acceleration mechanisms. In any case, it is reasonable to assume that all regions corresponding to different origins or mechanisms would

have some overlap between them, smoothing the transition areas between one region and another.

As regards the composition in charge of the primary nuclei, it has been established that it presents differences with respect to the distribution of the elements in the universe. However, even in this case, the knowledge of both distributions is not as detailed, and the interpretation of these differences is not immediate. For example, the presence of light elements in the cosmic radiation is lower than that of the natural abundance of elements in the universe, and this suggests that the cosmic radiation is relatively "young", that is, it has not had sufficient time to go through a fragmentation of the heavier nuclei through interstellar space, having suffered a relatively limited number of collisions.

Today it is quite accepted that most of the primary cosmic radiation, starting from energies of the order of GeV/nucleon, up to energies of the order of $10^{15}$ eV, is of "galactic" origin. The recent gamma observations produced by dedicated high-quality satellite measurements also contributed to this belief. They have shown that the flux of energetic gamma rays, produced to a large extent by the decay of neutral pions, in turn generated in hadronic collisions with nuclei present in the interstellar medium, is distributed throughout the entire Galaxy, with a greater intensity in its central area and gradually decreasing towards the outermost regions of the disc. This would go against a hypothesis of uniform distribution in intergalactic space, with entry into the volume of the Galaxy by the outside.

Starting from a certain energy onwards, the so-called "knee" region around $3 \times 10^{15}$ eV, we generally speak of the presence of extragalactic components, particularly for those energies above the "ankle" region at $3 \times 10^{18}$ eV.

What are the arguments in favour of an extragalactic origin of these extreme energy particles?

First, charged particles, assuming they were produced within our Galaxy, could not remain forever confined by the weak galactic magnetic field. In general, if we assume an average value of the magnetic field B within a given region, we can estimate the maximum energy of the particles that could remain confined in that region, as they would move on circular orbits with a radius smaller than the size of the region. The Larmor radius corresponding to a given magnetic field B is given by $R = p_T/qB$, where $p_T$ is the momentum of the particle perpendicular to the direction of the field. Table 15.1 shows the energy value of the protons that could be confined within typical regions of interest for the origin and propagation of cosmic rays, together with the known value of the magnetic field present in those regions.

Another argument in favour of a different origin lies just in the change in the observed power law, with an exponent that at $3 \times 10^{15}$ eV passes from a value of 2.7 to a value greater than 3. Although this difference may seem small, it implies a difference in the reduction of the flux by at least a factor of 2 for each decade of energy. An exponent value equal to 2.7 in fact implies a flux that is reduced by a factor 500 for an increase in energy by a factor 10, while an exponent equal to 3 leads to a reduction in the flux of a factor 1000 for the same increase in energy.

Finally, very recent measurements seem to indicate a geometric correlation between the incoming direction of the extreme energy particles and the large-scale

**Table 15.1** Typical dimensions of the regions of interest for the origin, propagation and possible confinement of cosmic rays

| Region | Typical dimensions | Average magnetic field | Max energy of protons |
|---|---|---|---|
| Solar system | 100 A.U. = 1.5 × $10^{13}$ m | $10^{-9}$ T | $4 \times 10^{12}$ eV |
| Interstellar medium (mean distance between stars) | 100 pc = 3 × $10^{18}$ m | $0.5 \times 10^{-9}$ T | $4 \times 10^{17}$ eV |
| Disc thickness of Milky Way | 2000 l.y. = 2 × $10^{19}$ m | $0.3 \times 10^{-9}$ T | $2 \times 10^{18}$ eV |
| Milky Way diameter | $10^5$ l.y. = 9.5 × $10^{20}$ m | $0.3 \times 10^{-9}$ T | $8 \times 10^{19}$ eV |

distribution of matter in the nearby universe. Associating the arrival direction of the primary particles with specific areas of the universe is possible only in the case of neutral radiation (gamma, neutrinos), or for charged particles with very high energy, which are little affected by the magnetic field.

## 15.2   Some Historical Considerations About the Acceleration Mechanisms and the Origin of Cosmic Rays

As we have seen in the first chapters, from the very beginning the question of the origin of cosmic radiation has been one of the crucial issues behind the enormous variety of experimental observations and specific phenomenological aspects. It has been correctly noted that almost everyone who contributed to the first studies concerning cosmic radiation also attempted to get a theoretical representation of what the origin of this radiation could be, even before its commonly accepted extraterrestrial origin. In many cases these first hypotheses proved to be without foundation over time, even when they were proposed by some protagonists of the research of the time. We have already mentioned Millikan's attempts to associate gamma radiation—hypothesized as the preponderant part of primary radiation—with nuclear processes originated by the *birth* of the elements. But in that period—since the late 1920s—there was no lack even of other *exotic* hypotheses, such as those of C. T. R. Wilson and Halliday, who discussed the role of lightning in the production of cosmic radiation particles, or those of Bothe and Kolhöster, who considered the role of the gravitational forces in the acceleration of particles.

Between the 1930s and 1960s a variety of approaches attempted to address the problem of the origin of cosmic rays and of the mechanisms capable of justifying the acceleration of these particles, also in relation to the different regions of the energy

spectrum of the primary radiation, from a few hundred MeV to energies in excess of $10^{19}$ eV.

Among the approaches that referred to a solar origin and in general to the interplanetary environment, we should mention that of Swann [Swann1933], Dauvillier [Dauvillier1934], Menzel and Salisbury [Menzel1948], Richtmeyer and Teller [Richtmeyer1949], Alfvén [Alfvén1949, Alfvén1959]. One of the first models based on electrodynamic acceleration processes was developed by Swann [Swann1933], assuming that these processes took place near sunspots. The mechanisms hypothesized in this approach are, however, generally applicable to the existence of variable magnetic fields. This approach was able to explain the origin of the low energy component, with an injection of particles by explosions in the active regions of the Sun and a subsequent acceleration. However, no predictions could be made about the spectrum in energy, and the mechanism was closely related to regions in the vicinity of stars. In other approaches, such as those proposed by Alfvén, the acceleration mechanism was based on plasma beams produced by explosions in the active regions of the Sun, also linked to the interpretation of Forbush variations. Assuming that low energy particles were present in abundance in the solar corona, as happens, they could have been accelerated by this mechanism, increasing their energy in a short time. The existence of cosmic rays of energy of the order of $10^{11}$–$10^{12}$ eV could thus be explained, but not that of particles of even higher energy, which, as we have seen, could not have been confined within the Solar System. Although these models initially made a qualitative account of some experimental evidence, a deeper analysis in subsequent years showed that several specific observations, concerning the abundance of low energy particles during periods of intense solar activity, or the charge distribution of particles, were not reconcilable with this production mechanism.

Another group of theoretical models referred to the interstellar medium as the source and place of the acceleration of cosmic radiation. This group includes the model proposed by Fermi [Fermi1949, Fermi1954] which we will discuss in more detail in the next section, as well as the theoretical approaches of Fan [Fan1951], Chandrasekhar and Fermi [Chandrasekhar1953], Morrison, Olbert and Rossi [Morrison1954] and Davis [Davis1956].

The origin of cosmic radiation in reference to intergalactic (or extragalactic) space was discussed as early as the 1950s [Bierman1949, Bagge1950, Teller1954, Cocconi1956]. A "universal" mechanism based on what is called "magnetic pumping" was also proposed in those years [Swann1954, Alfvén1959]. Finally, theories that explicitly referred to supernovae are also present as early as the 1950s [TerHaar1950, Colgate1960]. The hypothesis of supernovae as sources of the most energetic cosmic radiation was strongly revived in subsequent years, also based on observational evidence not available before and will be discussed in more detail at the end of this chapter.

## 15.3   Fermi Acceleration Mechanism

A mechanism capable of accelerating charged particles moving within the Galaxy was proposed by Fermi in 1949 [Fermi1949]. This mechanism is based on the existence of magnetic fields moving in interstellar space, generated by clouds of ionized gas moving with respect to the reference system of the Galaxy. The average density of matter in interstellar space is of the order of $10^{-24}$ g/cm$^3$, roughly corresponding to one atom per cubic centimetre. However, it is not uniform throughout the space within the Galaxy, and there may be regions where the density is considerably greater, 10–100 times greater than the average density. The regions concerned have very large dimensions, of the order of several light years, and overall, it has been estimated that they can occupy 5% of the entire volume of the Galaxy. Due to these dimensions, they are characterized by great stability.

Charged particles with a certain energy can move between these regions in motion, and occasionally penetrate them, colliding with one of the particles in the cloud or interacting with an irregularity in the magnetic field. The interaction with these clouds, in particular with the irregularities of the magnetic field, can produce variations (both in excess and in defect) in the energy of the particle. Due to the stability of the magnetic region and the mass enormously greater than that of the single particle, the process can be treated as a collision with a large mass "reflecting" body.

According to this approach, the probability of a net energy gain by the particle is higher than the probability of an energy loss, at least starting from a certain threshold energy onwards, of the order of 200 MeV for protons. The argument in favour of this consideration is based on the statistical balance that must be achieved between the degrees of freedom of the moving magnetic fields and those of the particle.

A classic analogy to describe this mechanism is to imagine the interaction of the charged particle, in motion with a velocity v, with the magnetic cloud, as an interaction with a body of enormously greater mass, which can move with velocity V directed against the particle or in the same direction of motion as the particle. In the first case the particle would acquire energy and move with speed v + 2 V, while in the second it would lose it, moving with speed v − 2 V. The crucial point of this mechanism is that interactions of the first type, in which the magnetic cloud moves against the particle, are on average more frequent than those in which the cloud and the particle move in the same direction. Some have suggested a representation taken from everyday life to understand the phenomenon: imagine a car moving along a road, in the presence of equal traffic in both directions. The car will meet on average more cars moving in the opposite direction than cars moving in the same direction (in which case it will overtake them if it has a higher speed). If the car were stationary on the side of the road, on average, the same number of cars would pass in both directions. It is therefore a consequence of the relative motion.

In general, since the motion is random in all directions, there will be an angle θ between the direction of motion of the particle and that of the cloud (Fig. 15.1) and the probability of a head-on interaction will be proportional to v + V cos θ, while
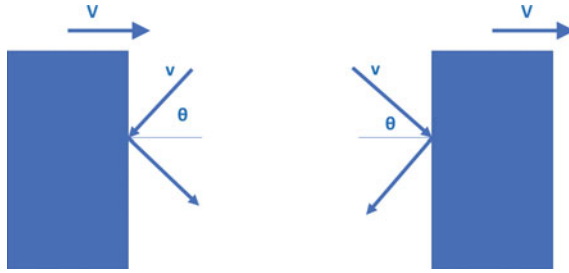
**Fig. 15.1** Schematic representation of the Fermi mechanism. A particle with initial velocity v can interact with the moving magnetic cloud with velocity V, with a component of its velocity directed in the same direction as the velocity of the cloud (right) or with a component directed in the opposite direction (left). In this second case, more likely on average, the particle can gain energy in each interaction

the probability for the interaction in the same direction will be proportional to v − V cos θ.

If the cloud moves with average speed V, and the total energy of the particle is W, the average energy gain for each collision is

$$dW = \left(\frac{V}{c}\right)^2 W = \beta^2 W$$

where $\beta = V/c$, and after N collisions, the energy of the particle will be

$$W = mc^2 e^{N\beta^2}$$

It can be shown that starting from these considerations, the energy distribution of the particles, accelerated by this mechanism, would follow a power law, even if the exponent would only be comparable with that observed experimentally.

Although the Fermi mechanism described (often referred to as the second order Fermi mechanism, since it depends on the factor $\beta^2$) can justify an acceleration of particles within galactic space, the time it takes for the particles to reach such high energies observed experimentally would be too long. Furthermore, the exponent of the power law that would be derived from these considerations is only qualitatively similar to that of the observed energy distribution. These, and other considerations, led in later times to not consider this mechanism valid as a complete and quantitative description of the acceleration mechanism of cosmic radiation. However, subsequent developments were based exactly on Fermi's original ideas, which therefore constitute a point of reference in the understanding of these phenomena (Fig. 15.2).

Particles could of course also be absorbed, interacting with matter. However, assuming a density of $10^{-24}$ g/cm$^3$, and the absorption cross section measured in the atmosphere, the average free path of these particles, before being absorbed, would be $7 \times 10^{23}$ m. This distance would be bridged, for particles moving at speed c, in a time of $2 \times 10^{15}$ s, equivalent to about 60 million years. These values ensure that there is

**Fig. 15.2**  Enrico Fermi.
*Source* AIP Emilio Segré
Visual Archive
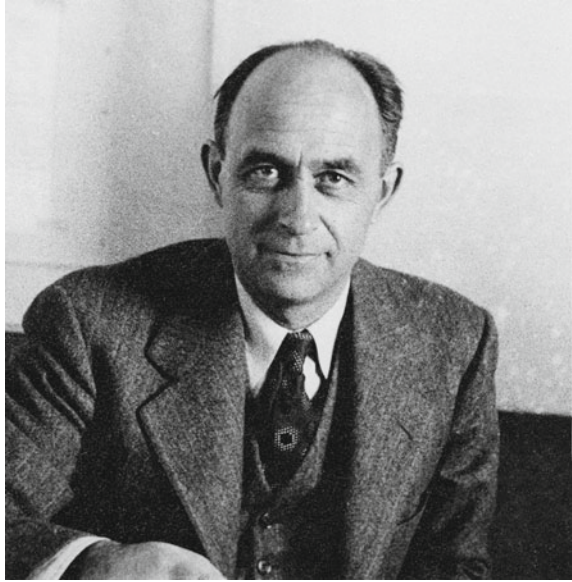


sufficient time during the life of the particle for it to be accelerated by the mechanism described. It can be estimated, in fact, from the distances between the regions with moving magnetic fields, that the average time interval between successive passages of the particle in these regions would be 1.3 years, and therefore the number of interactions with these regions over the course of its average life could be $10^7$.

As for the possibility that the gain in energy exceeds the losses, their average values were estimated by Fermi as a function of the initial energy of the particles, finding a threshold value above which the gain exceeds the loss, and the acceleration mechanism becomes effective. This value is about 200 MeV for protons, a value that can still be considered reasonable, assuming sources capable of producing protons of this energy. However, the threshold is much higher for heavier nuclei, increasing considerably with the atomic number of the nucleus considered. As an example, the threshold would be 20 GeV for oxygen nuclei and 300 GeV for iron nuclei, values that make this mechanism unlikely for a coherent explanation of the acceleration mechanism, valid for all nuclei. Fermi himself was aware of this limit, considering this mechanism as inadequate to explain the abundance of heavy nuclei in the cosmic radiation.

## 15.4   The Role of Supernovae

Some considerations about the possible role of supernovae in the production or acceleration of cosmic rays had already been made between the 1950s and 1960s [TerHaar1950, Colgate1960]. In the work of Colgate and Johnson [Colgate1960]

reference is made, for example, to the material ejected from the surface of an exploding supernova as the origin of cosmic rays, and to the fact that the nuclei at the surface of the star can acquire a much greater energy than the average energy released in the explosion, due to the different density between the innermost zone (core) and the outer mantle. The shock wave generated by the rapid increase in pressure in the core would be capable of imparting extremely high energies to the outermost layers.

Stellar events that are now called supernovae were observed long before their nature was understood. The sudden appearance of a very bright star in an area where no object was visible (*stella nova* in Latin) represents an event that even the peoples of the past had observed and recorded. Probably the first recorded observation (the object now called SN185) dates back to the year 185 AD, by Chinese astronomers. Very bright supernovae were observed in the year 1006 (SN1006, an object so bright as to be visible in broad daylight) and in the year 1054 (SN1054, in the Crab Nebula, an object comparable or even superior in brightness to that of the planet Venus). More precise observations of such events were then made by astronomers of 1500–1600, for example by Tycho Brahe in 1572 (SN1572) and by Kepler in 1604 (SN1604). Tycho Brahe could establish that the object had no relative motion with respect to other stars, and therefore could not be a nearby object, a matter of primary importance at that time, since celestial phenomena beyond a certain distance from the Earth were considered to belong to the place of immutability. These last two objects today represent the most recent supernovae directly observed within the Milky Way. The study of the residues of a supernova explosion allows, however, to date also events from the past that have not been directly observed.

The understanding of these events from an astrophysical point of view, however, came in much more recent times, when, around the end of the 1800s, the study of the spectra of the radiation emitted by novae stars turned out to be different from those of ordinary stars.

To date, the most recent supernova located within the Milky Way dates back to 1868, with a dating made only a few years ago. As for observations of supernovae in other galaxies, the first was SN1885A, observed by astronomers of the time in the Andromeda galaxy, although the nature of Andromeda, as an independent galaxy, located about 2.5 million light years from Earth, was established only in 1925. Observations of supernovae in other galaxies similar to ours have allowed us to estimate that the average rate at which these events occur in a galaxy like the Milky Way is about 3 per century. It should be noted however that entire regions of the Milky Way are not easily visible due to interstellar dust, so the immediate observation of a supernova in the visible can also escape.

A detailed observation from the astronomical point of view of a relatively "close" supernova (SN1987), observed in February 1987 in the Large Magellanic Cloud, about 160,000 light years away from us, allowed to confirm many of the hypotheses about the production of nuclei in these events.

If the term *nova* generically refers to a new bright star, the term *supernova* seems to have been used as early as 1931 by Baade and Zwicki, although other authors had used the same concept even before, with other names, such as "giant novae"

or "exceptional novae" or 'hauptnovae", in any case to denote energetic explosions much greater than ordinary novae.

In the case of supernovae, it has been estimated that the energy released is of the order of $10^{43}$–$10^{44}$ J, with a maximum brightness that can reach a billion times that of the Sun. Based on the light curves (trend of brightness over time) a classification of supernovae into two types (I and II) was introduced. Type I supernovae have a characteristic, well-defined, light curve, with a maximum reaching an absolute magnitude of 19.8. The rapid increase in brightness before the maximum is followed by a decrease at the same rate and then by a slower descent. The speed of the material ejected in the explosive process is of the order of $10^7$ m/s. Type II supernovae, which reach a maximum absolute brightness of 16.5, do not have a characteristic light curve, and the ejection rate is slower.

The explosion phenomena of supernovae have been understood, at least partially, within the overall evolutionary framework of the stars. The phenomena of nuclear fusion of light elements, present in the core of a star, allow to balance the gravitational force of the star. When the lighter elements, which serve as nuclear fuel, begin to run out, the star begins to contract, and its subsequent evolution depends on the star initial mass. For not too large mass values (roughly 1.5 times the mass of the Sun), the star contracts until it reaches enormously large densities ($10^6$ g/cm$^3$) and a pressure capable of balancing the gravitational contraction, making the whole a compact stable system. For masses greater than a certain limit (Chandrasekhar limit) the process of gravitational contraction does not stop, and the star continues its evolution towards a violent implosive collapse, with a reflection wave that produces the expulsion towards the outside of a substantial part of the star core.

The remnants of a supernova explosion (supernova remnants) will consist of a small super-dense collapsed core (a neutron star or a black hole) and a rapidly expanding gas nebula. Figure 15.3 shows a spectacular image of the Crab Nebula, the remnant (6 light years wide) of the explosion of the supernova SN1054, taken by the Hubble Space Telescope. The orange filaments are the tattered fragments of the star and consist mainly of hydrogen; blue light comes from electrons spinning, at speeds close to that of light, around magnetic field lines created by the pulsar located in the center, an ultra-compact remnant of the exploded star. The different colours reflect the various elements expelled during the explosion.

The amount of energy required per unit of time, necessary to maintain the level of cosmic radiation in the entire Galaxy, has been estimated in values of the order of $10^{34}$ W. Estimates of this order of magnitude had already been reported in the years '60 by Ginzburg, and further refined in more recent years [Strong2010], such as (0.7 ± 0.1) $10^{34}$ W.

If we ask ourselves what could be the source capable of providing such power, the answer, now discussed for several decades, is precisely that of the explosion of supernovae. If an energy of the order of $10^{44}$ J is released in the explosion of a supernova, and events of this kind occur on average every 30 years ($9.5 \times 10^8$ s), the resulting power is $10^{44}$ J/($9.5 \times 10^8$ s) ~ $10^{35}$ W, compatible with the above estimate, if we assume for example that 10% of the available energy is converted into the energy of the accelerated particles. Other sources, such as pulsars, are much

**Fig. 15.3** Crab Nebula, the remnant (6 light years wide) of the explosion of the supernova SN1054, taken by the Hubble Space Telescope. *Source* NASA, ESA, J. Hester and A. Loll (Arizona State University), HubbleSite: gallery, release, Public https://commons.wik imedia.org/w/index.php? curid=516106)
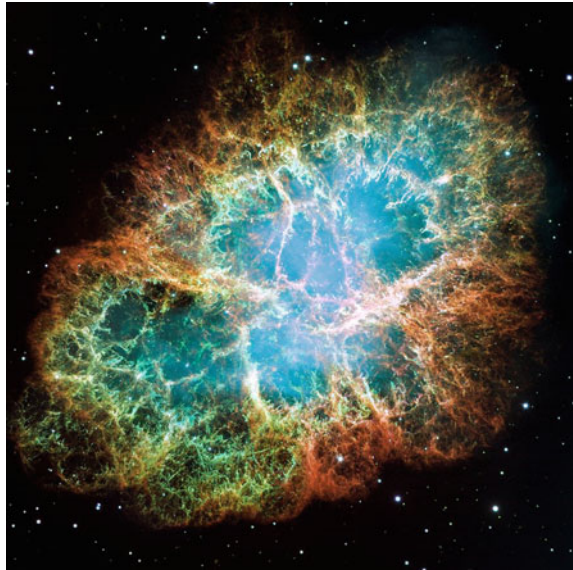


less energetic; they could be responsible, according to recent considerations, for a fraction of the electrons and positrons present in the high-energy cosmic radiation, but not for the prevailing part of the cosmic radiation, consisting of nuclei.

Regarding the question of the acceleration mechanism and the location of this acceleration process, significant progress has been made in recent decades, starting from the late 1970s [Axford1977, Bell1978, Blandford1978], on the basis of which it has been accepted that a version of the Fermi acceleration mechanism based on shock waves, has the characteristics necessary to explain the origin of most cosmic rays of a galactic nature. In this process, now commonly referred to as 'Diffusive Shock Acceleration" (DSA), it is assumed that the particles undergo numerous passages through the shock wave, gaining energy to each passage. The detailed description of this process, which goes beyond the scope of this chapter, can be found in several recent works on the subject [Drury1983, Blandford1987, Jones1991, Jones1994, Malkov2001]. We can only remember that this description leads to an energy distribution of the particles produced governed by a power law, with an exponent very similar to the one experimentally observed, without resorting to fine adjustments of the parameters involved. Furthermore, it does not require pre-acceleration phases of the particles, which can also originate with low energies.

In this context, there are aspects that limit the maximum available energy. First of all, these limitations derive from the size of the region in which the process takes place, due to the confinement of the particles up to a certain maximum energy, as we have seen in the introductory part of this chapter, and from other factors related to the diffusion of the particles. Another important parameter is the time, which must be long enough for the particles to be accelerated from very low energies to the required energy. Using reasonable values for these parameters, maximum achievable energies

are estimated, for protons, of the order of $10^{14}$ eV, which is even less than the energy corresponding to the knee in the energy spectrum of the primaries. It must be said, however, that if the higher energy part had a notable contribution from heavier nuclei, such as Iron, the achievable energies would be higher.

Another aspect that has been underlined [Bell1978] is that the value of the magnetic field in the region of interest for the acceleration of the particles could be significantly higher than the average galactic magnetic field, estimated to be 0.3 nT. Preliminary evidence of possible magnetic field increases in these regions has recently been obtained. This could further increase the maximum achievable energy value, up to values close to the "ankle" region.

For electrons, it must be considered that—although this mechanism may be valid for these particles—they significantly lose energy due to radiative processes, which limits the energy that can be reached. The electron injection phase in the acceleration process must also be hypothesized differently from that assumed for protons and nuclei.

A plausible synthesis of the origin of cosmic rays of a galactic nature therefore seems to be possible, assuming this acceleration mechanism in the vicinity of the residues of the supernova explosion. Using some of the aforementioned hypotheses, it is possible to justify the achievement of magnetic rigidity values of $10^{17}$ V; assuming a non-negligible presence of even heavier ions, up to Iron, this rigidity could correspond to energies up to about $3 \times 10^{18}$ eV.

## 15.5   The High-Energy Extragalactic Component

Based on the previous considerations, it is reasonable to assume that the highest energy component in the primary radiation spectrum, certainly that beyond the ankle region, cannot be of galactic origin. Knowledge of this part of the energy spectrum has significantly improved in recent years thanks to measurements obtained by the use of large detector arrays (AGASA, The Pierre Auger Observatory). The measurements themselves and their detailed interpretation are still ongoing, with discrepancies between the values measured by the two experiments at the very end of the spectrum, as discussed in one of the previous chapters. This may be due to the possible presence of the long hypothesized GZK cutoff, or to different mechanisms in that region. Certainly not a significant number of events due to high-energy showers are observed beyond the cutoff. Some retain as plausible that the same mechanism described in relation to the residues of supernova explosions could also be applied to Active Galactic Nuclei (AGN) [Hardcastle2010], although other possible mechanisms have recently been hypothesized, as well as the role of other phenomena with large energy emission, including gamma-ray bursts.

As regards the localization of the arrival directions of these extreme energy events, the study of which is possible in principle because at these energies the particles are not significantly deflected by the magnetic fields, attempts are underway to associate

the direction of arrival of these energetic particles to known sources of astrophysical interest. The first promising evidence of a significant correlation between the direction of these highly energetic primaries and the distribution of matter, obtained by the Pierre Auger Collaboration [Abreu2010], have been dampened by subsequent measurements, with a correlation that, although existing, is less significant than previously expected initially. However, the still not very precise knowledge of the intergalactic magnetic field can partially obscure any possible correlations.

The study of the origin and acceleration mechanisms of cosmic rays, both for the more energetic component—predictably of extragalactic origin—and for that of lower energy, discussed in the context of supernova explosions, is in any case a research field still very active today, with recent or pending measurements, and theoretical interpretations under discussion.

Some experiments in particular will certainly contribute to the understanding of these aspects, with detection facilities and measurement campaigns that will significantly extend the current set of observations available at the moment. Examples (not exhaustive) are the expansion of large arrays for the detection—even by hybrid techniques—of very high-energy atmospheric showers, high-energy gamma measurements from satellites and the detection of neutrinos in underwater laboratories.

# Chapter 16
# The Impact of Cosmic Rays in Applications and in Daily Life

**Abstract** This chapter provides an extensive list of different fields of application of cosmic ray muons in daily life and in applied research. These include: the production of radioactive isotopes in the Earth atmosphere and the associated dating techniques, also outside our Planet; the radiation dose delivered to living beings by the cosmic radiation; possible effects of cosmic rays on consumer electronics; muon tomography techniques based either on muon absorption, now employed for the investigation of large structures such as volcanoes, or on muon scattering, such as those widely employed for the scanning of containers in search of potentially dangerous fissile materials; the use of cosmic muons as probes to monitor the long-term stability of civil buildings. Additional topics concerned with cosmic ray muons, including those related to prospections of other natural and man-made structures, the role of cosmic rays in cloud formation, as well as recent proposals to use the arrival of cosmic showers as a tool to synchronize distant clocks are presented.

## 16.1 Introduction

The list of issues about the possible impact of the radiation of cosmic origin and its applications in various aspects of daily life, discussed in this chapter—although extensive—cannot be considered exhaustive. In recent years, an ever-increasing number of articles, technical reports, contributions to conferences, discussion forums on the Web have appeared on these issues, with the involvement of experts from different areas. For some of these issues, specialized conferences and workshops are today held periodically, others have also given rise to industrial applications. Despite this wide diffusion, or perhaps because of this, there is still a large territory in which to look for new applications, improve existing techniques or establish new links between research and application areas, all limited only by the imagination and creativity of the people involved.

## 16.2   Production of Radioactive Isotopes by Cosmic Rays and Dating Techniques

Particles in the primary radiation, in particular the most abundant ones (protons, helium nuclei …) interact, as we have seen, in the Earth's atmosphere, giving rise to showers of secondary particles. The interaction of these particles can also produce new isotopes: some of them are stable, others radioactive. Today we know that it is possible, through appropriate laboratory techniques, to detect even small quantities of these isotopes and to use these products, generated by cosmic rays, in various applications, especially as clocks capable of dating the age of objects. The concentration of an isotope in a material sample can in fact be used to determine the age of that material.

The best-known example in physics is the so-called radio carbon (or Carbon 14) dating, which is produced by cosmic rays in the atmosphere of the Earth, and which is found in every living organism (either animals or plants). The measurement of Carbon 14 in organic substances has revolutionized the archaeological dating technique: being able to date an artifact is extremely important for the study of past civilizations and in archaeological applications. Dating techniques based on the use of other isotopes can answer questions about how old the Earth is, how it formed, how and when certain living organisms first appeared or when they evolved into different forms. The age of the Earth can now be quantitatively estimated on the basis of measurements of the isotopes of lead and the content of radioactive uranium and thorium, whose relative proportions depend on the elapsed time and change on a time scale of billions of years. For dating applications on shorter time scales, such as those related to the history of civilizations and archeology, where times are measured on a scale of hundreds or thousands of years, dating can be obtained by studying the amount of Carbon 14. The Carbon 14 dating technique was introduced in the 1940s by Willard Libby [Libby1949a, Libby1949b], a chemist at the University of Chicago, Nobel laureate in 1960.

The carbon that we find on Earth consists almost exclusively of a mixture of two isotopes: Carbon 12 (at 98.9%) and Carbon 13 (at 1.1%). Other carbon isotopes with average lifetimes of minutes or even shorter can be created in the laboratory but are of no particular geological interest. Carbon 14, however, which is produced by cosmic rays in the Earth's atmosphere, is of special importance. To evaluate the importance of Carbon 14 dating we must consider that carbon is a critical element for life in all its forms, as all living organisms consist of a variety of carbon-based molecules; long chains of carbon atoms make up, together with other atoms, the DNA and complex molecules that are necessary for life and reproduction. The exchange of carbon dioxide between plants, animals, the atmosphere, the oceans is a necessary part of the cycle of life.

When cosmic rays penetrate the atmosphere, they interact with the air at the highest altitudes and already at a height of about 15 km from the surface of the ground, most of them have given rise to nuclear reactions in which neutrons can also be produced. Neutrons lose energy to the point where they can be captured by nitrogen nuclei to

produce Carbon 14, according to the process

$$^{14}N + n \rightarrow {}^{14}C + p$$
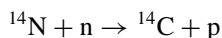
This new isotope, Carbon 14, is radioactive, with a half-life of 5730 years. It can decay into nitrogen after emitting an electron. Despite its radioactive properties, Carbon 14 retains all its chemical properties to combine with other atoms and form molecules; in particular, it can combine with oxygen and produce the radioactive carbon dioxide $^{14}CO_2$, which spreads throughout the biosphere. The molecules of $^{14}CO_2$ can in fact be diffused through the air currents in the atmosphere, can be found in the rain and eventually be absorbed by plants, which in turn are used as food by humans and other animals. Carbon dioxide can also end up in the water of rivers and oceans. In this regard, the time scale with which this Carbon 14 diffusion process takes place in the atmosphere is important. It has been estimated that it takes about 7 years for it to spread from the stratosphere to the regions of the atmosphere near the ground to reach living organisms or the water of rivers or oceans. This 7-year time is very small compared to the half-life of 5730 years (Fig. 16.1).

The quantity of $^{14}C$ present on Earth, which is produced by the processes described, with subsequent decay, sets the proportion of this isotope with respect to the $^{12}C + {}^{13}C$ isotopes to a very precise value in all living organisms, about 1 atom of $^{14}C$ every $10^{12}$ atoms of $^{12}C$. When the organism (plant or animal) dies, it no longer takes on additional $^{14}C$ from the outside, while the one contained within it progressively decays, shrinking more and more over time. The proportion $^{14}C/(^{12}C + {}^{13}C)$ therefore decreases over time.
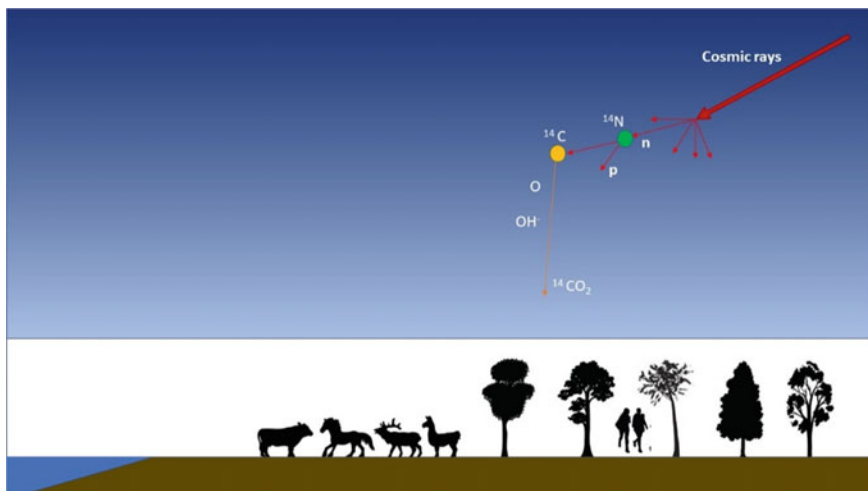


**Fig. 16.1** $^{14}C$ production mechanism in the Earth's atmosphere, induced by the interaction of primary cosmic rays. Among the products of nuclear interaction with the nuclei of the atmosphere, neutrons can in turn interact with a nucleus of $^{14}N$ producing $^{14}C$

A measurement of this ratio, carried out on a small sample of the material to be examined, can therefore provide the age of the sample, taking into account the law of radioactive decay, which regulates the number of $^{14}$C nuclei still present after a certain time interval t. The measurement of this ratio can be made, as in the original method introduced by Libby, by detecting the electrons emitted following the $^{14}$C decay process (and distinguishing them from the background produced by the cosmic rays themselves or by decays produced by other radioactive natural material placed in the proximity of the detector). Considering the activity of this isotope, it can be estimated that for each gram of carbon present in the sample in equilibrium conditions, 13.56 decays/min occur, a value already very low in itself, and which progressively decreases when the age of the sample is a few thousand years old, which makes the measurement difficult. For example, for a sample dating back to 3000 B.C. the activity would be reduced from 13.56 to a value of 7.39 per min per g.

The $^{14}$C decays by beta emission, according to the scheme

$$^{14}\text{C} \rightarrow {}^{14}\text{N} + \beta^- + \overline{\upsilon}$$
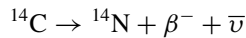
The emitted electrons have a continuous spectrum in energy, as occurs in beta decay, since in the final state the energy is distributed between the residual nucleus, the electron and the antineutrino, and the maximum energy of the electrons (endpoint) is only 156 keV, which makes it even more difficult to distinguish them from the background of other natural decays. These factors limit the applicability of the method, in the case of very ancient objects, since the measured values would be indistinguishable from the background.

Another technique for the detection of $^{14}$C, introduced in the 1970s, consists in taking a small amount of the sample (even a few milligrams), and using it in the source of an accelerator. The accelerated ions would then be deflected by a magnetic field, based on their energy, charge and mass, thus being able to distinguish $^{14}$C from other ions.

Realistically, the maximum age that can be sampled with these methods, in the best conditions, is a few tens of thousands of years, which still makes them suitable for dating finds of historical interest. It must be said, however, that the results of this technique can be affected by various factors, some due to natural causes, others related to human-induced phenomena. The variation in the flux of cosmic rays over the centuries or the solar cycle can induce variations in the amount of $^{14}$C, slightly distorting the dating estimates in case one wants to make precision measurements. For example, it is known that in the period between 1650 and about 1730, when sunspots were practically absent, the flux of low energy cosmic rays arriving on Earth was greater, as the corresponding amount of $^{14}$C found in the findings that date back to those years. However, a significant cause of variation in the $^{14}$C content in the atmosphere also derives from human activities. The use of fossil fuels has produced an increase in carbon content with a low $^{14}$C content in the atmosphere, altering the ratio by approximately 3%. Another major consequence on the relationship between the different isotopes of carbon in the atmosphere was produced by the nuclear tests carried out from the end of the Second World War up to the 1960s, which produced,

in the following years, an amount of $^{14}$C even double than the basic values. Currently, after nuclear testing in the atmosphere ceased in 1960, this quantity is slowly returning to its original value.

## 16.3   Cosmic Ray Dating Outside the Earth

Apart from the production of $^{14}$C, which certainly represents the most relevant aspect in terrestrial dating techniques using isotopes produced by cosmic rays, several other isotopes of some interest in longer time scale dating are also produced as a consequence of the arrival of primary cosmic rays on Earth and in the Solar System. On Earth, for example, $^{10}$Be (with a half-life of $1.4 \times 10^6$ years) or $^{26}$Al (half-life about $7.4 \times 10^5$ years) are isotopes of interest for this type of analysis. The relationship between these two isotopes, in particular, can be used to study their diffusion in geological processes.

Dating techniques linked to the existence of cosmic rays have also been applied to samples of the lunar soil. In the case of Moon, without an atmosphere, primary cosmic rays can interact directly with the ground, producing isotopes on the surface and up to a certain depth. The part of the ground close to the surface receives a greater dose of radiation than that localized at a certain depth; however, due to the impact of meteorites—microscopic or with a certain size—the lunar soil is continuously modified, since in the impact of a meteorite fragments of soil are expelled, leaving a certain area uncovered and covering instead other areas where the fragments are deposited after having travelled a certain path. This is made possible by the lack of an atmosphere and by a gravity smaller than on Earth.

Information on the time scale involved in these processes can also be extracted through the damage effect produced by cosmic rays in certain crystalline materials. The energy deposited in these crystals can be stored for very long times and subsequently released, in the form of light, when the crystal is heated. This is thermoluminescence, a technique widely used in the laboratory for dating finds of historical and archaeological interest, in particular ceramic artifacts. From samples of the lunar soil, up to a depth of 2 m, carried out during the Apollo missions in the early 1970s, it was possible to measure the exposure to cosmic rays of the different soil layers at various depths, and therefore to understand how the lunar soil is periodically "remixed", at least in its most superficial layers. It has been estimated, for example, that the most superficial layer (about 0.5 mm) is remixed on average every 10,000 years, while an average time of one million years is required to move and redistribute one centimeter of soil thickness. Modifications of the lunar soil below the depth of 10 cm, up to a maximum depth of one meter, require time scales of one billion years.

In the case of thermoluminescence, the result obtained is the consequence of a radiation dose absorbed over very long periods. Other useful information on objects located outside the terrestrial environment can be extracted from the study of the individual tracks generated by the passage of a primary particle. These tracks have been

observed, for example, in samples of material coming from comets, or in interplanetary dust, using etching techniques similar to those used in the case of nuclear emulsions to detect the passage of particles. The very existence of these tracks demonstrates, for example, the fact that these fragments were not exposed to very high temperatures, above about 500 °C, during their journey, including re-entering the atmosphere, otherwise the tracks originally present would have disappeared. The presence of some isotopes of the noble gases in specimens coming from interstellar dust also demonstrates their extraterrestrial character and their origin, due to interactions of primary cosmic rays in the material.

The period of time during which meteorites were exposed to the flux of primary cosmic rays indicates the period during which they existed as small objects (dimensions of the order of one meter) in a free state or bound to the surface of a body of larger dimensions. It therefore represents a sort of "age" of the meteorite itself and can be estimated in some cases precisely on the basis of the interaction of the cosmic rays in these bodies. This time interval, which often represents the time required for the meteorite to reach the asteroid zone in the Solar System to the Earth, can provide useful information about the mechanisms involved in operating this transport from one region to another of the Solar System. Galactic cosmic rays, that is, of high energy, mainly protons, can interact with these objects, up to depths of the order of one meter or a few meters, according to their energy, and following this interaction protons or neutrons can be emitted by the various elements present in the sample, by processes called spallation.

Due to these interactions, a large number of isotopes, stable or radioactive, of rare species in nature can be produced. They range from noble gas isotopes, such as $^3$He, $^{21}$Ne, $^{38}$Ar and $^{83}$Kr to other elements, such as $^{10}$Be, $^{26}$Al, $^{36}$Cl, and many others. The concentration of radioactive isotopes can give us information on the rate of interactions between cosmic rays and materials, while the accumulation of stable isotopes can measure the time elapsed since the bombardment with cosmic rays began, once the volume of the meteorite was exposed to their flux. As a result of these investigations, it has been estimated, for example, that almost all meteorites are older than one million years, which indicates that this is the minimum time required for their orbit to intersect that of the Earth, according to simulations of their trajectories. Although most meteorites show an age of some tens of millions of years, some of them, especially those rich in iron, have been shown to be much older, up to one billion years.

## 16.4   The Radiation Dose Produced by Cosmic Rays on Earth and in the Solar System

Ionizing radiation is one of the components of the environment in which we live, whether it is produced by natural or artificial causes. Examples of "natural" ionizing radiation, that is present in the environment independently of man, are those due

to cosmic rays or to the natural radioactivity of rocks, while "artificial" sources of radiation may be those related to diagnostics and therapy in the medical field, to the functioning of particle accelerators or to radioactive elements, which, although natural, are artificially produced, that is, as a result of human activities.

Cosmic rays, like other ionizing radiations, deposit a certain amount of radiation dose in the materials with which they interact, as well as in the tissues of living organisms. We will see in the next section the effect of such radiation dose in electronic circuits that are now used in most human activities, while we will discuss here the effect of the dose absorbed by people and due to radiation of cosmic origin.

Living beings coexist since their origin with a background level of natural radiation, but it is important to minimize as far as possible the dose of radiation absorbed by extra-natural causes. The overall effective dose absorbed by an organism in a certain time interval, which depends on the energy deposited per unit of mass, as well as on a biological damage factor for that specific radiation, can be expressed in Sievert. However, it is important to evaluate the absorbed dose per unit of time, which can conveniently be expressed in μSv/h (microSievert per hour). It has been estimated that the average effective dose to which an organism is subject—because of the cosmic radiation and of the terrestrial radioactivity, mainly due to Radon gas— is about 2.4 mSv/year (milliSievert per year), equivalent to 0.27 μSv/h. Slightly different values are reported depending on the territory. Current laws, sometimes slightly different from country to country, then establish, in accordance with the results of medicine, what are the maximum allowable doses for the different types of workers.

The various factors that contribute to determining the average dose absorbed by a person are slightly different depending on the environment, habits and other factors. As an example, the following figure shows, through a pie diagram, the various causes contributing to the radiation dose and the corresponding fraction to the overall dose, in the case of the Italian population (Fig. 16.2).

This diagram shows that the effect of cosmic rays at sea level, as regards the dose absorbed by an individual, amounts to just under 10% of the total average absorbed dose. This dose is essentially due—again referring to sea level—to the secondary radiation, since the primary component is essentially absorbed by the atmosphere. In fact, the presence of the Earth's atmosphere offers considerable protection against these radiations. With the exception of particular periods of solar activity (in which the low-energy components can make a notable contribution), the components that essentially produce this dose of radiation are the galactic, high-energy components.

At altitudes significantly higher than sea level, the intensity of the secondary radiation becomes higher, and consequently also the radiation dose. As an example, the dose due to cosmic rays doubles for altitudes around 2500 m, while it even becomes almost 5 times greater in the case of the Tibetan plateau, located at an altitude of over 4000 m. Slight variations can be expected going from locations near the equator to higher latitudes.

If such doses refer to populations that on average always live in the same territory, the case of people who frequently travel by plane is different, in particular civilian flight crews (pilots, on-board personnel) or military, who pass a consistent number of
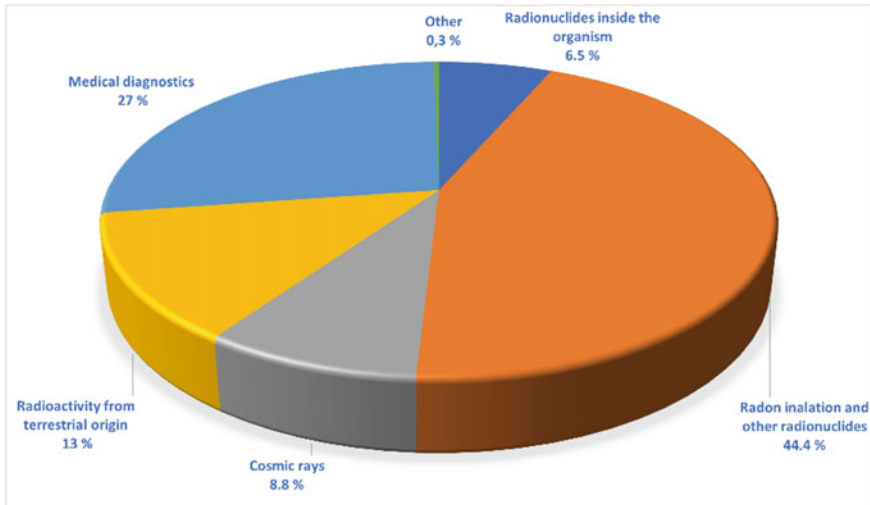
**Fig. 16.2** Percentage distribution of the various causes that contribute to the absorption of a certain dose of radiation in human organisms, in the case of the Italian population

hours each year at high altitudes. The central part of each scheduled flight takes place at cruising altitudes of around 10,000 m, with values ranging from 7000 to 12,000 m depending on the type of aircraft and route, while the initial and final phases of the flight, with a duration of 15–20 min each, take place between the initial (or final) altitude and the cruise altitude. For the personnel, this can lead to an increase in the total absorbed dose over the course of a year of 2–4 mSv, depending on the routes followed and the total number of flight hours, which corresponds to a total dose of 2–3 times greater than that absorbed by the rest of the population.

For this reason, staff people are subject to periodic routine medical checks, which also take this aspect into account. Small differences can be expected between flights that take place mainly at low latitudes and those that take place at latitudes close to those of the poles. In any case, these are still very low dose levels and statistical studies have so far shown no association between these doses of radiation and an increased incidence of cancer cases. A lower threshold is recommended in any case for pregnant women, for whom it is suggested not to exceed a dose level of 1 mSv throughout pregnancy, a dose that would be reached over a hundred flight hours at high altitudes and latitudes. As for frequent passengers, significant doses could accumulate only in the case of thousand flight hours per year. To give practical examples, a London–Singapore–Melbourne flight would involve a dose of 42 µSv, which means that it would take over 20 such flights in a year to accumulate a dose of 1 mSv. These estimates lead to consider as very marginal the risk from cosmic radiation in almost all cases.

The situation is completely different in the case of astronauts and space missions that take place outside the Earth's atmosphere, in the space surrounding the Earth or in any mission to other bodies in the Solar System. In this case the radiation dose

can derive from one or more of these different components: the primary radiation of galactic origin, composed mainly of protons and light nuclei of high energy, the particles emitted into interplanetary space by the Sun during intense periods of solar activity and finally the charged particles trapped around the Earth by the Earth's magnetic field. The first human missions in space flights began, as it is known, with the flight of the cosmonaut Gagarin, in 1961. Since then, in more than 60 years, a few hundred astronauts have spent more or less long periods in space, in orbit around to the Earth at various altitudes, and some flying to the Moon. The hypothesis of human missions on or around Mars has been and still is under discussion, in relation to which the assessment of the possible doses of radiation absorbed and strategies to improve radiation protection are particularly crucial.

As we have previously seen, the average dose that each individual receives while living on Earth, due to the various causes of radiation, including cosmic radiation, is about 2.7 mSv per year. This is a very low dose, and international standards require a person working in contact with radiation sources to take annual doses not exceeding 50 mSv. In the case of space missions, the limits set, assessed in such a way as to keep the risk of medical damage still low, are higher, in the order of 100 mSv.

What are the predictable radiation doses for space missions? In the case of the lunar missions, the travel times were around ten days overall, with absorbed doses from 2 to 12 mSv. A week-long orbital mission around the Earth, at an altitude of 400 km, would produce a dose of around 6 mSv. A stay on board the International Space Station, which orbits at an altitude of 300–400 km, would give rise to doses between 80 and 160 mSv, depending on the activity of the Sun in that period, therefore already potentially exceeding the permitted limits. A possible mission to Mars, for an estimated time of 3 years, could result in a dose of up to 1200 mSv. It is therefore evident that the dose of radiation due to the presence of cosmic rays is one of the limiting factors, if not the main one of any long-lasting human mission.

On the one hand, measures are possible to reduce the dose of radiation absorbed in space missions. In the case of long stays on the surface of the Moon or Mars, the possibility of choosing suitable areas where there is a weak magnetic field has been investigated, that could reduce, by deflecting them, the intensity of the incoming particles. The intensity of the magnetic field on these two bodies of the Solar System has been carefully monitored at different latitudes and longitudes, but it does not seem sufficient to provide an adequate shield from radiation. Recall that on Earth this shielding effect is provided both by the presence of the magnetic field and by the atmosphere, practically absent on the Moon and on Mars, even if on the latter there is a weak atmosphere consisting mainly (95%) of $CO_2$, at a pressure of about 1% compared to the terrestrial one.

Any people who remain for long periods on the surface of these celestial bodies should minimize the amount of time spent outdoors or on the surface, for example on the occasion of explorations to be done at ground, and it is required instead to spend a significant fraction of the time in underground environments or with an adequate protection from radiation.

We do not address in this context the aspect of the type of damage caused by radiation and the studies in this area, which are very active, with the participation of physicists, medical doctors and biologists.

As for the aspects to consider about the possible strategies to be used to reduce the absorbed dose and prevent possible radiation damage caused by cosmic rays during space missions, the experimental monitoring of the dose in the different environments in which astronauts are operating, and the theoretical evaluation of the effects of the materials present are among the main activities carried out for this purpose.

An essential part is in fact the radiation dosimetry, which consists in monitoring, characterizing and quantifying the radiation present in these environments. To this end, a large series of dosimeters accompany astronauts during missions in space. Detailed measurements on phantoms that incorporated radiation sensors arranged in correspondence to the different organs were carried out in space, to extract not only the average absorbed dose, but also its distribution within the body, corresponding to the organs of interest. Dosimetric measurements are also carried out in the various work environments of astronauts, particularly in the International Space Station, to assess the dose in each environment and identify the areas with less exposure, based on the structure of the station itself.

If on the one hand the first strategy to be used to reduce the effects of radiation is to limit the time spent in space, particularly outside the spacecraft in the case of extravehicular activity, on the other hand, solutions are also put into play to protect, as far as possible, people aboard spacecrafts. They are based on various strategies for shielding, adapted to the environments in which astronauts spend most of their time on board, with appropriate layer thickness and choice of materials. In the International Space Station many environments are shielded with polyethylene, a material rich in hydrogen. It must be taken into account that the primary high-energy particles can create secondary particles (neutrons and other charged particles) in the same material used for the shielding, and that sometimes the secondary ones can create more problems than the primary ones from the point of view of biological damage, if the thickness of the screen is not sufficient to contain them. From this point of view, light materials with high hydrogen and carbon content may be more suitable than heavy materials such as lead, in which more secondary are generated. Tests and calculations have shown that these materials are even more suitable than aluminum. Another suitable material is water, although its oxygen content makes it slightly heavier than polyethylene. The overall mass of the spacecraft and its components is a determining factor, since a greater mass to be brought into orbit or sent over a long distance requires larger thrusters and greater energies. It should be considered, however, that a certain amount of water, as well as organic liquids, is in any case on board a spacecraft, and that it can be housed in such a way as to contribute to the shielding of people. In any case, the thickness of the shielding materials (5–7 cm) provides a dose reduction of only 30–35%, while the remaining 65–70% is able to cross the shield and therefore contribute to the absorbed dose. In the case of permanence on the surface of other bodies, such as the Moon or Mars, the screens can also be chosen using other materials, without necessarily transporting them from the Earth. In addition to "absorbent" screens, other solutions based on the use of

magnetic fields to deflect incoming particles have also been studied; however, these solutions in turn involve the use of heavy materials to create a suitable magnetic field.

Further strategies to reduce not the dose of radiation absorbed but at least mitigate their effect, makes use of an appropriate diet and appropriate drugs, sometimes also used in the terrestrial environment in case of exposure to high doses of radiation.

From what has been discussed, even briefly, it is clear that the problem caused by cosmic radiations in any long-term stay in space is a problem that is not easy to solve and at the moment represents one of the major challenges posed to space travels.

## 16.5  Electronics and the Effect of Cosmic Radiations

Electronic circuits, especially those based on semiconductors, use electrical charges located in a certain area of the material as a means to define elementary binary information (0, 1). Any noise source that is able to modify these charge distributions can alter the information content. The noise source can come from the power line itself, from electromagnetic radiations or even from sources of ionizing radiation, including the cosmic radiation or any radioactive material placed near the circuit.

In a 16 kb memory chip, for example, introduced in 1977, the number of electrons in the single cell was of the order of $10^6$, comparable to the number of electrons created by the passage of an alpha particle along a path of a few microns, typical cell dimensions. This justifies the non-negligible probability that the passage of an ionizing radiation through the dimensions of the cell can induce a charge sufficient to alter the content existing at that moment.

In the 1970s it became clear that ionizing particles could momentarily alter the content of some bits in a memory chip, transforming "1" into "0" and vice versa (Fig. 16.3).

**Fig. 16.3**  In a set of memory cells, all initially set to 0, one of the cells can change its state, from 0 to 1, following the passage of an ionizing radiation (alpha particles, cosmic rays, …)
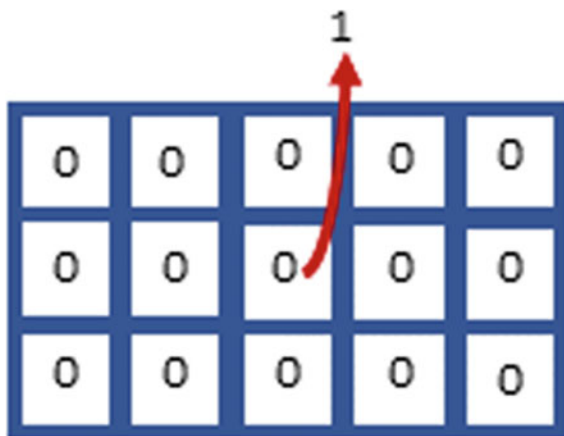
This type of effect, called "soft fail" (or failure), or single event upset, even if momentary, by altering the information contained in that bit, can produce a malfunctioning of the entire circuit or produce an incorrect information. Soft fail effects must be distinguished from permanent damage to the circuits due to the cumulatively absorbed radiation dose, effects which occur only with very high doses. The alteration of the content of an elementary cell does not necessarily lead, however, to the malfunctioning of the entire system, for example a computer that uses it. The computer may not use the contents of that cell during the operation in progress, or overwrite a new, correct information on that cell before reading the information which was altered.

In the first DRAM (Dynamic Random Access Memory) circuits, introduced in those years, the material of the ceramic package sometimes contained impurities, with the presence of very small quantities of alpha radioactive material, which could induce effects of this kind. The effect was then systematically studied, both to assess the purity conditions which the materials had to meet to reduce these effects below a certain value, and to understand how to improve immunity to these effects and possibly diagnose and correct them. Interestingly, from an anecdotal point of view, that effects of this kind in electronic components were imagined in a science fiction story by Isaac Asimov in the 1950s (*Caves of Steel*, 1952), i.e., 25 years before they were actually revealed, an event for which Asimov received recognition.

At sea level, the particles of cosmic radiation that are most likely to induce soft errors are neutrons. Although neutral, they can interact with the nuclei of the material, being captured and producing charged secondary particles that induce charges in the chip. In the 1990s, it was estimated by IBM that soft errors of the order of one per month could be induced in a 256 Mb memory of a PC due to cosmic rays. Of course, the flux of cosmic rays depends on altitude, so at higher altitudes, the rate of these errors also increases; this effect is enormously amplified aboard airplanes, which travel at high altitudes. Conversely, under considerable shielding (for example in underground laboratories) it has been verified that this rate is strongly reduced, even if a small contribution remains, also due to the natural radioactive material present in the rocks. The average rate of these possible errors also depends on the particular period within the solar cycle [Ziegler1996a, Ziegler1996b].

Certain cases have been documented with certainty in which the transformation of a bit into a memory location led to incorrect results or to the malfunctioning of a system. Among these, for example, the case of the counting of votes during an election, in which the system had assigned to one of the contenders a number of votes higher than the actual one, equal to 4096 ($2^{12}$), due to a bit flip which had triggered a bit from 0 to 1. It was also reported, on one occasion, the malfunctioning of the automatic pilot system of an airliner, which due to this caused the aircraft to momentarily lose altitude.

Proper chip design can help reduce the importance of these effects, through a suitable design of geometry, semiconductor type, and choice of package materials, such as avoiding the presence of $^{10}B$ and instead using materials enriched in $^{11}B$, which does not have this problem.

It is important in any case, since the rate of these errors cannot be reduced to zero, to carefully diagnose their presence and find solutions to correct the possible errors that result from them. From a hardware point of view, the circuits can be replicated—with consequent complexity and costs—in order to compare the result obtained from multiple copies of the circuits. A strategy sometimes used, especially in those situations where the reliability must be very high, such as in the applications of air or space flights, is to have three copies of the same circuit and, in case of discrepancy between the output of the three circuits, choose the value that two out of three have. Software techniques for the correction of this type of errors use, at the level of the compilation of the programs, a temporal replication of the program instructions with verification of the results obtained from sequences of instructions executed several times.

The diagnostics and possible correction of soft errors can be done, at least in some cases, by introducing redundant data into the ordinary data flow, and by introducing checks that evaluate and correct the error. For example, by introducing an additional bit and establishing an appropriate parity of the bits, it can be verified whether some bit flip has been introduced in the sequence of bits ordinarily assigned to the data (see Appendix N).

The rate of these soft errors, as we have said, depends, for a given system, on many environmental factors, linked to the location of the device and to the particular operating conditions (time of the year, solar cycle, occurrence of catastrophic solar events …). This explains why the estimates can vary widely between different studies. The error rate is sometimes expressed as the number of errors per unit of time (Failure in time, FIT = 1 error per $10^9$ h of component operation), or as the average time between two successive errors (Mean Time Between Failures, MTBF).

Quantitative evaluations of these effects by IBM in the 1990s led to estimates of possible soft errors on the order of 1 per month per 256 Mb of RAM installed in a PC, which corresponds to an error rate of $3.7 \times 10^{-9}$ per bytes per month ($1.5 \times 10^{-15}$ per byte per second).

Other evaluations report soft error rates in DRAM memories between 10 and 100 FIT per Mb. Based on this value, a system with 10 Gb memory should show such an error between 1000 and 10,000 h.

## 16.6  Muons and the Origin of Tomographic Techniques

Although as early as the 1930s it seems that some measurements of the muon flux in the London Underground were used to verify the thickness of the overlying rock, the first documented attempts to use cosmic muons as a probe to explore the interior of large solid structures probably date back to the mid-1950s [George1955], with some measurements carried out inside a tunnel, above which the layers of solid rock shielded a fraction of the muon component. Today, since a few years, an incredible variety of studies related to the use of secondary cosmic muons have appeared in the literature, with applications ranging from the exploration of volcanoes to archeology,

to the control of the content of potentially dangerous fissile materials. As this sector has received a significant boost in very recent years, many projects are still under development and further applications can be found by consulting the documentation available on the Web. In this context we will give in the following sections an overview of the main methodologies in which muon detection has proved useful for the exploration of the surrounding world. Further reviews discussing these issues can be found for example in [Checchia2016, Bonomi2017, LaRocca2018, Bonechi2020].

It is useful to distinguish in this field between those applications in which the absorption of muons is used to obtain information on the amount of material crossed by the particles, as described in the case of the search for hidden chambers inside the Egyptian pyramids, and other applications in which use is made of another phenomenon to which muons, as well as other charged particles, are also subject, the phenomenon of multiple scattering. This phenomenon, as we have seen, is particularly relevant in the case of materials with a high atomic number and can therefore detect the presence of these materials even within volumes that are difficult to access.

One of the studies that certainly marked the use of muons in these investigations is represented by the work of Alvarez and collaborators, published in 1970 [Alvarez1970], concerning the possibility of exploring one of the Egyptian pyramids in search of hidden chambers inside. The proposal to carry out measurements of this kind had already been advanced in 1965 by Luis Alvarez, an American physicist of Spanish origin, who was to receive the Nobel Prize in 1968 for studies related to particle physics. Furthermore, Alvarez's name is linked—in addition to the Manhattan project—to various scientific issues of an interdisciplinary nature, from the hypothesis of the extinction of dinosaurs following the impact of a large meteorite on Earth (based on observations of the content of Iridium in some rocky layers) to the study of ballistic information concerned with the murder of John Kennedy. Alvarez's proposal on muon experiments within a pyramid was sent—as the author himself testifies—to a group of cosmic ray physicists and archaeologists, to evaluate its feasibility, as well as to the political institutions of the countries involved. After it was approved, the installation of the detector and equipment necessary to operate it within the Pyramid of Chefren (Kafre) began in 1967.

Unlike other pyramids, even larger, such as the Pyramid of Cheops, which contains many internal chambers, it seemed that in case of the Chefren pyramid, despite being an enormous structure with sides equal to 215 m and an (original) height 143 m, only a single internal structure, called Chamber of Belzoni, were present. The question therefore arose whether this structure could also contain other rooms, which until then had remained hidden from exploration or looting. Knowing the location of the detector with respect to the pyramid structure, it would have been possible to evaluate, along each direction, the actual thickness of material crossed and the consequent absorption of the muon flux coming from that direction.

The detector used was based on a set of spark chambers, large area detectors with digital reading, capable of tracing and reconstructing the trajectories of the particles. During about two years of measurements, the detection apparatus had reconstructed about 100 million muons coming mainly from a cone around the vertical, allowing to
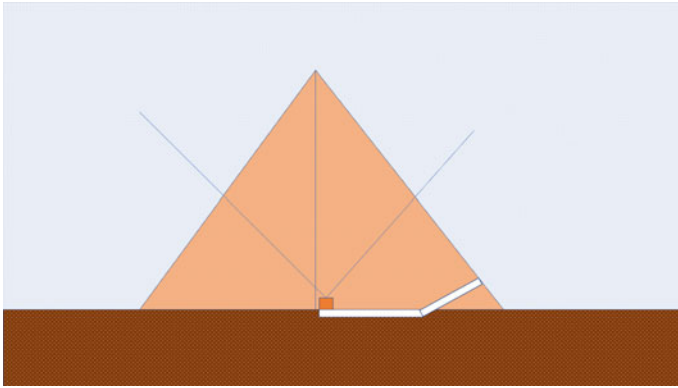
**Fig. 16.4** Schematization of the Pyramid of Chefren, 215 m side and 143 m high. In the only known chamber, the Berzoni chamber, located in a slightly displaced position with respect to the center of the base, a detector capable of reconstructing the trajectories of muons crossing the solid material of the structure can provide information on the presence of any hidden chambers. Experiment performed by Alvarez and collaborators [Alvarez1970]

measure their flux as a function of direction, and to exclude the presence of additional large chambers inside the pyramid (Fig. 16.4).

This experiment, although it gave a "negative" result, is of considerable importance in several respects. First of all, it opened the doors to a series of possible investigations in this direction, which were actually carried out in the following decades, and which in some cases led to archaeological discoveries of interest, such as the evidence of further hidden chambers in the structure of the Large Pyramid, or Pyramid of Khufu. In the latter case, complementary evidence was obtained from independent measurements, performed with nuclear emulsions located in one of the known chambers, with scintillators still located inside the same chamber and finally from gas detectors located outside the pyramid [Morishima2017, Procureur2023]. Following the original Alvarez experiment, the use of this technique has been generalized to apply it to the study of large natural structures, such as volcanoes or other geological structures. Measures of this type are still in progress on different structures and with slightly different purposes and are now a commonly accepted technique. But, more generally, the awareness that cosmic muons, as "natural" sources of radiation, could give information about the surrounding world, has led to numerous other applications, as we shall see, not necessarily based on the absorption of muons in a material solid, but on other possible phenomena characteristic of their interaction with the media.

It must also be said that Alvarez's experiment was often used as a model for conducting educational studies or simulations of the phenomenon. A few years ago, the "Pyramid Hunters" educational project was the winner of the 2016 edition of the "CERN Beamline for Schools" competition, dedicated to educational projects presented by school teams and to be conducted through the CERN facilities. In this study, proposed by a Polish team [Gutowski2018], in addition to a modelling of the

geometry of the Chefren Pyramid, in order to evaluate the absorption of muons in the different directions and compare it with the results of Alvarez and collaborators, some measurements was organized to experimentally assess in detail the absorption of muons in real pyramid blocks, using a beamline from the PS accelerator at CERN and a particle identification system.

In the following section we will review in greater detail some of the specific applications of cosmic muons in tomographic investigations.
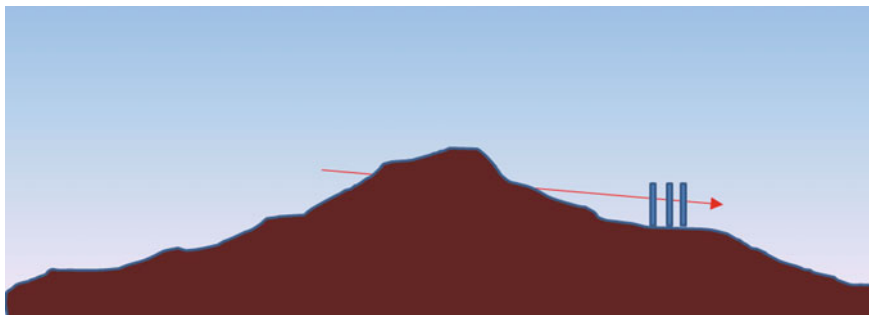
## 16.7   Tomographic Techniques Based on Cosmic Muon Absorption

The use of the technique based on the absorption of muons is particularly useful in the case of relevant structures, which require very penetrating probes to be able to give information on their interior. If the dimensions of the objects are of the order of one meter, or less, the use of X-rays (or possibly neutrons) may be a reasonable choice. The X-ray attenuation coefficients (energy 30 keV) are of the order of 30 $cm^2$/g in the case of lead, and therefore even a lead thickness of several cm can be crossed by a non-negligible fraction of these photons. However, for greater thicknesses, only highly penetrating particles, such as high-energy cosmic muons, can penetrate inside.

These considerations are the basis of the absorption-based imaging technique, which can also be applied to large solid structures, such as the summit of volcanoes. Even in this case, the measurement of the muon flux coming from the different orientations, especially if compared with the corresponding flux measured from the "open sky", that is from angular regions in which the muons do not cross any solid material, can give quantitative information on the fraction of muons absorbed, and therefore on the quantity of material crossed (density of the material integrated on the length of the path, usually called opacity). In the simplest case in which a constant density of the rock is assumed, this reduction in flux can highlight the presence of cavities inside the volcano.

This technique, introduced in the mid-90s [Nagamine1995], has been successfully applied in recent years to the study of various volcanoes (active and inactive) in various parts of the world [Tanaka2001, Tanaka2007a, Lesparre2010, Ambrosi2011, Marteau2012, Ambrosino2014, Ambrosino2015a, Carbone2014, Tanaka2014, Tanaka2016, LoPresti2018, Olah2018, Tioukov2019, LoPresti2020] and is still under development and further applications.

From an experimental point of view, the use of this technique requires a muon tracking detector (telescope), used in transmission mode (i.e., with the object to be explored positioned between the open sky and the detector, see Fig. 16.5). The result of measurements made with a setup of this kind provides two-dimensional density maps, with spatial resolutions that depend on the tracking capabilities of the telescope and on the amount of multiple scattering in the rock and materials surrounding the detector. Many aspects of the detector's performance, such as detection efficiency,

**Fig. 16.5** Schematic of the radiographic technique of the summit of a volcano, based on the absorption of cosmic muons. A muon tracking detector, hypothesized as a telescope consisting of three detection planes, sensitive to the position, is used to measure the flux of muons as a function of the arrival direction, obtaining information on the amount of solid material crossed by the muons along the various orientations

resolution, stability, sensitive area, as well as portability and cost, ultimately determine the difference between various projects and contribute to the feasibility of the measurements.

Although absorption tomography can only provide two-dimensional density maps, in principle the combined use of multiple telescopes, which view the volcano from different angles, coupled with numerical imaging algorithms, can also provide a 3D map. Attempts of this kind are currently in the design or construction phase.

It must be remembered that the exploration of volcanoes by tomographic techniques based on cosmic muons requires in any case long acquisition times (weeks/months) to provide reliable images. It is therefore a technique that can give information on the evolution of the internal structure of the volcano on this time scale, to provide, in a complementary way to other volcanological exploration techniques, useful information to predict in the medium term, possible changes and evolutions of the volcano activity. At the moment it is possible to see the detail of the internal structure with spatial resolutions of the order of ten meters, but this parameter is constantly evolving, based on the improvement of the detection equipment.

The use of the absorption tomographic technique has not been limited to the study of volcanoes, although these represent one of the most interesting challenges, but has also been widely extended to the study of smaller structures, such as underground cavities, caves, mines, tunnels, as well as other constructions of archaeological interest [Caffau1997, Menchaca2011, Gomez2016, Saracino2017, Fuji2017]. In many of these typical applications, the thickness of the rock that muons have to cross can be a few tens of meters, which leads to a much smaller reduction in flux than the typical crossing of the top of a volcano (hundreds of meters), with therefore shorter measurement times.

## 16.8  Muon Tomography and Scattering from High-Z Materials

Scattering muon tomography is based on the multiple scattering process that muons, as charged particles, can undergo when passing through a material. The value of the scattering angle, as we saw in a previous chapter, depends—with the same muon energy—on the characteristics and thickness of the material crossed, in particular on its atomic number. It is therefore understandable, at least in principle, that by measuring the deviation that muons undergo when crossing a sample of material, information on the main features of the sample can be obtained. However, the transition from a statement of principle to an established technique, capable of being used under realistic conditions, required an enormous amount of work, and is still in a development phase.

The first quantitative investigation using this technique to obtain a muography of the hidden content inside a given volume dates back to the early 2000s [Borozdin2003], using sets of drift chambers to reconstruct the trajectories of cosmic muons above and below the volume to be examined, and therefore measure, in each event, the deflection of the muon track. A schematic illustration of the technique is shown in Fig. 16.6.

Position-sensitive tracking detectors are arranged above and below the volume to be inspected, reconstructing two independent tracks that must be compared in each event. Muons that pass through any material with a high atomic number, located within the volume between the detectors, will be deflected, providing information on the amount of scattering and the 3D position in which the scattering process took place.

This technique has proved very promising since its inception, for several reasons. First of all, as it is based on the flux of cosmic muons existing in nature, it does not require artificially produced radiations, such as X-rays, usually used for scanning small objects; furthermore, muons have a much greater penetrating power than X-rays, and the technique can therefore also be used for volumes and objects larger than those that can be explored with X-rays. Finally, as it is based on scattering and not on absorption, each muon passing through the entire volume can contribute to the overall information, that is, to the reconstruction of the tomographic image. Since the scattering process depends on the atomic number Z of the element crossed, it is possible to some extent to discriminate between the presence of elements with low Z, intermediate Z and high Z, i.e., recognize the presence of elements with high Z even in the presence of a background produced by scattering due to low or intermediate Z materials. Even if the technique cannot distinguish between elements with similar atomic numbers, such as uranium and lead, this is rarely a problem, given the reasons with which this technique was proposed and the different fields of application in which it proved useful.

It should be remembered, in fact, that one of the problems that gave rise to the use of this technique is linked to the possibility that fissile material (Uranium or Plutonium) can be transported illegally inside containers, mixed with other commercial goods,

**Fig. 16.6** Sketch of muon
tomography based on muon
scattering. The track of a
muon, reconstructed before
and after the scattering
process, provides
information on the deflection
of the track and on the
localization of the scattering
process. The statistical
distribution of a high number
of muons can provide a 3D
tomography of the interior of
a volume, in principle
detecting the presence of
materials with a high atomic
number
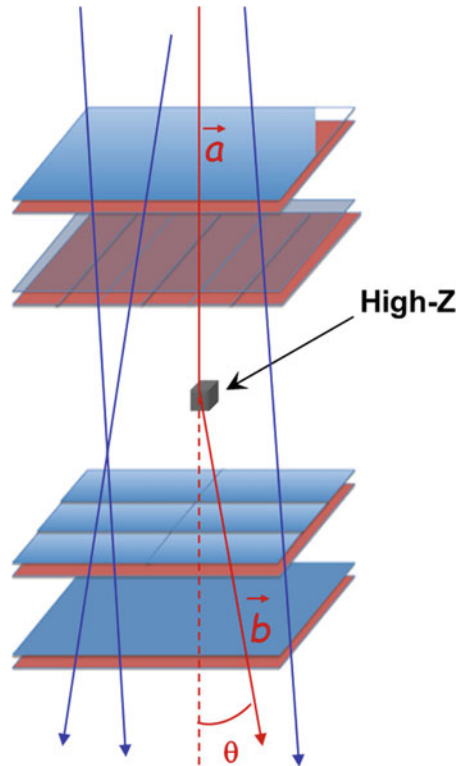


typically made up of lightweight materials. Systematic checking of each container
would take such a long time to be incompatible with the existing flow of goods.
For example, it is known that the number of containers used annually in the world
for the transport of goods is around 200 million, and of these only a small fraction
is controlled. Since the advent of containers as a standard means of transport on a
large scale, the need for inspection and control techniques that were fast and reliable
has been very strong. Muon tomography based on scattering has been suggested
as a viable way to achieve this aim, as it is capable of detecting in a reasonable
time the possible presence of small samples with a high atomic number (even cubic
decimetres) inside the entire container, that is, in volumes of about 50 $m^3$.

The use of this technique involves, as one can imagine from the previous figure,
the use of two muon tracking detectors with good performance, to be placed above
and below the volume to be inspected, in order to reconstruct the track of each
individual muon before and after the scattering process. In the simplest case, an
algorithm, called POCA (Point Of Closest Approach) can be used to determine the
3D coordinates of the scattering centre, as the midpoint of the segment of minimum
distance between the two skewed lines in space that represent the tracks of the muon
before and after scattering:

$$\mathbf{P}_{\text{POCA}} = (\mathbf{a} + \mathbf{b})/2$$

where **a** and **b** represent the vectors of the tracks reconstructed in the upper and lower part, as indicated in the previous figure.

Considering a large number of individually tracked muons, which come from any direction compatible with the geometrical acceptance of the detectors, it is possible to reconstruct two- and three-dimensional density maps of the inspected volume. The performance of such a tomograph can be evaluated in terms of its spatial and angular resolution (which in turn depends on the characteristics of the tracking detectors), of the overall detection efficiency, which allows to provide a response in a short scan time, and the percentage of false positives, i.e., false reporting of potentially dangerous areas within the volume.

In recent years, especially in the last decade, numerous prototypes of detectors for muon tomography, specifically designed for container inspection have been designed and built, both in small and full-scale dimensions [Schultz2004, Pesente2009, Riggi2010, Gnanvo2011, Baesso2014, Mahon2013, Xing-Ming2014, Anghel2015, Keizer2018, Riggi2018, Riggi2021b], making use of different detection technologies, from gas detectors to plastic scintillator strips with reading systems based on silicon photomultipliers and WLS fibers. As an example, Fig. 16.7 shows a tomographic result obtained from a full-scale prototype measuring 7 m × 3 m × 3 m, therefore capable of inspecting a volume equal to that of an entire 20′ container [Riggi2021b]. The figure shows the reconstructed XY density map, for a given Z (vertical axis) section; the horizontal dimensions of this map are 300 × 300 cm, corresponding to half of the overall volume. The other half of the volume, empty, was taken in this case as a reference to evaluate the background, with respect to which the excess density was extracted (difference between the left and right sides of the volume). To this extent, a lead block of 4 dm$^3$ size was placed within one of the two half volumes between the two detectors. The algorithm used for the data analysis was based on the POCA method, as previously described, i.e., reporting, for each event, the coordinates (X, Y, Z) of the POCA minimum approach point between the upper and lower tracks of the muon, with a cut on the minimum value of the scattering angle.

In the approach called POCA, a single scattering centre is assumed. However, there are more sophisticated algorithms [Schultz2007, Bandieramonte2015], with better performances, to determine the distribution of scattering centres and provide density maps of the explored volume.

Scattering-based muon tomography has also been used in recent years in numerous other applications, other than being a technique for inspecting containers. In particular, it has been suggested that the material produced during the operation of nuclear power plants and subsequently stored in sealed containers can be inspected using cosmic muons, without the need to open these containers [Jonkmans2013, Clarkson2014, Ambrosino2015b, Clarkson2015, Chatzidakis2016, Poulson2017]. Further applications of the same technique also refer to the integrity control of nuclear reactors, especially in the event of possible accidents [Borozdin2012, Perry2013, Fuji2013].
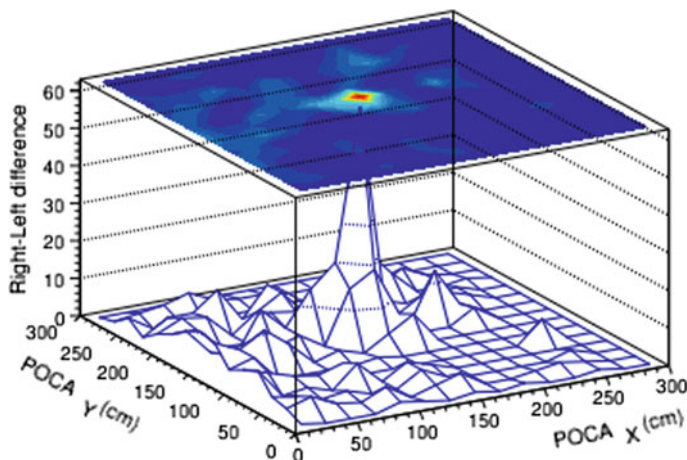
**Fig. 16.7**   A density map obtained by placing a 4 dm$^3$ lead block inside a volume equal to that of a standard 20′ container, obtained using a prototype portal for muon tomography [Riggi2021b]. The red spot marks the presence of the lead block

Another possible application is the control of any "orphan" radioactive sources that may be dispersed in the midst of scrap metal sent for their melting to steel mills [Bonomi2014, Furlan2014]. Incidents of this kind are more frequent than one might think, and can create serious contamination on the production line, so they must be diagnosed before the scrap metal is melted.

## 16.9   Imaging Techniques Based on Secondary Particle Production

While the tomographic techniques described above make use of the absorption or scattering process of muons, it has recently been suggested that also the interaction of muons in matter with consequent production of secondary (gamma, electrons) can give information on the characteristics of the material crossed [Reidy1978, Terada2015, Knezevic2019]. This information can be related to the type of secondary products, their energy distribution and their abundance. Muons, as we have seen, interact with matter through ionization processes, e$^+$e$^-$ pair production, bremsstrahlung and nuclear interaction. The relative importance of these processes depends on the energy of the muons. At energies typical of muons at sea level (some GeV) the nuclear interaction is irrelevant, and the predominant process is that of ionization, while for high energies the effects of production of pairs and bremsstrahlung start to become important, depending on the atomic number of the material present in the sample.

**Fig. 16.8** Cosmic muons, tracked by a position-sensitive detector, can generate secondary products (gamma, electrons) in a material, which are detected by a set of scintillators placed around the sample, and operating in coincidence with the tracking detector
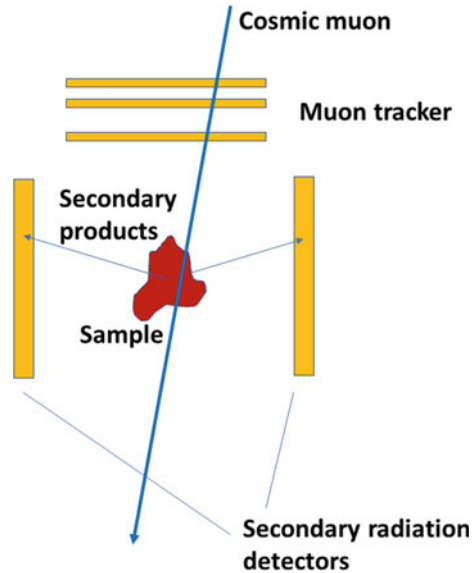
An apparatus that in principle can implement this method consists of muon tracking detectors, which define their trajectory, and a high-resolution Germanium gamma detector [Bikit2016] or a set of scintillators placed around the sample to be examined, so as to coincidentally detect the secondary products emitted following the interaction of the muon [Mrdja2016, Galgoczi2020], as schematized in Fig. 16.8. However, the potential of this method and its field of application still need to be systematically explored.

## 16.10  Monitoring of the Stability of Buildings by Tracking Cosmic Muons

Among the other possible applications that in recent years have attracted the interest of some research groups, it is certainly worth mentioning the possibility of monitoring, through a precision tracking of muons, possible deformations on a long time scale of buildings and civil structures.

In this case, it is a question of using two or more detectors, at least one of which is large and with good tracking capabilities, i.e., capable of reconstructing the trajectory of the detected muons, installing them in appropriate positions fixed to the structure, in order to detect any shifts in time of one with respect to the other. Figure 16.9 shows the diagram of a possible location, in the case of a building.

One of the detectors is placed on the ground or on the basement of the structure, while the other, even small and without any tracking capability, is located at a certain
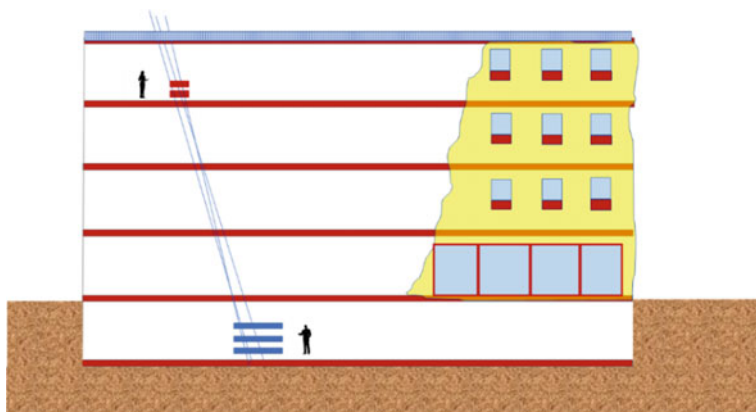
**Fig. 16.9** Two detectors, at least one of which with muon tracking capabilities, can be located in different positions of a building, to evaluate long time scale sub-millimetre relative deformations of the various parts of the structure

distance, anchored to that part of the structure whose possible displacement or deformation over time is to be explored. The two detectors must operate in coincidence, selecting those muons capable of passing through both detectors, even if separated by floors, walls, or other solid structures. A continuous measurement over time allows to extract, for example, the angular distribution of the muons detected in coincidence by the two detectors, discriminating them from those coincidence events originating from two independent muons, belonging to the same extensive atmospheric shower. These, in fact, may constitute a continuous background in the angular distribution, while the muons passing through both detectors will produce a well-defined peak in the angular distribution. Any displacement or deformation of the structure, on a long time scale (weeks or months) will produce a slight variation in the angular distribution and the displacement of the centroid of this peak will give information on the amount of deformation. In the case of very large distances between the two detectors, which would make it impractical to pass the signals from each detector to the coincidence circuit, it is also possible that each of the two detectors collect the data independently, labelling the arrival of each event using the GPS information and subsequently correlating off-line the collected data to search for coincidence events.

The use of this technique, for which some prototype measurements made in recent years are available [Bodini2007, Donzella2014, Bonomi2019, Abbrescia2019, Pinto2020b], is particularly useful compared to other techniques for monitoring the stability of a building when the parts of the structure whose stability is to be monitored are not in visual contact, in which case it would be possible to use laser-based alignment systems or mechanical deformation monitoring systems. The precision of the technique based on the reconstruction of cosmic muons depends on various factors, including the spatial or angular resolution of the detectors used, the relative distance between the detectors, the effects of multiple scattering in the crossing of the materials interposed between the detectors and the time of overall measurement.

Given the precision that must be achieved, and the long measurement times, it is important that the detection systems used are as stable as possible over time. It has been estimated that with measurement times of the order of the month and adequate detectors it is possible to achieve a precision such as to be able to highlight millimetric deformations of a large structure, which makes this technique suitable for monitoring civil structures (buildings of historical interest, bridges, viaducts …) on a long time scale.

## 16.11    Additional Possible Applications of Muon Tomography

Further application examples of muon tomography techniques, in its various aspects, have been proposed in recent years, both using absorption and scattering processes. For example, tomographic images of water towers were obtained [Bouteille2016, Jourde2016], as well as the amount of $CO_2$ stored inside cavities [Kudryvtsev2012, Klinger2015]. Examples of radiographs of industrial equipment obtained with muons are reported in [Giboy2005, Durham2015]. Recently, the problem of controlling reinforced concrete structures, in particular the deterioration of the internal metal part, has also received new attention, based on the possibility of using muon scattering tomography [Dobrowolska2020, Niederleithinger2021].

On a different side, it is worth mentioning the fact that cosmic ray-based tomography has recently been proposed and discussed also in the context of explorations of other bodies in the solar system [Tanaka2007b, Kedar2012, Kedar2013]. The use of the cosmic radiation for the purposes of tomographic imaging outside the Earth's atmosphere is completely different, as the interaction of primary cosmic rays produces different effects depending on the atmosphere present (or absent) in the particular planet or satellite considered and the consistency of the soil. In the case of celestial bodies totally devoid of atmosphere, such as the Moon, the primary cosmic rays strike the ground without producing extensive atmospheric showers. In other situations, such as Venus, the atmosphere is so dense that once the showers are generated at the top of this atmosphere, the secondary products are almost completely absorbed by the subsequent layers. The application of these techniques should therefore be discussed in relation to the particular structure of the celestial body considered.

Problems of this kind have been discussed above all in relation to the planet Mars, in which a very thin atmosphere (approximately 1/100 of the Earth's atmospheric pressure) exists. Under these conditions, the proportion between protons (or primary nuclei) and secondary component (pions, muons) is very different from that generated in the Earth's atmosphere, and, in particular, depends on the inclination of the particles. As an example, the flux of vertical muons is much less than that observed on Earth, while the situation is very different for directions close to the horizontal. In any case, there is a large overlap between primary protons and secondary products,

which should be appropriately identified and discriminated. Examples of this kind have been discussed [Tanaka2007b], also with possible applications to the prospection of Mount Olympus, the giant among the mountains existing in the solar system, a structure 25 km high and with a base of about 600 km.

## 16.12   The Impact of Cosmic Rays on Cloud Formation

It has been hypothesized in recent years that the arrival of cosmic rays in the Earth's atmosphere may also have an impact in determining the formation of clouds and in general in influencing the weather [Kirby2011]. When charged particles interact with the atmosphere, they can ionize volatile compounds, causing them to condense into droplets, around which clouds may begin to form. Although these elementary processes are known, it is not entirely clear whether they can have a really important impact on the climate, to the point of determining it and inducing climate changes, in relation to the intensity of cosmic radiation over time.

For an understanding of these effects under controlled conditions, particle beam experiments at CERN were started a few years ago, such as the Cosmic Leaving Outdoor Droplets experiment [CLOUD], in which a cloud chamber filled with ultrapure air and defined chemical compounds, which are believed to give rise to cloud formation, such as water vapor, ozone … is bombarded with beams of high-energy protons, extracted from the SPS accelerator. The gaseous atmosphere of the chamber is monitored following the bombardment with these ionizing particles, to analyse its content and evaluate the effect of radiation. The first results [Kirby2011, Lehtipalo2016], show some evidence that cosmic rays increase the formation of aerosols in the atmosphere, although the activity is still ongoing and the issue is the subject of debate, with varied opinions, some of the which deny that the importance of these mechanisms is competitive with other known cloud formation mechanisms.

## 16.13   Use of Extensive Air Showers in Time Synchronization

The problem of synchronizing systems operating in geographically distant locations is very common in various applications of today's technology. Usually, the best possibility of synchronizing the operation of systems that operate remotely is that which makes use of the GPS information available from the constellation of satellites orbiting the Earth. Recent developments in GPS technology make it possible to achieve very high resolutions, of the order of the nanosecond [Valat2020]. It should be remembered that precisely the synchronization of distant events using the GPS technique has allowed, as we have mentioned, the management of cosmic ray physics experiments, making it possible to carry out coincidence measurements between

detectors located at great distances. This is the case of large surface arrays where the average distance between the detectors is of the order of km, but also of experiments in which evidence of correlated events on a planetary scale is sought, as is the case with recent observations of gravitational waves in observatories located on different continents.

However, the ability to use satellite GPS signals requires that the satellites can be "seen" by an antenna, and that the area has adequate signal coverage. In many situations this is not taken for granted, such as in certain mountain locations, or in underground or submarine environments. The same difficulty in these environments would also arise in using alternative technologies to GPS, such as radio signals emitted by repeaters, or high intensity pulsed LED light signals. In cases where the GPS signal is intermittent, a high-precision local clock can in principle be used, which maintains synchronization for a certain period. However, the use of high precision clocks (nanoseconds), such as those based on Cesium atomic clocks, is enormously expensive if the system is to be replicated in multiple installations. There are less accurate and cheaper local clock systems (OCXO: Oven-Controlled Crystal Oscillator), with a limit drift of the order of microseconds per hour, which could be used to maintain synchronization for a certain period in the absence of a reliable GPS signal.

It has recently been suggested [Tanaka2022] that the detection of extensive air showers could be a local synchronization event to be used to further improve the accuracy of the local clock in the absence of a GPS signal. The muons of the atmospheric showers, in fact, travelling at speeds close to that of light, and following paths not too far from the primary axis, arrive within small time intervals, of the order of tens of nanoseconds, as we have seen while discussing the time profile of a shower. Each station, in addition to the local clock, should include a muon detector, for example a scintillator, and should be able to communicate with the other stations according to traditional technologies (Wi-Fi, optical systems …), even if not of high precision. The simultaneous arrival—within a few tens of nanoseconds—of muons in distant detectors would provide the synchronization signal to correct local clock drift. It has been estimated that with an appropriate distribution of the detectors and sensitive areas of the order of one square meter, synchronization between the various stations could be maintained within a hundred nanoseconds, with very low false synchronizations, depending on the amount of random coincidences between the different detectors. Of course, synchronization is limited to an area corresponding to the size of an extensive air shower, but it can be replicated by extending the stations, to cover very large areas, or by exploiting the ability of smartphones to detect muons via their CCD sensor, to create a virtual network extended to the whole planet Earth.

# Appendix A
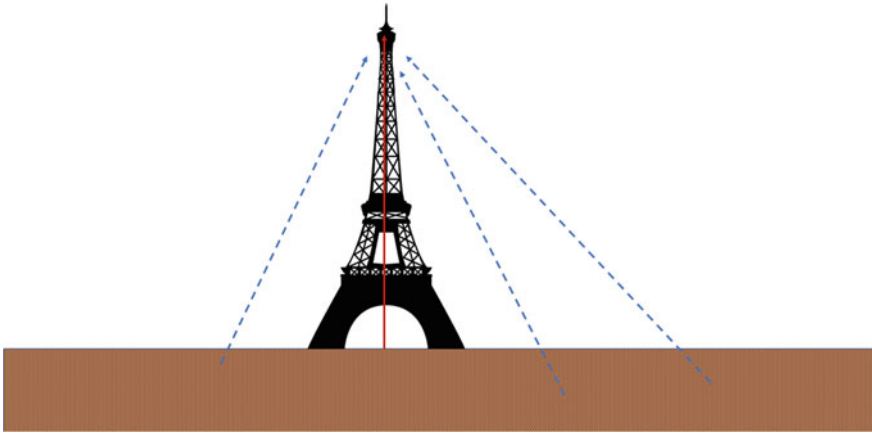# A Calculation of the Flux at the Top of the Eiffel Tower Due to Soil Radioactivity

Considering the presence of gamma-emitter radioactive isotopes in the terrestrial soil, we can try to evaluate, on the basis of the absorption coefficients of the gammas in the air and in the soil, reported in Chap. 1, what could be the effect of this radioactive material placed within a certain distance from the vertical corresponding to the centre of the Eiffel Tower, and a given depth in the subsoil. In assessing the flux due to the gammas coming from the ground, it must in fact be considered that at a certain height h (for example h = 300 m for the Eiffel Tower) not only the gammas emitted vertically but also those coming from the surrounding ground can contribute, within a large area (Fig. A.1).

How far from the vertical of the Eiffel Tower and to what depth in the soil is the contribution of gamma radioactivity still significant? We qualitatively expect that the contribution of the material placed very deep underground will not contribute, because of the average absorption coefficient in the rocks, estimated to be about 0.1 cm$^{-1}$ (see Table 1.1). As regards the dependence on the radial distance with respect to the vertical of the Tower, the contribution of the material close to the ground surface is not negligible even at large distances, due to the small value of the absorption coefficient in the air.

For a quantitative estimate we can numerically integrate the contribution due to the flux produced by the existing material within a given circular annulus between R and R + dR (where R is the radial distance with respect to the vertical passing through the centre of the Tower) and within a depth with respect to the surface between p and p + dp, assuming a uniform distribution of the radiation emitting centres distributed in the soil.

Figure A.2 shows the contribution that could be expected if all the radioactive material were distributed only on the surface of the ground (rather than also underground), as a function of the radial distance from the vertical.

As can be seen from this figure, the largest contribution comes from an area located at a certain distance, a few hundred meters, from the Tower, more than from the one below the Tower itself, due to the linear growth of the area of the circular

**Fig. A.1** Gamma radiation emitted by isotopes distributed on the ground or at moderate depths underground can reach great distances in the air. The contribution of this radiation present at the top of the Eiffel Tower, 300 m high, may also come from areas far from the vertical passing through the centre of the structure
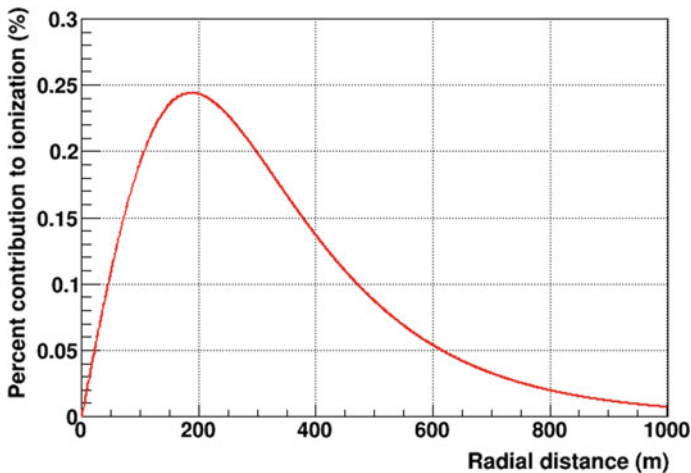


**Fig. A.2** Percentage contribution—for each meter of radial distance—to the total flux measured at the top of the Eiffel Tower (h = 300 m), as a function of the radial distance with respect to the vertical passing through the centre of the Tower, assuming that the radioactive material is distributed exclusively at the ground level. For the absorption of gamma in the air, a coefficient equal to 0.000044 cm$^{-1}$ was assumed (Table 1.1)

annulus with the radial distance R. The contribution due to the flux originating from a certain radial distance R is attenuated with a factor $\exp(-\mu d)/d^2$, where $\mu$ is the absorption coefficient due to air and $d = \sqrt{h^2 + R^2}$. It can realistically be assumed that at radial distances of about 1 km this contribution becomes negligible. As for the
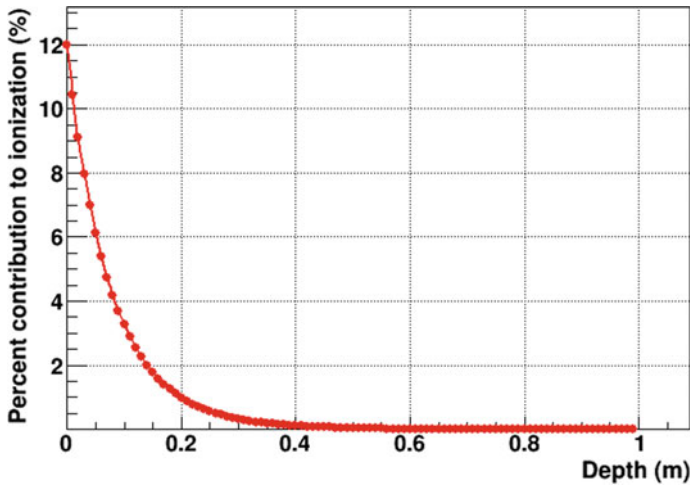
**Fig. A.3** Percentage contribution to the total flux measured at the top of the Eiffel Tower (h = 300 m), as a function of the depth, integrating from 0 to 1000 m in the radial distance. For the absorption of gamma in the soil, an absorption coefficient of 0.092 cm$^{-1}$ has been assumed

contribution due to the soil layers below the surface, we can integrate up to a radial distance of 1 km and evaluate the percentage contribution coming from the various layers placed at a certain depth. This result is shown in Fig. A.3.

In this case it can be seen that the main contribution comes from a very thin layer with respect to the soil, so much so that at depths greater than 30–40 cm the contribution becomes negligible. However, assuming an integration limit of 1 m for depth, it is possible to recalculate the contribution to the total flux as a function of the radial distance, shown in Fig. A.4, to be compared with that shown in Fig.A.2, obtained by assuming that all the contributions came from the soil surface. The trend is qualitatively similar, with a maximum slightly shifted towards smaller radial distances.

It can therefore be said by looking at these results that the effect on the ionization of the air measurable at a certain height with respect to the ground comes from the radioactive material distributed in the soil up to a depth of a few tens of centimeters but over a very large area, up to radial distances comparable to or greater than the height of the observation point itself, in this case about 1 km against the height of 300 m for the Eiffel Tower.

The overall result of the calculation, integrating both in depth, up to 1 m below the ground, and in radial distance from the Eiffel Tower, up to 1 km, has already been reported in Chap. 1 (Fig. 1.2), normalizing the vertical scale to the value obtained experimentally by Wulf at ground level.

Readers are invited to implement such calculations by themselves, employing a suitable programming tool and evaluating the precision of the numerical integration procedure.
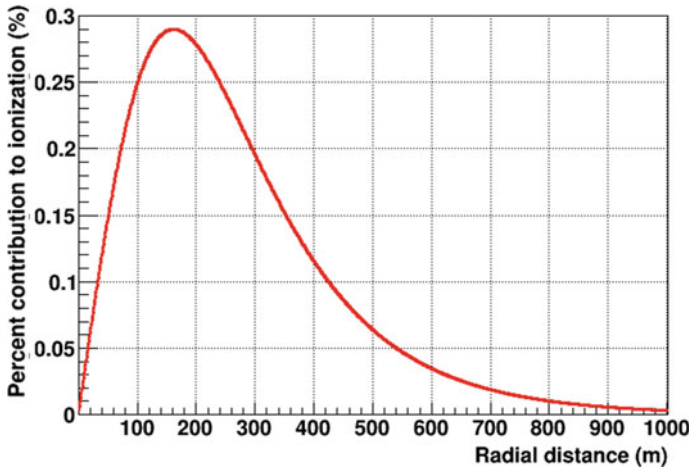
**Fig. A.4** Percentage contribution—for each meter of radial distance—to the total flux measured at the top of the Eiffel Tower (h = 300 m), as a function of the radial distance. For comparison with Fig. A.2, this time the flux has been integrated along the depth, up to a maximum value of 1 m

# Appendix B
# The Absorption Coefficient in Water and the Directionality of Cosmic Rays

In his third article of 1926 [Millikan1926c] Millikan evaluates the absorption coefficient of cosmic rays in water, able to reproduce the measured data, taking into account for the first time the assumption that they come from all directions (even if with equal intensity, a hypothesis that will be corrected later). Indicating with $I_0$ the intensity of this radiation outside the water, the intensity $I$ measured at a depth H will have a contribution $dI$ given by

$$dI = 2\pi I_0 \sin\theta \, d\theta e^{-\mu H \sec\theta}$$

and the overall intensity will be given by the following integral:

$$I = 2\pi I_0 \int_0^{\pi/2} \sin\theta e^{-\mu H \sec\vartheta} d\vartheta$$

If we denote $x = \sec\theta$, the previous integral can be written in the form

$$I = 2\pi I_0 \int_1^{\infty} \frac{1}{x^2} e^{-\mu H x} dx$$

Millikan uses a table of integrals of this type, published by Gold, to evaluate whether a single absorption coefficient $\mu$ obtained at the top of the curve is capable of reproducing the entire trend of the data, but realizes that no single coefficient is able to provide a result that reproduces the overall trend. Rather, the data indicate that this coefficient changes with depth, showing that radiations capable of reaching greater depth are more penetrating. Previous observations, according to Millikan, had too large uncertainties to point out deviations from a simple exponential law.

The previous integral can also be solved today using simple numerical methods, once the value of the absorption coefficient has been selected.
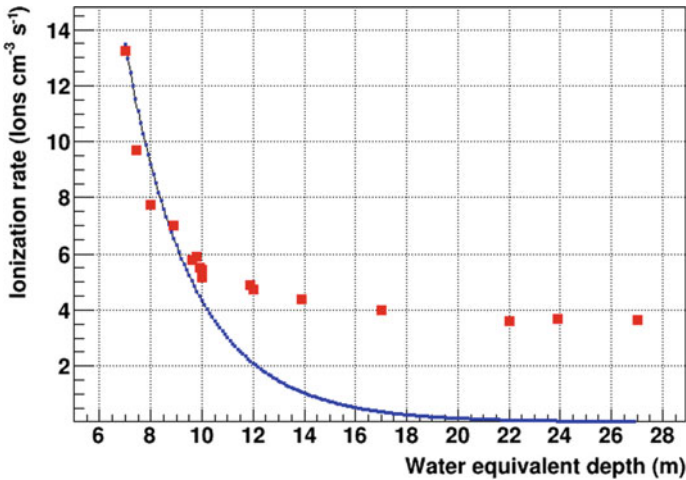
**Fig. B.1** Comparison between the experimental data obtained by Millikan [Millikan1926c] with one of the electroscopes used under the waters of lakes Muir and Arrowheads and the absorption curve calculated taking into account the (uniform) directionality of cosmic rays. The experimental values are reported as a function of the thickness of equivalent water, assuming the thickness of the atmosphere is 7 m. The absorption coefficient used is 0.003 cm$^{-1}$, which reproduces the first part of the curve

Figure B.1 shows such a calculation made with the previous equation (blue line), which takes into account the direction of the cosmic rays and therefore the different amount of water crossed, depending on the orientation. The curve was obtained by a numerical calculation of the integral in the previous equation, assuming an absorption coefficient equal to 0.003 cm$^{-1}$, which reproduces well the experimental values obtained by Millikan under the surface of the water (red symbols in the plot) to small depths. The curve was normalized to the highest value in the dataset. As can be seen from the comparison, the same curve does not reproduce the absorption of cosmic rays at greater depths, suggesting that the absorption coefficient is greater for radiations that have already passed through a certain thickness of water without being absorbed

Even in this case the reader is invited to implement his/her own numerical method to solve the integrals required in this calculation.

# Appendix C
# Geographic and Geomagnetic Latitude

Usually, the position of a place on Earth can be defined by its geographic coordinates (latitude and longitude). Latitude, as it is known, is the coordinate that expresses how much the position of the considered point is North (N) or South (S) of the equator, and therefore is measured from an angle that can take values between 0 and 90° N for the Northern hemisphere and between 0 and 90° S for the Southern hemisphere. The geographical longitude instead expresses the East (E) or West (W) coordinate with respect to the reference meridian, the one passing through Greenwich. The longitude value will therefore assume values between 0 and 180° E or between 0 and 180° W. In this context, the geographic North Pole and the geographic South Pole represent the imaginary points, of the northern and southern hemisphere respectively, in which the Earth's rotation axis intersects the surface. As a first approximation, it was believed, until the 19th century, that the position of the geographic poles was immutable. However, around the end of the 1800s, accurate astronomical measurements (by the American astronomer Chandler) made it possible to establish that the geographic North Pole moves, describing a small circumference, around an "average" position, with a period 435 days. This is due to the non-perfectly spherical shape of the Earth and the distribution of its mass. The effect, however, is small enough, of the order of ten meters, to have significant repercussions in determining the geographical position.

Another aspect, much more relevant, is the fact that the behaviour of the Earth as a magnet is characterized by magnetic poles that do not coincide with the geographical ones. As is well known, it was around 1600, with Gilbert, that the idea emerged that the Earth was itself a huge magnet, with its magnetic poles and its lines of force (Fig. C.1).

The North magnetic pole is the point where the Earth's magnetic field points exactly downward. Assuming that the Earth's magnetic field can be described in simplified form as that of an ideal magnet, we can define a further point, called the geomagnetic north pole, which represents the pole of this simplified dipole model of the Earth's complex magnetic field. The position of the North magnetic pole and the North geomagnetic pole are shown, as an example, as of 2017, with respect to
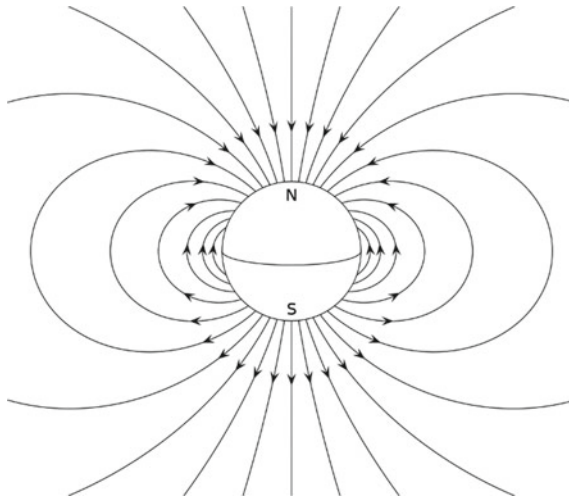
**Fig. C.1** Schematic of the Earth as a huge magnet, with the North and South magnetic poles and the field lines of force
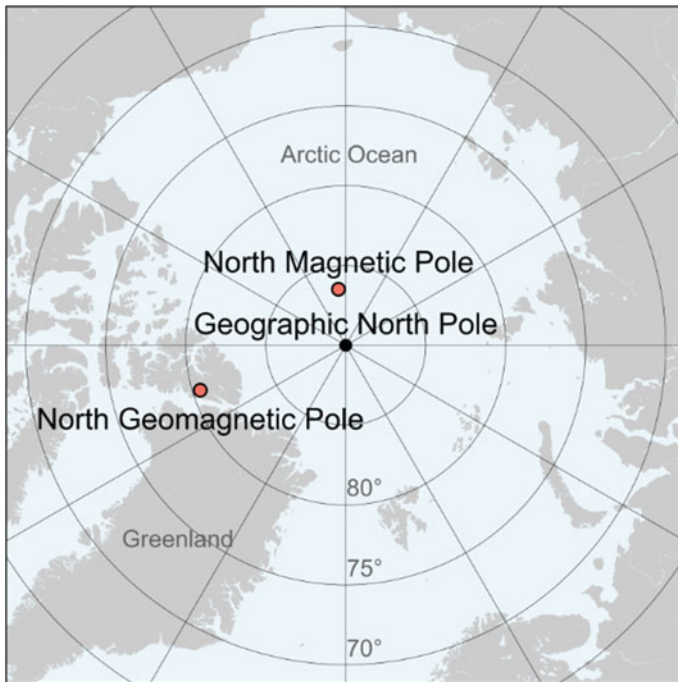


**Fig. C.2** Positions of the magnetic pole and the north geomagnetic pole in 2017. *Source* World Data Center for Geomagnetism, Kyoto [WDC]

the geographic North pole position, in Fig. C.2. As can be seen, these locations are very far from the geographic North Pole.

The position of the North magnetic pole shifts over time, even reaching geographic positions very far from the geographic North pole. For example, around 2001 its position was located at about 81° N 110° W, while over the course of 20 years, in 2021, it progressively moved around 86° N 157° W, with a rate of about 55 km per year. Fig. C.3 shows the "virtual path" of the position of the magnetic North pole over time, and, in more detail, in the last decades.

Moreover, it should be remembered that during the Earth's existence, the polarity of the Earth's magnetic field has reversed several times, on average every 450,000 years for the last 83 million years. The entire process of inversion of the magnetic field is a phenomenon that seems to have occurred over a period of time between 2000 and 12,000 years [Glatzmaier2015].

Finally, the magnetic North Pole and the magnetic South Pole are not exactly opposite, since the Earth's magnetic field is not exactly symmetrical. This means that the line passing through the two magnetic poles, North and South, does not cross the Earth through its centre. In recent decades, numerous highly detailed measurements of the Earth's magnetic field and its variations over time have been made.

On the basis of what has been outlined, one can then imagine a system of geomagnetic coordinates, similar to that of geographic coordinates, in which the poles are represented by the geomagnetic poles, and latitude and longitude are replaced by geomagnetic latitude and longitude. A map in geomagnetic coordinates, evaluated in 2020, is shown in Fig. C.4 [NOAA]. The reader may follow the evolution of these displacement in the next years.
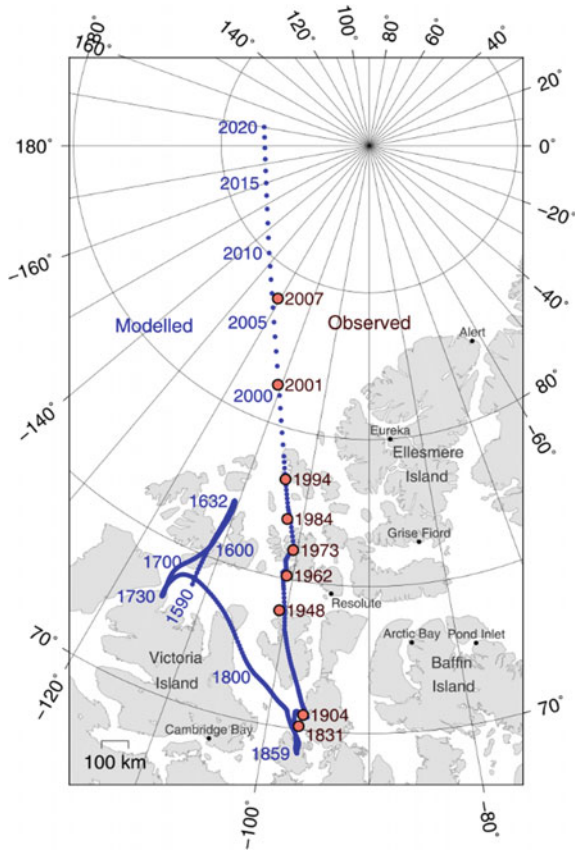
**Fig. C.3** North magnetic pole shift from 1600 onwards, particularly in recent decades, where more frequent and accurate measurements have been obtained. *Source* Wikimedia Commons. The observed positions of the poles are extracted from Newitt et al., *Location of the North Magnetic Pole in April 2007*, Earth Planets Space **61** (2009) 703. Model predictions are extracted from the National Geophysical Data Center. The geomagnetic pole path was created using GMT, CC BY 4.0, https://commons.wikimedia.org/w/index.php?curid=46888403
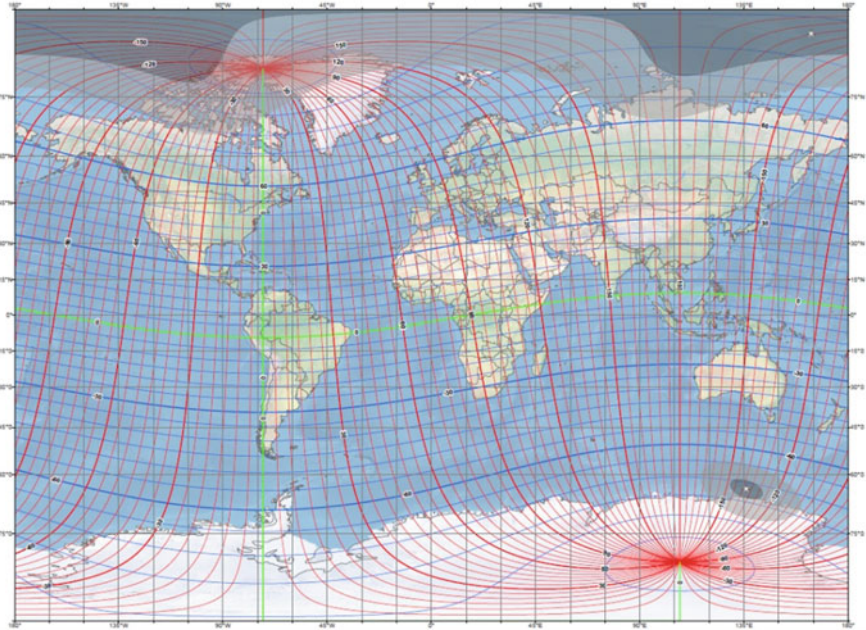
**Fig. C.4** Map in geomagnetic coordinates, showing the position of the geomagnetic poles in 2020 and the coordinate system with geomagnetic latitude (in blue) and longitude (in red). The lines corresponding to the geomagnetic equator and the geomagnetic meridian of reference are represented in green. *Source* National Center for Environmental Information (National Oceanic and Atmospheric Administration, NOAA) [NOAA]

# Appendix D
# The Magnetic Rigidity of Particles

A magnetic field exerts on a charged particle with a charge q, in motion, a force, perpendicular to the direction of its velocity **v** and of the magnetic field **B** (assumed to be uniform within a certain region), expressed by the Lorentz force, by means of the vector product:

$$\mathbf{F} = q\mathbf{v} \times \mathbf{B}$$

If the direction of the velocity is perpendicular to that of the magnetic field, the action of the force produces a change in the direction of the velocity without altering its modulus, resulting in a circular trajectory of radius R, which can be evaluated from the relationship

$$qvB = m\,v^2/R$$

The radius will then be (Fig. D.1)

$$R = m\,v/qB$$

While the previous relationship holds under the approximation of small speeds with respect to the speed of light, a similar relationship, correct from a relativistic point of view, is the one that links the radius of the trajectory to the relativistic momentum p:

$$R = p/q\,B$$
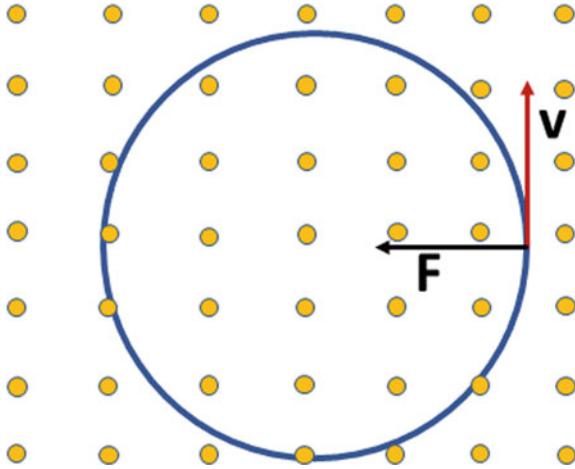
**Fig. D.1** A charged particle moving in a uniform magnetic field, with a direction perpendicular to its speed (represented by the yellow points in the plane of the figure), is subject to the Lorentz force, following a circular trajectory
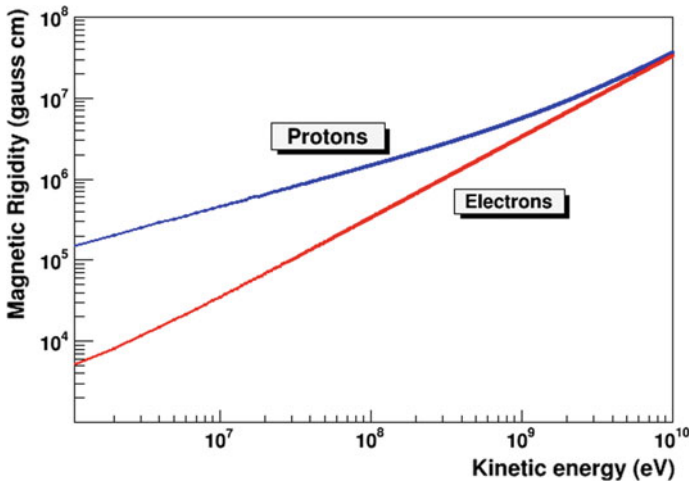


**Fig. D.2** Magnetic rigidity of protons and electrons as a function of their kinetic energy, from about 1 MeV to 10 GeV

The magnetic rigidity of a particle is then given by the product B R between the intensity of the magnetic field and the radius of curvature of its trajectory:

$$B R = p/q$$

where p is the particle momentum.

Considering the relationship between momentum and total energy, $E^2 = p^2c^2 + (mc^2)^2$, we can evaluate the magnetic rigidity of a particle as a function of its kinetic energy $K = E - mc^2$, for specific categories of particles.

Figure D.2 shows as an example the magnetic rigidity curve, expressed in (gauss cm), for electrons and protons of various energies, from about 1 MeV to 10 GeV.

For a given magnetic field, the p/q ratio is a measure of the angular deflection that particle will be subject to as it moves through that magnetic field. The greater the momentum of the particle, the less it will be curved.

If SI units are used, the product (BR) can be written in [Tesla × m] and the following relation holds

$$(BR) \, [Tesla \times m] = pc \, (MeV)/300$$

For example, a 6 GeV electron will have a value (BR) = 6000/300 = 20 [Tesla × m], and moving through a 2 T field, it will follow a circular path with radius R = 10 m.

The concept of magnetic rigidity is often used in evaluating the deflection of charged particles using suitable magnets in the context of particle accelerators, but it can also be used to understand the confinement properties of a charged particle of the cosmic radiation moving in the existing magnetic field in a large region of space, such as the interplanetary region of the Solar System, or the region corresponding to the size of the Milky Way. As an example, the magnetic field existing within the Solar System has an average value of about $6 \times 10^{-9}$ T $= 6 \times 10^{-5}$ gauss $= 60 \, \mu$G. On the other hand, typical values of the galactic magnetic field are of the order of a few $\mu$G in the regions around the Sun, to increase up to a few tens of $\mu$G in the innermost regions of the Milky Way.

To make a numerical estimate, we could consider protons of 3 GeV, which move in the interplanetary magnetic field: in this case (BR) = 10, therefore R = 1.67 × $10^9$ m, to be compared with the Sun-Earth distance equal to $1.5 \times 10^{11}$ m. Protons of much greater energy could reach values of magnetic rigidity such that they cannot be confined within the dimensions of the Solar System.

To perform additional calculations, one may consider different particles, such as muons or pions, and check the validity of non-relativistic approximation at low energy.

# Appendix E
# The Energy Loss of Charged Particles and the Estimate of the Muon Mass

The average energy loss by ionization of a charged particle can be described by the Bethe and Bloch relation [Leo1987, Knoll2000, Leroy2004, Grupen2008], which allows to evaluate the specific energy loss, i.e., the energy loss per unit of path in a material, based on the charge, mass and energy of the incident particle, together with the properties of the material (atomic number, atomic weight and density), as discussed in the chapter dedicated to the interaction of charged particles with matter. The loss of energy is therefore different, in the same material, for the different particles. As an example, the values of the specific energy loss (Stopping Power), evaluated in (MeV cm$^2$/g) in the case of protons interacting with an absorber made from Carbon, are shown in Fig. E.1 as a function of the proton momentum.
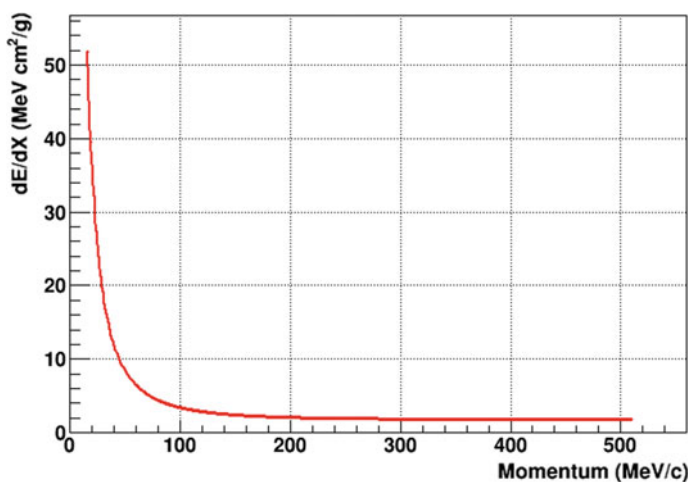


**Fig. E.1** Specific energy loss of protons on a $^{12}$C absorber, evaluated by the Bethe and Bloch relationship and expressed in MeV cm$^2$/g, as a function of the momentum of protons
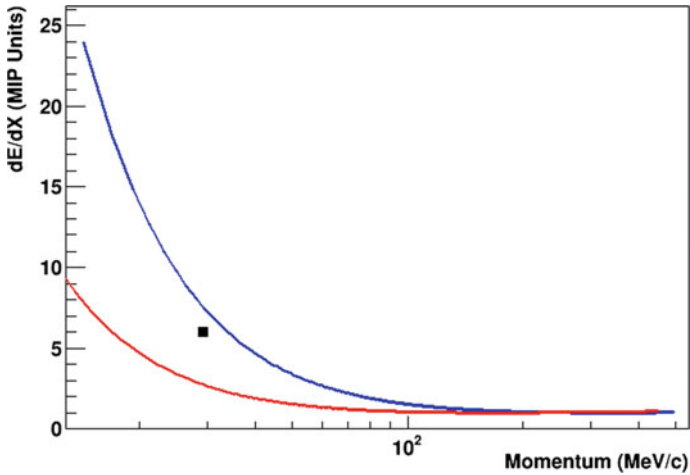
**Fig. E.2** Specific muon energy loss, normalized to the value obtained at the minimum ionization (MIP unit), as a function of the muon momentum. The two curves refer to two different hypotheses about the mass of muons: 100 electronic masses (lower curve, in red) and 200 electronic masses (upper curve, in blue). The black symbol shows the experimentally obtained value by Street and Stevenson [Street1937]

It can be seen how the specific energy loss decreases as the incident energy of the protons increases. At very high energies a minimum in the ionization loss is reached, beyond which this quantity starts to increase slowly, due to relativistic effects (*Relativistic Rise*). Particles with an energy close to that for which there is minimal ionization are often called *Minimum Ionizing Particles* (MIP). This dependence of the ionization density on their kinetic energy (or momentum) allows in principle to "identify" the particles, if one is able to measure both the momentum and the specific energy loss at the same time. However, this technique can only be used for low values of the incident energy, since at higher energies the curves corresponding to different particles tend to approach each other making their separation difficult or impossible.

Particles having the same charge, but different masses, therefore ionize in a different way. If we therefore consider muons, their ionization power depends on the mass they possess. A measurement of the ionization density for muons having a given momentum would allow in principle to determine their mass. The initial measurements of Neddermayer and Anderson could not separate the different curves corresponding to different hypotheses on the still unknown mass of the muons, as the detected muons had a very high momentum. Subsequent measurements, made by Street and Stevenson, optimized for low-energy muons, were able to separate these curves.

Figure E.2 shows the trend of the specific energy loss, normalized to the minimum ionization value, in the hypothesis of muons having a mass equal to 100 times the mass of the electron (lower curve, in red) or 200 times the mass of the electron (upper

curve, in blue). The experimentally obtained value (black symbol) is closer to the curve corresponding to 200 electronic masses.

Implementing energy loss calculations, as described by the Bethe-Bloch equation (Chap. 13), may result in a variety of activities, including the calculation of the energy loss on different materials and compounds, the evaluation of the particle range and the different behaviour of the energy loss at small and high incoming energy.

# Appendix F
# List of High-Altitude Observation Stations in the Mid-1950s

The following table shows a (non-exhaustive) list of the main observation stations built at high altitudes, totally or partially used for studies concerning cosmic radiation, as shown in a Report prepared in the mid-1950s [Korff1952, Korff1982].

| Station name | Location | Altitude | Coordinates (Lat/Long) |
| --- | --- | --- | --- |
| Observatorio del Infiernillo | Santiago, Chile | 4320 m | 33°.10′ S/70°17′ W |
| Observation Station | Mendoza, Argentina | 4000 m | 33° N/69° W |
| Montezuma Solar Station | Calama, Chile | 9000 ft | 22°40′ S/68° 56′ W |
| Laboratorio Fisica Cosmica | Chacaltaya, La Paz, Bolivia | 5200 m | 16° 19′ S/68° 10′ W |
| Instituto geofisico | Huancayo, Peru | 3350 m | 12°02′ S/75° 20′ W |
| Morococha | Junin, Peru | 4540 m | 11° 37′ S/76°08′ W |
| Timboroa Station | Timboroa, Kenya | 2880 m | 0° 0′/35° 31′ E |
| Kodaikanal Observatory | Kodaikanal, India | 2343 m | 10° 13′ N/77° 29′ E |
| Teoloyucan | Messico | 2300 m | 19° S/99° W |
| Mauna Loa Geophysical Observatory | Hawai | 13,453 ft | 19° 26′ N/155° 36′ W |
| Kole Kole Station | Hawai | 3067 m | 20.8° N/156.3° W |
| Sacramento Peak | New Mexico, USA | 9200 ft | 32°47′ N/105° 49′ W |
| Gulmarg Research Observatory | Gulgmarg, India | 9000 ft | 34° 03′ N/74° 24′ E |
| Capillo Peak Observatory | Albuquerque, New Mexico | 9200 ft | 34° 41′ N/106° 24′ W |
| Mount Fuji Weather Station | Shizuoka, Japan | 3772 m | 35° 21′ N/138°44′ E |
| Cactus Peak | Inyokern, California, USA | 5415 ft | 36° 04′ N/117° 48′ W |
| Mt. Norikura Cosmic ray Station | Neugawa-Mura, Japan | 2840 m | 36° 06′ N/137° 33′ W |

(continued)

(continued)

| Station name | Location | Altitude | Coordinates (Lat/Long) |
|---|---|---|---|
| Lake Sabrina | Bishop, USA | 2765 ft | 37.5° N/118° W |
| White Mountain Research Station | Big Pine, USA | 10,640 ft | 37° 30′ N/118° 10′ W |
| Tioga Pass Station | Yosemite, USA | 9941 ft | 37° 55′ N/119° 15′ W |
| High Altitude Harvard Observatory | Climax, USA | 11,190 ft | 39° 23′ N/106° 12′ W |
| Mt. Evans Laboratory | USA | 14,150 ft | 30° 35′ N/105° 38′ W |
| Echo Lake Laboratory | USA | 10,700 ft | 39° 39′ N/105° 35′ W |
| Observatoire du Pic du Midi | Bagneres de Bigorre, France | 2857 m | 42° 56′ N/0° 8′ E |
| Laboratoire de l'Aiguille du Midi | Chamonix, France | 3600 m | 43° N/7° E |
| Puy de Dome | Clermont Ferrand, France | 1450 m | 45° 47′ N/2° 58′ E |
| Observatoire Vallot | Chamonix, France | 4353 m | 45° 50′ N/0° 27′ E |
| Laboratorio Testa Grigia | Val D'Aosta, Italy | 3480 m | 45° 56′ N/7° 42′ E |
| Jungfraujoch High Altitude Station | Jungfraujoch, Switzerland | 3457 m | 46° 22′ N/7° 59′ E |
| Laboratorio della Marmolada | Canazei, Italy | 2030 m | 46° 28′ N/11° 53′ E |
| Astrophysikalische Observatorium | Switzerland | 2050 m | 46° 40′ N/0° 38′ E |
| Sonnblick Observatorium | Salzburg, Austria | 3106 m | 47° 03′ N/12° 57′ E |
| Observatorium Zugspitze | Germany | 2960 m | 47° 25′ N/10° 59′ E |
| Hafelekar | Sud Tirol, Austria | 2297 m | 47° 19′ N/11° 23′ E |
| Mt.Wrangell Observatory | Alaska | 14,000 ft | 62° N/144° W |
| Estacion de altura Peron | Mendoza, Argentina | 3852 m | 34° 10′ S/69° 40′ W |
| Observatorio Eva Peron | Mendoza, Argentina | 3100 m | 32° 49′ S/69° 10′ W |

# Appendix G
# An Estimate of the Particle Density in an Extensive Air Shower

The average density of particles present in an extensive air shower (number of particles per square meter) depends on the overall energy of the shower and varies over the region of the shower explored (whether it is close to the axis of the shower or at a large distance from it).

A numerical estimate of the average density of particles can be obtained by making use of a number of counters, of area S, placed at a certain distance, for example at the vertices of a rectangle (Fig. G.1, left) or in a triangular configuration (Fig. G.1, right), as reported in one of the papers by Cocconi and collaborators [Cocconi1944a].

The reasoning is based on the calculation of probabilities. If $p(S, \Delta)$ represents the probability that an area counter S will not be hit by a shower having an average particle density of $\Delta$, the probability that it will be hit will be $(1 - p)$. An increase dS of this surface leads to a decrease in the probability p, equal to $dp = - pS\Delta$. From this we then obtain $p = e^{-S\Delta}$.
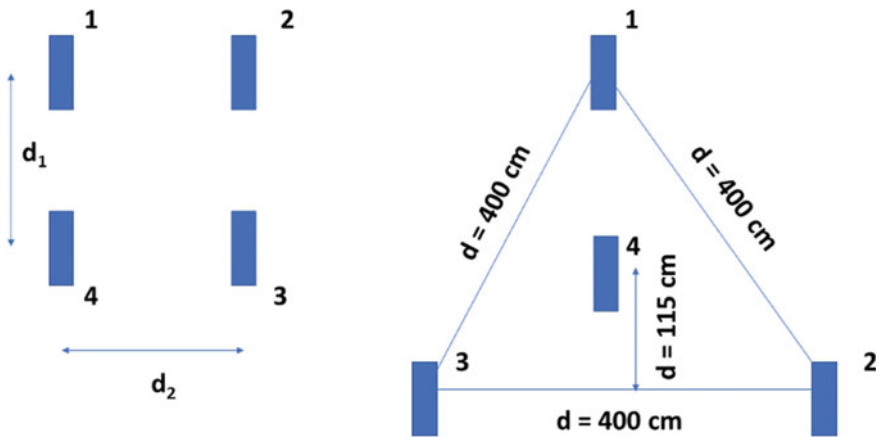


**Fig. G.1** Geometric configurations used by Cocconi and collaborators [Cocconi1944a] for the experimental estimation of the average density of particles in an extensive air shower

The probability that a single counter is hit will therefore be $(1 - p) = 1 - e^{-S\Delta}$, while the probability that n counters are hit simultaneously will be given by

$$(1 - p)^n = [1 - e^{-S\Delta}]^n$$

If we measure the coincidences $C_n$ and $C_{n-1}$ between n counters and $(n - 1)$ counters, the ratio between these quantities will be equal to the probability ratio, i.e.

$$C_n/C_{n-1} = [1 - e^{-S\Delta}]^n/[1 - e^{-S\Delta}]^{n-1} = 1 - e^{-S\Delta}$$

hence

$$e^{-S\Delta} = 1 - C_n/C_{n-1}$$

and therefore, the average density $\Delta$ can be obtained:

$$\Delta = -(1/S)\ln(1 - C_n/C_{n-1})$$

# Appendix H
# The Relationship Between Altitude and Atmospheric Depth

The Earth's atmosphere plays an important role in understanding the phenomena related to the study of the cosmic radiation. As a matter of fact, all possible interactions of the primary particles take place in it, as well as the generation, propagation and decay of the secondary ones.

The Earth's atmosphere is a complex system, the conditions of which vary over time. However, we can outline some of the basic properties of this system. We can consider the atmosphere as a large volume of gas, which at sea level has a density of about $10^{19}$ particles per $cm^3$. We know that the density, and therefore the average number of particles per unit of volume, decreases with increasing altitude. The composition of the atmosphere includes several gases, among which the most abundant are Nitrogen ($N_2$), with a percentage of 78.1%, Oxygen ($O_2$) for 20.9% and Ar, with a percentage of 0.9%. Small amounts of other substances, such as $CO_2$, make up the remaining 0.1%.

The atmospheric depth crossed is measured starting from the zone in which the density is negligible, and gradually increases towards the sea level, corresponding to a depth of about 1000 $g/cm^2$. It therefore represents the thickness of the atmosphere, expressed in surface density units.

In a simplified schematization, we can assume an isothermal static model of the atmosphere, according to which the density varies almost exponentially with altitude, according to a trend of the type

$$n(h) = n(h_0)e^{-h/h_s}$$

where n(h) and $n(h_0)$ represent the densities at heights h and $h_0$ respectively, and $h_S$ is a parameter that for a perfect exponential trend should be constant, expressed in cm from

$$h_s = KT/Mg$$
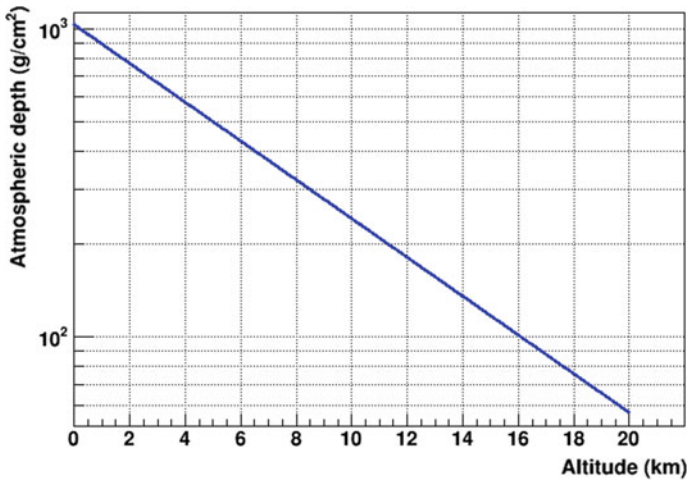
**Fig. H.1** Atmospheric depth crossed (in g/cm$^2$) as a function of the altitude with respect to sea level (in km), according to a simplified atmosphere model

where K is the Boltzmann constant, T the absolute temperature (in Kelvin), M the molecular weight (in g/mol) and g the Earth's acceleration of gravity (in cm$^{-1}$ s$^{-2}$).

A quantitative representation of this ideal trend is shown in Fig. H.1.

In a model of a real atmosphere, $h_S$ varies slightly with the atmospheric depth, from about $7 \times 10^5$ cm at the atmospheric depth of 10 g/cm$^2$ (corresponding to an altitude of about 30 km) to a value of about $8.2 \times 10^5$ cm at an atmospheric depth of 900 g/cm$^2$, corresponding to about 1500 m of altitude. Quantitative graphs of the relationship between altitude and atmospheric depth in the case of a real model of the atmosphere are shown in [Grieder2001].

# Appendix I
# Gaisser-Hillas Parameterization of the Longitudinal Profile of a Shower

The longitudinal profile of an extensive air shower (density of particles at various atmospheric depths X) can be expressed according to different parameterizations. One of the widely used functions was introduced by Gaisser and Hillas [Gaisser1977]:

$$N(X) = N_{max}\left(\frac{X}{X_{max}}\right)^{\frac{X_{max}}{\lambda}} e^{(X_{max}-X)/\lambda}$$

where X represents the atmospheric depth (expressed in g/cm$^2$), $N_{max}$ is the number of particles corresponding to the maximum $X_{max}$, while $\lambda$ represents a characteristic depth (usually assumed to be 70 g/cm$^2$). Figure I.1 shows this function, for a value of $\lambda$ assumed exactly equal to 70 g/cm$^2$, and for two different values of $X_{max}$ (200 and 400 g/cm$^2$).

The next figure shows the effect of the $\lambda$ parameter on the distribution, evaluated with the same value of $X_{max}$ (400 g/cm$^2$) and for two different values of $\lambda$ (50 and 90 g/cm$^2$).

The effect of these two parameters therefore determines the position of the maximum in the profile of N(X) and the width of this distribution.

In some cases, it is possible to introduce an additional parameter $X_0$, to take into account the fact that the first interaction does not occur at X = 0 [Pryke2001]. With this modification, the previous equation can be written as:

$$N(X) = N_{max}\left(\frac{X-X_0}{X_{max}-X_0}\right)^{\frac{X_{max}-X_0}{\lambda}} e^{(X_{max}-X)/\lambda}$$

The reader may use the previous equations to perform additional calculations as a function of the two parameters ($X_{max}$ and $\lambda$).
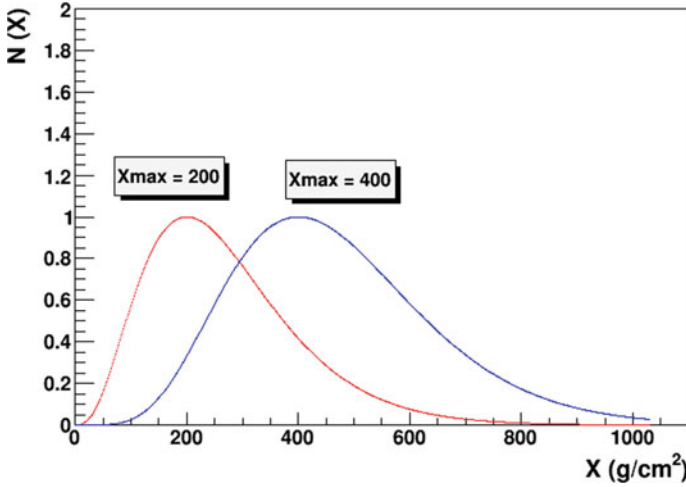
**Fig. I.1** The Gaisser-Hillas distribution that parameterizes the behaviour of the longitudinal development of a shower along the atmosphere, evaluated for a value of $\lambda$ equal to 70 g/cm$^2$ and for two different values of the parameter $X_{max}$ (200 and 400 g/cm$^2$)
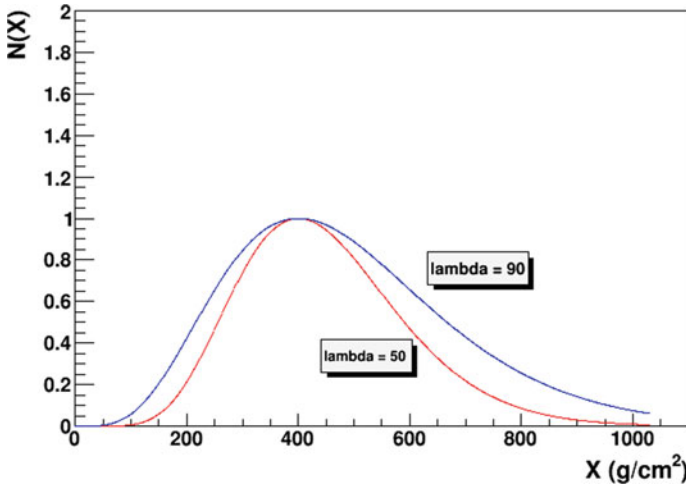


**Fig. I.2** Gaisser-Hillas distribution which parameterizes the behaviour of the longitudinal development of a shower along the atmosphere, evaluated for a value of $X_{max}$ equal to 400 g/cm$^2$ and for two different values of $\lambda$ (50 and 90 g/cm$^2$)

# Appendix J
# The Thickness of Air Crossed by a Particle in the Atmosphere

When a particle travels in the atmosphere, the effective thickness crossed depends on the inclination of the track with respect to the vertical. For particles that move vertically (perpendicular to the ground), the thickness crossed, in terms of surface density (g/cm$^2$) is given by the relationship between altitude and thickness, as described in Appendix H. For inclined tracks, the thickness actually crossed is larger. If we consider the approximation of a 'flat" Earth, which is a good approximation for not too large inclination angles (typically up to about 60 degrees), the actual thickness (slant depth) is given by

$$X_s = X \sec \vartheta = \frac{X}{\cos \vartheta}$$

When the angle of inclination with respect to the vertical becomes very large, the curvature of the Earth's surface cannot be ignored, and the previous approximation
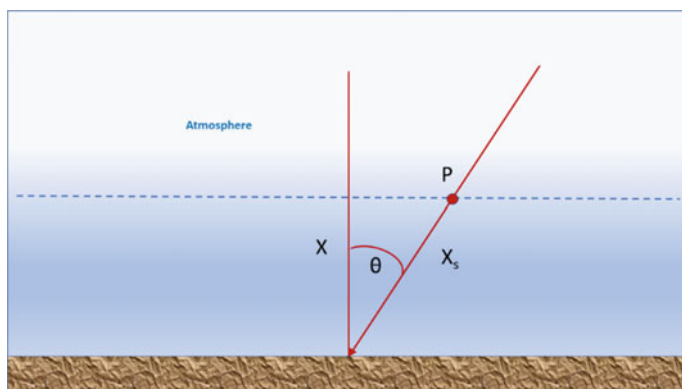


**Fig. J.1** Effective thickness traversed by a particle moving from a height X, with an inclination angle θ with respect to the vertical, in the approximation of a 'flat" Earth, valid for not too high inclination angles
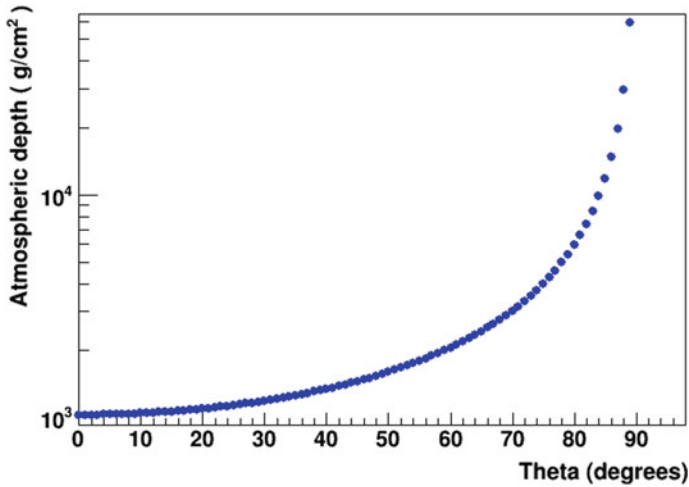
**Fig. J.2** Effective thickness traversed by a particle moving from a height X, with an angle of inclination θ with respect to the vertical, in the approximation of a 'curved" Earth, based on a parameterization of the Chapman function [Swider1967]

is no longer valid. This happens for example for the detection of almost horizontal muons, or for detectors placed at very high altitudes. Taking into account the entire thickness of the atmosphere crossed by particles moving horizontally, this is about 40 times larger than that crossed vertically.

In this case, a geometrical analysis of the situation leads to an expression of the true crossed thickness which can be expressed through the Chapman functions, or through approximations to these functions [Swider1967].

Figure J.2 shows the atmospheric depth crossed as a function of the angle of inclination with respect to the vertical. While for a vertically moving particle, the atmospheric depth is just over $1000$ g/cm$^2$, it becomes about 10 times greater for angles close to $85°$

The interested reader may further investigate the use of the Chapman functions or their approximate behaviour through a series of numerical calculations.

# Appendix K
# Evaluation of the Shower Direction from the Relative Timing of Several Detectors

With three detectors placed horizontally and not aligned, it is possible, by measuring the arrival time of the shower particles in each of the detectors, to determine with a certain approximation the axis of the shower, and therefore the incoming direction of the primary particle, using a technique of triangulation. With reference to Fig. K.1, we can imagine having 3 detectors (0, 1 and 2), placed horizontally on a plane, in the positions $(x_0, y_0)$, $(x_1, y_1)$, $(x_2, y_2)$, each of which detects one of the particles of the shower, at the time $T_0$, $T_1$, $T_2$.

Assuming as a first approximation that the different detected particles travel at the speed of light c, and that they move parallel, geometric considerations allow us
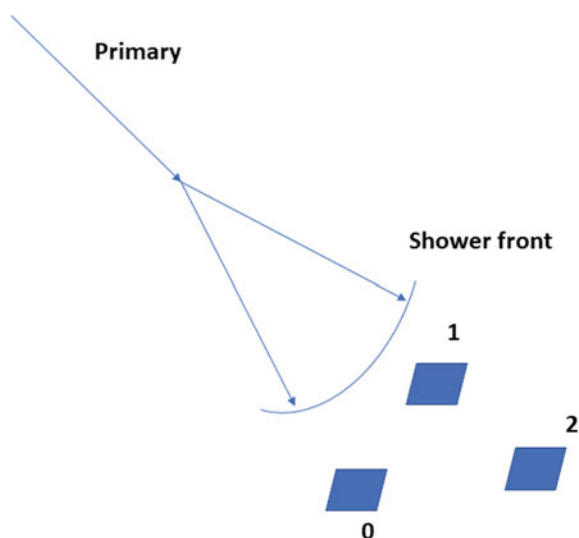


**Fig. K.1** Use of 3 detectors arranged on a horizontal plane (not aligned) to measure the differences in the arrival times of the particles in each of them and determine, based on geometric triangulation considerations, the direction of the shower axis

to determine the direction $(\theta, \varphi)$ of the axis in polar coordinates, using the following set of equations:

$$\cos \vartheta \sin \varphi = \frac{d_2 - d_1 \frac{y_2 - y_0}{y_1 - y_0}}{(x_2 - x_0) - (x_1 - x_0)\frac{y_2 - y_0}{y_1 - y_0}}$$

$$\cos \vartheta \cos \varphi = \frac{d_2 - d_1 \frac{x_2 - x_0}{x_1 - x_0}}{(y_2 - y_0) - (y_1 - y_0)\frac{x_2 - x_0}{x_1 - x_0}}$$

where $d_1 = c\,(T_1 - T_0)$, $d_2 = c(T_2 - T_0)$ and the two time-differences $(T_1 - T_0)$, $(T_2 - T_0)$ are measured experimentally.

Based on the relative distances and the time resolution with which it is possible to measure the differences in arrival times, a larger or smaller precision will be obtained in the reconstruction of the angles $\theta$ and $\varphi$. Use of this technique has been also exploited in educational experiments in cosmic ray physics [Aiola2012, Riggi2014].

In an array of several detectors, the measurement of the time differences between all the possible pairs of detectors gives rise to an oversized set of equations, which can be solved with minimization techniques to determine the optimal solution. For example, referring to the work of Clark et al. [Clark1961], which used such a procedure for managing the data obtained with an array of detectors, the direction of the shower, defined by the director cosines $l, m$, was evaluated by minimizing the quantity

$$\chi 2 = \frac{1}{(N-3)} \sum_{i=1}^{i=N} (ct_i + lx_i + my_i - ct_0)^2$$

where the positions of the N detectors involved in the event to be reconstructed are named $(x_i, y_i)$, $i = 1, 2, …, N$, the $t_i$ are the arrival times at the single detectors, and $t_0$ is the average time.

To further understand the limit and potential of this method, the reader may investigate the role of the time resolution on the overall precision of the method.

# Appendix L

# Parameterizations of the Muon Spectrum at Sea Level

The energy (or momentum) spectrum of secondary muons at sea level has been measured in a variety of experiments in the past. In many circumstances it is useful to have a parameterization of the dependence of the flux of secondary muons on the energy and on the angle of inclination, in order to use simple relationships that summarize different sets of measured data, and which can be used in further calculations, for example to model the expected cosmic ray flux in a simulation. One of the classic parametrizations used is that due to Gaisser [Gaisser1990], already mentioned in the text, which provides a dependency of the type:

$$\frac{dN}{dEd\Omega} = 0.14 E^{-2.7} \left( \frac{1}{1 + \frac{1.1 E \cos\theta}{115\,\text{GeV}}} - \frac{0.054}{1 + \frac{1.1 E \cos\theta}{850\,\text{GeV}}} \right) \text{cm}^{-2}\,\text{s}^{-1}\,\text{sr}^{-1}\,\text{GeV}^{-1}$$

where E and $\theta$ represent respectively the energy and the angle of inclination of the muons with respect to the vertical. An example of a spectrum obtained for vertical muons on the basis of this parameterization has already been reported in Chap. 10. Figure L.1 shows a comparison between the spectrum of vertical muons (on the left) and that of muons with an inclination of 70° (on the right).

The Gaisser parameterization is valid for sufficiently high energies and for not too large angles of inclination. Different parameterizations have been proposed in the following years, some of which generalize that of Gaisser, so as to make it applicable even in a range of smaller energies and at larger angles, where the effect of the Earth's curvature is not negligible. For example, one of these has been proposed by Guan et al. [Guan2015]. In this we use the angle $\theta^*$, linked to $\theta$ by the relation

$$\cos\theta^* = \sqrt{\frac{(\cos\theta)^2 + p_1^2 + p_2(\cos\theta)^{p_3} + p_4(\cos\theta)^{p_5}}{1 + p_1^2 + p_2 + p_4}}$$

where the coefficients $p_i$, determined by the best fit of the available experimental data, have the following values:
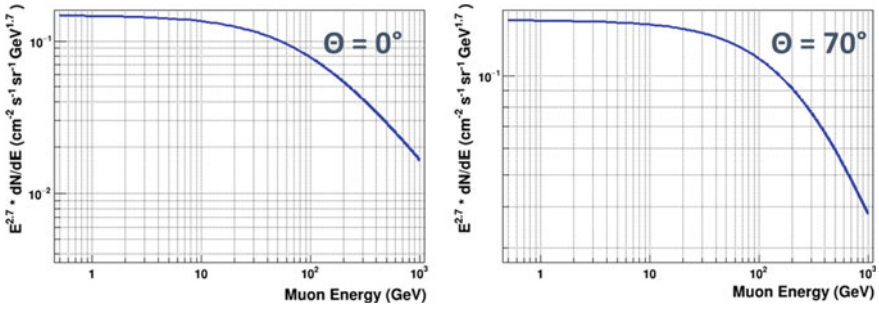
**Fig. L.1** Spectrum of vertical secondary muons (left) and inclined at 70° (right), multiplied by the factor $E^{2.7}$, based on the parameterization of Gaisser [Gaisser1990]
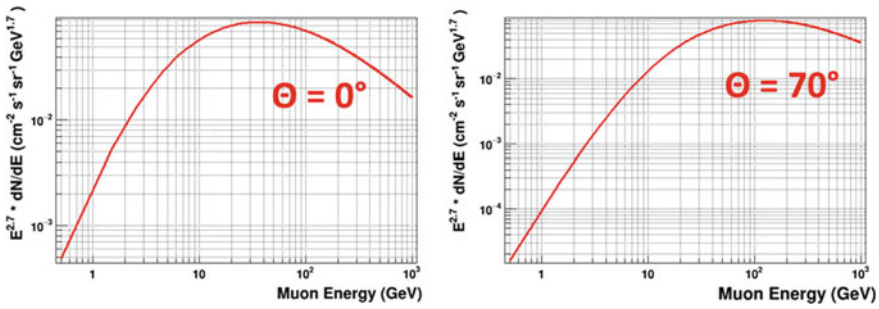


**Fig. L.2** Spectrum of vertical (left) and 70° inclined (right) secondary muons, multiplied by the factor $E^{2.7}$, based on the parameterization of Guan et al. [Guan2015]

| $p_1$ | $p_2$ | $p_3$ | $p_4$ | $p_5$ |
|---|---|---|---|---|
| 0.102573 | $-0.068287$ | 0.958633 | 0.0407253 | 0.817285 |

The Gaisser relation is then modified as follows:

$$\frac{dN}{dEd\Omega} = 0.14 \left[ E \left( 1 + \frac{3.64}{E(\cos\theta*)^{1.29}} \right) \right]^{-2.7}$$

$$\times \left( \frac{1}{1 + \frac{1.1E\cos\theta*}{115\text{GeV}}} - \frac{0.054}{1 + \frac{1.1E\cos\theta*}{850\text{GeV}}} \right) \text{cm}^{-2}\,\text{s}^{-1}\,\text{sr}^{-1}\,\text{GeV}^{-1}$$

If this parameterization is used, spectra similar to the previous ones are obtained for high muon energies, but with a very different trend for the low energy part, below some GeV, which reproduce the available experimental data. As an example, Figure L.2 shows the corresponding spectra calculated according to this parameterization, for the vertical muons (on the left) and for those inclined at 70° (on the right).
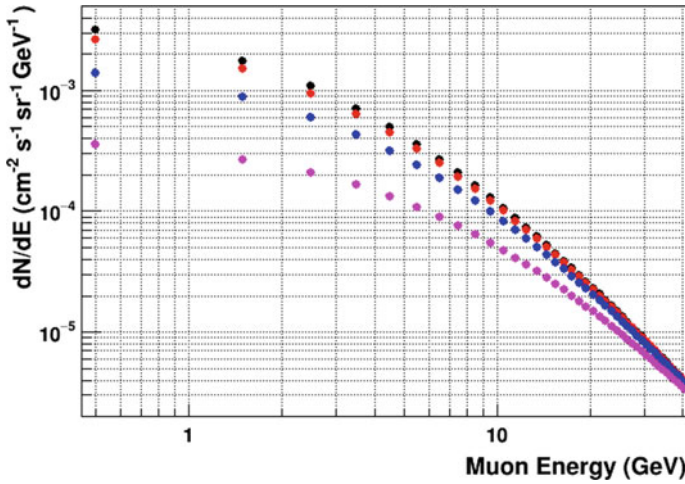
**Fig. L.3** Spectrum of secondary muons at angles of 0° (black symbols), 20° (red symbols), 40° (blue symbols) and 60° (purple symbols), based on the parameterization of Guan et al. [Guan2015]

Figure L.3 shows the dN/dE spectra (therefore without the multiplicative factor $E^{2.7}$) for different angles, from 0 to 60 degrees, again using the parameterization of Guan et al. [Guan2015]

Many other works, which report various theoretical calculations of the muon flux, their energy spectrum, charge ratio and dependence on orientation or geomagnetic latitude have been published after 1970. Among these, for example those discussed by [RamanaMurthy1972, Gaisser1974, Honda1995, Bugaev1998].

As an exercise to the reader, the comparison between different parameterizations of the muon spectrum may be further investigated, and approximate solution to the problem in specific momentum or angular ranges may be found.

# Appendix M
# The Flux of Underground Muons

The relationship between the muon flux and depth is often parameterized on the basis of semiempirical formulas, which take into account the available data, or a subset of these data obtained under certain conditions, and use a series of parameters, usually obtained from a fit of the experimental data. A frequently used relation has been proposed by Miyake [Miyake1963], which expresses the vertical intensity $I(X)$ as a function of the depth X as

$$I(X) = (X + a)^{-\alpha} \frac{K}{X + H} e^{-\beta X}$$

where the parameters a, K, H, $\alpha$ and $\beta$ are obtained from a fit of the experimental data and the depth X is expressed in m.w.e. (or hg/cm$^2$). Using the following set of parameters, the trend shown in Fig. M.1 (blue line) can be obtained.

| a | K | H | $\alpha$ | $\beta$ |
|---|---|---|---|---|
| 11 | 174 | 400 | 1.53 | $8 \times 10^{-4}$ |

In this relationship, the depth X (considered from the top of the atmosphere) is expressed in hg/cm$^2$ (or in m.w.e.), while the intensity is calculated in cm$^{-2}$ s$^{-1}$ sr$^{-1}$.

Alternatively, a slightly more elaborate formula, with a wider range of application ($10–10^4$ hg/cm$^2$) has been reported by Barbouti and Rastin [Barbouti1983]:

$$I(X) = K \frac{e^{-\beta X}}{(X + H)(X^{\alpha} + a)}$$

with the parameters shown in the following table:

| a | K | H | $\alpha$ | $\beta$ |
|---|---|---|---|---|
| 75 | 270.7 | 200 | 1.68 | $5.5 \times 10^{-4}$ |
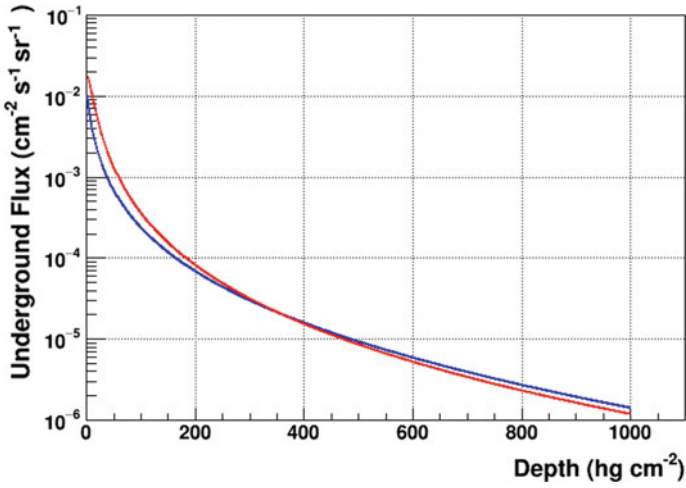
**Fig. M.1** Parameterizations of the vertical flux of underground muons as a function of depth, expressed in hg/cm$^2$. Blue line: parameterization due to Myake [Myake1963]; red line: parameterization due to Barbouti [Barbouti1983]

The resulting plot from this relationship is shown in the same figure by a red line.

The two parameterizations are quite similar especially in the intermediate region, while some differences can be observed for smaller depth values.

# Appendix N
# Detection of Bit-Flip Errors Originated by Cosmic Rays

The simplest technique to diagnose and possibly correct soft errors in a series of binary information, such as those that could be introduced by the passage of cosmic rays, by ionizing radiations, or simply by transmission disturbances in a line, is that of parity check. This technique was introduced as early as the 1950s to evaluate the correctness of a series of binary signals marked on a paper or magnetic tape. It basically involves adding a bit (parity bit) to the other bits present in a given sequence, making sure that the number of 0 s (or 1 s) present in the sequence is always even (or odd, depending on the convention adopted). These bit sequences could simply be those that make up a byte, or longer sequences.

In the case of a sequence of 8 bits (one byte), the most significant bit of the byte can be used as the parity bit and the other 7 bits to define one of the possible $2^7 = 128$ values (from 0 to 127), for example those used for the ASCII encoding of the various symbols (letters, digits 0–9, special characters). The parity bit P is set by the system based on the content of the other 7 bits and the convention adopted. In Fig. N.1, for
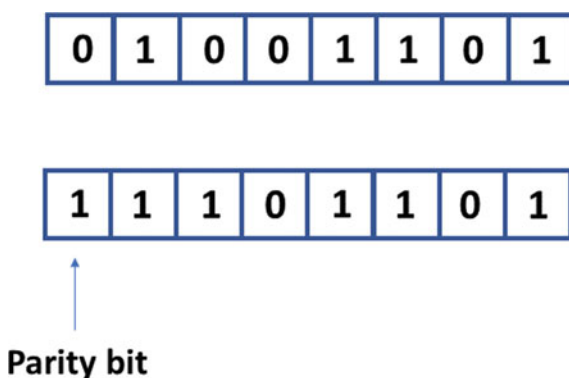


**Fig. N.1** In a 7-bit sequence, an additional bit (parity bit) can be added to make sure that the number of bits at 1 is always even or odd, depending on the chosen convention, and thus diagnose if one of the bits of the sequence has changed its initial state

example, assuming a convention according to which the number of bits 1 (including the parity bit) must be even, the 7-bit sequence "1001101" needs a parity bit set to 0 (so that the total number of bits 1 remains four) and therefore the total sequence of 8 bits would be "01001101". Similarly, the 7-bit sequence "1101101", in which the number of bits 1 is five (odd), requires a parity bit set to 1, in order to bring the total number of bits 1 to six (even). The complete sequence will therefore be "11101101".

The check upon arrival of a sequence of bits transmitted by a transmitting circuit, or present in a memory cell, is done by comparing the overall parity (number of bits 1) with that expected according to the assumed convention. If it is different, it can be diagnosed that a parity error has occurred, due to the fact that one of the bits in the sequence has changed state (from 1 to 0 or viceversa). It is important to note that diagnosing the error does not in itself lead to its correction, as we cannot know which of the different bits in the sequence has changed its state. The system, however, can be organized in such a way as to request a new sending of the same sequence, neglecting the data received previously. Another important remark is that the use of a parity bit can only diagnose errors in which only a single bit changes its state, while it cannot detect situations in which two bits both change state, which is generally much less probable, and which in certain cases can be further minimized with a suitable geometric arrangement of the cells corresponding to bits forming part of the same sequence.

# Notes to the Bibliography

There is nothing that can replace the reading and study of an author's original works. If this is particularly true for literary works, we may say that even for a scientific discipline a great help to understand the original ideas, the attempts to interpret the observed phenomenology and the overall path towards the current status of that discipline certainly derives from the knowledge of the texts in which those ideas and those attempts were originally described.

In the study of the cosmic radiation, there is a very peculiar atmosphere when reading the considerations about the first evidence of a cosmic radiation, the first attempts to interpret—often overcome by subsequent events—the perspectives of research, right from the written pages by the protagonists of this adventure. For the most part the results and theoretical considerations in the scientific tradition are communicated through short articles in specialized journals, through the proceedings of conferences dedicated to specific topics, through review articles that report the status of the knowledge on a given problem and summarize what it has been done in that field, more rarely—only when the status of knowledge in that area has reached a certain degree of maturity—even from textbooks.

Many of the authors who have made the history of cosmic ray physics have also ventured into the non-trivial challenge of communicating their personal involvement, the certainties and doubts they have reached, through works that are worth reading for many decades after being published. These works, of a general nature, dedicated to the history and evolution of cosmic ray physics in the first decades after their discovery, are complementary to the more recently published specialist textbooks on the subject. Without any completeness, we mention the following, from many of which the author has benefited enormously:

- Pierre Auger, *Rayon cosmiques*, University of Paris Press, Paris, 1941.
- T.E. Cranshaw, *Cosmic Rays*, Clarendon Press, 1963.
- Vitaly L. Ginzbug and S.I. Syrovatskii, *The origin of cosmic rays*, English ed. Pergamon Press Inc., New York, 1964.
- A. Michael Hillas, *Cosmic Rays*, Pergamon Press, Oxford, 1972.

- Lajos Janossy, *Cosmic Rays*, Clarendon Press, Oxford, 1950.
- Lajos Janossy, *Cosmic Rays and Nuclear Physics*, Pilot Press Ltd., 1948.
- Louis Leprince-Ringuet, *Cosmic Rays*, Prentice-Hall, New York, 1950.
- Robert Millikan, *Cosmic Rays, three lectures*, Cambridge University Press, 1939.
- Donald Joseph X. Montgomery, *Cosmic Ray Physics*, Princeton University Press, Princeton, 1949.
- Martin A. Pomerantz, *Cosmic rays*, Van Nostrand Reinhold, 1971.
- Bruno Rossi, *Cosmic Rays*, McGraw-Hill, New York, 1964.
- Bruno Rossi, *Moments in the life of a scientist*, Cambridge University Press, New York, 1990.
- Bruno Rossi, *High Energy particles*, Prentice Hall Inc., Englewood Cliffs, New Jersey, 1959.
- Arne Eld Sandström, *Cosmic ray physics*, North-Holland, Amsterdam; Interscience (Wiley), New York, 1965.
- G.B. Zhdanov, *Cosmic Rays*, Lawrence and Wishart, 1959.

More recent texts, either introductory or more advanced, among the many available in the literature are the following:

- Lev I. Dorman, *Cosmic Rays: Variations and Space Explorations*, American Elsevier, 1974.
- Lev I. Dorman, *Cosmic Rays in the Earth Atmosphere and Underground*, Springer, 2004.
- Michael W. Friedlander, *Cosmic rays*, Harvard University Press, 1989.
- S. Flügge, *Cosmic Rays I & II*, Springer Nature, 2012.
- T.K. Gaisser, *Cosmic Rays and Particle Physics*, Cambridge University Press, 1988.
- Peter K.F. Grieder, *Cosmic Rays at Earth, Researcher's Reference Manual and Data Book*, Elsevier Science, Amsterdam, 2001.
- Peter K.F. Grieder, *Extensive Air Showers, High-Energy Phenomena and Astrophysical Aspects. A tutorial, reference manual and data book, Volumes 1 & 2*, Springer, Berlin, Heidelberg, 2010.
- T.K. Gaisser and A.A. Watson, *The Highest Energy Cosmic Rays*, Cambridge University Press, 2004.
- D.V. Skobel'tsyn (Ed.), *Cosmic rays and nuclear interactions at high energies*, Springer, 2014.
- T.S. Stanev, *Cosmic Ray Physics*, John Wiley and Sons, 1998.

A guide to the bibliography concerned with general and historical works on Cosmic Ray Physics, updated in the mid-1960s, was published in the American Journal of Physics in 1967 (J.R. Winckler and D.J. Hofmann, *Resource Letter CR-1 on Cosmic Rays*, American Journal of Physics **35** (1967) 2), and contains information on the original articles that marked the main milestones in the history of this discipline in its first 50 years, together with a list of review articles on some aspects of this discipline and general books on the subject, either informative or by a more in-depth nature.

There is also a large number of articles, or textbooks, on the historical and educational aspects of cosmic ray physics, some of which were published just in the years that marked the centenary of their discovery. We cite, without any exhaustive aim, only a few, of interest to what is discussed in this text:

- Luisa Bonolis, *International scientific cooperation during the 1930s. Bruno Rossi and the development of the status of cosmic rays into a branch of physics*, Annals of Science 71 (2014) 355.
- Jonathan F. Ormes (Editor), *Centenary Symposium 2012: Discovery of Cosmic Rays*, Denver, June 26–28, 2012, AIP Conference Proceedings 1516 (2013) 1–301, reporting the proceedings of the Symposium organized in 2012 on the occasion of the 100th anniversary of the discovery of cosmic rays.
- Johannes Knapp, Michael Walter and Christian Spiering (Editors), *Centenary of cosmic ray discovery*, Astroparticle Physics 53 (2014) 1–190, which includes a collection of papers mainly of historical nature, on the occasion of the 100th anniversary of the discovery of cosmic rays.
- Mario Bertolotti, *Celestial messengers. Cosmic rays, the story of a scientific adventure*, Springer-Verlag, Berlin, Heidelberg, 2013.
- P. Carlson, *A Century of Cosmic Rays*, Physics Today **65** (2012) 30.
- Roger Clay and Bruce Dawson, *Cosmic bullets, High energy particles in astrophysics*, Basic Books, 1999.
- Alessandro De Angelis, *L'enigma dei raggi cosmici*, Springer, Milano, 2012.
- Lev I. Dorman and Irina V. Dorman, *Cosmic Ray History*, Nova Science Publisher Inc., 2014.
- Lev I. Dorman and Irina V. Dorman, *How cosmic rays were discovered and why they received this misnomer*, Advances in Space Research **53** (2014) 1388.
- M.W. Friedlander, *A Thin Cosmic Rain: Particles from Outer Space*, Harvard University Press, 2002.
- M.W. Friedlander, *Physics: A Century of Cosmic Rays*, Nature **483** (2012) 400.
- Karl-Heinz Kampert and Alan A.Watson, *Extensive air showers and ultra-high-energy cosmic rays: a historical review*, European Physical Journal H **37** (2012) 359.
- L. Marafatto, *In search of the cosmic rays*, Aracne Editrice, 2016.
- Y. Sekido and H. Elliott (Eds.), *Early History of Cosmic Ray Studies*, D. Reidel Publishing Company, Dordrecht, 1985.
- William F.G. Swann, *History of cosmic rays*, American Journal of Physics **29** (1961) 811.
- M. Walther and A.W. Wolfendale, *Early history of cosmic ray physics*, European Physical Journal H **37** (2012) 323.
- A.W. Wolfendale, *History of British contributions to the astrophysical aspects of cosmic rays and gamma rays since the second world war*, Quarterly Journal of the Royal Astronomical Society **29** (1988) 27.
- Q. Xu and M.L. Brown, *The early history of cosmic ray research*, American Journal of Physics **55** (1987) 23.

Among the periodic conferences dedicated to cosmic ray physics, it is certainly worth mentioning the series of the International Conference on Cosmic Ray Physics (ICRC), whose proceedings have been digitized and made accessible through the website: https://adsabs.harvard.edu/Proceedings/proceedings/ICRC.

The specific bibliographic references, cited throughout the text in square brackets, for example [Aab2017a], with the name of the first (or only) author and the year of publication, are shown below, following the alphabetical order. Even if it is a rather long list, it was preferred to group them together at the end of the text, rather than distributing them within each chapter, which would perhaps have allowed a more direct consultation, however at the expense of the possibility of comparing references by the same author but cited in different contexts. In the case of bibliographic indications pointing to Web sites, initials in capital letters have been used, for example [NIST]. For each reference, the name of the author was generally indicated, or authors, if limited in number, or the wording "et al." after the name of the first author, in the case of a large number of co-authors. In the case of articles published in scientific Journals, the name of the Journal, the Volume, the initial page and the Year of publication are shown below, while in the case of books, reference is made to the Publishing House and the place and year of publication. In a few cases, especially for historical articles, some of the previous indications may be missing, where it has not been possible to find all the details. With regard to the accessibility of this material, it should be remembered that many articles considered to be of historical interest are available on public servers, even if originally published in journals for which credentials or subscriptions are required. In recent years, the editorial policy of Open Access publishing has been introduced in several Journals, offering many of the relevant scientific articles freely available. Students and researchers should be able to access most of the bibliographic material through the accounts of the Institutions they belong to.

# Bibliography

[Aab2017a] A. Aab et al. (The Pierre Auger Collaboration), Observation of a large-scale anisotropy in the arrival directions of cosmic rays above $8 \times 10^{18}$ eV. Science **357**, 1266 (2017)

[Aab2017b] A. Aab et al. (The Pierre Auger Collaboration), Inferences on mass composition and tests of hadronic interactions from 0.3 to 100 EeV using the water-Cherenkov detectors of the Pierre Auger Observatory. Phys. Rev. **D96**, 122003 (2017)

[Aartsen2016] M.G. Aartsen et al., Anisotropy in cosmic-ray arrival directions in the southern hemisphere based on six years of data from the Icecube detector. Astrophys. J. **826**, 220 (2016)

[Abbasi2010] R. Abbasi et al., Measurement of the anisotropy of cosmic-ray arrival directions with Icecube. Astrophys. J. Lett. **718**, L194 (2010)

[Abbrescia2011] M. Abbrescia et al. (The EEE Collaboration), Observation of the February 2011 Forbush decrease by the EEE telescopes. Eur. Phys. J. Plus **126**, 61 (2011)

[Abbrescia2013] M. Abbrescia et al. (The EEE Collaboration), Time Correlation measurements from extensive air showers detected by the EEE telescopes. Eur. Phys. J. Plus **128**, 148 (2013)

[Abbrescia2015] M. Abbrescia et al. (The EEE Collaboration), Looking at the sub-TeV sky with cosmic muons detected in the EEE MRPC telescopes. Eur. Phys. J. Plus **130**, 187 (2015)

[Abbrescia2016] M. Abbrescia et al. (The EEE Collaboration), A study of upward going particles with the Extreme Energy Events telescopes. Nucl. Instrum. Methods Phys. Res. **A816**, 142 (2016)

[Abbrescia2018] M. Abbrescia et al. (The EEE Collaboration), Search for long distance correlations between extensive air showers detected by the EEE network. Eur. Phys. J. Plus **133**, 34 (2018)

[Abbrescia2019] M. Abbrescia et al. (The EEE Collaboration), The EEE MRPC telescopes as tracking tools to monitor building stability with cosmic muons. J. Instrum. **14**, P06035 (2019)

[Abbrescia2020] M. Abbrescia et al. (The EEE Collaboration), New high precision measurements of the cosmic charged particlerate beyond the Arctic Circle with the PolarquEEEst experiment. Eur. Phys. J. **C80**, 665 (2020)

[Abbrescia2021] M. Abbrescia (The EEE Collaboration), Search for multi-coincidence cosmic ray events over large distances with the EEE MRPC telescopes. J **4**, 838 (2021)

[Abbrescia2022] M. Abbrescia et al. (The EEE Collaboration), Detection of Rayleigh-Lamb waves generated by the 2022 Hunga-Tonga volcanic eruption with the POLA detectors at Ny-Alesund. Sci. Rep. **12**, 19978 (2022)

[Abbrescia2023] M. Abbrescia et al. (The EEE Collaboration), Measurement of the cosmic charged particle rate at sea level in the latitude range 35°–82° N. Eur. Phys. J. C (2023)

[Abdo2009] A.A. Abdo et al., The large scale cosmic-ray anisotropy as observed with Milagro. Astrophys. J. **698**, 2121 (2009)

[Abdollahi2013] S. Abdollahi et al., Study of atmospheric muons using a cosmic ray telescope. J. Phys. G: Nucl. Part. Phys. **40**, 025202 (2013)

[Abeysekara2019] A.U. Abeysekara et al., All-sky measurement of the anisotropy of cosmic rays at 10 TeV and mapping of the local interstellar magnetic field. Astrophys. J. **871**, 96 (2019)

[Abreu2010] P. Abreu et al. (The Pierre Auger Collaboration), Update on the correlation of the highest energy cosmic rays with nearby extragalactic matter. Astropart. Phys. **34**, 314 (2010)

[Aglietta1996] M. Aglietta et al., A measurement of the solar and sidereal cosmic-ray anisotropy at E~$10^{14}$ eV. Astrophys. J. **470**, 501 (1996)

[Aguilar2016] M. Aguilar et al. A(MS Collaboration), Antiproton flux, antiproton-to-proton ratio, and properties of elementary particle fluxes in primary cosmic rays measured with the Alpha Magnetic Spectrometer on the International Space Station. Phys. Rev. Lett. **117**, 091103 (2016)

[Aguilar2021] M. Aguilar et al., (The AMS Collaboration), *The Alpha Magnetic Spectrometer (AMS) on the International Space Station: Part II - Results from the First Seven Years.* Phys. Rep. **894**, 1 (2021)

[Aiola2012] S.Aiola, P.La Rocca, F.Riggi and S.Riggi, Detection of extensive cosmic air showers by small scintillation detectors with wavelength-shifting fibers. Eur. J. Phys. **33**, 1207 (2012)

[Aizu1959] H. Aizu et al., Heavy nuclei in the primary cosmic radiation at Prince Albert, Canada. I. Carbon, Nitrogen and Oxygen. Phys. Rev. **116**, 436 (1959)

[Aizu1961] H. Aizu et al., Heavy nuclei in the primary cosmic radiation at Prince Albert, Canada. II. Phys. Rev. **121**, 1206 (1961)

[Alexeev1973] E.N. Alexeev et al., The intensity of the μ->e decays at different depths underground, in *Proceedings of the 13th International Cosmic Ray Conference*, Denver, Colorado, vol. 3 (1973), p. 1936

[Alfvén1949] H. Alfvén, On the solar origin of the cosmic radiation. Phys. Rev. **75**, 1732 (1949)

[Alfvén1959] H. Alfvén, Momentum spectrum of cosmic radiation. Tellus **11**, 106 (1959)

[Allan1966] H.R. Allan, J.K. Jones, Radio pulses from extensive air showers. Nature **212**, 129 (1966)

[Allan1971] H.R. Allan, Radio emission from extensive showers. Prog. Elem. Part. Cosmic Ray Phys. **10**, 171 (1971)

[Allkofer1964] O.C. Allkofer, J. Trumper, The muon spectrum at 3000 m altitude. Z. Naturforsch. **A19**, 1304 (1964)

[Allkofer1965] O.C. Allkofer, E. Kraft, Das Spektrum der Muonen, der Protonen und der Elektronen in 5200 m Höhe. Nuovo Cimento **39**, 1051 (1965)

[Allkofer1967] O.C. Allkofer, R.D.Andresen, Nuovo Cimento **51B**, 329 (1967)

[Allkofer1970] O.C. Allkofer et al., *Proceedings of the VI Inter-American Seminar on Cosmic Rays*, vol. 4 (1970), p. 930

[Allkofer1971] O.C. Allkofer, K. Carstensen, W.D. Dau, The absolute cosmic ray muon spectrum at sea level. Phys. Lett. B **36**, 425 (1971)

[Allkofer1979] O.C. Allkofer et al., The muon charge ratio up to 7 TeV measured with the DEIS spectrometer, in *Proceedings of the 16th International Cosmic Ray Conference*, Kyoto (Japan), vol. 10 (1979), p. 56

[Aloisio2001] A. Aloisio et al., The ARGO-YBJ experiment in Tibet. Nuovo Cimento **24C**, 739 (2001)

[Alvarez1933] L. Alvarez, H.A. Compton, A positively charged component of cosmic rays. Phys. Rev. **43**, 835 (1933)

[Alvarez1970] L.W. Alvarez et al., Search for hidden chambers in the pyramids. Science **167**, 832 (1970)

[Ambrosi2011] G.Ambrosi et al., The MU-RAY project: volcano radiography with cosmic ray muons. Nucl. Instrum. Methods Phys. Res. **A628**, 120 (2011)

[Ambrosio1999] M. Ambrosio et al., Measurement of the energy spectrum of underground muons at Gran Sasso with a transition radiation detector. Astropart. Phys. **10**, 11 (1999)

[Ambrosino2014] F. Ambrosino et al., The MU-RAY project: detector technology and first data from Mt. Vesuvius. J. Instrum. **9**, C02029 (2014)

[Ambrosino2015a] F. Ambrosino et al., Joint measurement of the atmospheric muon flux through the Puy de Dôme volcano with plastic scintillators and Resistive Plate Chambers detectors. J. Geophys. Res. Solid Earth **120**, 7290 (2015)

[Ambrosino2015b] F. Ambrosino et al., Assessing the feasibility of interrogating nuclear waste storage silos using cosmic-ray muons. J. Instrum. **10**, T06005 (2015)

[Amenomori2004] M. Amenomori et al., Observation by an air-shower array in Tibet of the multi-TeV cosmic-ray anisotropy due to terrestrial orbital motion around the Sun. Phys. Rev. Lett. **93**, 061101 (2004)

[Amenomori2006] M. Amenomori et al., Anisotropy and corotation of galactic cosmic rays. Science **314**, 439 (2006)

[Amenomori2010] M. Amenomori et al., On temporal variations of the multi-TeV cosmic ray anisotropy using the Tibet III air shower array. Astrophys. J. **711**, 119 (2010)

[Amenomori2017] M. Amenomori et al., Northern sky galactic cosmic ray anisotropy between 10 and 1000 TeV with the Tibet air shower array. Astrophys. J. **836**, 153 (2017)

[Anchordoqui2019] L.A. Anchordoqui, Ultra-high-energy cosmic rays. Phys. Rep. **801**, 1 (2019)

[Anderson1932a] C.D. Anderson, Energies of cosmic-ray particles. Phys. Rev. **41**, 405 (1932)

[Anderson1932b] C.D. Anderson, The apparent existence of easily deflectable positives. Science **76**, 238 (1932)

[Anderson1933a] C.D. Anderson, The positive electron. Phys. Rev. **43**, 491 (1933)

[Anderson1933b] C.D. Anderson, S.H. Neddermayer, Positrons from gamma rays. Phys. Rev. **43**, 1034 (1933)

[Anderson1936] C.D. Anderson, S.H. Neddermayer, Cloud chamber observations of cosmic rays at 4300 meters elevation and near sea-level. Phys. Rev. **40**, 263 (1936)

[Anghel2015] V. Anghel et al., A plastic scintillator-based muon tomography system with an integrated muon spectrometer. Nucl. Instrum. Methods Phys. Res. **A798**, 12 (2015)

[Antoni2003] T. Antoni et al., The cosmic ray experiment KASCADE. Nucl. Instrum. Methods Phys. Res. **A513**, 490 (2003)

[Antonov1957] Yu.N. Antonov et al., Structure of the periphery of extensive atmospheric air showers. Soviet Physics JETP **5**, 172 (1957)

[Antonov1960] R.A. Antonov et al., Air showers at altitudes 9–12 km, in *Proceedings of the 6th International Cosmic Ray Conference*, Moscow, vol. 2 (1960), p. 96

[Antonov1964a] R.A. Antonov et al., Altitude variation of vertical extensive air showers in the upper part of the atmosphere. Sov. Phys. JETP **18**, 1279 (1964)

[Antonov 1964b] R.A. Antonov et al., Formation of high energy gamma quanta in extensive air showers with energy $10^{14}$–$10^{15}$ eV in the upper third of the atmosphere. Sov. Phys. JETP **19**, 20 (1964)

[Antonov1971] R.A. Antonov et al., Altitude variation of EAS in the upper atmosphere, in *Proceedings of the 12th International Cosmic Ray Conference*, Tasmania, vol. 6 (1971), p. 2194

[Antonov1975] R.A. Antonov et al., Altitude dependence of EAS in the upper atmosphere and the μ-meson shower intensity near sea level, in *Proceedings of the 14th International Cosmic Ray Conference*, Munich, vol. 8 (1975), p. 2714

[Antonov1983] R.A. Antonov et al., Altitude variation of EAS and particle lateral distribution function in the upper atmosphere, in *Proceedings of the 18th International Cosmic Ray Conference*, Bangalore, vol. 6 (1983), p. 19

[Apel2010] W.D. Apel et al., The KASCADE-Grande experiment. Nucl. Instrum. Methods Phys. Res. **A620**, 202 (2010)

[Apparao1967] K.M.V. Apparao, Upper limits on the abundance of antiprotons in the low energy galactic cosmic radiation. Nature **215**, 727 (1967)

[Armstrong1973] T.W. Armstrong et al., Calculations of neutron flux spectra induced in the Earth's atmosphere by galactic cosmic rays. J. Geophys. Res. **78**, 2715 (1973)

[Arneodo2019] F. Arneodo et al., Measurement of cosmic muons angular distribution in Abu Dhabi at sea level. Nucl. Instrum. Methods Phys. Res. **A936**, 242 (2019)

[Ashton1960] F. Ashton et al., in *Proceedings of the 6th International Cosmic Ray Conference*, Moscow, vol. 1 (1959), p. 302

[Askaryan1962] G.A. Askaryan, Excess negative charge of an electron-photon shower and its coherent radio emission. Sov. Phys. JETP **14**, 441 (1962)

[Auger1934] P. Auger, P. Ehrenfest, Corpuscules ultrapénétrants du rayonnement cosmique. Comptes Rendus **199**, 1609 (1934)

[Auger1938a] P. Auger, R. Maze, T. Grivet-Meyer, Grandes gerbes cosmique atmospherique contenantes des corpuscules ultrapénétrants. Comptes Rendus **206**, 1721 (1938)

[Auger1938b] P. Auger, R. Maze, Les grandes gerbes cosmiques de l'atmosphère. Comptes Rendus **207**, 228 (1938)

[Auger1939a] P. Auger, R. Maze, P. Ehrenfest Jr., A. Fréon, Les grandes gerbes de rayons cosmiques. J. Phys. Radium **10**, 39 (1939)

[Auger1939b] P. Auger, R. Maze, Robley, Comptes Rendus **208** (1939) 1641

[Auger1939c] P. Auger et al., Extensive cosmic-ray showers. Rev. Mod. Phys. **11**, 288 (1939)

[Auger1940] P. Auger, J. Daudin, Diurnal variations of extensive showers. Phys. Rev. **61**, 95 (1940)

[Auger1942] P. Auger, J. Daudin, Absorption of extensive atmospheric showers of cosmic rays in air and lead. Phys. Rev. **61**, 91 (1942)

[Auger1945] P. Auger, J. Dadin, Les grandes gerbes de l'air. J. Phys. Radium **6**, 233 (1945)

[Auger1949] R. Maze, A. Fréon, J. Daudin, P. Auger, Extensive and penetrating atmospheric showers. Rev. Mod. Phys. **21**, 914 (1949)

[AUGER_OBS] Web site of the Pierre Auger Observatory: www.auger.com

[Axford1977] W.I. Axford, E. Leer, G. Skadron, The acceleration of cosmic rays by shock waves, in *Proceedings of the 15th International Cosmic Ray Conference*, Plovdiv (Bulgaria), vol. 11 (1977), p. 132

[Babson1990] J. Babson et al., Cosmic ray muons in the deep ocean. Phys. Rev. D **42**, 3613 (1990)

[Baesso2014] P. Baesso et al., Toward a RPC-based muon tomography system for cargo containers. J. Instrum. **9**, C10041 (2014)

[Bagge1950] E. Bagge, Eine Deutung der Expansion des Kosmos. Z. Phys. **128**, 239 (1950)

[Bahmanabadi2005] M. Bahmanabadi et al., Experimental studies of positive and negative atmospheric muons with a cosmic ray telescope. Astropart. Phys. **24**, 183 (2005)

[Bahmanabadi2019] M. Bahmanabadi, A method for determining the angular distribution of atmospheric muons using a cosmic ray telescope. Nucl. Instrum. Methods Phys. Res. **A916**, 1 (2019)

[Bandieramonte2015] M. Bandieramonte et al., Clustering analysis for muon tomography data elaboration in the muon portal project. J. Phys: Conf. Ser. **608**, 012046 (2015)

[Baradzei1959] L.T. Baradzei et al., Momentum spectrum of particles of the hard component of cosmic rays at an altitude of 9 km. Sov. Phys. JETP **36**, 1151 (1959)

[Barber1949] W.C. Barber, East-West asymmetry and latitude effect of cosmic rays at altitudes up to 33000 feet. Phys. Rev. **75**, 590 (1949)

[Barbouti1983] A.I. Barbouti, B.C. Rastin, A study of the absolute intensity of muons at sea level and under various thicknesses of absorber. J. Phys. **G9**, 1577 (1983)

[Barkas1963] W.H. Barkas, Nuclear research emulsions, techniques and theory, in *Pure and Applied Physics, A Series of Monographs and Textbooks*, vol. 15 (Academic, New York, London, 1963)

[Barnóthy1939] J. Barnóthy, M. Forró, Cosmic ray particles at great depth. Phys. Rev. **55**, 870 (1939)

[Barradas2010] F. Barradas-Solad, P. Alameda-Melendez, Bringing particle physics to life: build your own cloud chamber. Sci. Sch. **14**, 36 (2010)

[Barrett1952] P.H. Barrett et al., Interpretation of cosmic ray measurements far underground. Rev. Mod. Phys. **24**, 133 (1952)

[Bartelt2018] V.K. Cirkel-Bartelt, *A Quest for Truth? Heroic Patterns in Early Cosmic Ray Physics*. https://doi.org/10.6094/helden.heroes.heros./2018/HS/06

[Bassi1953] P. Bassi, G. Clark, B. Rossi, Distribution of arrival times of air shower particles. Phys. Rev. **92**, 441 (1953)

[Batignani2011] G. Batignani et al., L'esperimento di Pacini sull'origine dei raggi cosmici. G. Fis. **42**, 1 (2011)

[Bazilevskaya2014] G.A. Bazilevskaya, Skobeltsyn and the early years of cosmic particle physics in the Soviet Union. Astropart. Phys. **53**, 61 (2014)

[Beedle1970] R.E. Beedle, W.R. Webber, Measurement of cosmic ray electrons in the energy range 4 MeV to 6 BeV at 2 g/cm² atmospheric depth at Ft. Churchill. Can. J. Phys. **46**, S1014 (1968)

[Bell1948] P.R. Bell, The use of anthracene as a scintillation counter. Phys. Rev. **73**, 1405 (1948)

[Bell1978] R. Bell, The acceleration of cosmic rays in shock front. Mon. Not. Roy. Astron. Soc. **182**, 147 (1978)

[Bellotti1999] R. Bellotti et al., Balloon measurements of cosmic ray muon spectra in the atmosphere along with those of primary protons and helium nuclei over midlatitude. Phys. Rev. D **60**, 052002 (1999)

[Belov2005] A. Belov et al., A study of the ground level enhancement of 23 February 1956. Adv. Space Res. **35**, 697 (2005)

[Belov2009] A.V. Belov, Forbush effects and their connection with solar, interplanetary and geomagnetic phenomena. Proc. IAU Symp. **257**, 439 (2008)

[Bennett1931] R.D. Bennett, J.C. Stearns, A.H. Compton, The constancy of cosmic rays. Phys. Rev. **38**, 1566 (1931)

[Bennett1932a] R.D. Bennett, J.C. Stearns, H. Compton, Diurnal variation of cosmic rays. Phys. Rev. **41**, 119 (1932)

[Bennett1932b] R.D. Bennett et al., Intensity of cosmic ray ionization in Western North America. Phys. Rev. **42**, 446 (1932)

[Běhounek1929] F. Běhounek, Atmospheric-electric researches made in 1928 during the Nobile Arctic Expedition in collaboration with Professor A. Pontremoli (Milan) and Professor F. Malmgren (Uppsala). Terr. Magn. Atmos. Electr. **34**, 173 (1929)

[Bergeson1975] H.E. Bergeson et al., The Fly's Eye, a novel technique for sensing extensive air showers, in *Proceedings of the 14th International Cosmic Ray Conference*, Munich, vol. 8 (1975), p. 3059

[Bergwitz1910] K. Bergwitz, Die Gammastrahlung des Erdkörpers und ihr Anteil an der spontanen Ionisierung der Atmosphäre. Jahresbericht des Braunschweiger Vereins für Naturwissenschaft **10**, 196 (1910)

[Bethe1934] H.A. Bethe, W. Heitler, On the stopping of fast particles and on the creation of positive electrons. Proc. Roy. Soc. **146**, 83 (1934)

[Bethe1953] H.A. Bethe, Molière's theory of multiple scattering. Phys. Rev. **89**, 1256 (1953)

[Beuermann1968] K.P. Beuermann, G. Wibberenz, Can. J. Phys. **46**, S1034 (1968)

[Bhat1978] P.N. Bhat, P.V. Murthy, Angular distribution of low-energy cosmic ray muons underground. J. Phys. G: Nucl. Phys. **4**, 453 (1978)

[Bhattacharyya1974] D.P. Bhattacharyya, Absolute sea-level integral muon spectra at zenith angles 45 °W and 60 °W near the geomagnetic equator in the momentum range (0.4÷3) GeV/c. Nuovo Cimento **B24**, 78 (1974)

[Biehl1949] A.T. Biehl et al., Cosmic-ray experiments at high altitudes over a wide range of latitudes. Phys. Rev. **76**, 914 (1949)

[Bierman1949] L. Bierman, E. Bagge, Über die Entstehung der solaren Komponente der Ultrastrahlung. Z. Naturforsch. **4a**, 303 (1949)

[Bikit2016] I. Bikit et al., Novel approach to imaging by cosmic ray muons. Europhys. Lett. **113**, 58001 (2016)

[Bjorklund1950] R. Bjorklund et al., High energy photons from proton-nucleon collisions. Phys. Rev. **77**, 213 (1950)

[Blackett1932] P.M.S. Blackett, G. Occhialini, Photography of penetrating corpuscular radiation. Nature **130**, 363 (1932)

[Blackett1933a] P.M.S. Blackett, G. Occhialini, Some photographs of the tracks of penetrating radiation. Proc. Roy. Soc. **A139**, 699 (1933)

[Blackett1933b] P.M.S. Blackett, The positive electron. Nature **132**, 917 (1933)

[Blackett1948] P.M.S. Blackett, A possible contribution to the light of the night sky from the Cherenkov radiation emitted by cosmic rays, in *Physical Society Gassiot Committee Report: The Emission Spectra of the Night Sky and Aurorae*, p. 34

[Blanco2006a] F. Blanco et al., Geiger counters offer powerful way to teach detection methods. Phys. Educ. **41**, 204 (2006)

[Blanco2006b] F. Blanco et al., Educational cosmic ray experiments with Geiger counters. Nuovo Cimento C **29**, 381 (2006)

[Blanco2008a] F. Blanco, P. La Rocca, F. Riggi, Educational experiments with cosmic rays, in *Science Education in Focus*, ed. by M.V. Thomase (Nova Publishers, New York, 2008). ISBN: 1-60021-949-7

[Blanco2008b] F. Blanco, P. La Rocca, F. Riggi, S. Riggi, Timing the random and anomalous arrival of particles in a Geiger counter with GPS devices. Eur. J. Phys. **29**, 355 (2008)

[Blanco2008c] F. Blanco et al., Cosmic ray measurements by scintillators with metal resistor semiconductor avalanche photo diodes. Phys. Educ. **43**, 536 (2008)

[Blanco2009] F. Blanco, P. La Rocca, F. Riggi, Cosmic ray physics from sea level to aircraft cruise altitudes. Eur. J. Phys. **30**, 685 (2009)

[Blandford1978] R.D. Blandford, J.P. Ostriker, Particle acceleration by astrophysical shocks. Astrophys. J. **221**, L29 (1978)

[Blandford1987] R. Blandford, D. Eichler, Particle acceleration at astrophysical shocks: a theory of cosmic ray origin. Phys. Rep. **154**, 1 (1987)

[Blau1925] M. Blau, Über die photographische Wirkung natürlicher H-Strahlen. Proc. Vienna Acad. Sci. Sect. IIa **134**, 427 (1925)

[Blau1932] M. Blau, H. Wambacher, Photographic detection of protons liberated by neutrons. Proc. Vienna Acad. Sci. Sect. II **141**, 617 (1932)

[Blau1937] M. Blau, H. Wambacher, Disintegration processes by cosmic rays with the simultaneous emission of several heavy particles. Nature **140**, 585 (1937)

[Blokh1977] Y.L. Blokh, L.I. Dorman, I.Y. Libin, Studies of the angular distribution and of the altitude dependence of the cosmic-ray muon and general components using scintillation telescopes. Nuovo Cimento **B37**, 198 (1977)

[Blumer2009] J. Blumer et al., Cosmic rays from the knee to the highest energies. Prog. Part. Nucl. Phys. **63**, 293 (2009)

[Bodini2007] I. Bodini et al., Cosmic ray detection based measurement systems. Meas. Sci. Technol. **18**, 3537 (2007)

[Bogomolov1971] E.A. Bogomolov et al., *Proceedings of the 12th International Cosmic Ray Conference*, Hobart (Australia), vol. 5 (1971), p. 1730

[Bogomolov1979] E.A. Bogomolov et al., *Proceedings of the 16th International Cosmic Ray Conference*, Kyoto (Japan), vol. 1 (1979), p. 330

[Bonechi2020] L. Bonechi et al., Atmospheric muons as an imaging tool. Rev. Phys. **5**, 100038 (2020)

[Bonolis2011a] L. Bonolis, Bruno Rossi and the racial laws of fascist Italy. Phys. Perspect. **13**, 58 (2011)

[Bonolis2011b] L. Bonolis, Walther Bothe and Bruno Rossi: the birth and development of coincidence methods in cosmic-ray physics. Am. J. Phys. **79**, 1133 (2011)

[Bonolis2014] L. Bonolis, From cosmic ray physics to cosmic ray astronomy: Bruno Rossi and the opening of new windows on the universe. Astropart. Phys. **53**, 67 (2014)

[Bonomi2014] G. Bonomi et al., Muon tomography as a tool to detect radioactive source shielding in scrap metal containers. Int. J. Mod. Phys.: Conf. Ser. **27**, 1460157 (2014)

[Bonomi2017] G. Bonomi, Progress in muon tomography, in *Proceedings of Science POS (EPS-HEP2017)*, p. 609

[Bonomi2019] G. Bonomi et al., Cosmic ray tracking to monitor the stability of historical buildings: a feasibility study. Meas. Sci. Technol. **30**, 045901 (2019)

[Borozdin2003] K.N. Borozdin et al., Radiographic imaging with cosmic ray muons. Nature **422**, 277 (2003)

[Borozdin2012] K.N. Borozdin et al., Cosmic ray radiography of the damaged cores of the Fukushima reactors. Phys. Rev. Lett. **109**, 152501 (2012)

[Bothe1929a] W. Bothe, W. Kolhörster, Das Wesen der Höhenstrahlung. Z. Phys. **56**, 751 (1929)

[Bothe1929b] W. Bothe, W. Kolhörster, The nature of the penetrating radiation. Nature **123**, 638 (1929)

[Bothe1930a] W. Bothe, W. Kolhörster, Berl. Ber. 450 (1930)

[Bothe1930b] W. Bothe, H. Becker, Künstliche Erregung von Kern–γ–Strahlen. Z. Phys. **66**, 289 (1930)

[Bothe1937] W. Bothe et al., Phys. Z. **38**, 964 (1937)

[Bothe1954] Walther Bothe Nobel Lecture, see the Web site: https://www.nobelprize.org/prizes/physics/1954/bothe/lecture/

[Bouteille2016] S. Bouteille et al., A Micromegas-based telescope for muon tomography: The WatTo experiment. Nucl. Instrum. Methods Phys. Res. **A834**, 223 (2016)

[Boys1889] C.V. Boys, Quartz as an insulator. Philos. Mag. **28**, 14 (1889)

[Bradt1948] H.L. Bradt, B. Peters, Investigation of the primary cosmic radiation with nuclear photographic emulsions. Phys. Rev. **74**, 1828 (1948)

[Bradt1950] H.L. Bradt, B. Peters, The heavy nuclei of the primary cosmic radiation. Phys. Rev. **77**, 54 (1950)

[Broadbent1950] D. Broadbent et al., The density spectrum and structure of extensive cosmic ray showers at sea level. Proc. Phys. Soc. **A63**, 864 (1950)

[Brode1936] R.B. Brode et al., The heavy particle component of the cosmic radiation. Phys. Rev. **51**, 581 (1936)

[Brooke1964] G. Brooke, A.W. Wolfendale, The momentum spectrum of cosmic ray protons near sea level in the momentum range 0.6–150 GeV/c. Proc. Phys. Soc. **83**, 843 (1964)

[Broser1947a] I. Broser, H. Kallmann, Uber die Anregung von Leuchtstoffen durch schnelle Korpuskularteilchen I. Zeitschrift fur Naturforschung **2a**, 439 (1947)

[Broser1947b] I. Broser, H. Kallmann, Ueber den Elementarprozess der Lichtanregung in Leuchtstoffen durch Alphateilchen, Schnelle Elektronen und Gammaquanten. Zeitschrift fur Naturforschung **2a**, 642 (1947)

[Brown1949] R. Brown et al., Observations with electron-sensitive plates exposed to cosmic radiation. Nature **163**, 47 (1949)

[Brownlee1968] R.G. Brownlee et al., Design of an array to record air showers of energy up to $10^{21}$ eV. Can. J. Phys. **46**, S259 (1968)

[Bugaev1998] E.V. Bugaev et al., Atmospheric muon flux at sea level, underground, and underwater. Phys. Rev. D **58**, 054001 (1998)

[Bunner1967] N.A. Bunner, *Cosmic Ray Detection by Atmospheric Fluorescence*, Ph.D. Thesis, Cornell University (1967)

[Caffau1997] E. Caffau et al., Underground cosmic ray measurement for morphological reconstruction of the Grotta Gigante natural cave. Nucl. Instrum. Methods Phys. Res. **A385**, 480 (1997)

[CALTECH] https://www.caltech.edu/about/news/caltech-to-remove-the-names-of-robert-a-millikan-and-five-other-eugenics-proponents

[Carbone2014] D. Carbone et al., An experiment of muon radiography at Mt. Etna (Italy). Geophys. J. Int. **196**, 633 (2014)

[Carlson1941] J.F. Carlson, M. Schein, On the production of mesotrons. Phys. Rev. **59**, 840 (1941)

[Carlson2011] P. Carlson, A. De Angelis, Nationalism and internationalism in science: the case of the discovery of cosmic rays. Eur. Phys. J. **H35**, 309 (2011)

[Castagnoli1997] C. Castagnoli et al., Multiple interactions of muons in the NUSEX detector and muon energy spectrum deep underground. Astropart. Phys. **6**, 187 (1997)

[Cerenkov1937] P. Cherenkov, Visible radiation produced by electrons moving in a medium with velocities exceeding that of light. Phys. Rev. **52**, 378 (1937)

[CERN-Courier1966] A.J. Herz, W.O. Lock, CERN Courier, May 1966, https://cerncourier.com/a/nuclear-emulsions/

[Chadwick1932a] J. Chadwick, Possible existence of a neutron. Nature **129**, 312 (1932)

[Chadwick1932b] J. Chadwick, The existence of a neutron. Proc. Roy. Soc. **136**, 692 (1932)

[Chamberlain1955] O. Chamberlain et al., Observation of antiprotons. Phys. Rev. **100**, 947 (1955)

[Chandrasekhar1953] S. Chandrasekhar, E. Fermi, Problems of gravitational stability in the presence of magnetic field. Astrophys. J. **118**, 113 (1953)

[Chatzidakis2016] S. Chatzidakis et al., Interaction of cosmic ray muons with spent nuclear fuel dry casks and determination of lower detection limit. Nucl. Instrum. Methods Phys. Res. **A828**, 37 (2016)

[Checchia2016] P. Checchia, Review of possible applications of cosmic muon tomography. J. Instrum. **11**, C12072 (2016)

[Chiba1992] N. Chiba et al., Akeno Giant Air Shower Array (AGASA) covering 100 km$^2$ area. Nucl. Instrum. Methods Phys. Res. **A311**, 338 (1992)

[Clark1957a] G.W. Clark et al., Preparation of large plastic scintillators. Rev. Sci. Instrum. **28**, 433 (1957)

[Clark1957b] G.W. Clark et al., An experiment on air showers produced by high-energy cosmic rays. Nature **180**, 353 (1957)

[Clark1961] G.W. Clark et al., Cosmic-ray air showers at sea level. Phys. Rev. **122**, 637 (1961)

[Clarkson2014] A. Clarkson et al., The design and performance of a scintillating-fibre tracker for the cosmic-ray muon tomography of legacy nuclear waste containers. Nucl. Instrum. Methods Phys. Res. **A745**, 138 (2014)

[Clarkson2015] A. Clarkson et al., Characterising encapsulated nuclear waste using cosmic-ray muon tomography. J. Instrum. **10**, P03020 (2015)

[Clay1927] J. Clay, Penetrating radiation. Proc. Acad. Sci. Amst. **30**, 1115 (1927)

[Clay1928] J. Clay, Penetrating radiation II. Proc. Acad. Sci. Amst. **31**, 1091 (1928)

[Clay1939] J. Clay, The absolute value of cosmic-ray ionization at sea level in different gases. Rev. Mod. Phys. **11**, 128 (1939)

[Clay1984] R.W. Clay et al., The Buckland Park Air Shower Array, in *Proceedings of the 19th International Cosmic Ray Conference*, La Jolla (USA), vol. 3 (1984), p. 414

[CLIMATE] https://www.climate4you.com/Sun.htm

[CLOUD] https://home.cern/science/experiments/cloud

[Cocconi1941] G. Cocconi, On the protonic nature of the cosmic radiation. Phys. Rev. **60**, 532 (1941)

[Cocconi1944a] G. Cocconi, A. Loverdo, V. Tongiorgi, Lo spettro di densità degli sciami estesi nell'aria. Nuovo Cimento **2**, 14 (1944)

[Cocconi1944b] G. Cocconi, A. Loverdo, V. Tongiorgi, Sulla costituzione degli sciami estesi nell'aria. Nuovo Cimento **2**, 28 (1944)

[Cocconi1946a] G. Cocconi, A. Loverdo, V. Tongiorgi, Experimental and theoretical evaluation of the density spectrum of extensive cosmic-ray showers. Phys. Rev. **70**, 846 (1946)

[Cocconi1946b] G. Cocconi, A. Loverdo, V. Tongiorgi, Penetrating particles in air showers. Phys. Rev. **70**, 852 (1946)

[Cocconi1946c] G. Cocconi, V. Tongiorgi, On the fine structure of the zenithal curves of the cosmic radiation. Phys. Rev. **70**, 850 (1946)

[Cocconi1949a] G. Cocconi, Results and problems concerning the extensive air showers. Rev. Mod. Phys. **21**, 26 (1949)

[Cocconi1949b] G. Cocconi, Some properties of the cosmic ray ionizing particles that generate penetrating showers. Phys. Rev. **75**, 1074 (1949)

[Cocconi1949c] G. Cocconi, Meson background in penetrating shower experiments. Phys. Rev. **76**, 984 (1949)

[Cocconi1949d] G. Cocconi, V. Cocconi Tongiorgi, The density spectrum of extensive air showers of cosmic rays. Phys. Rev. **75**, 1058 (1949)

[Cocconi1949e] G. Cocconi, V. Cocconi Tongiorgi, Angular distribution and multiplicity of neutrons associated with local cosmic-ray showers. Phys. Rev. **76**, 318 (1949)

[Cocconi1949f] G. Cocconi, V. Cocconi Tongiorgi, K. Greisen, The lateral structure of cosmic-ray air showers. Phys. Rev. **76**, 1020 (1949)

[Cocconi1956] G. Cocconi, Intergalactic space and cosmic rays. Nuovo Cimento **3**, 1433 (1956)

[Colgate1960] S.A. Colgate, M.H. Johnson, Hydrodynamic origin of cosmic rays. Phys. Rev. Lett. **5**, 235 (1960)

[Coltman1947] J.W. Coltman, F.H. Marshall, Photomultiplier radiation detector. Nucleonics **1**, 58 (1947)

[Compton1923] A.H. Compton, A quantum theory of the scattering of X-rays by light elements. Phys. Rev. **21**, 483 (1923)

[Compton1931] A.H. Compton, R.D. Bennett, J.C. Stearns, Ionization as a function of pressure and temperature. Phys. Rev. **38**, 1565 (1931)

[Compton1932a] A.H. Compton, R.D. Bennett, J.C. Stearns, Ionization by penetrating radiation as a function of pressure and temperature. Phys. Rev. **39**, 873 (1932)

[Compton1932b] A.H. Compton, Variation of cosmic rays with latitude. Phys. Rev. **41**, 111 (1932)

[Compton1932c] A.H. Compton, Progress of cosmic-ray survey. Phys. Rev. **41**, 681 (1932)

[Compton1933] A.H. Compton, A geographic study of cosmic rays. Phys. Rev. **43**, 387 (1933)

[Compton1934] A.H. Compton, H. Bethe, Composition of cosmic rays. Nature **134**, 734 (1934)

[Compton1935] A.H. Compton, I.A. Getting, An apparent effect of galactic rotation on the intensity of cosmic rays. Phys. Rev. **47**, 817 (1935)

[Compton1936a] A.H. Compton, Cosmic rays as electrical particles. Phys. Rev. **50**, 1119 (1936)

[Compton1936b] A.H. Compton, Recent developments in cosmic rays. Rev. Sci. Instrum. **7**, 71 (1936)

[Copeland2020] K. Copeland, *CARI-7 Documentation: Geomagnetic Cutoff Rigidity Calculations and Tables for 1965–2010*, DOT/FAA/AM-19/4 Office of Aerospace Medicine, Washington, DC

[Corlin1927] A. Corlin, Über den kosmischen Ursprung der durchdringenden Höhenstrahlung. Astron. Nachr. **9**, 137 (1927)

[Corlin1928] A. Corlin, The highly penetrating cosmic rays. Nature **121**, 322 (1928)

[Corlin1930] A. Corlin, Lund Medd. **121**, 39 (1930)

[Cosyns1940] M.G.E. Cosyins, Barometric coefficient of extensive air showers. Nature **145**, 668 (1940)

[Coulomb1785] C. de Coulomb, Troisième mémoire sur l'électricité et le magnétisme. De la quantité d'électricité qu'un corps isolé perd dans le temps donné, soit par le contact de l'air plus ou moins humide, soit le lond des soutiens plus ou moins idio-électriques, avec 1 planche. Mém. Acad. Roy. Sci. **88**, 612 (1785)

[Cowan1948] E.W. Cowan, Evidence for the existence of a low mass mesotron. Science **108**, 534 (1948)

[Critchfield1951] C.L. Critchfield, E.P. Ney, S. Oleska, Soft radiation at balloon altitudes. Phys. Rev. **85**, 461 (1951)

[Crookes1878] W. Crookes, On Electrical Insulation in high vacua. Proc. R. Soc. Lond. **28**, 347 (1879)

[Crookes1903] W. Crookes, Certain properties of the emanations of radium. Chem. News **87**, 241 (1903)

[Crookes1972] J.N. Crookes, B.C. Rastin, An investigation of the absolute intensity of muons at sea level. Nucl. Phys. B **39**, 493 (1972)

[Curie1898] M. Curie, Rayons émis par les composés de l'uranium et du thorium. Comptes Rendus **126**, 1101 (1898)

[Curie1899] M. Curie, Les rayons de Becquerel et le polonium. Rev. Gen. Sci. Pures Appl. **10**, 41 (1899)

[Curie1930] I. Curie, Sur le rayonnement γ nucléaire excité dans le glucinium et dans le lithium par les rayons αdu polonium. Compte Rendus Séances Academie Science Paris **193**, 1412 (1930)

[Curie1932a] I. Curie, F. Joliot, Émission de protons à grande vitesse par les substances hydrogénées sous l'influence des rayons γ très pénétrants. Compte Rendus Séances Academie Science Paris **194**, 273 (1932)

[Curie1932b] I. Curie, F. Joliot, Effet d'absorption de rayons γde très haute fréquence par projection de noyaux légers. Compte Rendus Séances Academie Science Paris **194**, 708 (1932)

[Curie1932c] I. Curie, F. Joliot, Sur la nature du rayonnement pénétrant excité dans les noyaux légers par les particules α. Compte Rendus Séances Academie Science Paris **194**, 1229 (1932)

[Curie1933] I. Curie, F. Joliot, Sur l'origin des electron positifs. Compte Rendus Séances Academie Science Paris **196**, 1581 (1933)

[Curran1944] S.C. Curran, W.R. Backer, *A photoelectric alpha particle detector*, U. S. Atomic Energy Commission Report MDDC 1296, 17 Nov 1944

[Curtiss1928] L.F. Curtiss, On the action of the Geiger counter. Phys. Rev. **31**, 1060 (1928)

[Daggs1952] W. Daggs, W. Parr, A. Krebs, Tests on scintillation G-M tubes. Nucleonics **10**, 54 (1952)

[Daion1959] M.I. Daion, L.I. Potapov, Underground muon spectrum at ~40 m water equivalent. Sov. Phys. JETP **36**, 488 (1959)

[Dauvillier1934] M.A. Dauvillier, Researches on cosmic rays at Scoresby Sund during the polar year. J. Phys. Radium **5**, 640 (1934)

[Davis1956] L. Davis, Modified Fermi mechanism for the acceleration of cosmic rays. Phys. Rev. **101**, 351 (1956)

[Davitaev1970] L.N. Davitaev et al., Intensity measurements of cosmic rays in water at large depths, in *Proceedings of the 11th International Conference on Cosmic Rays*, Budapest, Suppl. Acta Phys. Acad. Sci. Hung. **29**, 53 (1970)

[DeAngelis2010] A. De Angelis, Domenico Pacini, uncredited pioneer of the discovery of cosmic rays. La Rivista del Nuovo Cimento **33**, 713 (2010)

[DeAngelis2012] A. De Angelis, *L'enigma dei raggi cosmici* (Springer, Milano, 2012)

[DeAngelis2014] A. De Angelis, Atmospheric ionization and cosmic rays: studies and measurements before 1912. Astropart. Phys. **53**, 19 (2014)

[DeAngelis2018a] V.F. Hess, *Measurements of the Penetrating Radiation During Seven Balloon Flights* (Translated and commented by A. De Angelis, C.A.B. Schultz), arXiv:1808.02927v2 10 Aug 2018

[DeAngelis2018b] A. De Angelis, M. Mallamaci, Gamma-ray astrophysics. Eur. Phys. J. Plus **133**, 324 (2018)

[Degrange2013] B. Degrange, G. Fontaine, P. Fleury, Tracking Louis Leprince-Ringuet's contribution to cosmic ray physics. Phys. Today **66**, 8 (2013)

[DeShong1964] J.A. De Shong Jr., R.H. Hildebrand, P. Meyer, Ratio of electrons to positrons in the primary cosmic radiation. Phys. Rev. Lett. **12**, 3 (1964)

[Deutschmann1947] M. Deutschmann, Untersuchung der kosmischen Strahlenschauer mit Hilfe einer großen Wilson-Kammer. Z. Naturforsch. **2a**, 61 (1947)

[Dirac1928] P.A.M. Dirac, The quantum theory of the electron. Proc. Roy. Soc. **117**, 610 (1928)

[Dmietreva2006] A.N. Dmietreva et al., Measurement of integrated muon intensity at large zenith angles. Phys. At. Nucl. **69**, 865 (2006)

[Dobrowolska2020] M. Dobrowolska et al., Towards an application of muon scattering tomography as a technique for detecting rebars in concrete. Smart Mater. Struct. **29**, 055015 (2020)

[Donzella2014] A. Donzella et al., Historical building stability monitoring by means of a cosmic ray tracking system. Nuovo Cimento C **37**, 223 (2014)

[Dorman1974] L.I. Dorman, *Cosmic Rays, Variations and Space Explorations* (North Holland Publishing Company, Amsterdam, 1974)

[Drury1983] L. O'C Drury, An introduction to the theory of diffusive shock acceleration of energetic particles in tenuous plasmas. Rep. Prog. Phys. **46**, 973 (1983)

[Drury2012] L. O'C Drury, Origin of cosmic rays. Astropart. Phys. **39–40**, 52 (2012)

[Durham2015] J.M. Durham et al., Tests of cosmic ray radiography for power industry applications. AIP Adv. **5**, 067111 (2015)

[Earl1961] J.A. Earl, Cloud-chamber observations of primary cosmic ray electrons. Phys. Rev. Lett. **6**, 125 (1961)

[Ebert1901] H. Ebert, Über Elektricitätszerstreuung in grösseren Höhen. Ann. Phys. **310**, 718 (1901)

[EEE] Web site of the EEE Collaboration: https://eee.centrofermi.it/

[Elster1899] J. Elster, H. Geitel, Uber einen apparat zur messung der Elektricitatszerstreuung in der luft. Phys. Z. **1**, 11 (1899)

[Elster1900a] J. Elster, H. Geitel, Über Elektricitätszerstreuung in der Luft. Ann. Phys. **307**, 425 (1900)

[Elster1900b] J. Elster, H. Geitel, Weitere Versuche ber die Elektrizitätszerstreuung in abgeschlossenen Luftmengen. Phys. Z. **2**, 560 (1900)

[Elster1901] J. Elster, H. Geitel, Uber die radioaktivitat der im erdboden henthaltenen luft. Phys. Z. **3**, 574 (1901)

[ESPER] https://www.esperimentanda.com/come-costruire-una-camera-a-nebbia-a-diffusione-con-ghiaccio-secco-per-rivelare-particelle-subatomiche/

[Euler1940] H. Euler, H. Wergeland, Über die ausgedehnten Luftschauer der kosmischen Strahlung. Astrophisica Norvegica **3**, 165 (1940)

[Eve1906] A.S. Eve, On the radioactive matter in the earth and the atmosphere. Philos. Mag. Lond. **12**, 189 (1906)

[Eve1907] A.S. Eve, The ionization of the atmosphere over the ocean. Philos. Mag. Lond. **13**, 248 (1907)

[Fadhel2021] K.F. Fadhel et al., Estimating the lateral distribution of high energy cosmic ray particles by depending on Nishimura-Kamata-Greisen function. J. Phys. G: Conf. Series **1879**, 032089 (2021)

[Famoso2005] B. Famoso, P. La Rocca, F. Riggi, An educational study of the cosmic ray barometric effect with a Geiger counter. Phys. Educ. **40**, 461 (2005)

[Fan1951] C.Y. Fan, On Fermi's theory of the origin of the cosmic radiation. Phys. Rev. **82**, 211 (1951)

[Fanselow1969] J.L. Fanselow et al., Charge composition and energy spectrum of primary cosmic-ray electrons. Astrophys. J. **158**, 771 (1969)

[Fermi1949] E. Fermi, On the origin of cosmic radiation. Phys. Rev. **75**, 1169 (1949)

[Fermi1954] E. Fermi, Galactic magnetic fields and the origin of the cosmic radiation. Astrophys. J. **119**, 1 (1954)

[Fick2014] D. Fick, D. Hoffman, Werner Kolhoster (1887–1945): the German pioneer of cosmic ray physics. Astropart. Phys. **53**, 50 (2014)

[Fichtel1978] C.E. Fichtel, G.A. Simpson, D.J. Thomson, Diffuse gamma radiation. Astrophys. J. **222**, 833 (1978)

[Forbush1937] S.E. Forbush, On the effects in cosmic-ray intensity observed during the recent magnetic storm. Phys. Rev. **51**, 1108 (1937)

[Forbush1938] S.E. Forbush, On world-wide changes in cosmic-ray intensity. Phys. Rev. **54**, 975 (1938)

[Forbush1938] F. von Forstner et al., Using Forbush decreases to derive the transit time of ICMEs propagating from 1 AU to Mars. J. Geophys. Res. Space Phys. **123**, 39 (2018)

[Foster1949] J.S. Foster, Arthur Stewart Eve, 1862–1948. Obituary Note Fellows Roy. Soc. **6**, 396 (1949)

[Fradkin1956] M.I. Fradkin, On the problem of antiprotons in the primary stream of cosmic rays. Sov. Phys. JETP **2**, 87 (1956)

[Freier1948a] P. Freier, E.J. Lofgren, E.P. Ney, F. Oppenheimer, H.L. Bradt, B. Peters, Evidence for heavy nuclei in the primary cosmic radiation. Phys. Rev. **74**, 213 (1948)

[Freier1948b] P. Freier, E.J. Lofgren, E.P. Ney, F. Oppenheimer, The heavy component of the primary cosmic radiation. Phys. Rev. **74**, 1818 (1948)

[Fretter1948] W.B. Fretter, Penetrating showers in lead. Phys. Rev. **73**, 41 (1948)

[Fricke2017] R.G.A. Fricke, K. Schlegel, Julius Elster and Hans Geitel, Dioscuri of physics and pioneer investigators in atmospheric electricity. Hist. Geo- Space-Sci. **8**, 1 (2017)

[Fuji2013] H. Fuji et al., Performance of a remotely located muon radiography system to identify the inner structure of a nuclear plant. Prog. Theor. Exp. Phys. **7**, 073C01 (2013)

[Fuji2017] H. Fuji et al., Detection of on-surface objects with an underground radiography detector system using cosmic ray muons. Prog. Theor. Exp. Phys. **5**, 053C01 (2017)

[Fulks1974] G. Fulks, P. Meyer, Cosmic ray electrons in the atmosphere. J. Geophys. (Z. Geophys.) **40**, 751 (1974)

[Furlan2014] M. Furlan et al., Application of muon tomography to detect radioactive sources hidden in scrap metal containers. IEEE Trans. Nucl. Sci. **61**, 2204 (2014)

[Fyodorov1986] V.M. Fyodorov, Muon registration under water in the ocean with a Cherenkov detector. Nucl. Instrum. Methods Phys. Res. **A248**, 221 (1986)

[Gaisser1974] T.K. Gaisser, Calculation of Muon yields, response functions, and sea level integral energy spectrum using recent accelerator data and Feynman scaling. J. Geophys. Res. **79**, 2281 (1974)

[Gaisser1977] T.K. Gaisser, A.M. Hillas, Reliability of the method of constant intensity cuts for reconstructing the average development of vertical showers, in *Proceedings of the 15th International Cosmic Ray Conference*, Plovdiv, vol. 8 (1977),p. 353

[Gaisser1990] T.K. Gaisser, *Cosmic Rays and Particle Physics* (Cambridge University Press, 1990)

[Galbraith1953] W. Galbraith, J.V. Jelley, Light pulses from the night sky associated with cosmic rays. Nature **171**, 349 (1953)

[Galgoczi2020] G. Galgoczi et al., Imaging by muons and their induced secondary particles: a novel technique. J. Instrum. **15**, C06014 (2020)

[Geiger1909] H. Geiger, E. Marsden, On a diffuse reflection of the α-particles. Proc. Roy. Soc. **A82**, 495 (1909)

[Geiger1928a] H. Geiger, W. Müller, Elektronenzählrohr zur Messung schwächster Aktivitäten. Naturwissenschaften **16**, 617 (1928)

[Geiger1928b] H. Geiger, W. Müller, Das Elektronenzählrohr. Phys. Z. **29**, 839 (1928)

[Geiger1929a] H. Geiger, W. Müller, Technische Bemerkungen zum Elektronenzählrohr. Phys. Z. **30**, 489 (1929)

[Geiger1929b] H. Geiger, W. Müller, Demonstration des Elektronenzählrohrs. Phys. Z. **30**, 523 (1929)

[Geitel1901] H. Geitel, Über die Elektrizitätszerstreuung in abgeschlossenen Luftmengen. Phys. Z. **2**, 116 (1901)

[George1955] E.P. George, Cosmic rays measure overburden of tunnel. Commonw. Eng. 455 (1955)

[George1956] E.P. George, G.S. Shrikantia, Observation of the energy spectrum of the cosmic radiation below ground. Nucl. Phys. **1**, 54 (1956)

[Gerontidou2021] M. Gerontidou et al., World grid of cosmic ray vertical cut-off rigidity for the last decade. Adv. Space Res. **67**, 2231 (2021)

[Giacconi1962] R. Giacconi et al., Evidence for X-rays from sources outside the solar system. Phys. Rev. Lett. **9**, 439 (1962)

[Gibbs1988] G.K. Gibbs et al., The Chicago Air Shower Array (CASA). Nucl. Instrum. Methods Phys. Res. **A264**, 67 (1988)

[Giboy2005] W.B. Giboy et al., Industrial thickness gauging with cosmic-ray muons. Radiat. Phys. Chem. **74**, 454 (2005)

[Ginzburg1964] V.L. Ginzburg, S.I. Syrovatskii, *The Origin of Cosmic Rays* (Pergamon Press, Oxford, 1964)

[Glatzmaier2015] G.A. Glatzmaier, R.S. Coe, Magnetic polarity reversals in the core, *Treatise on Geophysics* (Elsevier, 2015)

[Gockel1908] A. Gockel, Th. Wulf, Beobachtungen über die Radioaktivität der Atmosphäre im Hochgebirge. Phys. Z. **9**, 907 (1908)

[Gockel1910] A. Gockel, Luftelektrische Beobachtungen bei einer Ballonfahrt. Phys. Z. **11**, 280 (1910)

[Gockel1911] A. Gockel, Messungen der durchdringenden Strahlung bei Ballonfahrten. Phys. Z. **12**, 595 (1911)

[Gockel1915] A. Gockel, Beiträge zur Kenntnis der in der Atmosphäre vorhandenen durchdringenden Strahlung. Phys. Z. **16**, 345 (1915)

[Gockel1923] A. Gockel, Ionization unserer Atmosphäre und Sonnentätigkeit. Phys. Z. **24**, 500 (1923)

[Goldader2010] J.D. Goldader, S. Choi, An inexpensive cosmic ray detector for the classroom. Phys. Teach. **48**, 594 (2010)

[Golden1978] R.L. Golden et al., A magnetic spectrometer for cosmic ray studies. Nucl. Instr. Meth. **148**, 747 (1978)

[Golden1979a] R.L. Golden et al., Results of a recent attempt to observe antiprotons in the cosmic rays, in *Proceedings of the 16th International Cosmic Ray Conference*, Kyoto (Japan), vol. 12 (1979), p. 76

[Golden1979b] R.L. Golden et al., Evidence for the existence of cosmic ray antiprotons. Phys. Rev. Lett. **43**, 1196 (1979)

[Gomez2016] H. Gomez et al., Studies in muon tomography for archeological internal structure scanning. J. Phys: Conf. Ser. **718**, 052016 (2016)

[Grant1931] K. Grant, Observations on the penetrating radiation in the Antarctic. Nature **127**, 924 (1931)

[Gnanvo2011] K. Gnanvo et al., Imaging of high-Z material for nuclear contraband detection with a minimal prototype of a muon tomography station based on GEM detectors. Nucl. Instrum. Methods Phys. Res. **A652**, 16 (2011)

[GRAND] Web site of the GRAND Collaboration: https://www3.nd.edu/~grand/

[GRAPES-3] Web site of the GRAPES-3 Collaboration: https://grapes-3.tifr.res.in/

[Gray1980] P.C. Gray, S.I. Akasofu, L.C. Lee, A model of the heliospheric magnetic field configuration. Planet. Space Sci. **28**, 609 (1980)

[Greisen1942] K.I. Greisen, The intensities of the hard and soft components of cosmic rays as functions of altitude and zenith angle. Phys. Rev. **61**, 212 (1942)

[Greisen1948] K.I. Greisen, On neutral mesons in cosmic rays. Phys. Rev. **73**, 521 (1948)

[Greisen1966] K. Greisen, End to the cosmic-ray spectrum? Phys. Rev. Lett. **16**, 748 (1966)

[Grieder1979] P.K.F. Grieder, Average development and properties of the hadronic, muonic and electromagnetic components in showers of $10^4$ to $10^8$ GeV derived from an all-component-model calculation, in *Proceedings of the 16th International Cosmic Ray Conference*, Kyoto, vol. 9 (1979), p. 178

[Grieder2001] P.K.F. Grieder, *Cosmic Rays at Earth* (Elsevier, Amsterdam, 2001)

[Grieder2009] P.K.F. Grieder, *Extensive Air Showers* (Elsevier, Amsterdam, 2009)

[Grigorov1961] N.L. Grigorov et al., Artificial Earth Satellites **10**, 96 (1961)

[Groom2001] D.E. Groom, N.V. Mokhov, S.I. Striganov, Muon stopping-power and range tables, 10 MeV–100 TeV. At. Data Nucl. Data Tables **78**, 183 (2001)

[Grupen2008] C. Grupen, B. Shwartz, *Particle Detectors* (Cambridge University Press, 2008)

[Guan2015] M. Guan et al., *A parametrization of the cosmic ray muon flux at sea level*, arXiv:1509.06176v1 [hep-ex], 21 Sept 2015

[Guillian2007] S. Guillian et al., Observation of the anisotropy of 10 TeV primary cosmic ray nuclei flux with the Super-Kamiokande-I detector. Phys. Rev. **D75**, 062003 (2007)

[Guo2018] J. Guo et al., Measurements of Forbush decreases at Mars: both by MSL on ground and by MAVEN in orbit. Astron. Astrophys. **611**, A79 (2018)

[Gutowski2018] B. Gutowski et al., The secret chambers in the Chefren pyramid. Phys. Educ. **53**, 045011 (2018)

[Hardcastle2010] M.J. Hardcastle, Which radio galaxies can make the highest energy cosmic rays? Mon. Not. Roy. Astron. Soc. **405**, 2801 (2010)

[Haskin1959] D.M. Haskin et al., *Proceedings of the 6th International Cosmic Ray Conference*, Moscow, vol. 3 (1959), p. 123

[Heck1998] D. Heck et al., *CORSIKA: A Monte Carlo Code to Simulate Extensive Air Showers*, Report Forschungszentrum Karlsruhe FZKA-6019 (1998)

[Heisenberg1936] W. Heisenberg, On the theory of showers in cosmic radiation. Z. Phys. **101**, 533 (1936)

[Heisenberg1938] W. Heisenberg, The absorption of the penetrating components of cosmic radiation. Ann. Phys. **33**, 596 (1938)

[Herz1966] A.J. Herz, W.O. Lock, The particle detectors. I. Nuclear emulsions. CERN Courier **6**, 83 (1966)

[Hess1911] V.F. Hess, On the absorption of gamma-radiation in the atmosphere. Phys. Z. **12**, 998 (1911)

[Hess1912] V.F. Hess, Uber Beobachtungen der durchdringenden Strahlung bei sieben Freiballon-fahrten. Phys. Z. **13**, 1084 (1912)

[Hess1913] V.F. Hess, The origins of penetrating radiation. Phys. Z. **14**, 612 (1913)

[Hess1917] V.F. Hess, M. Kofler, Ganzjährige Beobachtungen der durchdringenden Strahlung auf dem Obir (2044m). Phys. Z. **18**, 585 (1917)

[Hess1926] V.F. Hess, Uber den Ursprung der Höhenstrahlung. Phys. Z. **27**, 159 (1926)

[Hess1932] V.F. Hess, The cosmic ray observatory on the Hafelekar (2300 m) near Innsbruck (Austria) and its first results. Terr. Magn. Atmos. Electr. **37**, 399 (1932)

[Hess1937] V.F. Hess, A. Demmelmair, Cosmic rays and the aurora of January 25–26. Nature **140**, 316 (1937)

[Hess1938] V.F. Hess, R. Steinmaurer, A. Demmelmair, Meteorologische und solare Einflüsse auf die Intensität der Ultrastrahlung. Nature **141**, 686 (1938)

[Hewitt1978] J.E. Hewitt et al., Ames collaborative study of cosmic ray neutrons. Health Phys. **34**, 375 (1978)

[Higashi1966] S. Higashi et al., Cosmic ray intensities under sea-water at depths down to 1400 m. Nuovo Cimento **43A**, 334 (1966)

[Hilberry1941] N. Hilberry, Extensive cosmic-ray showers and the energy distribution of primary cosmic rays. Phys. Rev. **60**, 1 (1941)

[HISPARC] Web site of the HISPARC Collaboration: https://www.hisparc.nl/en/

[Hodson1952] A.L. Hodson, The altitude variation of penetrating showers. Proc. Phys. Soc. **A65**, 702 (1952)

[Hodson1953a] A.L. Hodson, Some aspects of the altitude variation of extensive air showers. Proc. Phys. Soc. **A66**, 49 (1953)

[Hodson1953b] A.L. Hodson, Penetrating particles in extensive air showers. Proc. Phys. Soc. **A66**, 65 (1953)

[Hofstadter1948] R. Hofstadter, Alkali halide scintillation counters. Phys. Rev. **74**, 100 (1948)

[Honda1995] M. Honda et al., Calculation of the flux of atmospheric neutrinos. Phys. Rev. D **52**, 4985 (1995)

[Horandel2013] J.R. Horandel, Early cosmic ray work published in German. *AIP Conference Proceedings*, vol. 1516 (2013), p. 52

[Hsiung1934] D.S. Hsiung, A coincidence test of the corpuscular hypothesis of cosmic rays. Phys. Rev. **46**, 653 (1934)

[Ichimura1993] M. Ichimura et al., Observation of heavy cosmic-ray primaries over the wide energy range from ∼100 GeV/particle to ∼100 TeV/particle: is the celebrated '"knee"' actually so prominent? Phys. Rev. D **48**, 1949 (1993)

[Ivanov2009] A.A. Ivanov et al., Measuring extensive air showers with Cherenkov light detectors of the Yakutsk array: the energy spectrum of cosmic rays. New J. Phys. **11**, 065008 (2009)

[IZMIRAN] Web site of the Moscow Neutron Monitor: http://cr0.izmiran.ru/mosc/

[JACEE1999] M.L. Cherry (JACEE Collaboration), Where is the bend in the cosmic ray proton spectrum?, in *Proceedings of the 26th International Cosmic Ray Conference*, Salt Lake City, USA, vol. 3 (1999), p. 187

[Janeselli1968] R. Janeselli, Doppia oscillazione diurna della pressione atmosferica e del gradiente verticale del campo elettromagnetico. Ann. Geophys. **21**, 305 (1968)

[Janossy1949] L. Janossy, C.B.A. McCusker, The nature of penetrating particles in air showers. Nature **163**, 182 (1949)

[Jelley1955] J.V. Jelley, Cherenkov radiation and its application. Br. J. Appl. Phys. **6**, 227 (1955)

[Jelley1965] J.V. Jelley et al., Radio pulses from extensive cosmic ray air showers. Nature **205**, 327 (1965)

[Jelley1981] J.V. Jelley, The atmospheric Cherenkov technique in γ-ray astronomy: the early days. Philos. Trans. Roy. Soc. Lond. **A301**, 611 (1981)

[Johnson1933a] T.H. Johnson, J. Street, A circuit for recording multiply-coincident discharges of Geiger-Müller counters. J. Franklin Inst. **215**, 239 (1933)

[Johnson1933b] T.H. Johnson, The azimuthal asymmetry of the cosmic radiation. Phys. Rev. **43**, 834 (1933)

[Johnson1934] T.H. Johnson, Coincidence counter studies of the corpuscular component of the cosmic radiation. Phys. Rev. **45**, 569 (1934)

[Johnson1935] T.H. Johnson, Progress of the directional survey of the cosmic ray intensities and its application to the analysis of the primary cosmic radiation. Phys. Rev. **48**, 287 (1935)

[Johnson1938] T.H. Johnson, Cosmic ray intensity and geomagnetic effects. Rev. Mod. Phys. **10**, 193 (1938)

[Johnson1941] T.H. Johnson, The East-West asymmetry of the cosmic radiation in high latitudes and the excess of positive mesotrons. Phys. Rev. **59**, 11 (1941)

[Johnston1967] M. Johnston (ed.) *The Cosmos of Arthur Holly Compton* (Knopf, 1967)

[Joliot1931] F. Joliot, Sur l'excitation des rayons γ nucléaires du bore par les particules α. Énergie quantique du rayonnement γ du polonium. Compte Rendus Séances Academie Science Paris **193**, 1415 (1931)

[Jones1965] J.K. Jones, The measurement of the time variation of small showers, in *Proceedings of the 9th International Conference on Cosmic Rays*, London, vol. 2 (1965), p. 787

[Jones1991] F.C. Jones, D.C. Ellison, The plasma physics of shock acceleration. Space Sci. Rev. **58**, 259 (1991)

[Jones1994] F.C. Jones, A theoretical review of diffusive shock acceleration. Astrophys. J. **90**, 561 (1994)

[Jonkmans2013] G. Jonkmans et al., Nuclear waste imaging and spent fuel verification by muon tomography. Ann. Nucl. Energy **53**, 267 (2013)

[Jordan1949] W.H. Jordan, P.R. Bell, Scintillation counters. Nucleonics **5**, 30 (1949)

[Jourde2016] K. Jourde et al., Monitoring temporal opacity fluctuations of large structures with muon tomography: a calibration experiment using a water tower tank. Sci. Rep. **6**, 23054 (2016)

[Judge1965] R.J.R. Judge, W.F. Nash, Measurement of the muon flux at various zenith angles. Nuovo Cimento **35**, 999 (1965)

[Kahlert2011] H. Kahlert, H. Krenn, L. Wilmes, Echophysics, the first European Center for the History of Physics in Poellau, Austria. Europhys. News **42**, 28 (2011)

[Kamata1958] K. Kamata, J. Nishimura, The lateral and the angular structure functions of electron showers. Prog. Theor. Phys. Suppl. **6**, 93 (1958)

[Kampert2012] K. Kampert, A. Watson, Extensive air showers and ultra-high-energy cosmic rays: a historical review. Eur. Phys. J. **H37**, 359 (2012)

[Karmakar1973] N. Karmakar et al., Measurements of absolute intensities of cosmic-ray muons in the vertical and greatly inclined directions at geomagnetic latitudes 16 °N. Nuovo Cimento **B17**, 173 (1973)

[Kedar2012] S. Kedar et al., Low cost, low power, passive muon telescope for interrogating Martian subsurface. Concepts Approach Mars Expl. **1679**, 4150 (2012)

[Kedar2013] S. Kedar et al., Muon radiography for exploration of Mars geology. Geosci. Instrum. Methods Data Syst. **2**, 157 (2013)

[Keil1960] E. Keil, E. Zeitler, W. Zinn, Zur Einfach- und Mehrfachstreuung geladener Teilchen. Z. Naturforsch. **A15**, 1031 (1960)

[Keizer2018] F. Keizer et al., A compact, high resolution tracker for cosmic ray muon scattering tomography using semiconductor sensors. J. Instrum. **13**, P10028 (2018)

[Kinoshita1910] S. Kinoshita, The photographic action of the α-particles emitted from radioactive substance. Proc. Roy. Soc. **A83**, 432 (1910)

[Kinoshita1915] S. Kinoshita, H. Ikeuti, The tracks of alpha particles in sensitive photographic films. Philos. Mag. **29**, 420 (1915)

[Kiraly2013] P. Kiraly, Two centenaries: the discovery of cosmic rays and the birth of Lajos Janossy. J. Phys: Conf. Ser. **409**, 012001 (2013)

[Kirby2011] J. Kirby et al., Role of sulphuric acid, ammonia and galactic cosmic rays in atmospheric aerosol nucleation. Nature **476**, 429 (2011)

[Klinger2015] J. Klinger et al., Simulation of muon radiography for monitoring $CO_2$ stored in a geological reservoir. Int. J. Greenh. Gas Control **42**, 644 (2015)

[Knezevic2019] J. Knezevic et al., Simple coincidence technique for cosmic-ray intensity exploration via low energy photon detection. Appl. Radiat. Isot. **151**, 157 (2019)

[Knoll2000] G.F. Knoll, *Radiation Detection and Measurements* (Wiley, New York, 2000)

[Kocharian1956] N.M. Kocharian et al., Meson component of the cosmic radiation at an altitude of 3200 m above sea level. Sov. Phys. JETP **3**, 350 (1956)

[Kocharian1959] N.M. Kocharian et al., Energy spectra and nuclear interactions of cosmic ray particles. Sov. Phys. JETP **8**, 933 (1959)

[Kolhörster1913a] W. Kolhörster, Uber eine Neukonstruktion des Apparates zur Messung der durchdringenden Strahlung nach Wulf und die damit bisher gewonnen Ergebnisse. Phys. Z. **14**, 1066 (1913)

[Kolhörster1913b] W. Kolhörster, Messungen der durchdringenden strahlung im freiballon in grösseren höhen. Phys. Z. **14**, 1153 (1913)

[Kolhörster1914] W. Kolhörster, Messungen der durchdringenden Strahlungen bis in Höhen von 9300 m. Verh. Dtsch. Phys. Ges. **16**, 719 (1914)

[Kolhörster1926] W. Kolhörster, Bemerkungen zu der Arbeit von R. A. Millikan: Kurzwellige Strahlen kosmischen Ursprungs. Ann. Phys. **14**, 621 (1926)

[Kolhörster1933] W. Kolhörster, The hardest cosmic rays and the electric charge of the Earth. Nature **132**, 407 (1933)

[Kolhörster1934] W. Kolhörster, Cosmic rays under 600 m of water. Nature **133**, 419 (1934)

[Kolhörster1938] W. Kolhörster et al., Gekoppelte Höhenstrahlen. Naturwissenschaften **26**, 576 (1938)

[Korff1952] S. Korff, The world's high altitude laboratories. Phys. Today **5**, 28 (1952)

[Korff1982] S. Korff, High altitude observatories for cosmic rays and other purposes, in [Sekido1982]

[Korff2013] S. Korff, How the Geiger counter started to crackle: electrical counting methods in early radioactivity research. Ann. Phys. **A88–A92**, 525 (2013)

[Kuhn1962] T.S. Kuhn, *The Structure of Scientific Revolutions* (University of Chicago Press, 1962)

[Kraushaar1962] W.L. Kraushaar, G.W. Clark, Search for primary cosmic gamma rays with the satellite Explorer XI. Phys. Rev. Lett. **8**, 106 (1962)

[Kraybill1948] H.I. Kraybill, Altitude dependence of high energy atmospheric showers. Phys. Rev. **73**, 632 (1948)

[Kraybill1949] H.I. Kraybill, Extensive air showers at high altitudes. Phys. Rev. **76**, 1092 (1949)

[Kraybill1954a] H.I. Kraybill, Density of extensive air showers at airplane altitudes. Phys. Rev. **93**, 1360 (1954)

[Kraybill1954b] H.I. Kraybill, The altitude and angular dependence of cosmic ray showers. Phys. Rev. **93**, 1362 (1954)

[Krebs1941] A. Krebs, Ein Demonstrationsversuch zur Emanationsdiffusion. Ann. Phys. **431**, 330 (1941)

[Krebs1955] A.T. Krebs, Early history of the scintillation counter. Science **122**, 17 (1955)

[Kudryvtsev2012] A. Kudryvtsev et al., Monitoring subsurface $CO_2$ injection and security of storage using muon tomography. Int. J. Greenh. Gas Control **11**, 21 (2012)

[Kulikov1958] G.V. Kulikov, G.B. Khristiansen, On the size spectrum of extensive air showers. Sov. Phys. JETP **35**, 441 (1959)

[Kuzmin1968] V.A. Kuzmin, G.T. Zatsepin, On cosmic ray interactions with photons. Can. J. Phys. **46**, S617 (1968)

[LaRocca2005] P. La Rocca, F. Riggi, *Analysis of Neutron and Muon Counting During a Forbush Decrease.* Report INFN/AE-05/2, 4 April 2005

[LaRocca2018] P. La Rocca, D. Lo Presti, F. Riggi, Cosmic ray muons as penetrating probes to explore the world around us, in *Cosmic Rays*, ed. by Z. Szadkowski (InTechOpen, 2018). https://doi.org/10.5772/intechopen.75426

[LaRocca2019] P. La Rocca et al. (The EEE Collaboration), Search for coincident air showers over large-scale distances with the EEE network. Nucl. Phys. **B306–308**, 175 (2019)

[LaRocca2020a] P. La Rocca et al. (The EEE Collaboration), Scientific and educational aspects of the EEE Project. J. Phys. G: Conf. Ser. **1561**, 012012 (2020)

[LaRocca2020b] P. La Rocca et al. (The EEE Collaboration), Search for long distance time correlations between cosmic air showers with the MRPC telescopes of the EEE network, in *Proceedings of Science POS (EPS-HEP2019)*, p. 051

[LaRocca2020c] P. La Rocca et al., First commissioning measurements with a reconfigurable cosmic ray mini-array. J. Instrum. **15**, T02003 (2020)

[Lattes1947a] C.M.G. Lattes, G.P.S. Occhialini, C.F. Powell, Observations of the tracks of slow mesons in photographic emulsions, Part I. Nature **160**, 453 (1947)

[Lattes1947b] C.M.G. Lattes, G.P.S. Occhialini, C.F. Powell, Observations of the tracks of slow mesons in photographic emulsions, Part II. Nature **160**, 486 (1947)

[Lawrence1991] M.A. Lawrence, R.J.O. Reid, A.A. Watson, The cosmic ray energy spectrum above $4 \times 10^{17}$ eV as measured by the Haverah Park array. J. Phys. **G17**, 733 (1991)

[Lehtipalo2016] K. Lehtipalo et al., The effect of acid-base clustering and ions on the growth of atmospheric nano-particles. Nat. Commun. **7**, 11594 (2016)

[Lemaitre1933] G. Lemaitre, S. Vallarta, On Compton's latitude effect of cosmic radiation. Phys. Rev. **43**, 87 (1933)

[Lemaitre1936a] G. Lemaitre, S. Vallarta, On the geomagnetic analysis of cosmic radiation. Phys. Rev. **49**, 719 (1936)

[Lemaitre1936b] G. Lemaitre, S. Vallarta, On the allowed cone of cosmic radiation. Phys. Rev. **50**, 493 (1936)

[Leo1987] W.R. Leo, *Techniques for Nuclear and Particle Physics Experiments* (Springer, Berlin/Heidelberg/New York, 1987)

[Leone2011] M. Leone, Particles that take photographs of themselves: the emergence of the triggered cloud chamber technique in early 1930s cosmic ray physics. Am. J. Phys. **79**, 454 (2011)

[Leroy2004] C. Leroy, P.G. Rancoita, *Principles of Radiation Interaction in Matter and Detection* (World Scientific Publishing Company, 2004)

[Lesparre2010] N. Lesparre et al., Geophysical muon imaging: feasibility and limits. Geophys. J. Int. **183**, 1348 (2010)

[Lewis1948] H.V. Lewis, J.B. Oppenheimer, S.A. Wouthuysen, The multiple production of mesons. Phys. Rev. **73**, 127 (1948)

[Libby1932] W.F. Libby, Simple amplifier for Geiger-Müller counter. Phys. Rev. **42**, 440 (1932)

[Libby1949a] W.F. Libby et al., Age determination by radiocarbon content: world-wide assay of natural radiocarbon. Science **109**, 227 (1949)

[Libby1949b] J.R. Arnold, W.F. Libby, Age determination by radiocarbon content: checks with samples of know ages. Science **110**, 678 (1949)

[Linke1904] F. Linke, Luftelektrische Messungen bei zwölf Ballonfahrten, Abhandlungen der Gesellschaft der Wissenschaften in Göttingen. Mathematisch-Physikalische Klasse **3**, 1 (1904)

[Linsley1961] J. Linsley, L. Scarsi, B. Rossi, Extremely energetic cosmic ray event. Phys. Rev. Lett. **6**, 485 (1961)

[Linsley1963] J. Linsley, Evidence for a primary cosmic ray particle with energy $10^{20}$ eV. Phys. Rev. Lett. **10**, 146 (1963)

[Linsley1977] J. Linsley, in *Proceedings of the 15th International Conference on Cosmic Rays*, Plovdiv, vol. 8 (1977), p. 207

[Longair2014] M. Longair, C. T. R. Wilson and the cloud chamber. Astropart. Phys. **53**, 55 (2014)

[Lorenz2012] E. Lorenz, R. Wagner, Very high energy gamma ray astronomy. Eur. Phys. J. **H37**, 459 (2012)

[LoPresti2018] D. Lo Presti et al., The MEV project: design and testing of a new high-resolution telescope for muography of Etna Volcano. Nucl. Instrum. Methods Phys. Res. A**904**, 195 (2018)

[LoPresti2020] D. Lo Presti et al., Muographic monitoring of the volcano-tectonic evolution of Mount Etna. Sci. Rep. **10**, 11351 (2020)

[Lovell1939] A.C.B. Lovell, J.G. Wilson, Investigation of cosmic ray showers of atmospheric origin using two cloud chambers. Nature **144**, 863 (1939)

[Lowder1991] D.M. Lowder et al., Observation of muons using the polar ice cap as a Cherenkov detector. Nature **144**, 863 (1939)

[Maghrabi2021] A. Maghrabi et al., Charged particle detector-related activities of the KACST radiation laboratory. J. Radiat. Res. Appl. Sci. **14**, 111 (2021)

[Mahon2013] D. Mahon et al., A prototype scintillating-fibre tracker for the cosmic-ray muon tomography of legacy nuclear waste containers. Nucl. Instrum. Methods Phys. Res. **A732**, 408 (2013)

[Malkov2001] M.A. Malkov, L. O'C Drury, Nonlinear theory of diffusive acceleration of particles by shock waves. Rep. Prog. Phys. **64**, 429 (2001)

[Mandeville1950a] C.E. Mandeville, H.O. Albrecht, Detection of scintillations from crystals with a photosensitive Geiger-Mueller counter. Phys. Rev. **79**, 1010 (1950)

[Mandeville1950b] C.E. Mandeville, H.O. Albrecht, Detection of beta-induced scintillations from crystals with a photosensitive Geiger-Mueller counter. Phys. Rev. **80**, 117 (1950)

[Mandeville1950c] C.E. Mandeville, H.O. Albrecht, Detection of gamma-induced scintillations from crystals with a photosensitive Geiger-Mueller counter. Phys. Rev. **81**, 164 (1950)

[Mandeville1950d] C.E. Mandeville, H.O. Albrecht, Crystals for the scintillation Geiger counter. Phys. Rev. **81**, 163 (1950)

[Mandeville1950e] C.E. Mandeville, M.V. Scherb, Photosensitive Geiger counters: their applications. Nucleonics **7**, 34 (1950)

[Marshall1947a] F.H. Marshall et al., The photomultiplier X-ray detector. Rev. Sci. Instrum. **18**, 504 (1947)

[Marshall1947b] F.H. Marshall, J.W. Coltman, The photomultiplier radiation detector. Phys. Rev. **72**, 528 (1947)

[Marteau2012] J. Marteau et al., Muon tomography applied to geosciences and volcanology. Nucl. Instrum. Methods Phys. Res. **A695**, 23 (2012)

[Maurin2014] D. Maurin et al., A database of charged cosmic rays. Astron. Astrophys. **A32**, 569 (2014)

[Mayer1913] F. Mayer, Über die Zerstreuung der α-Strahlen. Ann. Phys. **41**, 931 (1913)

[Mayneord1950] W.V. Mayneord, E.H. Belcher, Scintillation counting and its medical applications. Br. Radiol. Suppl. **2–3**, 259 (1950)

[Maze1938] R. Maze, Etude d'un appareil a grand pouvoir de resolution pour rayons cosmiques. J. Phys. Radium **9**, 162 (1938)

[Maze1948] R. Maze et al., High altitude measurements on extensive showers. Phys. Rev. **73**, 418 (1948)

[McLennan1903a] J.C. McLennan, E.F. Burton, Some experiments on the electrical conductivity of atmospheric air. Phys. Rev. **16**, 184 (1903)

[McLennan1903b] J.C. MacLennan, E.F. Burton, Phys. Z. **4**, 553 (1903)

[Meitner1933] L. Meitner, K. Philipp, Die bei neutronenanregung auftretenden elektronenbahnen. Naturwissenschaften **24**, 468 (1933)

[Menchaca2011] A. Menchaca-Rocha, Searching for cavities in the Teotihuacan Pyramid of the Sun using cosmic muon experiments and instrumentation, in *Proceedings of the 32nd International Cosmic Ray Conference, Beijing (China)*, vol. 4 (2011), p. 325

[Mendonca2019] R.R.S. Mendonca et al., Analysis of Cosmic Rays atmospheric effects and their relationships to cutoff rigidity and zenith angle using global muon detector network data. J. Geophys. Res. Space Phys. **134**, 9791 (2019)

[Menzel1948] D.H. Menzel, W.W. Salisbury, The origin of cosmic rays. Nucleonics **2**, 67 (1948)

[Meyer1961] P. Meyer, R. Vogt, Electrons in the primary cosmic radiation. Phys. Rev. Lett. **6**, 193 (1961)

[Meyer1970] B.S. Meyer et al., Cosmic ray muon intensity deep underground versus depth. Phys. Rev. D **1**, 2229 (1970)

[Michl1912] W. Michl, Akad Wiss. Wien **121**, 1431 (1912)

[Millikan1923] R.A. Millikan, I.S. Bowen, Penetrating radiation at high altitudes. Phys. Rev. **22**, 198 (1923)

[Millikan1925] R.A. Millikan, High frequency rays of cosmic origin. Nature **116**, 823 (1925)

[Millikan1926a] R.A. Millikan, I.S. Bowen, High frequency rays of cosmic origin. I. Sounding balloon observations at extreme altitude. Phys. Rev. **27**, 353 (1926)

[Millikan1926b] R.A. Millikan, R.M. Otis, High frequency rays of cosmic origin. II. Mountain peak and airplane observations. Phys. Rev. **27**, 645 (1926)

[Millikan1926c] R.A. Millikan, G.H. Cameron, High frequency rays of cosmic origin. III. Measurements in snow-fed lakes at high altitudes. Phys. Rev, **28**, 851 (1926)

[Millikan1928a] R.A. Millikan, G.H. Cameron, High altitude tests on the geographical, directional and spectral distribution of cosmic rays. Phys. Rev. **31**, 163 (1928)

[Millikan1928b] R.A. Millikan, G.H. Cameron, The origin of the cosmic rays. Phys. Rev. **32**, 533 (1928)

[Millikan1928c] R.A. Millikan, G.H. Cameron, New precision in cosmic ray measurements, yielding extension of spectrum and indication of bands. Phys. Rev. **31**, 921 (1928)

[Millikan1930a] R.A. Millikan, History of research in cosmic rays. Nature **126**, 14 (1930)

[Millikan1930b] R.A. Millikan, On the question of the constancy of the cosmic radiation and the relation of these rays to meteorology. Phys. Rev. **36**, 1595 (1930)

[Millikan1934] I.S. Bowen, R.A. Millikan, H.V. Neher, A very high altitude survey of the effect of latitude upon cosmic-ray intensities and an attempt at a general interpretation of cosmic-ray phenomena. Phys. Rev. **46**, 641 (1934)

[Millikan1935a] R.A. Millikan, *Electrons, Protons, Photons, Neutrons and Cosmic Rays* (Chicago, 1935)

[Millikan1935b] R.A. Millikan, H.V. Neher, The equatorial longitude effect in cosmic rays. Phys. Rev. **47**, 205 (1935)

[Millikan1936] R.A. Millikan, H.V. Neher, A precision world survey of sea level cosmic ray intensities. Phys. Rev. **50**, 15 (1936)

[Millikan1938a] I.S. Bowen, R.A. Millikan, H.V. Neher, New evidence as to the nature of the incoming cosmic rays, their absorbability in the atmosphere, and the secondary character of the penetrating rays found in such abundance at sea level and below. Phys. Rev. **53**, 217 (1938)

[Millikan1938b] I.S. Bowen, R.A. Millikan, H.V. Neher, New light on the nature and origin of the incoming cosmic rays. Phys. Rev. **53**, 855 (1938)

[Miyake1963] S. Miyake, Empirical formula for range spectrum of cosmic ray μ-mesons at sea level. J. Phys. Soc. Jpn. **18**, 1093 (1963)

[Miyake1973] S. Miyake, Underground muon angular distribution, in *Proceedings of the 13th International Conference on Cosmic Ray Physics*, Denver (USA), vol. 5 (1973), p. 3638

[Mizutani1979] K. Mizutani et al., Energy spectrum of cosmic rays deep underground, in *Proceedings of the 16th International Cosmic Ray Conference*, Tokyo, vol. 10 (1979), p. 40

[Mohanty2016] P.K. Mohanty et al., Transient weakening of Earth's magnetic shield probed by a cosmic ray burst. Phys. Rev. Lett. **117**, 171101 (2016)

[Montgomery1936] C.G. Montgomery, D.D. Montgomery, W.E. Ramsey, W.F.G. Swann, A search for protons in the primary cosmic-ray beam. Phys. Rev. **50**, 403 (1936)

[Morales2019] J.A. Morales-Soto et al., The lateral distribution function of cosmic-ray induced air showers studied with the HAWC observatory. *Proceedings of the 36th International Cosmic Ray Conference*, Madison (USA), POS (ICRC2019), p. 358

[Morishima2013] K. Morishima et al., Development of an automated nuclear emulsion analyzing system. Radiat. Meas. **50**, 237 (2013)

[Morishima2017] K. Morishima et al., Discovery of a big void in Khufu's pyramid by observation of cosmic-ray muons. Nature **552**, 386 (2017)

[Morrison1954] P. Morrison, S. Olbert, B. Rossi, The origin of cosmic rays. Phys. Rev. **94**, 440 (1954)

[Morton1949] G.A. Morton, J.A. Mitchell, Performance of 931-A type multiplier as a scintillation counter. Nucleonics **4**, 6 (1949)

[MPI] https://www.mpi-hd.mpg.de/hfm/CosmicRay/CosmicRaySites.html

[Mrdja2016] D. Mrdja et al., First cosmic ray images of bones and soft tissues. Europhys. Lett. **116**, 48003 (2016)

[Murdoch1960] H.S. Murdoch et al., The Sydney cosmic ray spectrometer, in *Proceedings of the 6th International Cosmic Ray Conference*, Moscow, vol. 1 (1960), p. 304

[Miyazaki1949] Y. Miyazaki, Cosmic rays at a great depth. Phys. Rev. **76**, 1733 (1949)

[Myssowsky1925] L. Myssowsky, L. Tuwim, Versuche über die Absorption der Höhenstrahlung im Wasser. Z. Phys. **35**, 299 (1926)

[Myssowsky1926] L. Myssowsky, L. Tuwim, Unregelmäßige Intensitätsschwankungen der Höhenstrahlung in geringer Seehöhe. Z. Phys. **39**, 146 (1926)

[Myssowsky1927] L. Myssowsky, L. Tuwim, Absorptionskurve der Höhenstrhlung im Wasser. Z. Phys. **44**, 369 (1927)

[Myssowsky1928] L. Myssowsky, L. Tuwim, Absorption in Blei, sekundäre Strahlen und Wellenlänge der Höhenstrahlung. Z. Phys. **50**, 273 (1928)

[Nagamine1995] K. Nagamine et al., Method of probing inner structure of geophysical substance with the horizontal cosmic ray muons and possible application to volcanic eruption prediction. Nucl. Instrum. Methods Phys. Res. **A356**, 585 (1995)

[NALTA] Web site of the NALTA Collaboration: http://neutrino.phys.washington.edu/~walta/NALTA.html

[Nash1956] W.F. Nash, A.J. Pointon, The momentum spectrum of μ-mesons at a depth of 40 m water equivalent. Proc. Phys. Soc. **A69**, 725 (1956)

[Neddermayer1937] S.H. Neddermayer, C.D. Anderson, Note on the nature of cosmic ray particles. Phys. Rev. **51**, 884 (1937)

[Neddermayer1938] S.H. Neddermayer, C.D. Anderson, Cosmic ray particles of intermediate mass. Phys. Rev. **54**, 88 (1938)

[Neher1940] H.V. Neher, W.H. Pickering, An attempt to measure the latitude effect of extensive cosmic ray showers. Phys. Rev. **58**, 665 (1940)

[Nesvizhevsky2017] V. Nesvizhevsky, J. Villain, The discovery of the neutron and its consequences (1930–1940). C. R. Phys. **18**, 592 (2017)

[Niederleithinger2021] E. Niederleithinger et al., Muon tomography of the interior of a reinforced concrete block: first experimental proof of concept. J. Nondestr. Eval. **40**, 65 (2021)

[Nishimura2013] J. Nishimura, The birth of cosmic ray work in Japan. AIP Conf. Proc. **1516**, 25 (2013)

[Nishina1937] Y. Nishina, M. Takeuchi, T. Ichimiya, On the nature of cosmic-ray particles. Phys. Rev. **52**, 1198 (1937)

[Nishina1941] Y. Nishina et al., Cosmic rays at a depth equivalent to 1400 meters of water. Phys. Rev. **59**, 401 (1941)

[NIST] https://www.nist.gov/pml/x-ray-and-gamma-ray-data

[NOAA] National Oceanic and Atmospheric Administration (NOAA) Web site: ngdc.noaa.gov

[NRIC] National Radiation Instrument Catalog, http://www.national-radiation-instrument-catalog.com/

[Ochi2003] N. Ochi et al., The status and future prospect of the LAAS project, in *Proceedings of the 28th International Conference on Cosmic Ray Physics*, Tsukuba (Japan), vol. 2 (2003), p. 1005

[Olah2018] L. Olah et al., High-definition and low noise muography of the Sakurajima volcano with gaseous tracking detectors. Sci. Rep. **8**, 1 (2018)

[Oppenheimer1933] J.R. Oppehneimer, M.S. Plesset, On the production of the positive electron. Phys. Rev. **43**, 53 (1933)

[ORAU] Oak Ridge Associated Universities Museum of Radiation and Radioactivity, https://www.orau.org/health-physics-museum/index.html

[Otis1923a] R.M. Otis, The variation of penetrating radiation with altitude. Phys. Rev. **22**, 198 (1923)

[Otis1923b] R.M. Otis, The penetrating radiation on Mt. Whitney. Phys. Rev. **22**, 199 (1923)

[Otis1924] R.M. Otis, R.A. Millikan, The source of penetrating radiation found in the earth's atmosphere. Phys. Rev. **23**, 778 (1924)

[OULU] Web site of the Oulu Neutron Monitor: http://cosmicrays.oulu.fi/

[Pacini1910] D. Pacini, Penetrating radiation on the sea. Le Radium **8**, 307 (1910)

[Pacini1912] D. Pacini, Penetrating radiation at the surface of and in water. Nuovo Cimento **6**, 93 (1912)

[Pal2012] S. Pal et al., Measurement of the integrated flux of cosmic ray muons at sea level using the INO-ICAL prototype detector. J. Cosmol. Astropart. Phys. **07**, 033 (2012)

[PDG] The Review of Particle Physics, R.L. Workman et al. (Particle Data Group), Prog. Theor. Exp. Phys. 083C01 (2022). PDG Web Site: pdg.lbl.gov

[Penzias1965] A.A. Penzias, R.W. Wilson, A measurement of the excess antenna temperature at 4080 Mc/s. Astrophys J **142**, 419 (1965)

[Perry2013] J. Perry et al., Imaging a nuclear reactor using cosmic ray muons. J. Appl. Phys. **113**, 184909 (2013)

[Peruzzi2007] G. Peruzzi, S. Talas, The Italian contributions to cosmic ray physics from Bruno Rossi to the G-stack. A new window into the inexhaustible wealth of nature. La Rivista del Nuovo Cimento **30**, 197 (2007)

[Pesente2009] S. Pesente et al., First results on material identification and imaging with a large-volume muon tomography prototype. Nucl. Instrum. Methods Phys. Res. **A604**, 738 (2009)

[Pethuraj2017] S. Pethuraj et al., Measurement of cosmic muon angular distribution and vertical integrated flux by 2m × 2 m RPC stack at IICHEP-Madhurai. J. Cosmol. Astropart. Phys. **9**, 021 (2017)

[Piccard1932] A. Piccard, E. Stahel, P. Kipfer, Messung der Ultrastrahlung in 16000 m Höhe. Naturwissenschaften **20**, 592 (1932)

[Pinto2020a] C. Pinto et al., A low cost reconfigurable mini-array facility for (under) graduate studies in cosmic ray physics. Proc. Sci. (POS-HEPS2019) **438** (2020)

[Pinto2020b] C. Pinto et al. (The EEE Collaboration), Measurements with cosmic muons to monitor the stability of a civil building on a long time-scale. J. Instrum. **15**, C03058 (2020)

[Pfotzer1936] G. Pfotzer, Dreifachkoinzidenzen der Ultrastrahlung aus vertikaler Richtung in der StratosphÄre. Z. Phys. **102**, 23 (1966)

[Pfotzer1972] G. Pfotzer, History of the use of balloons in scientific experiments. Space Sci. Rev. **13**, 199 (1972)

[Pfotzer1982] G. Pfotzer, Early evolution of coincidence counting, a fundamental method in cosmic ray physics, in [Sekido1982]

[Poluianov2017] S.V. Poluianov et al., GLE and sub-GLE redefinition in the light of high-altitude polar neutron monitors. Sol. Phys. **292**, 176 (2017)

[Porter1958] N.A. Porter et al., Observations on extensive air showers VII. The lateral distribution of energy in the electron-photon component. Philos. Mag. **3**, 826 (1958)

[Poulson2017] D. Poulson et al., Cosmic ray muon computed tomography of spent nuclear fuel in dry storage casks. Nucl. Instrum. Methods Phys. Res. **A842**, 48 (2017)

[Powell1950] C.F. Powell, Mesons. Rep. Prog. Phys. **13**, 350 (1950)

[Powell1959] C.F. Powell, P.H. Fowler, D.H. Perkins, *The Study of Elementary Particles by the Photographic Method* (Pergamon Press, New York, 1959)

[Pringle1950] R.W. Pringle, The scintillation counter. Nature **166**, 11 (1950)

[Procureur2023] S. Procureur et al., Precise characterization of a corridor-shaped structure in Khufu's Pyramid by observation of cosmic-ray muons. Nature Comm. **14**, 1144 (2023)

[Pryke2001] C.L. Pryke, A comparative study of the depth of maximum of simulated air shower longitudinal profiles. Astropart. Phys. **14**, 319 (2001)

[Pyle1999] R. Pyle et al., The use of $^3$He tubes in a neutron monitor latitude survey, in *Proceedings of the 26th International Cosmic Ray Conference*, Salt Lake City (USA), vol. 7 (1999), p. 386

[RamanaMurthy1972] P.V. Ramana Murthy, A. Subramanian, Test of scale invariance in pion production at high energies using cosmic ray primary nucleon and sea level muon intensities. Phys. Lett. **B39**, 646 (1972)

[Rasetti1941] F. Rasetti, Disintegration of slow mesotrons. Phys. Rev. **60**, 198 (1941)

[Ravel2013] O. Ravel, Early cosmic ray research in France. AIP Conf. Proc. **1516**, 67 (2013)

[Regener1932a] E. Regener, Über das Spektrum der Ultrastrahlung. Z. Phys. **74**, 433 (1932)

[Regener1932b] E. Regener, Intensity of cosmic radiation in the high atmosphere. Nature **130**, 364 (1932)

[Regener1932c] E. Regener, Messung der Ultrastrahlung in der Stratosphäre. Naturwissenschaften **20**, 695 (1932)

[Regener1933] E. Regener, Die Absorptionskurve der Ultrastrahlung und ihre Deutung. Phys. Z. **34**, 306 (1933)

[Reidy1978] J.J. Reidy et al., Use of muonic X rays for nondestructive analysis of bulk samples for low Z constituents. Anal. Chem. **50**, 40 (1978)

[Reinganum1911] M. Reinganum, Streuung und photographische Wirkung der α-Strahlen. Phys. Z. **12**, 1076 (1911)

[Riadigos2020] I. Riadigos et al., Atmospheric temperature effects in secondary cosmic rays observed with a 2 m$^2$ ground based tPRC detector. Earth Space Sci. **7**, 1131 (2020)

[Richtmeyer1949] R.D. Richtmeyer, E. Teller, On the origin of cosmic rays. Phys. Rev. **75**, 1729 (1949)

[Riggi2010] S. Riggi et al., GEANT4 simulation of plastic scintillator strips with embedded optical fibers for a prototype of tomographic system. Nucl. Instrum. Methods Phys. Res. **A624**, 583 (2010)

[Riggi2014] F. Riggi et al., An extensive air shower trigger station for the Muon Portal detector. Nucl. Instrum. Methods Phys. Res. **A764**, 142 (2014)

[Riggi2017] F. Riggi et al. (The EEE Collaboration), Time and orientation long-distance correlations between extensive air showers detected by the MRPC telescopes of the EEE Project. Il Nuovo Cimento **C40**, 196 (2017)

[Riggi2018] F. Riggi et al., The Muon Portal project: commissioning of the full detector and first results. Nucl. Instrum. Methods Phys. Res. **A912**, 16 (2018)

[Riggi2020] F. Riggi et al., Investigation of the cosmic ray angular distribution and the East-West effect near the top of Etna volcano with the MEV telescope. Eur. Phys. J. Plus **135**, 280 (2020)

[Riggi2021a] F. Riggi et al., A modular telescope facility to investigate the cosmic ray decoherence curve. J. Instrum. **16**, T08006 (2021)

[Riggi2021b] F. Riggi et al., Multiparametric approach to the assessment of muon tomographic results for the inspection of a full-scale container. Eur. Phys. J. Plus **136**, 139 (2021)

[Rogers1984] I.W. Rogers, M. Tristam, The absolute depth-intensity curve for cosmic ray muons underwater and the integral sea-level momentum spectrum in the range 1–100 GeV/c. J. Phys. G: Nucl. Part. Phys. **10**, 983 (1984)

[Rossi1930a] B. Rossi, Method of registering multiple simultaneous impulses of several Geiger counters. Nature **125**, 636 (1930)

[Rossi1930b] B. Rossi, On the magnetic deflection of cosmic rays. Phys. Rev. **36**, 606 (1930)

[Rossi1931a] B. Rossi, Magnetic experiments on the cosmic rays. Nature **128**, 300 (1931)

[Rossi1931b] B. Rossi, Measurements on the absorption of the penetrating corpuscular rays coming from inclined directions. Nature **128**, 408 (1931)

[Rossi1931c] B. Rossi, Ricerche sull'azione del campo magnetico terrestre sopra i corpuscoli della radiazione penetrante. Nuovo Cimento **8**, 85 (1931)

[Rossi1932a] B. Rossi, Absorptionsmessungen der durchdringenden Korpuskularstrahlung in einem Meter Blei. Naturwissenschaften **20**, 65 (1932)

[Rossi1932b] B. Rossi, Nachweis einer Sekundärstrahlung der durchdringenden Korpuskularstrahlung. Phys. Z. **33**, 304 (1932)

[Rossi1932c] B. Rossi, Ricerche sulla radiazione secondaria della radiazione corpuscolare pene-trante. Ric. Sci. **3**, 234 (1932)

[Rossi1932d] B. Rossi, La curva di assorbimento della radiazione corpuscolare penetrante. Ric. Sci. **3**, 435 (1932)

[Rossi1933a] B. Rossi, Über die Eigenschaften der durchdringenden Korpuskularstrahlung in Meeresniveau. Z. Phys. **82**, 151 (1933)

[Rossi1933b] B. Rossi, I risultati della missione scientifica in Eritrea per lo studio dei raggi cosmici. Ric. Sci. **4**, 365 (1933)

[Rossi1934a] B. Rossi, Directional measurements on the cosmic rays near the geomagnetic equator. Phys. Rev. **45**, 212 (1934)

[Rossi1934b] B. Rossi, Misure della distribuzione angolare di intensità della radiazione penetrante all'Asmara. La Ricerca Scientifica Supplement **1**, 579 (1934)

[Rossi1941] B. Rossi, D.B. Hall, Variation of the rate of decay of mesotrons with momentum. Phys. Rev. **59**, 223 (1941)

[Rossi1942] B. Rossi, N. Nereson, Experimental determination of the disintegration curve of mesotrons. Phys. Rev. **62**, 417 (1942)

[Rossi1943] N. Nereson, B. Rossi, Further measurements on the disintegration curve of mesotrons. Phys. Rev. **64**, 199 (1943)

[Rossi1964] B. Rossi, *Cosmic Rays* (McGraw-Hill, New York, 1964)

[Rossi1981] B. Rossi, Early days in cosmic rays. Phys. Today **34**, 34 (1981)

[Rossi1990] B. Rossi, *Moments in the Life of a Scientist* (Cambridge University Press, New York, 1990)

[Rutherford1903] E. Rutherford, H.L. Cooke, A penetrating radiation from the earth's surface. Phys. Rev. **16**, 183 (1903)

[Rutherford1908] E. Rutherford, H. Geiger, An electrical method of counting the number of α particles from radioactive substances. Proc. Roy. Soc. (Lond.) **A81**, 141 (1908)

[Ryan1979] J.M. Ryan et al., Atmospheric gamma ray angle and energy distribution from sea level to 3.5 g/cm$^2$ and 2 to 25 MeV. J. Geophys. Res. **84**, 5279 (1979)

[Rypdal1997] K. Rypdal, T. Brundtland, The Birkeland Terrella experiments and their importance for the modern synergy of laboratory and space plasma physics. J. Phys. **7**, 113 (1997)

[Sandström1965] A.E. Sandström, *Cosmic ray physics* (North Holland, Amsterdam, 1965)

[Sahni1915] R.R. Sahni, The photographic action of alpha, beta and gamma rays. Philos. Mag. **29**, 836 (1915)

[Saracino2017] G. Saracino et al., Imaging of underground cavities with cosmic ray muons from observations at Mt. Echia (Naples). Sci. Rep. **7**, 1181 (2017)

[Saraiva2020] J.P. Saraiva et al., The TRISTAN detector—2018–2019 latitude survey of cosmic rays. J. Instrum. **15**, C09024 (2020)

[Scarsi2005] L. Scarsi, *Bruno Rossi and the school of Arcetri*. Int. J. Mod. Phys. **A20**, 6539 (2005)

[Schein1941] M. Schein et al., The nature of the primary cosmic radiation and the origin of the mesotron. Phys. Rev. **59**, 615 (1941)

[Schmeiser1938] K. Schmeiser, W. Bothe, Die harten Ultrastrahlschauer. Ann. Phys. **424**, 161 (1938)

[Schönfelder1980] V. Schönfelder et al., The vertical component of 1–20 MeV gamma rays at balloon altitudes. Astrophys. J. **240**, 350 (1980)

[Schopper1967] E. Schopper et al., Handbuch der Physik. Kosmische Strahlung **XLVI**(2), 372 (1967)

[Schröder2017] F.G. Schröder, Radio detection of cosmic ray air showers and high energy neutrinos. Prog. Part. Nucl. Phys. **93**, 1 (2017)

[Schultz2004] L.J. Schultz et al., Image reconstruction and material Z discrimination via cosmic ray muon radiography. Nucl. Instrum. Methods Phys. Res. **A519**, 687 (2004)

[Schultz2007] L.J. Schultz et al., Statistical reconstruction for cosmic ray muon tomography. IEEE Trans. Image Process. **16**, 1985 (2007)

[Schuster2014] P.M. Schuster, The scientific life of Victor Franz Hess. Astropart. Phys. **53**, 33 (2014)

[Sekido1982] Y. Sekido, H. Elliott (eds.), *Early History of Cosmic Study* (D. Reidel Publishing Company, 1982)

[Setter1939] G. Setter, H. Wambacher, Z. Phys. **40**, 702 (1939)

[Shamos1966] M.H. Shamos et al., A new measurement of the intensity of cosmic ray ionization at sea level. J. Geophys. Res. **71**, 4651 (1966)

[Shapiro1941] M. Shapiro, Tracks of nuclear particles in photographic emulsions. Rev. Mod. Phys. **13**, 58 (1941)

[Shapiro1970] M.M. Shapiro, R. Silberberg, Heavy cosmic ray nuclei. Annu. Rev. Nucl. Sci. **20**, 323 (1970)

[Sheldon1963] W.R. Sheldon, N.M. Duller, Intensity of muons underground at large zenith angles. Nuovo Cimento **23**, 63 (1963)

[Sime2012] R.L. Sime, Marietta Blau in the history of cosmic rays. Phys. Today **65**, 8 (2012)

[Sime2013] R.L. Sime, Marietta Blau, Pioneer of photographic nuclear emulsions and particle physics. Phys. Perspect. **15**, 3 (2013)

[Skobeltsyn1927] D.V. Skobeltsyn, Die Intensitätsverteilung in dem Spektrum der γ-Strahlen von RaC. Z. Phys. **43**, 354 (1927)

[Skobeltsyn1929] D.V. Skobeltsyn, Uber eine neue Art sehr schneller β-Strahlen. Z. Phys. **54**, 686 (1929)

[Skobeltsyn1947] D.V. Skobeltsyn, G.T. Zatsepin, V.V. Miller, The lateral extension of Auger showers. Phys. Rev. **71**, 315 (1947)

[Smart2005] D.F. Smart, M.A. Shea, A review of geomagnetic cutoff rigidities for earth-orbiting spacecraft. Adv. Space Res. **36**, 2012 (2005)

[Snyder1949] H.S. Snyder, W.T. Scott, Multiple scattering of fast charged particles. Phys. Rev. **76**, 220 (1949)

[SPACEWEATHER] https://www.spaceweather.com

[Spiering2012] C. Spiering, Towards high-energy neutrino astronomy. Eur. Phys. J. **H37**, 515 (2012)

[Spillantini2013] P. Spillantini, Early cosmic ray research in Italy. AIP Conf. Proc. **1516**, 61 (2013)

[Stecker1968] F.W. Stecker, Effect of photomeson production by the universal radiation field on high energy cosmic rays. Phys. Rev. Lett. **21**, 1016 (1968)

[Steinke1930] E. Steinke, Über Schwankungen und Barometereffekt der kosmischen Ultrastrahlung im Meeresniveau. Z. Phys. **64**, 48 (1930)

[Steinmaurer1982] R. Steinmaurer, Erinnerungen an V. F. Hess, den Entdecker der Kosmischen Strahlung, und an die Ersten Jahre des Betriebes des Hafeleakr-Labors, in [Sekido1982]

[Stevenson1935] E.C. Stevenson, T.H. Johnson, Coincidence counter studies of the variation of intensities of cosmic ray showers and vertical rays with barometric pressure. Phys. Rev. **47**, 578 (1935)

[Størmer1907] C. Størmer, Sur les trajectoires des corpuscules électrisés dans l'espace sous l'action du magnétisme terrestre avec application aux aurores boréales. Arch. Sci. Phys. Nat. Genève **24**, 5, 113, 221, 317 (1907)

[Størmer1930] C. Størmer, Periodische Elektronenbahnen im Felde eines Elementarmagneten und ihre Anwendung auf Brüches Modellversuche und auf Eschenhagens Elementarwellen des Erdmagnetismus. Mit 32 Abbildungen. Z. Astrophys. **1**, 237 (1930)

[Størmer1955] C. Størmer, *The Polar Aurora* (Oxford University Press, 1955)

[STRATOCAT] https://stratocat.com.ar/indexe.html

[Street1935] J.C. Street, R.H. Woodward, E.C. Stevenson, Phys. Rev. **47**, 891 (1935)

[Street1937] J.C. Street, E.C. Stevenson, New evidence for the existence of a particle of mass intermediate between the proton and the electron. Phys. Rev. **52**, 1003 (1937)

[Strohmayer2006] B. Strohmayer, *Marietta Blau, Stars of Disintegration: Biography of a Pioneer of Particle Physics* (Ariadne, 2006)

[Strong2010] A.W. Strong et al., Global cosmic-ray-related luminosity and energy budget of the Milky Way. Astrophys. J. **722**, L58 (2010)

[Suga1962] K. Suga et al., Bolivian Air Shower Joint Experiment. J. Phys. Soc. Jpn. **17**(Suppl. AIII) (1962)

[Swanenburg1981] B.N. Swanenburg et al., Second COS B catalog of high energy gamma-ray sources. Astrophys. J. **243**, L69 (1981)

[Swann1933] W.F.G. Swann, Applications of Liouville's theorem to electron orbits in the Earth magnetic field. Phys. Rev. **44**, 224 (1933)

[Swann1935] W.F.G. Swann, The corpuscular theory of the primary cosmic radiation. Phys. Rev. **48**, 641 (1935)

[Swann1936] W.F.G. Swann, Can protons represent the primary cosmic radiation at sea level? Phys. Rev. **49**, 478 (1936)

[Swann1939a] W.F.G. Swann, The nature of cosmic ray phenomena at high altitudes. Phys. Rev. **56**, 209 (1939)

[Swann1939b] W.F.G. Swann, Showers produced by penetrating rays and allied phenomena. Rev. Mod. Phys. **11**, 242 (1939)

[Swann1940] W.F.G. Swann, A theory of cosmic-ray phenomena based upon a single primary component. Phys. Rev. **58**, 200 (1940)

[Swann1941a] W.F.G. Swann, A single component for the primary cosmic radiation. Phys. Rev. **59**, 770 (1941)

[Swann1941b] W.F.G. Swann, Further evidence for a single component in the primary cosmic radiation. Phys. Rev. **59**, 836 (1941)

[Swann1954] W.F.G. Swann, On H. Alfvén's theory of the effect of magnetic storms on cosmic ray intensity. Phys. Rev. **93**, 905 (1954)

[Swann1961] W.F.G. Swann, History of cosmic rays. Am. J. Phys. **29**, 811 (1961)

[Swider1967] W. Swider, M.E. Gardner, Environmental Research Paper No. 272, Air Force Cambridge Research, Bedford, MA (1967)

[TA] Telescope Array Web site: http://www.telescopearray.org/

[Tanaka2001] H.K.M. Tanaka et al., Development of the cosmic ray muon detection system for probing the internal structure of a volcano. Hyperfine Interact. **138**, 521 (2001)

[Tanaka2007a] H.K.M. Tanaka et al., Imaging the conduit size of the dome with cosmic ray muons: the structure beneath Showa-Shinzan lava dome. Geophys. Res. Lett. **10**, L031389 (2007)

[Tanaka2007b] H.K.M. Tanaka, Monte-Carlo simulations of atmospheric muon production: implication of the past Martian environment. Icarus **19**, 603 (2007)

[Tanaka2014] H.K.M. Tanaka et al., Radiographic visualization of magma dynamics in an erupting volcano. Nat. Commun. **5**, 3381 (2014)

[Tanaka2016] H.K.M. Tanaka et al., Instant snapshot of the internal structure of Unzen lava dome with airborne muograhy. Sci. Rep. **6**, 39741 (2016)

[Tanaka2022] H.K.M. Tanaka, Cosmic time synchronizers (CTS) for wireless and precise time synchronization using extended air showers. Sci. Rep. **12**, 7078 (2022)

[Teller1954] E. Teller, Theory of origin of cosmic rays. Rep. Prog. Phys. **17**, 154 (1954)

[Tennent1967] R.M. Tennent, The Haverah Park extensive air shower array. Proc. Phys. Soc. **92**, 622 (1967)

[Terada2015] K. Terada et al., A new X-ray fluorescence spectroscopy for extraterrestrial materials using a muon beam. Sci. Rep. **4**, 5072 (2015)

[TerHaar1950] D. Ter Haar, Cosmogonical problems and stellar energy. Rev. Mod. Phys. **22**, 119 (1950)

[Thompson1974] D.J. Thompson, A three-dimensional study of 30 to 300 MeV atmospheric gamma rays. J. Geophys. Res. **79**, 1309 (1974)

[Thompson2012] L. Thompson, *The Discovery of Air-Cherenkov Radiation*, CERN Courier, 18 July 2012

[Tioukov2019] V. Tioukov et al., First muography of Stromboli volcano. Sci. Rep. **9**, 1 (2019)

[Tongiorgi1948a] V. Tongiorgi Cocconi, On the presence of neutrons in the extensive air showers. Phys. Rev. **73**, 923 (1948)

[Tongiorgi1948b] V. Tongiorgi Cocconi, On the origin of the neutrons associated with the extensive air showers. Phys. Rev. **74**, 226 (1948)

[Tonwar2013] S.C. Tonwar, Cosmic ray research in India, 1912–2012. AIP Conf. Proc. **1516**, 72 (2013)

[Treat1948] J.E. Treat, K.I. Greisen, Penetrating particles in extensive air showers. Phys. Rev. **74**, 414 (1948)

[Valat2020] D. Valat, J. Delporte, Absolute calibration of timing receiver chains at the nanosecond uncertainty level for GNSS time scales monitoring. Metrologia **57**, 025019 (2020)

[Vavilov1970] Yu.N. Vavilov et al., Bulletin of the Russian Academy of Science. Phys. Ser. **34**, 1759 (1970)

[Vernov1967] S.N. Vernov et al., Radio emission of extensive air showers of cosmic rays. JETP Lett. **5**, 127 (1967)

[Walker1981] R. Walker, A.A. Watson, Measurement of the elongation rate of extensive air showers produced by primary cosmic rays of energy above $2 \times 10^{17}$ eV. J. Phys. G: Nucl. Phys. **7**, 1297 (1981)

[Walter2012] M. Walter, A.W. Wolfendale, Early history of cosmic particle physics. Eur. J. Phys. **H37**, 323 (2012)

[Watase1937] Y. Watase, Cosmic ray showers. Nature **139**, 671 (1937)

[Watson2010] A. Watson, The discovery of the Cherenkov radiation and its use in the detection of extensive air showers, in *Proceedings of the Cosmic Ray International Seminars (CRIS2010)*, Catania, Nucl. Phys. Proc. Suppl. **B212–213**, 13 (2010)

[WDC] World Data Center for Geomagnetism, Kyoto, https://wdc.kugi.kyoto-u.ac.jp/index.html

[Webber1974] W.R. Webber, J.A. Lezniak, The comparative spectra of cosmic ray protons and Helium nuclei. Astrophys. Space Sci. **30**, 361 (1974)

[Wibberenz1962] G. Wibberenz, Identifizierung von Protonen, Müonen und Elektronen in der weichen Komponente der Ultrastrahlung und Messung ihrer Energiespektren. Z. Phys. **167**, 284 (1962)

[Williams1940] E. Williams, G. Roberts, Evidence for transformation of mesotrons into electrons. Nature **145**, 102 (1940)

[Williams1948] E. Williams, The structure of large cosmic ray air showers. Phys. Rev. **74**, 1689 (1948)

[Wilson1896] C.T.R. Wilson, Proc. R. Soc. Lond. **59**, 338 (1896)

[Wilson1897] C.T.R. Wilson, Condensation of water vapour in the presence of dust-free air and other gases. Philos. Trans. **189**, 265 (1897)

[Wilson1898] C.T.R. Wilson, On the condensation nuclei produced in gases by the action of Roentgen rays, uranium rays, ultra-violet light and other agents. Proc. R. Soc. Lond. **64**, 127 (1898)

[Wilson1899] C.T.R. Wilson, On the comparative efficiency as condensation nuclei of positively and negatively charged ions. Proc. R. Soc. Lond. **65**, 289 (1899)

[Wilson1900a] C.T.R. Wilson, On the leakage of electricity through dust-free air. Proc. Camb. Philos. Soc. **11**, 32 (1900)

[Wilson1900b] C.T.R. Wilson, Atmospheric electricity. Nature **62**, 149 (1900)

[Wilson1901a] C.T.R. Wilson, On the ionisation of atmospheric air. Proc. R. Soc. Lond. **A68**, 151 (1901)

[Wilson1901b] C.T.R. Wilson, On the spontaneous ionisation of gases. Proc. R. Soc. Lond. **A69**, 277 (1901)

[Wilson1912] C.T.R. Wilson, On an expansion apparatus for making visible the tracks of ionising particles in gases and some results obtained by its use. Philos. Trans. R. Soc. **A87**, 277 (1912)

[Wilson1943] V.C. Wilson, D.J. Hughes, Cloud chamber and counter studies of cosmic rays underground. Phys. Rev. **63**, 161 (1943)

[Winckler1950] J.R. Winckler et al., A directional and latitude survey of cosmic rays at high altitude. Phys. Rev. **79**, 656 (1950)

[Winn1986] M.M. Winn et al., The cosmic-ray energy spectrum above $10^{17}$ eV. J. Phys. G: Nucl. Part. Phys. **12**, 653 (1986)

[Wolferton2019] M. Wolferton, *How the First American Science Writer Found (Then Lost) God in the Cosmic Rays*, https://www.sciencehistory.org/distillations

[Wulf1909a] T. Wulf, A new electrometer. Phys. Z. **10**, 251 (1909)

[Wulf1909b] T. Wulf, Uber die in der Atmosphäre vorhandene Strahlung von Hoher Durchdringungsfähigkeit. Phys. Z. **10**, 997 (1909)

[Wulf1910] T. Wulf, Beobachtungen űber die Strahlung hoher Durchdringungsfähigkeit auf dem Eiffelturm. Phys. Z. **11**, 811 (1910)

[Xing-Ming2014] F. Xing-Ming et al., A position resolution MRPC for muon tomography. Chin. Phys. C **38**, 046003 (2014)

[Xu1987] Q. Xu, L.M. Brown, The early history of cosmic ray research. Am. J. Phys. **55**, 23 (1987)

[Yock1986] P.C.M. Yock, Heavy cosmic rays at sea level. Phys. Rev. D **34**, 698 (1986)

[Yodh2013] G.B. Yodh, Early history of cosmic rays at Chicago. AIP Conf. Proc. **1516**, 37 (2013)

[Yoshida1959] S. Yoshida, M. Wada, Storm-time increase of cosmic ray intensity. Nature **183**, 381 (1959)

[Zanini2001] A. Zanini et al., Neutron spectrometry at various altitudes in atmosphere by passive detector technique. Nuovo Cimento C **24**, 691 (2001)

[Zanini2009] A. Zanini et al., Cosmic rays at high mountain observatories. Adv. Space Res. **44**, 1160 (2009)

[Zatsepin1951] G.T. Zatsepin, Dokl. Akad. Nauk SSSR **80**, 577 (1951)

[Zatsepin1966] G.T. Zatsepin, V.A. Kuz'min, Upper limit of the spectrum of cosmic rays. ZhETF Pisma Redaktsiiu **4**, 114 (1966)

[Zhou1999] D. Zhou et al., Cosmic ray abundance at aircraft altitudes in the Earth's atmosphere, in *Proceedings of the 26th International Cosmic Ray Conference*, Salt Lake City (USA), vol. 3 (1999), p. 101

[Ziegler1996a] J.F. Ziegler et al., IBM experiments in soft fails in computer electronics (1978–1994). IBM J. Res. Dev. **40**, 3 (1996)

[Ziegler1996b] J.F. Ziegler, Terrestrial cosmic rays. IBM J. Res. Dev. **40**, 19 (1996)

[Ziegler1989] Ch.A. Ziegler, Technology and the process of scientific discovery: the case of cosmic rays. Technol. Cult. **30**, 939 (1989)